Some Clinical Aspects of Critical Flicker Fusion Perimetry: an in-depth analysis

Knut Luraas
Doctor of Philosophy

Cardiff University
June 2012

Knut Luraas
Doctor of Philosophy
Cardiff University 2012

Some Clinical Aspects of Critical Flicker Fusion Perimetry: an in-depth analysis

The thesis evaluated, in three studies, the clinical potential of Critical Flicker Fusion perimetry (CFFP) undertaken using the Octopus 311 perimeter.

The influence of the learning effect on the outcome of CFFP was evaluated, in each eye at each of five visits each separated by one week, for 28 normal individuals naïve to perimetry, 10 individuals with ocular hypertension (OHT) and 11 with open angle glaucoma (OAG) all of whom were experienced in Standard Automated perimetry (SAP). An improvement occurred in the height, rather than in the shape, of the visual field and was largest for those with OAG. The normal individuals reached optimum performance at the third visit and those with OHT or with OAG at the fourth or fifth visits.

The influence of ocular media opacity was investigated in 22 individuals with age-related cataract who were naïve to both SAP and CFFP. All individuals underwent both CFFP and SAP in each eye at each of four visits each separated by one week. At the third and fourth visit, glare disability (GD) was measured with 100% and 10% contrast EDTRS LogMAR visual acuity charts in the presence, and absence, of three levels of glare using the Brightness Acuity Tester. The visual field for CFF improved in height, only. Little correlation was present between the various measures of GD and the visual field, largely due to the narrow range of cataract severity.

The influence of optical defocus for both CFFP and SAP was investigated, in one designated eye at each of two visits, in 16 normal individuals all of whom had taken part in the first study. Sensitivity for SAP declined with increase in defocus whilst that for CFFP increased. The latter was attributed to the influence of the Granit-Harper Law arising from the increased size of the defocused stimulus.

CFF perimetry, SAP, TOP, learning effect, ocular media opacity, defocus

To
Marit and Herbjørn Luraas, my parents

Acknowledgements

I would like to thank the following persons for their help and input to this thesis.

Firstly, I would like to extend my very special thanks to my supervisor, Prof John M. Wild, for his endless patience; his guidance; and his scientific, as well as his personal, support.

Secondly, I am very grateful to ophthalmologists Dr Hans Hafskolt, MD, and Dr Erik Holmberg, MD, for their contribution in recruiting patients with ocular hypertension and patients with glaucoma.

I also wish to thank Mr Jan Birger Håvardsrud, BSc, and Mr Ivan Grischott for their computer assistance; Mr David Shaw, MSc, Senior Medical Statistician, for the Analyses of Variances and Mr Tom Reiersen, BSc, for his linguistic advice.

I would also like to thank the staff of my optometric practice who worked hard during my commitment to this thesis.

I also wish to thank my friends Mr Sven Them-Enger, MSc, Mr Bonnie Uchermann, MSc, and Dr Per Lundmark, PhD, for their inspiration and encouragement during the period of my studies.

Finally, I would especially like to thank my wife, Jorån, and also Lene, Gry and Astri, my children, for all their personal support and encouragement during this demanding, but enjoyable, period.

LIST OF CONTENTS

LIST OF TABLES

LIST OF FIGURES

KEY TO THE ABBREVIATIONS USED IN THE TEXT

ACG	**Angle Closure Glaucoma**
ANOVA	**Analysis of Variance**
ARVO	**Association for Research in Vision and Ophthalmology**
CD	**Cumulative defect curve**
CFF	**Critical flicker fusion**
CLV	**Corrected Loss Variance**
CLUS	**Cluster depth**
CO	**Comparison**
CPSD	**Corrected Pattern Standard Deviation**
CV	**Cup Volume**
D	**Diopter**
dB	**Decibels**
DD	**Diffuse Defect**
DG	**Disability glare**
ED	**Examination Duration**
FDT	**Frequency-Doubling Technology**
FOSC	**Frequency-of-seeing curve**
GANT	**Graphical Analysis of Numerical trends**
GATE	**German Adaptive Thresholding Estimation**
GATT	**Graphical analysis of topographical trends**
GHT	**Glaucoma Hemifield Test**
HFA	**Humphrey Field Analyzer**
HRP	**High-pass Resolution Perimetry**
HRT	**Heidelberg Retina Tomograph**
Hz	**Hertz (cycles per second)**
IOP	**Intra ocular pressure**
IQR	**Interquartile range**
K	**Koniocellular**
K-cell	**Small bistratified cells (koniocellular pathway)**
LD	**Localised Defect**
LED	**Light-emitting diode**
LGB	**Lateral geniculate body**
LGN	**Lateral geniculate nucleus**
LI	**Learner's Index**
LOCS	**Lens Opacities Classification System**
LTF	**Long-Term fluctuation**
LV	**Loss Variance**
LWS	**Long-wavelength sensitivity**
M	**Magnocellular**
M-cell	**Parasol cells (magnocellular pathway)**
MD	**Mean Defect/ Mean Deviation**
MHR	**Mean hit rate**
MOBS	**Modified ninary search**
MS	**Mean Sensitivity**
MWS	**Medium-wanelength sensitivity**
NV	**Normal value**
OAG	**Open angle glaucoma**

OHT	**Ocular hypertension**
ONH	**Optic nerve head**
P	**Parvocellular**
PC	**Persone computer**
PCLUS	**Percentage of the cluster depth**
PCO	**Pennsylvania College of Optometry**
P-cell	**Midget cells (parvocellular pathway)**
PSD	**Pattern Standard Deviation**
Q	**Skewness**
RBP	**Rarebit perimetry**
RF	**Reliability factor**
RGC	**Retinal ganglion cell**
RNFL	**Retinal nerve fiber layer**
SAP	**Standard automated perimetry**
SAPRO	**Spatially adaptive program**
SC	**Spatial correlation**
SF	**Short-term fluctuation**
SITA	**Swedish Interactive Threshold Algorithm**
SIZ	**Cluster size**
SKD	**Stato-kinetic dissociation**
SKP	**Semi-automated kinetic perimetry**
sLV	**Square root of the Loss Variance**
SWAP	**Short-wavelength Automated Perimetry**
SWS	**Short-wavelength sensitive**
TMP	**Temporal Modulation Perimetry**
TOP	**Tendency Oriented Perimetry**
ZATA	**Zippy Adaptive Threshold Algoritm**
ZEST	**Zippy Estimation of Sequential Testing**
VA	**Value table**
V.A.	**Visual acuity**

CHAPTER 1

AUTOMATED PERIMETRY

1.1 Introduction

The purpose of this Thesis was threefold. Firstly, to determine the learning effect for CFF perimetry in normal individuals, in individuals with OAG and in individuals with OHT. Secondly, to determine the influence of age-related cataract on the outcome of CFF perimetry. Thirdly, to determine the influence of optical defocus on the outcome of CFF perimetry. These studies were carried out using the Octopus 311 perimeter.

1.1.1 The visual field

The visual field is that portion of the external environment of the observer in which the steadily fixating eye(s) detects visual stimuli (Weijland et al 2004). The maximum extent of the visual field for a normal fixating eye is approximately 60° nasally, 90° temporally, 70° inferiorly and 60° superiorly from the straight ahead fixating position (Anderson and Patella 1999). The full field for the eye can be restricted by the facial anatomy such as the extent of the nose, the facial bones, deep set eyes and prominent brows (Meyer et al 1993; Anderson and Patella 1999).

The visual field has been described as an 'island of vision in a sea of blindness' by Traquair (1927). The island/ hill of vision serves as a three-dimensional model of the visual field, representing its height (the z-axis describes sensitivity to the stimulus) and its angular extent in all directions. Fixation is referenced to the 'origin' (x=0, y=0) and corresponds to the fovea which exhibits, under photopic conditions, the greatest sensitivity to the stimulus (i.e., the peak, or highest point of the island). The sensitivity decreases as the island slopes towards the sea, corresponding to increased eccentricity, and the slope of the island is steeper nasally than

temporally and steeper superiorly than inferiorly. The normal physiological blind spot (described by Mariotte in 1666), which corresponds to the location of the optic nerve head, is centred slightly below the horizontal midline, 1.5°, and 15.5° temporally relative to fixation. It measures approximately 5.5º in width and 7.5º in height and corresponds to linear dimensions of 1.5mm horizontally and 1.8mm vertically on the fundus (Reed and Drance 1972; Choplin and Edwards 1998).

The 'island of vision in the sea of blindness' is an excellent, easily understood way to explain a patient's visual field. A sinking of the 'island of vision' into 'the sea of blindness' (i.e., a reduction in the height) illustrates a generalised depression/ diffuse reduction across the entire visual field. A focal, or localised, defect (scotoma) corresponds to a region, of variable size and depth, in the 'island of vision', depending upon the severity of the underlying cause. A constriction of the visual field occurs when there is a total loss of sensitivity in the periphery and manifests as an island with steep cliffs at its edges.

Examination of the visual field, perimetry, conventionally involves the measurement of the differential light threshold (ΔL), the minimum luminance necessary for the detection of a small spot of white light (the stimulus) presented on a white background of a given luminance (L). The outcome is expressed as ΔL/L. The reciprocal of the differential light threshold is termed the differential light sensitivity (L/ΔL). Two types of perimetry are available, kinetic perimetry and static perimetry.

Kinetic perimetry involves the movement of a stimulus of constant size and luminance, along given meridians of the visual field, from the 'non-seen' to 'seen' and expresses the threshold in terms of the position within the visual field at which the given stimulus is first detected. The line

joining locations of equal threshold is called an isopter (Groenouw 1893) and is analogous to a contour line for the description of height. The procedure is repeated using a stimulus of different sizes and luminance. By careful selection of the appropriate stimulus sizes and luminances, a quasi three-dimensional estimation, described in terms of isopters (contour lines), of the 'island of vision' can be achieved. The stimulus is traditionally presented under the manual control of the perimetrist. The Goldmann bowl perimeter, designed by Hans Goldmann in 1945, is the 'Gold Standard' method for kinetic perimetry and enables calibrated stimulus and background luminances. However, the procedure is limited by the lack of standardization of the stimulus velocity and by the reaction time of the patient, both of which can materially influence the size of any given isopter. The Goldmann perimeter is slowly being replaced by the semi-automated kinetic perimetry as the 'Gold Standard'.

Static threshold perimetry uses a stationary stimulus of constant size which is presented at a given stimulus location and which is adjusted in given steps of luminance either from the 'non-seen' to 'seen' or from the 'seen' to 'non-seen' or both. Threshold is technically defined as the stimulus luminance, which is perceived with a probability of 50%. The procedure is repeated at various locations across the visual field in order to obtain a topographical representation of the field.

Prior to the automation of static threshold perimetry, the length of the examination was such that the technique was not clinically viable. The first automated perimeter, the Octopus Automated Perimeter, was described by Fankhauser et al in 1972. The ensuing principles of threshold static perimetry were developed using this perimeter (Fankhauser, Koch and Roulier 1972; Koch, Roulier and Fankhauser 1972; Spahr 1975; Fankhauser 1979). Subsequently, other automated perimeters were described including the Competer (Heijl and Krakau 1975), the Fieldmaster

(Keltner, Johnson and Balestrery 1979), the Perimetron (Heijl and Drance 1981), the Peritest (Greve, Dannheim and Bakker 1982), the Dicon (Mills 1984), and the Humphrey Field Analyzer (Heijl 1985). As a consequence, static threshold perimetry has become the accepted method of clinical assessment of the visual field. Compared to the original manual control of the technique, the topography of the visual field can be estimated considerably more quickly and the results are more reproducible. The software and hardware enables standardization of the stimulus parameters and the capacity for data storage and statistical analysis. Although automation of static threshold perimetry has been optimized, the test remains a subjective outcome which is prone to the vagaries of the patient's understanding of the task, co-operation and accuracy of response.

Static threshold perimetry has the advantage over kinetic perimetry in that it is more sensitive and precise for the detection of small isolated focal defects such as those which usually appear in the early stages of glaucoma (Drance, Wheeler and Pattullo 1967; Armaly 1971; Schmied 1980).

Examination of the visual field is undertaken to determine, and wherever possible localize, functional damage in the visual pathway. Visual field defects have different origins and can be pre-retinal (due to ocular media opacities), within the inner or outer retina, in the optic nerve, at the chiasm, in the lateral geniculate body, in the optic tract, in the optic radiations, or at the occipital cortex. The visual field loss arising from a retinal lesion usually corresponds in size and shape to the lesion which, itself, is usually directly observable and may or may not cross the vertical midline. Visual field defects arising from lesions at the optic nerve head reflect damage to the retinal nerve fibre layer and include nasal steps, arcuate defects, altitudinal defects, and temporal wedge defects. These latter defects usually manifest within the central visual field, defined as a radius of 30° from fixation. Visual field defects involving the optic nerve anterior to

the chiasm are monocular and, although generally producing central or ceco-central defects, can manifest in any format (Choplin and Edwards 1998). Lesions involving the chiasm produce bitemporal (hemianopic) field loss which respects the vertical midline. The superotemporal field will be initially affected when the lesion lies inferior to the chiasm, such as a pituitary adenoma, and the inferotemporal fields will be initially affected when the lesion lies superior to the chiasm such as a craniopharyngioma (Kanski 2003). Lesions posterior to the chiasm (i.e. involving the optic tract, lateral geniculate nucleus, optic radiation or visual cortex) do not cross the vertical meridian and the salient localising feature is the homonymous nature of the field loss (affecting the same side of the visual field). Such field loss may manifest as hemianopia or a quadrantopsia and, additionally in the case of the occipital lobe lesions, as altitudinal (double quadrantic) defects. Lesions affecting the temporal and parietal lobes usually damage the optic radiations and will produce homonymous field loss manifesting (initially at least) as superior and inferior quadrantanopic defects, respectively. The similarity (congruity) of the visual field loss between the two eyes increases with increasing posterior manifestation of the lesion (Anderson and Patella 1999).

One of the most common causes of field loss is that of glaucoma. Glaucoma is one of the leading causes of blindness and is estimated to affect more than 66 million people worldwide (Quigley 1996; Fraser, Bunce and Wormald 1999; Musch et al 1999; Gasch, Wang and Pasquale 2000). The number of individuals exhibiting either open angle glaucoma (OAG) or angle closure glaucoma (ACG) will increase to 79.6 million by 2020; and, of these, 74% will have OAG. It was estimated that by 2010, women would comprise 55% of all cases of OAG, 70% of all cases of ACG, and 59% of all cases of glaucoma (Quigley and Broman 2006). Asians would represent 47% of those with glaucoma and 87% of those with ACG (Quigley and Broman 2006). Approximately 2% of the 40+ population have glaucoma (Klein et al 1992). However, only 50%

of those with glaucoma are aware of their condition (Sommer et al 1991; Quigley 1996). Glaucoma is a chronic and progressive multifactorial optic neuropathy characterized by excavation of the optic nerve head (ONH) and retinal nerve fibre layer (RNFL) thinning which result in loss of visual function (Garway-Heath et al 2000; Burk and Rendon 2001). Raised intraocular pressure and increasing age have each been identified as major risk factors for the development of OAG. However, 33% to 50% of those with OAG manifest an IOP within the normal range (Sommer et al 1991). Such estimates have not yet been validated.

Kinetic perimetry is an indispensable diagnostic method in neuro-ophthalmology, in advanced glaucoma and in situations where it is difficult to obtain reliable results with static perimetry.

The purpose of the following review is to describe the fundamentals of static automated perimetry with particular reference to the procedures for the measurement, and the analysis, of a single visual field examination in individuals with OAG. The literature concerning the methods, and the relative efficacy of those methods, for the identification of progressive visual field loss by static automated perimetry and the literature concerning the correlation between function (i.e. outcomes from perimetry) and structure (i.e. the outcomes from imaging) are beyond the scope of the review and of the thesis.

1.1.2 The basics of perimetry

The variation of sensitivity across the visual field, known as the sensitivity gradient, is influenced by a number of factors including the background luminance, the stimulus size, and the stimulus duration.

1.1.3 Units of Measurements

Under scotopic conditions, the amount of light needed to detect a stimulus is constant. Under low photopic background conditions ($1.3cdm^{-2}$ to $10cdm^{-2}$), the behaviour of the differential light threshold can be described by the Rose de Vries Law ($\Delta L/L^{0.5}$ = constant) (Fankhauser 1979; Tate 1985). Above $10cdm^{-2}$, the Weber-Fechner Law is operative namely:

$\Delta L/L=K$ where K is a constant.

Thus, the differential light threshold increases in a linear relation to the background luminance, The standard background luminance used by most perimeters is $10cdm^{-2}$ which lies within that described by the Weber-Fechner Law (Aulhorn and Harms 1972).

On a logarithmic scale: Sensitivity (dB) = k + 10 log ($\Delta L/L$)

The sensitivity of the human visual system ranges from approximately one asb to 1,000,000asb. For this reason, sensitivity is measured on a logarithmic scale (in decibels [dB]). The dB scale is a logarithmic scale where, in perimetry, 0dB is referenced to the maximum stimulus luminance of the perimeter and where 1dB represents a 0.1 log unit of attenuation of the maximum luminance and 10dB represents a 1.0 log unit attenuation of the maximum luminance. The maximum stimulus luminance (0dB) for the Goldmann perimeter is 1000asb, for the current Octopus (300 and 900 series) perimeters 4800asb, and that of the Humphrey Field Analyzers 10,000asb.

1.1.4 Background Luminance and Dynamic Range

To maximise the detection of shallow defect depths within the visual field, it is desirable to achieve the maximum possible dynamic range of the perimeter. A low background luminance and a large stimulus luminance maximizes the dynamic range (Fankhauser 1979; Heijl 1985; Choplin, Sherwood and Spaeth 1990; Zalta 1991). The dynamic range is defined as the measurement range over which the neuro-visual system can be tested, using specific equipment with a given set of experimental variables (Fankhauser 1979). The stimulus size will also influence the dynamic range of a perimeter. For example, an increase in the stimulus size from Goldmann I to III increases the dynamic range by 12 dB for a background luminance of 1.3cdm^{-2} at an eccentricity of 50º (Fankhauser 1979). To obtain a satisfactory dynamic range and minimize the adaptation time needed prior to the examination, the background luminance of 10cdm^{-2}, which lies within Weber-Fechner Law, is considered to represent a compromise between the background luminance/ adaptation time and the maximal dynamic range (Heijl 1985).

Stimuli with high luminances may result in erroneous measures of sensitivity caused either by intra-ocular light scatter or by seepage from the boundaries of the stimulus (Fankhauser and Haeberlin 1980a; Dengler-Harles et al 1990). Those early perimeters which used LED sources for the stimulus utilized a lower background luminance due to the reduced luminance of the available LEDs.

1.1.5 Stimulus Size

Spatial summation and temporal summation both influence the visibility of the stimulus. Spatial summation describes the relationship between the differential light threshold and the size and luminance of the stimulus, whereby a dim large stimulus and a brighter smaller stimulus are

equally visible. Spatial summation varies with stimulus location, (Wilson 1970; Anderson and Patella 1999) and can be expressed as:

$$A^{k} \; x \, I = C$$

where A is the area of the stimulus, I is the stimulus luminance and C is a constant at the given location. The value of the exponent k varies with location from 0.55 to 0.9 (Anderson and Patella 1999).

The six stimulus sizes for the Goldmann bowl perimeter are designated by Roman numerals: size 0 to size V. Each stimulus increases in diameter by a factor of 2 and in area by a factor of 4 (Table 1.1) compared to the immediately previous smaller stimulus. The Goldmann stimulus sizes have been adopted for automated perimetry. The default stimulus size for static threshold perimetry is Goldmann size III. This stimulus size is affected less than size I by optical defocus (Heijl 1985), and media opacities (Sloan 1961; Wood, Wild and Crews 1987a). The use of smaller stimuli reduces the dynamic range, especially in the periphery (Zalta and Burchfield 1990), but provides the opportunity to measure the visual field with a higher spatial resolution (Bek and Lund-Andersen 1989). The variability of the threshold estimate within 30° eccentricity increases with successive reduction in stimulus size compared to size III and reduces for successive increases in stimulus size compared to size III (Gilpin et al 1990; Wall, Kardon and Moore 1993).

1.1.6 Stimulus Duration

Temporal Summation describes the relationship between the differential light sensitivity and stimulus duration. Temporal summation is expressed as:

$$\Delta L \times T^{k} = C$$

where ΔL is the differential light threshold, T is the stimulus duration, k is the summation coefficient and C is a constant. There are several laws that describe Temporal Summation including: Pieron's Law (k=0.3), Piper's Law (k=0.5), Goldmann's approximation (k=0.8) and Bloch's Law or Bunsen-Roscoe's Law (k=1) (Baumgardt 1959; Greve 1973). Bloch's Law describes the fact that the differential light sensitivity increases linearly with increase in stimulus duration until the duration exceeds a critical value after which, sensitivity is independent of the duration (Bloch 1885). Temporal summation decreases with increasing stimulus size (Barlow 1958; Saunders 1975) and increasing background luminance (Barlow 1958; Saunders 1975; Daly and Normann 1985).

The critical stimulus duration in the normal population varies between 60 and 100msec (Barlow 1958; Greve 1973; Saunders 1975). Short stimulus durations reduce the examination time and are useful for patients with poor fixation (Greve 1973) but increase the variability of the threshold estimate. The Octopus perimeters use stimulus duration of 100msec whilst the Humphrey Field Analyzers use stimulus duration of 200msc. The stimulus duration for the Octopus perimeters is such as to achieve complete temporal summation but is shorter than the latency time for voluntary eye movements (Weijland et al 2004).

Goldmann stimulus size (Roman numerals)	Stimulus diameter (degrees)	Stimulus area (mm^2) at a viewing distance of 30cm
0	0.05°	0.0625
I	0.11°	0.25
II	0.22°	1
III	0.43°	4
IV	0.86°	16
V	1.72°	64

Table 1.1 The spatial characteristics of each of the six Goldmann stimuli sizes.

1.1.7 Stimulus Generation

The mode of stimulus generation varies between different types of perimeter. The Octopus 100, 300 and 900 series and the Humphrey Field Analyzers utilize projection of a halogen source. An alternative approach, employed on the Dicon, Henson and Medmont perimeters, utilizes LED stimuli. LEDs have a long life span and, if desirable, can be temporally modulated at high frequencies. However, each LED requires individual calibration and the given type of perimeter is limited by the number of LEDs incorporated into the design which, in turn, limits the spatial possibilities of the stimulus array. The Octopus 1-2-3 and now the Octopus 300 series use(d) a direct projection system in which the LED generated stimulus, background illumination and fixation target are projected onto the retina from optical infinity (Weijland et al 2004). Most other perimeters employ a spherical bowl as a background although the HFA 700 Series uses an aspheric bowl.

In some of the early LED perimeters, the LEDs were not covered by the diffusing surface of the background and caused localised changes in retinal adaptation (Heijl 1985; Britt and Mills 1988) and an increase in variability in areas of high sensitivity (Desjardins and Anderson 1988) arising from the resulting “black-hole” effect (Britt and Mills 1988). Other early perimeters such as the

Fieldmaster 200 (Mills 1984) and the Tübingen 2000 used fibre optic waveguides emanating from a single light source to generate each stimulus. As with LED stimuli, the use of fibre optics limited the number of stimulus locations. The technology was also expensive to manufacture.

1.1.8 Spatial Configuration of Stimuli

The overall aim of the visual field examination is to balance the requirement to maximize the potential for the detection, and the optimum description, of visual field loss with that of a realistic examination time.

Clearly, the number of stimulus locations within any given visual field examination largely determines the length of the examination. However, the number of, and the extent of the separation between, the stimuli determine the resolution with which the defect can be detected and/ or described. A circular defect of 9° in diameter has a 95% probability of detection when 50 regularly distributed stimulus locations are evenly placed out to 30° eccentricity (Greve 1975). The probability of detection is 100% using 452 stimulus locations for a defect of 7.5°. It is 95% for a defect of 3° in diameter (Greve 1975). The relation between sensitivity for detection and the number of stimulus locations is logarithmic, whilst that for specificity is linear. Thus, large numbers of stimulus locations are not required to reach high levels of sensitivity (Henson, Chauhan and Hobley 1988).

Visual field defects in glaucoma usually occur within the central field and correspond to the anatomy of the retinal nerve fiber layer and its projection to the optic nerve (Werner and Drance 1977; Caprioli and Spaeth 1985). The prevalence of glaucomatous field loss in the peripheral field manifesting with a normal central field is 1% (Blum, Gates and James 1959) or 4% (Ballon et al 1992). Glaucomatous field loss initially presents in one hemisphere either as a nasal step or

as a deep, frequently absolute, paracentral defect or as a combination of both. Temporal wedge defects also reflect the retinal nerve fiber layer anatomy, but are seen less than 5% of the time (Walsh 1996). The initial paracentral and/ or nasal step defect progresses to an arcuate defect and eventually to an altitudinal defect. At some point, the opposite hemifield becomes involved. In the advanced stages of damage, the superior and inferior loss coalesces and results in isolated central and temporal islands of residual vision within the central field. The occurrence of purely generalized/ diffuse field loss in glaucoma is equivocal (Drance et al 1987; Heijl 1989; Langerhorst et al 1989; Asman and Heijl 1994).

The given arrangement of stimulus locations for any given visual field examination is termed the Program. The 'Gold Standard' stimulus program is Program 32 which was introduced with the first Octopus perimeters in 1975. The stimuli are presented in terms of a square grid which is offset by 3º both from the horizontal and from the vertical midlines, respectively, and in which the inter-stimulus separation is 6º. The corresponding program for the Humphrey Field Analyzers is Program 30-2. A focal defect of 8.4º in diameter can be detected with 100% probability using stimulus size III and either Program 32 or 30-2. However, the probability of detection reduces to 79% for a defect of 6º in diameter (Fankhauser and Bebie 1980). Nevertheless, a resolution of 6º is frequently insufficient for the identification of the physiological blind spot (King et al 1986). Program G1 of the Octopus is specially designed for glaucoma and the number of stimulus locations is weighted towards the paracentral and nasal step regions. In the paracentral region (out to 10º eccentricity) the grid has an inter-stimulus separation of 2.8º and between 10º and 30º eccentricity an inter-stimulus separation of 6º (Weijland et al 2004). A modification of Program 30-2 is that of Program 24-2 which omits all the locations in the outer annulus of the grid with the exception of the two locations immediately above and below the horizontal midline, respectively, at the extreme nasal periphery.

The concept of spatially adaptive programs is an attractive notion whereby the stimulus separation is reduced (i.e. the resolution is increased) in areas of suspected, or actual, reduced sensitivity. The Spatially Adaptive Program (SAPRO) was developed for the Octopus perimeters (Haeberlin and Fankhauser 1980) whereby the spatial resolution changed from 6º to 3º resolution. However, the use of such spatially adaptive programs does not improve the sensitivity and specificity of the visual field examination compared to that achieved by the standard 6º resolution (Asman et al 1988).

A custom test allows the examiner to design stimulus programs with a given number of stimuli and, therefore, a given spatial resolution. A stimulus grid of 9º by 9º containing 100 stimulus locations with an inter-stimulus resolution of 1º can identify areas of reduced sensitivity which would be undetected by the conventional resolution of 6º (Westcott et al 1997).

1.2 Threshold Algorithms

The threshold algorithm (strategy) is the name given to the method for determining the estimate of threshold. Classically threshold is estimated by compilation of a frequency-of-seeing (FOS) curve whereby the frequency of a positive response (ordinate) is plotted as a function of stimulus luminance (abscissa). The curve has a sigmoid appearance with a linear part in the middle. The frequency of a 'seen' response is never 0% due to the presence of false-positive responses and never reaches 100% due to the presence of false-negative responses. Threshold is generally taken as the luminance which corresponds to a 50% frequency-of-seeing.

The classical method for compiling the FOS curve for estimation of the differential light threshold is the Method of Limits. The stimulus luminance is adjusted in small intervals or steps either in an ascending or a descending manner until it is perceived with a probability of 50%.

The method is time consuming when the initial stimulus luminance is far from the threshold. Conversely, the procedure is rapid if the initial stimulus luminance is close to the threshold (Taylor 1971).

The current approach, the adaptive method, varies the stimulus luminance in ascending *and* descending steps until the estimate of threshold is obtained. The procedure is termed the staircase or bracketing method (Wetherill and Levitt 1965). The most frequently used algorithms in perimetry generally employ a double crossing of the threshold whereby, if the initial stimulus is not seen, the luminance is increased in unit steps until the a positive response is obtained. The stimulus luminance is then decreased in steps (which are half that of those used for the first estimation) until a negative response is obtained. The threshold is thereby crossed twice. The threshold can, of course, be approached from the opposite direction. Wherever possible, the number of stimuli necessary to estimate the threshold are minimized with the intention of shortening the examination duration and thereby reducing the inherent variability in the threshold estimate arising from fatigue (Searle et al 1991; Hudson, Wild and O'Neill 1994; Gonzalez de la Rosa and Pareja 1997; Anderson and McKendrick 2007). However, the variability in the estimation of threshold, itself, reduces with increase in the number of crossings of threshold, with reduction in step size and with the number of threshold estimations.

The various threshold algorithms used in automated perimetry can be divided, depending upon their date of introduction, into first, second and third generation algorithms. The second generation algorithms exhibit a reduction in examination duration, compared to that of the first generation, at the cost of some loss of accuracy of the threshold estimate whilst the third generation algorithms have utilised the advances in computer processing speed to exhibit a reduction in examination duration without loss of accuracy in the threshold estimate.

1.2.1 First Generation Algorithms

The Threshold algorithm for the Octopus series of perimeters commences the examination at each of four 'primary' stimulus locations (anchor points) located near the centre of each quadrant of the visual field (Spahr 1975; Zulauf, LeBlanc and Flammer 1994; Weijland et al 2004). The initial luminance of each stimulus is 4dB dimmer than the age-corrected normal value. If the response is negative, the subsequent stimulus luminance is increased by 6dB. The process continues with an increase of the stimulus luminance in steps of 8dB until a positive response is obtained. Following the crossing of threshold, the stimulus luminance is reduced in steps of 4dB until the threshold is crossed for the second time. After the second crossing of threshold, the stimulus luminance is increased again in 2dB steps until the threshold is crossed for the third time. The latter value is adjusted by 1dB in the opposite direction to the last response (Weijland et al 2004). If the response to the initial stimulus luminance is positive, the luminance is decreased in steps of 2dB until a negative response is obtained after which the luminance is increased in 1dB steps until a positive response is obtained. The sensitivity at the four anchor positions is used, in conjunction with the prior knowledge of the slope of the age-corrected sensitivity gradient, to calculate the magnitude of the initial luminance for the threshold estimate of each of the surrounding locations in the corresponding quadrant. The bracketing procedure then continues, as before, in 4-2-1 dB steps. The initial luminances for the next set of subsequent locations are calculated, in each case, from the median value of the three previously thresholded neighbouring locations and from the slope of the age-corrected sensitivity gradient (Weijland et al 2004).

The Full Threshold algorithm of the Humphrey Field Analyzer initially obtains a threshold estimate twice at each of four stimuli (seed points) situated 9° from both the horizontal and vertical meridians, respectively. The initial luminance at each of these four seed locations is

25dB and threshold is crossed twice in 4dB and 2dB steps, respectively. The final 2dB crossing of threshold can occur in either an ascending or descending direction. The threshold is taken as the mean of the last positive and first negative response. The initial value for the immediate adjacent stimulus locations is 2 dB brighter than the expected value derived from knowledge of the sensitivity at the primary locations and of the slope of the hill of vision (Wild et al 1999a).

.

1.3 Second Generation Algorithms

The Dynamic Strategy algorithm for the Octopus perimeters reduces the examination duration by 30-40% in areas of normal sensitivity and by 40-50% in areas of severe loss compared with the Threshold algorithm (Weber and Klimaschka 1995).

The luminance steps for the Dynamic Strategy algorithm are adapted to the sensitivity at the given stimulus location from a knowledge of the width of the FOS curve. With increasing severity of visual field loss, the step size increases from 2dB to 10dB and threshold is crossed only once. The threshold estimate is calculated as the mean of the two last two stimulus luminances (Weber and Klimaschka 1995). The Dynamic Strategy algorithm exhibits lower between-examination variability than the Threshold algorithm for sensitivities in the normal range but higher between-examination variability for relative defects (Weber and Klimaschka 1995). Alternatively, the short-term fluctuation of the Dynamic Strategy is higher than the Threshold algorithm, but the long-term fluctuation is similar (Zulauf, Fehlmann and Flammer 1996). The ratio of benefit (accuracy) versus cost (time) is largely in favour of the Dynamic Strategy algorithm (Weber and Klimaschka 1995).

1.3.1 FASTPAC

The FASTPAC algorithm was introduced for the Humphrey Field Analyser as a shorter alternative to the Full Threshold algorithm. The FASTPAC algorithm utilizes a 3dB step size and a single crossing of threshold. The threshold is obtained at the initial seed locations as for the Full Threshold algorithm after which the initial starting luminance for the secondary locations is 2dB dimmer than the expected threshold when the expected value is an odd number and 1dB brighter when the expected value is an even number. The threshold is designated as the last seen stimulus luminance (Flanagan et al 1993). In comparison to the Full Threshold algorithm, the FASTPAC algorithm reduces the examination duration by 35% to 40%. The impact of errors arising from an incorrect estimate of threshold at a given seed location, and which can lead to a masking of relative loss, is greater for the FASTPAC algorithm than for the Full Threshold algorithm (Glass, Schaumberger and Lachenmayr 1995). The Short-term fluctuation is approximately 25% higher than that for the Full Threshold algorithm (Flanagan et al 1993; Flanagan, Wild and Trope 1993; Glass, Schaumberger and Lachenmayr 1995; Schaumberger, Schafer and Lachenmayr 1995). The visual field indices (See Sections 1.11.1 and 1.11.2), Mean Sensitivity (MS) and Mean Deviation (MD) are similar between the two algorithms (Schaumberger, Schafer and Lachenmayr 1995). However, the Pattern Standard Deviation (PSD) and the Corrected Pattern Standard Deviation (CPSD) indices are either smaller (Schaumberger, Schafer and Lachenmayr 1995) or larger (Flanagan, Wild and Trope 1993) than those for the Full Threshold algorithm.

1.4 Third Generation Algorithms

1.4.1 Swedish Interactive Threshold Algorithms (SITA)

The Swedish Interactive Threshold Algorithms became commercially available in 1997 for the HFA 700 series. Two algorithms are available: the SITA Standard is analogous to the Full

Threshold algorithm and the SITA Fast is analogous to the FASTPAC algorithm (Olsson, Rootzen and Heijl 1988; Olsson et al 1993; Bengtsson et al 1997; Olsson et al 1997; Bengtsson, Heijl and Olsson 1998; Bengtsson and Heijl 1998a; Bengtsson and Heijl 1998b). Both algorithms reduce the examination duration in normal individuals: the SITA Standard algorithm is approximately 50% shorter compared to the Full Threshold algorithm and the SITA Fast algorithm, 50% shorter compared to the FASTPAC algorithm. The SITA Fast algorithm is 41% shorter than the SITA Standard algorithm (Anderson and Patella 1999; Wild et al 1999a). The examination duration of both SITA algorithms increases (i.e. the saving of time compared to the Full Threshold algorithm becomes less) as the severity of the glaucomatous field loss increases, particularly for the SITA Fast algorithm (Wild et al 1999a; Sekhar et al 2000; Budenz et al 2002). The SITA Fast algorithm exhibits greater test-retest variability in those areas (Artes et al 2002).

The reduction in the examination duration for both SITA algorithms is achieved by a complex statistical model. The majority of the time-saving arises from a reduction in the number of stimulus presentations which is achieved by the use of a Bayesian approach. The latter uses two prior likelihood models (density functions) of the sensitivity for each given stimulus location: one model describes the distribution of the probability for the given value of sensitivity in the normal field and the other describes the distribution of the probability for the given value of sensitivity in the glaucomatous field. The initial luminance at the seed locations is identical to that of the Full Threshold algorithm. The initial luminance at any given immediately surrounding location is based upon the expected normal value of sensitivity which, itself, is derived from the prior density function for normal sensitivity. The initial step size is +/-4dB from this value. Subsequent luminance levels are based upon the nature of the response, on knowledge of the characteristics of the associated FOS curve at the given location and on the correlation of

sensitivity with immediate neighbouring locations. The FOS curve is steep with a narrow width and of variability in normal eyes, but flattens as sensitivity declines. The FOS curve in glaucomatous eyes exhibits a shallower slope with a resultant increased variability of response (Chauhan et al 1993; Olsson et al 1993). The prior density function at each location is modified as a consequence of responses from the given individual to produce a corresponding posterior density function. The latter are constantly updated following each response, regardless of stimulus location, to produce an estimate of the likely threshold at the given location. In the case of reduced values of sensitivity, the prior density function for the probability of the given sensitivity in the glaucomatous eye is utilized. The height of the peak of the posterior density function represents the likely threshold estimate whilst the width represents the potential error in the estimate. The accuracy of the estimate is evaluated in the case of the SITA Standard algorithm by the use of 4dB steps, and, once threshold has been crossed, by the use of 2dB steps. Threshold is taken as the 50% 'seen' value of sensitivity on the FOS curve. The corresponding step size for the SITA Fast algorithm is 4dB. The staircase procedure is terminated once the estimated threshold exhibits accuracy within a predetermined error (the error related factor). Threshold estimation with the SITA Standard algorithm cannot be terminated unless there has been at least one crossing of the threshold (Bengtsson et al 1997). However, the threshold estimation with the SITA Fast algorithm can be terminated at any given location without a crossing of threshold (Bengtsson et al 1997; Bengtsson and Heijl 1998b).

The examination duration of the algorithms is also shortened by adapting the inter-stimulus interval to the response time of the individual and by estimation of false-positive responses based upon the reaction time of the individual (Bengtsson et al 1997; Anderson and Patella 1999).

The Mean Sensitivity in the normal eye is 0.8dB and 1.3dB larger for the SITA Standard and the and SITA Fast algorithm, respectively, compared to the Full Threshold algorithm (Wild et al 1999a). The Mean Sensitivity in the normal eye for the SITA Fast algorithm is 1.47 dB greater than that for the FASTPAC algorithm and 0.5dB larger than that for the SITA Standard Algorithm (Wild et al 1999a). In the glaucomatous eye, both SITA Standard and SITA Fast algorithms generate a marginally higher Mean sensitivity compared to the Full Threshold and FASTPAC algorithms but with a statistically deeper defect depth (Wild et al 1999). Both SITA algorithms exhibit better test-retest variability for sensitivities above 25dB than for the Full Threshold algorithm. Below 25dB, the SITA Standard algorithm exhibits slightly better test-retest variability, and the SITA Fast algorithm slightly poorer test-retest variability compared to the Full Threshold algorithm. The higher sensitivity values, the statistically deeper defect depths (Aoki, Takahashi and Kitahara 2007) arising from the narrow confidence intervals for normality, and, in general, the better test-retest variability compared to the Full Threshold algorithms has been attributed to the reduction in the perimetric fatigue effect arising from the reduction in examination duration (Sharma et al 2000; Artes et al 2002).

1.4.2 Tendency Orientated Perimetry (TOP)

Tendency Oriented Perimetry (TOP) was introduced in 1996 (Gonzalez de la Rosa et al 1996) for the Octopus perimeters and utilizes the correlation of sensitivity between neighbouring stimulus locations.

The TOP strategy subdivides the various stimulus locations within the given stimulus program into four overlapping sub-matrices such that, in the case of Program 32, each sub-matrix comprises 19 stimulus locations with a between-stimulus separation of 15° (Anderson 2003). Each matrix is examined in sequential order. The stimulus luminance at each of the locations in the first sub-matrix is presented at half (8/16) that of the age-corrected value of normal

sensitivity at the given location. Each location in the first sub-matrix is examined once. If a positive response is obtained at the given location, the sensitivity is recorded as the value of the starting luminance less (i.e. dimmer) 4/16 of the age-corrected value of normal sensitivity at the location i.e., ([8/16 + 4/16] of the age-corrected value of normal sensitivity). If a negative response is obtained at the given location, the sensitivity is recorded as the value of the starting luminance plus (i.e. brighter) 4/16 of the age-corrected value of normal sensitivity at the location i.e., ([8/16 - 4/16] of the age-corrected value of normal sensitivity).

As a consequence of the responses derived for the locations in the first sub-matrix, the expected (i.e., age-corrected) value of sensitivity at any given location in the second sub-matrix is modified by the average of the response(s) derived by the first sub-matrix at any locations situated within 9º vertically and 9º horizontally of the given location in the second sub-matrix. The stimulus luminance at each of the locations in the second sub-matrix is presented at the expected value of sensitivity at the given location. If a positive response is obtained at the given location, the sensitivity is recorded as this value pluss 3/16 of the normal age corrected value. If a negative response is obtained at the given location, the sensitivity is recorded as 4/16 of the expected value of normal sensitivity at the given location.

The locations in the third sub-matrix are adjusted by the average of the response derived by the second sub-matrix at any locations situated within 9º vertically and 9º horizontally of the given location. The stimulus luminance at each of the locations in the third sub-matrix is presented at 2/16 of that of the expected value of the sensitivity at the given location. The threshold estimate for all the locations within the third sub-matrix is recorded as +/- 2/16 of the expected value of normal sensitivity at the given location depending upon whether a positive or a negative response was obtained.

The cycle is repeated for those locations in the fourth sub-matrix and sensitivity is recorded as +/- 1/16 of the expected value of normal sensitivity at the given location depending upon whether a positive or a negative response was obtained. The final adjustment recalculates the estimates based upon the established correlations between adjacent locations.

The TOP strategy is appropriate for patients in whom time-consuming perimetry is not possible or who exhibit advanced loss (Maeda, Nakaura and Negi 2000). The algorithm can be easily applied to other perimetric methods such as SWAP, Pulsar perimetry and Critical Flicker Fusion (CFF) perimetry, (Chapters 2, 4, 5 and 6). The TOP algorithm yields shallower defects compared to the Threshold algorithm (Lachkar et al 1998; Maeda, Nakaura and Negi 2000) and the SITA Fast algorithm of the HFA (King et al 2002). The examination duration is between 75% and 80% less compared to the Threshold strategy both in normal individuals and in individuals with OAG (Morales, Weitzman and Gonzalez de la Rosa 2000; Kratochvilová 2002; Gonzales de la Rosa et al 2003).

1.4.3 German Adaptive Thresholding Estimation (GATE-i/GATE)

The GATE-i algorithm (Schiefer et al 2009) commences by determining the sensitivity at each of five predefined seed locations. The measured sensitivity at each seed location is then compared to the corresponding age-corrected normal value. The smallest deviation, across the five locations, between the measured and age-corrected values of sensitivity is then used to adjust the overall height of the expected visual field. The initial stimulus luminance at each subsequent stimulus location is 2dB brighter than the expected value from the adjusted hill of vision. If a positive response is obtained, the luminance is reduced in 4dB steps until a negative response is obtained after which the luminance is increased in 2dB steps until a positive response is obtained. If the initial luminance yields a negative response, the subsequent stimulus is presented

at the maximum luminance. If the latter yields a negative response, the threshold estimation at the given location is terminated. If the maximum luminance yields a positive response, the subsequent stimulus is presented at 4dB brighter than the initial presentation and the luminance is increased in 4dB steps until a positive response occurs. The stimulus is then presented 2dB dimmer than the level at which the previous positive response occurred. The threshold is defined as the mean of the last positive and negative response.

The GATE algorithm is similar to the GATE-i algorithm but differs only in that the reference field for the initial stimulus presentations is based upon the previously determined thresholds for the given individual rather than upon the age-corrected normal values.

The characteristics of the threshold recorded with the GATE-i and GATE algorithms compare favourably with those obtained with the Full Threshold algorithm despite the approximate halving of the examination duration. The Mean Sensitivities of 60 individuals (40 with OAG, 10 with suspected OAG and 10 with OHT) derived with Program 24-2 and with the SITA Standard, GATE-i and GATE algorithms were 1.2dB, 0.6dB and 0.0dB higher, respectively, than with the Full Threshold algorithm. The standard deviation of the difference in the Mean Sensitivity obtained at two examinations within a period of 14 days was 3.9dB for the Full Threshold algorithm, 4.5dB for GATE-i, 4.2dB for GATE and 3.1dB for the SITA Standard algorithm. Test-retest agreements, as measured by the 95% reference interval of the differences, were -7.69dB to 7.69dB, -9.76dB to 9.0dB, -8.40dB to 8.56dB and -7.01dB to 7.44dB, respectively. The examination durations were 9.0, 5.7, 4.7 and 5.6 minutes, respectively (Schiefer et al 2009).

1.4.4 Zippy Adaptive Threshold Algorithm (ZATA)

The Zippy Adaptive Threshold Algorithm (ZATA) was introduced for the Henson 8000 perimeter. Two versions of ZATA are available: Standard and Fast. Both algorithms use data from prior examinations to reduce the time for threshold estimation. The algorithm reduces the examination duration in normal eyes and in eyes with severe field loss. However, at the time of submission of this thesis, no peer reviewed publications report on the performance of these algorithms.

1.4.5 Continuous light increment perimetry (CLIP) SPARK Precision and SPARK Light

Continuous light increment perimetry (CLIP) SPARK Precision and SPARK Light are third generation fast threshold algorithms available for use with the Oculus Easyfield perimeter. At the time of submission of this thesis, no detailed descriptions of these algorithms have been published.

CLIP uses a 'modified ramp stimulus' whereby the stimulus luminance is continuously increased from an infrathreshold level 'according to the patient's reaction time' until it is seen (Wabbels, Diehm and Kolling 2005). The test is 'constantly modified according to patient performance'. CLIP yields a higher Mean Sensitivity than the 4-2dB algorithm of the Easyfield perimeter in individuals with glaucomatous field loss and tends to underestimate the depth of deep focal loss. The examination duration for CLIP was 5.6 minutes for 55 stimulus locations compared with that of 8.9 minutes for the 4-2dB algorithm (Wabbels, Diehm and Kolling 2005). The mean point-wise sensitivity difference in individuals with glaucomatous field loss between the SITA Fast and the Full Threshold algorithms of the Humphrey Field Analyzer (0.84 dB) was significantly lower than that found between CLIP and the 4-2dB algorithm of the Easyfield

perimeter the Oculus FT strategy (1.71 dB) (Capris et al 2008). The examination duration for the SITA Fast (367+/-71 sec) and CLIP (453+/-98 sec) algorithms were approximately 55% and 35% shorter than those found with the respective/ equivalent first generation algorithms. The CLIP algorithm has also been found suitable for the examination of children above the age of 8 years (Wabbels and Wilscher 2005).

According to Oculus (http://www.oculus.de/us/sites/detail) the SPARK Precision strategy offers faster and more reliable threshold perimetry' and a 'complete visual field test of glaucoma patients can be performed in only 3 minutes per eye, 'The measurement excels in the stability of the results for improved progression analysis.' The SPARK Light strategy is for follow-up or for screening examinations. In those individuals with a previous visual field examination, the quality of the results is similar to those of the SPARK Precision algorithm but with a further halving of the examination duration. A SPARK Training strategy which lasts approximately 40 seconds is also available to reduce the effect of the learning effects in the standard perimetry. The performance of these algorithms against the more established algorithms has yet to be evaluated.

1.5 Suprathreshold static perimetry

Current suprathreshold perimetry uses a stimulus that is presented at a suprathreshold level referenced to the sensitivity gradient of the normal field. The sensitivity gradient is either that of the age-corrected normal or that derived for the individual and calculated from several individual threshold estimates i.e., threshold-related. The technique is limited by the lack of separation of abnormalities in height and shape of the field from abnormalities in shape only, i.e., the separation of focal loss from that arising from cataract. The sensitivity and specificity of the technique is also dependent upon the magnitude of the suprathreshold increment. Too small an increment results in poor specificity whilst too large an increment results in poor sensitivity. The

use of an 8dB increment with age-corrected suprathreshold perimetry, for example, with the Humphrey Field Analyzer can mask shallow defects, particularly those paracentrally, which can be detected with the FASTPAC (Stewart, Shields and Ollie 1989; Mills et al 1994) and SITA algorithms. The similarity between the outcomes of suprathreshold and threshold perimetry increases as the severity of the defect increases particularly those exhibiting absolute loss as encountered in lesions of the optic tract and those more posteriorly (Lewis, Johnson and Keltner 1986; Sponsel et al 1995; Siatkowski et al 1996; Artes et al 2003; Topouzis et al 2004; McKendrick and Turpin 2005b).

1.6 Reliability parameters

The utility of the visual field examination as a diagnostic tool is dependent upon the ability and co-operation of the patient in determining the threshold estimate. The reliability of the response can be sampled in terms of the Short-term Fluctuation and the response to several quality control parameters, namely the fixation loss catch trials and the false-positive and the false-negative catch trials.

1.7 Fixation monitoring

Fixation stability is essential during the visual field examination. Fixation can be monitored with varying degrees of sophistication via the monitor of the perimeter, via the Heijl-Krakau method and via eye tracking.

The Heijl-Krakau method of monitoring fixation is used in many perimeters including that of the HFA. The technique establishes the position of the blind spot within the visual field at the outset of the examination and monitors fixation by projecting a Goldmann size III stimulus into the blind spot location at various intervals throughout the examination (Heijl and Krakau 1975). If

the individual does not respond to the stimulus, fixation is assumed to be correct. However, a positive response indicates an eye movement. Continual positive responses in the presence of steady fixation indicate an inappropriate localization of the blind spot at the outset of the examination, most usually due to head tilt. They can also be associated with excessive incorrect responses to the false-positive catch trials. In order to prevent the occurrence of pseudo fixation losses, it is important initially to map the correct position and size of the blind spot (Sanabria, Feuer and Anderson 1991; Fankhauser 1993). Optical effects, caused either by high positive or high negative corrective lenses can move the apparent position of the blind spot away from the intended location fixation and it is vital to detect such problems early in the test (Sanabria, Feuer and Anderson 1991). Media opacities can also reduce the accuracy of the Heijl-Krakau technique (Fankhauser and Haeberlin 1980a). In the HFA series of perimeters, the number of fixation loss catch trials comprises 5% of the total number of stimulus presentations.

The Octopus perimeters use an infrared illumination system to produce two Purkinje I reflexes, one either side of the pupil centre. With the Octopus 300 series which employs direct projection onto the retina, small sustained re-adjustments of fixation can be compensated for by appropriate rotation in the x and y direction of the optical head of the perimeter. If an eye movement is made, the Octopus perimeters discount the response from the individual. If the patient blinks or closes the eyelids during a stimulus presentation, the Octopus perimeters re-present the stimulus at the given location at a later time in the examination (Interzeag AG 1998; Weijland et al 2004).

Some models of the HFA 700 Series are equipped with gaze monitoring. An infra-red system measures the distance between the pupil centre and the Purkinje I reflex. Image analysis determines the distance between the pupil centre and the corneal reflex. A deviation in the location of the pupil relative to the corneal reflex indicates a change in the direction of gaze.

Such deviations are only recorded during a stimulus presentation. An equivalent method is also used to monitor the vertex distance of the forehead. The gaze tracker system provides a continuous print-out of the quality of fixation during each stimulus presentations. An upward deflection indicates an eye movement, the amplitude of which is truncated at 10°, and a downward deflection a loss of quality of the image due to blinking, lid closure, tear film rupture etc.

The concept of a movable (kinetic) fixation target is employed with the Dicon series of perimeters to improve fixation stability. The individual is required to maintain fixation on the fixation target which moves in between stimulus presentations and stops immediately prior to the presentation of the next stimulus. It is claimed that kinetic fixation is more interesting and reduces the fatigue effect (Reitner et al 1996). However, it results in significantly higher fixation errors compared to convention fixation in normal individuals and in individuals with glaucomatous field loss (Asman et al 1999).

1.8 False-positive and False-negative catch trials

A false-positive response can be evaluated in two ways. The original method uses the catch-trial approach based upon the 'non-presentation' of a stimulus in time with the rhythm of the test procedure and in conjunction with any mechanical noise associated with the stimulus presentation. A false-positive response may occur when the patient either does not understand the examination procedure or is anxious and concerned about not seeing all the stimuli. The alternative method, available in the Humphrey Field Analyzer 700 series, is based upon the time at which a positive response occurs during the periods of the examination when the individual is not expected to respond (Olsson et al 1997). The software evaluates whether a positive response has occurred at either, or both, of two of three different time periods. The first recording period

for the occurrence of false-positive responses corresponds to that between the onset of the stimulus and the minimum reaction time of 180msec. The second period is that during which the individual is expected to respond to the presence of the stimulus (the 'response window') and lasts from a minimum of 180msec (but is modified depending upon the individual's reaction time) after the onset of the stimulus to a designated proprietary time point. The third period is that of the second recording period for the occurrence of false-positive responses and lasts from a given time after the end of the response window to the onset of the subsequent stimulus. Positive responses that occur following a positive response during the response window are excluded as are those which occur between the given time after the end of the response window and the given time to the onset of the subsequent stimulus. In a validation study by Wall et al (2008), the average number of false-positive catch trials was 9.9 (SD = 0.3) with an average sampling time of 9 seconds per examination (SD = 2.0). The mean duration of the recording time for the presence of false-positive responses was 141 seconds (SD = 29 sec) per test. The mean frequency of false-positive responses, for the reponse time method, 2.2%, was similar to the mean of 3.1% incorrect responses to the false-positive catch trials. In those individuals with glaucomatous field loss who exhibit incorrect responses by both methods, the outcome of the response time method underestimates what the traditional method by approximately 50% (3.58% vs. 7.72%, p=0.007). The response time method also underestimates the frequency of induced errors, particularly among normal individuals (Newkirk et al 2006).

False-negative responses are assessed by the catch-trial method which involves the presentation of the stimulus, at a given stimulus location, at a known level above (brighter) than the threshold estimate derived earlier in the examination. The suprathreshold increment for SAP with the Humphrey Field Analyzer is 9dB. For CFF perimetry with the Octopus perimeters, the

suprathreshold increment is 100Hz. A False-negative response can occur due to lack of understanding of the examination procedure or to a lack of attention/ fatigue.

Age (Bickler-Bluth et al 1989), visual acuity and pupil diameter do not influence the outcome of the false-positive or the false-negative catch trials for SAP (Katz and Sommer 1988). The frequency of incorrect responses to the false-positive catch trials is higher with poor fixation, especially in inexperienced patients (Bickler-Bluth et al 1989; Reynolds, Stewart and Sutherland 1990; Sanabria, Feuer and Anderson 1991). A high frequency of incorrect responses to the false-positive catch trials is associated with a hyper-normal value of Mean Sensitivity and of Mean Defect both in normal individuals (Katz and Sommer 1990; Cascairo, Stewart and Sutherland 1991; Demirel and Vingrys 1994) and an underestimation of the defect depth in individuals with glaucoma (Katz and Sommer 1990). The frequency of incorrect responses to the false-negative catch trials increases for SAP as the severity of the field loss, in general, increases (Katz and Sommer 1988; Katz and Sommer 1990; Reynolds, Stewart and Sutherland 1990; Bengtsson 2000; Bengtsson and Heijl 2000). The increase in the frequency of incorrect responses to the false-negative catch trials occurs partially as a consequence of the increase in the within-examination variability of the threshold estimate with decline in sensitivity: the suprathreshold increment can lie inside the range of variability associated with the given value of sensitivity at the given stimulus location.

The upper limit of acceptability for the incorrect responses to the fixation loss catch trials for SAP is generally considered to be 20% (Katz, Sommer and Witt 1991). Short-wavelength automated perimetry is undertaken with a size V stimulus to ensure maximum SWS isolation and the same stimulus is used for the Heijl-Krakau method of monitoring fixation. The larger stimulus size can overlap the borders of the blind spot and, as a consequence, a positive response

may be obtained. Thus, the upper limit of acceptability for the incorrect responses to the fixation loss catch trials can be higher for SWAP than for SAP. The upper limit for the incorrect responses to the false-positive catch trials for SAP was originally considered to be 20% (Vingrys and Demirel 1998) or 33% (Katz, Sommer and Witt 1991; Anderson and Patella 1999; Sherafat et al 2003) but, with the advent of the reaction time-based assessment, is now considered to be 20% (Bengtsson and Heijl 2000). The corresponding value for the incorrect responses to the false-negative catch trials for SAP is generally considered to be 33% (Katz, Sommer and Witt 1991; Anderson and Patella 1999). However, due to the inherent increase in variability with increasing field loss, these values should be modulated, on an individual basis, for those with suspected or manifest glaucoma (Bengtsson 2000; Coops and Henson 2005).

The Octopus 300 Series utilises the Reliability Factor which expresses the number of incorrect responses to the false-positive and the false-negative catch trials as a fraction of the total number of catch trials. The RF should, ideally, be < 15% (Weijland et al 2004).

1.9 Presentation of Perimetric Sensitivity

1.9.1 Numerical and Greyscale Threshold Printouts

The print-out for each type of perimeter always contains a display in which the value of the threshold estimate at each stimulus location is annotated in terms of sensitivity, expressed in dBs, in a spatial configuration representing that employed in the stimulus program. With some threshold algorithms, the values of a second threshold estimate at any given stimulus location are displayed underneath the initial value.

The Grey scale printout displays the values of sensitivity within the spatial configuration as an interpolated grey scale. The Grey scale is intended to facilitate the interpretation of the spatial

representation of sensitivity. By convention, lighter shades of grey represent higher sensitivities and darker shades represent lower sensitivities with black indicating the lowest levels of sensitivity. The greyscale levels are usually organized into groups of 5dB in width. For the Octopus perimeters, the greyscale values range from 0 to 45dB assigned in 9 levels of grey whilst that of the Humphrey Field Analyzers cover a range from 0 to 51dB in 10 levels of grey. In addition, the attenuation in dBs is referenced to the maximum stimulus luminance superimposed upon a given background luminance. The grey scale is neither age nor eccentricity corrected. As such, the appearance of the grey scale in the normal eye darkens with increase in eccentricity. It also darkens with increase in age, particularly with increase in eccentricity, to reflect the reduction in the height and shape (a 'peripheral' steepening). The grey scale can appear to be normal in the presence of early loss, particularly with the SITA algorithms and particularly in the paracentral regions. However, in the presence of severe loss, the grey scale becomes increasingly representative of the visual field as the general height adjustment (i.e., the method of removing the abnormality in height) becomes increasingly unreliable (Asman, Wild and Heijl 2004). The grouping of the greyscale levels for short-wavelength automated perimetry is the same as that for standard automated perimetry. As a consequence of the difference in the magnitude of the normal values of sensitivity between the two types of perimetry, the appearance of the greyscale for short-wavelength automated perimetry in the normal eye is darker than that for standard automated perimetry (Wild 2001).

1.9.2 Total Deviation/ Comparison values

The numerical values of sensitivity, alone, are insufficient for the accurate interpretation of the visual field. A second level of analytical complexity is that of the Total Deviation/ Comparison analysis whereby the measured value of sensitivity at any given stimulus location is compared with that of the corresponding age-corrected value of sensitivity. With the Humphrey Field

Analyzer series, the outcome at each stimulus location is called the Total Deviation value. A negative value represents the extent to which the measured value of sensitivity is lower than that of the age-corrected value and a positive value the extent to which a measured value of sensitivity is higher than that of the age-corrected value. The corresponding approach for the Octopus series of perimeters is termed the Comparison value; however, the sign convention is reversed. A positive value represents the extent to which the measured value of sensitivity is lower than that of the age-corrected value and a negative value the extent to which a measured value of sensitivity is higher than that of the age-corrected value. A value within ± 4 dB of the age-corrected normal value is represented as a "+" symbol. A value worse (i.e., more) than +4dB is represented as the given value; however, a measured value of sensitivity of zero is designated by a black square. The Octopus perimeters also have an option for an interpolated greyscale representation of the Comparison values whereby each value is expressed as a percentage from 100% to 0% divided into 9 levels of grey. Thus, an entirely normal field will appear as a completely white rendition and a field with absolute loss at each stimulus locations as completely.

1.9.3 Pattern Deviation/ Corrected Comparison values

A continuation of this second level of analytical complexity is that of the Pattern Deviation analysis for the Humphrey Field Analyzers and the Corrected Comparison analysis for the Octopus perimeters whereby the measured value of sensitivity, corrected for the general height adjustment, at any given stimulus location is compared with that of the corresponding age-corrected value of sensitivity. The outcome of the analysis is displayed in an identical format for each type of perimeter to that of Total Deviation and Comparison analysis, respectively. The general height adjustment (Asman, Wild and Heijl 2004) provides an estimate of the magnitude of the diffuse/ generalised loss and corrects the value of sensitivity at each stimulus location,

accordingly. Diffuse/ generalised loss largely arises from cataract but can also occur from a variety of other causes such as an uncorrected or inaccurately corrected, refractive error, a naturally occurring small pupil or a pharmacologically constricted pupil etc. Following the general height adjustment, any attenuation of sensitivity is considered to be non-optical and to be of focal origin. The basic tenet of the general height adjustment is dependent upon the acceptance that glaucomatous, or for that matter any other cause of, visual field loss does not exhibit a diffuse component. However, as stated in section 1.1.8, the absence of a diffuse component of glaucomatous field loss is equivocal (Lachenmayr and Drance 1992; Lachenmayr, Drance and Airaksinen 1992b; Asman and Heijl 1994; Chauhan et al 1997; Henson, Artes and Chauhan 1999). The method of estimation of the magnitude of the general height adjustment varies between types of perimeter. For the Humphrey Field Analyzers, the general height adjustment arising from examination of the central field is based upon the 52 stimulus locations of Program 24-2 (the two locations immediately above and below the blind spot are omitted). The Total Deviation values are ranked in order from most positive/ least negative to most negative value. The general height is defined as the 7^{th} most positive/ least negative ranked value (Heijl, Lindgren and Olsson 1987b). This value represents the 87^{th} percentile of the distribution of the ranked deviation values. For the Octopus series of perimeters, the general height adjustment is based upon the mean of the 12^{th} to the 16^{th} highest ranked values of sensitivity and is expressed as the Diffuse Defect (see Section 1.11.6).

1.9.4 Total Deviation/ Comparison Probability analysis

The Total Deviation/ Comparison Probability analysis determines the probability of the respective Deviation/ Comparison value at the given stimulus location lying within the distribution of values encountered for the age-corrected normal eye. A statistically significant

value is highlighted in terms of a square with the 'greyness' of the square becoming increasingly darker as the probability level successively changes through four levels from $p<0.05$ to $p<0.005$.

1.9.5 Pattern Deviation/ Corrected Comparison Probability analysis

The outcome of the corresponding probability analysis for the Pattern Deviation/ Corrected comparison values is displayed in an identical manner to that for the Total Deviation/ Comparison Probability analysis. The presence of a statistically significant value, in effect, indicates the presence of focal abnormality with the severity of the abnormality increasing as the 'blackness' of the symbol increases.

The probability levels displayed by the various probability analyses represent those up to the 5^{th} percentile. The use of continuous scale probability plots has been advocated (Wall et al 2009) whereby the probability level, regardless of statistical significance, is displayed at each stimulus location. Although normal individuals frequently exhibit sensitivities between the 5^{th} and the 20^{th} percentiles, the stimulus locations exhibiting such an occurrence are randomly arranged. However, as would be expected the extent of focal loss is larger with the use of the continuous scale probability scale.

The outcome of probability analysis using stimulus size V recorded with the Full Threshold algorithm is similar to that using stimulus size III recorded with the SITA Standard algorithm in individuals with glaucoma (Wall et al 2008). The use of stimulus size V with its inherent lower variability (Wall, Kutzko and Chauhan 1997; Wall et al 2009) and greater dynamic range and number of steps (Wall et al 2010) would be a viable alternative to stimulus size III.

1.10 Cumulative Defect curve

The Cumulative Defect (CD) curve, also known as the Bebié Curve, is a method for rapidly visualising the characteristics and the depth of the visual field loss (Bebie, Flammer and Bebie 1989). The CD curve illustrates, graphically, the sensitivity across each of the locations in ranked order from the highest (left) to the lowest (right) and compares this to the mean, and to the 5% and 95% confidence limits, of the age-corrected normal curve. A diffuse/ generalised loss of sensitivity is represented by a downward displacement of the entire curve 'parallel' to the mean age-corrected normal curve. Focal loss is indicated by a localised downward displacement of the curve, the extent of which describes the area and depth of the loss. The separation of the initial manifestation of focal from the diffuse loss can be difficult with the CD curve (Funkhouser, Fankhauser and Weale 1992). In addition, the CD curve does not display the spatial localization of the visual field loss (Asman and Olsson 1995) and, for this reason, it is necessary to interpret the curve outcome in conjunction with the spatial display of the sensitivity values (Kaufmann and Flammer 1989).

1.11 Global Indices

The Octopus perimeters initially provided four global indices: the Mean Defect (MD), Loss Variance (LV), Short-term Fluctuation (SF) and Corrected loss variance (CLV) (Flammer et al 1985; Flammer 1986; Flammer et al 1987). These indices correspond to those subsequently introduced for the Humphrey Field Analyzer, namely the Mean Deviation (MD), the Pattern Standard Deviation (PSD), the Short-term Fluctuation (SF) and the Corrected Pattern Standard Deviation (CPSD) (Heijl, Lindgren and Olsson 1987b). Each type of index is a summary measure which describes a given feature of the visual field. The indices are optimally used in combination with spatial information particularly that of the Pattern Deviation/ Corrected Comparison probability analysis.

1.11.1 Mean Sensitivity

The mean sensitivity (MS) is the arithmetic mean of the sensitivity across all the given stimulus locations.

$$MS = \frac{1}{n}\sum_{i=1}^{n} x_i$$

and

$$x_i = \frac{1}{m}\sum_{k=1}^{m} x_{ik}$$

i, is the stimulus location; x_i is the sensitivity at stimulus location *i*, n is the number of stimulus locations excluding those in the blind spot region and m is the number of threshold estimates, k, at location *i*.

The MS declines with increase in age (Hermann et al 2008). It is influenced by diffuse/ generalised loss; small areas of localised loss exert little influence on the MS (Flammer 1986).

1.11.2 Mean Defect and Mean Deviation

The Mean Defect, used in the Octopus series of perimeters, is the arithmetic mean of the difference between the age-corrected value of normal sensitivity and the measured value of sensitivity across all the stimulus locations. For the normal visual field, the Mean Defect approaches zero. An increasingly positive value indicates an increasingly abnormal field. A negative value indicates a field which is better than the age-corrected field (Flammer 1986). The Mean Defect is defined as:

$$MD = \frac{1}{n}\sum_{i=1}^{n} (z_i - x_i)$$

where n is the number of stimulus locations excluding those in the blind spot region; z_i is the age-corrected normal value of sensitivity at stimulus location i and x_i is the measured value of sensitivity. MD primarily describes the extent of the diffuse/ generalised visual field loss but also reflects that of increasingly severe localized loss.

The Mean Deviation, used in the Humphrey Field Analyzer, is the weighted mean of the difference between the measured sensitivity at each stimulus location and the age-corrected normal value across all the stimulus locations. The more centrally located values are weighted to reflect the lower variability of the threshold estimate at these locations compared to those situated more peripherally. The Mean Deviation primarily describes the extent of the diffuse/ generalised visual field loss but also reflects that of increasingly severe localized loss.
(Heijl, Lindgren and Olsson 1987b) An increasingly negative value indicates an increasingly abnormal field. The Mean Deviation is defined as:

$$MD = \left(\frac{1}{n} \sum_{i=1}^{n} \frac{(x_i - z_i)}{S_{1i}^{\ 2}} \right) / \left(\frac{1}{n} \sum_{i=1}^{n} \frac{1}{S_{1i}^{\ 2}} \right)$$

where n is the number of stimulus locations, excluding those in the blind spot region, x_i is the measured value of sensitivity at stimulus location i, z_i is the age-corrected normal value of sensitivity at stimulus location i and $S_{1i}^{\ 2}$ is the variance of normal sensitivity at stimulus location i.

The weighting function exerts little influence on the Mean Defect (Funkhouser and Fankhauser 1991) or on the Mean Deviation (Flanagan, Wild and Trope 1993) in glaucomatous field loss.

1.11.3 Loss Variance and Pattern Standard Deviation

The Loss Variance (LV), used in the Octopus series of perimeters, is the variance of the difference between the normal age-corrected value of sensitivity and the measured value of sensitivity across all the stimulus locations. As a variance, the value is expressed in dB^2. It is an indicator of localized loss and the value initially increases as the localised loss increases but then declines as the localised loss becomes increasingly widespread. The Loss variance is defined as:

$$LV = \frac{1}{(n-1)} \sum_{i=1}^{n} (z_i - x_i - MD)^2$$

where n is the number of stimulus locations excluding those in the blind spot region, z_i is the age-corrected normal value of sensitivity at stimulus location i, x_i is the measured value of sensitivity and MD is the Mean Defect.

The Pattern Standard Deviation (PSD), used in the Humphrey Field Analyzer, is the Standard Deviation of the difference between the measured sensitivity at each stimulus location and the age-corrected normal value across all the stimulus locations and incorporates the weighting function used in the calculation of the Mean Deviation. The Pattern Standard Deviation is defined as:

$$PSD = \sqrt{\left(\frac{1}{n} \sum_{i=1}^{n} S_{1i}{}^2 \right) \left(\frac{1}{n-1} \sum_{i=1}^{n} \frac{(x_i - z_i - MD)^2}{S_{1i}{}^2} \right)}$$

where n is the number of stimulus locations, excluding those in the blind spot region, x_i is the measured value of sensitivity at stimulus location i, z_i is the age-corrected normal value of

sensitivity at stimulus location *i*, MD is the Mean Deviation and S_{1i}^{2} is the variance of normal sensitivity at stimulus location *i*. The PSD initially increases as the localised loss increases but declines as the localised loss becomes increasingly widespread.

As would be expected from the mathematics of the two functions, the difference between the LV and the PSD increases as the severity of the focal loss increases.

1.11.4 Short-term Fluctuation (SF)

The Short-term Fluctuation is the variation of the threshold estimate at any given location during a given visual field examination (Bebie, Fankhauser and Spahr 1976; Flammer et al 1984; Flammer, Drance and Zulauf 1984). The SF can be calculated for any given number of stimulus locations and for the Octopus perimeters is expressed as:

$$SF = \sqrt{\frac{1}{n}\sum_{i=1}^{n}(SD_i)^2}$$

where n is the number of stimulus locations, *i* is the given stimulus location, and SD is the standard deviation of the threshold estimates at location *i* (Flammer 1986).

For the first and second generation algorithms, the Humphrey Field Analyzer calculates the Short-term Fluctuation by measuring the threshold twice at ten pre-determined stimulus locations and calculates the weighted mean of the standard deviations at these ten locations. The weighting function is to account for the increase in the Short-term Fluctuation with increase in eccentricity (Brenton and Phelps 1986; Heijl, Lindgren and Olsson 1987a). The Short-term Fluctuation is expressed as:

$$SF = \sqrt{\left\{\frac{1}{10}\sum_{i=1}^{10} {S_{2i}}^2\right\}\left\{\frac{1}{10}\sum_{i=1}^{10}\frac{(x_{i1}-x_{i2})^2}{2(Si^2)}\right\}}$$

where x_{i1} is the first value of sensitivity and, x_{i2} is the second value of sensitivity at stimulus location *i* and ${S_{2i}}^2$ is the variance of the normal sensitivity at stimulus location *i*.

Weighting with $\frac{1}{{S_{2i}}^2}$ minimises the Short-term Fluctuation in normal individuals (Heijl, Lindgren and Olsson 1987b) and in individuals with glaucoma (Flanagan, Wild and Trope 1993). The Short-term Fluctuation for the Octopus series of perimeters is approximately 0.3dB greater than for the weighted Short-term Fluctuation of the Humphrey Field Analyzer (Brenton and Argus 1987) although the stimulus parameters are not the same between the two types of perimeter. The Short-term Fluctuation is independent of stimulus duration (Pennebaker et al 1992) but decreases with increase in stimulus size (Gilpin et al 1990). It is independent of background luminance in the low photopic range which is that used in most perimeters (originally the Octopus perimeters used 1.27cdm^{-2} but now some use the 10cdm^{-2} featured in the Humphrey Field Analyzers) but increases with mesopic illumination at or below 0.1cdm^{-2} (Croswell et al 1991). It varies with the type of threshold algorithm being greater for the algorithms with larger step sizes and fewer reversals compared to that of the 4dB-2dB double crossing of threshold (Bebie, Fankhauser and Spahr 1976; Flanagan, Wild and Trope 1993; Weber and Klimaschka 1995). An increased Short-term Fluctuation is considered to be an early manifestation of glaucomatous damage (Werner and Drance 1977; Flammer et al 1984). The Short-term Fluctuation is also greater at the border of deep focal loss (Haefliger and Flammer 1991).

The third generation threshold algorithms do not incorporate the facility for the measurement of the Short-term Fluctuation. The reason for this is unknown but is presumably due to the balance between the additional examination time requirement and the clinical value of the index.

1.11.5 Corrected LV and Corrected PSD

Corrected Loss Variance (CLV), used in the first and second generation algorithms of the Octopus series of perimeters, is the LV corrected for the square of the Short-term Fluctuation (SF) (Flammer 1986). CLV is expressed in dB^2 and is defined as:

$$CLV = LV - \frac{1}{n}(SF)^2$$

The Corrected Pattern Standard Deviation (CPSD) used in the first and second generation algorithms of the Humphrey Field Analyzer, is defined as:

$$CPSD^2 = PSD^2 - kSF^2$$

where k is a constant greater than one and compensates for the non-uniform spatial arrangement of the stimulus locations used for the estimation of the SF. CPSD is considered to be the most accurate descriptor of glaucomatous visual field loss (Hayashi et al 2001).

Programs 30-2 and 24-2 generate similar PSD and CPSD indices and the weighting function produces a larger PSD and CPSD (Flanagan, Wild and Trope 1993). Weighting of hemifield and cluster analyses improves the sensitivity and specificity (Asman and Heijl 1992b).

1.11.6 The Diffuse Defect (DD)

An index to describe the extent of diffuse loss, the Individual General Sensitivity index, was first proposed in 1989 (Langerhorst et al 1989). A similar index was the Diffuse Loss Index (Funkhouser, Fankhauser and Weale 1992).

The Diffuse Defect (DD) is the difference between the general height of the age-corrected normal visual field and that of the individual's visual field (Buerki and Monhart 2007).

The DD is defined as:

$$DD = \frac{1}{\Delta i + 1} \sum_{i=20\%}^{i=27\%} (a_i - b_i)$$

where a_i is the value of sensitivity of the given ranked value of the measured sensitivity and b_i is the 50th percentile of the distribution of the corresponding value in the age-corrected normal eye. The DD is based upon the 12th (20%) to the 16th (27%) highest ranked values.

1.11.7 The Local Defect (LD)

The area underneath Cumulative Deficit curve derived from the measured sensitivity having adjusted for the DD is known as the Abnormal Response Area (ARA). The ARA is defined as:

$$ARA = \sum_{i=23\%}^{i=100\%} (a_i - b_i - DD)$$

where a_i is the value of sensitivity of the given ranked value of the measured sensitivity and b_i is the 50th percentile of the distribution of the corresponding value in the age-corrected normal eye

and DD is the diffuse defect. The ARA is based upon the 14th (20%) to the 59th (100%) highest ranked values of the measured sensitivity.

The Local Defect is defined as:

$$LD = \frac{ARA}{\Delta i}$$

Since the first 20% of the ranked values are omitted from the calculation of the DD, both the DD and the LD are less influenced by inappropriately high values of sensitivity arising from false positive responses (Buerki and Monhart 2007). However, the use of a higher ranked value for the general height adjustment limits the use of the technique in advance field loss (Asman, Wild and Heijl 2004). As would be expected, the LD correlates with the sLV and the PSD (Buerki and Monhart 2007).

1.11.8 Glaucoma Progression Index

The Glaucoma Progression Index (GPI) (Bengtsson and Heijl 2008) can be calculated for any given field and, as its name suggests, is an index for use in the identification of progressive glaucomatous loss. However, it can be used as an indication of the severity of field loss at any given examination. The GPI is based upon the Pattern Deviation probability map and scored from 100% which represents a normal field to 0% which represents absolute loss. A sensitivity, at any given location, lying within the normal range by Pattern Deviation probability analysis is scored as 100% and that of absolute loss is scored as 0%. A sensitivity, at any given location, exhibiting a Pattern Deviation probability analysis of $p \leq 0.05$ is expressed as a percentage, namely

$$100 - [(\left|\text{Total Deviation}\right|/\text{age-corrected normal sensitivity}) \times 100].$$

The outcome at any given location is weighted for cortical magnification whereby the inner-most stimulus locations are weighted most highly. The GPI is the mean of the weighted scores.

The hypothesised advantage of the GPI was that it would be 'largely independent' of cataract and would provide a more appropriate measure of progressive loss than the corresponding Mean Deviation index (Bengtsson and Heijl 2008). However, the GPI has been shown to improve in patients with glaucomatous field loss following cataract extraction and IOL implantation; the improvement in the group mean was 4.3% compared to that for the MD of 13.6% (Ang, Shunmugam and Azuara-Blanco 2010). The GPI was implemented on the Humphrey Field Analyzer and has become known as the Visual Field Index (VFI). Following phacoemulsification cataract extraction and IOL implantation in 41 individuals with nuclear sclerotic cataract and in 12 individuals with posterior subcapsular cataracts, all of whom had glaucomatous field loss), the VFI remained unchanged whilst the postoperative MD exhibited a statistically significant, but clinically insignificant, improvement and the PSD a statistically significant, but clinically insignificant, worsening (Rao et al 2011b). The utility of the VFI when regressed against time to follow-up, compared to that of the corresponding Mean Deviation is equivocal (Artes et al 2011). As the VFI is based upon Pattern Deviation Probability values, a 'ceiling effect' is present which limits the diagnostic sensitivity for detection of progressive early damage (Artes et al 2011). The relationship, in Chinese eyes with glaucoma, between progressive loss identified with the VFI and that of progressive reduction in the retinal nerve fibre layer thickness, as measured with the StratusOCT, and increase in the neuro-retinal rim area is poor (Leung et al 2011). However, given the logarithmic nature of the decibel scale of

sensitivity and the linear scale of a structural measure this is hardly surprising (Hood et al 2007; Gardiner, Demirel and Johnson 2011). Indeed, various linear-based indices have been recently proposed in an attempt to improve the identification of progressive glaucomatous damage and the understanding of the structure-function relationship (Gardiner, Demirel and Johnson 2011).

1.11.9 Long-Term Fluctuation (LF)

The Long-term Fluctuation (LF) is the variability of the threshold estimate between examinations and occurs over days, months or years. However, the LF is not quantified in clinical perimetry despite the need to separate the inherent variability in the threshold estimate from the 'true' reduction in sensitivity due to the presence of progressive disease (Bebie, Fankhauser and Spahr 1976; Flammer, Drance and Schulzer 1983; Flammer et al 1984; Flammer, Drance and Schulzer 1984; Parrish, Schiffman and Anderson 1984; Ross et al 1984; Wilensky and Joondeph 1984; Lewis, Johnson and Keltner 1986; Brenton and Argus 1987; Katz and Sommer 1987; Heijl, Lindgren and Olsson 1987a). Classically, the LF consists of two components: the Homogeneous LF (LTF_{HOM}) and the Heterogeneous LF (LTF_{HET}). The LTF_{HOM} refers to the uniform variability of sensitivity across the field (Hutchings et al 2001). The LTF_{HET} refers to the local variability of sensitivity at different visual field locations (Zulauf et al 1991; Hutchings et al 2001). The calculation of the LF excludes the short-term fluctuation, the learning effect and age (Bebie, Fankhauser and Spahr 1976; Flammer, Drance and Zulauf 1984; Blumenthal et al 2000). The LF is weakly correlated with the SF for both SAP (Hutchings et al 1993) and SWAP (Hutchings et al 2001). Other measures of long-term variability increase with increase in age (Katz and Sommer 1987; Heijl, Lindgren and Olsson 1987a) with increase in the interval between examinations (Katz and Sommer 1986) and with increase in eccentricity

in the normal (Heijl, Lindgren and Olsson 1987a; Rutishauser and Flammer 1988) and in the glaucomatous eye (Zulauf et al 1991; Boeglin, Caprioli and Zulauf 1992).

1.11.10 Other Indices

Various other indices have been proposed over the years including the Third Central Moment (M3), Skewness (Q) Defect Volume (DV) and Spatial Correlation (SC) indices. The M3 index described the sensitivity at the stimulus locations which deviated most from the age-matched normal value (Flammer 1986). The Skewness (Q) index also attempted to describe early loss and was a standardization of the M3 index with respect to LV (Brechner and Whalen 1984; Flammer 1986) (Pearson, Baldwin and Smith 1988). The DV index described the volume of the three-dimensional representation of the normal age-corrected field minus the volume of the measured visual field (Langerhorst et al 1985; van Den Berg et al 1985). The SC index described the extent of clustering of the visual field loss across the visual field. The SC index increased as the visual field loss became increasingly clustered (Flammer 1986).

Although the concept of Cluster analysis is effective in detecting localized visual field loss and in distinguishing a normal visual field from a glaucomatous visual field (Asman and Heijl 1992a; Mandava et al 1993). Cluster deteriorating occur more frequently in the superior hemifield than in the inferior hemifield in glaucoma (Chauhan, Henson and Hobley 1988).

Cluster size (SIZ), depth (CLUS), centroid (mean x-y coordinate), the number of clusters and the total size and depth have also been supported (Chauhan, Drance and Lai 1989). PCLUS quantifies the percentage of the MD that was clustered. The sensitivity and specificity of the cluster indices, SIZ, CLUS, and PCLUS, have been compared with the global indices MD and CLV (Chauhan, Drance and Douglas 1990). Cluster indices are effective in determining progressive loss compared to the normal points as well as in determining further deterioration in

abnormal visual fields (Chauhan, Drance and Douglas 1990). The specificity demonstrates the best results in the superior hemifield (Asman and Heijl 1992a; Asman and Heijl 1992b).

1.11.11 Learner's Index (LI)

The presence of a learning effect with SAP (Wood et al 1987b; Werner, Adelson and Krupin 1988; Heijl, Lindgren and Olsson 1989; Wild et al 1989; Autzen and Work 1990; Kulze, Stewart and Sutherland 1990; Werner et al 1990; Marchini, Pisano and Bertagnin 1991 Gardiner et al 2008; Searle et al 1991; Wild et al 1991; Heijl and Bengtsson 1996) with SWAP using the Full Threshold (Rossetti et al 2006; Wild et al 2006; Gardiner, Demirel and Johnson 2008; Zhong et al 2008) and the SITA SWAP algorithms (Fogagnolo et al 2010) and with Frequency Doubling Technology perimetry (Centofanti et al 2008; Pierre-Filho et al 2010) is well established. The learning effect occurs because the patient becomes increasingly familiar with the requirements of the perimetric task and manifests as an improvement in sensitivity, a decrease in measurement variability over time and a reduction in the examination duration. A Learner's index was developed to detect regions of low sensitivity possibly due to perimetric inexperience (Olsson, Asman and Heijl 1997). The central visual field was divided into five concentric zones, and the mean of the deviations from the age-corrected normal values were determined for each zone. The variance and covariance between results were used to construct a linear discriminant function, the LI (Olsson, Asman and Heijl 1997). However, the LI has not been the subject of further study.

1.11.12 Glaucoma Hemifield Test (GHT)

The Glaucoma Hemifield Test (GHT) is specifically designed to detect localized glaucomatous visual field loss and is available for the Humphrey Field Analyzers (Asman and Heijl 1992a;

Asman and Heijl 1992b). The GHT divides each of the upper and lower hemifields into 5 mirror-imaged zones, each of which include between 3 and 6 stimulus locations, based upon the configuration of the retinal nerve fibre layer. Subsequently, each zone is scored according to the number of Pattern Deviation probability values, and compared to its mirror image. The results of the GHT are displayed as one of five possible text phrases. 'Outside normal limits' is displayed when the difference between any one, or more, pairs of zones, is greater than that corresponding to the 99th percentile in age-corrected normal individuals. It is also displayed if the combined score of one, or more, pairs of zones exhibits a combined score exceeding that of the 99.5th percentile in age-corrected normal individuals. A 'Borderline' classification is displayed if the criteria for 'Outside normal limits' are not reached, but the difference between any one, or more, pairs of zones, is greater than that corresponding to the 97th percentile in age-corrected normal individuals. A 'General reduction of sensitivity' is displayed if the criteria for 'Outside normal limits' are not reached, but that the reduction in the General Height is greater than that of the 99.5th percentile in age-corrected normal individuals. 'Abnormally high sensitivity' is displayed if the General Height exceeds that of the 5th percentile in age-corrected normal individuals. 'Within normal limits' is displayed when none of the above criteria are met.

Criteria based on the GHT and on the Pattern Deviation Probability map demonstrate high sensitivity and specificity for detecting early glaucomatous visual field changes (Katz, Sommer and Gaasterland 1991; Johnson et al 2002).

1.12 Novel techniques of perimetry

It is has long been established that substantial retinal ganglion cell damage occurs prior to the manifestation of visual field loss derived by standard automated perimetry, at least when the latter is expressed in dBs (Harwerth et al 1999; Kerrigan-Baumrind et al 2000; Harwerth et al

2004). The topic is extensively reviewed by (Anderson 2006; Hood et al 2007; Harwerth et al 2010). As a consequence of the apparent lack of sensitivity of standard automated perimetry for the detection of early glaucomatous damage, a number of other perimetric tests have been developed and are reviewed by (McKendrick 2005a).

The modality for each of the newer perimetric tests is based upon one, or more, of three possible, but not necessarily independent, hypotheses for retinal ganglion cell loss in early OAG. The latter are well reviewed by (Spry et al 2005; Anderson 2006) and (McKendrick 2005a).

The first explanation for retinal ganglion cell loss, based upon histological evidence, suggests that retinal ganglion cells with large diameter axons are preferentially damaged in early glaucoma (Quigley, Dunkelberger and Green 1988; Glovinsky, Quigley and Dunkelberger 1991). However, such evidence has been disputed (Morgan 1994; Morgan, Uchida and Caprioli 2000). The second hypothesis arises from the psychophysical literature which suggests that selective testing of functional properties exhibited by retinal ganglion cells (M-cells) which project to the magnocellular layers of the lateral geniculate nucleus (and which are larger than those projecting to the parvocellular layers (P-cells) such as motion (Silverman, Trick and Hart 1990; Anderson and O'Brien 1997; Bosworth et al 1998; Sample et al 2000a; Spry et al 2005) and flicker (Tyler 1981; Van Toi, Grounauer and Burckhardt 1990; Lachenmayr et al 1991; Yoshiyama and Johnson 1997; Matsumoto et al 1999; Matsumoto et al 2006), identifies glaucomatous damage at an earlier stage than testing of non-selective ganglion cell function. The third hypothesis, the reduced redundancy hypothesis, is also compatible with the second hypothesis, and is based upon the concept that all types of retinal ganglion cells are equally affected by the glaucomatous disease process(es) but that sparsely represented cell types (which exhibit lower degrees of overlap between adjacent receptive fields than the more abundant types)

demonstrate functional abnormality, earlier, since loss of only a small number of cells will impair retinal receptive field coverage. The latter hypothesis is consistent with that for Short-wavelength automated perimetry which is mediated, at least in part, by the scarcely represented small bistratified ganglion cells which are of similar size to eccentricity-matched M-cells and which project to the koniocellular layers of the lateral geniculate nucleus (K cells).

1.12.1 Short Wavelength Automated Perimetry (SWAP)

Short Wavelength Automated Perimetry (SWAP) was developed in the 1980s and 1990s (Hamill et al 1984; Sample, Weinreb and Boynton 1986; Heron, Adams and Husted 1988; Sample and Weinreb 1992; Sample et al 1993; Johnson et al 1993a; Johnson et al 1993b; Sample, Martinez and Weinreb 1994; Johnson et al 1995; Keltner and Johnson 1995; Wild et al 1995). SWAP stimulates the short-wavelength sensitive (SWS) pathway by the use of a narrow band blue stimulus in conjunction with a broad band yellow background, to suppress the involvement of the medium- and long-wavelength sensitive pathways, which is presented at a background luminance at least one log unit higher than that used for standard automated perimetry in order to saturate rod involvement. A Goldmann size V stimulus is used to increase the isolation of the SWS pathway

The early studies of SWAP involved the use of differing stimulus and background parameters (Heron, Adams and Husted 1988; de Jong et al 1990; Sample and Weinreb 1990; Sample and Weinreb 1992; Hudson, Wild and Archer-Hall 1993; Moss, Wild and Whitaker 1995; Wild et al 1995; Wild, Moss and O'Neill 1996). However, the stimulus parameters for the commercially available technique are now standardized. The Humphrey Field Analyzers use a 440nm stimulus with a bandwidth of 27nm mediated by an Omega filter and a 100cdm^{-2} background mediated by a Schott OG 530 filter. The Octopus series of perimeters use identical characteristics with the

exception that the stimulus is mediated by an Omega 440nm filter with a bandwidth of 14nm. The duration of the stimulus is 200 msec for both types of perimeter.

Initially, SWAP was considered to exhibit glaucomatous visual field loss in advance of that derived by standard automated perimetry (de Jong et al 1990; Hart et al 1990; Sample and Weinreb 1990; Sample and Weinreb 1992; Casson, Johnson and Shapiro 1993; Johnson et al 1993a; Johnson et al 1993b). However, such studies consisted of small case series and frequently lacked robust definitions for field loss and for progressive field loss.

The promise of SWAP for the detection of abnormality prior to that identified by standard automated perimetry lasted over the ensuing decade and the evidence base for this has recently been reviewed (Jampel et al 2011).

The apparent advantage of SWAP over standard automated perimetry was counter intuitive to the increased between-individual normal variability (Wild et al 1995; Wild et al 1998) and to the increased within- and between-examination variability for SWAP, relative to standard automated perimetry, in normal individuals (Wild et al 1998; Blumenthal et al 2003), in individuals with ocular hypertension and in individuals with open-angle glaucoma (Hutchings et al 2001; Blumenthal et al 2003). The increased between-individual normal variability, expressed in terms of the coefficient of variation, to account for the differences in the dynamic range of the two techniques, was shown to be greater by, on average, 2.7 times, than that for standard automated perimetry (Wild et al 1998). The implication from these findings is that, for the detection of glaucomatous abnormality, a larger deviation from the age-corrected normal value is required for SWAP to achieve statistical significance than occurs for standard automated perimetry (Wild et al 1998). In addition, forward light scatter arising from cataract influences the visual field to a

greater extent for SWAP compared to that of SAP (Kim et al 2001). However, anterior cortical cataract exerts greater effect on SAP compared to SWAP whilst the opposite effect occurs with posterior subcapsular cataract (Moss, Wild and Whitaker 1995).

The SITA SWAP algorithm, introduced in 2003, exhibits a 22% reduction in the between-individual normal variability of the SITA SWAP algorithm compared to that of the Full Threshold algorithm with a consequent reduction of 14% and 11% in the probability value necessary to achieve the 5% significance level in the Total Deviation and Pattern Deviation analysis (Bengtsson and Heijl 2003). However, in a study of 101 individuals with either ocular hypertension or suspect or early OAG, the identification glaucomatous visual field loss was similar between the SITA SWAP and Full Threshold SWAP algorithms and both exhibited equivalent diagnostic sensitivity to the SITA Fast algorithm (Bengtsson and Heijl 2006).

With the current approach for the reference diagnosis to be based upon the outcome from stereo-photography of the optic nerve head (Ng et al 2009) or from the results of retinal nerve fibre layer thickness derived by spectral domain optical coherence tomography (Liu et al 2011), it is becoming increasingly accepted that, in cross sectional studies, SWAP generates similar diagnostic sensitivities to standard automated perimetry for the detection of glaucomatous optic neuropathy regardless as to whether the comparison is that of SITA SWAP to SITA Standard (Tafreshi et al 2009 ; Liu et al 2011) or Full Threshold SWAP to SITA Standard (Sample et al 2006) and or both SITA SWAP and Full Threshold SWAP to SITA Standard (Ng et al 2009).

In one of the few prospective longitudinal studies of standard automated perimetry and SWAP, in individuals with ocular hypertension and normal fields by standard automated perimetry at baseline, it was concluded that standard automated perimetry appeared to be at least as diagnostically sensitive as SWAP for conversion to glaucomatous field loss (van der Schoot et al

2010). The study involved 416 individuals who had undergone standard automated perimetry and Full Threshold SWAP every 6 months for between 7 and 10 years or until the manifestation of repeatable visual field loss by standard automated perimetry. Twenty-four eyes of 21 individuals exhibited conversion by standard automated perimetry. Of these 24 eyes, 22 did not show an earlier conversion by SWAP. Field loss by standard automated perimetry preceded that by SWAP in 15 of the 22 eyes. In only 2 eyes did SWAP exhibit an earlier conversion (by up to 18 months).

1.12.2 High-pass Resolution Perimetry (HRP)

High-pass resolution perimetry (HRP) was developed to examine P cell ganglion cell sampling density (Frisén 1987; Frisén 1993). The stimulus is a 'vanishing optotype' stimulus that contains predominantly high spatial frequencies and is ring-shaped with dark borders (15cd/m²) surrounding a lighter centre (25cd/m²). The background luminance is 20cd/m². The duration of the stimulus is 165ms (Wall et al 2004). The size of the stimulus is changed, over a range of 14 sizes, in a single-reversal staircase procedure with each stimulus being larger/ smaller than the previous stimulus by a factor of 1.26. The Ring program comprises 50 stimulus locations within the central visual field.

The test was developed on the basis that, as detection and resolution thresholds are the same for a high-pass ring stimulus, the threshold estimate would be directly proportional to ganglion cell sampling density (Frisén 1987; Frisén 1987a). However, the detection and resolution thresholds are not the same beyond the fovea and aliasing is clearly present (Anderson, Ennis and McDowell 1999) and indicates that the threshold is more likely to provide an estimate of ganglion cell receptive field size rather than spacing or density (Thibos, Cheney and Walsh 1987).

Nevertheless, HRP detects glaucomatous visual field progression earlier than SAP (Chauhan et al 1993; Graham and Drance 1995; Martinez, Sample and Weinreb 1995; Chauhan et al 1999). Alternatively, the two techniques may yield similar outcomes (Artes and Chauhan 2005). HRP may (Meyer and Funk 1995) or may not (Lachenmayr et al 1991) (Sample et al 2006) be more diagnostically sensitive than standard automated perimetry for the detection of early glaucomatous visual field loss. HRP has been validated in pseudotumor cerebri (Wall et al 1991; Wall and White 1998), optic neuritis (Wall 1991) and hemianopsia (Martin-Boglind 1993). It continues to be used in its country of origin, Sweden, (Kalaboukhova, Fridhammar and Lindblom 2006; Martin 2007; Frisén and Jensen 2008) but has never gain widespread acceptance elsewhere.

1.12.3 Rarebit Perimetry (RBP)

The use of the Goldmann size III stimulus oversamples the visual field in that it covers many, receptive fields. As a consequence, the identification of abnormal function of any one finite retinal ganglion cell is hindered by those ganglion cells which remain functional and which generate normal receptive fields at the given location of the stimulus. Rarebit Perimetry (RBP) uses a stimulus that presents a minimum of information (rare bits) (Frisén 2002) with the intention of locating minute gaps in the retinal neuronal matrix arising from dead/ dysfunctional/ or disconnected neurons. Indeed, the stimuli used for RBP are much closer in size to an individual ganglion cell receptive field in human (Hackett and Anderson 2011).

In the initial version of RBP, two high luminance micro-dots (150 cdm^{-2}), each half the normal minimum angle of resolution, are presented for 200 msec on a dark background (1 cdm^{-2}) within each of 30 circular stimulus areas of 5° in diameter within 30° eccentricity. Each circular stimulus area is probed five times (i.e. 10 microdots) with a separation of 4° between each pair of

dots. The observer is required to indicate the number of micro-dots seen per presentation (i.e., two, one or none) and the outcome is defined in terms of the hit/ miss (i.e seen/ not seen) score. The results can be presented as the overall Mean or Median Hit Rate (MHR) (Frisén 2002); graphically, as the proportion of missed probes, represented by the proportionate diameter of a dark circle, within each of the circular stimulus areas of 5° (Frisén 2002); and as the number of stimulus areas with a hit rate of less than 90% (Martin and Wanger 2004).

The group median hit rate in 27 normal individuals (aged between 20 – 70 years) was 96% (range between 88% - 100%) with the hit rate declining by 1% per decade of age (Frisén 2002).

The initial studies of RBP indicate that the techniques is equivalent to that of standard automated perimetry in the detection of glaucomatous field loss (Martin and Wanger 2004; Brusini et al 2005) and to Frequency Doubling Technology Perimetry in individuals with ocular hypertension (Corallo et al 2008). In the latter study, the greatest area under the ROC curve, of 0.95, and optimal sensitivity, of 97.4%, were obtained when an abnormal outcome to RBP was defined as at least one of an MHR <80%; >15 areas with a non-hit rate of >10%; ≥2 areas with a non-hit rate of >50%; and at least one area with a non-hit rate of ≥70%. It is also comparable to standard automated perimetry in detecting the homonymous hemianopia in stroke patients with occipital lobe infarcts (Gedik, Akman and Akova 2007).

A more recent version of the software, version 4.0, differs from earlier versions in that the examination of the central field is divided into 24 rectangular zones of different sizes, as opposed to the 30 circular zones of 5° diameter (Chin et al 2011). The rectangular areas increase in size from 6° x 8° degrees centrally to 6° x 14° peripherally. The software also includes foveal and separate left and right ‘flank’ stimulus programs. The foveal program incorporates 10 square

examination areas each subtending 1.5° x 1.5° and the two microdots are separated by 1° and can be displayed by data projector (Winther and Frisén 2010).

The Mean Hit Rate, using the Version 4.0 software, of 54 normal individuals from Singapore, was 86.3 ± 13.95% for the central field and 91.6 ± 6.35% for the foveal field. The decline in Mean Hit Rate was 4.7% per decade of age. The Mean Hit Rate increased by 3.5 between two examinations separated by one month (Chin et al 2011). These values compare favourably from a similar study, using Version 4.0, of 75 European normal individuals with a mean age of 52.9 ±13.7 years. The group mean Mean Hit Rate was 91% (±5.7%) and the age-related decline in Mean Hit Rate was 2.1% per decade (Salvetat et al 2007). A learning effect was present between the first and the second or third examination. The decline in the Mean Hit Rates with age compares with that in Europeans of 1.5% per decade of age with Version 3.0 (Brusini et al 2005).

The outcome of RBP is adversely affected by optical defocus (Salvetat et al 2007) and by cataract (Salvetat et al 2007; Nilsson et al 2010). In the latter study of 25 patients before and after cataract extraction and IOL implantation, the median value of the MHR increased from 77 (IQR 60-98) pre-operatively to 93 (IQR 85.9-96) postoperatively. The corresponding values for the foveal test were 8 (IQR 0-52) and 93.5 (47-100). In individuals with OAG, the correlation between MHR and peripapillary retinal nerve fibre layer thickness determined by Time-Domain OCT is relatively modest (r=0.39 to 0.47) (Katsanos et al 2008). RBP exhibits lower between-examination variability for five examinations over a five week period than that for standard automated perimetry for both stimulus size I and stimulus size III (Vislisel et al 2011).

RBP yields acceptable, but lower sensitivity and specificity compared to standard automated perimetry, in the detection of visual field loss resulting from idiopathic intracranial hypertension (Celebisoy, Oztürk and Köse 2010).

Critical Flicker Fusion perimetry (CFF), Flicker Defined Form (FDF) technology, Frequency-Doubling Technology perimetry (FDT), Moorfields Motion Displacement test (MDT) and Temporal Modulation perimetry (TMP) are all novel perimetric techniques preferentially based on the Magnocellular pathway and will be discussed in Chapter 2.

1.13 Factors potentially affecting the outcome of the perimetric examination

1.13.1 Perimetric Artefacts

The successful outcome of any visual field examination is a combination of the skill of the perimetrist, the understanding of, and co-operation in, the requirements of the visual field examination by the patient and the expertise of the clinician in interpreting the statistical analysis. The outcome of any given examination can be influenced by one or more artefacts which can either lead to the impression of visual field loss or to the apparent exacerbation of existing loss.

1.13.2 Physical Factors

The facial structure can cause apparent abnormality of the visual field. The most predominant causes are a prominent nose, prominent brows, long eyelashes, deep set eyes, ptosis and dermatochalasis (Meyer et al 1993). A superior visual field defect, or a restriction of the supero-temporal quadrant of the visual field, can be caused by either ptosis or dermatochalasis (Kosmin 1997). These visual field defects may mimic a superior arcuate scotoma or a supero-temporal

defect (Riemann, Hanson and Foster 2000). When necessary, the upper lid should be taped to prevent artefacts caused by ptosis. Improved instruction by the perimetrist may also be necessary (Riemann, Hanson and Foster 2000).

Lens rim artefacts can occur from the use of reduced aperture trial lenses, from thick rims and from incorrect placement (Zalta 1989). The latter can result in an induced prismatic effect (Atchison 1987; Miller and Gelber 1990). Trial lenses should be used in accordance with the instruction from the manufacturer of the perimeter (Weijland et al 2004). It is also important to maintain the correct position of the patient during the examination (Anderson and Patella 1999).

1.14 Physiological Factors

1.14.1 Age

Age adversely influences the visual field derived by static automated perimetry. The process is generally considered to be linear for SAP with a reduction in sensitivity of between 0.4 and 1.1 dB per decade of age out to 30º eccentricity (Brenton and Phelps 1986; Haas, Flammer and Schneider 1986; Heijl, Lindgren and Olsson 1987a; Zulauf, LeBlanc and Flammer 1994; Wild et al 1998). The decline increases within increase in eccentricity and is largest in the peripheral and superior areas compared to the paracentral and inferior areas (Haas, Flammer and Schneider 1986; Jaffe, Alvarado and Juster 1986). The net effect of age reduces the height and steepens the hill of vision (Haas, Flammer and Schneider 1986; Jaffe, Alvarado and Juster 1986; Heijl, Lindgren and Olsson 1987a). The effect is greatest after the age of fifty (Johnson and Choy 1987) and largely arises from a neural loss (Johnson and Choy 1987; Johnson, Adams and Lewis 1989). Indeed, a nonlinear function provides the best description of the effect of age on the Mean Sensitivity derived by standard automated perimetry in that the Coefficients of Determination (R^2) for linear, bilinear, and nonlinear functions were 0.21, 0.20, and 0.26, respectively (Spry

and Johnson 2001). The decline in sensitivity was 0.43 dB/decade before the age of 53.4 years and 1.02 dB/decade beyond that age.

The age-related decline in sensitivity derived by SWAP is between 1.3dB per decade for both the Full and SITA SWAP algorithms to 2.2dB per decade (Johnson et al 1988; Johnson and Marshall 1995; Wild et al 1995) compared with approximately 0.8 dB per decade for standard automated perimetry (Heijl, Lindgren and Olsson 1987a; Flanagan et al 1993) The reason for the difference in the slopes between the two methods is unknown. However, several explanations have been postulated, e.g. the reduced redundancy of the SWS pathway (Johnson 1994), preferential damage to the SWS cones due to the exposure of UV light (Ham et al 1982), age-related cortical changes, both in terms of number of neurons and in the morphology (Scheibel et al 1975; Devaney and Johnson 1980), loss of retinal ganglion cells (Dolman, McCormick and Drance 1980; Balazsi et al 1984) and reduction both in photoreceptor density (Gartner and Henkind 1981; Farber et al 1985) and foveal cone photopigment (Keunen, van Norren and van Meel 1985; Kilbride et al 1986).

When the slope of the decline in sensitivity with age for the given type of perimetry is corrected for the magnitude of the corresponding dynamic range, short-wavelength automated perimetry shows the largest age effects, followed by Frequency Doubling Technology (FDT), and lastly by standard automated perimetry (Gardiner, Johnson and Spry 2006).

1.14.2 Refractive Defocus

Optical defocus of the retinal image decreases the visibility of the stimulus (Campbell and Green 1965). Therefore, it is recommended that the visual field examination should be undertaken with the distance refractive correction, in trial lens form, together with any near correction, as

appropriate. For standard automated perimetry, Goldmann III (0.43°) stimuli, or larger, are less affected by optical defocus at the fovea than are smaller stimuli (Adams, Heron and Husted 1987; Atchison 1987; Anderson and Patella 1999). Nevertheless, even with Goldmann size III, the reduction in sensitivity is between 0.80dB and 1.50dB per 1.00DS of defocus with the effect diminishing with increase in eccentricity (Atchison 1987; Goldstick and Weinreb 1987; Heuer et al 1987). The influence of optical defocus on the outcome of Frequency Doubling Perimetry is approximately 0.5dB per 1.00DS for the 10° stimulus (Artes et al 2003) and -0.63dB to -0.74dB per 1.00DS of defocus for the 2° stimulus (Anderson and Johnson 2003).

1.14.3 Pupil Size

In normal individuals, sensitivity increases with increase in pupil size, modulated with thymoxamine 0.5% and with phenylephrine 10% (Wood et al 1988) at background luminances of both 10 and 45 asb (Wood et al 1988), with the effect increasing with increase in eccentricity (Wood et al 1988). The increase in sensitivity in normal individuals measured with the Tubingen Automated Perimeter (10cdm^{-2} background luminance) with change in pupil size modulated with dapiprazole 0.5% and phenylephrine 2%, increased for the central field out to 20° eccentricity, as a whole, by 0.21 dB/mm (95% CI 0.09–0.33 dB/mm) with the increase in sensitivity becoming less with increase in eccentricity (Martin et al 2005). In individuals with OAG receiving pilocarpine 2% therapy, and following administration of phenylephrine 10% , the MD improved by an average of 3.14dB (SD 1.89) and the PSD and by 1.42 dB and 1.73 dB, respectively. The increase in sensitivity increased with increase in eccentricity (Rebolleda et al 1992). However, following pupil dilation with tropicamide 1%, the MD in normal individuals worsened by 0.83dB (SD 0.92) (Lindenmuth et al 1990). As would be expected, the use of pilocarpine 2% produces a worsening of the MD in normal individuals (Lindenmuth et al 1989).

1.14.4 Media Opacities

Any ocular media opacity, such as a corneal scar or a cataract, will blur, absorb and scatter the amount of light reaching the retina with a resultant attenuation in the differential light sensitivity.

Light scatter affects the differential light sensitivity more than light absorption (Bettelheim and Chylack 1985). Light scatter can be divided into backward light scatter, i.e. light reflected away from the crystalline lens and forward light scatter, i.e. stray light reaching the retina. Forward light scatter resulting in the loss of retinal image contrast, described as disability glare (DG) (Philipson 1969). The latter is assumed to be the primary cause of image degradation both for a narrow and wide angle glare source (Dengler-Harles et al 1990) resulting from cataract (Bettelheim and Chylack 1985; Wood et al 1989). Indeed, the outcomes of standard automated perimetry and of short-wavelength automated perimetry are more prone to the effects of intraocular stray light, induced by commercially available opacity-containing filters, than are Frequency Doubling perimetry and Grating Resolution perimetry (Anderson et al 2009).

The degree of image degradation is dependent both upon the extent and the position of the opacity within the ocular media. Posterior capsular cataract produces a proportionately greater attenuation of sensitivity because it is located close to the nodal point of the eye (Baraldi, Enoch and Raphael 1987). Nuclear/Colour opalescence cataract occurs with aging and results in increased absorption. Absorption of light is dependent upon the wavelength and preferentially attenuates the shorter wavelengths (Sample, Boynton and Weinreb 1988; Lam, Alward and Kolder 1991; Moss, Wild and Whitaker 1995). Indeed, cataract generally causes a diffuse loss of sensitivity (Guthauser and Flammer 1988; Budenz, Feuer and Anderson 1993) and the co-morbidity of increasing age-related cataract can impair the interpretation of progressive glaucomatous visual field loss (Bengtsson et al 1997).

The outcome of studies comparing the visual field for standard automated perimetry before and after cataract extraction by phacoemulsification and intra-ocular lens implantation in individuals with OAG or in otherwise normal individuals are in general agreement. Either modest (Smith, Katz and Quigley 1997; Kook et al 2004; Siddiqui, Khairy and Azuara-Blanco 2007) or little clinical improvement occurs in the MD (Stewart et al 1995; Koucheki et al 2004; Carrillo et al 2005) with clinically similar, but generally worse, values for either or both the PSD and the CPSD of the glaucomatous field (Stewart et al 1995; Smith, Katz and Quigley 1997; Hayashi et al 2001; Koucheki et al 2004; Siddiqui, Azuara-Blanco and Neville 2005) and either for the pointwise Total Deviation (Carrillo et al 2005) or the pointwise Pattern Deviation values (Koucheki et al 2004). In otherwise normal eyes, the improvement in the MD for short-wavelength automated perimetry was greater by a factor of 2.4 times than that for standard automated perimetry (Kim et al 2001). A similar finding to standard automated perimetry is present for Frequency Doubling Technology perimetry in individuals with OAG namely a minimal (Arvind et al 2005) or modest (Siddiqui, Azuara-Blanco and Neville 2005) improvement in the MD together with a clinically insignificant worsening in the PSD (Arvind et al 2005; Siddiqui, Azuara-Blanco and Neville 2005). The presence of advanced cataract, particularly that of posterior sub-capsular cataract can cause false-positive outcomes for the C-20-5 screening mode of the Frequency Doubling Technology perimeter (Casson and James 2006).

1.14.5 Medical Therapy

Ocular adverse effects associated with systemic medications have been reviewed by Santaella and Fraunfelder (2007) and by Li et al (2008). The principal systemic drugs which result in visual field loss are chloroquine/ hydroxychloroquine, ethambutol and vigabatrin.

The characteristcs of the field loss attributable to hydroxychloroquine in relation to Programs 10-2 and 24-2 of standard automated perimetry and of Frequency Doubling perimetry has been discussed by (Anderson, Blaha and Marx 2011) and (Tanga et al 2011), respectively; in relation to the progressive nature of the damage despite withdrawal of drug (Michaelides et al 2011); and in relation to recommendations for screening by (Marmor et al 2011) on behalf of the American Academy of Ophthalmology. The latter consider that objective tests, such as multifocal electroretinogram, spectral domain optical coherence tomography, and fundus autofluorescence, can be more sensitive than perimetry with Program 10-2. As a consequence, it is now recommended that, where available, at least one of these objective procedures should be undertaken for routine screening in conjunction with perimetry using Program 10-2. However, a review of 3 cases of chloroquine and 26 cases of hydroxychloroquine toxicity over a 30 year period showed that mfERG failed to diagnose some early patients who either had an abnormal fundus or an abnormal outcome to perimetry with Program 10-2. The three recommended tests, multifocal electroretinogram, spectral domain optical coherence tomography, and fundus autofluorescence, failed to identify all of the cases of retinal toxicity. Multifocal electroretinography was the most sensitive of the three tests (Farrell 2012).

Recent studies of ethambutol toxicity (Menon et al 2009) suggest that visual field loss developes in 7.7% of cases (8/104 eyes) and that the field loss is reversible in 80% of eyes one month after withdrawal of ethambutol (Menon et al 2009) and that, in addition to the standard central or cecocentral defect, bitemporal loss can occur which mimics chiasmal decompression (Kho, Al-Obailan and Arnold 2011). However prospective study of 44 patients (88 eyes) on ethambutol therapy at a dose of 15–20 mg/kg/day for 2 months under a Directly Observed Treatment Strategy (category I) for primary tuberculosis suggest that visual acuity, contrast sensitivity, and

multifocal ERG are sensitive tests to detect ethambutol toxicity in its subclinical stages (Kandel et al 2012).

The visual field loss arising from the anti-epileptic drug vigabatrin is a bilateral concentric constriction which, within the central field out to 30° eccentricity, manifests by static perimetry as a binasal annulus at the extremity of the central field and which extends centripetally towards fixation with varying amounts of sparing of the temporal field (Eke, Talbot and Lawden 1997; Wild et al 1999). The median value for the prevalence of the field loss is 31% (IQR 21–52) (Maguire et al 2010).

The phenothiazines bind to melanin granules and can cause a severe phototoxic retinopathy; however, the associated visual field loss has not been documented.

Tamoxifen retinopathy manifests as crystalline deposits in the inner retina and exhibits a central scotoma (Li, Tripathi and Tripathi 2008). The utility of short-wavelength sensitive and Frequency Doubling Technology perimetry in relation to the detection of tamoxifen attributed dysfunction has been discussed by (Eisner, Austin and Samples 2004). A comparison of the standardised mean deviation indices between the two types of perimetry indicated a duration-dependent abnormality for short-wavelength sensitive perimetry before completion of the standard 5 year treatment regimen. It was concluded that tamoxifen appeared to affect some types of visual pathways preferentially or selectively, particularly the SWS cone pathways. However, standard automated perimetry was not used as a control.

A probable link exists between amiodarone and a bilateral optic neuropathy that is very similar to non-arteritic ischaemic optic neuropathy. The cGMP-specific phosphodiesterase type 5

inhibitors (erectile dysfunction drugs) have been also implicated in the development of non-arteritic ischaemic optic neuropathy (Li, Tripathi and Tripathi 2008).

Long-term treatment with linezolid, a synthetic antimicrobial drug, may result in an optic neuropathy, symmetric painless decrease of visual acuity and colour vision, and bilateral central scotoma (Rucker et al 2006).

Alcohol ingestion in normal individuals prior to the visual field examination reduces the reliability of the examination performance as manifest by the increase in the number of incorrect responses to the false-positive and false-negative catch trials (Zulauf, Flammer and Signer 1986) and in the worsening of the MD, PSD and CPSD (Wild, Betts and Shaw 1990).

Moderate cigarette smoking is associated with both diffuse and localized reduction in sensitivity for standard automated perimetry in that smokers exhibited a significantly lower foveal threshold and Mean Sensitivity, and a significantly higher PSD and higher CPSD compared to non-smokers. However, such outcomes were not present for short-wavelength automated perimetry (Akarsu et al 2004).

1.15 Psychological Factors

1.15.1 Learning Effect

The learning effect in perimetry is also discussed in Section 4.2 whereby sensitivity improves and both the variability of the threshold estimate and the examination duration reduce as the individual becomes increasingly familiar with the examination procedure.

For SAP, the learning effect is present in normal individuals (Wood et al 1987b; Heijl, Lindgren and Olsson 1989; Wild et al 1989; Autzen and Work 1990), in individuals with OHT and in patients with OAG. The learning effect from the first to the second examination in normal individuals manifests as an improvement in the MS and MD of approximately 1-2dB (Wood et al 1987b; Heijl, Lindgren and Olsson 1989; Wild et al 1989; Autzen and Work 1990; Searle et al 1991).

The learning effect is present for the first eye examined at the initial visit (Searle et al 1991); and is transferred between eyes at the first visit (Searle et al 1991); it is present between visits, both within- (Searle et al 1991) and between-eyes (Wilensky and Joondeph 1984; Heijl, Lindgren and Olsson 1989; Searle et al 1991; Heijl and Bengtsson 1996), generally up to at least the end of the second or third visit (Wood et al 1987b; Heijl, Lindgren and Olsson 1989; Searle et al 1991). The improvement in sensitivity increases with increase in eccentricity (Wood et al 1987b; Heijl, Lindgren and Olsson 1989; Wild et al 1989; Werner et al 1990; Searle et al 1991) and is greatest in areas of relative loss (Heijl, Lindgren and Olsson 1989; Wild et al 1989; Kulze, Stewart and Sutherland 1990).

The learning effect is often greatest in the superior field, and may be caused by either patients learning to raise their upper eyelid (Wood, Wild and Crews 1987a) or instructions from the examiner. The learning effect seems to be independent of age (Heijl, Lindgren and Olsson 1989; Kulze, Stewart and Sutherland 1990).

The learning effect, over two visits within one week, in young normal individuals is proportionately less, in terms of both the MD and the PSD, for the SITA Standard algorithm compared to the Full Threshold algorithm (Yenice and Temel 2005).

A learning effect is also present for short-wavelength automated perimetry using the Full Threshold algorithm in normal individuals (Blumenthal et al 2000; Zhong et al 2008) and in individuals with either OHT (Rossetti et al 2006; Wild et al 2006; Zhong et al 2008) or OAG (Wild et al 2006; Zhong et al 2008) and experienced in standard automated perimetry. The learning effect for the Full Threshold algorithm can last upto the third (Zhong et al 2008) or fourth (Wild et al 2006) examinations and is independent of prior experience in standard automated perimetry (Zhong et al 2008). However, the learning effect is absent over five weekly visits, save that of the foveal threshold, for short-wavelength automated perimetry using the SITA algorithm in individuals with ocular hypertension experienced in standard automated perimetry (Fogagnolo et al 2010).

The learning effect for temporal perimetry will be reviewed in Chapter 2.

1.15.2 Fatigue Effect

The fatigue effect is the term used to describe the reduction in performance with increase in duration of the visual field examination (Heijl and Drance 1983; Hudson, Wild and O'Neill 1994; Gonzalez de la Rosa and Pareja 1997). The fatigue effect largely occurs with the first generation algorithms and is present in normal individuals (Searle et al 1991; Hudson, Wild and O'Neill 1994), in individuals with OAG (Wild et al 1991; Hudson, Wild and O'Neill 1994) and in individuals with neuro-ophthalmic disease (Heijl and Drance 1983; Johnson et al 1988). In the normal eye, the fatigue effect constitutes a worsening of the Mean Defect/ Mean Deviation index of between 1dB (Johnson et al 1988) to 2.5dB (Hudson, Wild and O'Neill 1994). In individuals with OAG, the fatigue effect is approximately 3.0dB (Johnson et al 1988) and in individuals with ocular hypertension it is approximately 2.0dB (Hudson, Wild and O'Neill 1994). The fatigue effect is greater for the second eye in normal individuals (Searle et al 1991) and in OHT

(Hudson, Wild and O'Neill 1994). The fatigue effect is greatest in the peripheral region of the central visual field (Hudson, Wild and O'Neill 1994), especially in glaucoma (Johnson et al 1988) patients exhibiting focal defects (Heijl and Drance 1983). The threshold estimate for Frequency Doubling Technology perimetry worsens (i.e. declines) over six consecutive repeated examinations (Artes et al 2003). The outcome of kinetic perimetry also declines with fatigue, as modulated by four successive identical examinations of the III4e-isopter position derived by semi-automated kinetic perimetry. Fatigue increases the variability of the isopter position and is greatest for individuals with OAG, less for those with postchiamsal lesions and less still for those with retinitis pigmentosa (Nowomiejska et al 2012). An increase in reaction time was the most important factor influencing the increased variability of response and, as such, offers promise as a reliability indicator of Semi-automated kinetic perimetry (SKP) (Nowomiejska et al 2012).

1.15.3 Perimetrist and environmental factors

The nature of the instruction by the perimetrist prior to the examination can influence the threshold estimate by up to 2.04dB in younger patients and up to 6.57dB in older patients (Kutzko, Brito and Wall 2000). An educational video shown prior to the initial visual field examination increases the number of outcomes deemed to be 'reliable' particularly for the eye which is examined second (Sherafat et al 2003). The supervision of individuals with a low educational level and/ or an age greater than 70 years and/ or a prior visual field examination with a high number of incorrect responses to either/ or the fixation loss and false-positive catch trials improves the reliability of the outcome from the visual field examination (Van Coevorden et al 1999). The number of incorrect responses to the fixation loss and false-negative catch trials, the proportion of false-positive responses and the number of locations exhibiting a probability level of $p \leq 0.05$ by Pattern Deviation analysis derived with Program 24-2 and the SITA Standard algorithm were statistically significantly lower in medical students undergoing visual field

examination for the first time and who were exposed to the playing of music by Mozart immediately prior to the visual field examination compared to the control of an absence of music (Fiorelli et al 2006). However, in older individuals with glaucomatous field loss, exposure to music by Mozart prior to the visual field examination does not afford any advantage, in terms of improvement in the reliability parameters, over either no music or noise cancellation (Shue et al 2011).

CHAPTER 2

TEMPORALY MODULATED PERIMETRY

2.1 Introduction

Even though imaging techniques such as Optical Coherence Tomography, Laser Scanning Ophthalmoscopy and Nerve Fibre Layer Polarimetry are now in routine clinical use, perimetry still remains an important technique for the detection and monitoring of abnormalities of the eye and the visual pathway, particularly that of open angle glaucoma (OAG). The relationship between the functional outcome (i.e., perimetry) and the structural outcome (i.e., damage to the optic nerve head (ONH) and to the retinal nerve fibre layer (RNFL)) has been the subject of numerous studies (Reus and Lemij 2004; Rao et al 2011a; Leite et al 2012; Medeiros et al 2012) and yields only statistically moderate relationships (Coefficients of Determination, R^2, in the region of 0.36). Nevertheless, it is generally agreed that, in the case of early OAG, structural damage is detectable before functional loss (Johnson et al 2000). However, in the later stages of the disease, progressive loss of the visual field can be seen at an earlier stage than progressive change in the structure of either the ONH or the RNFL (Johnson et al 2002; de la Rosa et al 2007).

Standard Automated Perimetry (SAP) is the most common method for assessment of the visual field. However, it is widely accepted that between 25% and 50% of the retinal ganglion cells may be damaged before the corresponding visual field loss is detectable by SAP (Quigley, Dunkelberger and Green 1988; Harwerth et al 1999; Garway-Heath et al 2000; Kerrigan-Baumrind et al 2000; Harwerth et al 2004; Anderson 2006; Hood et al 2007; Harwerth et al 2010). As a consequence, ‘new’ perimetric methods have been introduced over the last two decades with the aim of identifying functional abnormality at an earlier stage than that by SAP.

The development of these newer perimetric techniques is based upon the use of visual functions which are mediated by the different axonal pathways of the various types of retinal ganglion cells. The retinal nerve fibre layer contains the axons of at least four major types of retinal ganglion cells. The parasol ganglion cells, the midget ganglion cells and the small bi-stratified ganglion cells project, via separate parallel visual pathways, to the Magnocellular, Parvocellular and Koniocellular layers of the laterale geniculate nucleus, respectively. The parasol ganglion cells (also known as the Magnocellular [M] ganglion cells) represent approximately 10% of the total number of retinal ganglion cells and are primarily responsive to temporally modulated stimuli (Merigan, Byrne and Maunsell 1991). At the fovea, the M cells constitute approximately 5% of the total retinal ganglion cell population and approximately 20% at the periphery (beyond 6°) (Dacey 1993; Dacey 1994). The Magnocellular retinal ganglion cells have fibres with larger diameters and larger receptive fields compared to the midget retinal ganglion cells (also known as the Parvocellular [P] retinal ganglion cells) (Kaplan and Shapley 1982; Shapley and Perry 1986; Dacey 1993).

The Parvocellular retinal ganglion cells have the smallest dendritic trees and constitute 80% of the total ganglion cell population (Shapley and Perry 1986; Dacey 1993). They are primarily responsive to high spatial frequencies, to low temporal frequencies, to colour and to contrast (Lennie 1980; Livingstone and Hubel 1987; Livingstone and Hubel 1988; Shapley 1990).

The small bi-stratified ganglion cells comprise approximately 5% of the total retinal ganglion cell population (de Monasterio et al 1985; Curcio et al 1991; Dacey 1993; Calkins 2001). They are responsive to blue-yellow opponent visual information (Dacey and Lee 1994).

A fourth subset of retinal ganglion cells contain melanopsin which are photosensitive and exhibit maximum sensitivity to short-wavelength stimuli (Hankins, Peirson and Foster 2008). These ganglion cells mediate regulation of circadian rhythms and are also involved with pupil constriction (Zaidi et al 2007).

It has been suggested from histological (Quigley 1987; Quigley, Dunkelberger and Green 1988; Glovinsky, Quigley and Dunkelberger 1991; Chaturvedi, Hedley-Whyte and Dreyer 1993; Glovinsky, Quigley and Pease 1993; Kerrigan-Baumrind et al 2000) and psychophysical studies (Johnson and Samuels 1997) that the larger diameter ganglion cell axons are selectively damaged in the glaucomatous disease process. However, these findings have been questioned in experimental glaucoma models (Morgan, Uchida and Caprioli 2000; Morgan 2002) and it has been suggested that retinal ganglion cell loss in early glaucoma is non-selective. Nevertheless, since any sparsely represented retinal ganglion cell type exhibits less degree of overlap between adjacent receptive fields than a more abundant type, the axons of such types may be more vulnerable to identifiable functional abnormality earlier in the glaucomatous disease process (Spry et al 2005).

As discussed in Section 1.12.1, Short Wavelength Automated Perimetry (SWAP) stimulates the Short-Wavelength Sensitive (SWS) pathway and therefore the Koniocellular retinal ganglion cells (Sample and Weinreb 1992; Johnson et al 1993a; Johnson et al 1993b; Sample, Bosworth and Weinreb 1997).

Frequency Doubling Technology (FDT) perimetry (Johnson and Samuels 1997; Maddess et al 1999), Flicker Defined Form (FDF) technology (Rogers-Ramachandran and Ramachandran 1998; Goren and Flanagan 2008), Temporal Modulation Perimetry (TMP) (Casson, Johnson and

Nelson-Quigg 1993; Casson, Johnson and Shapiro 1993; Yoshiyama and Johnson 1997), Critical Flicker Fusion (CFF) perimetry (Yoshiyama and Johnson 1997; Rota-Bartelink 1999; Matsumoto et al 2006), and Motion Automated Perimetry (MAP) (Silverman, Trick and Hart 1990; Wall, Jennisch and Munden 1997 ; Bosworth et al 1998), all target the M-pathway.

Pulsar perimetry (Gonzalez-Hernandez et al 2000; González-Hernández et al 2004; Zeppieri et al 2010; Salvetat et al 2011) stimulates both the parvocellular and the magnocellular visual pathways.

2.2 Types of non-standard 'temporal' perimetry

2.2.1 Frequency-Doubling technology perimetry (FDT)

The initial commercially available version of the Frequency Doubling Technology perimeter (Carl Zeiss Meditec, Inc., Dublin, CA) utilized a 0.25 cycles per degree sinusoidal grating, presented within a 10° x 10° stimulus patch, which underwent counterphase flicker at 25Hz. Contrast is modulated until the grating is detected. With such stimulus parameters, the grating appears to exhibit twice the spatial frequency (Kelly 1966; Kelly 1981; Maddess and Henry 1992). Threshold is determined by a modified binary search (MOBS) staircase algorithm. The suprathreshold stimulus is age-corrected and is presented at one of two contrasts which should be seen by 95% and 99%, respectively, of the corresponding age-corrected normal population (Johnson and Samuels 1997). The specificity and sensitivity of the former is between 85-100% and between 78-92%, respectively, whilst that of the latter is between 80-90% and between 85-95% (Johnson 2008).

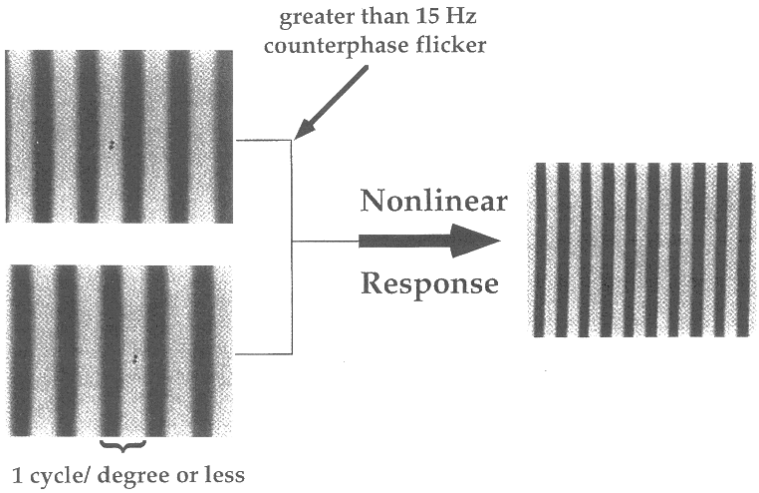

Figure 2.1 The stimulus for the Frequency-Doubling Technology perimeter illustrating the principal of the Frequency-Doubling illusion (Carl Zeiss Meditec, Inc., Dublin, CA).

The technology is based upon the assumption that the outcome is mediated by a specific subset of retinal ganglion cells, the M_y-cells. These latter cells exhibit non-linear response properties (Livingstone and Hubel 1987; Livingstone and Hubel 1988) and are thought to be selectively damaged by the glaucomatous process (Quigley 1987; Quigley, Dunkelberger and Green 1988; Glovinsky, Quigley and Dunkelberger 1991; Kerrigan-Baumrind et al 2000). However, higher order cortical visual areas are also involved in the processing (White et al 2002; Zeppieri et al 2008).

The commercially available second generation version of the Frequency Doubling Technology perimeter, the Humphrey Matrix perimeter, utilizes a 0.5 cycles per degree sinusoidal grating, presented within a 5° x 5° stimulus patch, which undergoes counterphase flicker at 18Hz. (Anderson et al 2005; Johnson 2008) The dynamic range of the device is compatible with that of the Humphrey FDT perimeter (Anderson et al 2005; Artes et al 2005). Threshold is determined by the Zippy Estimation by Sequential Testing (ZEST) algorithm, which is an adaptive Bayesian method for determining sensitivity. As with the SITA algorithms, the method combines prior

knowledge about the expected distribution of sensitivity (Anderson and Johnson 2006). ZEST is a fast, accurate and reliable algorithm for the determination of threshold in normal and in glaucomatous eyes (Turpin et al 2002; Turpin et al 2003).

It was suggested that the initial FDT perimeter exhibited a higher sensitivity and specificity for the detection of open OAG (Johnson and Samuels 1997; Casson et al 2000; Cello, Nelson-Quigg and Johnson 2000; Holló, Szabó and Vargha 2001; Khong et al 2001; Serguhn and Spiegel 2001; Wu et al 2001) compared to that of either SAP (Wu et al 2001), scanning laser polarimetry, nerve fiber layer photographs (Paczka et al 2001) or SWAP (Bowd et al 2001). However, more recent studies indicate that the outcome of the Humphrey Matrix is similar to that for SAP in the detection of glaucomatous abnormality (Anderson et al 2005; Spry, Hussin and Sparrow 2005; Brusini et al 2006; Mastropasqua et al 2006; Hong et al 2007; Bozkurt, Ylmaz and Irkec 2008; Racette et al 2008) particularly for the detection of moderate to advanced visual field loss (Burgansky-Eliash et al 2007; Hong et al 2007). Nevertheless, it is also claimed that FDT perimetry is predictive in determining glaucomatous visual field progression (Medeiros, Sample and Weinreb 2004; Haymes et al 2005; Kogure, Toda and Tsukahara 2006).

As would be expected, FDT can detect field loss arising from rhegmatogenous retinal detachment (Sheu et al 2001), optic neuritis (Fujimoto and Adachi-Usami 2000), and other neuro-ophthalmological disease (Thomas et al 2001). However, the utility of the original FDT, in regard to the larger stimulus, for the detection of macular abnormalities (Sheu et al 2001) or in regard to the stimulus-offset relative to the vertical midline for the detection of hemianopic defects (Thomas et al 2001) is limited.

Optical defocus (Artes et al 2003) and forward light scatter influence, adversely, the outcome of FDT perimetry. Age-related cataract has an adverse effect on the MD (Tanna et al 2004; Casson and James 2006) and schould be considered during the interpretation of the visual field (Anderson and Johnson 2003; Kim and Kee 2008) in order to avoid false-positive outcomes/ diagnoses.

2.2.2 Flicker Defined Form (FDF) technology

The Flicker Defined Form (FDF) stimulus (Rogers-Ramachandran and Ramachandran 1998) stimulates the magnocellular pathway. The FDF stimulus creates an illusory edge contour which arises from a high temporal frequency driven illusory stimulus based upon phase differences between the stimulus and the background (Flanagan et al 1995; Rogers-Ramachandran and Ramachandran 1998). The commercially available Heidelberg Edge Perimeter (FDF, Heidelberg Engineering, Germany) utilises this stimulus. The test consists of flickering random dots on a background of 50cdm^{-2} mean luminance. The stimulus is 5° in diameter and is created by a phase reversal of the black and white dots that flicker in counterphase to the background dots at a temporal frequency of 15Hz. (Figure 2.2)

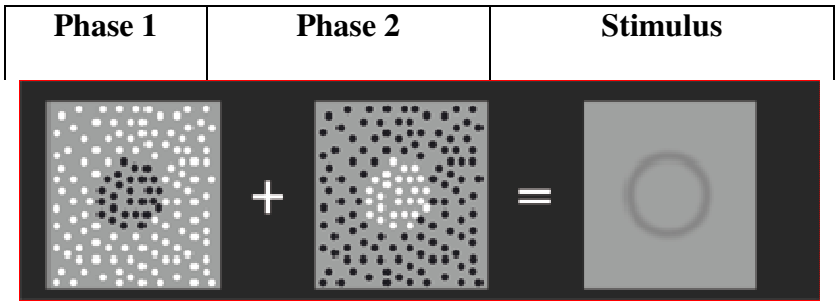

Figure 2.2 The Flicker Defined Form stimulus utilized by the Heidelberg Edge Perimeter (Phase 1 + Phase 2 = The Illusory Edge stimulus).

The visual field indices, Mean Deviation and Pattern Standard Deviation, for the Edge perimeter exhibit only a modest correlation with those derived by SAP using the Humprey Visual Field Analyser (Perez et al 2010a) for individuals with OAG (Perez et al 2010b). The lack of agreement between the two types of perimetry may be explained by the presence of a leaning effect over three visits for the Edge stimulus (Lamparter et al 2011).

2.2.3 Pulsar Perimetry

Pulsar perimetry purports to evaluate both the parvocellular and the magnocellular visual pathways (Gonzalez-Hernandez et al 2000; González-Hernández et al 2004). In this context, the Pulsar perimeter evaluates the threshold of various visual functions, the high spatial and high temporal frequencies.

The prototype of the Pulsar Perimeter consisted of a 19 inch screen with a resolution of 1024x768 pixels, a frame rate of 60Hz and a colour temperature is 6500ºK. The screen luminance is 100asb. The 5º circular stimulus decreases in contrast towards the edge and oscillates at 30Hz below and above the luminance of the background (i.e. is initially iso-luminant to the background). The stimulus duration is 500msec.

The contrast of the Pulsar stimulus at each stimulus location (V) depends upon the global contrast (C), the distance from fixation (D), spatial resolution (SF) and the radius (R) of the stimulus, where

$$V = C.\cos([2\pi.SF.D] - \pi)(1 - [D/R])$$

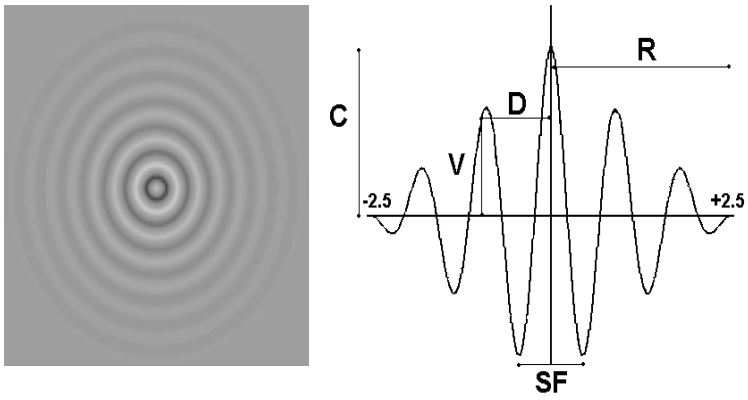

Figure 2.3 The stimulus used in the clinical version (T30W) of the prototype Pulsar perimeter.

The spatial resolution (dLog) varies over twelve logarithmic levels (between 0.5 cycles/degree and 6.3 cycles/degree) and is described as:

$$dLog = 10Log[spatialresolution/0.5]$$

Where dLog corresponds to the spatial resolution level.

The contrast varies between 6% and 100% (0-31 dB), over 32 logarithmic levels.

The contrast level is defined as:

-20Log ([central amplitude contrast - background luminance] / [background luminance])

Pulsar perimetry had greater sensitivity in the detection of early visual field loss in patients with OHT compared to SAP (Vidal-Fernández et al 2002; Gonzalez-Hernandez et al 2004; Zeppieri et al 2010). The between-examination variability is lower for Pulsar Perimetry compared to both standard automated perimetry and FDT perimetry (Gonzalez-Hernandez et al 2007a). The Pulsar perimeter is seemingly able to detect more cases of apparent progressive glaucomatous damage than either confocal scanning laser ophthalmoscopy or nerve fibre layer polarimetry (Gonzalez de la Rosa et al 2009).

2.2.4 Flicker perimetry

There are three types of flickering stimulus utilized in perimetry: Temporal Modulation perimetry, Critical Flicker Fusion perimetry and Luminance Pedestal Flicker perimetry. All three types stimulate M ganglion cell function.

Temporal Modulation perimetry (TMP) measures contrast thresholds for a fixed temporal frequency, i.e, the minimum luminance at which a flickering stimulus of a given temporal frequency is perceived to exhibit flicker (Tyler, Ryu and Stamper 1984).

TMP is assumed to detect glaucomatous damage earlier than standard automated perimetry, but the assumption is equivocal. At 25Hz, TMP does not exhibit any increased sensitivity, compared with SAP, in the identification of field loss in glaucoma suspect individuals or in those with OAG manifesting established field loss by SAP (Feghali et al 1991). However, Casson et al (1993) suggest that TMP demonstrates significantly greater abnormality in early glaucoma, at all temporal frequencies, and identifies those cases of ocular hypertension that will develop glaucoma (Casson, Johnson and Shapiro 1993). Although it has been discussed which temporal frequencies provide the optimum diagnostic outcome (Tyler 1981; Casson, Johnson and Nelson-

Quigg 1993), it appears that all temporal frequencies are able to detect glaucomatous damage in a similar manner (Casson and Johnson 1993; Casson, Johnson and Shapiro 1993; Yoshiyama and Johnson 1997). Individuals with normal visual function seem to demonstrate a greater age-related decline in sensitivity for high temporal frequencies compared to low and medium temporal frequencies (Casson, Johnson and Nelson-Quigg 1993).

Luminance Pedestal Flicker perimetry presents a flickering stimulus, superimposed on a pedestal of a steady luminance, and determines the temporal frequency necessary to distinguish the stimulus from the pedestal (Anderson and Vingrys 2000; Anderson and Vingrys 2002). The technique is currently incorporated in the commercially available Medmont M600 (Medmont, Camberwell, Australia) perimeter However, the clinical utility of Luminance Pedestal Flicker perimetry in patients with either OAG or OHT has not been investigated.

Critical Flicker Fusion perimetry represents the highest temporal frequency at which a flickering stimulus of constant luminance is initially perceived as a continuous (non-flickering) stimulus (Allen 1926; Pieron 1962; Midena 1989). The literature is equivocal as to whether the end point for CFF should be determined by increasing the temporal frequency until fusion is reported (Mahneke 1957) or by reducing the temporal frequency until flicker is perceived (Knox 1945).

In normal individuals, the CFF increases linearly with increase in the logarithm of the stimulus area. This relationship is often referred to as the Granit-Harper Law. The linearity of this relationship has been confirmed by several researchers (Berger 1953; Kugelmass and Landis 1955; Roehrig 1959b) for stimulus diameters up to 13.6° and out to 50º eccentricity (Brown 1945) in terms of spatial summation and in terms of the increase in stimulus size arising from optical defocus (Roehrig 1959a). Subsequent research has questioned the Granit-Harper Law,

showing that, for eccentricities beyond 15°, the relationship becomes non-linear (Hartmann, Lachenmayr and Brettel 1979).

CFF varies regionally and reaches a maximum at an eccentricity at 40° in the temporal visual field and at an eccentricity of 25° to 30° in the nasal field (Hylkema 1942).

CFF increases linearly with increase in the logarithm of the background luminance. The maximum CFF increases with increase in stimulus size and reaches a maximum at an eccentricity of 40° in the temporal visual field and at an eccentricity of 25° to 30° in the nasal field (Hylkema 1942). This outcome is described by the Ferry-Porter Law over a broad range of luminances (Brooke 1951).

The background luminance appears to have minimal influence on CFF, for a foveal stimulus. When stimuli are varied from 0.5 minutes up to 400 minutes, the maximum influence occurs with a circular test area of 1 minute diameter (Fry and Bartley 1936; Berger 1954). A high luminance CFF stimulus of 2° in diameter exhibits an increase in sensitivity over a broad range of photopic luminances and decline in sensitivity at low luminances (Ross 1936a).

CFF increases with increase in stimulus duration between 100msec and approximately 1 sec (Granit and Harper 1930).

CFF is affected by light and dark-adaptation. Some researchers have found that CFF decreases with the light adapted eye (Peckham and Arner 1952). Others have found opposite results in animals and humans, both based on retinal action potential and with an increase in light adaptation (Granit and Riddell 1934; Granit and Therman 1935; Granit 1935b). It has been

demonstrated that the effect of increased dark adaptation from the fovea to 90º in the periphery for luminances from 0.0003 to 7.3 mL shows a decrease in CFF and adverse the effect with the light adapted eye (Lythgoe and Tansley 1929).

From a clinical point of view, different methods of flicker perimetry have been reported to detect retinal (Phipps, Guymer and Vingrys 1999; Vingrys and Pesudovs 1999; Stavrou and Wood 2005) and macular abnormalities (Mayer et al 1992a; Mayer et al 1992b; Mayer et al 1994; Phipps et al 2004). Several studies have also reported that this method is superior to SAP in the detection of glaucomatous field loss (Lachenmayr et al 1991; Lachenmayr et al 1991; Lachenmayr and Drance 1992; Lachenmayr and Gleissner 1992; Lachenmayr, Drance and Airaksinen 1992b; Lachenmayr 1994; Lachenmayr et al 1994; Matsumoto et al 2006). The relationship between the MS for SAP (dB) and that for CFF (Hz), based upon patients with retinal detachment and patients with open-angle glaucoma, is curvilinear (Figure 2.4) (Matsumoto et al 1999).

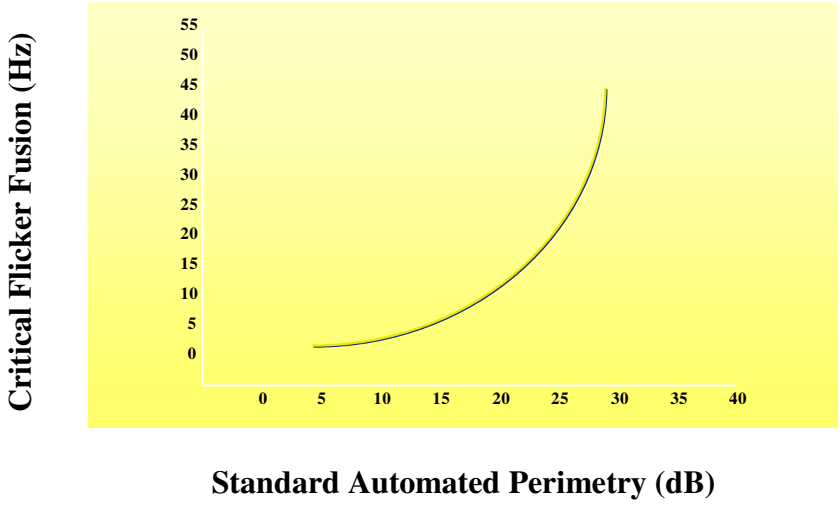

Figure 2.4 Shows that a small dB loss in SAP (at the steep end of the curve) corresponds to an important drop in CFF perimetry (Hz).

CFF perimetry is currently clinically possible, and commercially available, with the Octopus 311 and forms the topic for this thesis. The outcome of CFF perimetry in relation to the learning effect, media opacities and refractive defocus is described in detail in Chapters 4, 5.and 6, respectively.

2.2.5 Moorfield Motion Displacement test (MDT)

The motion detection threshold test presents a vertical bar of 85% Michelson contrast on a 10-cdm^{-2} white background at each of 32 stimulus locations (Oleszczuk, Bergin and Sharkawi 2012). Three oscillations of 200 msec each modulate the lateral displacement of each bar. Threshold is the discernible displacement detected for 50% of the presentations. The test is developed as a simple effective test for the detection of glaucoma (Baez et al 1995) and is relatively immune to the effects of intra-ocualar light scatter (Bergin et al 2011; Oleszczuk, Bergin and Sharkawi 2012)

CHAPTER 3

RATIONALE AND DESCRIPTION FOR THE RESEARCH

3.1 Previous work

Several studies have evaluated the efficiency of CFF perimetry in detecting early field loss in OAG and in OHT (Lachenmayr et al 1991; Yoshiyama and Johnson 1997; Matsumoto et al 1999; Matsumoto et al 2006) and it is claimed that CFF perimetry can detect abnormality in advance of SAP. However, it is only recently that, with the availability of CFF automated perimetry, that the viability of these claims can be investigated in routine clinical populations.

A learning effect for CFF Perimetry is seemingly present in normal individuals (Bernardi, Costa and Shiroma 2007). The latter findings were published during the course of this Thesis. The group mean global, central, and peripheral sensitivity improved from the first to the third examinations. However, the age profile of the cohort was not clinically representative of those attending either a glaucoma or a retina clinic. In the absence of knowledge of the impact of the learning effect on the outcome of CFF perimetry in patients, the potential of the technique for identifying visual field loss prior to that with SAP remains unknown.

Any cause of media opacities of the eye, such as a corneal scar or a cataract will blur, absorb and scatter, both backwards and forwards, the amount of light reaching the retina and hence reduce the visibility of the retinal image (Essock et al 1984; Baraldi, Enoch and Raphael 1987). The outcomes of SAP (Guthauser and Flammer 1988; Lam, Alward and Kolder 1991; Budenz, Feuer and Anderson 1993), of SWAP (Moss and Wild 1994; Moss, Wild and Whitaker 1995; Kim et al 2001) and of FDT (Artes et al 2003; Tanna et al 2004; Casson and James 2006) are adversely influenced by stray light arising from cataract; SWAP exhibits the greatest attenuation

presumably due to the higher background luminance. CFF perimetry is seemingly less influenced by media opacities compared to these techniques (Lachenmayr and Gleissner 1992; Takada et al 2004). However, the resistance of the CFF stimulus to intra-ocular light scatter arising from age-related cataract (Lachenmayr and Gleissner 1992; del Romo, Douthwaite and Elliott 2005; Shankar and Pesudovs 2007) has not been validated/ confirmed with the rigour of current research practice particularly in regard to perimetry.

Optical defocus decreases the visibility of the stimulus primarily by reducing the contrast of the retinal image (Campbell and Green 1965; Adams, Heron and Husted 1987; Atchison 1987). The CFF stimulus modulates the frequency of the flickering stimulus from slow (1-5Hz) to fast (towards 50Hz). The influence of defocus in a clinical setting is unknown, but might be expected to be relatively minimal (Lachenmayr and Gleissner 1992). It was therefore considered clinically important to investigate the influence of defocus on the CFF stimulus.

3.2 Rationale

This Thesis describes three separate studies of CFF perimetry undertaken at the authors's optometric practice, Rjukan Synssenter Optometri, in Rjukan, Norway, between 2005 and 2011. The first study investigated the learning effect for CFF perimetry in normal individuals, in individuals with OAG and in individuals with OHT. The second study investigated the influence of age-related cataract on the outcome of CFF perimetry. The third study investigated the influence of optical defocus on the outcome of CFF perimetry.

3.3 The learning effect for critical flicker fusion perimetry in normal individuals, in individuals with OHT and in individuals with OAG (Chapter 4).

The study used a systematic examination protocol comprising 5 examinations each separated by one week. The study considered, specifically, the within- and between-individual differences in performance within- and between-visits in 28 normal individuals, in 10 individuals with OHT and in 11 individuals with OAG, with the Octopus 311 using Program G1 and the TOP algorithm.

3.4 The comparative performance of SAP and CFF perimetry in individuals with age-related cataract (Chapter 5).

The influence of age-related cataract on the outcome of CFF perimetry and SAP (Octopus 311, Program G1 and the TOP algorithm) was investigated in 22 individuals with either monocular cataract or with a marked difference in the severity of the cataract between the two eyes. Individuals underwent CFF perimetry and SAP in both eyes on each of four occasions each separated by one week. Measurement of forward light scatter was undertaken at the third and fourth visits. Forward light scatter was assessed by measuring logMAR visual acuity at high and low contrast levels in the absence of, and in the presence of, three levels of glare using the Brightness Acuity Test. Back scatter was assessed in terms of LOCS III (Chylack et al 1993).

3.5 The influence of defocus on the outcome of CFF perimetry (Chapter 6).

The influence of defocus on the outcome of CFF perimetry (Octopus 311, Program G1 and the TOP algorithm) was investigated in 16 normal individuals all of whom had participated in the study of the learning effect on CFF perimetry described in Chapter 4. CFF perimetry and SAP was undertaken in one eye on two occasions each separated by one week. At one visit, two randomly selected levels of defocus from plano, +1.00DS, +2.00DS or +4.00DS were

superimposed upon the distance correction. The remaining two defocus levels were used at the second visit.

3.6 Logistics

3.6.1 Background

The author is an Optometrist, registered since 1980 with the Norwegian Department of Health. From 1981 to the present date, he has worked in private optometric practice in Rjukan, Norway. In 2004, he obtained, by Distance Learning, the degree of Master of Science in Clinical Optometry from Pennsylvania College of Optometry (PCO), Philadelphia, USA.

In 2005, the author enrolled for a research degree as a part of the innovative joint Cardiff University and PCO programme for individuals who had obtained a Masters Degree in Clinical Optometry from PCO. It was envisaged that the research would be undertaken in the author's practice without the necessity for the purchase of expensive dedicated equipment.

By the end of the first year of research, the author was required to submit a First Year Continuation Report on his research, to date, and to undergo a vive voce examination of the Report. Following his successful vive voce examination, the author continued his research for the degree PhD of Cardiff University.

The research was conducted under the academic supervision of Prof John Wild of Cardiff University.

3.7 Methods

The research was undertaken in the author's practice. All three studies were approved by the Norwegian Ethical Committee for Medical Research (Regional Komité for medisinsk forskningsetikk Sør-Norge [REK Sør]) and the Norwegian Data Protection Registrar (Datatilsynet).

Normal individuals and individuals with age-related cataract were recruited from the author's practice. The individuals with either OAG or with OHT were recruited from the clinics of two ophthalmologists, Dr Hans Hafskolt and Dr Erik Holmberg, .at Rjukan Hospital.

An ophthalmic examination was undertaken on each individual prior to enrolment in the given study to ascertain their suitability. At enrolment, each participant gave signed consent after having been informed of the appropriate procedures, risks and possible consequences of the given study.

Normal individuals were classified as normal on the basis of the ophthalmic examination undertaken by the author and on the basis of the digital stereo-images of the fundus evaluated by Prof . Wild.

Individuals with OAG were diagnosed by either of the two ophthalmologists on the basis of the appearance of the ONH and by Prof. Wild on the basis of the appearance of the visual field and of the digital stereo-images of the ONH.

Individuals with age-related cataract were diagnosed and classified according to the Lens Opacity Classification System (LOCS III) by the author and by Prof. Wild who evaluated the digital images of the crystalline lens obtained from slit lamp photography.

Despite the large number of individuals (approximately 6,000) attending the author's practice and the enthusiastic assistance from Drs. Hafskolt and Holmberg, the recruitment of individuals with OAG and the individuals with OHT was time consuming and only partially successful. Many potential participants did not meet the strict inclusion criteria for each of the studies. General health conditions, such as diabetes or a family history of glaucoma, reduced the number of potential participants. Due to the fact that Rjukan is in a rural part of Norway and individuals can travel up to 160 kilometres for a return trip to the practice, and that two of the three studies required a minimum of 4 visits each separated by one week, it was very difficult to persuade and to motivate individuals to participate in any given study. Frequently, work commitments or demands of private life were reasons cited for a lack of willingness to participate in any given study.

The author planned and coordinated the visits of the individuals recruited into all three studies. In total, 87 individuals provided 1146 visual fields. The author undertook all the visual field examinations himself. The time spent conducting the visual field examinations was approximately 200 hours. The author was trained in the operation of the Octopus 311 by Prof Wild over a period of three days prior to the onset of the first study. In addition, Prof Wild also followed up the process of the examinations by visiting the author at his optometric practice on three separate occasions. The results from each individual in each of the various studies were also regularly monitored by Prof Wild.

Supervision by Prof Wild was provided via weekly telephone conferences, through meetings at conferences e.g. that of the Association for Research in Vision and Ophthalmology (ARVO) and through 1-2 visits per year by the author to the Cardiff School of Optometry and Vision Sciences.

The author presented his research at meetings of the Association for Research in Vision and Ophthalmology, Fort Lauderdale, Florida, in 2007, 2009 and 2010; at the Octopus Users Symposium, Berne, Switzerland, in 2008; and at the meeting of the Imaging and Perimetric Society, Teneriffe, Spain in 2010.

Despite the time-consuming nature of the recruitment phase of the research and of the clinical examinations, the experience of undertaking visual field examinations on such pleasant individuals will never be forgotten.

CHAPTER 4

THE LEARNING EFFECT FOR CRITICAL FLICKER FUSION PERIMETRY

4.1 Introduction

CFF perimetry is currently clinically possible, and commercially available, with the Octopus 311 perimeter. The default adaptation level (31.4 asb), stimulus size (Goldman III) and maximum stimulus luminance (4800 asb) are the same as those employed for SAP with the Octopus 300 series perimeters. The default stimulus duration for CFF perimetry, however, is 1000msec. The maximum temporal frequency of the stimulus is 60Hz. The suprathreshold increment for the false-negative catch trials is 5Hz. The temporal frequency for the false-positive catch trials is 100Hz. CFF perimetry with the Octopus perimeter can be undertaken with all the stimulus programs and threshold algorithms that are available for SAP. The results of CFF perimetry for any given patient with the Octopus perimeters are displayed and evaluated statistically in the same manner as for SAP.

4.2 The learning effect for Standard Automated Perimetry in normal individuals

The presence of a learning effect for SAP (also shown in Section 1.15.1) has long been documented (Wood et al 1987b; Werner, Adelson and Krupin 1988; Heijl, Lindgren and Olsson 1989; Wild et al 1989; Autzen and Work 1990; Kulze, Stewart and Sutherland 1990; Marchini, Pisano and Bertagnin 1991; Searle et al 1991; Wild et al 1991; Heijl and Bengtsson 1996). It was shown that the learning effect occurs as the observer becomes increasingly familiar with the requirements of the perimetric task and manifests as an improvement in sensitivity, a decrease in measurement variability, and a reduction in examination duration, over successive examinations.

It is present in normal individuals (Wood et al 1987b; Heijl, Lindgren and Olsson 1989; Searle et al 1991), in individuals with OHT (Wild et al 1989; Werner et al 1990; Wild et al 1991) and in individuals with OAG (Werner, Adelson and Krupin 1988; Kulze, Stewart and Sutherland 1990; Marchini, Pisano and Bertagnin 1991; Wild et al 1991; Heijl and Bengtsson 1996). The learning effect is present for the first eye examined at the first visit (Searle et al 1991) is transferred between eyes at the first visit (Searle et al 1991) and is present between visits, both within- (Searle et al 1991) and between-eyes (Heijl, Lindgren and Olsson 1989; Searle et al 1991; Heijl and Bengtsson 1996), generally up to at least the end of the second or third visit (Wood et al 1987b; Heijl, Lindgren and Olsson 1989; Searle et al 1991; Heijl and Bengtsson 1996). The improvement in sensitivity increases with increase in eccentricity (Wood et al 1987b; Heijl, Lindgren and Olsson 1989; Wild et al 1989; Werner et al 1990; Searle et al 1991; Heijl and Bengtsson 1996) and is greatest in areas of relative loss.

A learning effect is also present for SWAP in normal individuals (Wild, Moss and O'Neill 1996; Zhong et al 2008) and in individuals with OAG or with OHT regardless of the prior experience of SAP (Rossetti et al 2006; Wild et al 2006; Zhong et al 2008; Fogagnolo et al 2010). The learning effect for SWAP can also be present over several years (Gardiner, Demirel and Johnson 2008).

A learning effect is also present for FDT in normal individuals (Contestabile et al 2007; Pierre-Filho et al 2010) and in individuals with either OAG (Hong et al 2007; Pierre-Filho et al 2010) or with OHT (Matsuo et al 2002; Centofanti et al 2008).

Pulsar perimetry exhibits a greater learning effect than either SAP or FDT in individuals with OAG and in individuals with OHT (Gonzalez-Hernandez et al 2007a). Similarly, Flicker Defined

Form (FDF) perimetry demonstrates a significant learning effect over the first three 3 examinations (Lamparter et al 2011).

The learning effect for CFF Perimetry has received little attention. The only study, to date, was undertaken on a case series of 20 normal, and relatively young individuals (mean age: 28.7 years (ranging from 19 to 41 years) who underwent repeated perimetry in one eye, only, on six occasions (Bernardi, Costa and Shiroma 2007). The first three examinations covered an interval of between one and 30 days (sic) and the last three examinations were undertaken on the same day. The group mean Mean Sensitivity increased from the first to the second and third examinations by approximately 1.3Hz. ($p=0.014$). Unfortunately, the young age and the normality of the participants used in this study, together with the lack of robustness of the study design, namely the interval between examinations, were such as to render the information of little clinical value.

The learning effect presents a major clinical problem in the management of OAG in that it frequently exerts a substantial influence on the appearance of the recorded visual field at the initial examinations, resulting in an overestimation of the severity of the actual field loss, and also renders these examinations of little value in the determination of progressive visual field loss (Wild et al 2006). Clearly, if CFF perimetry is to have an impact clinically the characteristics of the learning effect must be delineated.

4.3 The learning effect for Critical Flicker Fusion Perimetry in normal individuals

4.4 Aims

The overall aim of the study was twofold. Firstly, to determine the characteristics of any learning effect for CFF Perimetry in normal individuals, in individuals with OHT and in individuals with OAG, over five consecutive visits each separated by an interval of one week using the Octopus 311 and Program G1 and the TOP threshold algorithm. Secondly, to compare the outcome at the fifth visit with that determined on a sixth occasion, one week later, using the Dynamic threshold algorithm.

More specifically, the primary aim was to determine, over the five visits, the between-individual between-visit differences in performance. The performance was considered in terms of four different types of analysis. Firstly, any change in each of the visual field indices Mean Sensitivity, Mean Defect, square root of the Loss Variance, Diffuse Defect and Local Defect determined using separate ANOVAs for each index. Secondly, in terms of the change in sensitivity at each stimulus location as a function of stimulus eccentricity. Thirdly, in terms of the change in sensitivity at each stimulus location as a function of defect depth. Fourthly, in terms of the change in sensitivity at each stimulus location expressed in terms of the Comparison and of the Corrected Comparison probability level.

4.5 Methods

The study was a prospective observational case series study.

4.6 Case Series

The case series comprised 49 consecutively presenting Caucasian individuals who met the inclusion criteria for enrolment in the study and who had volunteered to take part in the study.

All individuals were provided with verbal and written information concerning the nature of the study and had given written consent, in accordance with the requirements, and approval, of the Norwegian Research and Ethics Committee (REK, Regional komité for medisinsk forskningsetikk Sør-Norge (REK Sør) and the Norwegian Datatilsynet (Enclosure number 1, 2, and 5) which are in turn, in accordance with the tenets of the Declaration of Helsinki.

The case series consisted of three groups of individuals. The first group comprised 28 normal individuals (14 males) who attended the optometric practice, Rjukan Synssenter, Rjukan, Norway, and who were deliberately stratified by age to achieve approximately equal numbers for each decade of age after the age of 50 years. The mean age of the normal individuals was 62.4 years (SD 8.7) and the median 62.5 years (IQR 13.5). A case series of 28 individuals was based upon the detection of a 3Hz difference in the Mean Defect between successive examinations with 95% power. [(11 participants aged between 50 and 59 years, 10 between 60 and 69 years and 7 between 70 and 79 years)] (Table 4.1).

The second group comprised 10 individuals with OHT (4 males) who were recruited from the clinics of one or both of two consultant ophthalmologists, Dr Hans Hafskolt and Dr Erik Holmberg of the Rjukan Hospital, Rjukan, Norway. The mean age of these individuals was 67.6 years (SD 7.5) and the median 67.5 years (IQR 9.7). [(one participant aged between 50 and 59 years, 5 aged between 60 and 69 years and 4 aged between 70 and 79 years)] (Table 4.1).

The third group comprised 11 individuals with OAG (8 males) who were also recruited from the clinics of the two ophthalmologists at Rjukan Hospital. The mean age was 62.9 years (SD 7.8) and the median 63.0 years (IQR 7.5).) [(one participant aged between 40 and 49 years, 2 participants aged between 50 and 59 years, 6 aged between 60 and 69 years and 2 aged between 70 and 79 years)] (Table 4.1).

Age (years)	Normal	OHT	OAG
40 – 49			1
50 – 59	11	1	2
60 – 69	10	5	6
70 – 79	7	4	2

Table 4.1 The number of individuals, by decade of age, within each of the three diagnostic groups.

At the enrolment visit, potential participants underwent a standard ophthalmic examination to confirm the inclusion criteria. The confirmatory examination in each eye included determination of visual acuity; refraction; SAP with the Octopus 311 perimeter using Program G1 and the Dynamic algorithm, central corneal thickness using the Sonogage Corneogage 2 ultrasonic pachometer (Sonogage Inc. Cleveland, USA); Goldmann applanation tonometry; gonioscopy; indirect ophthalmoscopy, usually with a +78 dioptre lens; stereo-photography of the optic nerve head and posterior pole using the Kowa Nonmyd α-D, non-mydriatic fundus camera (Kowa Company. Ltd., Japan). The assessment of IOP, the measurement of central corneal thickness and gonioscopy all required the installation of a topical anaesthetic (Oxibuprocaine 0.4%). Slit lamp indirect ophthalmoscopy and photography of the posterior pole required pupil dilation with one drop of Tropicamide 0.5%.

Potential participants were to be excluded from the study if they exhibited in either eye: a corrected visual acuity worse than 6/9; a distance refractive error greater than +/-5.0 dioptres sphere and/or greater than +/- 2.5 dioptres cylinder; a pupil diameter smaller than 3 mm; a central corneal thickness-corrected IOP of greater than 20mmHg for the normal individuals; a narrow anterior chamber angle; media opacities worse than NC3.0, NO3.0, C2.0 or P2.0 by the

Lens Opacities Classification System III (LOCS III) (Chylack et al 1993); any previous ocular surgery for the normal individuals; and any ocular disorder or ocular disease other than OHT or OAG, in the appropriate group. In addition, individuals were also excluded if they exhibited migraine with aura; diabetes; neurological disorder or disease; systemic disease other than systemic hypertension manifesting as Grade 1 hypertensive retinopathy; hyperthyroid disease; a family history of glaucoma (other than those comprising the groups with OHT or with OAG); or previous experience of CFF perimetry.

The images of the optic nerve head and of the posterior pole and the results of the visual field plots for the normal individuals were all designated as normal by Professor Wild who was masked to the assumed normality of the potential participant.

The diagnosis of either OHT or OAG had been made on the appearance of the ONH. Nine of the eleven individuals with OAG had undergone laser trabecularplasty (LTP) in both eyes. Of these nine, two individuals were being treated with a combination of topical beta-blocker, prostaglandin analogue and carbonic anhydrase inhibitor; three individuals were treated with a combination of topical beta-blockers and carbonic anhydrase inhibitor only; and six individuals were being treated with prostaglandin analogue agents.

Eight of the ten individuals with OHT had undergone LTP. Five of these ten individuals were also being treated with either a topical beta-blocker or with a prostaglandin analogue.

The five year risk of each individual with OHT for conversion to OAG, based upon the initial presenting IOP, was calculated using the S.T.A.R. II (S.T.A.R. Scoring Tool for Assessing Risk) (Gordon et al 2002; Kass et al 2002; Weinreb et al 2004; Medeiros et al 2005; Gordon et al

2007). Two individuals had a risk in one eye of 43% and 53%, respectively. Six had a risk below 20% in one or both eyes, three patients had a risk of greater than 33% in one eye (Table 4.2).

Patient ID	Age year	IOP mm Hg	CCT µm	PSD dB	C/D	Risk %
R 2356	65	20	624	1.94	0.2	**2.1**
L 2356	65	31	607	2.77	0.2	**12.3**
R 2530	54	25	506	2.97	0.2	**33.6**
L 2530	54	25	501	2.14	0.2	**23.5**
R 3117	75	24	562	2.85	0.4	**25.6**
L 3117	75	20	562	2.07	0.3	**10.1**
R 851	63	20	483	2.04	0.3	**27.8**
L 851	63	27	475	1.48	0.2	**34.2**
R 4175	71	17	503	1.61	0.3	**21.0**
L 4175	71	28	528	2.76	0.3	**43.1**
R 652	66	26	569	3.00	0.5	**28.3**
L 652	66	24	580	2.92	0.4	**16.6**
R 6070	74	22	517	1.84	0.6	**33.8**
L 6070	74	23	516	2.92	0.5	**52.8**
R1212	60	24	545	1.76	0.6	**18.6**
L 1212	60	24	552	1.81	0.5	**16.3**
R 3596	79	16	593	2.85	0.3	**7.0**
L 3596	79	25	585	2.86	0.3	**18.0**
R 562	69	18	583	2.90	0.4	**10.0**
L 562	69	25	579	2.53	0.3	**13.3**

Table 4.2 The risk of developing OAG within a 5 year period following the baseline examination for the 10 individuals with OHT calculated in terms of the magnitudes of age, IOP, CCT, PSD and vertical cup to disc ratio.

The characteristics of the individuals with OAG are given in Table 4.3. In terms of the associated visual field loss in the worst eye, classified using the system of Hodapp (Hodapp et al 1993), six individuals manifested early loss, two moderate loss and three severe loss. The appearance of the optic nerve head and of the Corrected Probability plot of the visual field in each eye are given in Table 4.4.

Patient	Age Year	ONH	SAP	Diagnosis	IOP mm Hg	CCT µm	MD dB	sLV dB	C/D	Hodapp
R85112	66	G	G	OAG	10	508	7.1	10.2	0.8	**Moderate**
L85112	66	G	N	OAG	10	499	0.8	3.7	0.7	**Early**
R2917	59	G	G	OAG	17	531	1.5	11.9	0.4	**Early**
L2917	59	N	N	N	12	590	-2.3	4.3	0.2	**Normal**
R82921	59	G	G	OAG	36	557	4.0	7.4	0.4	**Early**
L82921	59	G	G	OAG	42	574	4.7	7.2	0.5	**Early**
R2124	68	G	G	OAG	35	600	3.5	6.0	0.7	**Early**
L2124	68	G	G	OAG	14	760	13.9	7.6	0.8	**Advanced**
R3226	65	G	G	OAG	14	564	10.4	9.6	0.6	**Moderate**
L3226	65	G	G	OAG	14	561	14.3	9.5	0.7	**Advanced**
R2347	61	G	G	OAG	14	570	6.4	5.5	0.6	**Early**
L2347	61	G	G	OAG	17	546	13.4	8.7	0.8	**Advanced**
R4629	74	N	N	N	16	482	1.7	2.2	0.4	**Normal**
L4629	74	G	N	OAG	17	491	1.7	3.6	0.5	**Early**
R4207	60	G	N	N	18	572	-1.2	1.9	0.5	**Normal**
L4207	60	G	N	OAG	18	557	0.8	3.6	0.8	**Early**
R5037	73	G	G	OAG	19	550	11.3	11.1	0.7	**Moderate**
L5037	73	G	G	OAG	19	543	10.7	10.7	0.9	**Moderate**
R83530	45	G	N	OAG	25	581	2.1	2.2	0.8	**Early**
L83530	45	N	N	OAG	24	592	1.3	1.8	0.7	**Normal**
R344	63	G	N	OAG	21	586	-1.2	1.9	0.4	**Early**
L344	63	G	N	OAG	21	580	-0.6	2.3	0.3	**Early**

Table 4.3 The diagnostic characteristics (age, the appearance of the optic nerve head, the appearance of the visual field and the magnitudes of the presenting IOP, the CCT, the MD_{SAP} and the sLV_{SAP}, and the Cup to disc ratio, respectively), in each eye of the 11 individuals with OAG.

Participant ID	Right eye ONH	Right eye Visual field	Left Eye ONH	Left eye Visual field
1 85112	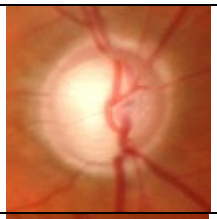	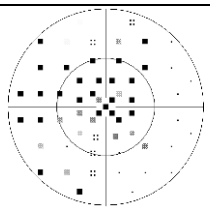		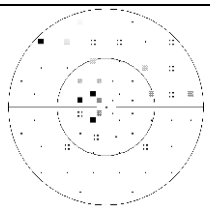
2 2917		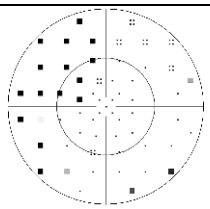		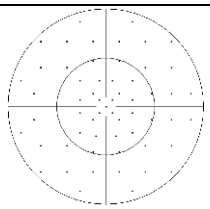
3 82921		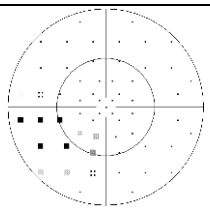	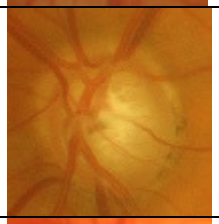	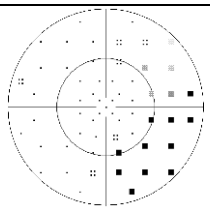
4 2124	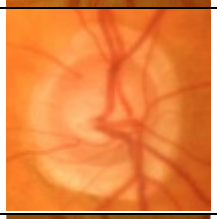	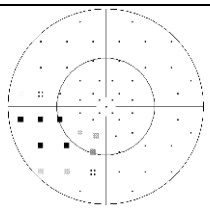	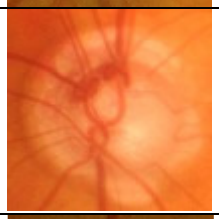	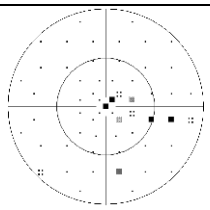
5 3226		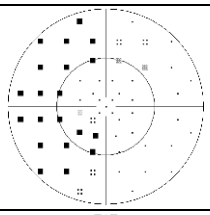	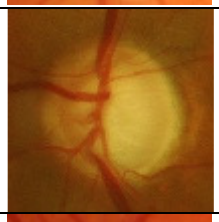	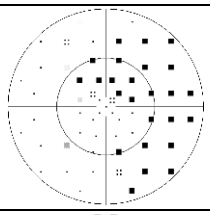
6 2347	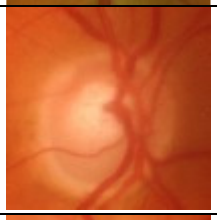	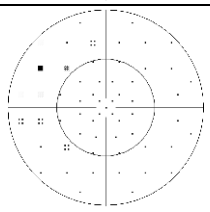		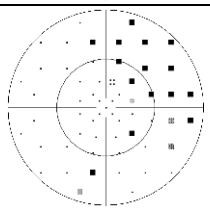
7 4629	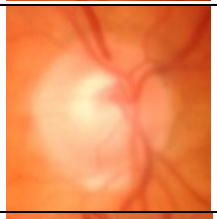	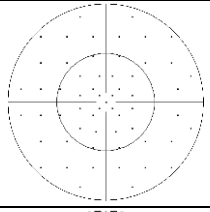	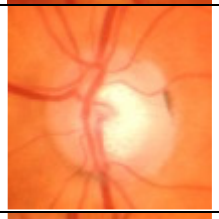	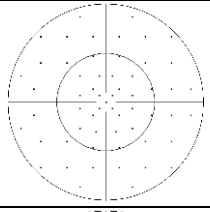
8 4207	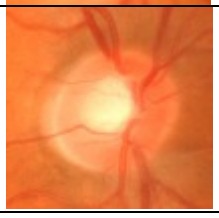	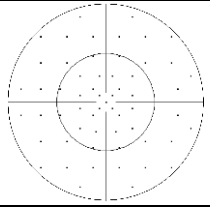	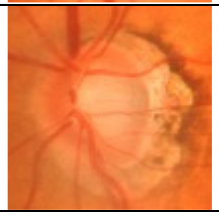	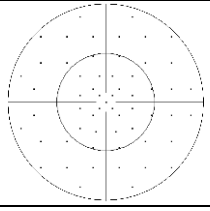

Participant ID	Right eye ONH	Right eye Visual field	Left Eye ONH	Left eye Visual field
9 5037	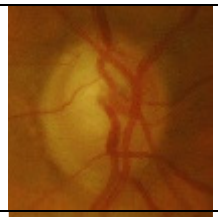	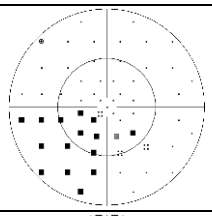		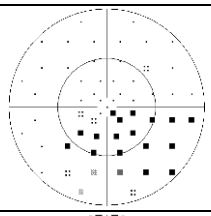
10 83530		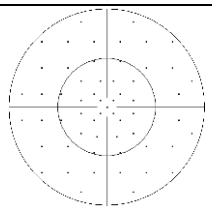		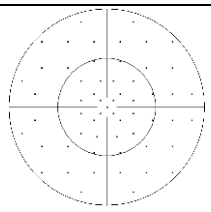
11 344	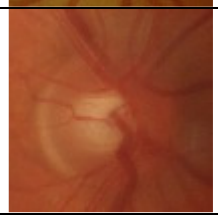	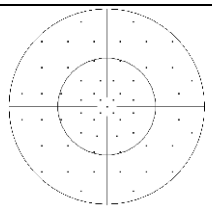	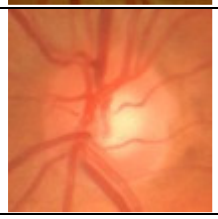	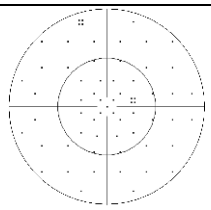

Table 4.4 The appearance of the optic nerve head and of the Corrected Comparison probability map, derived by SAP, at the enrolment visit for each eye of each of the 11 individuals with OAG.

4.7 Perimetric Protocol

Following enrolment, each participant underwent examination of each eye with CFF perimetry 14 days after the initial ophthalmic examination. At this first perimetry visit, both eyes were examined using CFF perimetry and Program G1 and the TOP algorithm of the Octopus 311. The right eye was always examined before the left eye. Distance refractive correction, in the form of full aperture trial lenses, was used for each eye. The non-examined eye was occluded with an opaque patch. The influence of the fatigue effect was reduced by the provision of rest periods of approximately one minute in duration at 3 minute intervals during the examination of each eye and by a 5 minute rest period between examination of each eye. Fixation was monitored continuously by the automatic eye tracker of the perimeter and was also viewed via the video monitor.

Each participant then attended for a further four perimetry visits (Table 4.5). The protocol at each of the four visits was identical to that at the first visit. Each visit was separated by an interval of one week. The same instructions were given at each visit. The visual field examinations at all five visits were undertaken by the author.

At the end of the fifth visit, the participants were invited to attend for a sixth visit, one week later. All 49 participants responded in the affirmative to this invitation. At this sixth visit, the visual field was examined by the author, in exactly the same manner to that of previous five visits, using the Dynamic algorithm.

	Enrolment	**Session 1**	**Session 2**	**Session 3**	**Session 4**	**Session 5**	**Session 6**
Method	SAP	CFF	CFF	CFF	CFF	CFF	CFF
Interval from immediate previous session (days)		14	7	7	7	7	7
Program/ algorithm	G1/ Dynamic	G1/ TOP	G1/ TOP	G1/ TOP	G1/ TOP	G1/ TOP	G1/ Dynamic

Table 4.5 The summary of the perimetric protocol at enrolment and at each of the subsequent six visits.

4.8 Analysis

4.9 The between-individual between-visit (Visits One to Five) performance (Primary Aim)

The first analysis of any potential learning effect consisted of separate Analyses of Variance of the visual field indices Mean Sensitivity, Mean Defect, square root of the Loss Variance, Diffuse Defect and Local Defect and for the examination duration. Age and diagnostic group were considered as separate between-subject factors and visit and eye as separate within-subject factors. Statistical sugnificans for this study and those in the remainder of the Thesis was considered to be $p \leq 0.05$.

The second analysis of any potential learning effect involved the change in sensitivity, at each given stimulus location between Visits One and Visits Two and between Visit Two and Visit Five, respectively, as a function of eccentricity. This was undertaken for the normal individuals and for the individuals with OHT, only.

The third analysis investigated the changes in sensitivity, across all stimulus locations, between Visit One and Visit Two and between Visit Two and Visit Five, respectively, as a function of the magnitude of sensitivity at the initial visit of the given paired comparison. The 10^{th}, 50^{th} and 90^{th} percentiles of the distribution of the change in sensitivity were calculated for each magnitude of sensitivity for each of the three groups, separately, and combined.

The fourth analysis investigated the changes in the Comparison probability value across all given stimulus locations between Visit One and Visit Two and between Visit Two and Visit Five, respectively, for each of the three groups, separately, and combined. The analysis was not expected to necessitate the evaluation of the corresponding differences in the Corrected Comparison probability analysis since the inclusion criterion for the ocular media precluded

those individuals likely to yield visual fields in which the height adjustment would have resulted in a change to the Corrected Comparison probability value.

4.10 The between-individual difference in the TOP and Dynamic algorithms (Visits Five and Visit Six) (Secondary Aim)

Any difference in the magnitude of sensitivity between the TOP algorithm undertaken at Visit Five and the Dynamic algorithm undertaken at Visit Six was analysed in an identical manner to that undertaken for the within- and between-individual between-visit change in performance.

4.11 The within-individual between-visit change in performance (Primary Aim)

The within-individual between-visit change in performance was evaluated in three ways. Firstly, in terms of the absolute change in each of the visual field indices between Visit One and Visit Two compared to that between Visit Two and Visit Five. Secondly, in terms of the proportionate change in Mean Sensitivity between Visit One and Visit Two compared to that between Visit Two and Visit Five. Thirdly, in terms of the diagnostic outcome as defined by the Comparison and Corrected Comparison probability analysis.

The selection of a comparison between Visits One and Visits Two and between Visit Two and Visit Five, respectively, was utilised for two reasons. Firstly, the majority of the learning effect for other types of perimetry is considered to have occurred over the first two visits and clinicians are used to placing less quantitative emphasis on the results from these initial examinations. Secondly, to reduce the amount of potential analysis to manageable proportions.

4.12 Results

4.12.1 Age-related decline in Mean Sensitivity

The slope of the age-related decline in MS, together with the magnitude of the Coefficient of Determination (R^2) for each eye at each of the five visits and for the Dynamic algorithm at Visit Six of the 28 normal individuals is given in Table 4.6. The corresponding slope at each stimulus location at Visit Five and at Visit Six for each eye is shown in Figure 4.1a and Figure 4.1b respectively.

Mean Sensitivity Slope		Visit 1	Visit 2	Visit 3	Visit 4	Visit 5	Visit 6
Right	**Slope**	-0.129	-0.101	-0.131	-0.155	-0.250	-0.175
	R^2	0.011	0.006	0.009	0.009	0.017	0.010
Left	**Slope**	-0.105	-0.107	-0.132	-0.164	-0.194	-0.287
	R^2	0.002	0.007	0.008	0.011	0.015	0.032

Table 4.6 The slope of the age-related decline in MS_{CFF} (Hz per year), and the corresponding Coefficient of Determination, R^2, for each eye of the 28 normal individuals at each of the five visits for the TOP algorithm and at Visit Six for the Dynamic algorithm.

The slope of the age-related decline in MS for the TOP algorithm steepened in the right eye for visits four and five and in the left eye for visits three, four and five implying a greater improvement in MS for the younger individuals.

The slope of the age-related decline in MS for the Dynamic Algorithm was notably steeper than that of the TOP algorithm over each of the first four visits for each eye and particularly so for the left eye. It appeared to be broadly similar to that at the fifth visit.

In general, the age-related decline in MS at Visit Five as a function of stimulus eccentricity, derived by the TOP algorithm (Figure 4.1a) exhibited some tendency to exhibit a steeper slope

with increase in eccentricity, superiorly and nasally, this effect was more apparent for the field of the right eye. This tendency was also apparent for the Dynamic Algorithm, particularly for the left eye (Figure 4.1b).

4.12.2 The between-individual between-visit (Visits One to Five) change in the Visual Field Indices

4.12.3 Mean Sensitivity (MS)

The summary statistics for the MS over the six visits are shown in Table 4.7 for each eye of the 28 normal individuals (Top), each eye of the 10 individuals with OHT (Middle) and each eye of the 11 individuals with OAG (Bottom). The distribution of the MS, at each visit, as a function of eye, across each of the three groups, is also illustrated in terms of Box and Whisker plots in Figure 4.2.

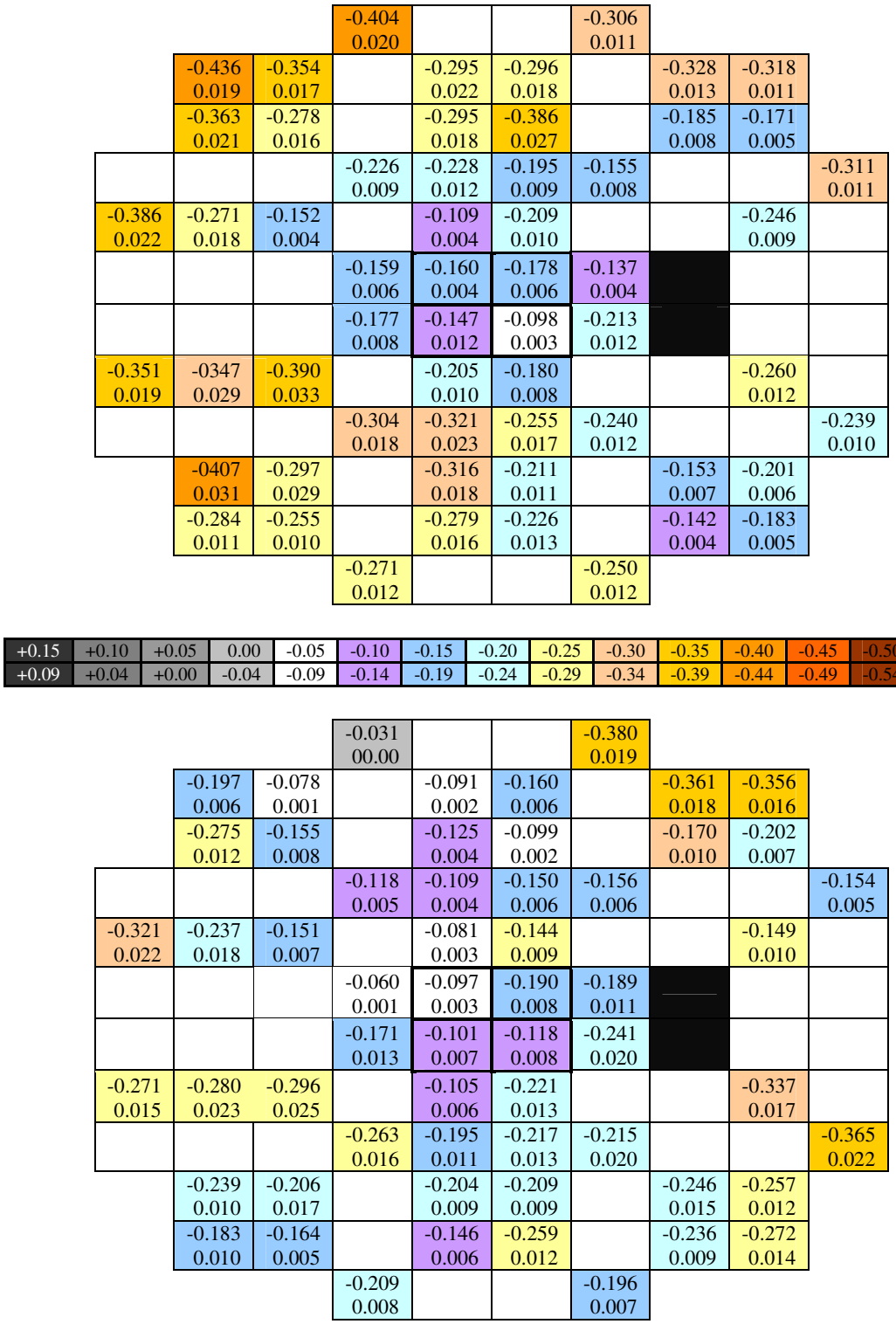

Figure 4.1 a The decline of the group MS_{CFF} (Hz per year) at each stimulus location with increase in age for the right eye (top) and left eye (bottom) of the 28 normal individuals at Visit Five for the TOP algorithm. The lower value at each location indicates the Coefficient of Determination (R^2). The stimulus locations for the left eye are displayed in right eye format in order to aid the between-eye comparison. The absence of values within a white cell corresponds to the absence of a stimulus location. The increasing 'warmth' of the colours represents an increasing steepening (i.e. negativity) of the slope.

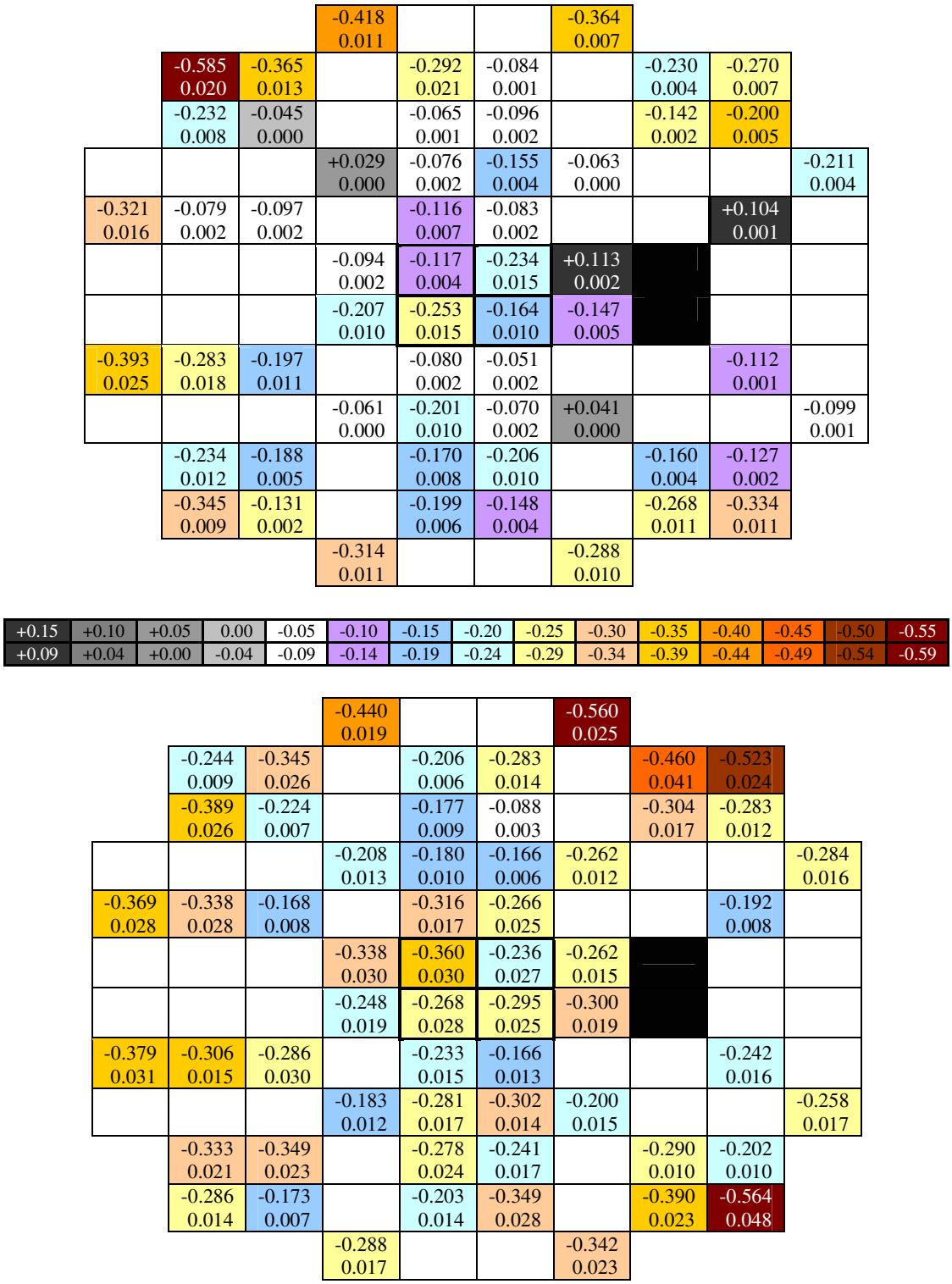

Figure 4.1 b The decline of the group MS_{CFF} (Hz per year) at each stimulus location with increase in age for the right eye (top) and left eye (bottom) eye of the 28 normal individuals at Visit Six for the Dynamic Algorithm. The lower value at each location indicates the Coefficient of Determination (R^2). The stimulus locations for the left eye are displayed in right eye format in order to aid the between-eye comparison. The absence of values within a white cell corresponds to the absence of a stimulus location. The increasing 'warmth' of the colours represents an increasing steepening (i.e. negativity) of the slope.

Mean Sensitivity (Hz)	Visit 1 TOP	Visit 2 TOP	Visit 3 TOP	Visit 4 TOP	Visit 5 TOP	Visit 6 Dynamic
Right Mean	34.58	35.10	34.82	35.00	34.71	38.21
SD	3.34	3.38	3.76	4.43	5.20	4.77
Left Mean	34.05	35.04	35.24	35.29	35.26	38.01
SD	5.46	3.39	4.09	4.32	4.38	4.44
Right Median	34.80	34.85	35.45	35.55	35.70	37.50
IQR	3.83	5.25	4.83	5.32	4.52	7.40
Left Median	34.75	35.70	36.20	36.10	36.15	37.95
IQR	5.85	4.15	3.62	4.33	5.08	7.25

Mean Sensitivity (Hz)	Visit 1 TOP	Visit 2 TOP	Visit 3 TOP	Visit 4 TOP	Visit 5 TOP	Visit 6 Dynamic
Right Mean	30.66	33.51	33.47	33.65	34.54	37.62
SD	6.04	6.34	6.68	6.95	7.57	8.18
Left Mean	32.35	33.88	34.47	34.19	33.83	37.27
SD	5.70	5.68	6.45	7.68	8.39	9.99
Right Median	32.25	35.65	35.35	37.00	36.75	39.55
IQR	3.85	1.65	2.48	3.55	1.50	4.25
Left Median	33.70	35.05	36.10	36.35	36.30	39.55
IQR	3.60	1.05	2.65	2.30	3.40	4.48

Mean Sensitivity (Hz)	Visit 1 TOP	Visit 2 TOP	Visit 3 TOP	Visit 4 TOP	Visit 5 TOP	Visit 6 Dynamic
Right Mean	27.5	30.28	30.33	30.61	31.12	35.07
SD	6.7	5.58	6.23	6.41	7.12	7.85
Left Mean	26.99	29.32	30.15	29.92	31.12	34.03
SD	7.19	7.00	7.14	7.07	6.89	7.13
Right Median	27.5	30.8	30.7	31.5	31.9	35.1
IQR	8.8	7.35	5.65	6.35	10.6	8.9
Left Median	24.3	27.6	29.4	30.6	32.2	32.7
IQR	9.75	8.85	8.4	9.2	8.1	7.65

Table 4.7 The summary statistics (mean, SD, median, IQR) of the MS_{CFF} (Hz) at each visit for the right eye and for the left eye for the 28 normal individuals (Top) for the 10 individuals with OHT (Middle) and for the 11 individuals with OAG (bottom).

Overleaf: Figure 4.2 The Box and Whisker plots of the distribution of the MS_{CFF} of each eye at each of the fifth visits using the TOP algorithm and at the sixth visit using the Dynamic algorithm for the 28 normal individuals (Top), the 10 individuals with OHT (Middle) and for the 11 individuals with OAG (Bottom). The median is represented by the bold line, the 25^{th} and 75^{th} percentiles by the lower and upper edges of the box, respectively, and the lowest and highest values by the lower and upper extremities of the whiskers, respectively. The results for the right eye over Visits One to Five are colour coded for the TOP algorithm in blue and in white for the left eye. The results at Visit Six for the Dynamic algorithm are coded in red for the right eye and in white for the left eye.

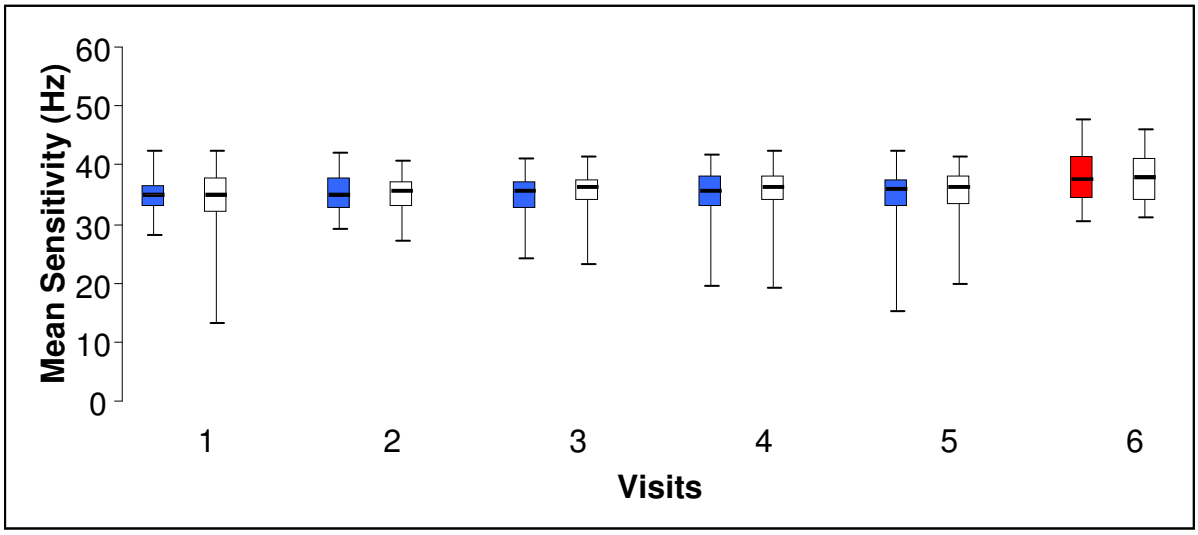
Mean Sensitivity (Hz)
60
50
40
30
20
10
0
1
2
3
4
5
6
Visits

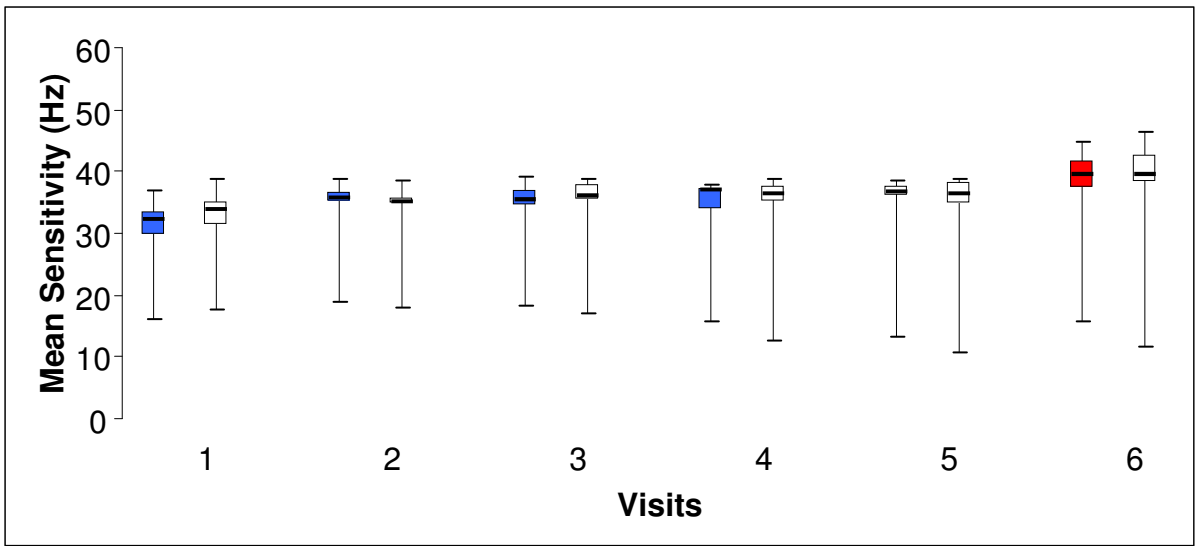
Mean Sensitivity (Hz)
60
50
40
30
20
10
0
1
2
3
4
5
6
Visits

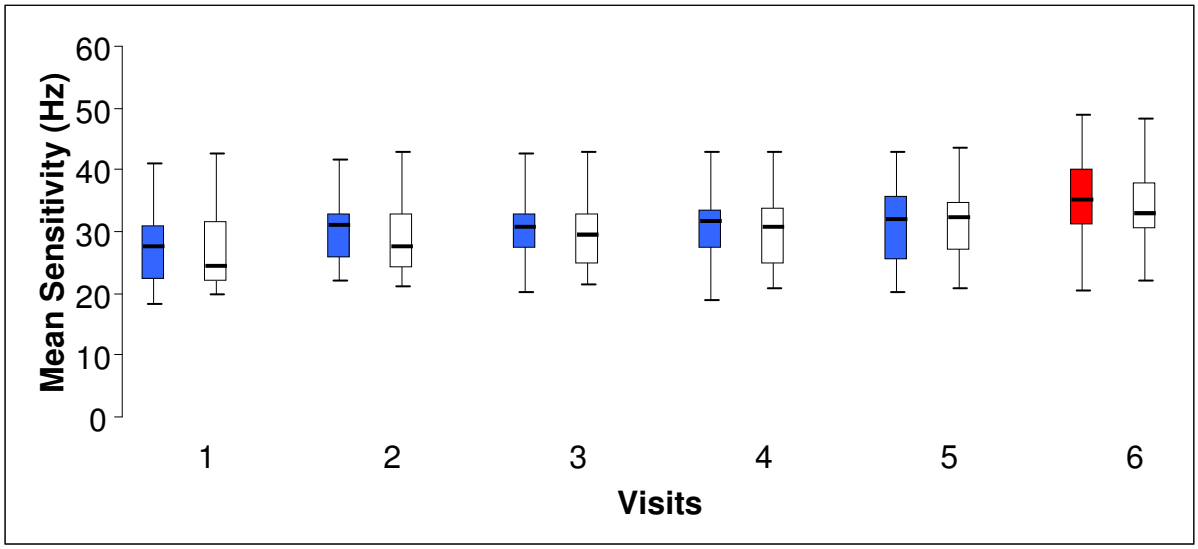
Mean Sensitivity (Hz)
60
50
40
30
20
10
0
1
2
3
4
5
6
Visits

The ANOVA summary table for the MS with the TOP algorithm over the five visits is given in Table 4.8. The group mean MS differed across the three groups (p=0.003) and, as would be expected, was lowest for the group with OAG. This difference was seemingly independent of age (p=0.120). As would also be expected, the group mean Mean Sensitivity declined with increase in age (p=0.003).

The group mean MS improved across the five visits (p<0.001). No difference in the magnitude of the improvement over the five visits could be detected across the three diagnostic groups (p=0.213), or with age (p=0.502).

Effect	Degrees of Freedom Numerator	Degrees of Freedom Denominator	F value	P value
Age	1	49	10.64	**0.002**
Gender	1	49	0.30	0.588
Diagnosis	2	49	6.65	**0.003**
Eye	1	441	0.10	0.750
Visit	4	441	5.53	**<0.001**

Effect	Degrees of Freedom Numerator	Degrees of Freedom Denominator	F value	P value
Age	1	49	10.64	**0.002**
Gender	1	49	0.30	0.588
Diagnosis	2	49	6.81	**0.003**
Visit	4	441	5.53	**<0.001**

Effect	Degrees of Freedom Numerator	Degrees of Freedom Denominator	F value	P value
Age	1	49	10.29	**0.003**
Diagnosis	2	49	6.65	**0.003**
Visit	4	441	5.53	**<0.001**
Age x Diagnosis	2	49	2.22	0.120
Age x Visit	4	441	0.84	0.502
Diagnosis x Visit	8	441	1.36	0.213

Table 4.8 The Analysis of Variance Summary Table for the MS_{CFF} index over the five visits.

The ANOVA summary table for the MS for the difference between the TOP algorithm at Visit Five and the Dynamic algorithm at Visit Six is given in Table 4.9. The group mean MS was higher for the Dynamic Algorithm ($p<0.001$).

Effect	Degrees of Freedom Numerator	Degrees of Freedom Denominator	F value	P value
Age	1	49	8.57	**0.005**
Gender	1	49	0.33	0.571
Diagnosis	2	49	2.39	0.102
Eye	1	147	0.12	0.719
Algorithm	1	147	90.14	**<0.001**

Effect	Degrees of Freedom Numerator	Degrees of Freedom Denominator	F value	P value
Age	1	49	8.57	**0.005**
Gender	1	49	0.33	0.571
Diagnosis	2	49	2.39	0.102
Algorithm	1	147	90.06	**<0.001**

Effect	Degrees of Freedom Numerator	Degrees of Freedom Denominator	F value	P value
Age	1	49	8.20	**0.006**
Diagnosis	2	49	2.21	0.120

Effect	Degrees of Freedom Numerator	Degrees of Freedom Denominator	F value	P value
Age	1	49	7.09	**0.011**
Algorithm	1	147	90.06	**<0.001**
Age x Algorithm	1	147	0.00	0.999

Effect	Degrees of Freedom Numerator	Degrees of Freedom Denominator	F value	P value
Algorithm	1	147	90.06	**<0.001**

Table 4.9 The Analysis of Variance Summary Table for the MS_{CFF} index between the TOP algorithm at Visit Five and the Dynamic algorithm at Visit Six.

4.12.4 Mean Defect

The summary statistics for the MD over the six visits are shown in Table 4.10 for each eye of the 28 normal individuals (Top), the 10 individuals with OHT (Middle) and the 11 individuals with OAG (Bottom). The distribution of the MD is also illustrated in terms of Box and Whisker plots for each eye of each of the three groups in Figure 4.3.

Mean Defect (Hz)	Visit 1 TOP	Visit 2 TOP	Visit 3 TOP	Visit 4 TOP	Visit 5 TOP	Visit 6 Dynamic
Right Mean	1.53	0.98	1.27	1.09	1.39	-2.12
SD	3.16	3.32	3.61	4.27	4.86	4.55
Left Mean	2.36	1.09	0.85	0.81	0.84	-1.88
SD	5.42	3.34	3.95	4.11	4.08	3.89
Right Median	1.4	0.7	0.95	0.3	0.8	-1.65
IQR	3.20	5.22	4.14	3.95	4.70	7.10
Left Median	1.85	0.55	-0.35	-0.05	-0.05	-2.95
IQR	5.19	4.45	4.32	2.97	3.67	5.64

Mean Defect (Hz)	Visit 1 TOP	Visit 2 TOP	Visit 3 TOP	Visit 4 TOP	Visit 5 TOP	Visit 6 Dynamic
Right Mean	4.79	1.95	1.97	1.8	0.91	-2.13
SD	5.68	6.28	6.61	6.84	7.36	8.30
Left Mean	3.08	1.57	0.97	1.25	1.59	-1.83
SD	5.39	5.50	6.40	7.48	8.24	10.04
Right Median	3.25	0.45	-0.45	-1.05	-1.5	-4.05
IQR	3.45	2.75	3.35	5.15	2.42	4.57
Left Median	2.4	0.5	-1.1	-1.2	-1.1	-4.5
IQR	3.7	2.1	3.37	1.92	4.2	6.45

Mean Defect (Hz)	Visit 1 TOP	Visit 2 TOP	Visit 3 TOP	Visit 4 TOP	Visit 5 TOP	Visit 6 Dynamic
Right Mean	8.54	5.81	5.69	5.4	5.04	0.97
SD	6.06	5.2	5.63	5.91	6.68	7.38
Left Mean	9.04	6.76	5.86	6.1	5.06	1.99
SD	6.41	6.39	6.59	6.59	6.34	6.56
Right Median	8.2	5.2	4.5	4.7	4.3	1.5
IQR	8.65	6.95	5.5	6.75	10.05	9.2
Left Median	11.4	8.9	5.9	5.1	4.7	2.6
IQR	8.25	8.85	7.85	9.55	8.95	7.1

Table 4.10 The summary statistics (mean, SD, median, IQR) of the MD_{CFF} (Hz) at each visit for the right eye and for the left eye for the 28 normal individuals (Top) for the 10 individuals with OHT (Middle) and for the 11 individuals with OAG (bottom).

Overleaf: Figure 4.3 The Box and Whisker plots of the distribution of the MD_{CFF} of each eye at each of the first Five Visits using the TOP algorithm and at the Sixth Visit using the Dynamic algorithm for the 28 normal individuals (top), the 10 individuals with OHT (middle) and the 11 individuals with OAG (bottom). The median is represented by the bold line, the 25^{th} and 75^{th} percentiles by the lower and upper edges of the box, respectively, and the lowest and highest values by the lower and upper extremities of the whiskers, respectively. The results for the right eye over Visits One to Five are colour coded for the TOP algorithm in blue and in white for the left eye. The results at Visit Six for the Dynamic algorithm are coded in red for the right eye and in white for the left eye.

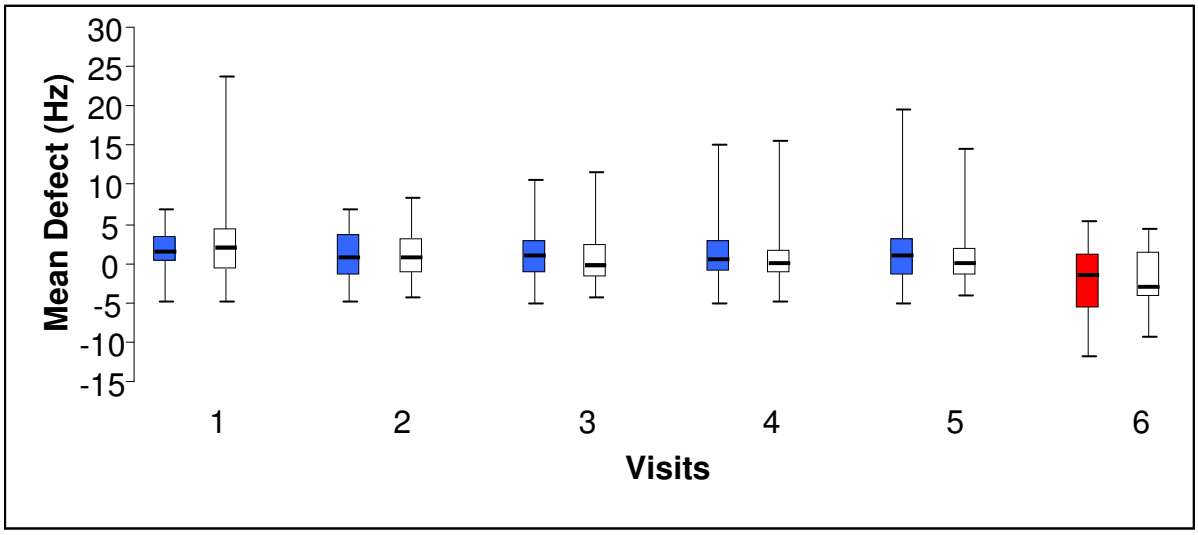
Mean Defect (Hz)
30
25
20
15
10
5
0
-5
-10
-15
1
2
3
4
5
6
Visits

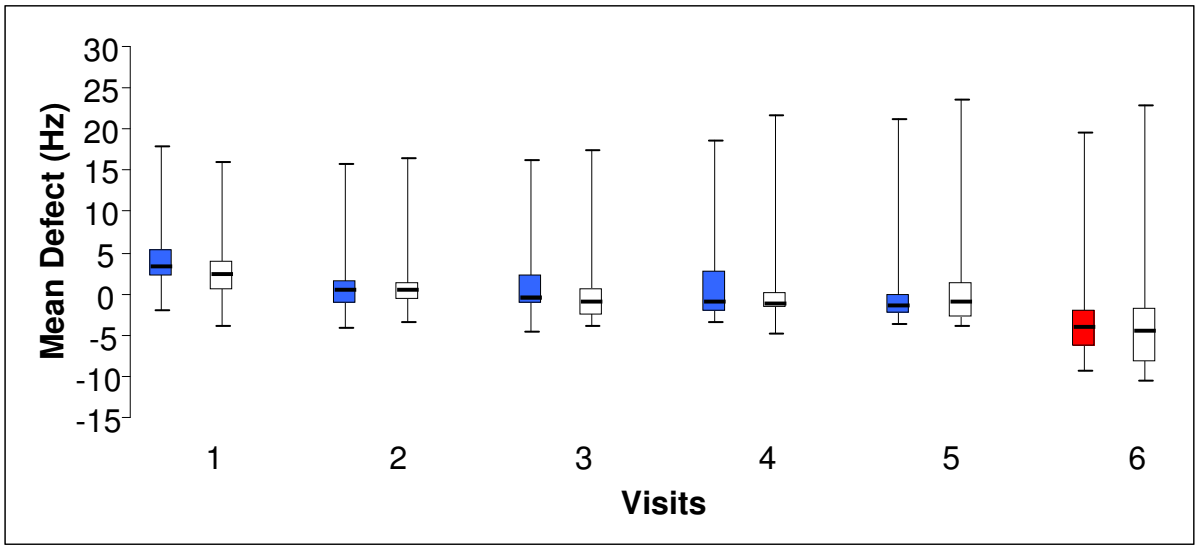
Mean Defect (Hz)
30
25
20
15
10
5
0
-5
-10
-15
1
2
3
4
5
6
Visits

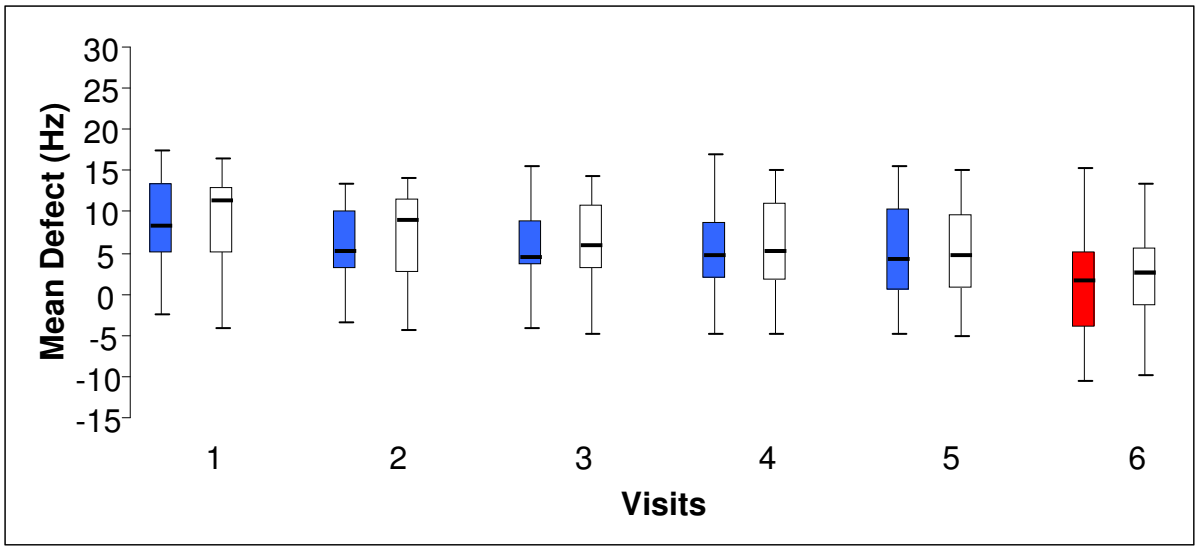
Mean Defect (Hz)
30
25
20
15
10
5
0
-5
-10
-15
1
2
3
4
5
6
Visits

The ANOVA summary table for the MD with the TOP algorithm over the five visits is given in Table 4.11. The group mean MD differed across the three groups (p=0.004) and, as would be expected, was worst for the group with OAG.

The group mean MD improved across the five visits (p<0.001). No difference in the magnitude of the improvement could be detected across the three diagnostic groups (p=0.312).

Effect	Degrees of Freedom Numerator	Degrees of Freedom Denominator	F value	P value
Age	1	49	2.10	0.153
Gender	1	49	0.29	0.593
Diagnosis	2	49	6.64	**0.003**
Eye	1	441	0.04	0.851
Visit	4	441	6.36	**<0.001**

Effect	Degrees of Freedom Numerator	Degrees of Freedom Denominator	F value	P value
Age	1	49	2.10	0.153
Gender	1	49	0.29	0.593
Diagnosis	2	49	6.64	**0.003**
Visit	4	441	6.36	**<0.001**

Effect	Degrees of Freedom Numerator	Degrees of Freedom Denominator	F value	P value
Age	1	49	1.91	0.174
Diagnosis	2	49	6.49	**0.003**
Visit	4	441	6.36	**<0.001**

Effect	Degrees of Freedom Numerator	Degrees of Freedom Denominator	F value	P value
Diagnosis	2	49	6.14	**0.004**
Visit	4	441	8.41	**<0.001**
Diagnosis x Visit	8	441	1.18	0.312

Table 4.11 The Analysis of Variance Summary Table for the MD_{CFF} index over the five visits.

The ANOVA summary table for the difference between the group mean MD for the TOP algorithm at Visit Five and the Dynamic algorithm at Visit Six is given in Table 4.12. The group mean MD was more negative (i.e. more normal) for the Dynamic algorithm (p<0.001).

Any difference in the magnitude of the group mean MD could not be detected across the three diagnostic groups (p=0.146).

Effect	Degrees of Freedom Numerator	Degrees of Freedom Denominator	F value	P value
Age	1	49	2.30	0.136
Gender	1	49	0.39	0.537
Diagnosis	2	49	2.46	0.096
Eye	1	147	0.15	0.701
Algorithm	1	147	91.42	**<0.001**

Effect	Degrees of Freedom Numerator	Degrees of Freedom Denominator	F value	P value
Age	1	49	2.30	0.136
Gender	1	49	0.39	0.537
Diagnosis	2	49	2.46	0.096
Algorithm	1	147	91.33	**<0.001**

Effect	Degrees of Freedom Numerator	Degrees of Freedom Denominator	F value	P value
Age	1	49	2.06	0.158
Diagnosis	2	49	2.26	0.116
Algorithm	1	147	91.33	**<0.001**

Effect	Degrees of Freedom Numerator	Degrees of Freedom Denominator	F value	P value
Diagnosis	2	49	2.00	0.146
Algorithm	1	147	91.33	**<0.001**

Effect	Degrees of Freedom Numerator	Degrees of Freedom Denominator	F value	P value
Algorithm	1	147	91.33	**<0.001**

Table 4.12 The Analysis of Variance Summary Table for the MD_{CFF} index between the TOP algorithm at Visit Five and the Dynamic algorithm at Visit Six.

4.12.5 Square root of the Loss Variance (sLV)

The summary statistics for the sLV over the six visits are shown in Table 4.13 for each eye of the 28 normal individuals (top), each eye for the 10 individuals with OHT (middle) and each eye for the 11 individuals with OAG (bottom). The distribution of the sLV is also illustrated in terms of Box and Whisker plots for each eye of each of the three groups in Figure 4.4.

Square root of Loss Variance (sLV) (Hz)	Visit 1 TOP	Visit 2 TOP	Visit 3 TOP	Visit 4 TOP	Visit 5 TOP	Visit 6 Dynamic
Right Mean	3.33	3.25	3.30	3.17	3.22	4.65
SD	1.38	1.35	1.17	1.50	1.40	1.34
Left Mean	3.20	3.28	3.19	3.30	3.27	4.15
SD	1.07	1.12	1.33	1.09	1.25	0.90
Right Median	3.06	2.92	3.15	2.91	2.81	4.33
IQR	1.13	1.21	1.31	1.61	1.49	1.61
Left Median	3.18	3.17	2.78	3.21	2.97	4.30
IQR	1.25	1.39	1.28	1.09	1.09	1.43

Square root of Loss Variance (sLV) (Hz)	Visit 1 TOP	Visit 2 TOP	Visit 3 TOP	Visit 4 TOP	Visit 5 TOP	Visit 6 Dynamic
Right Mean	3.81	3.32	3.73	3.63	3.41	5.65
SD	2.49	2.17	2.75	2.49	2.23	2.2
Left Mean	3.91	3.84	3.43	3.4	3.29	5.4
SD	1.74	1.5	2.22	2.23	1.80	1.97
Right Median	3.20	3.01	2.92	2.78	3.02	5.42
IQR	1.35	1.4	2.29	1.59	0.89	1.15
Left Median	3.32	3.37	2.59	2.99	2.81	5.06
IQR	1.96	1.34	0.83	0.56	1.31	0.75

Square root of Loss Variance (sLV) (Hz)	Visit 1 TOP	Visit 2 TOP	Visit 3 TOP	Visit 4 TOP	Visit 5 TOP	Visit 6 Dynamic
Right Mean	6.39	6.7	6.35	6.97	6.59	8.06
SD	3.15	3.85	3.44	3.81	4.03	3.65
Left Mean	6.38	6.36	6.16	6.16	6.31	8.23
SD	3.74	3.64	3.57	3.72	4.19	4.07
Right Median	5.91	7.54	5.29	7.54	6.21	7.16
IQR	4.53	5.49	5.31	6.25	7.02	5.81
Left Median	5.00	4.96	5.86	5.21	5.12	7.00
IQR	6.60	5.79	6.09	6.50	6.99	7.94

Table 4.13 The summary statistics (mean, SD, median, IQR) of the sLV_{CFF} (Hz) at each visit for the right eye and for the left eye for the 28 normal individuals (Top) for the 10 individuals with OHT (Middle) and for the 11 individuals with OAG (bottom).

Overleaf: Figure 4.4 The Box and Whisker plots of the distribution of the sLV_{CFF} for each eye at each of the first Five Visits using the TOP algorithm and at the Sixth Visit using the Dynamic algorithm for the 28 normal individuals (top), for the 10 individuals with OHT (middle) and for the 11 individuals with OAG (bottom). The median is represented by the bold line, the 25^{th} and 75^{th} percentiles by the lower and upper edges of the box, respectively, and the lowest and highest values by the lower and upper extremities of the whiskers, respectively. The results for the right eye over Visits One to Five are colour coded for the TOP algorithm in blue and in white for the left eye. The results at Visit Six for the Dynamic algorithm are coded in red for the right eye and in white for the left eye.

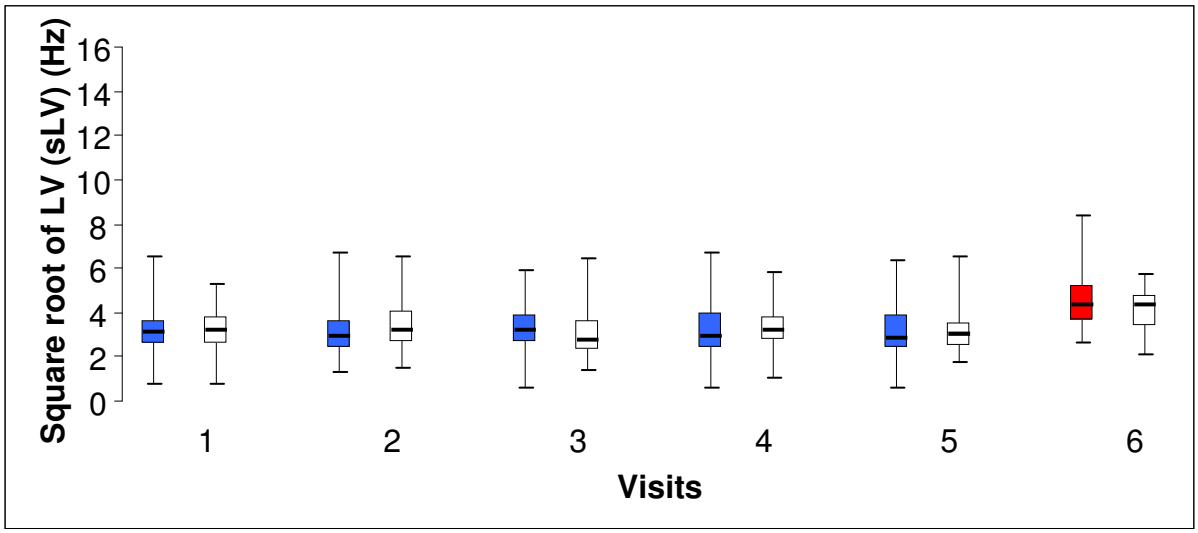
Square root of LV (sLV) (Hz)
16
14
12
10
8
6
4
2
0
1
2
3
4
5
6
Visits

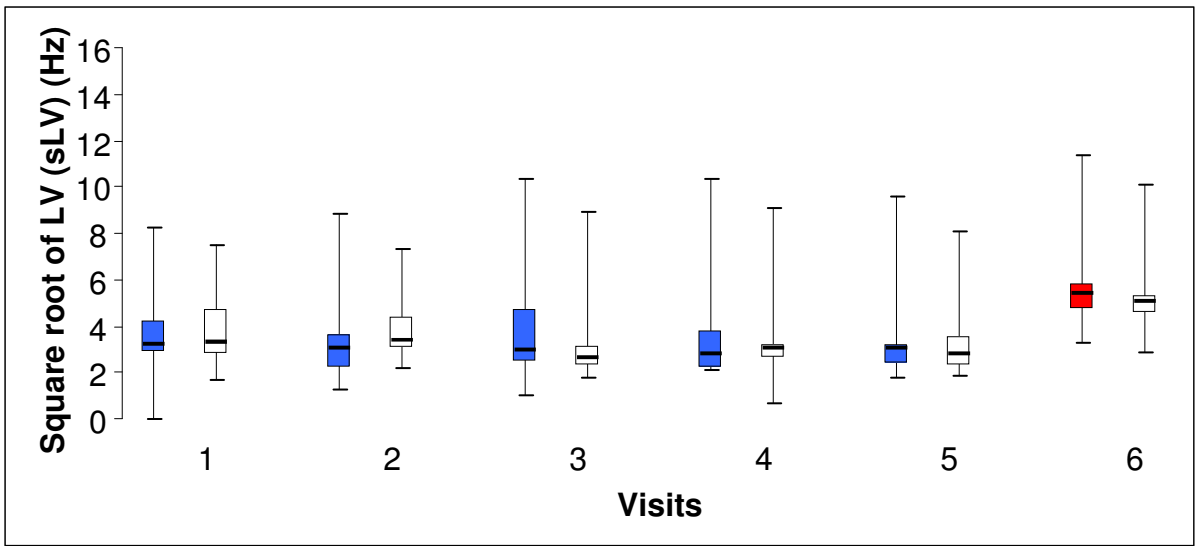
Square root of LV (sLV) (Hz)
16
14
12
10
8
6
4
2
0
1
2
3
4
5
6
Visits

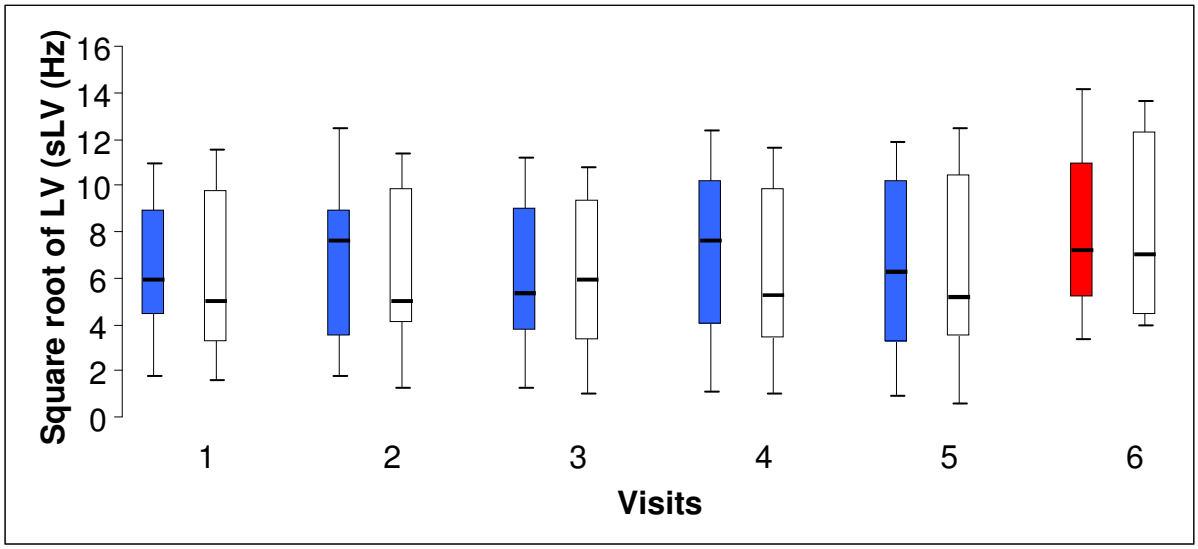
Square root of LV (sLV (Hz)
16
14
12
10
8
6
4
2
0
1
2
3
4
5
6
Visits

The ANOVA summary table for the sLV with the TOP algorithm over the five visits is given in Table 4.14. The group mean of the sLV differed across the three groups ($p<0.001$) and, as would be expected, was largest for the group with OAG. It increased with age ($p=0.041$)

The group mean of the sLV remained the same across the five visits ($p=0.976$).

Effect	Degrees of Freedom Numerator	Degrees of Freedom Denominator	F value	P value
Age	1	49	5.02	**0.030**
Gender	1	49	0.99	0.325
Diagnosis	2	49	15.24	**<0.001**
Eye	1	441	0.45	0.501
Visit	4	441	0.12	0.976

Effect	Degrees of Freedom Numerator	Degrees of Freedom Denominator	F value	P value
Age	1	49	5.02	**0.030**
Gender	1	49	0.99	0.325
Diagnosis	2	49	15.24	**<0.001**
Eye	1	441	0.45	0.501

Effect	Degrees of Freedom Numerator	Degrees of Freedom Denominator	F value	P value
Age	1	49	5.02	**0.030**
Gender	1	49	0.99	0.325
Diagnosis	2	49	15.24	**<0.001**

Effect	Degrees of Freedom Numerator	Degrees of Freedom Denominator	F value	P value
Age	1	49	4.39	**0.041**
Diagnosis	2	49	14.48	**<0.001**
Age x Diagnosis	2	49	1.58	0.217

Table 4.14 The Analysis of Variance Summary Table for the sLV_{CFF} index over the five visits.

.

The ANOVA summary table for the group mean of the sLV between the TOP algorithm at Visit Five and the Dynamic algorithm at Visit Six is given in Table 4.15.

The group mean of the sLV increased with increase in age (p=0.011), As would be expected, it varied across the groups (p<0.001) being largest for the group with OAG. It was lager for the Dynamic algorithm (p<0.001) and the difference between the two algorithms was seemingly independent of age (p=0.190) and of diagnosis (p=0.098).

Effect	Degrees of Freedom Numerator	Degrees of Freedom Denominator	F value	P value
Age	1	49	7.76	**0.008**
Gender	1	49	1.00	0.322
Diagnosis	2	49	16.46	**<0.001**
Eye	1	147	0.83	0.364
Algorithm	1	147	58.99	**<0.001**

Effect	Degrees of Freedom Numerator	Degrees of Freedom Denominator	F value	P value
Age	1	49	7.76	**0.008**
Gender	1	49	1.00	0.322
Diagnosis	2	49	16.46	**<0.001**
Algorithm	1	147	58.66	**<0.001**

Effect	Degrees of Freedom Numerator	Degrees of Freedom Denominator	F value	P value
Age	1	49	6.96	**0.011**
Diagnosis	2	49	15.67	**<0.001**
Algorithm	1	147	58.66	**<0.001**
Age x Diagnosis	2	49	1.06	0.354
Age x Algorithm	1	147	1.73	0.190
Diagnosis x Algorithm	2	147	2.36	0.098

Table 4.15 The Analysis of Variance Summary Table for the sLV_{CFF} index between the TOP algorithm at Visit Five and the Dynamic algorithm at Visit Six.

4.12.6 Diffuse Defect

The summary statistics for the DD over the six visits are shown in Table 4.16 for each eye of the 28 normal individuals (Top), each eye for the 10 individuals with OHT (Middle) and each eye for the 11 individuals with OAG (Bottom). The distribution of the DD is also illustrated in terms of Box and Whisker plots for each eye of each of the three groups in Figure 4.5.

Diffuse Defect (Hz)	Visit 1 TOP	Visit 2 TOP	Visit 3 TOP	Visit 4 TOP	Visit 5 TOP	Visit 6 Dynamic
Right Mean	1.13	0.50	0.80	0.77	1.07	-3.15
SD	2.66	2.49	2.81	3.44	4.23	4.56
Left Mean	1.63	0.82	0.50	0.43	0.47	2.59
SD	5.02	3.03	2.97	3.55	3.20	4.09
Right Median	0.90	0.55	0.30	-0.25	0.50	-2.45
IQR	4.09	3.52	3.49	3.85	4.20	5.87
Left Median	0.40	0.50	-0.20	0.50	0.60	-3.60
IQR	4.02	4.90	2.77	2.67	3.17	5.52

Diffuse Defect (Hz)	Visit 1 TOP	Visit 2 TOP	Visit 3 TOP	Visit 4 TOP	Visit 5 TOP	Visit 6 Dynamic
Right Mean	3.17	1.27	0.93	0.81	-0.03	-4.41
SD	4.45	4.34	3.99	3.87	4.67	6.55
Left Mean	2.33	0.49	-0.11	0.2	1.15	-3.92
SD	4.36	4.24	3.88	4.73	6.64	8.55
Right Median	2.2	-0.2	-0.35	-0.95	-1.6	-5.85
IQR	4.42	2.04	3.02	5.04	1.6	5.25
Left Median	1.85	-0.85	-1.2	-1.35	-1.0	-4.55
IQR	4.49	2.22	2.35	1.33	3.94	7.4

Diffuse Defect (Hz)	Visit 1 TOP	Visit 2 TOP	Visit 3 TOP	Visit 4 TOP	Visit 5 TOP	Visit 6 Dynamic
Right Mean	5.49	2.31	2.7	2.15	1.53	-2.44
SD	4.45	3.06	3.89	3.91	4.17	6.01
Left Mean	5.82	3.28	2.7	3.13	1.78	1.86
SD	4.4	4.01	4.02	3.86	3.57	4.6
Right Median	6.1	1.9	2.9	1.1	1.0	-1.4
IQR	4.65	1.95	5.0	3.1	4.05	7.75
Left Median	6.3	3.8	3.3	4.0	0.7	-2.7
IQR	5.35	5.4	5.75	5.05	4.25	3.7

Table 4.16 The summary statistics (mean, SD, median, IQR) of the DD_{CFF} (Hz) at each visit for the right eye and for the left eye for the 28 normal individuals (Top) for the 10 individuals with OHT (Middle) and for the 11 individuals with OAG.

Overleaf: Figure 4.5 The Box and Whisker plots of the distribution of the DD_{CFF} of each eye at each of the first Five Visits using the TOP algorithm and at the Sixth Visit using the Dynamic algorithm for the 28 normal individuals (top), the 10 individuals with OHT (middle) and the 11 individuals with OAG (bottom). The median is represented by the bold line, the 25^{th} and 75^{th} percentiles by the lower and upper edges of the box, respectively, and the lowest and highest values by the lower and upper extremities of the whiskers, respectively. The results for the right eye over Visits One to Five are colour coded for the TOP algorithm in blue and in white for the left eye. The results at Visit Six for the Dynamic algorithm are coded in red for the right eye and in white for the left eye.

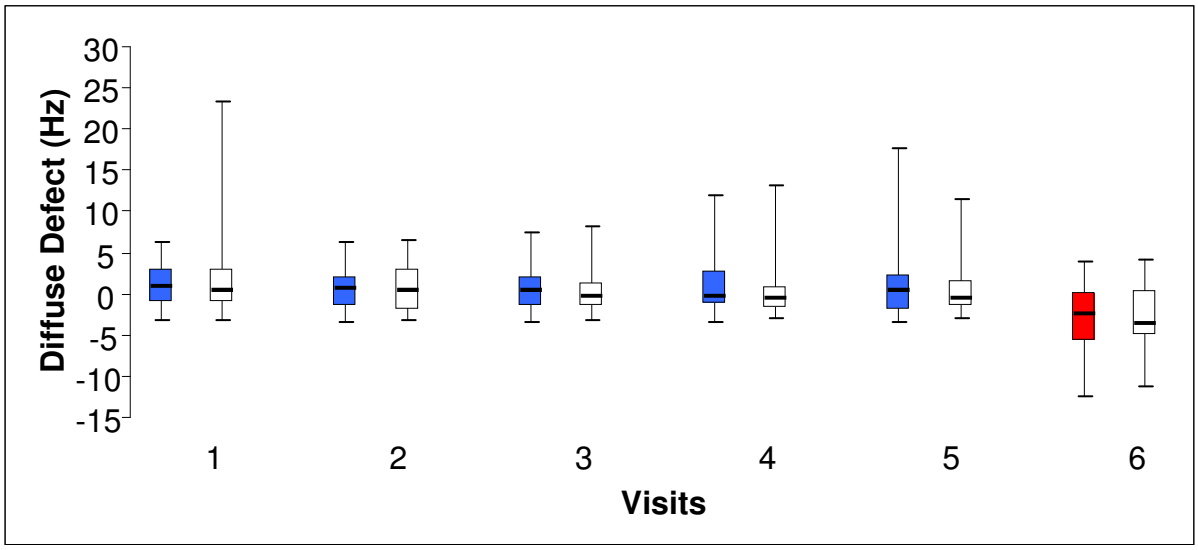
Diffuse Defect (Hz)
30
25
20
15
10
5
0
-5
-10
-15
1
2
3
4
5
6
Visits

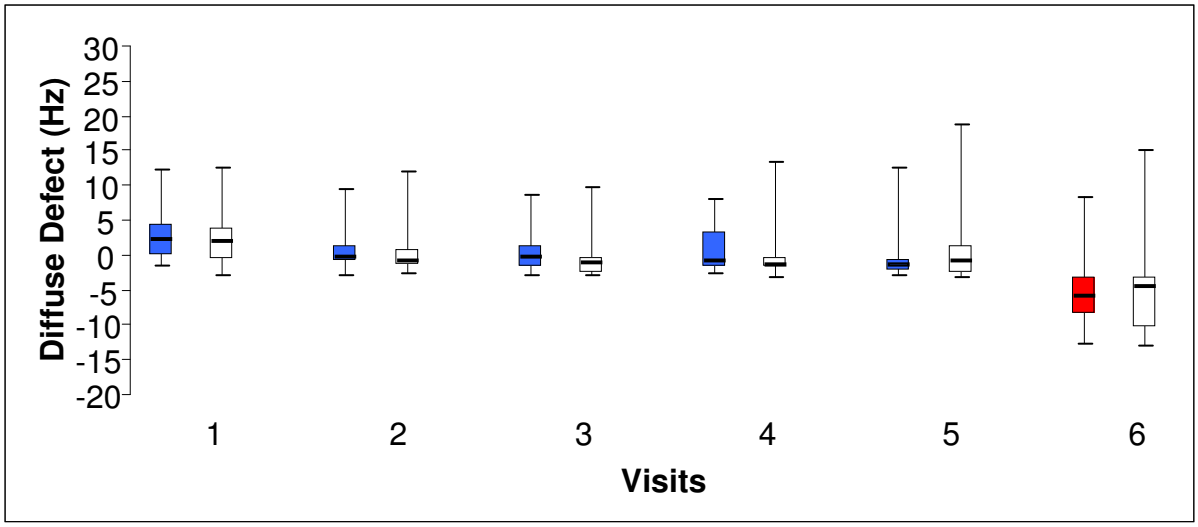
Diffuse Defect (Hz)
30
25
20
15
10
5
0
-5
-10
-15
-20
1
2
3
4
5
6
Visits

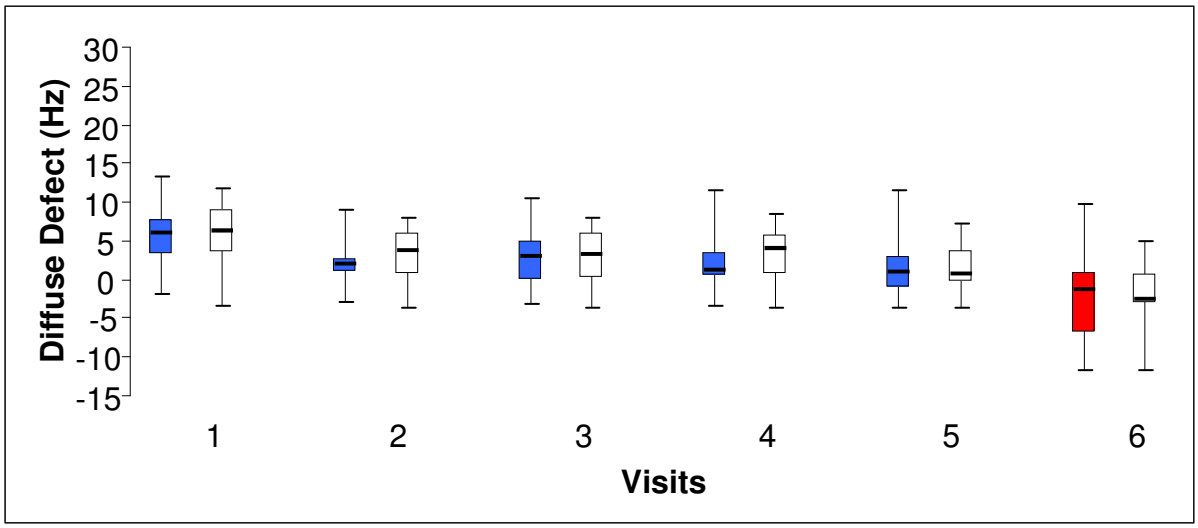
Diffuse Defect (Hz)
30
25
20
15
10
5
0
-5
-10
-15
1
2
3
4
5
6
Visits

The ANOVA summary table for the mean DD with the TOP algorithm over the five visits is given in Table 4.17. The difference in the group mean DD across the three groups exhibited marginal significance (p=0.077). The group mean DD improved across the five visits (p<0.001). The improvement varied across the three groups (p=0.041) and was greatest for the group with OAG.

Effect	Degrees of Freedom Numerator	Degrees of Freedom Denominator	F value	P value
Age	1	49	0.52	0.476
Gender	1	49	0.01	0.939
Diagnosis	2	49	2.62	0.083
Eye	1	441	0.01	0.930
Visit	4	441	7.38	**<0.001**

Effect	Degrees of Freedom Numerator	Degrees of Freedom Denominator	F value	P value
Age	1	49	0.54	0.464
Diagnosis	2	49	2.79	0.071
Eye	1	441	0.01	0.930
Visit	4	441	7.38	**<0.001**

Effect	Degrees of Freedom Numerator	Degrees of Freedom Denominator	F value	P value
Age	1	49	0.54	0.464
Diagnosis	2	49	2.79	0.071
Visit	4	441	7.38	**<0.001**

Effect	Degrees of Freedom Numerator	Degrees of Freedom Denominator	F value	P value
Diagnosis	2	49	2.71	0.077
Visit	4	441	7.38	**<0.001**
Diagnosis x Visit	8	441	2.04	**0.041**

Table 4.17 The Analysis of Variance Summary Table for the DD_{CFF} index over the five visits.

The ANOVA summary table for the group mean DD for the difference between the TOP algorithm at Visit Five and the Dynamic algorithm at Visit Six is given in Table 4.18. The group

mean for the DD was independent of age (p=0.459), was similar between the two eyes (p=0.429). Any difference in magnitude of the group mean DD across the three diagnostic groups could not be detected (p=0.429). It was higher for the Dynamic algorithm (p<0.001).

Effect	Degrees of Freedom Numerator	Degrees of Freedom Denominator	F value	P value
Age	1	49	0.88	0.353
Gender	1	49	0.02	0.900
Diagnosis	2	49	0.50	0.608
Eye	1	147	0.63	0.429
Algorithm	1	147	152.14	**<0.001**

Effect	Degrees of Freedom Numerator	Degrees of Freedom Denominator	F value	P value
Age	1	49	0.86	0.357
Diagnosis	2	49	0.63	0.429
Eye	1	147	0.50	0.610
Algorithm	1	147	152.14	**<0.001**

Effect	Degrees of Freedom Numerator	Degrees of Freedom Denominator	F value	P value
Age	1	49	0.56	0.459
Eye	1	147	0.63	0.429
Algorithm	1	147	152.14	**<0.001**

Effect	Degrees of Freedom Numerator	Degrees of Freedom Denominator	F value	P value
Eye	1	147	0.63	0.429
Algorithm	1	147	152.14	**<0.001**

Effect	Degrees of Freedom Numerator	Degrees of Freedom Denominator	F value	P value
Algorithm	1	147	151.49	**<0.001**

Table 4.18 The Analysis of Variance Summary Table for the DD_{CFF} index between the TOP algorithm at Visit Five and the Dynamic algorithm at Visit Six.

4.12.7 Local Defect

The summary statistics for the LD over the six visits are shown in Table 4.19 for each eye of the 28 normal individuals (Top) each eye for the 10 individuals with OHT (Middle) and each eye for the 11 individuals with OAG (Bottom). The distribution of the LD is also illustrated in terms of Box and Whisker plots for each eye of each of the three groups in Figure 4.6.

Local Defect (Hz)	Visit 1 TOP	Visit 2 TOP	Visit 3 TOP	Visit 4 TOP	Visit 5 TOP	Visit 6 Dynamic
Right Mean	0.41	0.43	0.32	0.39	0.35	0.89
SD	0.78	0.86	0.68	0.84	0.68	0.99
Left Mean	0.30	0.32	0.41	0.28	0.41	0.48
SD	0.47	0.80	0.83	0.51	0.92	0.53
Right Median	0.00	0.00	0.00	0.00	0.00	0.70
IQR	0.30	0.60	0.22	0.30	0.20	1.15
Left Median	0.05	0.00	0.00	0.05	0.00	0.35
IQR	0.42	0.25	0.20	0.32	0.10	0.82

Local Defect (Hz)	Visit 1 TOP	Visit 2 TOP	Visit 3 TOP	Visit 4 TOP	Visit 5 TOP	Visit 6 Dynamic
Right Mean	1.42	0.77	1.38	1.37	1.05	2.74
SD	2.81	2.4	3.33	3.82	3.32	3.6
Left Mean	0.68	0.73	1.1	1.16	0.67	2.06
SD	1.3	1.42	2.71	3.2	2.04	3.13
Right Median	0.10	0.00	0.00	0.00	0.00	1.75
IQR	0.32	0.00	0.80	0.22	0.00	1.30
Left Median	0.10	0.00	0.00	0.00	0.00	0.90
IQR	0.57	0.80	0.00	0.00	0.07	1.72

Local Defect (Hz)	Visit 1 TOP	Visit 2 TOP	Visit 3 TOP	Visit 4 TOP	Visit 5 TOP	Visit 6 Dynamic
Right Mean	3.25	3.80	3.04	3.54	3.74	3.64
SD	3.25	4.25	3.09	3.67	4.15	3.09
Left Mean	3.53	3.62	3.69	3.28	3.54	4.06
SD	3.9	3.84	3.42	3.7	4.24	4.12
Right Median	2.50	2.30	3.00	2.80	2.40	2.90
IQR	5.05	6.05	5.45	6.70	6.55	5.50
Left Median	1.40	1.60	3.20	1.10	0.90	2.10
IQR	6.90	6.30	5.10	6.55	8.05	7.05

Table 4.19 The summary statistics (mean, SD, median, IQR) of the LD_{CFF} (Hz) at each visit for the right eye and for the left eye for the 28 normal individuals (Top) for the 10 individuals with OHT (Middle) and for the 11 individuals with OAG (bottom).

Overleaf: Figure 4.6 The Box and Whisker plots of the distribution of the LD_{CFF} of each eye at each of the first Five Visits using the TOP algorithm and at the Sixth Visit using the Dynamic algorithm for the 28 normal individuals (top), the 10 individuals with OHT (middle) and the 11 individuals with OAG (bottom). The median is represented by the bold line, the 25^{th} and 75^{th} percentiles by the lower and upper edges of the box, respectively, and the lowest and highest values by the lower and upper extremities of the whiskers, respectively. The results for the right eye over Visits One to Five are colour coded for the TOP algorithm in blue and in white for the left eye. The results at Visit Six for the Dynamic algorithm are coded in red for the right eye and in white for the left eye.

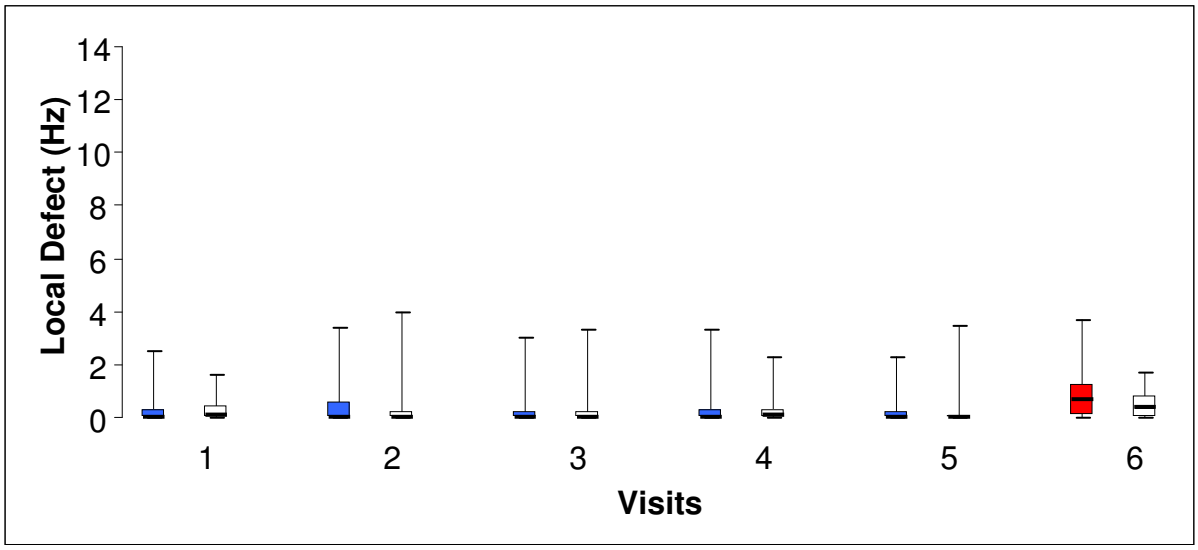
Local Defect (Hz)
14
12
10
8
6
4
2
0
1
2
3
4
5
6
Visits

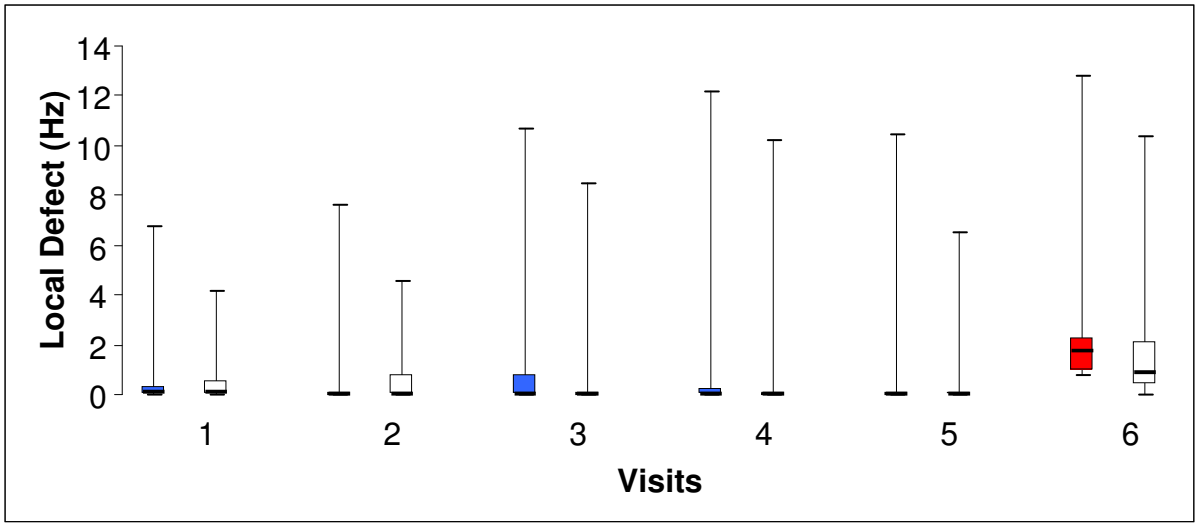
Local Defect (Hz)
14
12
10
8
6
4
2
0
1
2
3
4
5
6
Visits

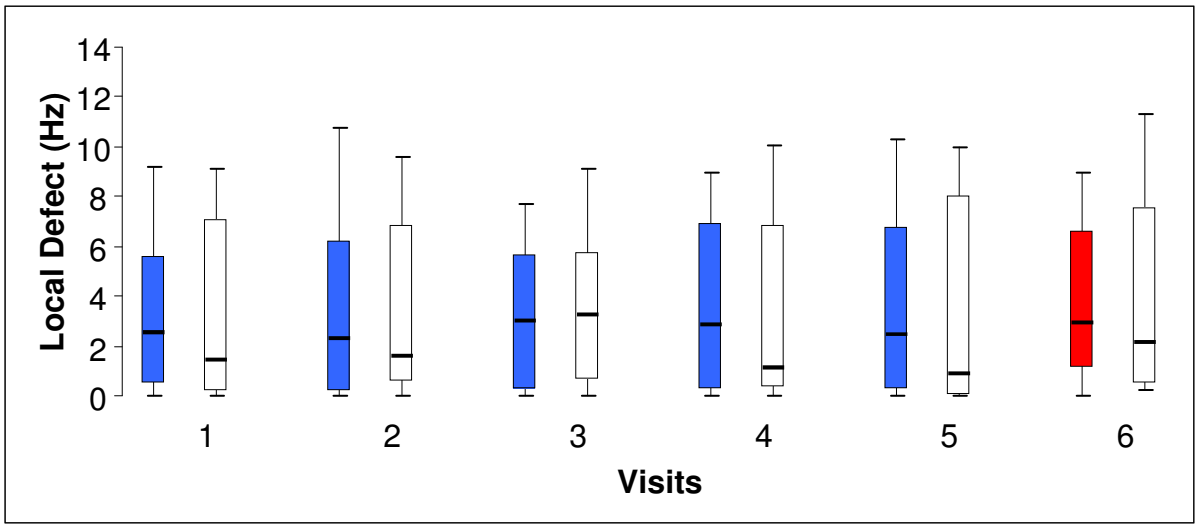
Local Defect (Hz)
14
12
10
8
6
4
2
0
1
2
3
4
5
6
Visits

The ANOVA summary table for the LD with the TOP algorithm over the five visits is given in Table 4.20. The group mean LD differed across the three groups ($p<0.001$) and, as would be expected, was worst for the group with OAG. The group mean LD did not improve across the five visits ($p=0.999$).

Effect	Degrees of Freedom Numerator	Degrees of Freedom Denominator	F value	P value
Age	1	49	3.74	**0.059**
Gender	1	49	1.05	0.311
Diagnosis	2	49	13.99	**<0.001**
Eye	1	441	0.36	0.551
Visit	4	441	0.02	0.999

Effect	Degrees of Freedom Numerator	Degrees of Freedom Denominator	F value	P value
Age	1	49	3.74	**0.059**
Gender	1	49	1.05	0.311
Diagnosis	2	49	13.99	**<0.001**
Eye	1	441	0.36	0.551

Effect	Degrees of Freedom Numerator	Degrees of Freedom Denominator	F value	P value
Age	1	49	3.74	**0.059**
Gender	1	49	1.05	0.311
Diagnosis	2	49	13.99	**<0.001**

Effect	Degrees of Freedom Numerator	Degrees of Freedom Denominator	F value	P value
Age	1	49	3.18	0.081
Diagnosis	2	49	13.18	**<0.001**
Age x Diagnosis	2	49	1.24	0.299

Table 4.20 The Analysis of Variance Summary Table for the LD_{CFF} over the five visits.
.

The ANOVA summary table for the difference between the group mean LD for the TOP algorithm at Visit Five and the Dynamic algorithm at Visit Six is given in Table 4.21. As would be expected, the group mean LD varied across the groups ($p<0.001$) being largest for the group with OAG. It was larger for the Dynamic algorithm ($p=0.004$). The increase in the group mean

LD with increase in age almost reached statistical significance (p=0.055); however, the magnitude of the increase with age was different between the two algorithms (p=0.009).

Effect	Degrees of Freedom Numerator	Degrees of Freedom Denominator	F value	P value
Age	1	49	4.63	**0.036**
Gender	1	49	1.44	0.237
Diagnosis	2	49	11.90	**<0.001**
Eye	1	147	0.92	0.338
Algorithm	1	147	8.69	**0.004**

Effect	Degrees of Freedom Numerator	Degrees of Freedom Denominator	F value	P value
Age	1	49	4.63	**0.036**
Gender	1	49	1.44	0.237
Diagnosis	2	49	11.90	**<0.001**
Algorithm	1	147	8.63	**0.004**

Effect	Degrees of Freedom Numerator	Degrees of Freedom Denominator	F value	P value
Age	1	49	3.86	**0.055**
Diagnosis	2	49	10.90	**<0.001**
Algorithm	1	147	8.63	**0.004**
Age x Diagnosis	2	49	1.45	0.244
Age x Algorithm	1	147	2.95	**0.009**
Diagnosis x Algorithm	2	147	3.48	**0.033**

Effect	Degrees of Freedom Numerator	Degrees of Freedom Denominator	F value	P value
Algorithm	1	147	8.63	**0.004**

Table 4.21 The Analysis of Variance Summary Table for the LD_{CFF} index between the TOP algorithm at Visit Five and the Dynamic algorithm at Visit Six.

4.12.8 Examination Duration

The summary statistics for the examination duration over the six visits are shown in Table 4.22 for each eye of the 28 normal individuals (Top), for each eye of the 10 individuals with OHT (Middle) and for each eye of the 11 individuals with OAG glaucoma (Bottom). The distribution

of the examination duration is also illustrated in terms of Box and Whisker plots for each eye of each of the three groups in Figure 4.7.

Examination Duration (Seconds)	Visit 1 TOP	Visit 2 TOP	Visit 3 TOP	Visit 4 TOP	Visit 5 TOP	Visit 6 Dynamic
Right Mean	339	272	210	233	250	905
SD	144	108	60	63	104	302
Left Mean	264	246	247	247	223	814
SD	97	102	130	103	51	224
Right Median/	301	227	205	218	208	851
IQR	150	93	25	46	57	446
Left Median/	241	220	204	208	207	751
IQR	74	54	65	50	46	321

Examination Duration (Seconds)	Visit 1 TOP	Visit 2 TOP	Visit 3 TOP	Visit 4 TOP	Visit 5 TOP	Visit 6 Dynamic
Right Mean	309	245	252	233	237	803
SD	99	95	44	81	129	189
Left Mean	253	236	207	225	231	920
SD	114	100	40	112	129	312
Right Median	286	209	263	210	198	759
IQR	120	40	64	37	41	178
Left Median	226	204	197	186	189	810
IQR	28	46	28	29	43	438

Examination Duration (Seconds)	Visit 1 TOP	Visit 2 TOP	Visit 3 TOP	Visit 4 TOP	Visit 5 TOP	Visit 6 Dynamic
Right Mean	242	234	248	227	223	932
SD	31	36	67	32	49	416
Left Mean	263	227	209	229	214	766
SD	66	46	33	48	35	202
Right Median	244	231	222	216	203	801
IQR	20	60	77	30	52	374
Left Median	241	216	203	207	210	733
IQR	81	63	27	54	42	179

Table 4.22 The summary statistics (mean, SD, median, IQR) of the examination duration (Seconds) at each visit for the right eye and for the left eye for the 28 normal individuals (Top) for the 10 individuals with OHT (Middle) and for the 11 individuals with OAG (bottom).

Overleaf: Figure 4.7 The Box and Whisker plots of the distribution of the examination duration of each eye at each of the first Five Visits using the TOP algorithm and at the Sixth Visit using the Dynamic algorithm for the 28 normal individuals (top), the 10 individuals with OHT (middle) and the 11 individuals with OAG (bottom). The median is represented by the bold line, the 25^{th} and 75^{th} percentiles by the lower and upper edges of the box, respectively, and the lowest and highest values by the lower and upper extremities of the whiskers, respectively. The results for the right eye over Visits One to Five are colour coded for the TOP algorithm in blue and in white for the left eye. The results at Visit Six for the Dynamic algorithm are coded in red for the right eye and in white for the left eye.

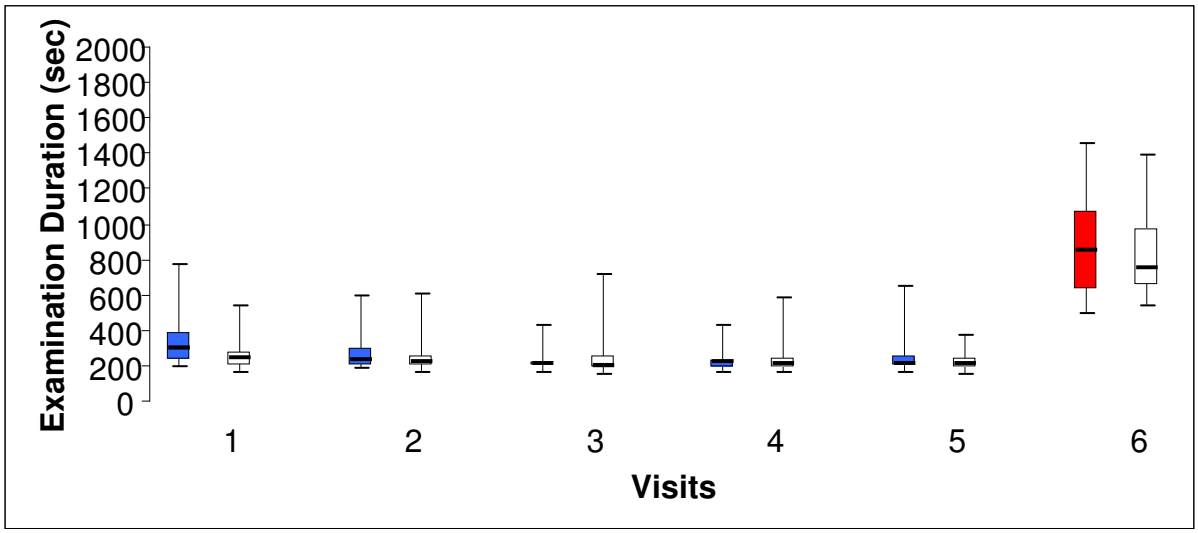
Examination Duration (sec)
2000
1800
1600
1400
1200
1000
800
600
400
200
0
1
2
3
4
5
6
Visits

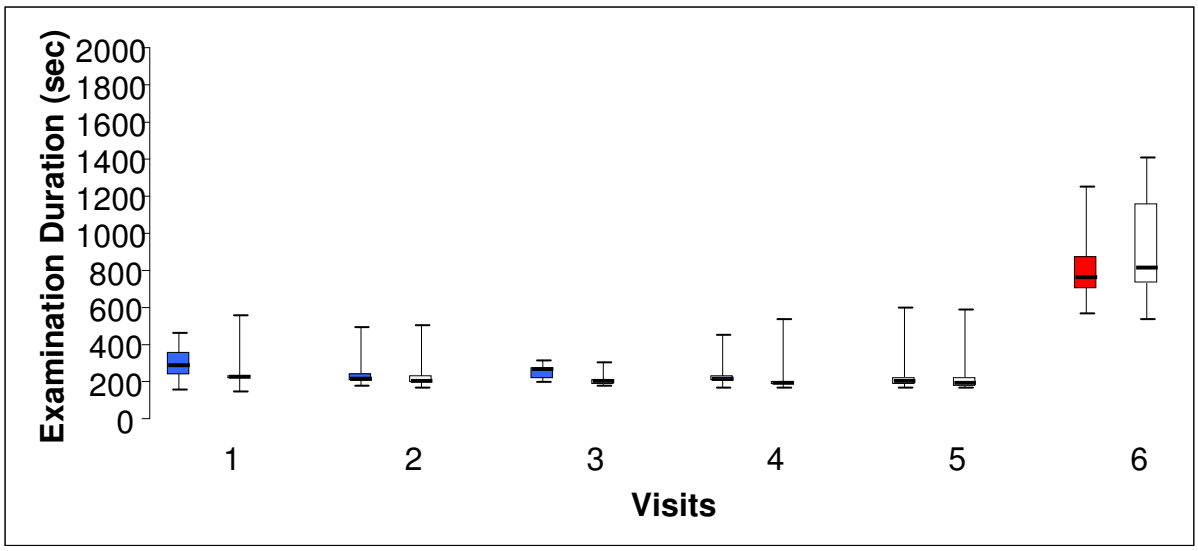
Examination Duration (sec)
2000
1800
1600
1400
1200
1000
800
600
400
200
0
1
2
3
4
5
6
Visits

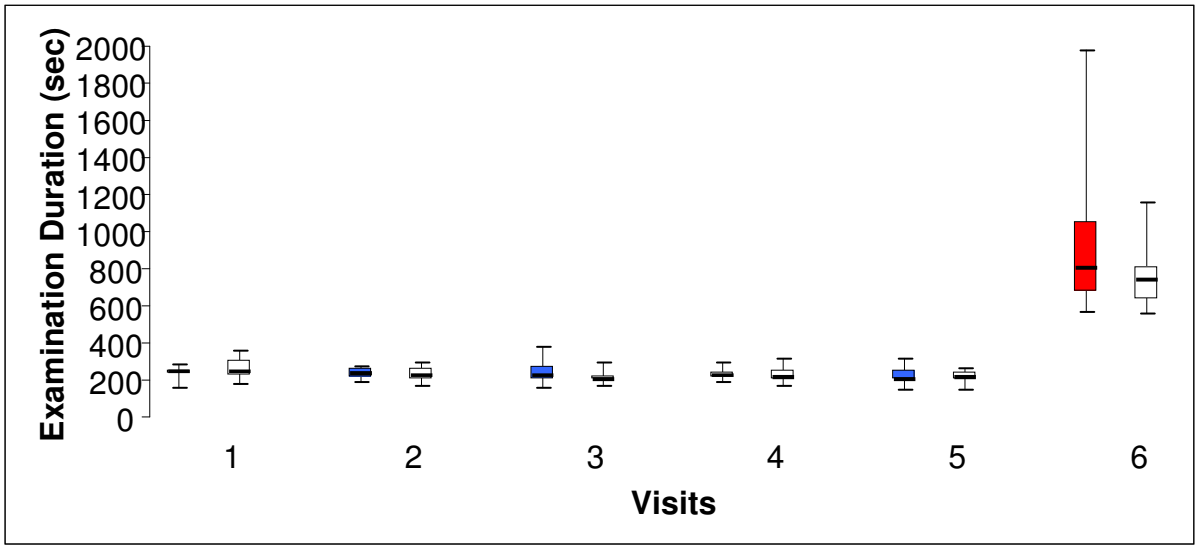
Examination Duration (sec)
2000
1800
1600
1400
1200
1000
800
600
400
200
0
1
2
3
4
5
6
Visits

The ANOVA summary table for the examination duration with the TOP algorithm over the five visits is given in Table 4.23. The group mean examination duration was similar across the three groups (p=0.370). It decreased over the five visits (p<0.001) and was longer for the first eye examined (p<0.008).

Effect	Degrees of Freedom Numerator	Degrees of Freedom Denominator	F value	P value
Age	1	49	3.78	**0.058**
Gender	1	49	1.28	0.264
Diagnosis	2	49	1.01	0.370
Eye	1	441	7.05	**0.008**
Visit	4	441	5.67	**<0.001**

Effect	Degrees of Freedom Numerator	Degrees of Freedom Denominator	F value	P value
Age	1	49	2.92	0.094
Gender	1	49	1.34	0.253
Eye	1	441	7.05	**0.008**
Visit	4	441	5.67	**<0.001**

Effect	Degrees of Freedom Numerator	Degrees of Freedom Denominator	F value	P value
Age	1	49	2.45	0.124
Eye	1	441	7.05	**0.008**
Visit	4	441	5.67	**<0.001**

Effect	Degrees of Freedom Numerator	Degrees of Freedom Denominator	F value	P value
Eye	1	441	7.05	**0.008**
Visit	4	441	5.67	**<0.001**
Eye x Visit	4	441	1.26	0.284

Table 4.23 The Analysis of Variance Summary Table for the examination duration over the five visits.

The ANOVA summary table for the difference between the group mean examination duration for the TOP algorithm at Visit Five and the Dynamic algorithm at Visit Six is given in Table 4.24. As would be expected, the group mean examination duration was considerably longer for the Dynamic algorithm (p<0.001) and the difference between the two algorithms was seemingly independent of age (p=0.812) of diagnosis (p=0.875) and of eye (p=0.112).

Effect	Degrees of Freedom Numerator	Degrees of Freedom Denominator	F value	P value
Age	1	49	0.09	0.766
Gender	1	49	0.64	0.426
Diagnosis	2	49	0.13	0.875
Eye	1	147	2.55	0.112
Algorithm	1	147	563.57	**<0.001**

Effect	Degrees of Freedom Numerator	Degrees of Freedom Denominator	F value	P value
Age	1	49	0.06	0.812
Gender	1	49	0.49	0.488
Eye	1	147	2.55	0.112
Algorithm	1	147	563.57	**<0.001**

Effect	Degrees of Freedom Numerator	Degrees of Freedom Denominator	F value	P value
Gender	1	49	0.46	0.503
Eye	1	147	2.55	0.112
Algorithm	1	147	563.57	**<0.001**

Effect	Degrees of Freedom Numerator	Degrees of Freedom Denominator	F value	P value
Eye	1	147	2.55	0.112
Algorithm	1	147	563.57	**<0.001**

Effect	Degrees of Freedom Numerator	Degrees of Freedom Denominator	F value	P value
Algorithm	1	147	553.95	**<0.001**

Table 4.24 The Analysis of Variance Summary Table for the examination duration between the TOP algorithm at Visit Five and the Dynamic algorithm at Visit Six.

4.12.9 Catch Trials

The Group mean (SD) for the incorrect responses to the False-positive (FP) and False-negative (FN) catch trials over the six visits for each eye of the 28 normal individuals, for the 10 individuals with OHT and for the 11 individuals with OAG are shown in Table 4.25.

FP and FN Catch trials	Visit 1 TOP	Visit 2 TOP	Visit 3 TOP	Visit 4 TOP	Visit 5 TOP	Visit 6 Dynamic
Right FP	10%	11%	6%	5%	10%	14%
SD	19%	21%	13%	12%	15%	15%
Left FP	13%	9%	2%	9%	6%	11%
SD	19%	14%	6%	17%	10%	12%
Right FN	1%	0%	1%	2%	2%	0%
SD	4%	2%	5%	7%	6%	1%
Left FN	2%	1%	0%	2%	1%	0%
SD	7%	3%	0%	7%	5%	1%

FP and FN Catch trials	Visit 1 TOP	Visit 2 TOP	Visit 3 TOP	Visit 4 TOP	Visit 5 TOP	Visit 6 Dynamic
Right FP	11%	5%	5%	18%	8%	22%
SD	16%	11%	10%	32%	12%	18%
Left FP	10%	5%	8%	8%	5%	19%
SD	17%	16%	17%	14%	11%	17%
Right FN	9%	3%	6%	2%	1%	1%
SD	17%	9%	19%	5%	5%	2%
Left FN	9%	0%	0%	0%	3%	3%
SD	20%	0%	0%	0%	9%	9%

FP and FN Catch trials	Visit 1 TOP	Visit 2 TOP	Visit 3 TOP	Visit 4 TOP	Visit 5 TOP	Visit 6 Dynamic
Right FP	12%	8%	13%	10%	4%	19%
SD	19%	15%	17%	17%	9%	16%
Left FP	11%	6%	20%	10%	15%	25%
SD	17%	10%	25%	19%	22%	16%
Right FN	7%	0%	2%	6%	0%	4%
SD	12%	0%	6%	11%	0%	5%
Left FN	0%	4%	0%	2%	2%	3%
SD	0%	9%	0%	6%	5%	7%

Table 4.25 The summary statistics of the incorrect responses to the False-positive and False-negative catch trials at each visit for each eye of the 28 normal individuals (top) of the 10 individuals with OHT (middle) and for the 11 individuals with OAG (bottom).

The relative lack of incorrect responses to the various catch trials was insufficient to warrant analysis by ANOVA. The number of individuals across each of the three groups exhibiting greater than 30% incorrect responses to the FP catch trials for each eye over each of the six visits together with the frequency of the false responses are shown in Table 4.26.

Within the limitations of the dataset (Table 4.26), the Dynamic algorithm at Visit Six yielded, across the three groups, a slightly greater frequency of incorrect responses to the FP catch trials than the TOP algorithm at Visit Five.

False Positive responses	Visit	Normal individuals		Individuals with OHT		Individuals with OAG	
		Right eye	Left eye	Right eye	Left eye	Right eye	Left eye
>30%	**1**	5	3	1	1	2	1
>30%	**2**	4	2	0	1	1	0
>30%	**3**	2	0	0	1	1	2
>30%	**4**	1	3	3	1	1	1
>30%	**5**	4	0	0	0	0	2
>30%	**6**	5	2	2	1	2	1

Table 4.26 The number of individuals across each of the three groups exhibiting greater than 30% incorrect responses to the FP catch trials for each eye over each of the six visits together with the frequency of the false-responses.

4.12.10 The ratio of the Peripheral Mean Sensitivity (PMS) to the Central Mean Sensitivity (CMS)

The ratio of the Peripheral Mean Sensitivity (PMS) to the Central Mean Sensitivity (CMS) over the six visits for each eye of the 28 normal individuals (top), of the 10 individuals with OHT (middle) and the 11 individuals with OAG (bottom) is shown in Table 4.27.

Peripheral/Central MS	Visit 1 TOP	Visit 2 TOP	Visit 3 TOP	Visit 4 TOP	Visit 5 TOP	Visit 6 Dynamic
Right Mean	0.94	0.93	0.93	0.92	0.93	0.96
SD	0.07	0.07	0.07	0.05	0.07	0.08
Left Mean	0.93	0.93	0.92	0.93	0.93	0.96
SD	0.07	0.06	0.07	0.05	0.08	0.05
Right Median	0.95	0.93	0.94	0.94	0.95	0.97
IQR	0.06	0.10	0.09	0.06	0.10	0.11
Left Median	0.94	0.94	0.92	0.92	0.93	0.97
IQR	0.09	0.06	0.07	0.08	0.09	0.07

Peripheral/Central MS	Visit 1 TOP	Visit 2 TOP	Visit 3 TOP	Visit 4 TOP	Visit 5 TOP	Visit 6 Dynamic
Right Mean	0.94	0.93	0.87	0.89	0.92	1.03
SD	0.12	0.11	0.18	0.20	0.20	0.05
Left Mean	0.92	0.93	0.93	0.91	0.90	0.93
SD	0.09	0.13	0.16	0.21	0.20	0.23
Right Median	0.94	0.97	0.94	0.95	0.99	1.06
IQR	0.06	0.03	0.09	0.04	0.06	0.05
Left Median	0.93	0.97	0.98	0.97	0.95	1.01
IQR	0.06	0.06	0.05	0.05	0.08	0.07

Peripheral/Central MS	Visit 1 TOP	Visit 2 TOP	Visit 3 TOP	Visit 4 TOP	Visit 5 TOP	Visit 6 Dynamic
Right Mean	0.90	0.87	0.91	0.89	0.89	0.97
SD	0.11	0.10	0.09	0.13	0.14	0.11
Left Mean	0.86	0.86	0.89	0.88	0.89	0.94
SD	0.14	0.14	0.15	0.15	0.13	0.16
Right Median	0.88	0.88	0.94	0.92	0.94	1.01
IQR	0.18	0.12	0.11	0.14	0.19	0.12
Left Median	0.91	0.90	0.94	0.89	0.96	0.95
IQR	0.12	0.17	0.14	0.10	0.21	0.20

Table 4.27 The ratio of the PMS_{CFF} to the CMS_{CFF} in each eye of the 28 normal individuals (top), the 10 individuals with OHT (middle) and the 11 individuals with OAG (bottom) at each of the Six Visits.

The Group Mean and Median ratio of the PMS to the CMS for the TOP threshold algorithm were essentially similar at each of the five visits. The ratio based upon the mean was slightly lower than that of the median particularly for the group with OHT and the group with OAG. A ratio of less than one indicates that the MS was higher centrally than peripherally. The ratio for the Dynamic algorithm at Visit Six was greater than that for the TOP algorithm at Visit Five.

4.13 The change in sensitivity at each given stimulus location (i.e. the variation with eccentricity) for the TOP algorithm between Visit Two and Visit One, and between Visit Five and Visit Two, and that between the Dynamic algorithm at Visit Six and the TOP algorithm at Visit Five.

The summary statistics of the change in MS at each stimulus location between Visit Two and Visit One for the right eye (top) and for the left eye (bottom) of the 28 normal individuals are shown in Figure 4.8 (mean [SD]) and in Figure 4.9 (median [IQR]), respectively, and for the right eye (top) and left eye (bottom) of the 10 individuals with OHT in Figure 4.10 and Figure 4.11, respectively. In general, the median tended to slightly underestimate the between-visit change in MS, relative to that indicated by the mean, in the field of each eye. Nevertheless, both measures suggested a slightly higher MS at Visit Two which was more apparent for the individuals with OHT, and that the magnitude of the change was approximately similar with increased eccentricity for the field of each eye in both groups of individuals.

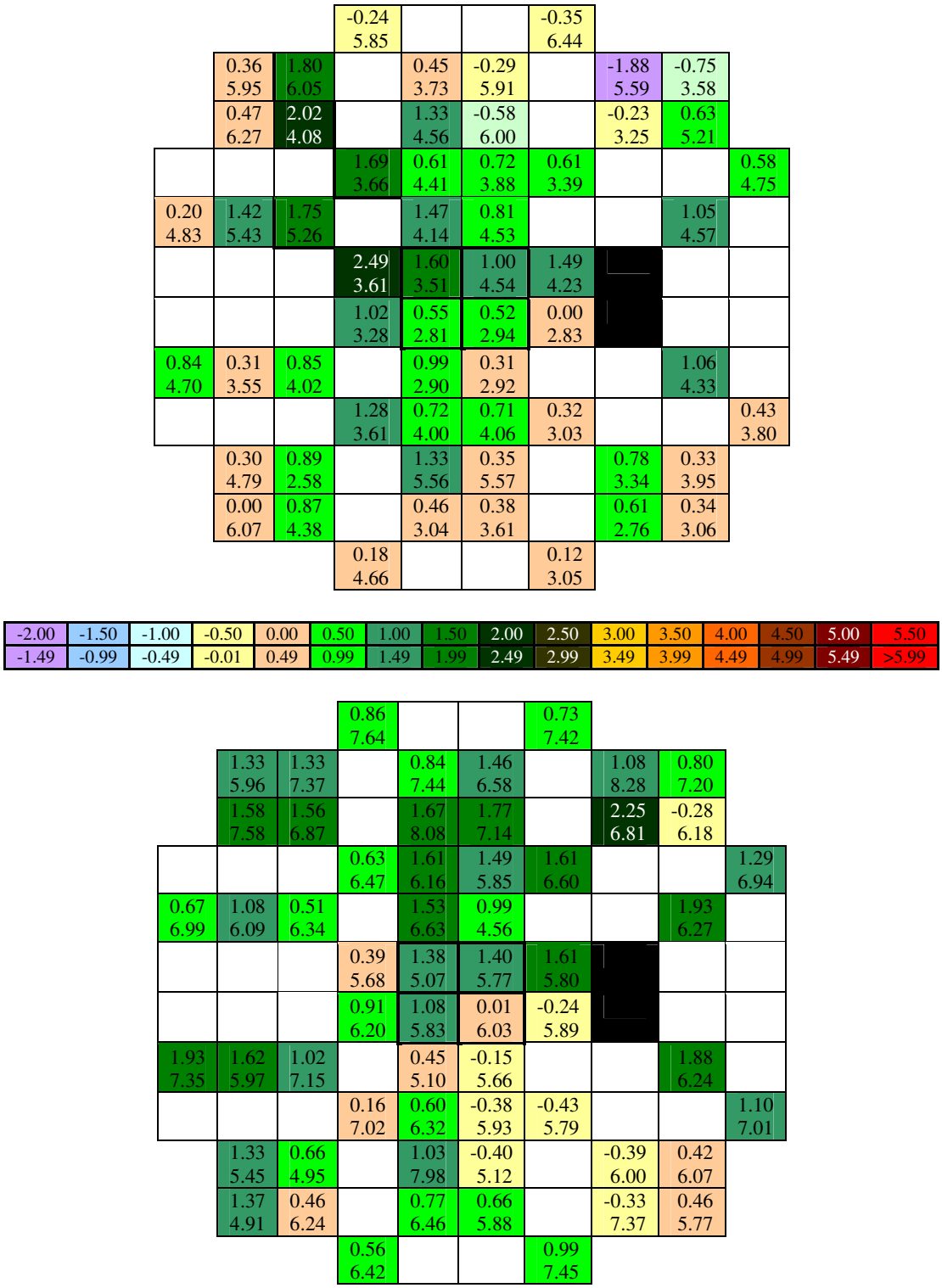

Figure 4.8 The group mean (SD) of the difference in MS_{CFF} at each stimulus location between Visit Two and Visit One for the right eye (top) and left eye (bottom) for the 28 normal individuals. The stimulus locations for the left eye are displayed in right eye format to aid the between-eye comparison. The lower value indicates the SD. An increasing 'warmth' of the colour at each stimulus location indicates an improvement in sensitivity at Visit Two.

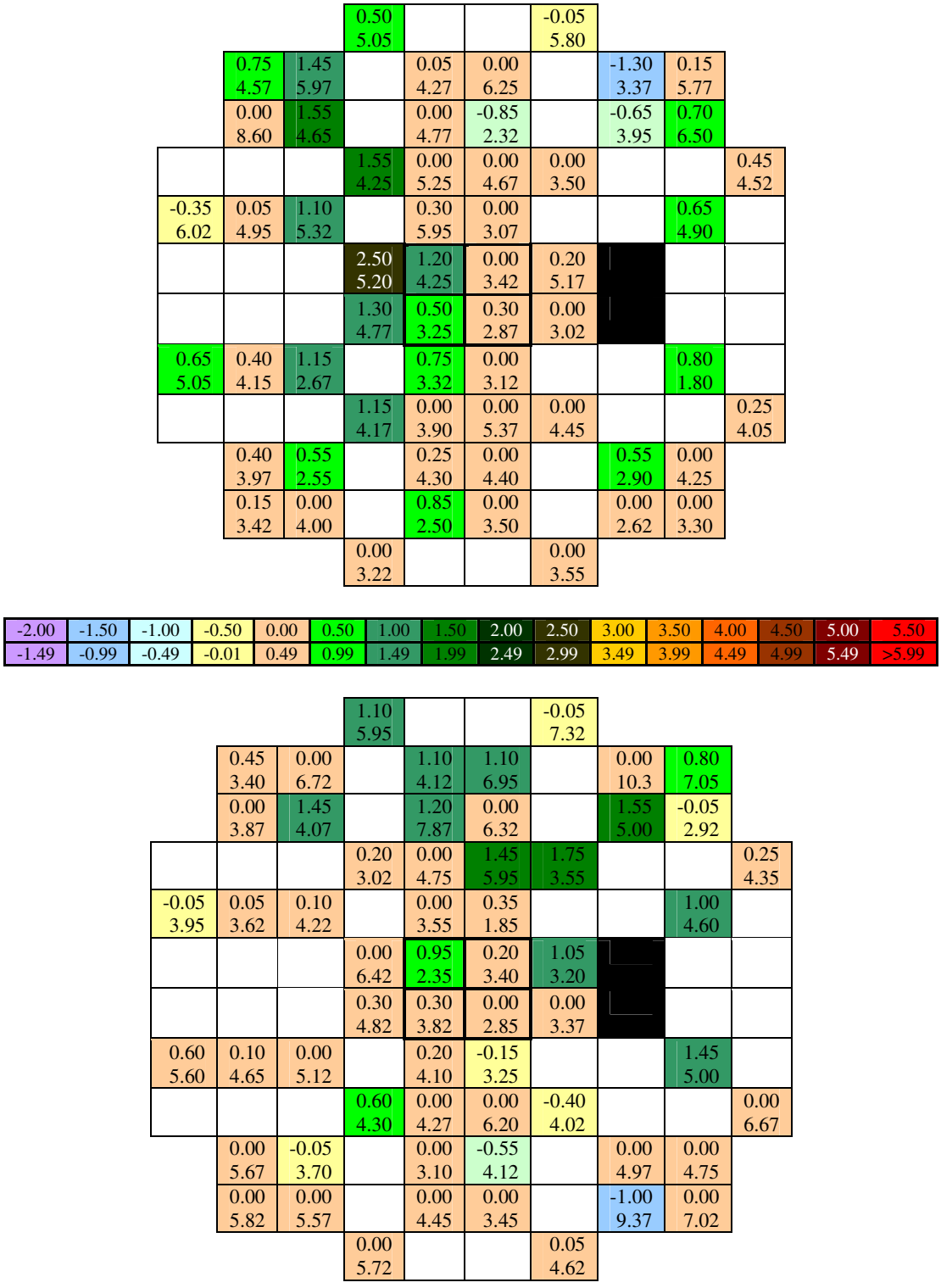

Figure 4.9 The group median (IQR) of the difference in MS_{CFF} at each stimulus location between Visit Two and Visit One for the right eye (top) and left eye (bottom) for the 28 normal individuals. The stimulus locations for the left eye are displayed in right eye format to aid the between-eye comparison. The lower value indicates the IQR. An increasing 'warmth' of the colour at each stimulus location indicates an improvement in sensitivity at Visit Two.

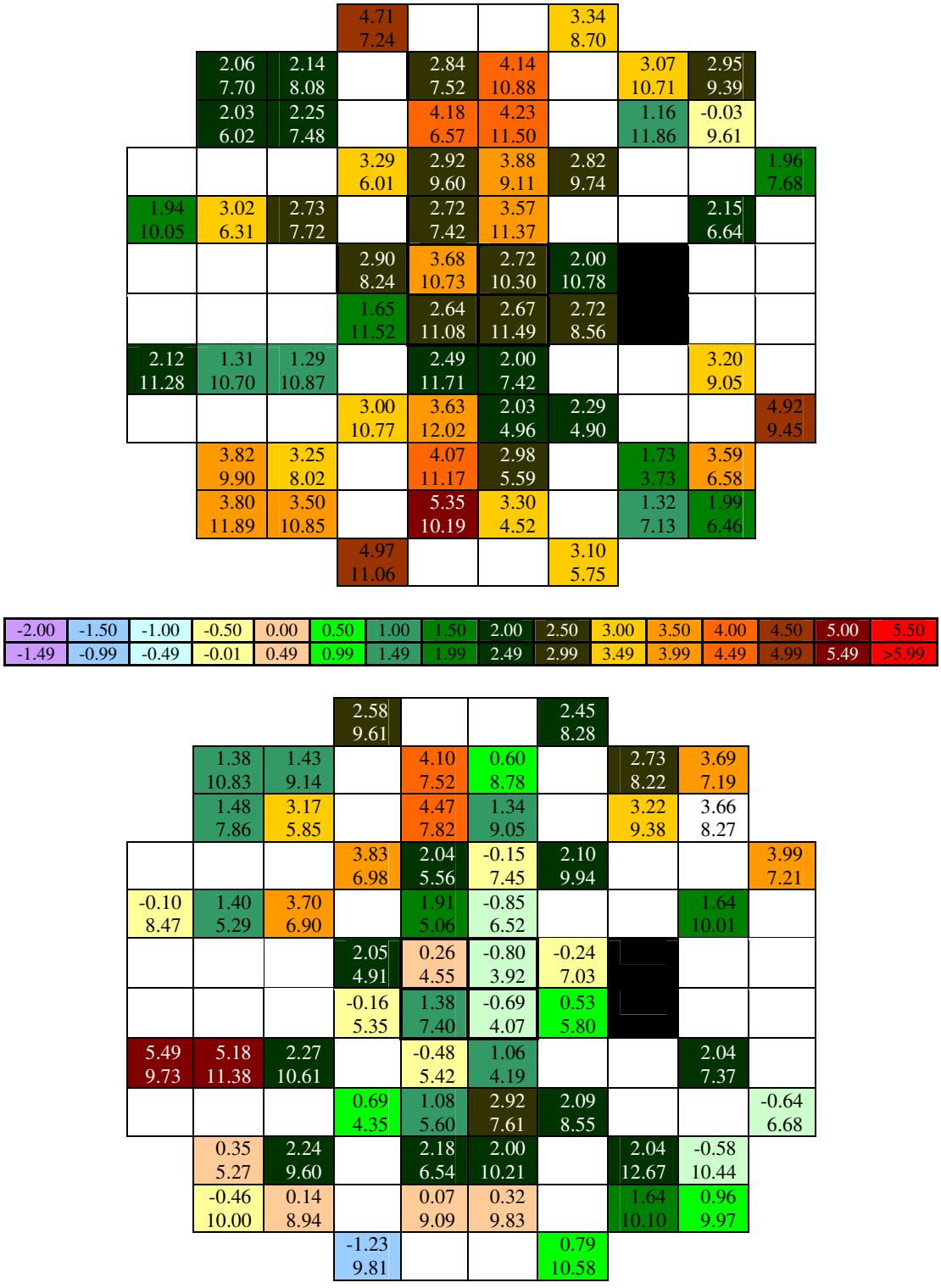

Figure 4.10 The group mean (SD) of the difference in MS_{CFF} at each stimulus location between Visit Two and Visit One for the right eye (top) and left eye (bottom) for the 10 individuals with OHT. The stimulus locations for the left eye are displayed in right eye format to aid the between-eye comparison. The lower value indicates the SD. An increasing 'warmth' of the colour at each stimulus location indicates an improvement in sensitivity at Visit Two.

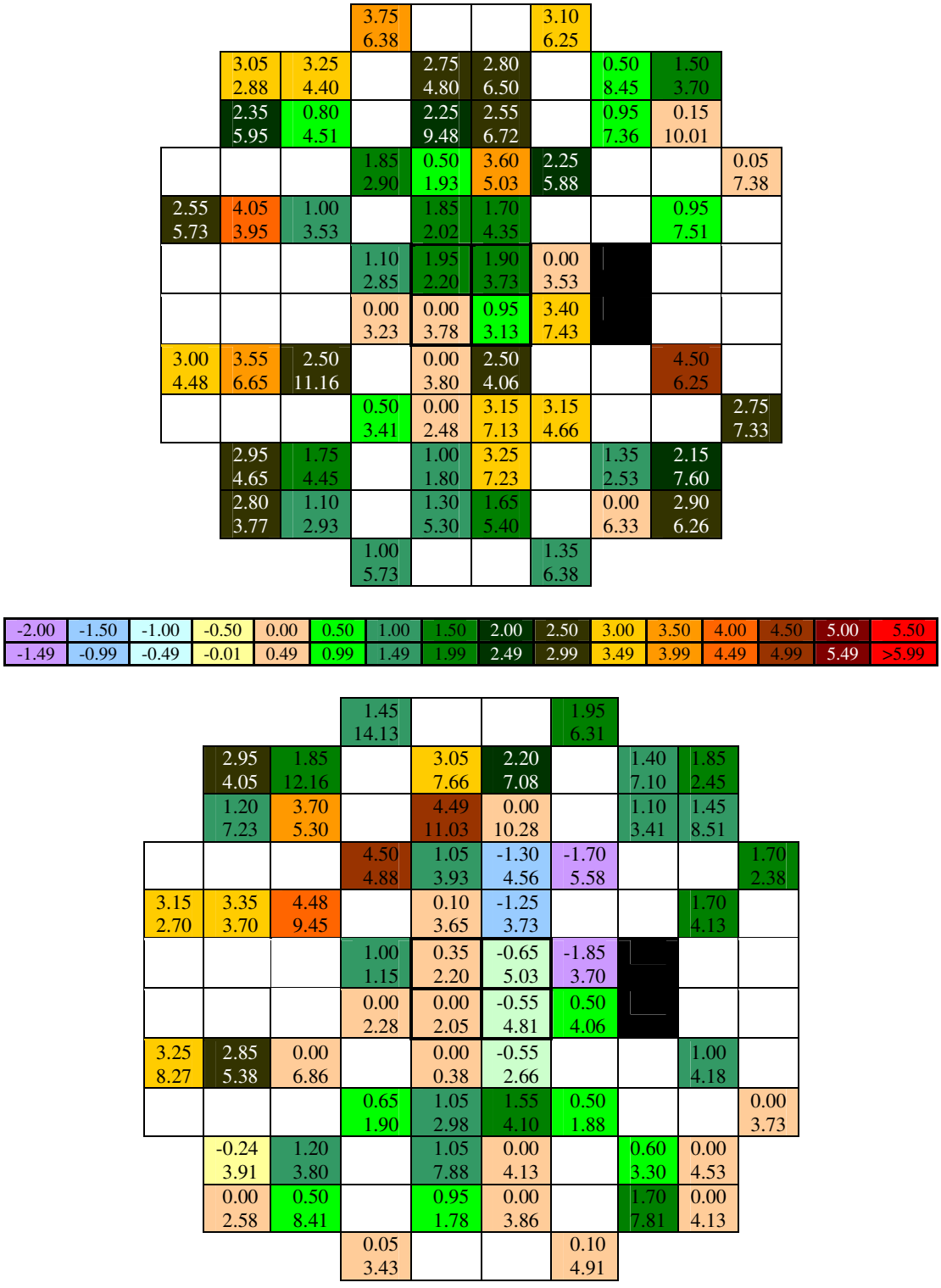

Figure 4.11 The group median (IQR) of the difference in MS_{CFF} at each stimulus location between Visit Two and Visit One for the right eye (top) and left eye (bottom) for the 10 individuals with OHT. The stimulus locations for the left eye are displayed in right eye format to aid the between-eye comparison. The lower value indicates the IQR. An increasing 'warmth' of the colour at each stimulus location indicates an improvement in sensitivity at Visit Two.

Similarly, the summary statistics of the change in MS at each stimulus location between Visit Five and Visit Two for the right eye (top) and left eye (bottom) for the 28 normal individuals are shown in Figure 4.12 (mean [SD]) and in Figure 4.13 (median [IQR]), respectively, and for the right eye (top) and left eye (bottom) for the 10 individuals with OHT in Figure 4.14 and Figure 4.15, respectively.

In general, the median again tended to slightly underestimate the magnitude of the between-visit change in sensitivity relative to that indicated by the mean, in the field of each eye. Both measures suggested an approximately similar magnitude of the MS at each examination with increase in eccentricity for the field of each eye.

The summary statistics of the change in MS at each stimulus location between the TOP algorithm at Visit Five and the Dynamic algorithm at Visit Six for the right eye (top) and left eye (bottom) for the 28 normal individuals are shown in Figure 4.16 (mean [SD]) and in Figure 4.17 (median [IQR]), respectively, and for the right eye (top) and left eye (bottom) for the 10 individuals with OHT in Figure 4.18 and Figure 4.19, respectively.

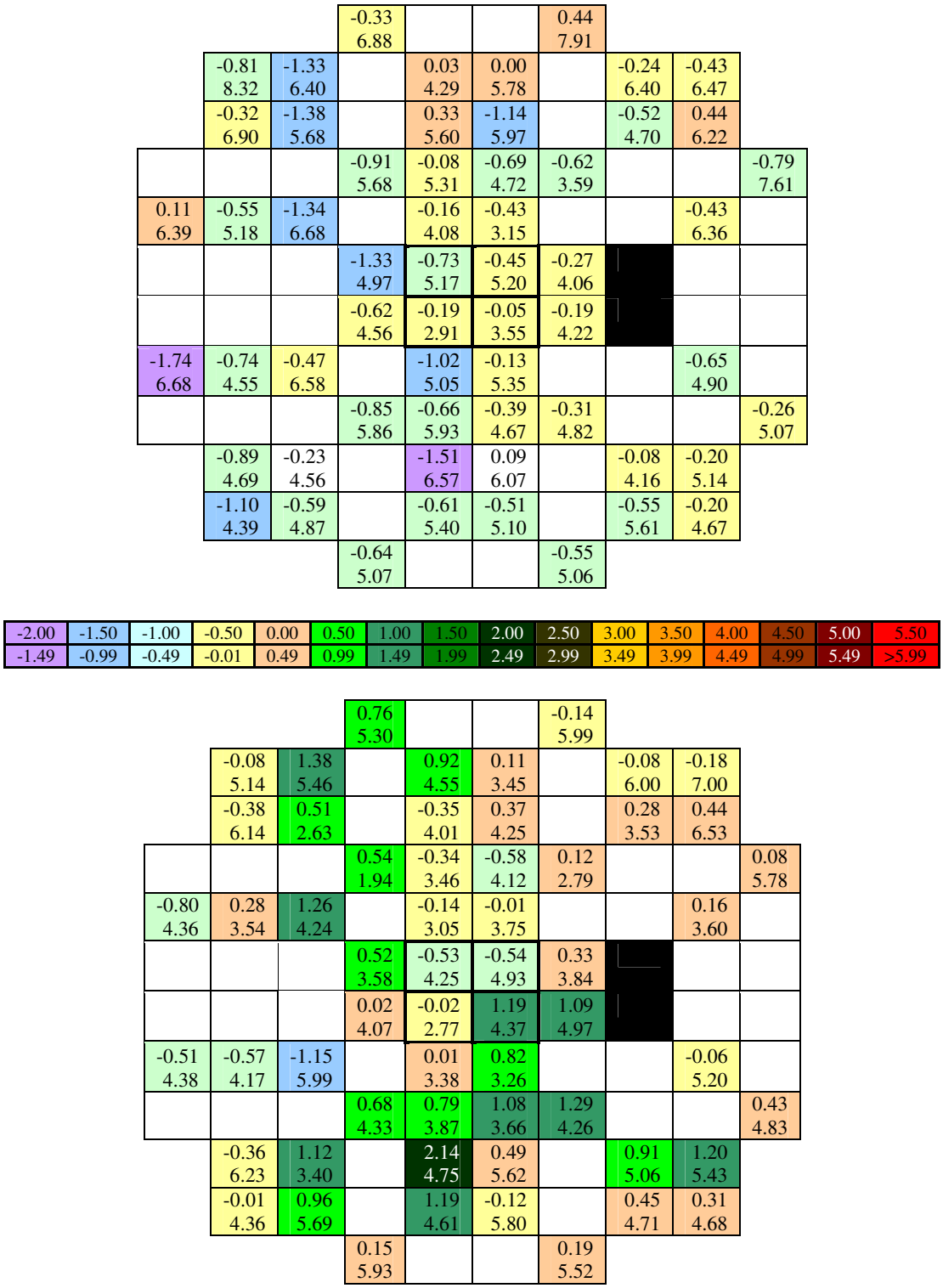

Figure 4.12 The group mean (SD) of the difference in MS_{CFF} at each stimulus location between Visit Five and Visit Two for the right eye (top) and left eye (bottom) for the 28 normal individuals. The stimulus locations for the left eye are displayed in right eye format to aid the between-eye comparison. The lower value indicates the Standard Deviation. An increasing 'warmth' of the colour at each stimulus location indicates an improvement in sensitivity at Visit Five.

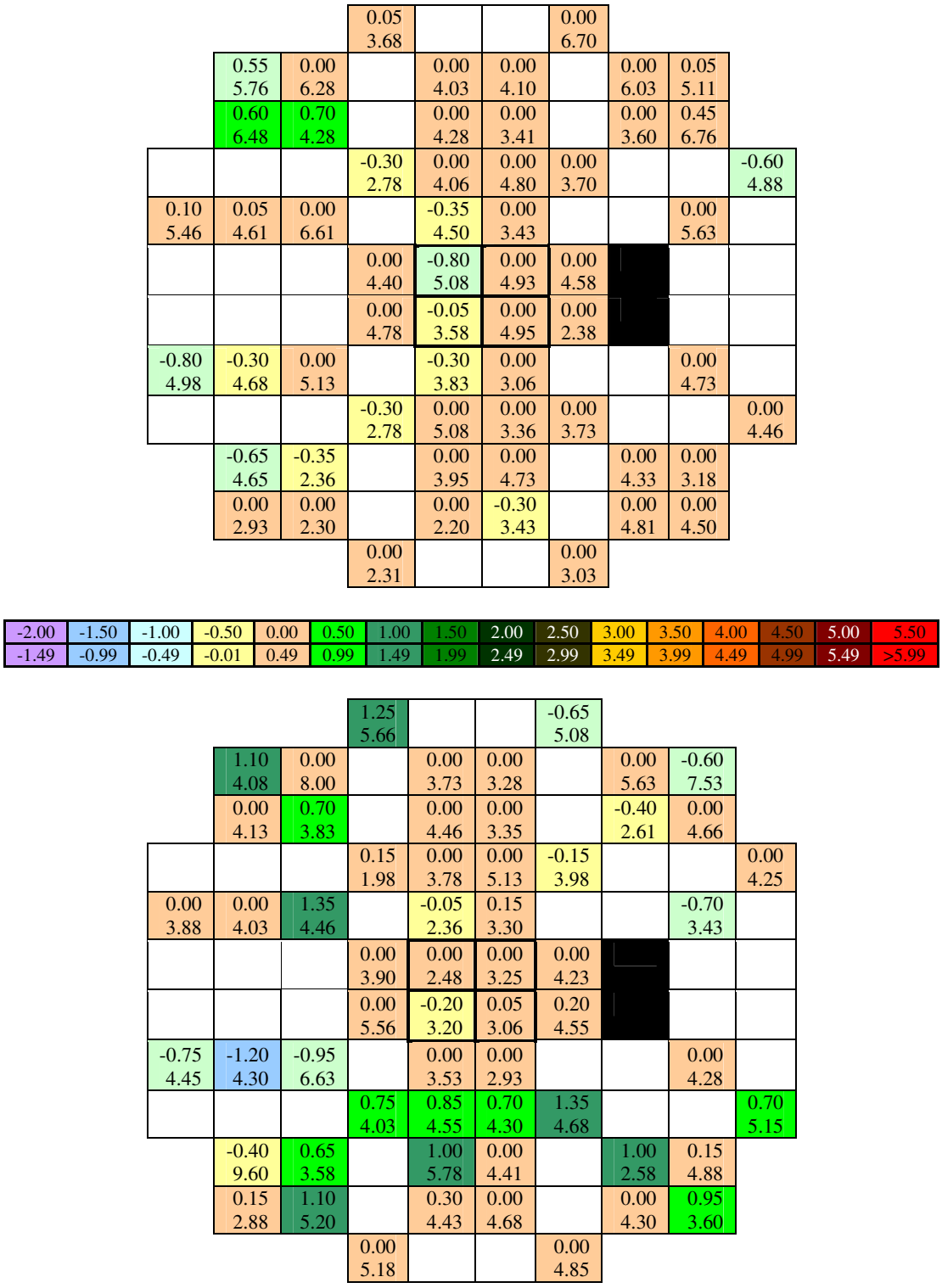

Figure 4.13 The group median (IQR) of the difference in MS_{CFF} at each stimulus location between Visit Five and Visit Two for the right eye (top) and left eye (bottom) for the 28 normal individuals. The stimulus locations for the left eye are displayed in right eye format to aid the between-eye comparison. The lower value indicates the IQR. An increasing 'warmth' of the colour at each stimulus location indicates an improvement in sensitivity at Visit Five.

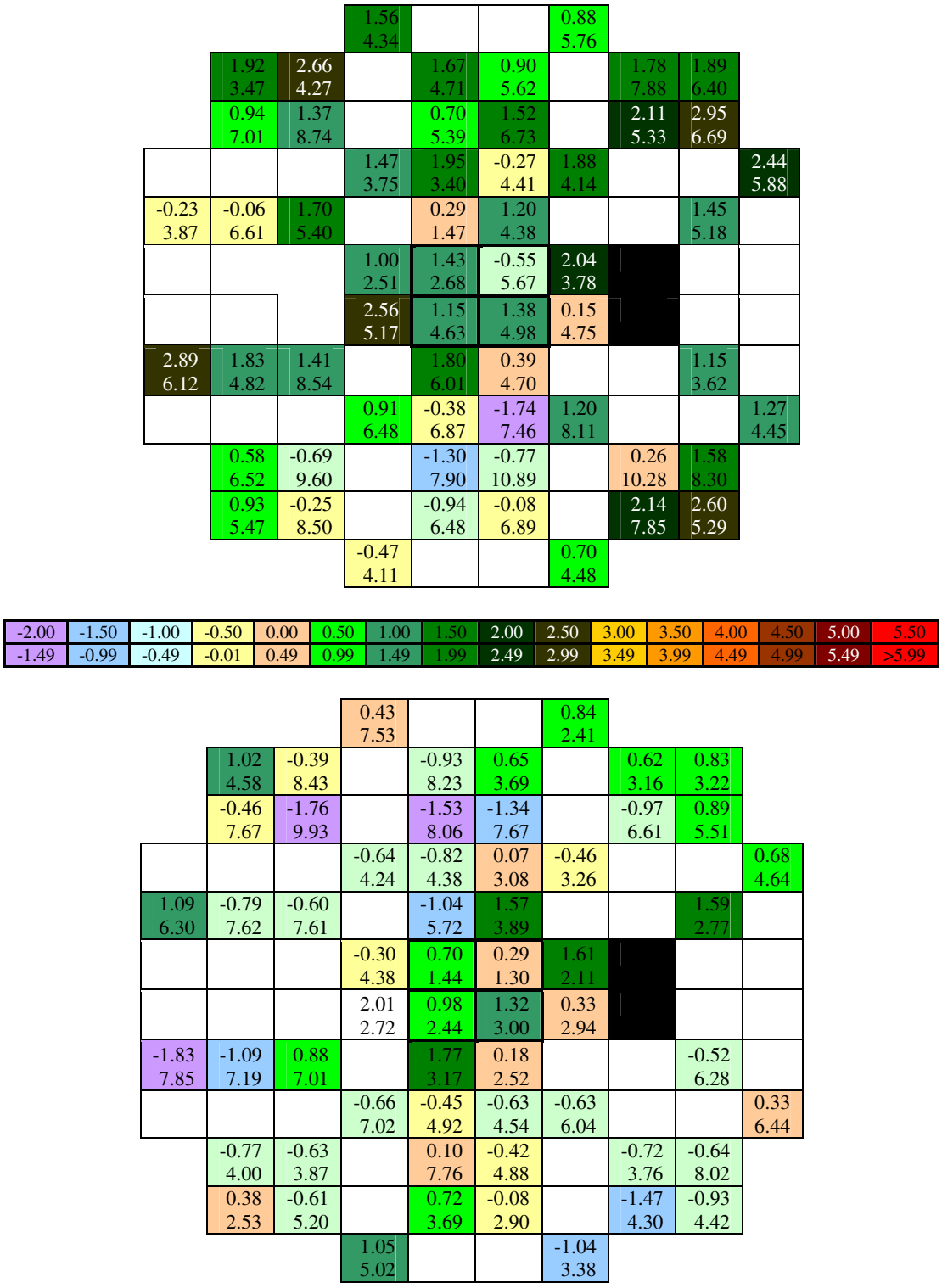

Figure 4.14 The group mean (SD) of the difference in MS_{CFF} at each stimulus location between Visit Five and Visit Two for the right eye (top) and left eye (bottom) for the 10 individuals with OHT. The stimulus locations for the left eye are displayed in right eye format to aid the between-eye comparison. The lower value indicates the Standard Deviation. An increasing 'warmth' of the colour at each stimulus location indicates an improvement in sensitivity at Visit Five.

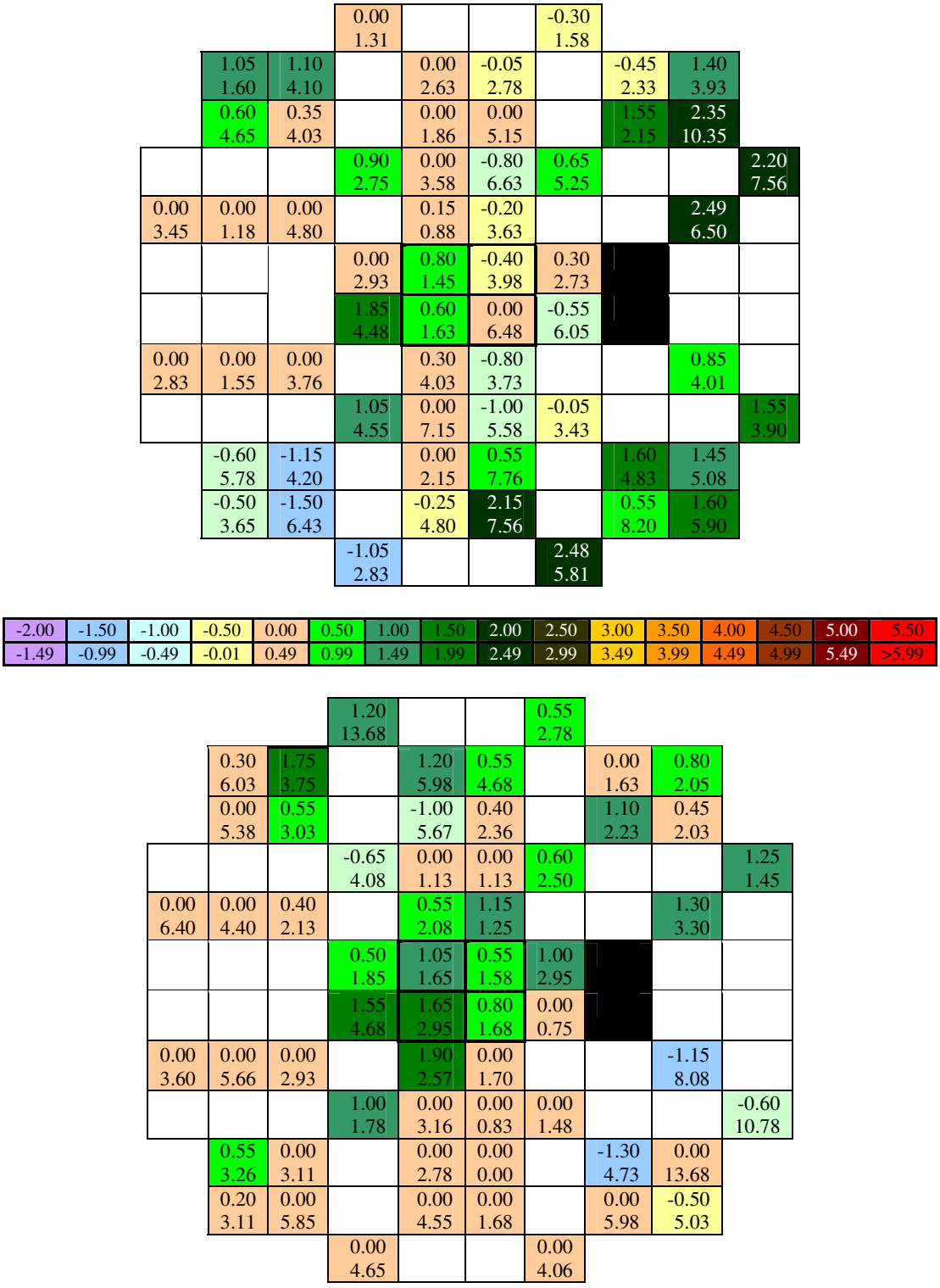

Figure 4.15 The group median (IQR) of the difference in MS_{CFF} at each stimulus location between Visit Five and Visit Two for the right eye (top) and left eye (bottom) for the 10 individuals with OHT. The stimulus locations for the left eye are displayed in right eye format to aid the between-eye comparison. The lower value indicates the IQR. An increasing 'warmth' of the colour at each stimulus location indicates an improvement in sensitivity at Visit Five.

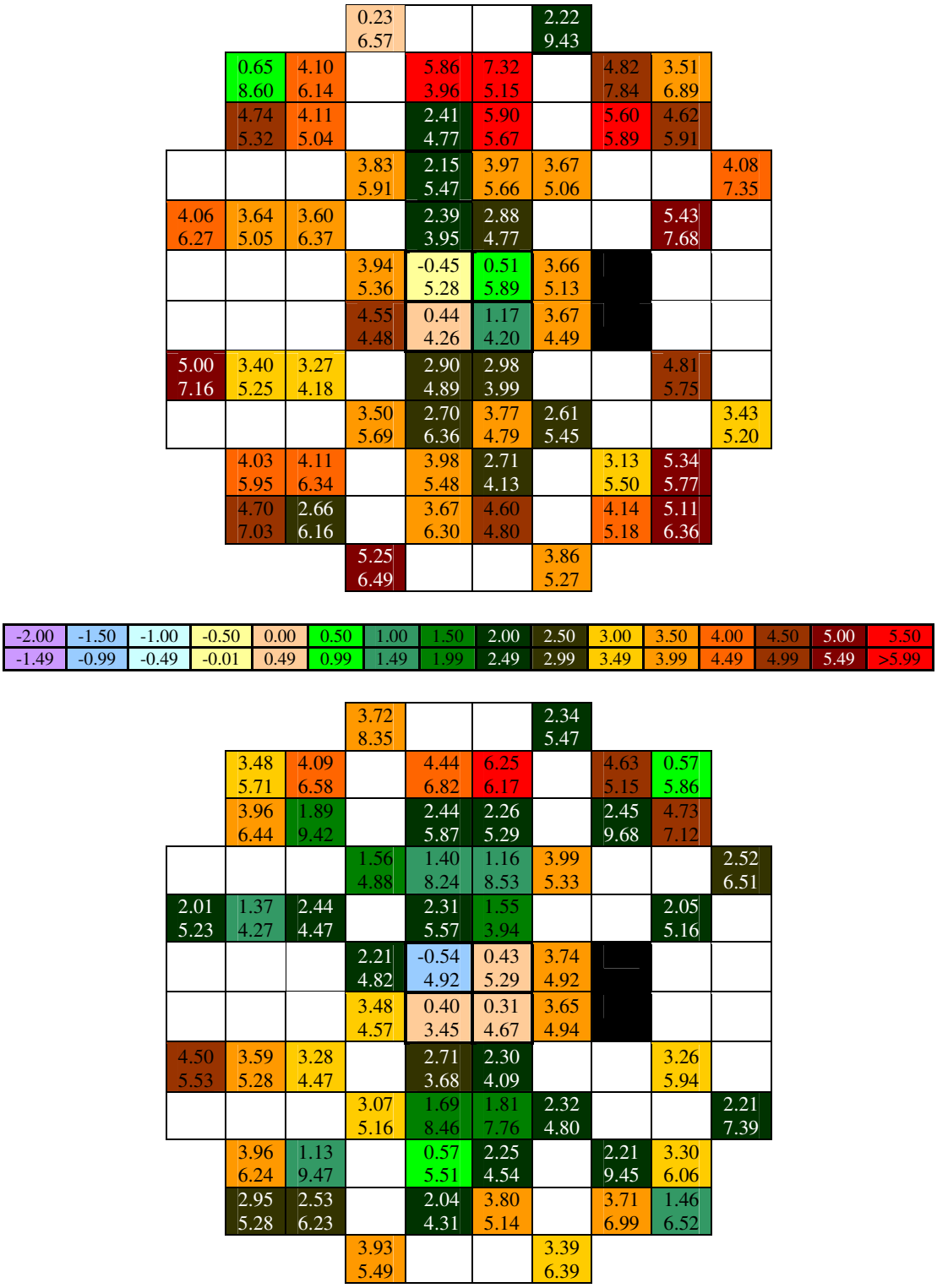

Figure 4.16 The group mean (SD) of the difference in MS_{CFF} at each stimulus location for the TOP algorithm at visit Five and the Dynamic algorithm at visit Six for the right eye (top) and left eye (bottom) for the 28 normal individuals. The stimulus locations for the left eye are displayed in right eye format to aid the between-eye comparison. The lower value indicates the Standard Deviation. An increasing 'warmth' of the colour at each stimulus location indicates an improvement in sensitivity for the Dynamic algorithm at Visit Six.

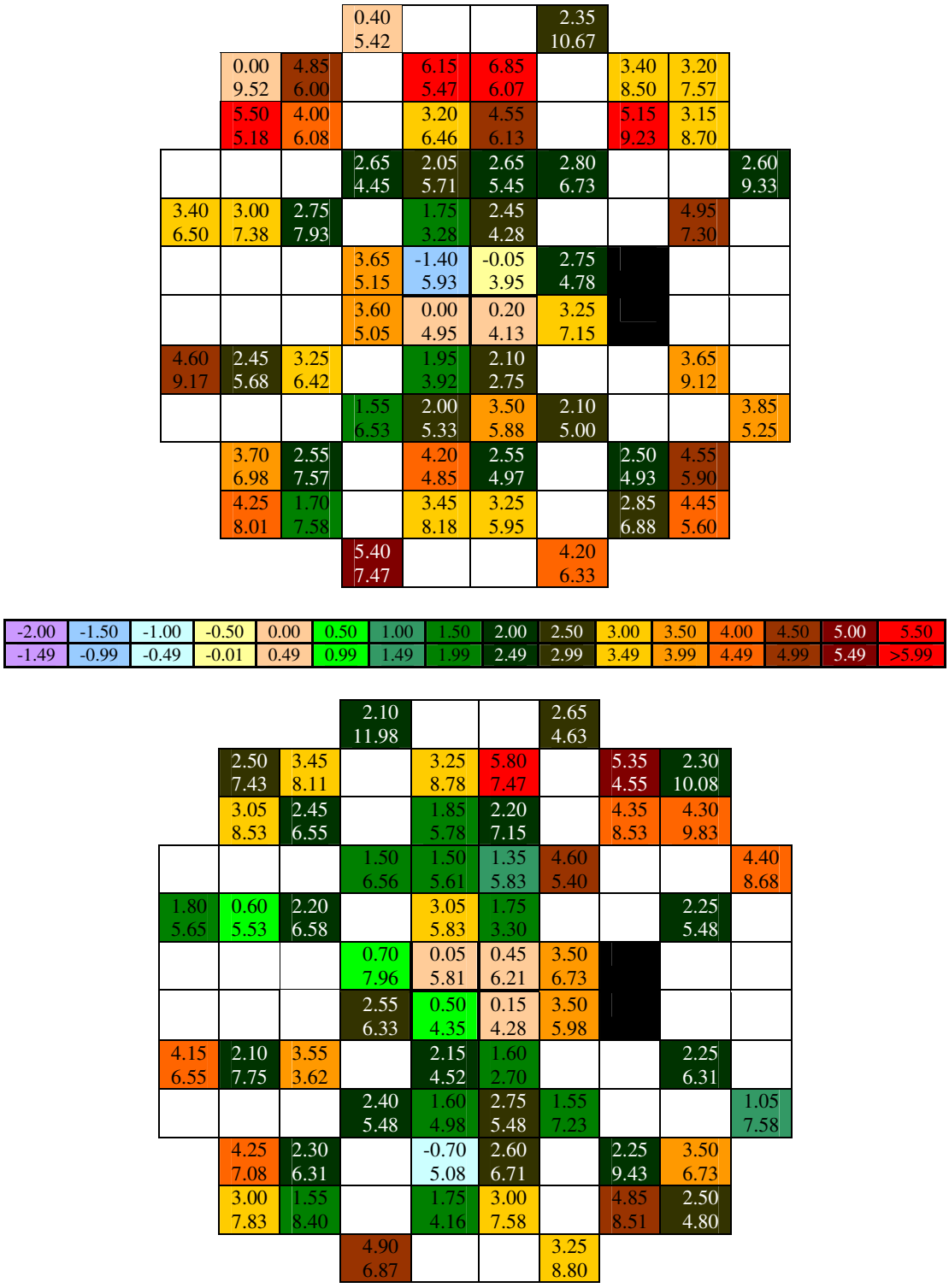

Figure 4.17 The group median (IQR) of the difference in MS_{CFF} at each stimulus location for the TOP algorithm at visit Five and the Dynamic algorithm at visit Six for the right eye (top) and left eye (bottom) for the 28 normal individuals. The stimulus locations for the left eye are displayed in right eye format to aid the between-eye comparison. The lower value indicates the IQR. An increasing 'warmth' of the colour at each stimulus location indicates an improvement in sensitivity for the Dynamic algorithm at Visit Six.

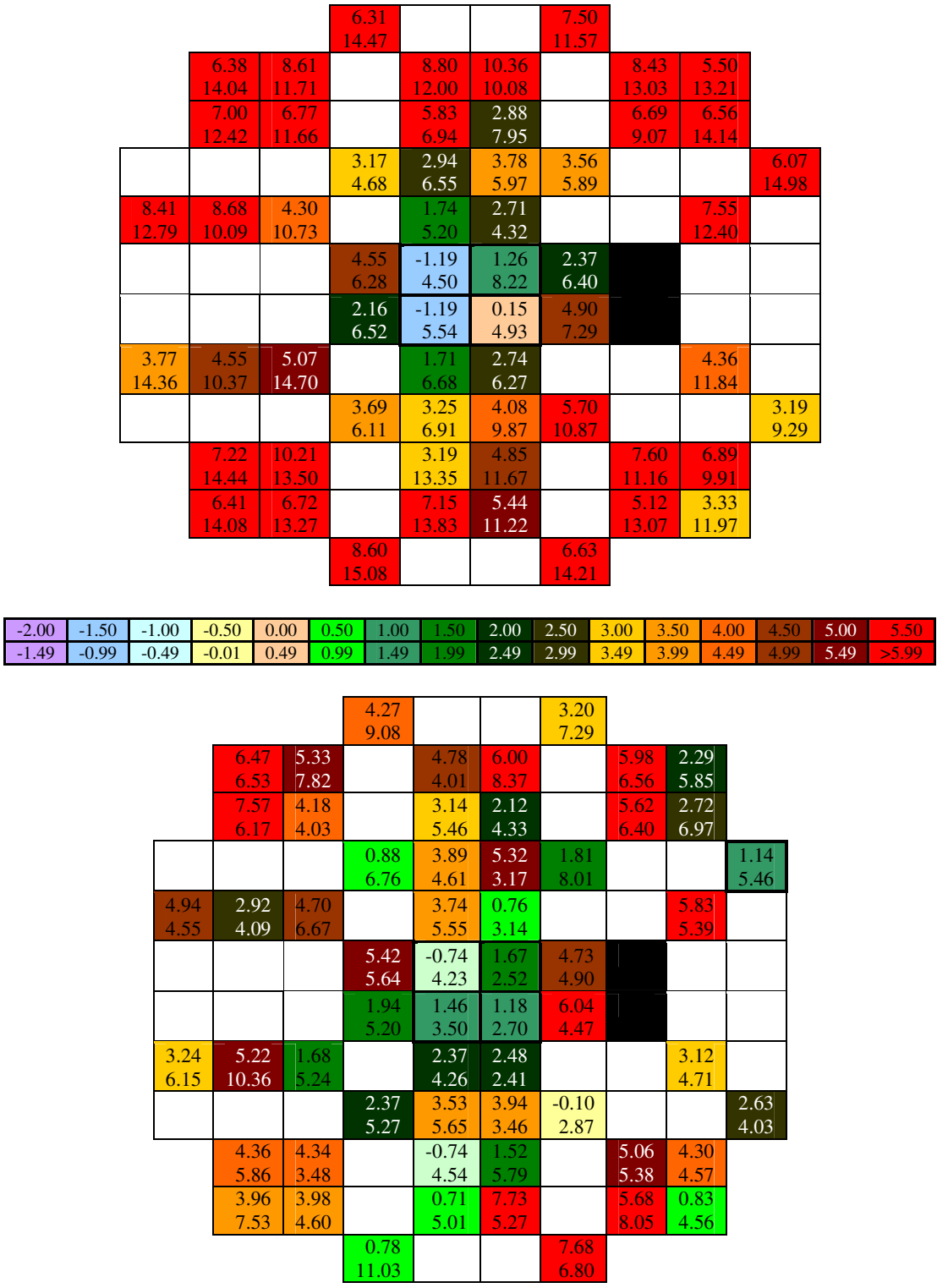

Figure 4.18 The group mean (SD) of the difference in MS_{CFF} at each stimulus location for the TOP algorithm at visit Five and the Dynamic algorithm at visit Six for the right eye (top) and left eye (bottom) for the 10 individuals with OHT. The stimulus locations for the left eye are displayed in right eye format to aid the between-eye comparison. The lower value indicates the Standard Deviation. An increasing 'warmth' of the colour at each stimulus location indicates an improvement in sensitivity for the Dynamic algorithm at Visit Six.

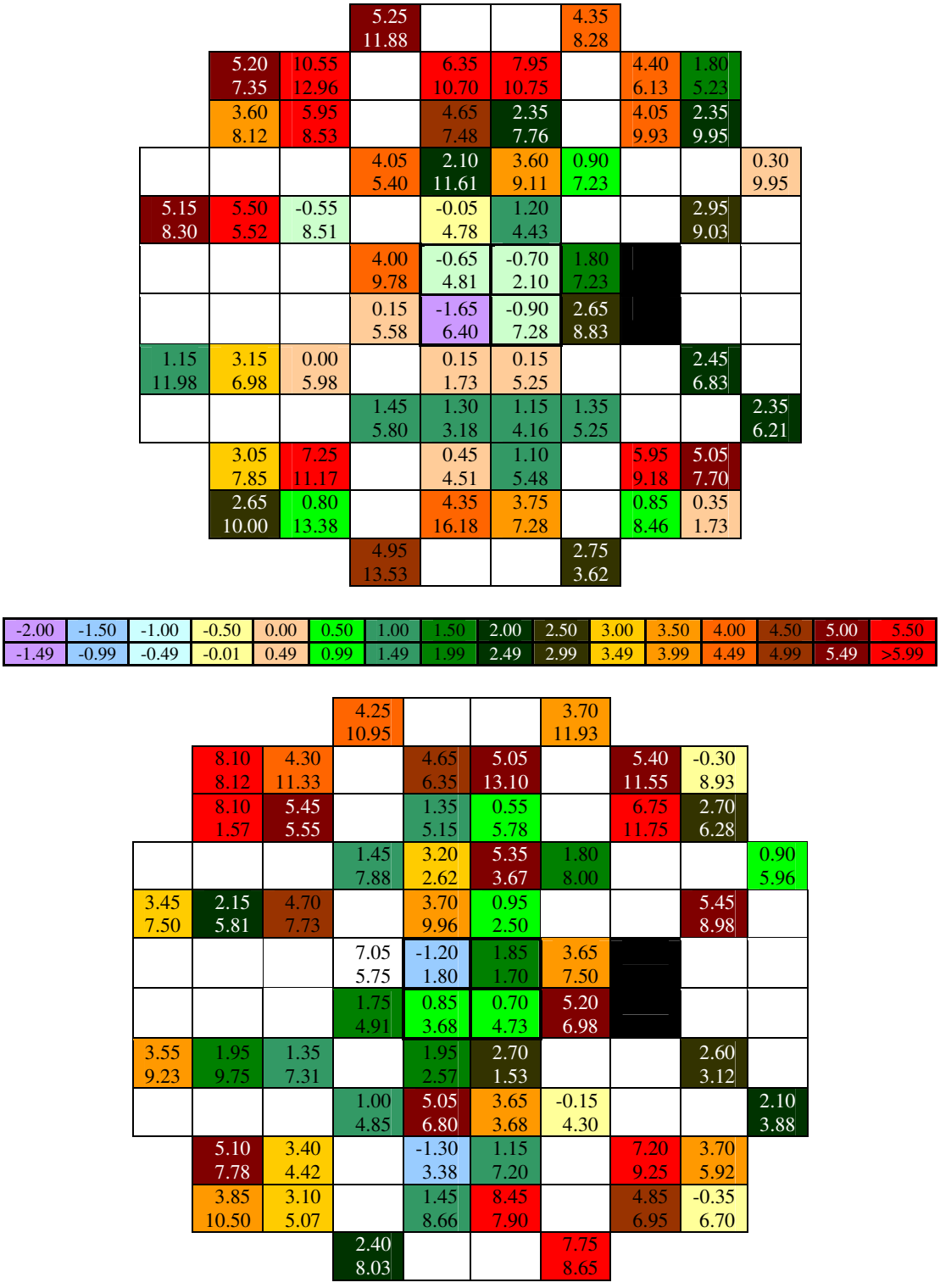

Figure 4.19 The group median (IQR) of the difference in MS_{CFF} at each stimulus location for the TOP algorithm at visit Five and the Dynamic algorithm at visit Six for the right eye (top) and left eye (bottom) for the 10 individuals with OHT. The stimulus locations for the left eye are displayed in right eye format to aid the between-eye comparison. The lower value indicates the IQR. An increasing 'warmth' of the colour at each stimulus location indicates an improvement in sensitivity for the Dynamic algorithm at Visit Six.

In general, the mean tended to slightly underestimate the difference between the TOP and the Dynamic algorithm in MS, relative to that indicated by the median, in the field of each eye. Both measures suggested, for the field of each eye, an increase in the disparity (i.e. the greater MS for the Dynamic algorithm) between the two algorithms with increase eccentricity and was more pronounced for the individuals with OHT.

4.14 The change in sensitivity, across all stimulus locations, between Visit Two and Visit One, between Visit Five and Visit Two, and between the Dynamic algorithm at Visit Six and the TOP algorithm at Visit Five, respectively, as a function of the magnitude of sensitivity at the initial visit of the given paired comparison.

The change in sensitivity, across all stimulus locations, between Visit Two and Visit One as a function of the magnitude of sensitivity at Visit One for the 28 normal individuals, the 10 individuals with OHT, the 11 individuals with OAG and for all three groups, combined, is given in Figure 4.20. The corresponding changes between Visit Five and Visit Two are given in Figure 4.21 and between the Dynamic algorithm at Visit Six and the TOP algorithm at Visit Five is given in Figure 4.22.

The 50^{th} percentile of the distribution of the change in sensitivity at each location for the normal individuals between Visits Two and One as a function of the sensitivity at Visit One (i.e. the defect depth) exhibited a tendency, within the limitations of the size of the case series, to exhibit a positive slope with reduction in sensitivity indicating an increasingly preferential improvement for the lower values of sensitivity at Visit Two. The corresponding slope was more positive for the left eye. A similar result was present for the individuals with OHT. However, the slopes for each eye of the individual with OAG remained flat, i.e. approximated to zero. The slopes for all three groups, combined, were, by definition, based upon a larger number of individuals than those for each individual group and, as a consequence, clearly exhibited the trend for an

increasing improvement in sensitivity at Visit Two with increasing defect depth manifested at Visit One (i.e. a positive slope).

Within the limitation of the data set, the slope of the 50th percentile of the distribution of the change in sensitivity at each location between Visit Five and Visit Two tended to zero for each eye of each group and for all three groups, combined, indicating little change between the two visits.

The 50th percentile of the distribution of the change in sensitivity at each location for the normal individuals between the Dynamic algorithm recorded at Visit Six and the TOP algorithm recorded at Visit Five as a function of the sensitivity recoded with the TOP algorithm exhibited a positive slope in each eye indicating an increasingly greater sensitivity for the Dynamic algorithm compared to the TOP algorithm with increasing defect depth as defined by the TOP algorithm.

The corresponding slope for the individuals with OHT tended to zero for each eye whilst that for the individuals with OAG exhibited a slight positive slope. The slopes for all three groups, combined, clearly exhibited the trend for an increasingly higher sensitivity for the Dynamic algorithm compared to the TOP algorithm with increasing defect depth as defined by the TOP algorithm.

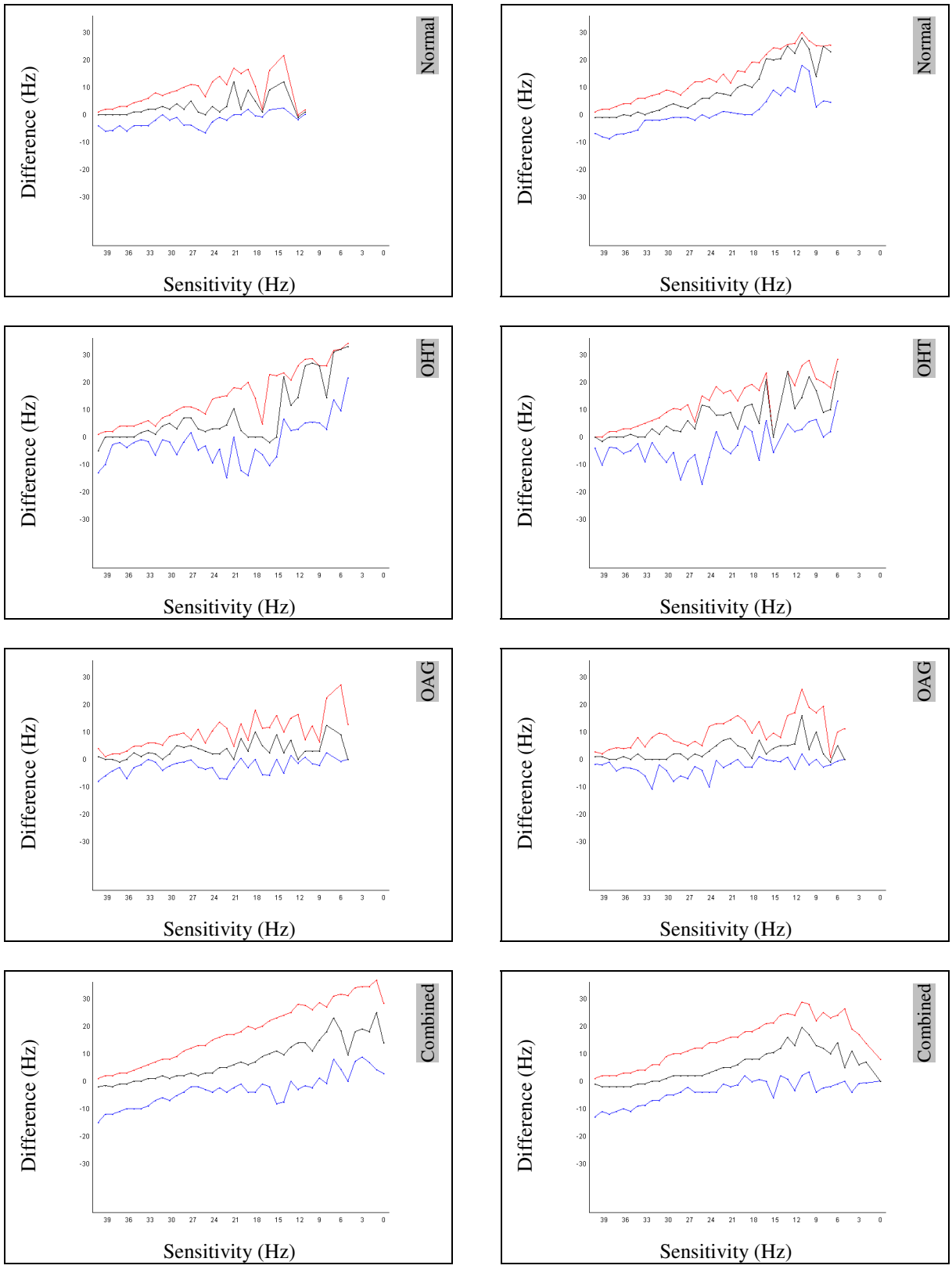

Figure 4.20 The 90th (red), 50th (black) and 10th (blue) percentiles of the distribution of the differences in sensitivity across all stimulus locations between Visits Two and Visit One as a function of the sensitivity at the corresponding stimulus location recorded at Visit One for the right (left column) and left (right column) eye, for the normal individuals (top), the individuals with OHT (middle top), the individuals with OAG (middle bottom) and for all three groups, combined (bottom), using the Octopus 311, Program G1, TOP algorithm.

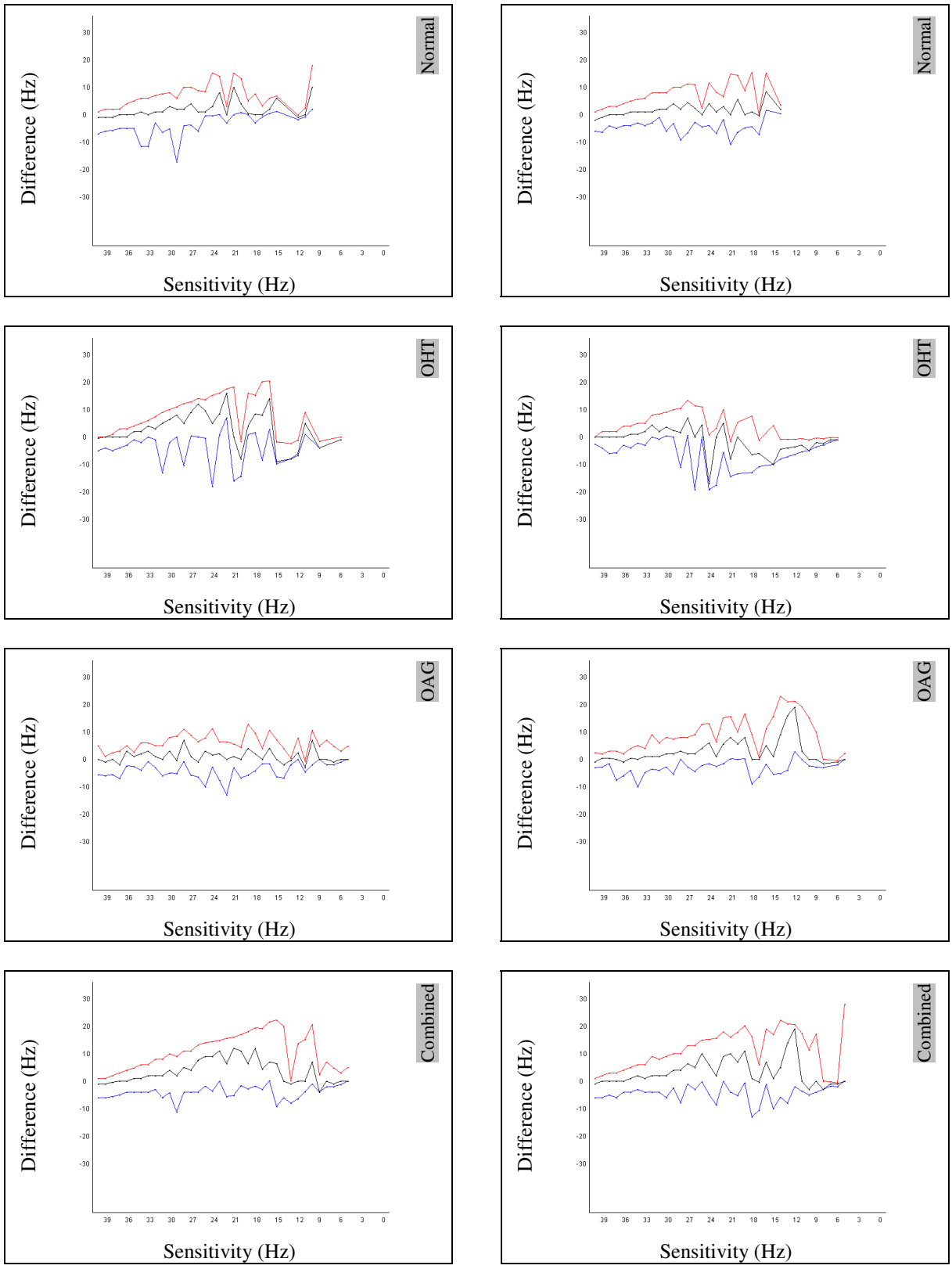

Figure 4.21 The 90th (red), 50th (black) and 10th (blue) percentiles of the distribution of the differences in sensitivity across all stimulus locations between Visits Five and Visit Two as a function of the sensitivity at the corresponding stimulus location recorded at Visit Two for the right (left column) and left (right column) eye, for the normal individuals (top), the individuals with OHT (middle top), the individuals with OAG (middle bottom) and for all three groups, combined (bottom), using the Octopus 311, Program G1, TOP algorithm.

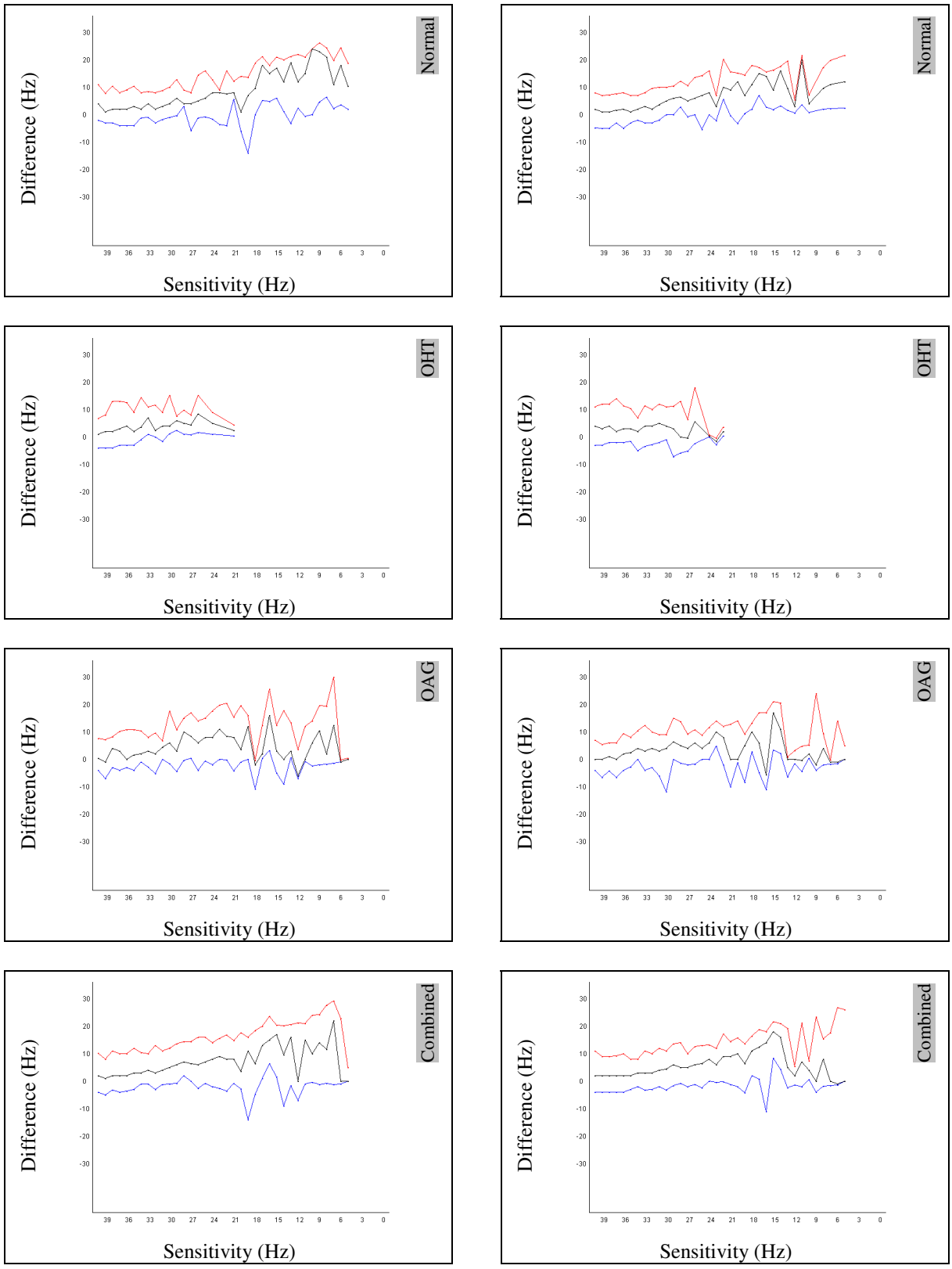

Figure 4.22 The 90th (red), 50th (black) and 10th (blue) percentiles of the distribution of the differences in sensitivity across all stimulus locations between the Dynamic algorithm at Visit Six and the TOP algorithm at Visit Five as a function of the sensitivity at the corresponding stimulus location recorded at for the TOP algorithm at Visit Five for the right (left column) and left (right column) eye, normal individuals (top), the individuals with OHT (middle top), the individuals with OAG (middle bottom) and for all three groups, combined (bottom), using the Octopus 311, Program G1, TOP algorithm.

4.15 The difference in the Comparison Probability value and in the Corrected Comparison Probability value, respectively, across all given stimulus locations between Visit One and Visit Two, between Visit Two and Visit Five and between the TOP algorithm at visit Five and the Dynamic algorithm at visit Six, respectively for each of the three groups, separately, and combined.

The Comparison probability values across all given stimulus locations at Visit Two compared with those at Visit One for the 28 normal individuals, for the 10 individuals with OHT and for the 11 individuals with OAG, and for the three groups, combined, is given in Table 4.28. The corresponding values at Visit Two compared to those at Visit Five are given in Table 4.29. The corresponding values between the TOP algorithm at Visit Five and the Dynamic algorithm at Visit Six are given in Table 4.30. A grater number of data entries below the shaded line (of unity) represents an improvement from Visit One to Visit Two in one or more probability levels at the given location.

The extent of the improvement between Visits One and Two in the Comparison probability value across the normal individuals, as a group, (Table 4.28) was relatively small in each eye, (right eye, 65 locations exhibiting an improvement and 37 locations exhibiting a deterioration, from a total of 1652 locations, i.e. overall, a 1.8 fold improvement,; left eye, 106 locations exhibiting an improvement, 66 locations exhibiting a deterioration i.e. overall, a 1.6 fold improvement). Thus, the field of the right eye showed an improvement of one or more probability levels at 2.3 stimulus locations per individual and a deterioration at 1.3 locations per individual. The field of the left eye showed an improvement at 3.8 locations per individual and a deterioration at 2.4 locations per individual.

The improvement between Visits One and Two in the Comparison probability value across the 10 individuals with OHT, as a group, (Table 4.28) was also modest (right eye, 72 locations exhibiting an improvement, 56 locations exhibiting a deterioration i.e. overall, a 1.3 fold overall

improvement; left eye, 69 locations exhibiting an improvement, and 49 locations exhibiting a deterioration i.e. overall, a 1.4 fold overall improvement). The field of the right eye showed an improvement of one or more probability levels at 7.2 stimulus locations per individual and a deterioration at 5.6 locations per individual. The field of the left eye showed an improvement at 6.9 locations per individual and a deterioration at 4.9 locations per individual.

The improvement between Visits One and Two in the Comparison probability value across the 11 individuals with OAG, as a group, (Table 4.28) was the largest of the three groups, both in absolute and in proportionate terms (right eye, 121 locations exhibiting an improvement, 34 locations exhibiting a deterioration i.e. overall, a 3.5 fold overall improvement; left eye, 123 locations exhibiting an improvement, and 59 locations exhibiting a deterioration i.e. overall, a 2.1 fold overall improvement). The field of the right eye showed an improvement of one more probability levels at 11.0 stimulus locations per individual and a deterioration at 3.1 locations per individual. The field of the left eye showed an improvement at 11.1 locations per individual and a deterioration at 5.3 locations per individual.

One facet of the improvement, apparent, across each of the three groups, particularly for the left eye, was the number of stimulus locations exhibiting abnormality at $p<0.005$ at Visit One which exhibited normality at Visit Two.

Visit One \ Visit Two	NS	<5%	<2%	<1%	<0.5%
NS	1533	13	7	5	2
<5%	30	8	3	0	2
<2%	12	6	6	1	0
<1%	6	0	2	1	4
<0.5%	8	0	0	1	2

Visit One \ Visit Two	NS	<5%	<2%	<1%	<0.5%
NS	1474	31	13	14	3
<5%	24	5	3	0	1
<2%	11	0	1	0	1
<1%	10	0	1	0	0
<0.5%	57	3	0	0	0

Visit One \ Visit Two	NS	<5%	<2%	<1%	<0.5%
NS	453	10	11	3	10
<5%	14	1	1	1	8
<2%	9	4	3	2	9
<1%	2	3	2	1	1
<0.5%	33	1	2	2	4

Visit One \ Visit Two	NS	<5%	<2%	<1%	<0.5%
NS	469	6	6	4	29
<5%	11	0	1	0	1
<2%	19	0	1	0	2
<1%	4	0	1	0	0
<0.5%	28	4	0	2	2

Visit One \ Visit Two	NS	<5%	<2%	<1%	<0.5%
NS	411	8	2	2	2
<5%	42	6	2	2	4
<2%	13	6	3	2	6
<1%	19	1	2	2	4
<0.5%	19	5	6	8	72

Visit One \ Visit Two	NS	<5%	<2%	<1%	<0.5%
NS	370	18	11	2	10
<5%	29	12	2	0	9
<2%	16	2	4	1	4
<1%	7	2	3	5	2
<0.5%	39	11	9	5	76

Visit One \ Visit Two	NS	<5%	<2%	<1%	<0.5%
NS	2397	31	20	10	14
<5%	86	15	6	3	14
<2%	34	16	12	5	15
<1%	27	4	6	4	9
<0.5%	60	6	8	11	78

Visit One \ Visit Two	NS	<5%	<2%	<1%	<0.5%
NS	2313	55	30	20	42
<5%	64	17	6	0	11
<2%	46	2	6	1	7
<1%	21	2	5	5	2
<0.5%	124	18	9	7	78

Table 4.28 The Comparison probability value across all the given stimulus locations at Visit Two compared with that at Visit One for the right eye (left column) and for the left eye (right column) for the 28 normal individuals (top), for the 10 individuals with OHT (middle top) and for the 11 individuals with OAG (middle bottom), and for the three groups, combined (bottom). The shading indicates the number of locations exhibiting identical probability levels at the two examinations. The data entries above the grey line indicate a statistically more severe field loss at Visit Two compared to that at Visit One and those below the line a statistically less severe field loss at Visit Two compared to Visit One, i.e. an improvement from Visit One to Visit Two.

No overall improvement in the Comparison probability value was present between Visits Two and Five for the normal individuals, as a group, (Table 4.29) (right eye, 44 locations exhibiting an improvement and 100 locations exhibiting a deterioration, i.e. overall, a 2.3 fold overall deterioration; left eye, 52 locations exhibiting an improvement, 84 locations exhibiting a deterioration i.e. overall, a 1.6 fold deterioration). The field of the right eye thus showed an improvement of one more probability levels at 1.6. stimulus locations per individual and a deterioration at 3.5 locations per individual. The field of the left eye showed an improvement at 1.8 locations per individual and a deterioration at 3.0 locations per individual.

Little improvement occurred between Visits Two and Five in the Comparison probability value across the 10 individuals with OHT, as a group, (Table 4.29) (right eye, 42 locations exhibiting an improvement, 23 locations exhibiting a deterioration i.e. a 1.8 fold overall improvement; left eye, 40 locations exhibiting an improvement, and 25 locations exhibiting a deterioration i.e. overall, a 1.6 fold overall improvement). The field of the right eye showed an improvement of one or more probability levels at 4.2 stimulus locations per individual and a deterioration at 2.3 locations per individual. The field of the left eye showed an improvement at 4.0 locations per individual and a deterioration at 2.5 locations per individual.

The improvement between Visits Two and Five in the Comparison probability value across the 11 individuals with OAG, as a group, (Table 4.29) was again the largest of the three groups, both in absolute and in proportionate terms (right eye, 51 locations exhibiting an improvement, 46 locations exhibiting a deterioration i.e. overall no improvement; left eye, 110 locations exhibiting an improvement, and 42 locations exhibiting a deterioration i.e. overall, a 2.6 fold overall improvement). The field of the right eye showed an improvement of one or more probability levels at 4.6 stimulus locations per individual and a deterioration at 4.1 locations per individual.

The field of the left eye showed an improvement at 10 locations per individual and a deterioration at 3.8 locations per individual.

Across the three groups, combined, the probability values for the field of the right eye tended to be lower at Visit Five compared with Visit Two whereas the reverse applied for the field of the left eye.

For the TOP algorithm, across the normal individuals, (Table 4.30 Top left) 101 locations for the field of the right eye exhibited a smaller Comparison Probability value (i.e. a statistically deeper defect), compared to the Dynamic algorithm and 41 locations a larger probability value, (i.e. a statistically less deep defect), resulting in overall, a 2.4 fold greater emphasis in the magnitude of the statistical probability associated with the height of the field compared to the Dynamic algorithm. Similarly, (Table 4.30 Top right) the statistical probability was less severe for the field of the left eye with the Dynamic Algorithm (97 locations exhibited a statistically deeper Comparison Probability value for the TOP algorithm compared to the Dynamic algorithm and 27 locations a less severe defect, i.e. overall, a 3.6 fold difference).

Across the 10 individuals with OHT, as a group, (Table 4.30) the Comparison Probability values were almost identical (2 locations for the field of the right eye exhibited a statistically deeper loss by Comparison Probability analysis for the TOP algorithm compared to the Dynamic algorithm and 5 locations the reverse). For the field of the left eye, 3 locations exhibited a statistically deeper loss by Comparison Probability value for the TOP algorithm compared to the Dynamic algorithm and 15 locations a larger probability value).

Visit Two \ Visit Five	NS	<5%	<2%	<1%	<0.5%
NS	1489	29	15	11	39
<5%	21	4	1	2	1
<2%	11	2	7	0	1
<1%	1	2	0	4	1
<0.5%	1	2	1	3	4

Visit Two \ Visit Five	NS	<5%	<2%	<1%	<0.5%
NS	1507	18	16	14	20
<5%	28	3	2	1	4
<2%	12	2	4	0	8
<1%	2	2	0	1	1
<0.5%	5	1	0	0	1

Visit Two \ Visit Five	NS	<5%	<2%	<1%	<0.5%
NS	497	3	1	1	6
<5%	14	2	1	0	3
<2%	10	0	2	0	6
<1%	9	1	0	0	2
<0.5%	6	1	1	0	24

Visit Two \ Visit Five	NS	<5%	<2%	<1%	<0.5%
NS	522	2	1	0	8
<5%	13	0	1	0	4
<2%	12	1	0	0	8
<1%	7	0	1	2	1
<0.5%	5	1	0	0	1

Visit Two \ Visit Five	NS	<5%	<2%	<1%	<0.5%
NS	481	12	11	2	5
<5%	16	2	1	3	1
<2%	7	1	1	3	5
<1%	4	4	0	3	6
<0.5%	4	4	3	8	65

Visit Two \ Visit Five	NS	<5%	<2%	<1%	<0.5%
NS	428	11	8	2	6
<5%	28	8	4	0	3
<2%	24	4	3	2	2
<1%	7	2	2	0	4
<0.5%	26	8	4	5	58

Visit Two \ Visit Five	NS	<5%	<2%	<1%	<0.5%
NS	2467	44	27	14	47
<5%	51	8	3	5	5
<2%	28	3	10	3	12
<1%	14	7	0	7	9
<0.5%	11	7	5	11	93

Visit Two \ Visit Five	NS	<5%	<2%	<1%	<0.5%
NS	2457	31	25	16	34
<5%	69	11	7	1	11
<2%	48	7	7	2	18
<1%	16	4	3	3	6
<0.5%	36	10	4	5	60

Table 4.29 The change in the Comparison probability value across all the given stimulus locations between Visit Five and Visit Two for the right eye (left column) and for the left eye (right column) for the 28 normal individuals (top), for the 10 individuals with OHT (middle top) and for the 11 individuals with OAG (middle bottom), and for the three groups, combined (bottom). The shading indicates the number of locations exhibiting identical probability levels at the two examinations. The data entries above the grey line indicate statistically more severe field loss at Visit Five compared to that at Visit Two and those below the line statistically less severe field loss at Visit Two compared to Visit Five, i.e. an improvement from Visit Two to Visit Five.

Across the 11 individuals with OAG, as a group, (Table 4.30) 72 locations for the field of the right eye exhibited a smaller Comparison Probability value for the TOP algorithm compared to the Dynamic algorithm and 17 locations a larger probability value, i.e. a 4.2 fold reduction in the magnitude of the statistical probability associated with the height of the field recorded with the Dynamic Algorithm. Similarly, the magnitude of the statistical probability associated with the height of the field was reduced for the field of the left eye with the Dynamic Algorithm (68 locations exhibited a smaller Comparison Probability value for the TOP algorithm compared to that of the Dynamic algorithm and 26 locations a larger probability value, i.e. a 2.6 fold reduction.

The reduced magnitude of the statistical probability associated with the height of the field recorded with the Dynamic algorithm compared to that of the TOP algorithm is readily apparent in the data for all three groups, combined, and primarily occurs in the normal individuals and in those with OAG from the number of locations which lies within the normal range for the Dynamic algorithm but are abnormal with the TOP algorithm. Thus, it would appear that the Dynamic algorithm will underestimate the statistical height of the normal visual field compared to that of the TOP algorithm.

TOP Algorithm \ Dynamic Algorithm	NS	<5%	<2%	<1%	<0.5%
NS	1502	16	11	6	5
<5%	28	2	1	0	1
<2%	20	0	2	0	1
<1%	14	0	2	0	0
<0.5%	34	0	1	2	4

TOP \ Dynamic Algorithm	NS	<5%	<2%	<1%	<0.5%
NS	1522	13	6	3	3
<5%	28	2	1	0	0
<2%	16	1	1	0	1
<1%	15	1	0	1	0
<0.5%	33	3	0	0	2

TOP Algorithm \ Dynamic Algorithm	NS	<5%	<2%	<1%	<0.5%
NS	555	2	3	0	0
<5%	1	0	0	0	0
<2%	1	0	0	0	0
<1%	0	0	0	0	0
<0.5%	0	0	0	0	28

TOP \ Dynamic Algorithm	NS	<5%	<2%	<1%	<0.5%
NS	542	4	5	1	3
<5%	2	0	1	0	1
<2%	1	0	1	0	0
<1%	0	0	0	0	0
<0.5%	0	0	0	0	29

TOP Algorithm \ Dynamic Algorithm	NS	<5%	<2%	<1%	<0.5%
NS	497	6	3	1	0
<5%	23	1	1	0	2
<2%	12	3	2	1	2
<1%	8	0	3	2	1
<0.5%	15	3	1	4	58

TOP \ Dynamic Algorithm	NS	<5%	<2%	<1%	<0.5%
NS	490	10	2	1	7
<5%	26	2	2	1	1
<2%	12	4	1	0	2
<1%	8	0	0	1	0
<0.5%	13	2	2	1	61

TOP Algorithm \ Dynamic Algorithm	NS	<5%	<2%	<1%	<0.5%
NS	2554	24	17	7	5
<5%	52	3	2	0	3
<2%	33	3	4	1	3
<1%	22	0	5	2	1
<0.5%	49	3	2	6	90

TOP \ Dynamic Algorithm	NS	<5%	<2%	<1%	<0.5%
NS	2554	27	13	5	13
<5%	56	4	4	1	2
<2%	29	5	3	0	3
<1%	23	1	0	2	0
<0.5%	46	5	2	1	92

Table 4.30 The change in the Comparison probability value across all the given stimulus locations between the Dynamic Algorithm at Visit Six and the TOP Algorithm at Visit Five for the right eye (left column) and for the 28 normal individuals (top), for the 10 individuals with OHT (middle top) and for the 11 individuals with OAG (middle bottom), and for the three groups, combined (bottom). The data entries above the grey line indicate statistically more severe field loss at Visit Six using the Dynamic algorithm compared to that at Visit Five using the TOP algorithm and those below the line a statistically less severe field loss at Visit Six using the Dynamic algorithm compared to Visit Five using the TOP algorithm.

All 49 individuals across the three groups exhibited identical Comparison and Corrected Comparison probability maps in both eyes at each of the 6 visits. It was subsequently learned that the corrected comparison map was not calculated for CFF. This outcome avoided the necessity to evaluate the learning effect in terms of the changes in Corrected Comparison Probability level.

4.16 The within-individual between-visit change in performance of the visual field indices between Visits One to Two and Visit Two to Five.

The within-individual between-visit change in performance was considered firstly, in terms of the absolute change, for each of the visual field indices, between Visit One and Visit Two compared to that between Visit Two and Visit Five; and, secondly, in terms of the proportionate change in the MS index, only, between Visit One and Visit Two compared to that between Visit Two and Visit Five. Such an analysis was undertaken to compare, for each individual, the magnitude of the learning effect occurring between the first two examinations with that occurring over the remaining visits.

4.16.1 Mean Sensitivity

The difference in the MS from Visit One to Visit Two compared to that between Visit Two and Visit Five for each eye of the 28 normal individuals is shown graphically in Figure 4.23. The corresponding difference in proportionate terms are given in Table 4.31.

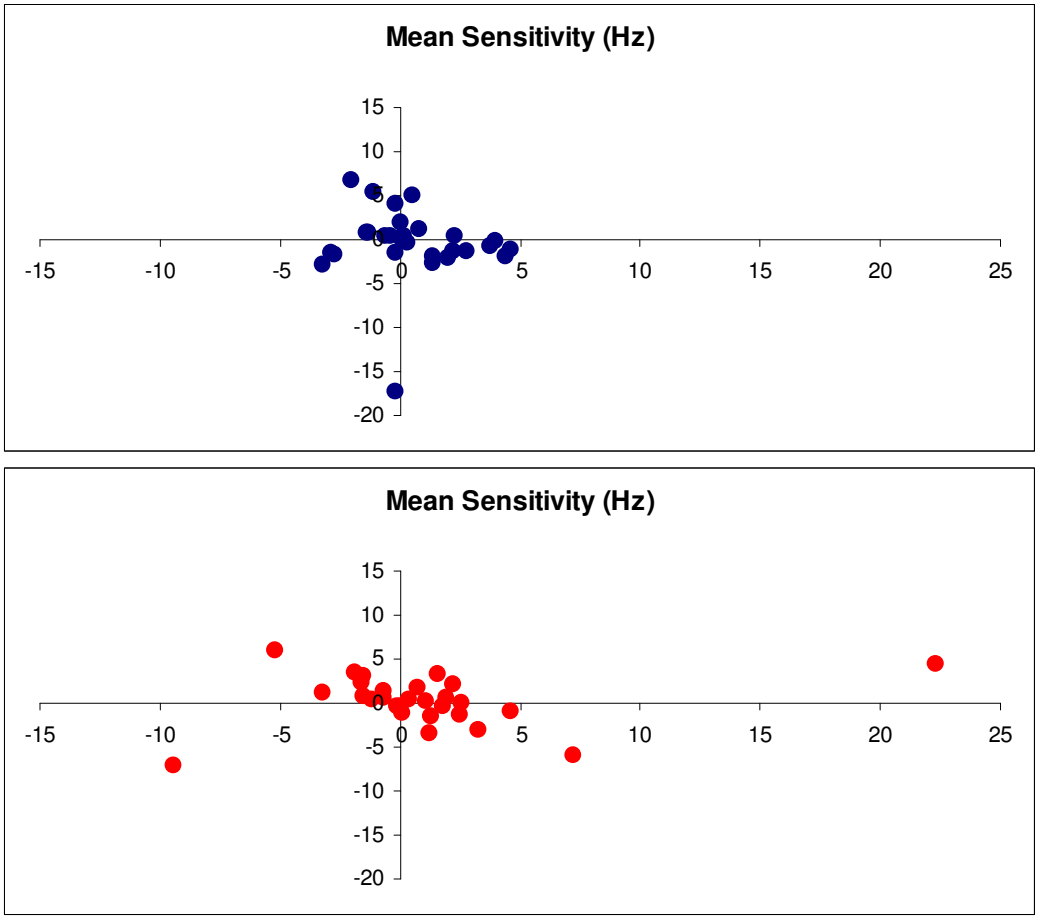

Figure 4.23 The scatter plot of the difference in the magnitude of the MS_{CFF} (Hz) between Visit One and Visit Two (abscissa) against the difference in the magnitude between Visit Two and Visit Five (ordinate) for each of the 28 normal individuals for the right (top), and left (bottom) eyes. Data points in the top left quadrant represent a deterioration from Visit One to Visit Two and an improvement from Visit Two to Visit Five. Data points in the top right quadrant represent an improvement from Visit One to Visit Two and also from Visit Two to Visit Five. Data points in the bottom right quadrant represent an improvement from Visit One to Visit Two and a deterioration from Visit Two to Visit Five. Data points in the bottom left quadrant represent a deterioration both from Visit One to Visit Two and from Visit Two to Visit Five.

A wide variation in performance between Visits One and Two was present amongst the normal individuals both between-eyes of an individual and between individuals for a given eye. A similar variation was present between Visits Two and Five, not only between-eyes of an individual and between individuals for a given eye but also between the two pairs of visits.

The difference in the MS from Visit One to Visit Two compared to the difference between Visit Two and Visit Five for each eye of the 10 individuals with OHT is shown graphically in Figure 4.24. The corresponding difference in proportionate terms is given in Table 4.32. Six of the 10 individuals with OHT exhibited an improvement in each eye from Visit One to Visit Two. Of these six individuals, two also exhibited an improvement in each eye from Visit Two to Visit Five.

The difference in the MS from Visit One to Visit Two compared to the difference between Visit Two and Visit Five for each eye of the 11 individuals with OAG is shown graphically in Figure 4.25. The corresponding difference in proportionate terms is given in Table 4.33. Seven of the 11 individuals with OAG exhibited an improvement in each eye from Visit One to Visit Two (Table 4.33). Of these seven individuals, five also exhibited an improvement in each eye from Visit Two to Visit Five. The magnitude of the improvement varied both between-eyes of an individual and between individuals for a given eye and also between the two pairs of visits

Case Number	Right Eye Absolute Change (Hz) V1 to V2	Right Eye Proportionate Change (%) V1 to V2	Right Eye Absolute Change (Hz) V2 to V5	Right Eye Proportionate Change (%) V2 to V5	Left Eye Absolute Change (Hz) V1 to V2	Left Eye Proportionate Change (%) V1 to V2	Left Eye Absolute Change (Hz) V2 to V5	Left Eye Proportionate Change(%) V2 to V5
1	2.80	8.41%	-1.40	-3.88%	0.10	0.28%	-1.10	-3.06%
2	-2.00	-5.71%	6.70	20.30%	22.30	170.23%	4.50	12.71%
3	-2.90	-8.26%	-1.50	-4.66%	-1.60	-5.06%	2.40	8.00%
4	-0.20	-0.65%	4.10	13.40%	1.20	3.93%	-3.40	-10.73%
5	-0.60	-1.53%	0.40	1.03%	-0.70	-1.82%	0.50	1.32%%
6	0.50	1.45%	5.00	14.25%	-1.90	-5.21%	3.50	10.12%
7	3.80	11.55%	-0.70	-1.91%	1.90	5.57%	0.50	1.39%
8	-3.20	-8.82%	-2.90	-8.76%	2.60	8.52%	0.00	0.00%
9	-1.10	-3.44%	5.30	17.15%	-5.20	-14.73%	5.90	19.60%
10	-2.70	-7.56%	-1.80	-5.45%	3.30	10.09%	-3.00	-8.33%
11	0.00	0.00%	0.20	0.53%	-1.20	-2.99%	0.30	0.77%
12	-0.20	-0.61%	-17.30	-53.23%	-9.40	-25.68%	-7.20	-26.47%
13	4.60	13.81%	-1.10	-2.90%	-0.10	-0.27%	-0.30	-0.80%
14	0.00	0.00%	2.00	6.33%	1.60	5.23%	3.20	9.94%
15	-0.20	-0.54%	-1.50	4.07%	0.40	1.05%	0.30	0.78%
16	0.30	0.81%	-0.30	-0.80%	-3.20	-8.29%	1.20	3.39%
17	-0.40	-0.94%	0.40	0.95%	-1.50	-3.55%	0.80	1.96%
18	1.40	3.74%	-2.00	-5.15%	2.50	6.51%	-1.30	-3.18%
19	-1.40	-3.92%	0.80	2.33%	2.20	6.90%	2.20	6.45%
20	2.20	6.21%	-1.40	-3.72%	1.30	3.74%	-1.60	-4.43%
21	0.20	0.49%	0.40	0.98%	0.00	0.00%	-0.30	-0.74%
22	1.40	4.83%	-2.60	-8.55%	4.60	14.42%	-0.90	-2.47%
23	4.00	13.65%	-0.10	-0.30%	1.10	3.50%	0.10	0.31%
24	2.00	6.13%	-2.20	-6.36%	-0.70	-2.19%	1.30	4.15%
25	2.30	6.53%	0.40	1.07%	1.80	5.11%	-0.30	-0.81%
26	-1.30	-3.88%	0.80	2.48%	0.70	2.16%	1.80	5.44%
27	4.40	12.87%	-1.90	-4.92%	-1.50	-4.32%	3.10	9.34%
28	0.80	2.83%	1.10	3.78%	7.20	26.18%	-5.90	-17.00%

Table 4.31 The absolute (Hz) and proportionate change (%) in MS_{CFF} for each eye of the 28 individuals between Visit One and Visit Two and between Visit Two and Visit Five. The green shading denotes an improvement from the first to the second visit of either given paired comparison. The red shading denotes a deterioration from the first to the second field of either given paired comparison.

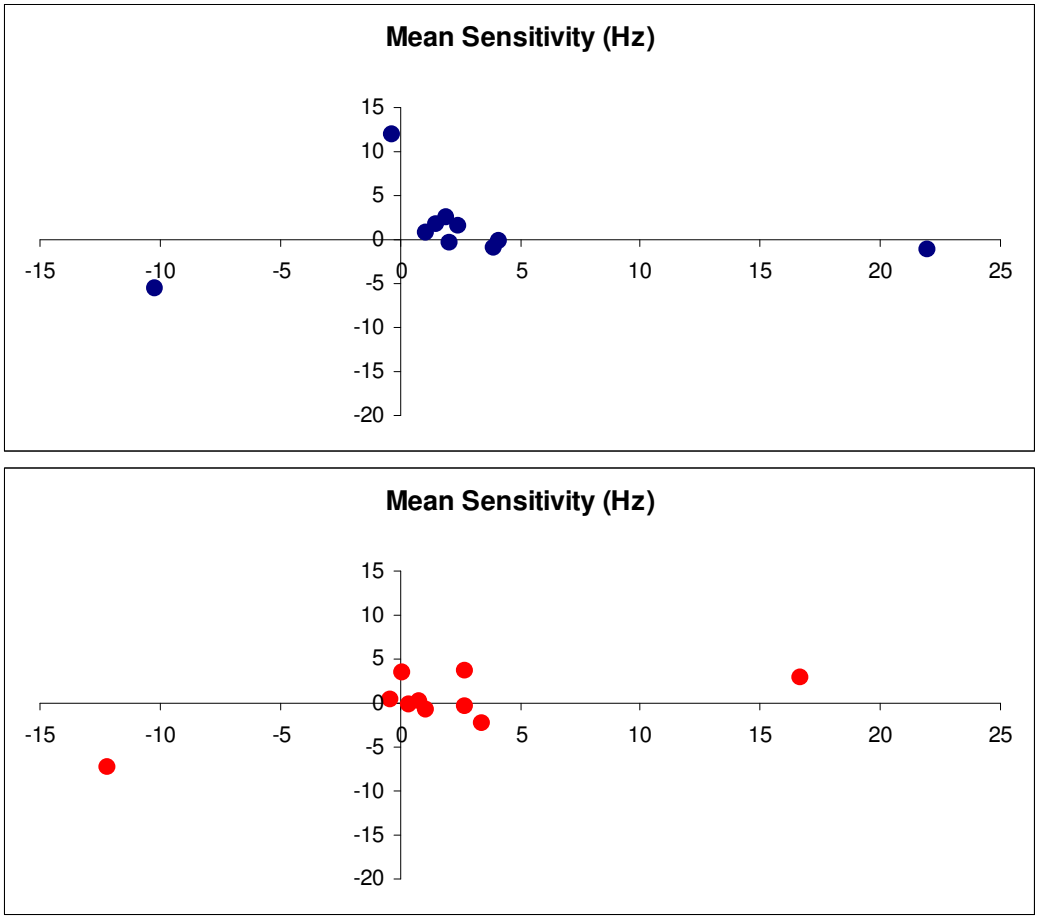

Figure 4.24 The scatter plot of the difference in the magnitude of the MS_{CFF} (Hz) between Visit One and Visit Two (abscissa) against the difference in the magnitude between Visit Two and Visit Five (ordinate) for each of the 10 individuals with OHT for the right (top), and left (bottom) eyes. A negative value represents deterioration in performance. Data points in the top left quadrant represent a deterioration from Visit One to Visit Two and an improvement from Visit Two to Visit Five. Data points in the top right quadrant represent an improvement from Visit One to Visit Two and also from Visit Two to Visit Five. Data points in the bottom right quadrant represent an improvement from Visit One to Visit Two and a deterioration from Visit Two to Visit Five. Data points in the bottom left quadrant represent a deterioration both from Visit One to Visit Two and from Visit Two to Visit Five.

Case Number	Right Eye Absolute Change (Hz) V1 to V2	Right Eye Proportionate Change (%) V1 to V2	Right Eye Absolute Change (Hz) V2 to V5	Right Eye Proportionate Change (%) V2 to V5	Left Eye Absolute Change (Hz) V1 to V2	Left Eye Proportionate Change (%) V1 to V2	Left Eye Absolute Change (Hz) V2 to V5	Left Eye Proportionate Change(%) V2 to V5
1	3.90	12.23%	-0.90	-2.51%	3.40	10.97%	-2.30	-6.90%
2	-10.20	-35.17%	-5.60	-29.79%	-12.20	-40.26%	-7.40	-40.88%
3	1.10	3.08%	0.70	1.90%	2.70	8.39%	3.60	10.32%
4	1.50	4.49%	1.70	4.87%	2.70	8.18%	-0.30	-0.84%
5	4.10	12.89%	-0.10	-0.28%	1.10	3.20%	-0.70	-1.97%
6	2.40	7.36%	1.50	4.29%	0.40	1.16%	-0.10	-0.29%
7	2.10	5.69%	-0.40	-1.03%	-0.40	-1.03%	0.30	0.78%
8	22.00	137.50%	-1.10	-2.89%	16.70	93.82%	2.90	8.41%
9	1.90	5.65%	2.50	7.04%	0.80	2.20%	0.10	0.27%
10	-0.30	-1.17%	12.00	47.24%	0.10	0.29%	3.40	9.69%

Table 4.32 The absolute (Hz) and proportionate change (%) in MS_{CFF} for each eye of the 10 individuals with OHT between Visit One and Visit Two and between Visit Two and Visit Five. The green shading denotes an improvement from the first to the second field of either given paired comparison. The red shading denotes a deterioration from the first to the second field of either given paired comparison.

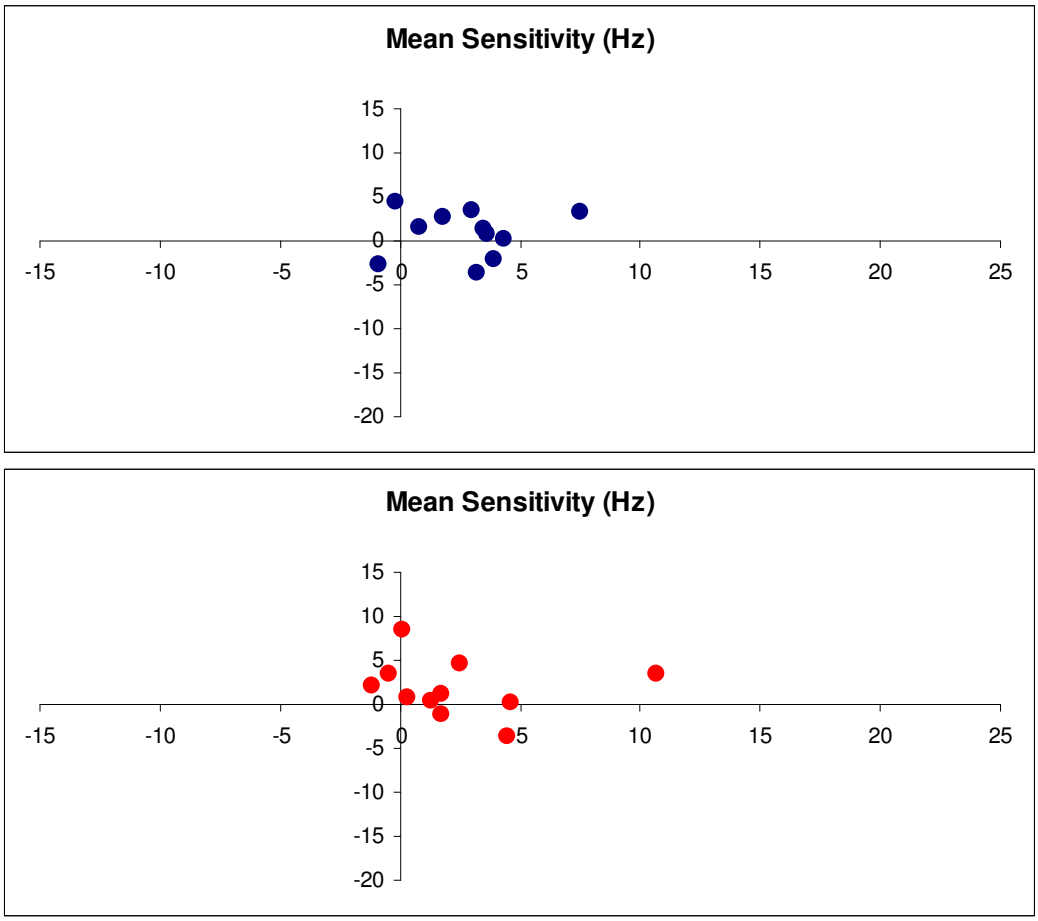

Figure 4.25 The scatter plot of the difference in the magnitude of the MS_{CFF} (Hz) between Visit One and Visit Two (abscissa) against the difference in the magnitude between Visit Two and Visit Five (ordinate) for each of the 11 individuals with OAG for the right (top), and left (bottom) eyes. A negative value represents a deterioration in performance. Data points in the top left quadrant represent a deterioration from Visit One to Visit Two and an improvement from Visit Two to Visit Five. Data points in the top right quadrant represent an improvement from Visit One to Visit Two and also from Visit Two to Visit Five. Data points in the bottom right quadrant represent an improvement from Visit One to Visit Two and a deterioration from Visit Two to Visit Five. Data points in the bottom left quadrant represent a deterioration both from Visit One to Visit Two and from Visit Two to Visit Five.

Case Number	Right Eye Absolute Change (Hz) V1 to V2	Right Eye Proportionate Change (%) V1 to V2	Right Eye Absolute Change (Hz) V2 to V5	Right Eye Proportionate Change (%) V2 to V5	Left Eye Absolute Change (Hz) V1 to V2	Left Eye Proportionate Change (%) V1 to V2	Left Eye Absolute Change (Hz) V2 to V5	Left Eye Proportionate Change(%) V2 to V5
1	3.60	16.98%	0.80	3.23%	4.60	13.33%	0.20	0.51%
2	4.30	21.18%	0.20	0.81%	-1.20	-5.36%	2.10	9.91%
3	-0.90	-2.64%	-2.70	-8.13%	1.70	6.56%	-1.10	-3.99%
4	-0.20	-0.61%	4.50	13.72%	1.30	3.95%	0.40	1.17%
5	0.80	1.96%	1.50	3.60%	0.30	0.71%	0.70	1.64%
6	3.50	12.03%	1.30	3.99%	0.10	0.42%	8.50	35.86%
7	3.20	13.73%	-3.60	-13.58%	4.50	22.50%	-3.70	-15.10%
8	7.50	27.68%	3.30	9.54%	10.70	50.95%	3.40	10.73%
9	1.80	6.55%	2.60	8.87%	2.50	12.63%	4.70	21.08%
10	3.90	21.31%	-2.10	-9.46%	1.70	7.00%	1.10	4.23%
11	3.00	10.79%	3.50	11.36%	-0.50	-1.67%	3.50	11.86%

Table 4.33 The absolute (Hz) and proportionate change (%) in MS_{CFF} for each eye of the 11 individuals with OAG between Visit One and Visit Two and between Visit Two and Visit Five. The green shading denotes an improvement from the first to the second field of either given paired comparison. The red shading denotes a deterioration from the first to the second field of either given paired comparison.

4.16.2 Mean Defect

The difference in the MD from Visit One to Visit Two compared to the difference from Visit Two to Visit Five for each eye of the 28 normal individuals, for each eye of the 10 individuals with OHT and for each eye of the 11 individuals with OAG is shown graphically in Figures 4.26 to Figure 4.28.

As would be expected from the analysis of the MS, a wide variation in performance between Visits One and Two was present amongst the normal individuals both between-eyes of an individual and between individuals for a given eye. A similar variation was present for the MD, sLV, DD and LD between Visits Two and Five not only between-eyes of an individual and between individuals for a given eye but also between the two pairs of visits.

The difference in the MD from Visit One to Visit Two compared to the difference from Visit Two to Visit Five for each eye of the 10 individuals with OHT showed that five of the individuals with OHT exhibited an improvement in each eye both from Visit One to Visit Two and from Visit Two to Visit Five. Three of the 10 individuals showed an improvement from Visit One to Visit Two and a deterioration from Visit Two to Visit Five in the right eye. For the left eye, four of the individuals showed an improvement both from Visit One to Visit Two and from Visit Two to Visit Five whilst four individuals improved from Visit One to Visit Two but deteriorated from Visit Two to Visit Five.

The difference in the MD from Visit One to Visit Two compared to the difference from Visit Two to Visit Five for each eye of the 11 individuals with OAG showed that six individuals exhibited an improvement in the right eye from Visit One to Visit Two and from Visit Two to Visit Five. Seven individuals exhibited the corresponding improvements in the left eye.

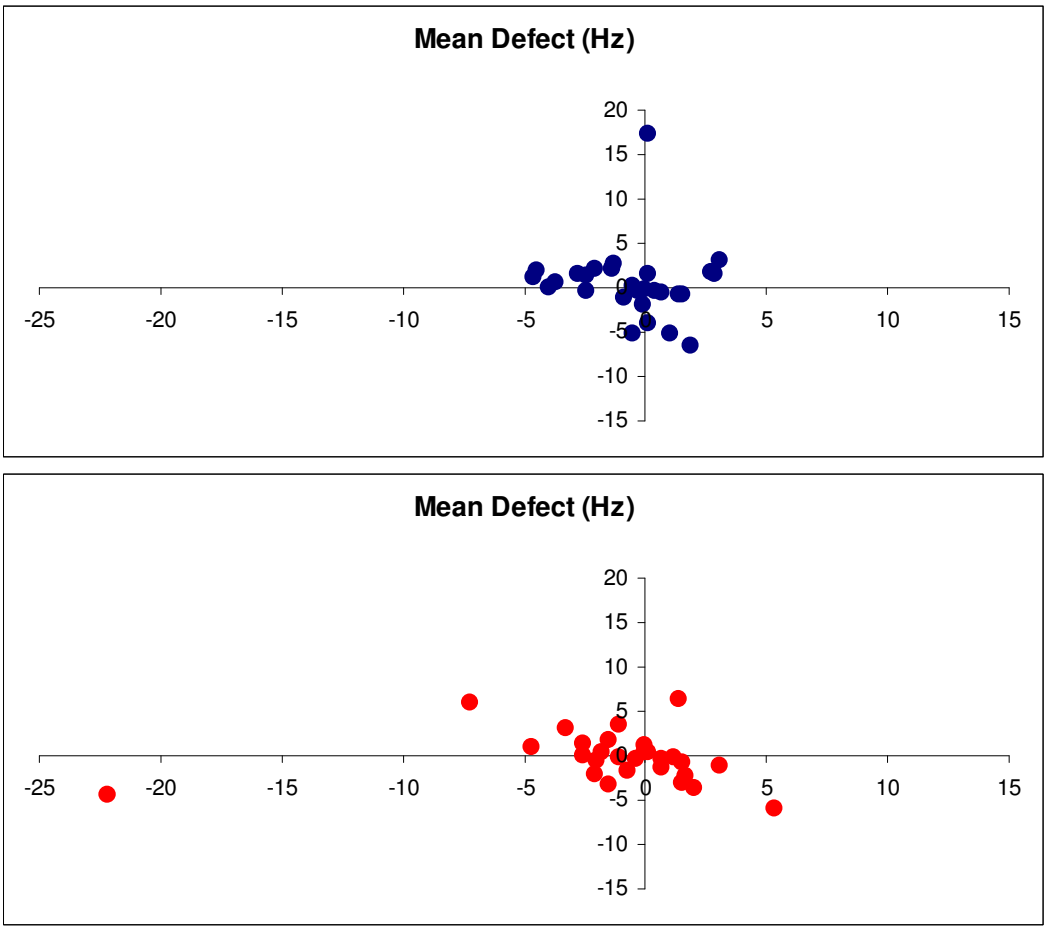

Figure 4.26 The scatter plot of the difference in the magnitude of the MD_{CFF} (Hz) between Visit One and Visit Two (abscissa) against the difference in the magnitude between Visit Two and Visit Five (ordinate) for each of the 28 normal individuals for the right (top), and left (bottom) eyes. A negative value represents an improvement in performance. Data points in the top left quadrant represent an improvement from Visit One to Visit Two and a deterioration from Visit Two to Visit Five. Data points in the top right quadrant represent a deterioration from Visit One to Visit Two and also from Visit Two to Visit Five. Data points in the bottom right quadrant represent a deterioration from Visit One to Visit Two and an improvement from Visit Two to Visit Five. Data points in the bottom left quadrant represent an improvement both from Visit One to Visit Two and from Visit Two to Visit Five.

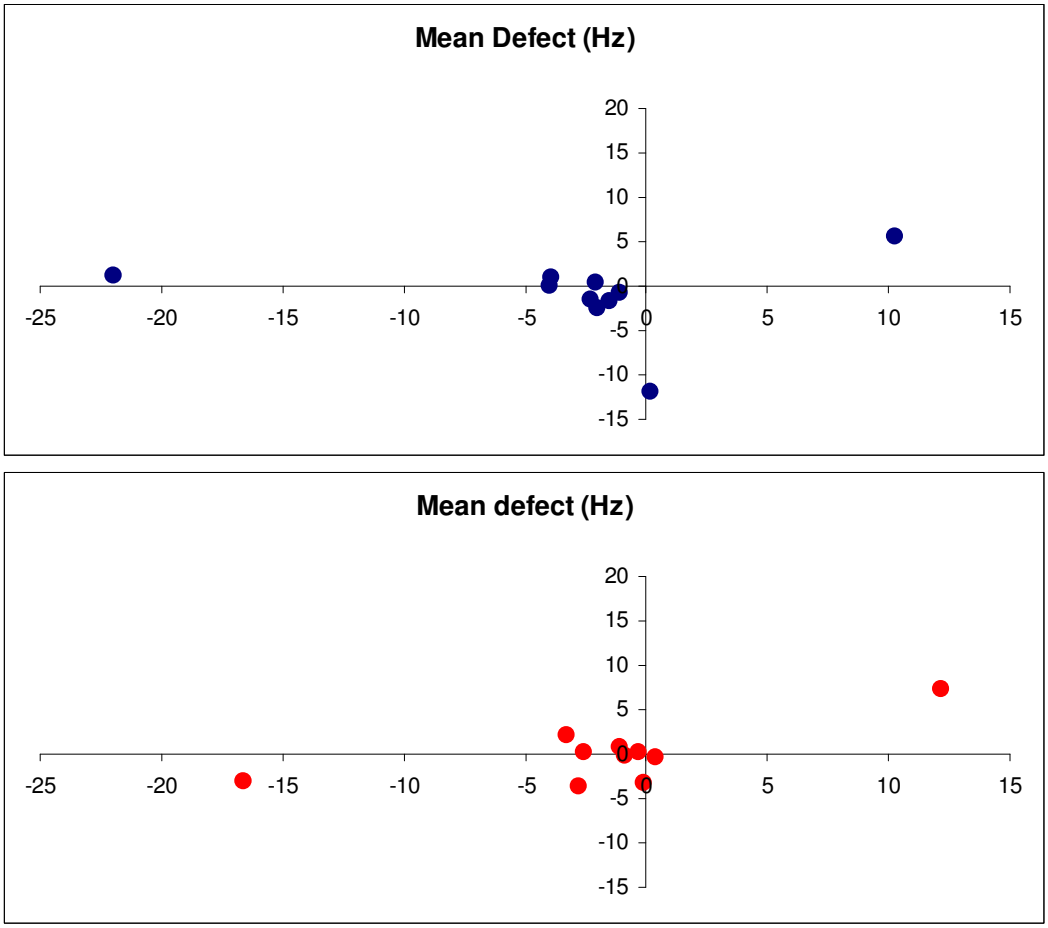

Figure 4.27 The scatter plot of the difference in the magnitude of the MD_{CFF} (Hz) between Visit One and Visit Two (abscissa) against the difference in the magnitude between Visit Two and Visit Five (ordinate) for each of the 10 individuals with OHT for the right (top), and left (bottom) eyes. A negative value represents an improvement in performance. Data points in the top left quadrant represent an improvement from Visit One to Visit Two and a deterioration from Visit Two to Visit Five. Data points in the top right quadrant represent a deterioration from Visit One to Visit Two and also from Visit Two to Visit Five. Data points in the bottom right quadrant represent a deterioration from Visit One to Visit Two and an improvement from Visit Two to Visit Five. Data points in the bottom left quadrant represent an improvement both from Visit One to Visit Two and from Visit Two to Visit Five.

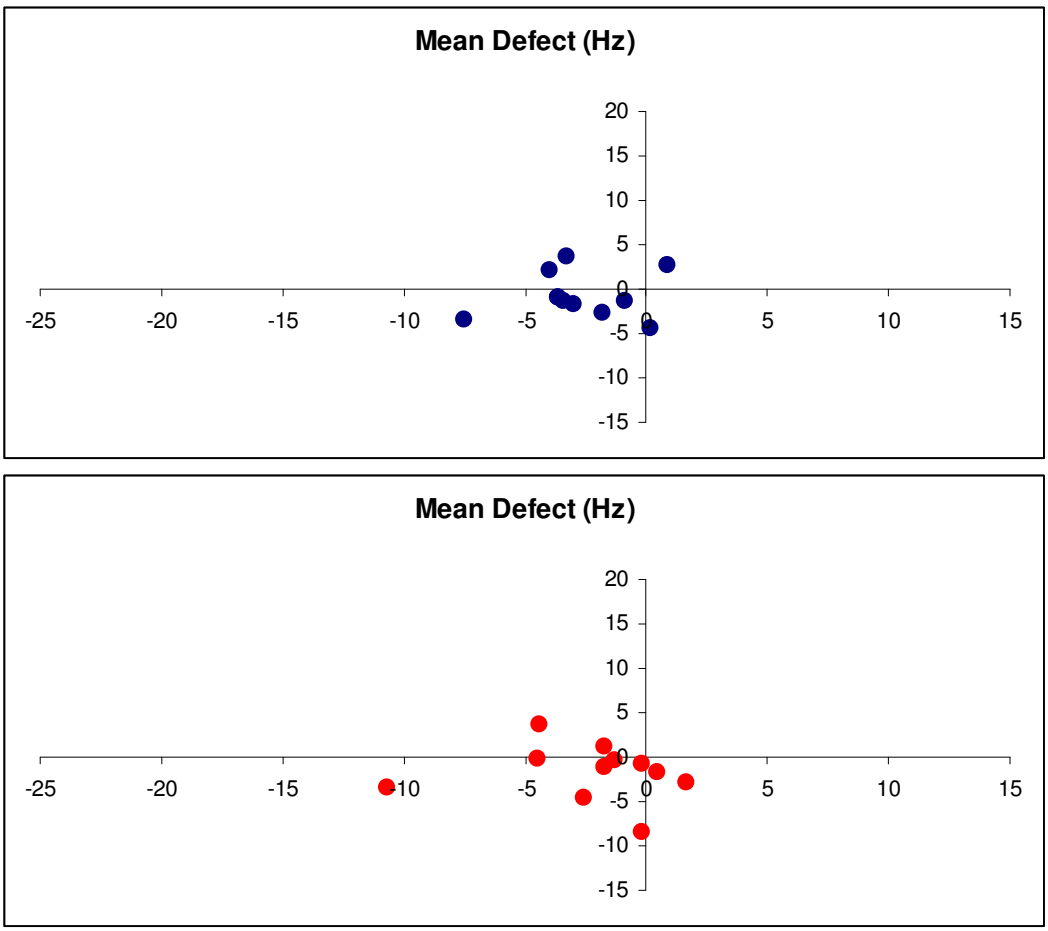

Figure 4.28 The scatter plot of the difference in the magnitude of the MD_{CFF} (Hz) between Visit One and Visit Two (abscissa) against the difference in the magnitude between Visit Two and Visit Five (ordinate) for each of the 11 individuals with OAG for the right (top), and left (bottom) eyes. A negative value represents an improvement in performance. Data points in the bottom left quadrant represent an improvement from Visit One to Visit Two and a deterioration from Visit Two to Visit Five. Data points in the top right quadrant represent a deterioration from Visit One to Visit Two and also from Visit Two to Visit Five. Data points in the bottom right quadrant represent a deterioration from Visit One to Visit Two and an improvement from Visit Two to Visit Five. Data points in the bottom left quadrant represent an improvement both from Visit One to Visit Two and from Visit Two to Visit Five.

4.16.3 Square root of the Loss Variance

The difference in the sLV from Visit One to Visit Two compared to the difference from Visit Two to Visit Five for each eye of the 28 normal individuals in, of the 10 individuals with OHT and of the 11 individuals with OAG are shown in Figures 4.29, 4.30, and 4.31, respectively.

The difference in the sLV from Visit One to Visit Two compared to the difference from Visit Two to Visit Five for each eye of the 10 individuals with OHT showed that, for the right eye, five exhibited an improvement from Visit One to Visit Two and a deterioration from Visit Two to Visit Five and 3 individuals an improvement from Visit Two to Visit Five and a deterioration from Visit One to Visit Two. For the left eye, three individuals showed an improvement both from Visit One to Visit Two and from Visit Two to Visit Five. Five individuals deteriorated from Visit One to Visit Two but improved from Visit Two to Visit Five.

The difference in the sLV from Visit One to Visit Two compared to the difference from Visit Two to Visit Five for each eye of the 11 individuals with OAG showed that, for the right eye, two individuals exhibited an improvement from Visit One to Visit Two and from Visit Two to Visit Five and three individuals exhibited an improvement between Visit One and Visit Two and a deterioration from Visit Two to Visit Five. For the left eye, four individuals exhibited an improvement from Visit One to Visit Two and from Visit Two to Visit Five.

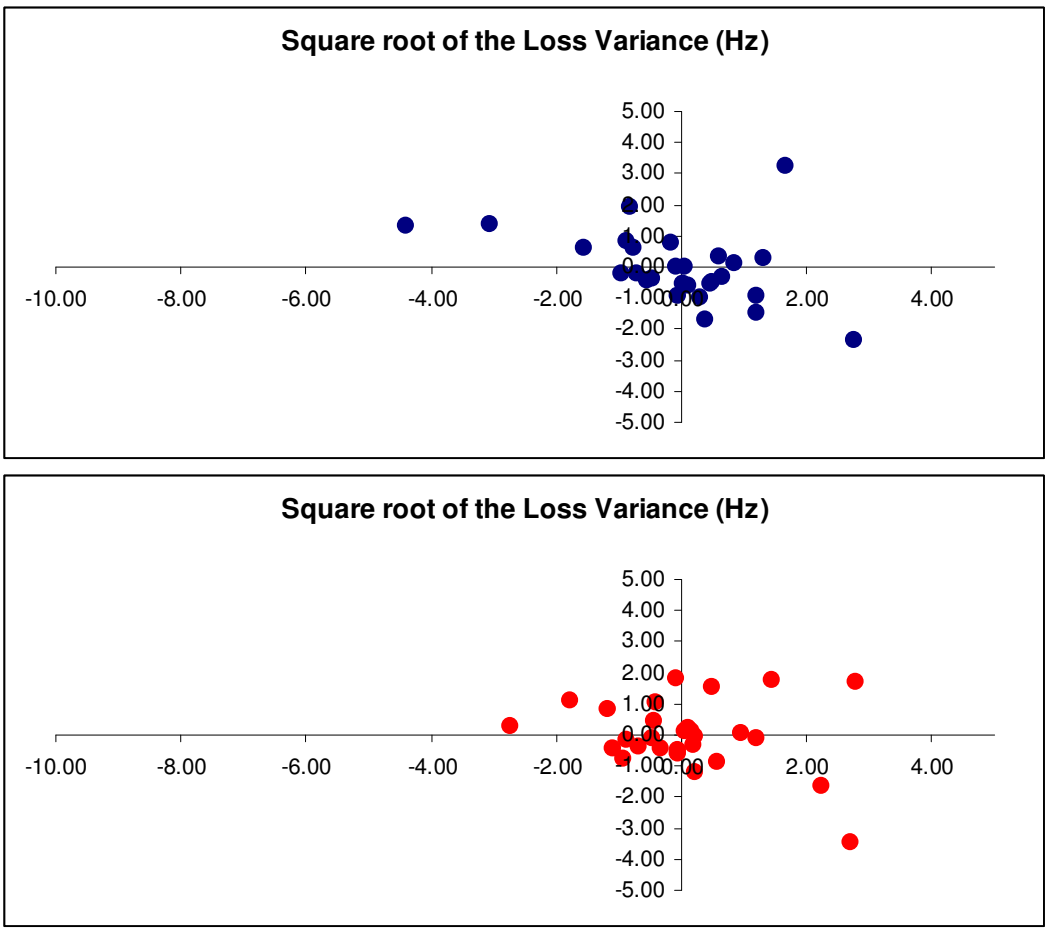

Figure 4.29 The scatter plot of the difference in the magnitude of the sLV_{CFF} (Hz) between Visit One and Visit Two (abscissa) against the difference in the magnitude between Visit Two and Visit Five (ordinate) for each of the 28 normal individuals for the right (top), and left (bottom) eyes. A negative value represents an improvement in performance. Data points in the superior left quadrant represent an improvement from Visit One to Visit Two and a deterioration from Visit Two to Visit Five. Data points in the superior right quadrant represent deterioration from Visit One to Visit Two and also from Visit Two to Visit Five. Data points in the inferior right quadrant represent deterioration from Visit One to Visit Two and an improvement from Visit Two to Visit Five. Data points in the inferior left quadrant represent an improvement both from Visit One to Visit Two and from Visit Two to Visit Five.

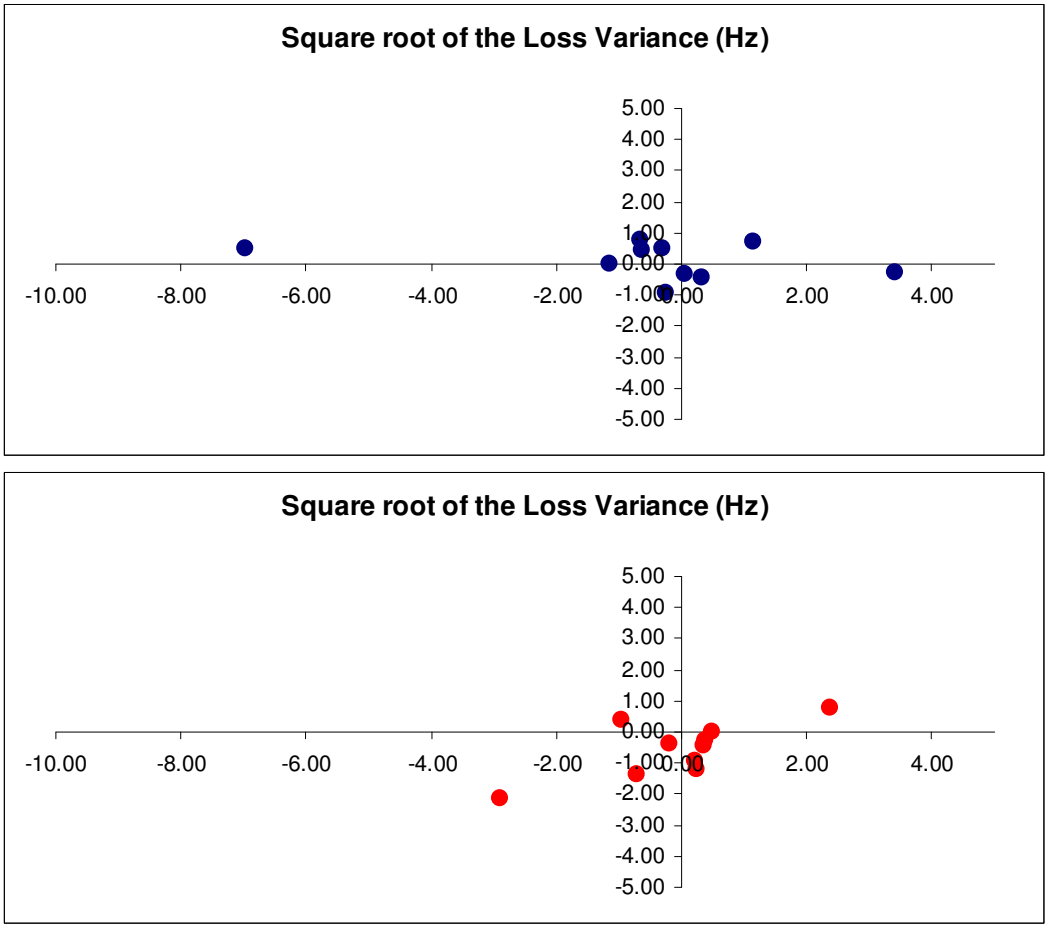

Figure 4.30 The scatter plot of the difference in the magnitude of the sLV_{CFF} (Hz) between Visit One and Visit Two (abscissa) against the difference in the magnitude between Visit Two and Visit Five (ordinate) for each of the 10 individuals with OHT for the right (top), and left (bottom) eyes. A negative value represents an improvement in performance. Data points in the superior left quadrant represent an improvement from Visit One to Visit Two and a deterioration from Visit Two to Visit Five. Data points in the superior right quadrant represent deterioration from Visit One to Visit Two and also from Visit Two to Visit Five. Data points in the inferior right quadrant represent deterioration from Visit One to Visit Two and an improvement from Visit Two to Visit Five. Data points in the inferior left quadrant represent an improvement both from Visit One to Visit Two and from Visit Two to Visit Five.

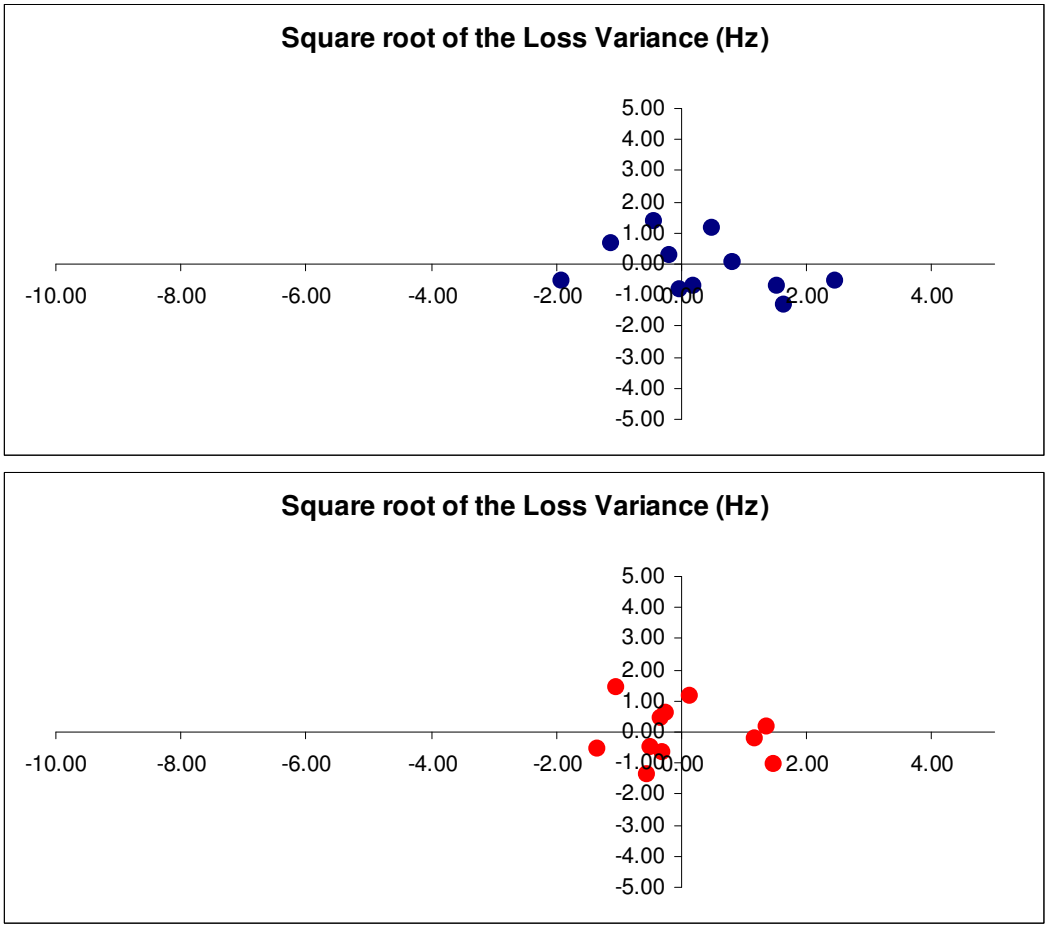

Figure 4.31 The scatter plot of the difference in the magnitude of the sLV_{CFF} (Hz) between Visit One and Visit Two (abscissa) against the difference in the magnitude between Visit Two and Visit Five (ordinate) for each of the 11 individuals with OHT for the right (top), and left (bottom) eyes. A negative value represents an improvement in performance. Data points in the superior left quadrant represent an improvement from Visit One to Visit Two and a deterioration from Visit Two to Visit Five. Data points in the superior right quadrant represent deterioration from Visit One to Visit Two and also from Visit Two to Visit Five. Data points in the inferior right quadrant represent deterioration from Visit One to Visit Two and an improvement from Visit Two to Visit Five. Data points in the inferior left quadrant represent an improvement both from Visit One to Visit Two and from Visit Two to Visit Five.

4.16.4 Diffuse Defect

The difference in the DD from Visit One to Visit Two compared to the difference between Visit Two and Visit Five for each eye of the 28 normal individuals, of the 10 individuals with OHT and of the 11 individuals with OAG is shown graphically in Figure 4.32 to Figure 4.34, respectively.

The difference in the DD from Visit One to Visit Two compared to the difference from Visit Two to Visit Five for each eye of the 10 individuals with OHT showed that, for the field of the right eye, three individuals exhibited an improvement in each eye from Visit One to Visit Two and from Visit Two to Visit Five and five individuals an improvement from Visit One to Visit Two and a deterioration from Visit Two to Visit Five. For the left eye, five showed an improvement from Visit One to Visit Two and from Visit Two to Visit Five and three individuals improvement from Visit One to Visit Two but a deterioration from Visit Two to Visit Five.

The difference in the DD from Visit One to Visit Two compared to the difference from Visit Two to Visit Five for each eye of the 11 individuals with OAG showed that six of the individuals exhibited an improvement from Visit One to Visit Two and from Visit Two to Visit Five for both eyes and three individuals an improvement between Visit One and Visit Two and a deterioration between Visit Two and Visit Five for both eyes.

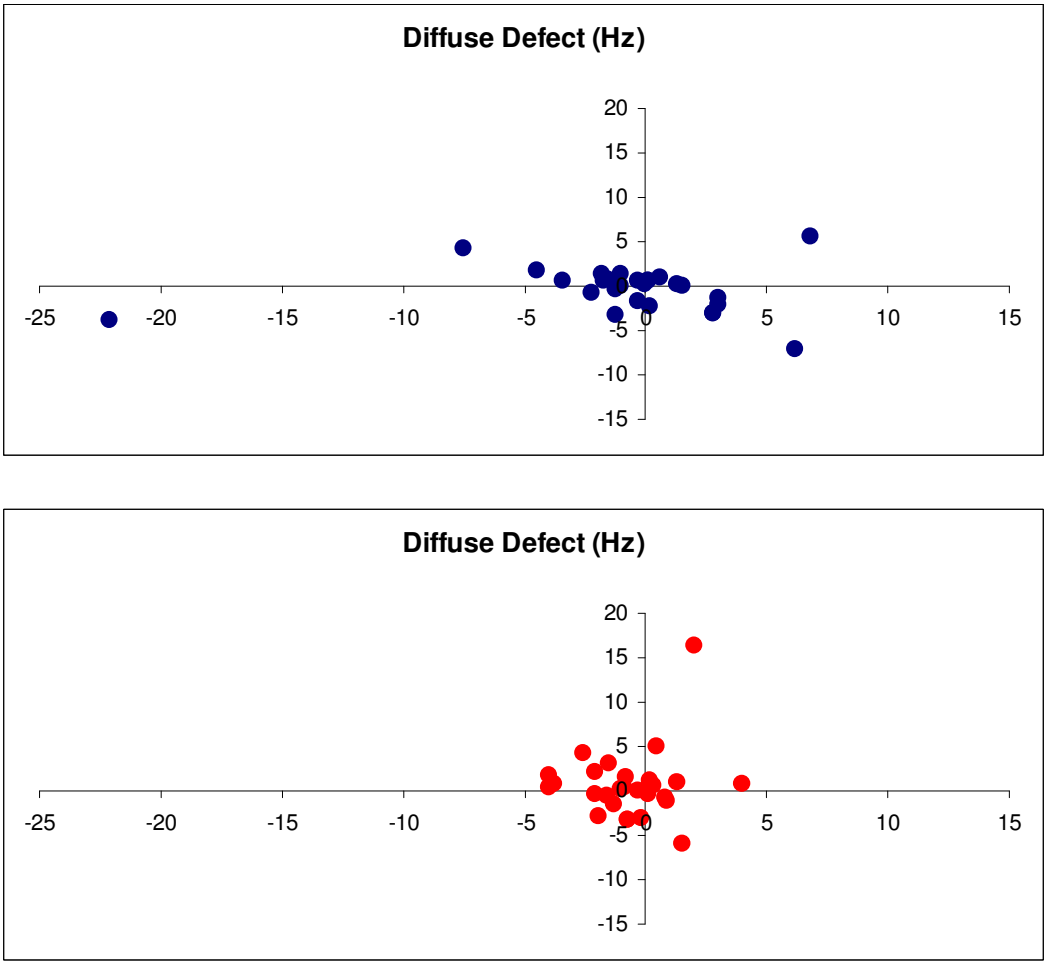

Figure 4.32 The scatter plot of the difference in the magnitude of the DD_{CFF} (Hz) between Visit One and Visit Two (abscissa) against the difference in the magnitude between Visit Two and Visit Five (ordinate) for each of the 28 normal individuals for the right (top), and left (bottom) eyes. A negative value represents an improvement in performance. Data points in the superior left quadrant represent an improvement from Visit One to Visit Two and deterioration from Visit Two to Visit Five. Data points in the superior right quadrant represent deterioration from Visit One to Visit Two and also from Visit Two to Visit Five. Data points in the inferior right quadrant represent deterioration from Visit One to Visit Two and an improvement from Visit Two to Visit Five. Data points in the inferior left quadrant represent an improvement both from Visit One to Visit Two and from Visit Two to Visit Five.

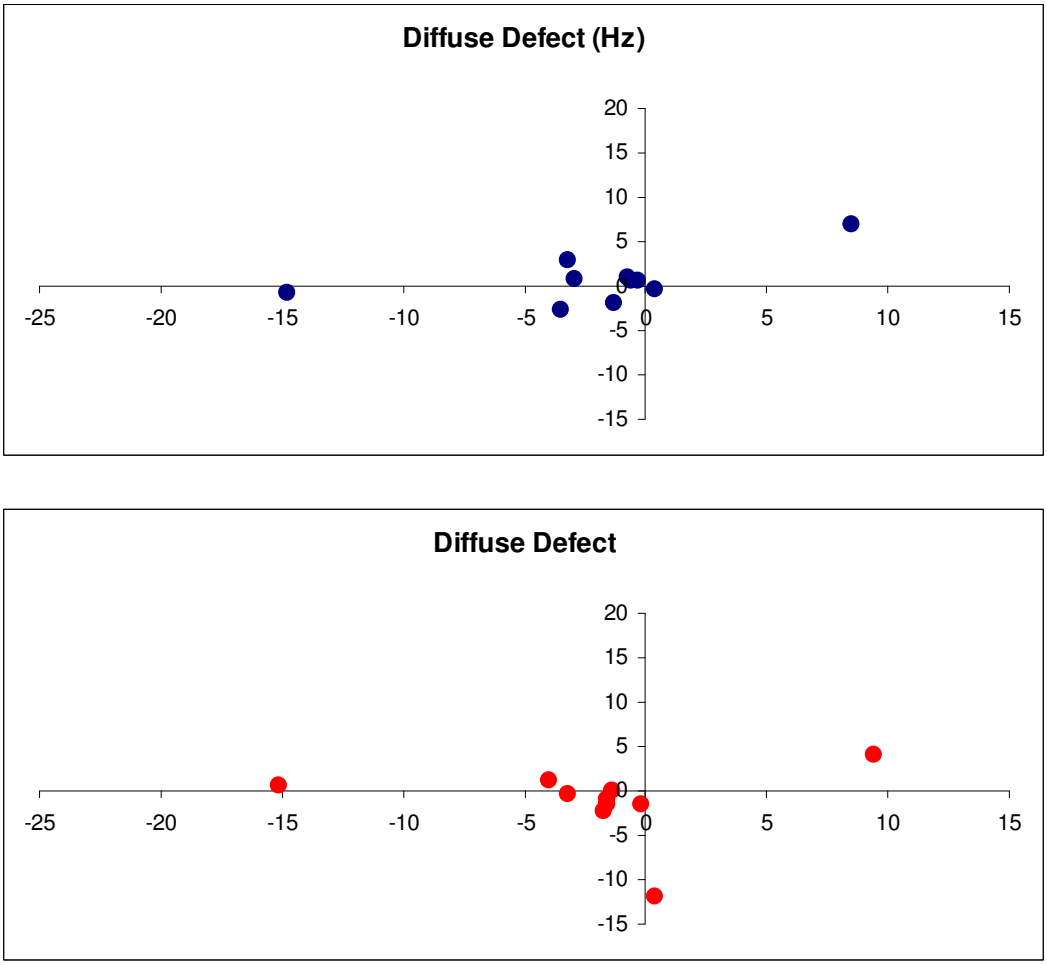

Figure 4.33 The scatter plot of the difference in the magnitude of the DD_{CFF} (Hz) between Visit One and Visit Two (abscissa) against the difference in the magnitude between Visit Two and Visit Five (ordinate) for each of the 10 individuals with OHT for the right (top), and left (bottom) eyes. A negative value represents an improvement in performance. Data points in the superior left quadrant represent an improvement from Visit One to Visit Two and deterioration from Visit Two to Visit Five. Data points in the superior right quadrant represent deterioration from Visit One to Visit Two and also from Visit Two to Visit Five. Data points in the inferior right quadrant represent deterioration from Visit One to Visit Two and an improvement from Visit Two to Visit Five. Data points in the inferior left quadrant represent an improvement both from Visit One to Visit Two and from Visit Two to Visit Five.

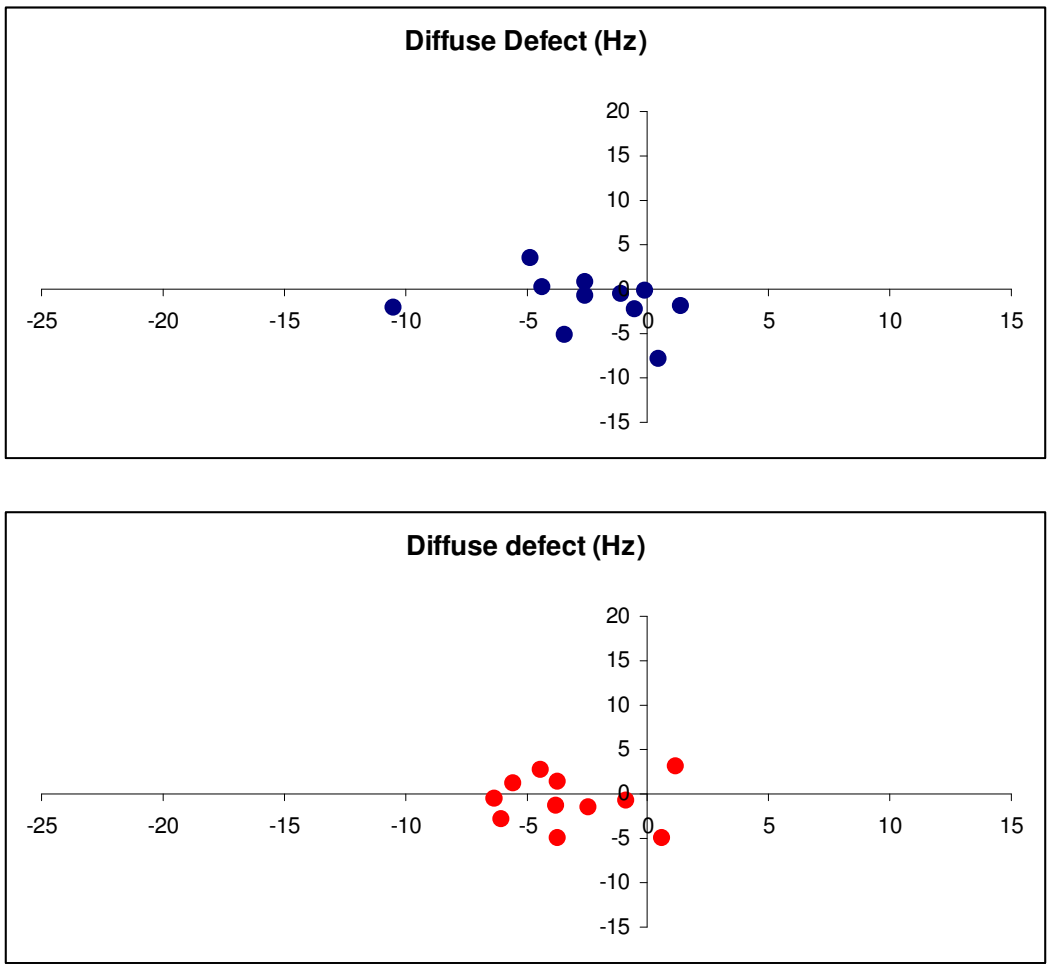

Figure 4.34 The scatter plot of the difference in the magnitude of the DD_{CFF} (Hz) between Visit One and Visit Two (abscissa) against the difference in the magnitude between Visit Two and Visit Five (ordinate) for each of the 11 individuals with OAG for the right (top), and left (bottom) eyes. A negative value represents an improvement in performance. Data points in the superior left quadrant represent an improvement from Visit One to Visit Two and deterioration from Visit Two to Visit Five. Data points in the superior right quadrant represent deterioration from Visit One to Visit Two and also from Visit Two to Visit Five. Data points in the inferior right quadrant represent deterioration from Visit One to Visit Two and an improvement from Visit Two to Visit Five. Data points in the inferior left quadrant represent an improvement both from Visit One to Visit Two and from Visit Two to Visit Five.

4.16.5 Local Defect

The difference in the LD from Visit One to Visit Two compared to the difference from Visit Two to Visit Five for each eye of the 28 normal individuals, of the 10 individuals with OHT and of the 11 individuals with OAG is shown graphically in Figure 4.35 to Figure 4.37, respectively.

The difference in the LD from Visit One to Visit Two compared to the difference from Visit Two to Visit Five for each eye of the 10 individuals with OHT showed that seven individuals for the right eye and eight individuals for the left eye exhibited little change in the LD between visits.

The difference in the LD from Visit One to Visit Two compared to the difference from Visit Two to Visit Five for each eye of the 11 individuals with OAG showed that only three of the individuals for the right eye and one individual for the left eye exhibited an improvement from Visit One to Visit Two and from Visit Two to Visit Five individuals exhibited an improvement for the left eye between Visit One and Visit Two and a deterioration between Visit Two and Visit Five.

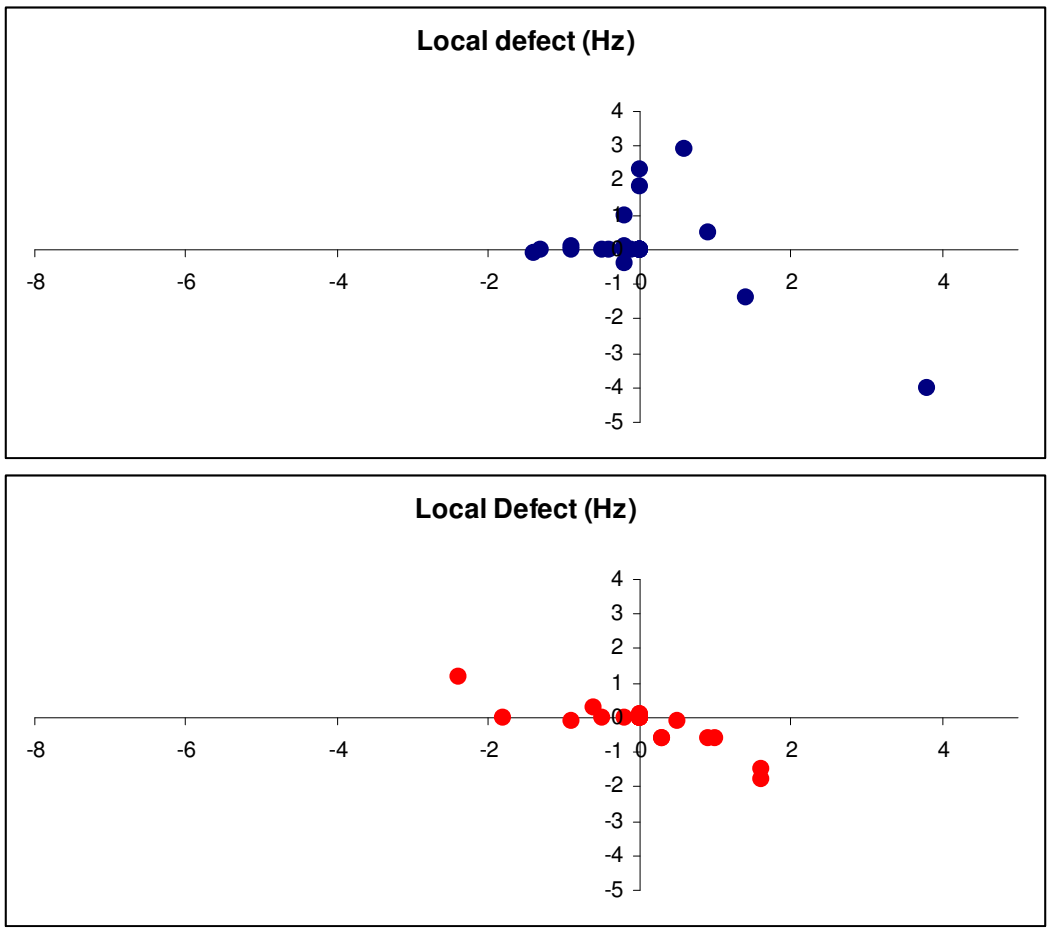

Figure 4.35 The scatter plot of the difference in the magnitude of the LD_{CFF} (Hz) between Visit One and Visit Two (abscissa) against the difference in the magnitude between Visit Two and Visit Five (ordinate) for each of the 28 normal individuals for the right (top), and left (bottom) eyes. A negative value represents an improvement in performance. Data points in the superior left quadrant represent an improvement from Visit One to Visit Two and deterioration from Visit Two to Visit Five. Data points in the superior right quadrant represent deterioration from Visit One to Visit Two and also from Visit Two to Visit Five. Data points in the inferior right quadrant represent deterioration from Visit One to Visit Two and an improvement from Visit Two to Visit Five. Data points in the inferior left quadrant represent an improvement both from Visit One to Visit Two and from Visit Two to Visit Five.

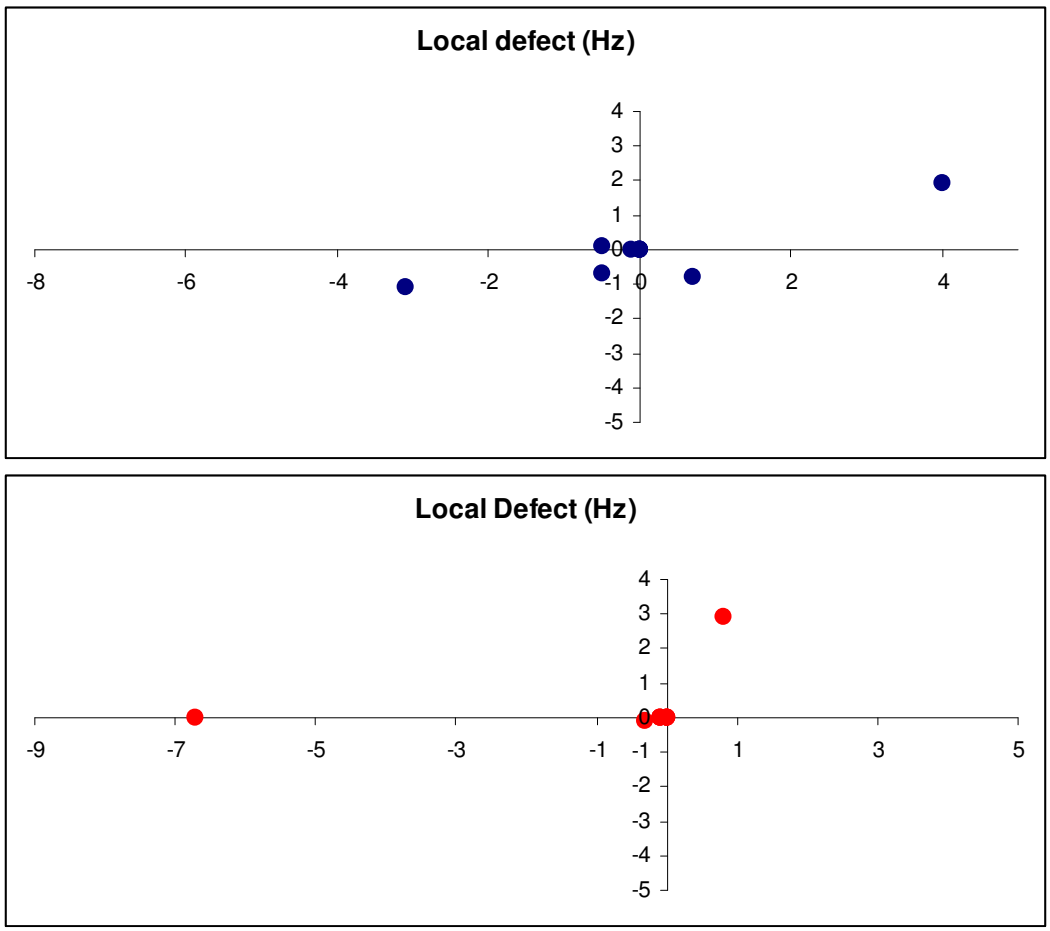

Figure 4.36 The scatter plot of the difference in the magnitude of the LD_{CFF} (Hz) between Visit One and Visit Two (abscissa) against the difference in the magnitude between Visit Two and Visit Five (ordinate) for each of the 10 individuals with OHT for the right (top), and left (bottom) eyes. A negative value represents an improvement in performance. Data points in the superior left quadrant represent an improvement from Visit One to Visit Two and deterioration from Visit Two to Visit Five. Data points in the superior right quadrant represent deterioration from Visit One to Visit Two and also from Visit Two to Visit Five. Data points in the inferior right quadrant represent deterioration from Visit One to Visit Two and an improvement from Visit Two to Visit Five. Data points in the inferior left quadrant represent an improvement both from Visit One to Visit Two and from Visit Two to Visit Five.

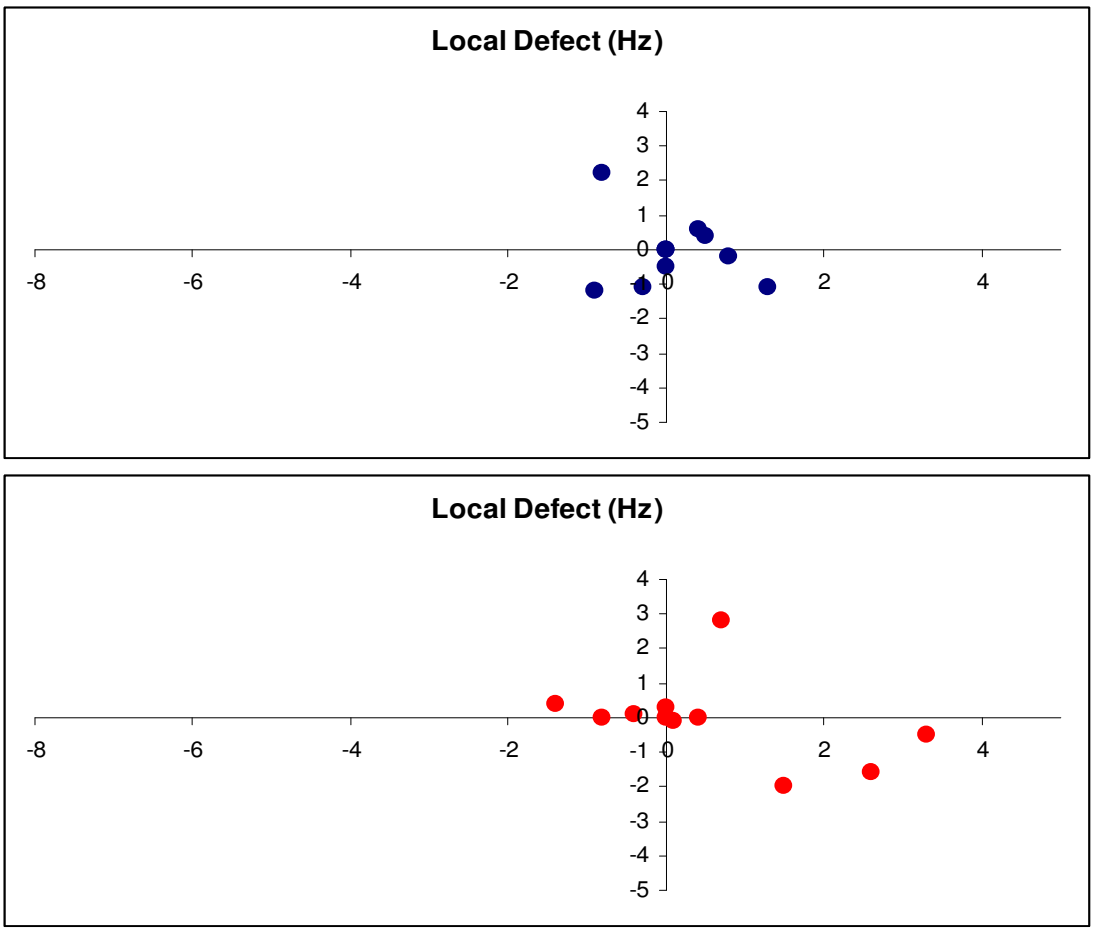

Figure 4.37 The scatter plot of the difference in the magnitude of the LD_{CFF} (Hz) between Visit One and Visit Two (abscissa) against the difference in the magnitude between Visit Two and Visit Five (ordinate) for each of the 11 individuals with OAG for the right (top), and left (bottom) eyes. A negative value represents an improvement in performance. Data points in the superior left quadrant represent an improvement from Visit One to Visit Two and deterioration from Visit Two to Visit Five. Data points in the superior right quadrant represent deterioration from Visit One to Visit Two and also from Visit Two to Visit Five. Data points in the inferior right quadrant represent deterioration from Visit One to Visit Two and an improvement from Visit Two to Visit Five. Data points in the inferior left quadrant represent an improvement both from Visit One to Visit Two and from Visit Two to Visit Five.

4.17 Discussion

The major finding from this study is that, when considered in terms of each diagnostic group, separately and combined, sensitivity derived by CFF perimetry, and expressed in terms of either the MS or the MD, improved across the central field (i.e. out to 30º eccentricity from fixation) in each eye over a training regime of five examinations each separated by an interval of one week. Although these visual field indices were statistically significantly different between the three groups, the ANOVA could not detect any difference between the groups in the magnitude of the improvement over the five visits. The DD also improved over the five visits; however, the improvement in the DD was greater for the individuals with OHT compared to the normal individuals and greater for the individuals with OAG compared to those with OHT. This suggests that diffuse visual field is present in OHT and in OAG and that it is the diffuse component which is largely responsible for the improvement in the height of the field. The lack of an improvement in the sLV and LD over the five visits suggests a uniform increase of the height, rather any change in the shape, of the field for CFF perimetry, over the five visits. The data also suggest that the normal individuals reached optimum performance at the third visit whilst the individuals with OHT and the individuals with OAG, both groups of which were experienced in SAP, reached optimum performance at the fourth or fifth visit.

The analysis of the pointwise change in sensitivity over the five visits, as a function of eccentricity, showed no clear evidence of any eccentricity dependent improvement in sensitivity thereby adding further credence to the hypothesis of a uniform change in the height of the field over the five visits. In addition, no improvement occurred in the PMS to CMS ratio.

The analysis of the pointwise change in sensitivity over the five visits, as a function of the magnitude of the initial sensitivity, exhibited an increasing improvement in sensitivity with

decline in the initial sensitivity to approximately 10Hz which, within the remit of the data sets, was more evident for the group with OAG. Such an outcome is consistent with the improvement in the DD.

The analysis of the pointwise change in the Comparison Probability level, showed very little overall improvement in probability level over the five visits. However, the group with OAG manifested the greatest improvement. Such a finding suggests that, in general, the magnitude of the improvement in sensitivity, at any given location, across the five visits lay within the magnitude of the confidence interval for the given probability level manifested at the initial visit. Thus, the magnitude of the learning effect, at least in Comparison Probability terms, has very little influence on the clinical diagnostic outcome of CFF perimetry. Such an outcome could be explained either in terms of the small magnitude of the learning effect or in terms of (excessively) wide confidence limits for abnormality with CFF perimetry. In proportionate terms, the change in MS for CFF perimetry was similar to that for SAP which suggests that the explanation can be attributed to wider confidence limits for CFF.

It should be noted that all 49 individuals across the three groups exhibited identical Comparison and Corrected Comparison differences and probability maps in both eyes at each of the 6 visits. The reason for the absence of a general height adjustment for CFF perimetry is unknown. It can be speculated that the reason arises from the commonly held assumption that CFF perimetry, which targets the magnocellular pathway, is unaffected by abnormalities which affect the general height (e.g. cataract, defocus, etc) and, therefore, such an adjustment is unnecessary. If such speculation is correct, then the rationale for the inclusion in the Seven-in-One printout of the Corrected Comparison difference and probability maps, which are identical to those of the Comparison, must be questioned

The improvement in the MS, MD and DD indices for the normal individuals exhibited a sustained improvement over the first four visits. The greatest improvement in these indices for the individuals with OHT and for the individuals with OAG occurred between Visits One and Two but a continued improvement was evident over Visits Three and Four.

The examination duration reduced over the five visits and was shorter for the second eye examined at any given examination. The latter finding indicated a between-eye transfer of the learning effect at each visit. Such a finding is compatible with that for SAP over the first two visits (Wild et al 2006; Castro, Kawase and Melo 2008), and for FDT (Horani et al 2002), and indicates the absence of the influence of the fatigue effect (Hudson, Wild and O'Neill 1994) whereby sensitivity declines with increase in the examination duration, particularly in the second eye.

In terms of individual performance across the five visits, the widest variation between individuals for each of the indices, expressed in absolute terms, occurred in the group of normal individuals. It was lower for, but similar between, the individuals with OHT and the individuals with OAG.

It would thus seem that the normal individuals who had only experienced one examination in each eye for SAP at enrolment and who were naïve to CFF perimetry exhibited the least improvement and the widest between-individual variation in performance. Such variation ranged from a deterioration at successive examinations from the baseline to an increasing improvement at all examinations. Surprisingly, the individuals with OHT and the individuals with OAG, although familiar with SAP exhibited the greatest improvement in the outcome to CFF. These

findings suggest that sustained prior experience with SAP possibly aids the outcome of CFF perimetry.

The age related decline in Mean Sensitivity for CFF perimetry in the normal eye at the first visit using the Dynamic algorithm has previously been shown to be -0.141Hz per year (Bernardi, Costa and Shiroma 2007). This published value compares favourably with that recorded at Visit One in the current study of -0.129 Hz for the field of the right eye and -0.105Hz for the field of the left eye.

The improvement in the Group Mean Sensitivity for the normal individuals from Visit One to Visit Three was 0.2Hz for the field of the right eye and 1.2Hz for the field of the left eye. The corresponding improvement in the median was 0.6Hz and 1.5Hz, respectively. These figures compare with a mean of 1.2Hz for the case series of 20 younger individuals (Bernardi, Costa and Shiroma 2007).

The greatest improvement in CFF perimetry for the individuals with OHT and for the individuals with OAG occurred between Visits One and Two. This finding is compatible with that present in SAP (Wood et al 1987b; Heijl, Lindgren and Olsson 1989; Wild et al 1989) and SWAP (Wild, Moss and O'Neill 1996; Zhong et al 2008). However, a sustained improvement was also present at Visits Three and Four. Such a finding is compatible with that for SWAP in individuals with OHT and in individuals with OAG who were experienced in SAP (Wild et al 2006) whereby the learning effect for SWAP was present over the first four of an identical protocol of five examinations each separated by one week.

The PMS/CMS ratio was similar across the five visits. The stability of the ratio is in contrast to that reported for SAP which manifests as a greater improvement peripherally compared to centrally (Heijl, Lindgren and Olsson 1987a; Wood et al 1987b; Wild et al 1989). It is also compatible with the consept of an overall improvement in the height of the visual field for CFF.

The wide variation in performance between the normal individuals in the current study may explain some of the magnitude of the potential increased confidence intervals for normality compared to those for SAP.

The learning effect could have been investigated over almost any number of successive examinations over almost any time period. The use of 5 visits each separated by a one week interval has become a standard designin perimetric research, and represents a trade-off between the opportunity for improvement over a sustained training regime and clinical reality (Heijl, Lindgren and Olsson 1989; Rossetti et al 2006; Wild et al 2006). Clearly, the results for the current study are only applicable to such a protocol.

The magnitudes of each of the indices were notably different between the TOP algorithm at Visit Five and the Dynamic algorithm at Visit Six for each diagnostic group. The Dynamic algorithm yielded a higher MS, a less positive MD and DD (i.e.better) and a larger sLV and DD (i.e. worse) than the TOP algorithm. The difference between the two algorithms for each respective index was in general, greatest for the individuals with OHT and the individuals with OAG. The difference in the magnitudes of the outcomes of the two algorithms indicates a difference in the estimate of the threshold between the two algorithms and a further difference in the magnitude of the normal values associated with each algorithm. The reason for the latter is unknown. The Dynamic algorithm also yielded fewer locations exhibiting abnormality in terms of the

Comparison Probability level i.e. the TOP algorithm yielded a statistically deeper defect depth. This would suggest a difference in the width of the confidence intervals between the two algorithms which again implies a difference in the magnitude of the normal values associated with each algorithm.

The TOP algorithm for CFF utilizes a ceiling effect which is 9/8 of the age-corrected normal value above (i.e. overall, a higher sensitivity) the normal value. This approach reduces the potential for abnormally high sensitivities compared to that of the Dynamic algorithm which does not employ a cut-off. Thus, it is possible that some of the higher sensitivities encountered with the Dynamic algorithm can be explained by the lack of truncation. However, it is more likely that the difference arises from the differences in the threshold estimate between the two algorithms. Indeed, the Dynamic algorithm has been shown to yield a larger MS for SAP compared to the TOP algorithm of approximately 1-2dB (Morales, Weitzman and Gonzalez de la Rosa 2000). It was discussed in Chapter One that the TOP algorithm for SAP also tends to underestimate the severity of focal visual field loss compared with the Dynamic algorithm and the findings of the current study, when expressed in terms of sLV, would suggest the same outcome for CFF perimetry. However, the defect depth expressed in terms of Comparison Probability values yields a statistically deeper defect depth for the TOP algorithm, particularly in OAG.

Although not a formal aim of the study, it was interesting to note that the outcome for SAP recorded with the Dynamic strategy, immediately prior to enrolment in the study, yielded either greater or deeper, or both, field loss in 6 of the 11 individuals with OAG compared with that for CFF recorded at the sixth visit (Figure 4.38). Of the remaining 5 individuals, 4 exhibited equivalence between the two types of perimetry. Such an outcome is likely to reflect the

increased confidence limits for CFF perimetry compared with SAP and contradicts the concept that CFF perimetry is a more sensitive indicator of functional damage than SAP. The difference in threshold estimate between the TOP and Dynamic algorithms and the additional difference influencing the magnitudes of the normal values poses a potential problem in the interpretation a series of visual fields using a mixture of the two algorithms.

SAP		CFF	
Right	**Left**	**Right**	**Left**
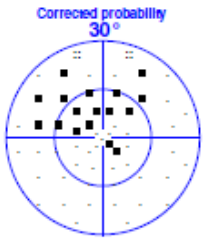 **MD 7.1 sLV 10.2**	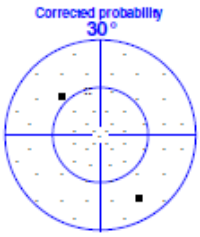 **MD 0.8 sLV 3.7**	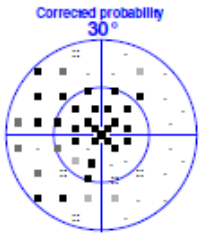 **MD 15.2 sLV 9.9**	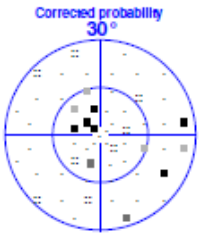 **MD 7.3 sLV 5.6**
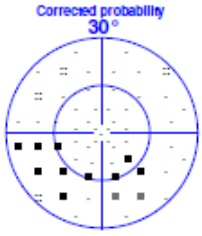 **MD 4.0 sLV 7.4**	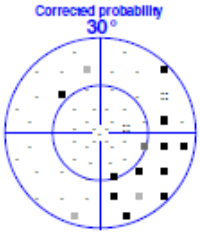 **MD 4.7 sLV7.2**	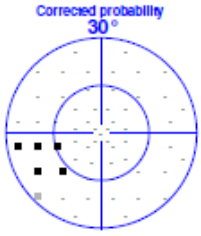 **MD 3.0 sLV 9.3**	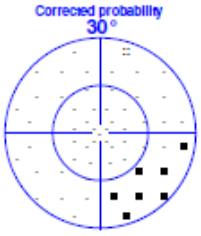 **MD 4.1 sLV 9.2**
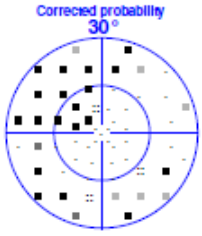 **MD 8.1 sLV 9.3**	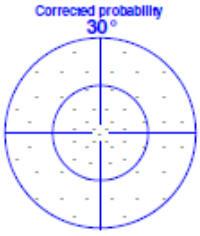 **MD -2.0 sLV 1.6**	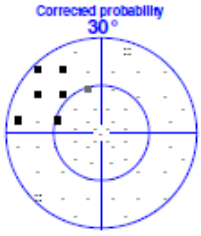 **MD 1.5 sLV 11.9**	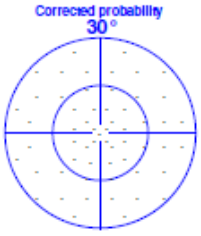 **MD -2.3 sLV 4.3**
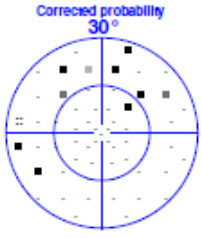 **MD 3.5 sLV 6.0**	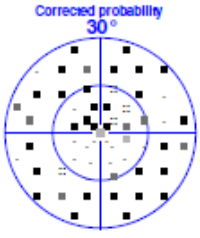 **MD 13.9 sLV 7.6**	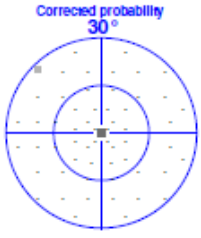 **MD -3.4 sLV 7.16**	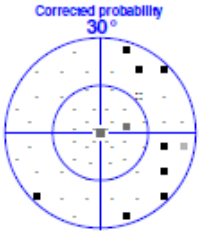 **MD 2.6 sLV 11.5**

SAP		CFF	
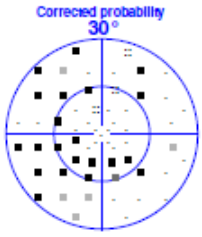	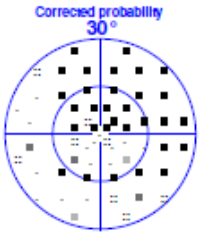	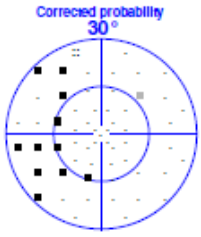	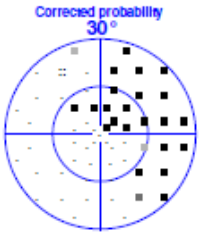
MD 10.4 **sLV 9.6**	**MD 14.3** **sLV 9.5**	**MD 7.1** **sLV 12.2**	**MD 13.5** **sLV 13.4**
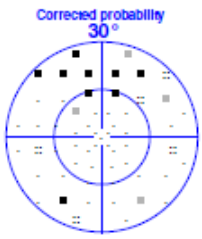	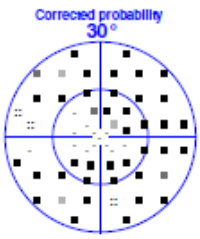	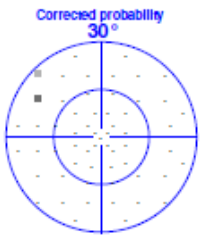	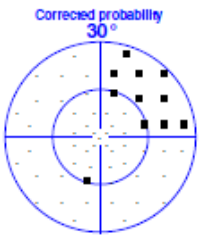
MD 6.4 **sLV 5.5**	**MD 13.4** **sLV 8.7**	**MD -4.9** **sLV 5.9**	**MD 4.1** **sLV 13.6**
		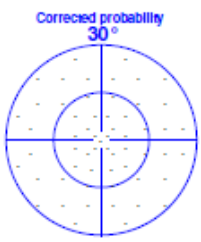	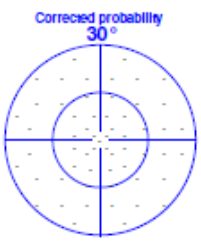
MD 1.7 **sLV 2.2**	**MD 1.7** **sLV 3.5**	**MD -6.8** **sLV 5.0**	**MD -5.2** **sLV 4.1**
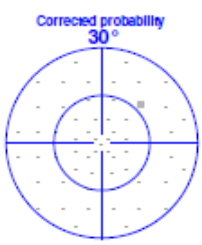	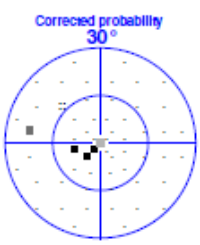	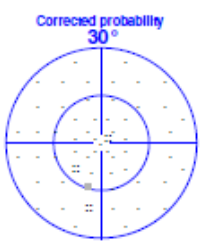	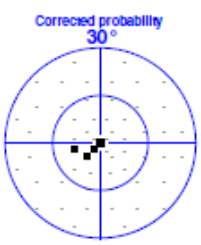
MD -1.2 **sLV 1.9**	**MD 0.8** **sLV 3.6**	**MD 1.5** **sLV 5.2**	**MD -0.5** **sLV 7.0**

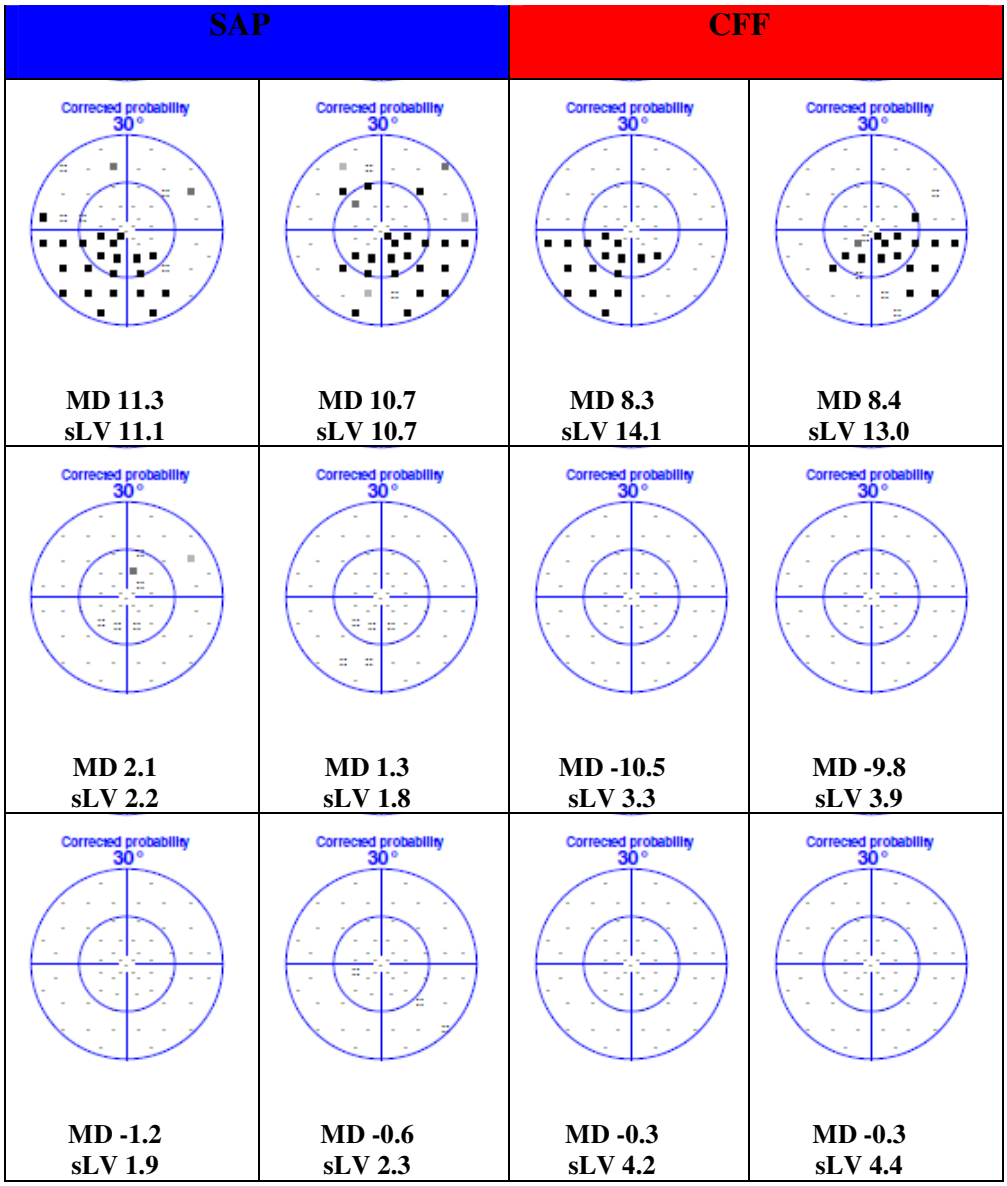

Figure 4.38 The Corrected Comparison probability map, derived by SAP, for the field of the right eye (extreme left hand column) and of the left eye (left column) and by CFF perimetry for the field of the right eye (right column) and of the left eye (extreme right column) for the 11 individuals with OAG.

4.18 Conclusion

The presence of a learning effect for CFF perimetry in individuals with OHT and in individuals with OAG, and which is sustained over four visits, together with the likelihood for increased confidence limits of normality compared to SAP and the uncertainty as to whether CFF

perimetry identifies visual field abnormality in advance of SAP, currently suggests that CFF perimetry offers little clinical advantage compared to SAP.

CHAPTER 5

THE INFLUENCE OF AGE-RELATED CATARACT ON CRITICAL FLICKER FUSION PERIMETRY

5.1 Introduction

5.2 Ocular media

Opacities in the ocular media will influence the amount of light reaching the retina thereby affecting the outcome of the visual field examination. Cataract causes image blur; increased absorption and therefore decreased retinal illumination; increased intraocular light scatter and therefore increased veiling glare. The effect of media opacities on the visual field has been documented both for manual kinetic and manual static perimetry (Bigger and Becker 1971; Greve 1973; Greve 1979; Lyne and Phillips 1996); for SAP (Lam, Alward and Kolder 1991; Hayashi et al 2001; Koucheki et al 2004; Rehman Siddiqui, Khairy and Azuara-Blanco 2007; Mutlu, Akay and Bayer 2009); for HRP (Martin 1997; Martin et al 2008); for SWAP (Moss, Wild and Whitaker 1995; Kim et al 2001); for RBP (Salvetat et al 2007; Nilsson et al 2010) and for FDT perimetry (Kook et al 2004; Tanna et al 2004; Simakova and Boĭko 2010).

Cataract reduces the sensitivity for SAP (Lam, Alward and Kolder 1991; Stewart et al 1995; Klein, Klein and Jensen 1996) and can mask glaucomatous visual field loss (Heider, Seez and Schnaudigel 1991; Bengtsson et al 1997; Smith, Katz and Quigley 1997; Chen and Budenz 1998; Hayashi et al 2001). Several studies of individuals with cataract, examined pre- and post-operatively following cataract extraction and IOL implantation have reported an improvement in the MD (Tanna et al 2004; Siddiqui, Azuara-Blanco and Neville 2005; Ueda et al 2006), but not in the PSD (Tanna et al 2004; Ueda et al 2006) which can also be worse post-operatively (Siddiqui, Azuara-Blanco and Neville 2005). The number of incorrect responses to the false-

positive catch trials is lower following cataract extraction and IOL implantation for advance age-related cataracts and for mild posterior subcapsular cataract (Casson and James 2006). The presence of age-related cataract, and the subsequent extraction and IOL implantation, also leads to difficulty in determining the presence of progressive visual field loss.

A number of studies suggest that CFF (Dudzinski, Zawojska and Kinasz 2003; del Romo, Douthwaite and Elliott 2005) or CFF perimetry (Gleissner and Lachenmayr 1992; Lachenmayr and Gleissner 1992) is relatively unaffected by cataract and that CFF can successfully predict visual outcome after cataract surgery (Douthwaite, Vianya-Estopà and Elliott 2007; Shankar and Pesudovs 2007). Unfortunately, the studies of CFF/ CFF perimetry and cataract were undertaken either with customised equipment (del Romo, Douthwaite and Elliott 2005; Shankar and Pesudovs 2007) and/ or with simulated cataract (Lachenmayr and Gleissner 1992; Matsumoto et al 1996), or both, and are such as to render the information of minimal clinical quantitative value. Thus, there is a pressing need to determine the extent to which the CFF stimulus in clinical perimetry is resistant to image degradation arising from age-related cataract.

As was discussed in the previous Chapter, the influence of the learning effect on the outcome of SAP is well documented for normal individuals, for individuals with OHT and individuals with OAG. However, the characteristics of the learning effect for individuals with cataract is unknown. In addition, the influence of age-related cataract on the learning effect for CFF perimetry is also unknown. Clearly, if CFF perimetry is to have an impact clinically, the extent of the resistance to image degradation in age-related cataract must also be delineated.

5.3 Intraocular light scatter

Light entering the eye will be scattered as a result of opacities in the ocular media. This light scatter can be subdivided into light scattered towards the retina (forward light scatter) and light

scattered backwards from the retina (backscatter). Forward light scatter results in a veiling luminance superimposed upon the retinal image thereby reducing the contrast of the image on the retina. The visual loss in cataract is principally due to increased forward light scatter (Hess and Woo 1978; Paulsson and Sjøstrand 1980; Bettelheim and Ali 1985; van den Berg 1991; de Waard et al 1992; Brown 1993). The veiling luminance can lead to a variety of complaints, including poor distance vision, monocular diplopia, poor night vision, and changes in colour perception (McAlinden et al 2011).

Glare Disability (GD) is a quantitative measure of the effect of the forward light scatter, arising from a glare source, on a patient's visual function. It can be measured clinically by determining VA under a variety of levels of disability glare. GD can be defined as the reduction in (logMAR) VA in the presence of the glare source. Individuals with cataract generally exhibit a GD which is greater than that predicted from their VA in normal illumination, alone (Cinotti 1979; Paulsson and Sjøstrand 1980; Maltzman, Horan and Rengel 1988; Neumann et al 1988a; Elliott, Gilchrist and Whitaker 1989; Koch 1989; Elliott and Hurst 1990).

Disability glare testing in individuals with age-related cataract is becoming more frequent as a clinical measure of visual disability. The outcome from such tests is also used to justify cataract surgery. Disability glare is the reduction in VA or contrast sensitivity resulting from a nearby glare source and is the result of forward intraocular light scatter. Many practitioners have suggested that VA should be complemented by contrast sensitivity and disability glare testing (Miller et al 1972 ; Hess and Woo 1978; Paulsson and Sjøstrand 1980; LeClaire et al 1982).
An evaluation of five commercially available glare tests to determine how accurately each device predicted outdoor Snellen acuity within one Snellen line in cataract individuals with cataract showed that the Brightness Acuity Test (BAT) produced the best result (73%) folloved by the

InnoMed True Vision Analyzer (TVA) (69%), the VisTech VCT 8000 (56%), the Miller-Nadler (47%) and the EyeCon (15%) (Neumann et al 1988).

The BAT is a hand-held instrument that consists of a hemispheric bowl with an internally illuminated surface. The individual holds the device to their eye and views the chart through a central 12 mm aperture (Figure. 5.78)

The high intensity setting on the BAT has been reported to give inappropriately high predictions of disability glare (Neumann et al 1988; Prager et al 1989) and can reduce contrast beyond a chart's limits of the chart with some early cataract patients (Elliott and Hurst 1990; Regan 1991).

A combination of the Pelli-Robson/BAT test has been shown to be the most repeatable, with the coefficient of repeatability of 0.18 log units (Elliott, Bullimore and Bailey 1991; Elliott and Bullimore 1993).

The new commercially available straylight meter, the Oculus C-Quant instrument (Oculus Optikergeräte GmbH, Münchholzhäuser, Wetzlar) shows good correlation between decreased quality of vision and presence, type and severity of age-related cataract (Franssen, Coppens and van den Berg 2006; Beerthuizen et al 2007; de Vries et al 2008).

The effect on the perimetric threshold caused by the presence of forward light scatter, secondary to cataract, is a major clinical problem in the management of OAG in that it attenuates the height of the recorded visual field, resulting in a mimicking, and therefore an overestimation, of diffuse damage to the visual field. Although the influence of cataract on the visual field can be minimised mathematically by the general height adjustment (Heijl, Lindgren and Olsson 1987b;

Asman and Heijl 1992a; Asman, Wild and Heijl 2004), the adjustment cannot differentiate the attenuation arising from optical causes from that due to neural causes. The concept of diffuse loss as an initial stage of OAG is equivocal (Drance et al 1987; Heijl 1989; Langerhorst et al 1989; Lachenmayr et al 1991; Henson, Artes and Chauhan 1999) largely because of the inability of the height adjustment to separate the optical from the neural attenuation. Quantification of the influence of forward light scatter on the perimetric profile by disability glare would enable some separation of the optical and diffuse components of diffuse loss at any given examination or over successive examinations.

5.4 The influence of age-related cataract on Critical Flicker Fusion Perimetry

5.5 Aims

The overall aim of the study was twofold. The primary aim was to determine the influence of age-related cataract on the outcome of commercial available Critical Flicker Fusion (CFF) perimetry using an experimental protocol which was intended to minimise the influence of any potential learning effect, i.e., repeated CFF perimetry at each of four consecutive visits each separated by an interval of one week. It was hypothesised that, if the CFF stimulus was unaffected by cataract, the height and shape probability analysis would have a clinically identical appearance to one another. The clinically identical appearance would cover a scenario where all the stimulus locations exhibit normality, in an experienced observer, through to a scenario where any number of locations could exhibit apparent abnormality depending upon the extent of the previous experience of CFF perimetry. As further confirmation of the resistance to cataract, it was hypothesised that forward intra-ocular light scatter, expressed as GD, would correlated with the outcomes of SAP but not with that of CFF perimetry.

The secondary aim was to determine the characteristics of any learning effect in the presence of the age-related cataract. More specifically, the secondary aim was to determine, over the four visits, the between-individual differences in performance for both CFF and SAP.

5.6 Methods

The study was a prospective observational case series study.

5.7 Case Series

The case series comprised 22 (11 males) consecutively presenting Caucasian individuals who exhibited an age-related cataract in each eye and who otherwise met the inclusion criteria for enrolment in the study and who had volunteered to take part in the study.

Prior to the enrolment visit, potential participants underwent a standard ophthalmic examination to confirm the inclusion criteria. The confirmatory examination in each eye included determination of visual acuity, refraction; SAP with the Octopus 311 perimeter using Program G1 and the Dynamic algorithm, central corneal thickness measurement using the Sonogage Corneogage 2 ultrasonic pachometer (Sonogage Inc. Cleveland); Goldmann applanation tonometry; gonioscopy, indirect ophthalmoscopy, usually with a +78 dipotre lens, photography of the crystalline lens, stereo-photography of the optic nerve head and posterior pole using the Kowa Nonmyd α-D (Kowa Company. Ltd., Japan) non-mydriatic fundus camera. The assessment of IOP, the measurement of central corneal thickness and gonioscopy all required the installation of a topical anaesthetic (Oxibuprocaine 0.4%). Photography of the crystalline lens, slit lamp indirect ophthalmoscopy and photography of the posterior pole required pupil dilation with one drop of Tropicamide 0.5%. The images of the crystalline lens, of the optic nerve head

and of the posterior pole and the results of the visual field examinations were all designated as normal by Prof Wild who was masked to the clinical characteritics of the potential participant.

Potential participants were to be excluded from the study if they exhibited in either eye: a distance refractive error greater than +/-5.0 dioptres sphere and/or greater than +/- 2.5 dioptres cylinder; a pupil diameter smaller than 3 mm; a central corneal thickness-corrected IOP of greater than 20 mm Hg; a narrow anterior chamber angle; previous ocular surgery; and any ocular disorder or ocular disease. In addition, individuals with migraine with aura; diabetes; neurological disorder or disease; systemic disease, other than systemic hypertension manifesting as Grade 1 hypertensive retinopathy, or hyperthyroid disease; a family history of glaucoma or of diabetes; and previous experience of CFF perimetry were also excluded.

All individuals were provided with verbal and written information concerning the nature of the study and given written consent, in accordance with the requirements, and approval, of the Norwegian Research and Ethics Committee (REK, Regional komité for medisinsk forskningsetikk Sør-Norge (REK Sør) and the Norwegian Datatilsynet (Enclosure number 3 and 5) which is, in turn, in accordance with the tenets of the Declaration of Helsinki.

The mean age of the twenty-two individuals was 69.7 years (SD 9.1), the median 71.0 years (IQR 13.5) and the range from 50 to 79 years (Table 5.1).

Age (years)	Cataract Individuals	NC	ACC	PSC	Mixed
50 – 59	2			2	
60 – 69	6	1	4	1	
70 – 79	14	7	3	2	2

Table 5.1 The number of individuals, and distribution of age, classified by cataract type.

5.8 Perimetric Protocol

Fourteen days after enrolment, each participant attended for the first visit of the study. At this visit, both eyes were examined using both SAP and CFF perimetry and Program G1 and the TOP algorithm of the Octopus 311. The order of the type of perimetry was held constant between the two eyes of an individual but was randomized between individuals. The examination procedure for both types of perimetry was undertaken in an identical fashion to that described in Chapter Four. The field of the right eye was always examined before that of the left eye. Distance refractive correction, in the form of full aperture trial lenses, was used for each eye. The non-examined eye was occluded with an opaque patch. The influence of the fatigue effect was reduced by the provision of rest periods of approximately one minute in duration, at 3 minutes intervals, during the examination of each eye, and by a 5 minute rest period between the examinations of each eye and by a further 5 minute rest period between the two types of perimetry. Fixation was monitored continuously by the automatic eye tracker of the Octopus 311 perimeter and was also viewed via the video monitor of the perimeter.

Each participant then attended for a further three perimetry visits (Table 5.2). The protocol at each of these three visits was identical to that at the first visit with the exception that the order of perimetry for each individual was alternately reversed over each of these three visits. Each visit was separated by an interval of one week. The same instructions were given at each visit and the visual field examinations at all four visits were undertaken by the author.

	Enrolment	Session 1	Session 2	Session 3	Session 4
Method	SAP	CFF and SAP*	SAP and CFF*	CFF and SAP*	SAP and CFF*
Interval between sessions (days)		14	7	7	7
Program/ algorithm	G1/ Dynamic	G1/ TOP	G1/ TOP	G1/ TOP	G1/ TOP

Table 5.2 The summary of the perimetric protocol at enrolment and at each of the subsequent four visits. The asterisk denotes that the perimetry could also have been undertaken in reverse order.

5.9 Glare disability protocol

At the third and fourth visits, and after the perimetry, each individual also underwent assessment of glare disability using high (100%) and low (10%) contrast Log MAR visual acuity charts each contained within a light box (Good-Lite, Model No. ESV1200, Standardized Viewer, Input: 12VDC, 1A) (Figure 5.1 [top]) in the absence, and then in the presence, of each of the three different levels of disability glare generated with the Brightness Acuity Tester (BAT Brightness Acuity Tester, MARCO Ophthalmic, INC, Jacksonville, FL) (Figure 5.1 [bottom]). The equivalence of the luminance of each light box was verified using a Hagner Universal Photometer/Radiometer S-171 02 (Solna, Sweden).

The individual viewed the given test chart at a distance of 4m and wore their distance refraction in both eyes in full aperture trial lens form. The non-examined eye was always occluded with a white opaque occluder. The examined eye viewed the 100% contrast chart through the BAT. Log MAR visual acuity was recorded in the 'Off' position, i.e., with a glare source, and then at each of the three BAT disability glare settings, 'Low' (41 cdm^{-2}) 'Medium'(343 cdm^{-2}) and 'High'

(1371 cdm^{-2}). An adaptation period of 30 seconds between BAT settings was used. The contralateral eye was then examined in an identical manner. The order of the eye examined was randomized between individuals. The procedure was then repeated for the 10% contrast chart. Four charts at each of the two contrast levels enabled a different randomly assigned chart to be used at each of the two contrast levels for each of the four brightness settings reduced the possibility of individuals recognising any previous letter combinations.

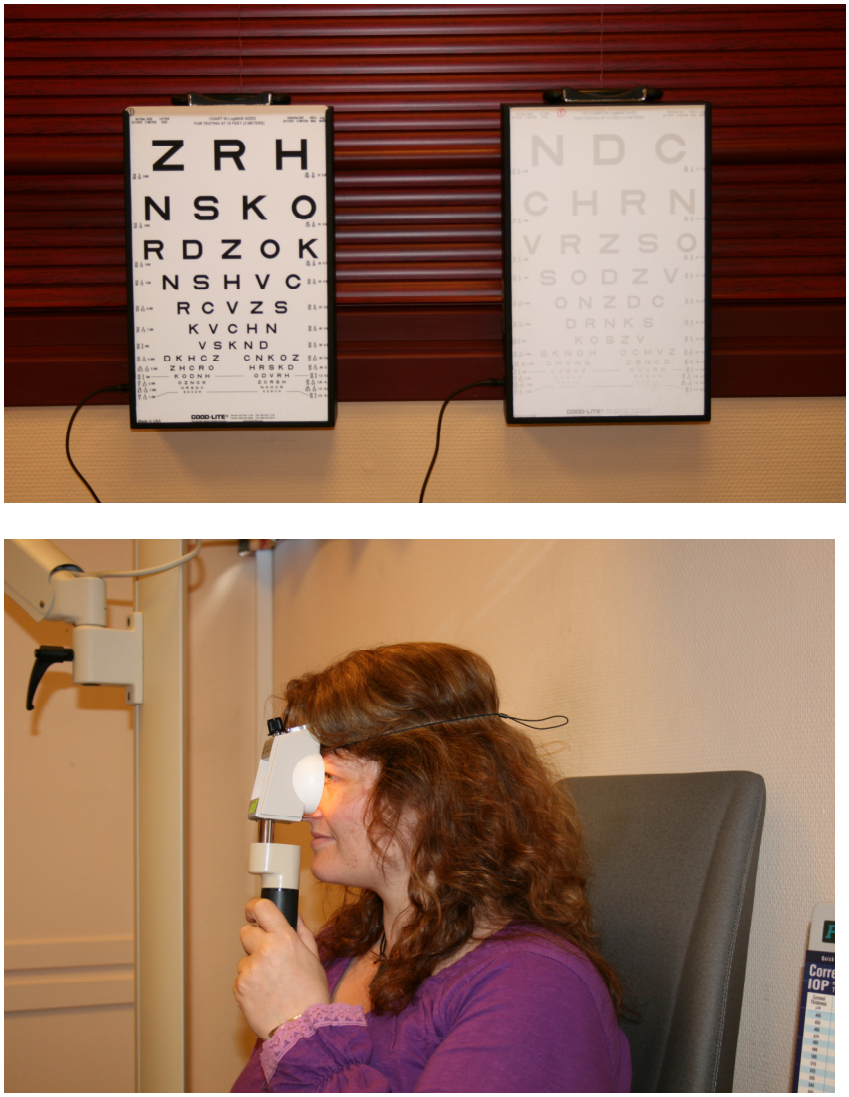

Figure 5.1 The high and low contrast ETDRS charts contained within the light boxes (top). The Brightness Acuity Test (BAT) (bottom).

The measurement of disability glare was repeated at Visit Four in an identical manner to that at Visit Three with the exception that the order of the examined eye was reversed and that the 10% contrast chart was used before the 100% chart.

The GD for each of the three glare sources at each of the two contrasts of the EDTRS chart was calculated from the values obtained at Visit 4 as:

$$\log \text{MARVA}_{\text{with glare}} - \log \text{MARVA}_{\text{without glare}}$$

The characteristics of the age-related cataract(s), based upon the LOCS III grading; the Snellen visual acuity recorded at the enrolment examination; the MD and the sLV (Program G1 and the TOP algorithm) for SAP recorded at Visit Four; for each eye of the 22 individuals are given in Table 5.3.

Gender/ Age	LOCS III Right	LOCS III Left	VA Right	VA Left	MD4 Right	MD4 Left	sLV4 Right	sLV4 Left	Worst eye
M - 79 y	C2/P 2	C1	0.5	1.0	-1.0	-1.9	1.2	1.1	Right
FM - 61 y	C2	C3	0.7	0.6	9.9	7.2	72	39	Left
M - 50 y	P 1	P 1	0.9	0.9	-2.1	0	0.6	1.1	Left
FM - 71 y	C3	C2	0.5	0.5	1.0	1.1	4.6	9.0	Right
M - 76 y	C2/NO2	C2/NO2	0.6	0.7	0.5	1.3	2.2	2.9	Right
FM - 60 y	C3	C2	0.7	0.7	0.3	-0.1	0.8	1.8	Right
M - 75 y	NO2/NC2	NO2/NC2	0.6	0.6	4.3	3.6	6.0	4.6	Left
FM - 68 y	NO1/NC1	NO1/NC1	0.9	0.8	-1.8	-1.4	1.6	2.1	Left
FM - 50 y	P3	P1	0.8	1.0	2.8	0.1	7.3	0.8	Right
FM - 60 y	P4	P1	0.3	1.0	7.0	1.8	14.8	11.0	Right
FM - 79 y	NO3/NC3	NO3/NC4	0.6	0.6	5.4	10.2	11.9	19.4	Left
FM - 70 y	P4	P2	0.7	0.7	0.9	0	5.4	3.7	Right
M - 79 y	NO3/NC3	NO3/NC3	0.8	0.7	-0.5	-1.8	10.5	1.2	Left
FM - 77 y	NO4/NC4	NO4/NC4	0.6	0.6	0.7	2.6	5.1	5.1	Left
FM - 77 y	NO3/NC3	NO4/NC4	0.7	0.6	0.3	0.8	2.5	5.1	Left
M - 63 y	C2	C3	0.7	0.7	-0.2	-0.3	0.9	4.0	Left
M - 76 y	C3	C2	0.9	1.0	-1.4	-2.3	1.5	0.6	Right
M - 71 y	P3	P2	0.8	1.0	0.8	-0.4	7.0	4.0	Right
FM - 71 y	NO2/NC2	NO3/NC3	0.9	0.7	0.7	0.9	3.5	2.9	Left
M - 79 y	NO4/NC4	NO3/NC3	0.6	0.8	1.5	0.7	9.2	4.5	Right
M - 65 y	C4	C3	0.8	1.0	2.4	-0.6	13.7	3.8	Right
M - 77 y	C3	C3	1.0	0.9	0	0.9	3.2	3.3	Left

Table 5.3 The "Worst eye" classified in terms of, the LOCS III grading; the Snellen visual acuity; the Mean Defect (MD) and the square root of the Loss Variance (sLV), at the fourth visit (SAP, Program G1 and the TOP algorithm); for each eye of the 22 individuals with age-related cataract.

5.10 Analysis

The relationship between the visual field and GD was investigated by the use of scatter plots of MD as a function of Glare Disability resulting from each of the three glare sources.

The analysis of the between-individuals between visits of the learning effect for each type of perimetry was considered in terms of the four different types of analysis described in Chapter Four. Firstly, any change in each of the visual field indices Mean Sensitivity, Mean Defect,

square root of the Loss Variance, Diffuse Defect and Local Defect determined using separate ANOVAs for each index. Secondly, in terms of the change in sensitivity at each stimulus location as a function of stimulus eccentricity. Thirdly, in terms of the change in sensitivity at each stimulus location as a function of the initial sensitivity. Fourthly, in terms of the change in sensitivity at each stimulus location expressed in terms of the Comparison and of the Corrected Comparison probability levels.

The within-individual between-visit change in performance was considered, in the same way, as for Chapter Four. Firstly, in terms of the absolute change, for each of the visual field indices, from Visit One to Visit Two compared to that from Visit Two to Visit Four; and, secondly, in terms of the proportionate change in the MS index, only, from Visit One and Visit Two compared to that from Visit Two to Visit Four. Such an analysis was again undertaken to compare, for each individual, the magnitude of the learning effect occurring between the first two examinations with that occurring over the remaining visits. The analysis for the learning effect was undertaken prior to that for GD in order to identify the improvement in perimetric performance.

5.11 Results

5.11.1 The between-individual between-visit (Visits One to Four) performance of the Visual Field Indices

5.11.2 Mean Sensitivity

The summary statistics for the MS derived by SAP, MS_{SAP}, (Top) and that derived by CFF perimetry, (Bottom) over the four visits are shown in Table 5.4 for each eye of the 22 individuals

with age-related cataract. The distributions of MS_{SAP} and of MS_{CFF} by eye, are also illustrated in terms of Box and Whisker plots in Figure 5.2.

Mean Sensitivity (dB)	Visit 1 TOP	Visit 2 TOP	Visit 3 TOP	Visit 4 TOP
Right Mean SD	23.26 3.86	24.23 3.22	24.42 4.23	25.14 2.82
Left Mean SD	23.93 3.76	25.03 3.33	24.88 3.99	25.41 3.03
Right Median IQR	24.55 5.10	25.30 4.52	25.65 5.07	25.95 1.45
Left Median IQR	24.90 4.02	25.95 3.25	25.95 3.05	26.55 2.70

Mean Sensitivity (Hz)	Visit 1 TOP	Visit 2 TOP	Visit 3 TOP	Visit 4 TOP
Right Mean SD	32.18 5.14	34.54 4.82	33.81 4.82	33.41 5.42
Left Mean (SD)	31.60 5.84	32.09 6.25	32.36 5.31	32.53 5.26
Right Median IQR	32.85 7.63	35.40 3.28	35.75 6.68	35.05 8.13
Left Median IQR	33.30 7.00	33.30 7.10	33.85 8.05	31.95 7.53

Table 5.4 The summary statistics (mean, SD, median and IQR) of the MS_{SAP} (top) and MS_{CFF} perimetry (bottom) at each visit for the right eye and for the left eye of the 22 individuals with age-related cataract.

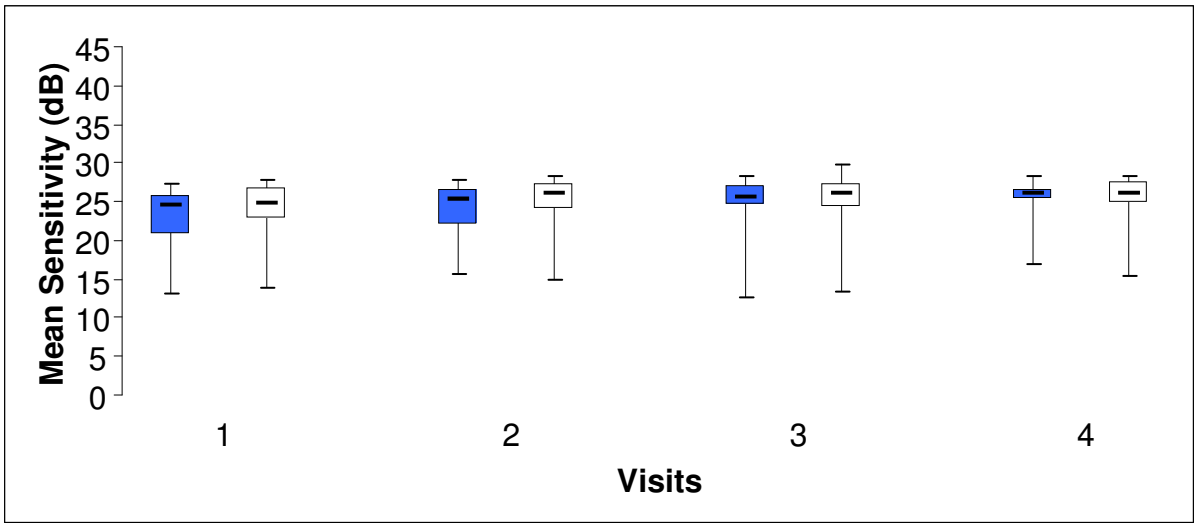

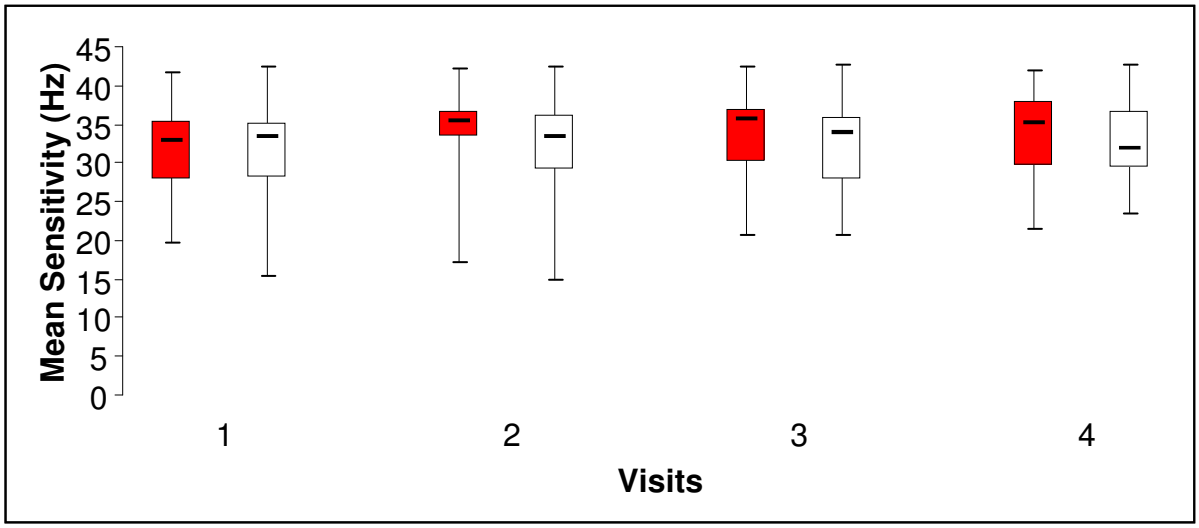

Figure 5.2 The Box and Whisker plots of the distribution of the Mean Sensitivity for SAP (top) and CFF Perimetry (bottom) of each eye at each of the four visits using the TOP algorithm for the 22 individuals with age-related cataract. The median is represented by the bold line, the 25th and 75th percentiles by the lower and upper edges of the box, respectively, and the lowest and highest values by the lower and upper extremities of the whiskers, respectively. The results for the right eye over Visits One to Four are colour coded for the TOP algorithm in blue for SAP and in red for CFF perimetry. The results for the left eye are colour coded in white for SAP and for CFF perimetry.

The ANOVA summary table for MS_{SAP}, with the TOP algorithm over the four visits is given in Table 5.5 The MS_{SAP} was, as would be expected, lowest in the worst of the two eyes (p=0.008). It was also higher in the right eye than in the left eye (p=0.020). It improved across the four visits (p<0.001).

Effect	Degrees of Freedom Numerator	Degrees of Freedom Denominator	F value	P value
Age	1	22	1.79	0.195
Gender	1	22	4.35	**0.049**
Eye	1	154	5.53	**0.020**
Order of Perimetry	1	22	0.20	0.662
Visit	3	154	8.89	**<0.001**
Worst Eye	1	154	7.30	**0.008**

Effect	Degrees of Freedom Numerator	Degrees of Freedom Denominator	F value	P value
Age	1	22	1.70	0.206
Gender	1	22	4.17	**0.053**
Eye	1	154	5.53	**0.020**
Visit	3	154	8.89	**<0.001**
Worst Eye	1	154	7.30	**0.008**

Effect	Degrees of Freedom Numerator	Degrees of Freedom Denominator	F value	P value
Gender	1	22	2.96	1.00
Eye	1	154	5.53	**0.020**
Visit	3	154	8.89	**<0.001**
Worst Eye	1	154	7.30	**0.008**
Visit x Eye	3	154	0.24	0.869
Visit x Worst Eye	3	154	0.40	0.991
Eye x Worst Eye	1	22	1.77	0.197
Gender x Worst Eye	1	154	6.88	**0.010**
Eye x Gender	1	154	1.04	0.310

Table 5.5 The Analysis of Variance Summary Table for the MS_{SAP} index over the Four Visits.

The ANOVA summary table for the MS_{CFF} with the TOP algorithm over the four visits is given in Table 5.6 The MS_{CFF} declined with age (p=0.019) and this reduction in sensitivity with age was greater for the right eye (p=0.023). The MS_{CFF} was lower in the left eye than in the right eye (p<0.001) and was higher when CFF was performed first at any given visit (p=0.025). It improved across the four visits (p=0.013).

Effect	Degrees of Freedom Numerator	Degrees of Freedom Denominator	F value	P value
Age	1	22	6.30	**0.020**
Gender	1	22	0.05	0.830
Eye	1	154	16.60	**<0.001**
Order of Perimetry	1	22	5.81	**0.025**
Visit	3	154	3.74	**0.013**
Worst Eye	1	154	0.28	0.595

Effect	Degrees of Freedom Numerator	Degrees of Freedom Denominator	F value	P value
Age	1	22	6.40	**0.019**
Eye	1	154	16.60	**<0.001**
Order	1	22	5.75	**0.025**
Visit	3	154	3.74	**0.0125**
Worst Eye	1	154	0.28	0.595

Effect	Degrees of Freedom Numerator	Degrees of Freedom Denominator	F value	P value
Age	1	22	6.40	**0.019**
Eye	1	154	16.57	**<0.001**
Order	1	22	5.75	**0.025**
Visit	3	154	3.73	**0.013**
Age x Eye	1	154	5.31	**0.023**
Age x Order	1	22	0.74	0.398
Age x Visit	3	154	0.17	0.919
Eye x Order	1	154	3.32	0.070
Eye x Visit	3	154	1.62	0.188
Order x Visit	3	154	1.10	0.350

Table 5.6 The Analysis of Variance Summary Table for the MS_{CFF} index over the Four Visits.

5.11.3 Mean Defect

The summary statistics for the MD for SAP, MD_{SAP}, (top) and for CFF perimetry, MD_{CFF}, (bottom) over the four visits are shown in Table 5.7 for each eye of the 22 individuals with age-related cataract. The distribution of the MDs, as a function of eye, is also illustrated in terms of Box and Whisker plots in Figure 5.3.

Mean Defect (dB)	Visit 1 TOP	Visit 2 TOP	Visit 3 TOP	Visit 4 TOP
Right Mean	3.07	2.12	1.93	1.15
(SD)	3.81	3.25	4.26	2.98
Left Mean	2.42	1.32	1.55	0.94
(SD)	3.69	3.24	3.83	2.93
Right Median	1.50	0.95	0.65	0.30
IQR	4.65	4.22	2.52	1.42
Left Median/	1.05	0.35	0.40	0.05
IQR	3.45	2.62	2.02	2.02

Mean Defect (Hz)	Visit 1 TOP	Visit 2 TOP	Visit 3 TOP	Visit 4 TOP
Right Mean	2.91	0.59	1.31	1.71
(SD)	4.59	4.43	4.36	5.04
Left Mean	3.48	3.03	2.77	2.58
(SD)	5.70	5.97	4.99	5.11
Right Median	2.60	-0.55	0.10	0.55
IQR	7.10	3.75	5.57	7.27
Left Median	2.15	2.60	1.90	3.75
IQR	6.40	6.00	7.12	7.82

Table 5.7 The summary statistics (mean, SD, median and IQR) of the MD_{SAP} (top) and MD_{CFF} perimetry (bottom) at each visit for the right eye, and for the left eye, of the 22 individuals with age-related cataract.

Overleaf: Figure 5.3 The Box and Whisker plots of the distribution of the MD_{SAP} (top) and MD_{CFF} (bottom) of each eye at each of the Four Visits using the TOP algorithm for the 22 individuals with age-related cataract. The median is represented by the bold line, the 25^{th} and 75^{th} percentiles by the lower and upper edges of the box, respectively, and the lowest and highest values by the lower and upper extremities of the whiskers, respectively. The results for the right eye over Visits One to Four are colour coded for the TOP algorithm in blue for SAP and red for CFF perimetry. The results for the left eye are colour coded in white for SAP and in white for CFF perimetry.

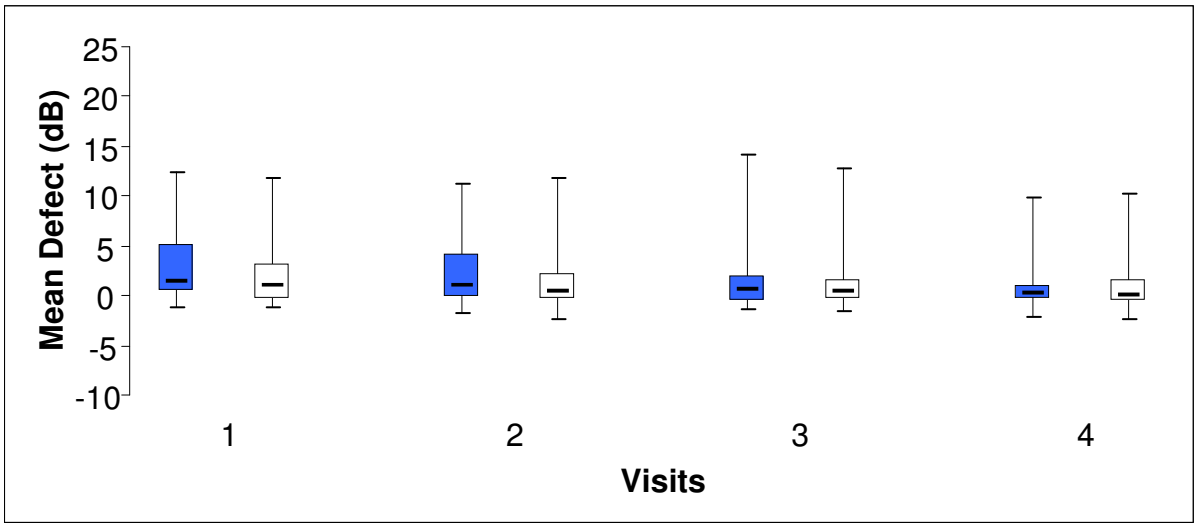

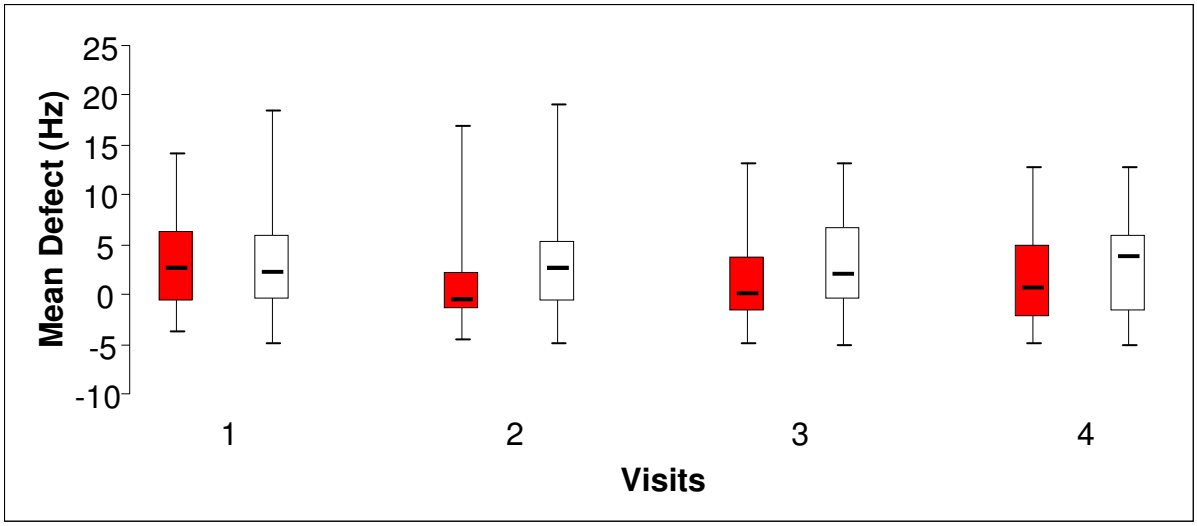

The ANOVA summary table for the MD_{SAP} with the TOP algorithm over the four visits is given in Table 5.8. The MD_{SAP} was, as would be expected, worst for the worse eye (p=0.004) and this finding was more marked for females (p=0.001). As would be also expected from the ANOVA of the MS_{SAP}, MD_{SAP} was worse for the right eye than for the left eye (p=0.030). The MD_{SAP} improved across the four visits (p<0.001).

Effect	Degrees of Freedom Numerator	Degrees of Freedom Denominator	F value	P value
Age	1	22	0.21	0.652
Gender	1	22	4.46	**0.046**
Eye	1	154	4.80	**0.030**
Order of Perimetry	1	22	0.20	0.661
Visit	3	154	9.08	**<0.001**
Worst Eye	1	154	8.49	**0.004**

Effect	Degrees of Freedom Numerator	Degrees of Freedom Denominator	F value	P value
Age	1	22	0.18	0.676
Gender	1	22	4.27	**0.051**
Eye	1	154	4.80	**0.030**
Visit	3	154	9.08	**<0.001**
Worst Eye	1	154	8.49	**0.004**

Effect	Degrees of Freedom Numerator	Degrees of Freedom Denominator	F value	P value
Gender	1	22	4.07	0.056
Eye	1	154	4.80	**0.030**
Visit	3	154	9.08	**<0.001**
Worst Eye	1	154	8.49	**0.004**
Visit x Eye	3	154	0.33	0.803
Visit x Worst Eye	3	154	0.02	0.995
Gender x Visit	3	154	2.10	0.103
Eye x Worst Eye	1	22	1.60	0.220
Gender x Worst Eye	1	154	6.89	**0.001**
Eye x Gender	1	154	1.10	0.296

Table 5.8 The Analysis of Variance Summary Table for the MD_{SAP} index over the Four Visits.

The ANOVA summary table for the MD_{CFF} with the TOP algorithm over the four visits is given in Table 5.9. The MD_{CFF} was lower for the left eye than for the right eye ($p<0.001$) and was worse when CFF was performed first at any given visit ($p=0.034$). It improved across the four visits ($p=0.019$).

Effect	Degrees of Freedom Numerator	Degrees of Freedom Denominator	F value	P value
Age	1	22	1.39	0.251
Gender	1	22	0.04	0.849
Eye	1	154	16.32	**<0.001**
Order of Perimetry	1	22	5.71	**0.026**
Visit	3	154	3.44	**0.018**
Worst Eye	1	154	0.28	0.598

Effect	Degrees of Freedom Numerator	Degrees of Freedom Denominator	F value	P value
Age	1	22	1.36	0.256
Eye	1	154	16.32	**<0.001**
Order	1	22	5.67	**0.026**
Visit	3	154	3.44	**0.018**
Worst Eye	1	154	0.28	0.598

Effect	Degrees of Freedom Numerator	Degrees of Freedom Denominator	F value	P value
Age	1	22	1.36	0.256
Eye	1	154	16.29	**<0.001**
Order	1	22	5.67	**0.026**
Visit	3	154	3.43	**0.019**

Effect	Degrees of Freedom Numerator	Degrees of Freedom Denominator	F value	P value
Eye	1	154	16.29	**<0.001**
Order	1	22	5.09	**0.034**
Visit	3	154	3.43	**0.019**
Eye x Order	1	154	3.15	0.078
Eye x Visit	3	154	1.61	0.189
Order x Visit	3	154	0.95	0.418

Table 5.9 The Analysis of Variance Summary Table for the MD_{CFF} index over the Four Visits.

5.11.4 Square root of the Loss Variance (sLV)

The summary statistics for the Square root of the sLV_{SAP} and sLV_{CFF} over the four visits are shown in Table 5.10 for each eye of the 22 individuals with age-related cataract. The distributions of the sLV_{SAP}, are also illustrated in terms of Box and Whisker plots in Figure 5.4.

Square root of Loss Variance (sLV) (dB)	Visit 1 TOP	Visit 2 TOP	Visit 3 TOP	Visit 4 TOP
Right Mean	2.88	2.76	2.44	2.17
SD	1.52	2.18	1.95	1.67
Left Mean	2.78	2.33	2.51	1.98
SD	1.92	1.95	2.08	1.31
Right Median	2.42	1.92	1.71	1.82
IQR	2.16	2.26	0.92	1.32
Left Median	2.10	1.71	1.75	1.59
IQR	1.79	1.47	1.52	1.10

Square root of Loss Variance (sLV) (Hz)	Visit 1 TOP	Visit 2 TOP	Visit 3 TOP	Visit 4 TOP
Right Mean	4.02	3.86	3.64	3.57
SD	1.80	2.11	2.23	2.52
Left Mean	4.02	3.96	4.05	3.79
SD	2.12	2.21	2.47	2.01
Right Median	3.42	3.23	2.85	2.87
IQR	1.86	1.13	1.24	1.63
Left Median	3.55	3.58	3.68	3.44
IQR	1.78	2.20	1.52	2.48

Table 5.10 The summary statistics of the sLV_{SAP} (top) and sLV_{CFF} (bottom) at each visit for the right eye and for the left eye of the 22 individuals with age-related cataract.

Overleaf: Figure 5.4 The Box and Whisker plots of the distribution of the sLV_{SAP} (top) and sLV_{CFF} (bottom) of each eye at each of the four visits using the TOP algorithm of the 22 individuals with age-related cataract. The median is represented by the bold line, the 25^{th} and 75^{th} percentiles by the lower and upper edges of the box, respectively, and the lowest and highest values by the lower and upper extremities of the whiskers, respectively. The results for the right eye over Visits One to Four are colour coded for the TOP algorithm in blue for SAP and in red for CFF perimetry. The results for the left eye are colour coded in white for SAP and for CFF perimetry.

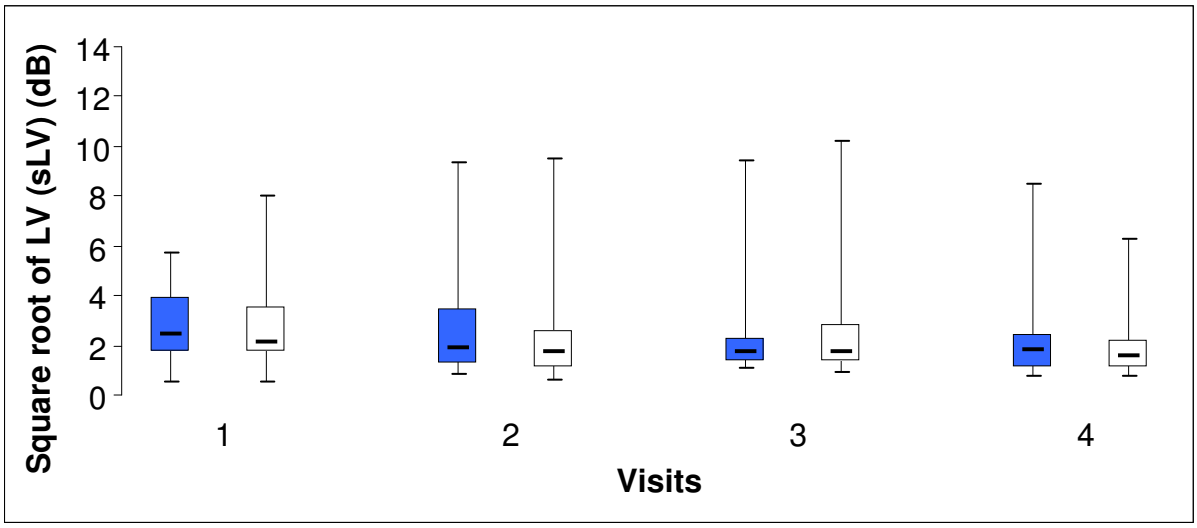

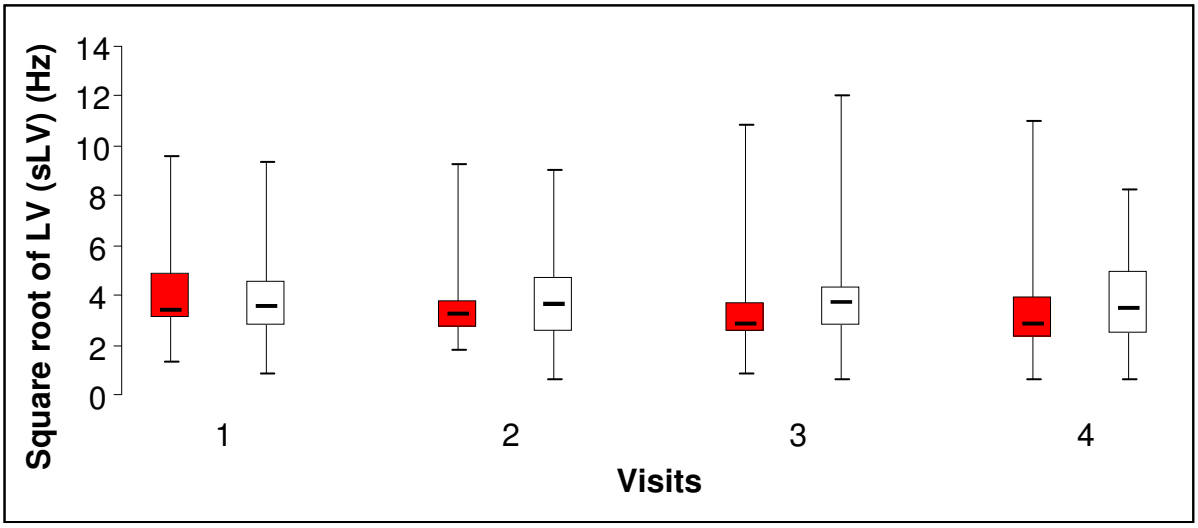

The ANOVA summary table for the sLV_{SAP} with the TOP algorithm is given in Table 5.11. The sLV_{SAP} improved over the four visits (p=0.003).

Effect	Degrees of Freedom Numerator	Degrees of Freedom Denominator	F value	P value
Age	1	22	0.93	0.345
Gender	1	22	0.39	0.537
Eye	1	154	1.52	0.219
Order of Perimetry	1	22	6.78	**0.016**
Visit	3	154	1.00	0.393
Worst Eye	1	154	1.56	0.213

Effect	Degrees of Freedom Numerator	Degrees of Freedom Denominator	F value	P value
Age	1	22	0.69	0.415
Eye	1	154	1.52	0.219
Order	1	22	6.39	**0.019**
Visit	3	154	1.00	0.393
Worst Eye	1	154	1.56	0.213

Effect	Degrees of Freedom Numerator	Degrees of Freedom Denominator	F value	P value
Gender	1	22	4.24	**0.052**
Eye	1	154	1.29	0.258
Order	1	22	1.10	0.305
Visit	3	154	5.02	**0.002**

Effect	Degrees of Freedom Numerator	Degrees of Freedom Denominator	F value	P value
Gender	1	22	3.70	0.068
Eye	1	154	1.29	0.258
Visit	3	154	5.02	**0.002**

Effect	Degrees of Freedom Numerator	Degrees of Freedom Denominator	F value	P value
Gender	1	22	3.70	0.068
Visit	3	154	4.98	**0.003**
Gender X Visit	3	154	0.51	0.678

Table 5.11 The Analysis of Variance Summary Table for the sLV_{SAP} index over the Four Visits.

The ANOVA summary table for the sLV_{CFF} with the TOP algorithm over the four visits is given in Table 5.12. sLV_{CFF} was higher when SAP was undertaken before CFF perimetry (p=0.023).

Effect	Degrees of Freedom Numerator	Degrees of Freedom Denominator	F value	P value
Age	1	22	1.39	0.251
Gender	1	22	0.04	0.849
Eye	1	154	16.32	**<0.001**
Order of Perimetry	1	22	5.71	0.026
Visit	3	154	3.44	**0.018**
Worst Eye	1	154	0.28	0.598

Effect	Degrees of Freedom Numerator	Degrees of Freedom Denominator	F value	P value
Age	1	22	1.36	0.256
Eye	1	154	16.32	**<0.001**
Order	1	22	5.67	**0.026**
Visit	3	154	3.44	**0.018**
Worst Eye	1	154	0.28	0.598

Effect	Degrees of Freedom Numerator	Degrees of Freedom Denominator	F value	P value
Eye	1	154	1.52	0.219
Order	1	22	6.01	**0.023**
Visit	3	154	1.00	0.393
Worst Eye	1	154	1.56	0.214

Table 5.12 The Analysis of Variance Summary Table for the sLV_{CFF} index over the Four Visits.

5.11.5 Diffuse Defect

The summary statistics for the DD_{SAP} (top) and DD_{CFF} (bottom) over the four visits are shown in Table 5.13 for each eye of the 22 individuals with age-related cataract. The distribution of the DD, as a function of eye, are also illustrated in terms of Box and Whisker plots in Figure 5.5.

Diffuse Defect (dB)	Visit 1 TOP	Visit 2 TOP	Visit 3 TOP	Visit 4 TOP
Right Mean	2.18	1.19	1.35	0.91
SD	2.58	1.41	2.68	1.76
Left Mean	1.57	0.82	0.99	0.74
SD	1.96	1.55	2.18	1.91
Right Median	1.15	1.00	0.55	0.55
IQR	2.60	1.32	1.57	1.35
Left Median	1.10	0.50	0.80	0.50
IQR	1.70	1.40	1.57	1.52

Diffuse Defect (Hz)	Visit 1 TOP	Visit 2 TOP	Visit 3 TOP	Visit 4 TOP
Right Mean	1.78	-0.18	0.44	1.00
SD	3.44	3.25	2.90	3.35
Left Mean	2.22	2.11	1.46	1.65
SD	3.91	4.25	3.40	3.68
Right Median	1.10	-1.05	-0.35	0.30
IQR	5.30	2.80	4.30	6.22
Left Median	1.50	1.65	0.85	2.05
IQR	5.70	4.87	6.40	6.97

Table 5.13 The summary statistics of the DD_{SAP} (top) and DD_{CFF} (bottom) at each visit for the right eye and for the left eye of the 22 individuals with age-related cataract.

Overleaf: Figure 5.5 The Box and Whisker plots of the distribution of the DD_{SAP} (top) and DD_{CFF} (bottom) of each eye at each of the four visits using the TOP algorithm for the 22 individuals with age-related cataract. The median is represented by the bold line, the 25^{th} and 75^{th} percentiles by the lower and upper edges of the box, respectively, and the lowest and highest values by the lower and upper extremities of the whiskers, respectively. The results for the right eye over Visits One to Four are colour coded for the TOP algorithm in blue for SAP and red for CFF perimetry. The results for the left eye are colour coded in white for SAP and for CFF perimetry.

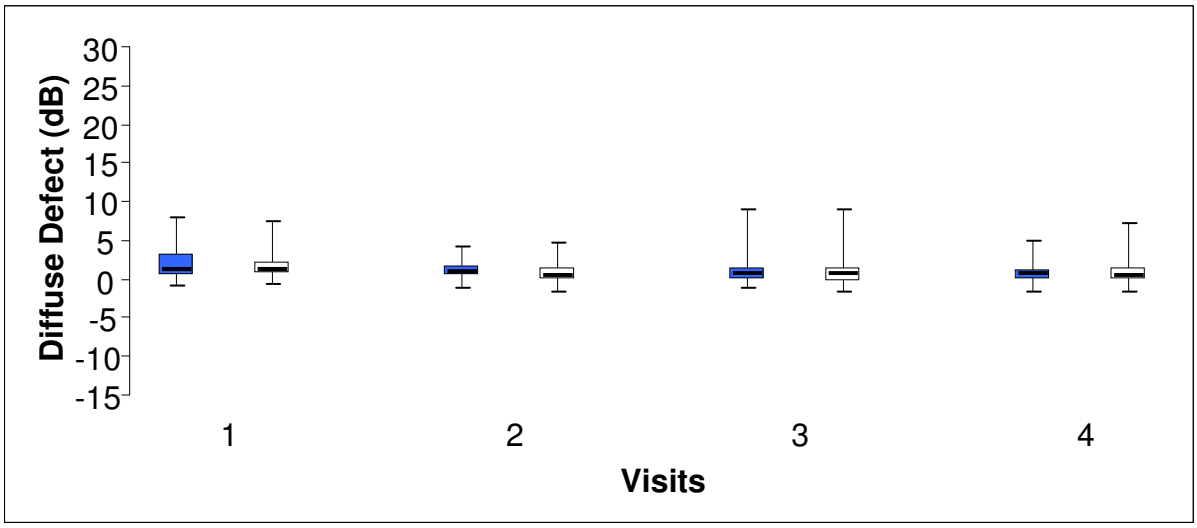

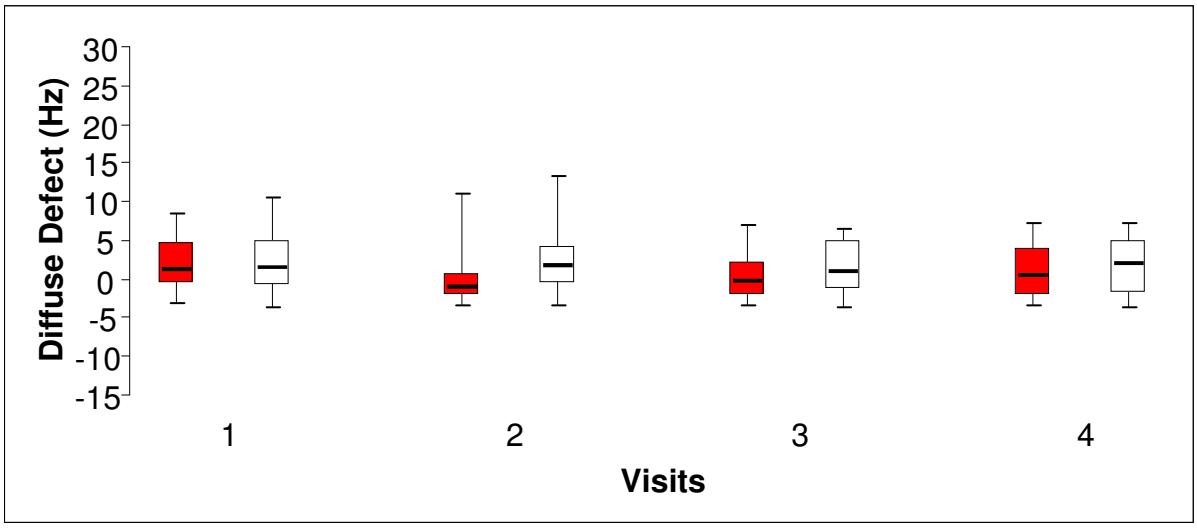

The ANOVA summary table for the DD_{SAP} with the TOP algorithm over the four visits is given in Table 5.14 The DD_{SAP} was lower for the left eye than for the right eye ($p=0.016$) and was worst for the worst eye ($p<0.002$). It improved across the four visits ($p<0.001$) and the improvement over the four visits was greater for females ($p=0.007$).

Effect	Degrees of Freedom Numerator	Degrees of Freedom Denominator	F value	P value
Age	1	22	0.02	0.882
Gender	1	22	3.25	0.085
Eye	1	154	5.97	**0.016**
Order of Perimetry	1	22	0.08	0.787
Visit	3	154	8.77	**<0.001**
Worst Eye	1	154	10.43	**0.002**

Effect	Degrees of Freedom Numerator	Degrees of Freedom Denominator	F value	P value
Gender	1	22	3.32	0.082
Eye	1	154	5.97	**0.016**
Order	1	22	0.08	0.778
Visit	3	154	8.77	**<0.001**
Worst Eye	1	154	10.43	**0.002**

Effect	Degrees of Freedom Numerator	Degrees of Freedom Denominator	F value	P value
Gender	1	22	3.43	0.078
Eye	1	154	5.97	**0.016**
Visit	3	154	8.77	**<0.001**
Worst Eye	1	154	10.43	**0.002**
Visit x Eye	3	154	0.33	0.804
Visit x Worst Eye	3	154	0.09	0.963
Gender x Visit	3	154	4.24	**0.007**
Eye x Worste Eye	1	22	0.95	0.341
Gender x Worst Eye	1	154	6.36	**0.013**
Eye x Gender	1	154	3.03	0.084

Table 5.14 The Analysis of Variance Summary Table for the DD_{SAP} index over the Four Visits.

Effect	Degrees of Freedom Numerator	Degrees of Freedom Denominator	F value	P value
Age	1	22	1.53	0.229
Gender	1	22	0.00	0.960
Eye	1	154	13.75	**<0.001**
Order of Perimetry	1	22	4.17	**0.053**
Visit	3	154	2.73	**0.046**
Worst Eye	1	154	0.19	0.664

Effect	Degrees of Freedom Numerator	Degrees of Freedom Denominator	F value	P value
Age	1	22	1.59	0.220
Eye	1	154	13.75	**<0.001**
Order	1	22	4.19	**0.053**
Visit	3	154	2.73	**0.046**
Worst Eye	1	154	0.19	0.664

Effect	Degrees of Freedom Numerator	Degrees of Freedom Denominator	F value	P value
Age	1	22	1.59	0.220
Eye	1	154	13.73	**<0.001**
Order	1	22	4.19	0.527
Visit	3	154	2.73	**0.046**

Effect	Degrees of Freedom Numerator	Degrees of Freedom Denominator	F value	P value
Eye	1	154	13.73	**<0.001**
Order	1	22	3.68	0.068
Visit	3	154	2.73	**0.046**
Eyex Order	1	154	1.23	0.269
Eye x Visit	3	154	2.05	0.110
Order x Visit	3	154	0.82	0.484

Table 5.15 The Analysis of Variance Summary Table for the DD_{CFF} index over the Four Visits.

The ANOVA summary table for the DD_{CFF} with the TOP algorithm over the four visits is given in Table 5.15. The DD_{CFF} was lower for the left eye than for the right eye ($p<0.001$). It improved across the four visits $p=0.046$).

5.11.6 Local Defect

The summary statistics for the LD_{SAP} (top) and LD_{CFF} (bottom) over the four visits are shown in Table 5.16 for each eye of the 22 individuals with age-related cataract. The distribution of the LD, as a function of eye, is also illustrated in terms of Box and Whisker plots in Figure 5.6.

Local Defect (dB)	Visit 1 TOP	Visit 2 TOP	Visit 3 TOP	Visit 4 TOP
Right	1.74	1.68	1.27	1.03
SD	1.85	2.90	2.69	2.00
Left	1.70	1.26	1.31	0.94
SD	2.45	2.55	2.82	1.84
Right Median	1.20	0.45	0.10	0.25
IQR	2.35	1.90	0.83	1.20
Left Median	0.70	0.10	0.25	0.20
IQR	1.90	1.35	1.28	0.78

Local Defect (Hz)	Visit 1 TOP	Visit 2 TOP	Visit 3 TOP	Visit 4 TOP
Right	1.06	0.75	0.82	0.89
SD	1.89	1.91	2.18	2.64
Left	1.25	1.33	1.21	1.07
SD	2.57	2.33	2.39	1.95
Right Median	0.05	0.00	0.00	0.00
IQR	1.28	0.10	0.25	0.15
Left Median	0.15	0.10	0.25	0.10
IQR	0.88	0.90	0.85	0.90

Table 5.16 The summary statistics of the LD_{SAP} (top) and LD_{CFF} (bottom) at each visit for the right eye and for the left eye of the 22 individuals with age-related cataract.

Overleaf: Figure 5.6 The Box and Whisker plots of the distribution of the LD_{SAP} (top) and LD_{CFF} (bottom) for each eye at each of the four visits using the TOP algorithm for the 22 individuals with age-related cataract. The median is represented by the bold line, the 25^{th} and 75^{th} percentiles by the lower and upper edges of the box, respectively, and the lowest and highest values by the lower and upper extremities of the whiskers, respectively. The results for the right eye over Visits One to Four are colour coded for the TOP algorithm in blue for SAP and red for CFF. The results for the left eye are colour coded in white for both SAP and CFF.

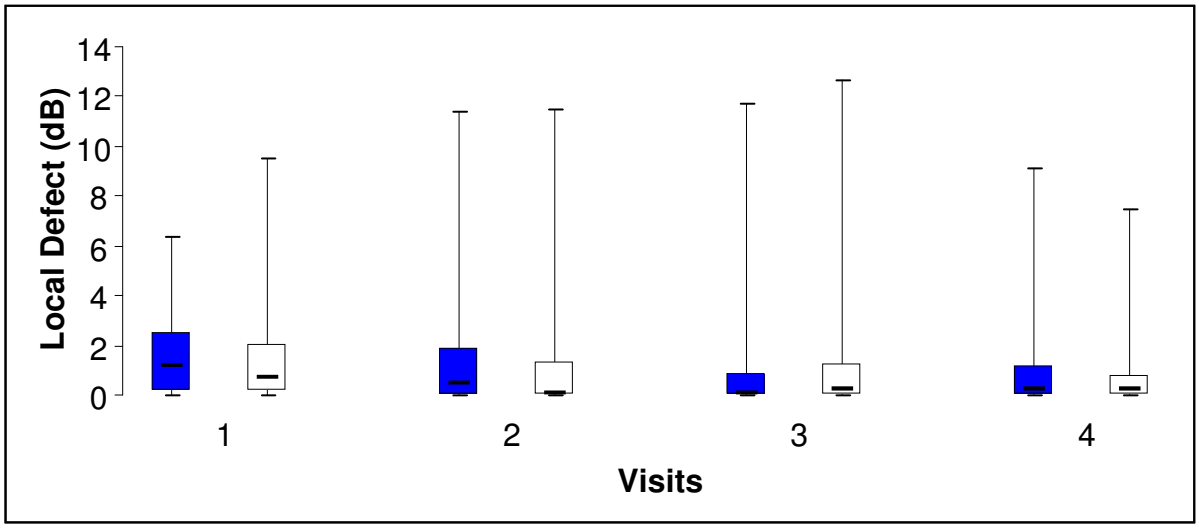
Local Defect (dB)
14
12
10
8
6
4
2
0
1
2
3
4
Visits

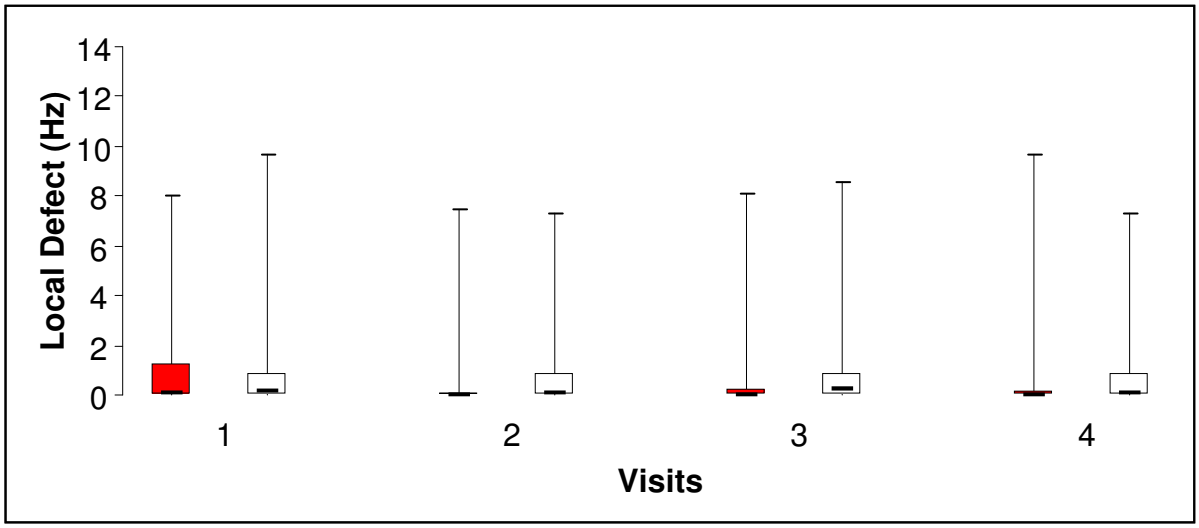
Local Defect (Hz)
14
12
10
8
6
4
2
0
1
2
3
4
Visits

Effect	Degrees of Freedom Numerator	Degrees of Freedom Denominator	F value	P value
Age	1	22	0.10	0.749
Gender	1	22	3.69	0.068
Eye	1	154	0.55	0.460
Order of Perimetry	1	22	1.18	0.290
Visit	3	154	3.24	**0.024**
Worst Eye	1	154	1.27	0.262

Effect	Degrees of Freedom Numerator	Degrees of Freedom Denominator	F value	P value
Gender	1	22	3.59	0.071
Eye	1	154	0.55	0.460
Order	1	22	1.13	0.300
Visit	3	154	3.24	**0.024**
Worst Eye	1	154	1.27	0.262

Effect	Degrees of Freedom Numerator	Degrees of Freedom Denominator	F value	P value
Gender	1	22	3.59	0.071
Order	1	22	1.13	0.300
Visit	3	154	3.23	**0.024**
Worst Eye	1	154	1.26	0.263

Effect	Degrees of Freedom Numerator	Degrees of Freedom Denominator	F value	P value
Gender	1	22	3.10	0.092
Visit	3	154	3.23	**0.024**
Worst Eye	1	154	1.26	0.263

Effect	Degrees of Freedom Numerator	Degrees of Freedom Denominator	F value	P value
Gender	1	22	3.10	0.092
Visit	3	154	3.23	**0.024**
Gender x Visit	3	154	0.66	0.578

Table 5.17 The Analysis of Variance Summary Table for the LD_{SAP} index over the Four Visits.

The ANOVA summary table for the LD_{SAP} with the TOP algorithm over the four visits is given in Table 5.17. The LD_{SAP} improved across the four visits p=0.024).

Effect	Degrees of Freedom Numerator	Degrees of Freedom Denominator	F value	P value
Age	1	22	0.09	0.772
Gender	1	22	0.19	0.667
Eye	1	154	6.39	**0.013**
Order of Perimetry	1	22	4.17	**0.053**
Visit	3	154	0.33	0.802
Worst Eye	1	154	1.35	0.247

Effect	Degrees of Freedom Numerator	Degrees of Freedom Denominator	F value	P value
Age	1	22	0.09	0.772
Gender	1	22	0.19	0.667
Eye	1	154	6.35	**0.013**
Order	1	22	4.17	**0.053**
Worst Eye	1	154	1.34	0.249

Effect	Degrees of Freedom Numerator	Degrees of Freedom Denominator	F value	P value
Gender	1	22	0.14	0.710
Eye	1	154	6.35	0.013
Order	1	22	4.08	**0.056**
Worst Eye	1	154	1.34	0.249

Effect	Degrees of Freedom Numerator	Degrees of Freedom Denominator	F value	P value
Eye	1	154	6.35	**0.013**
Order	1	22	3.95	**0.060**
Worst Eye	1	154	1.34	0.249

Effect	Degrees of Freedom Numerator	Degrees of Freedom Denominator	F value	P value
Eye	1	154	6.30	**0.013**
Order	1	22	3.95	**0.059**
Eye x Order	1	154	5.68	**0.018**

Table 5.18 The analysis of Variance Summary Table for the LD_{CFF} index over the Four Visits.

The ANOVA summary table for the LD_{CFF} with the TOP algorithm over the four visits is given in Table 5.18. The LD_{CFF} was lower for the left eye than for the right eye (p=0.013) and this difference was more pronounced when CFF perimetry was performed last (p=0.018)

5.11.7 Examination Duration

The summary statistics for the examination duration for SAP (top) and CFF perimetry (bottom) over the four visits are shown in Table 5.19 for each eye of the 22 individuals with age-related cataract. The distribution of the examination duration, as a function of eye, is also illustrated in terms of Box and Whisker plots in Figure 5.7.

Examination Duration SAP (Seconds)	Visit 1 TOP	Visit 2 TOP	Visit 3 TOP	Visit 4 TOP
Right Mean	163	152	155	153
SD	25	14	36	29
Left Mean	160	146	151	150
SD	21	19	31	27
Right Median	157	150	147	145
IQR	19	20	18	24
Left Median	156	138	144	138
IQR	27	22	19	31

Examination Duration CFF (Seconds)	Visit 1 TOP	Visit 2 TOP	Visit 3 TOP	Visit 4 TOP
Right Mean	272	228	234	233
SD	58	53	69	70
Left Mean	265	224	229	221
SD	76	47	59	58
Right Median	265	215	212	222
IQR	56	55	62	55
Left Median	244	209	213	199
IQR	61	41	59	69

Table 5.19 The summary statistics of the examination duration (seconds) for SAP (Top) and CFF (Bottom) at each visit for the right eye and for the left eye of the 22 individuals with age-related cataract.

Overleaf: Figure 5.7 The Box and Whisker plots of the distribution of the examination duration for SAP (top) and CFF (bottom) for each eye at each of the four visits using the TOP algorithm for the 22 individuals with age-related cataract. The median is represented by the bold line, the 25th and 75th percentiles by the lower and upper edges of the box, respectively, and the lowest and highest values by the lower and upper extremities of the whiskers, respectively. The results for the right eye over Visits One to Four are colour coded for the TOP algorithm in blue for SAP and red for CFF. The results for the left eye are colour coded in white for both SAP and CFF.

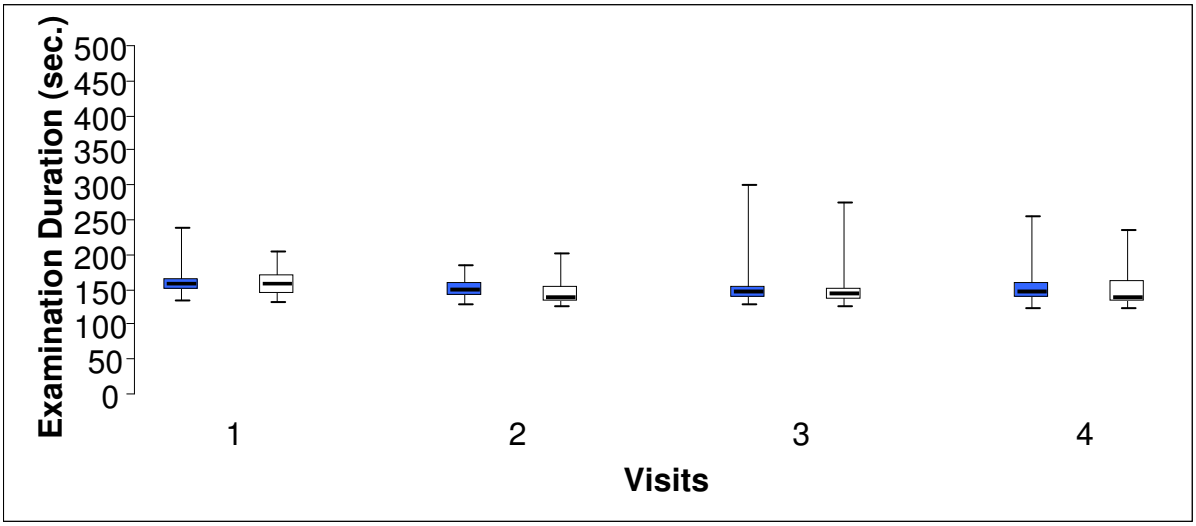

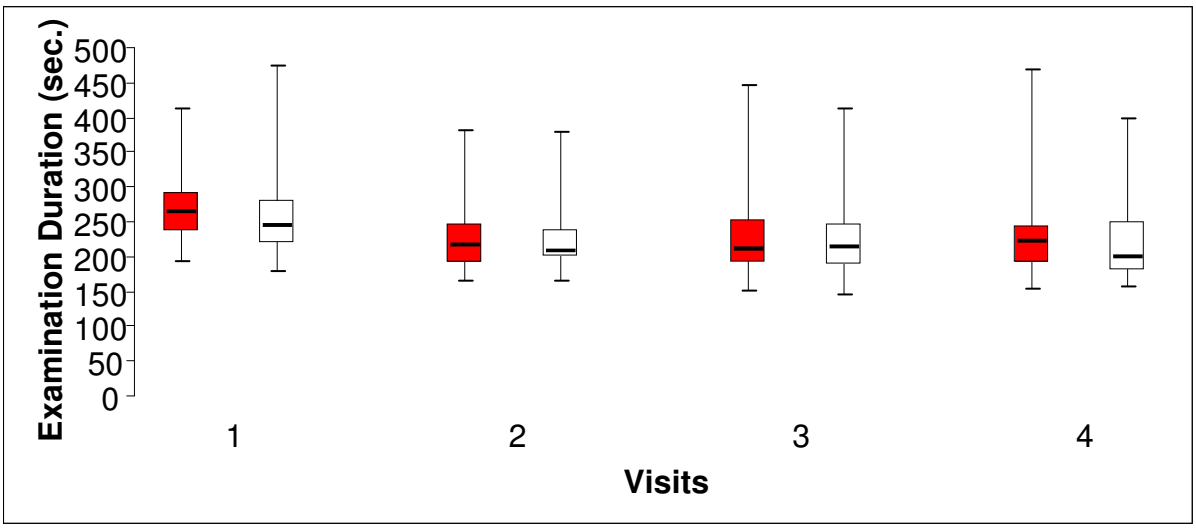

The ANOVA summary table for the examination duration$_{SAP}$ with the TOP algorithm over the four visits is given in Table 5.20 The examination duration$_{SAP}$ became shorter over the four examinations (p=0.006).

Effect	Degrees of Freedom Numerator	Degrees of Freedom Denominator	F value	P value
Age	1	22	1.69	0.207
Gender	1	22	3.75	0.066
Eye	1	154	2.29	0.132
Order of Perimetry	1	22	0.04	0.850
Visit	3	154	4.36	**0.006**
Worst Eye	1	154	0.00	0.961

Effect	Degrees of Freedom Numerator	Degrees of Freedom Denominator	F value	P value
Age	1	22	1.69	0.207
Gender	1	22	3.75	0.066
Eye	1	154	2.29	0.132
Order	1	22	0.04	0.850
Visit	3	154	4.36	**0.006**

Effect	Degrees of Freedom Numerator	Degrees of Freedom Denominator	F value	P value
Age	1	22	1.74	0.201
Gender	1	22	3.86	0.062
Eye	1	154	2.29	0.132
Visit	3	154	4.36	**0.006**

Effect	Degrees of Freedom Numerator	Degrees of Freedom Denominator	F value	P value
Gender	1	22	2.69	0.115
Eye	1	154	2.29	0.132
Visit	3	154	4.36	**0.006**

Effect	Degrees of Freedom Numerator	Degrees of Freedom Denominator	F value	P value
Gender	1	22	2.69	0.115
Visit	3	154	4.29	**0.006**

Effect	Degrees of Freedom Numerator	Degrees of Freedom Denominator	F value	P value
Visit	3	154	4.29	**0.006**

Table 5.20 The Analysis of Variance Summary Table for the examination duration (SAP) index over the Four Visits.

The ANOVA summary table for the examination duration$_{CFF}$ with the TOP algorithm over the four visits is given in Table 5.21 The examination duration$_{CFF}$ also became shorter over the four examinations ($p<0.001$).

Effect	Degrees of Freedom Numerator	Degrees of Freedom Denominator	F value	P value
Age	1	22	1.13	0.298
Gender	1	22	4.88	**0.038**
Eye	1	154	1.25	0.265
Order of Perimetry	1	22	0.05	0.833
Visit	3	154	9.41	**<0.001**
Worst Eye	1	154	0.006	0.811

Effect	Degrees of Freedom Numerator	Degrees of Freedom Denominator	F value	P value
Age	1	22	1.10	0.305
Gender	1	22	4.82	**0.039**
Eye	1	154	1.25	0.265
Visit	3	154	9.41	**<0.001**
Worst Eye	1	154	0.06	0.811

Effect	Degrees of Freedom Numerator	Degrees of Freedom Denominator	F value	P value
Age	1	22	1.10	0.305
Gender	1	22	4.82	**0.039**
Eye	1	154	1.25	0.265
Visit	3	154	9.41	**<0.001**

Effect	Degrees of Freedom Numerator	Degrees of Freedom Denominator	F value	P value
Gender	1	22	4.83	0.063
Eye	1	154	1.25	0.265
Visit	3	154	9.41	**<0.001**

Effect	Degrees of Freedom Numerator	Degrees of Freedom Denominator	F value	P value
Gender	1	22	3.83	0.063
Visit	3	154	9.33	**<0.001**
Gender x Visit	3	154	2.07	0.106

Table 5.21 The Analysis of Variance Summary Table for the examination duration (CFF) index over the Four Visits.

5.11.8 The ratio of the Peripheral Mean Sensitivity (PMS) to the Central Mean Sensitivity (CMS)

The summary statistics for the ratio of the Peripheral Mean Sensitivity (PMS) to the Central Mean Sensitivity (CMS) for SAP (top) and for CFF perimetry (bottom) over the four visits are shown in Table 5.22a and 5.22b for each eye of the 22 individuals with age-related cataract.

Peripheral/Central MS	Visit 1 TOP	Visit 2 TOP	Visit 3 TOP	Visit 4 TOP
Right (SD)	0.85 (0.12)	0.85 (0.14)	0.86 (0.15)	0.89 (0.08)
Left (SD)	0.84 (0.13)	0.87 (0.13)	0.86 (0.17)	0.89 (0.10)
Right Median/ IQR	0.87 (0.11)	0.91 (0.04)	0.90 (0.05)	0.92 (0.05)
Left Median/ IQR	0.89 (0.11)	0.90 (0.05)	0.92 (0.08)	0.91 (0.04)

Table 5.22a The ratio of the PMS to the CMS for the 22 individuals with age-related cataract derived by SAP.

Peripheral/Central MS	Visit 1 TOP	Visit 2 TOP	Visit 3 TOP	Visit 4 TOP
Right (SD)	0.91 (0.12)	0.93 (0.13)	0.92 (0.13)	0.91 (0.13)
Left (SD)	0.89 (0.14)	0.90 (0.15)	0.91 (0.14)	0.92 (0.12)
Right Median/ IQR	0.92 (0.08)	0.95 (0.07)	0.95 (0.06)	0.95 (0.09)
Left Median/ IQR	0.92 (0.11)	0.95 (0.09)	0.96 (0.15)	0.95 (0.10)x

Table 5.22b The ratio of the PMS to the CMS for the 22 individuals with age-related cataract derived by CFF perimetry.

The ANOVA summary table for the ratio of the Peripheral Mean Sensitivity (PMS) to the Central Mean Sensitivity (CMS) for SAP with the TOP algorithm over the four visits is given in Table 5.23 The ratio became greater over the four visits (p=0.021) indicating a greater learning effect in the peripheral zone.

Effect	Degrees of Freedom Numerator	Degrees of Freedom Denominator	F value	P value
Age	1	22	2.88	0.104
Gender	1	22	0.00	0.970
Eye	1	154	0.09	0.771
Order of Perimetry	1	22	0.68	0.420
Visit	3	154	3.35	**0.021**
Worst Eye	1	154	3.03	0.084

Effect	Degrees of Freedom Numerator	Degrees of Freedom Denominator	F value	P value
Age	1	22	3.02	0.100
Eye	1	154	0.09	0.771
Order	1	22	0.69	0.415
Visit	3	154	3.35	**0.021**
Worst Eye	1	154	3.03	0.084

Effect	Degrees of Freedom Numerator	Degrees of Freedom Denominator	F value	P value
Age	1	22	3.02	0.100
Order	1	22	0.69	0.415
Visit	3	154	3.35	**0.021**
Worst Eye	1	154	3.03	0.084

Effect	Degrees of Freedom Numerator	Degrees of Freedom Denominator	F value	P value
Age	1	22	3.09	0.093
Visit	3	154	3.35	**0.021**
Worst Eye	1	154	3.03	0.084
Age x Worst Eye	1	154	0.39	0.531
Age x Visit	3	154	0.88	0.451
Visit x Worst Eye	3	154	0.14	0.935

Table 5.23 The Analysis of Variance Summary Table for the PMS to the CMS (SAP) index over the Four Visits.

Effect	Degrees of Freedom Numerator	Degrees of Freedom Denominator	F value	P value
Age	1	22	0.05	0.817
Gender	1	22	0.77	0.391
Eye	1	154	3.59	0.060
Order of Perimetry	1	22	0.13	0.725
Visit	3	154	1.30	0.278
Worst Eye	1	154	0.20	0.652

Effect	Degrees of Freedom Numerator	Degrees of Freedom Denominator	F value	P value
Gender	1	22	0.92	0.348
Eye	1	154	3.59	0.060
Order	1	22	0.14	0.712
Visit	3	154	1.30	0.278
Worst Eye	1	154	0.20	0.652

Effect	Degrees of Freedom Numerator	Degrees of Freedom Denominator	F value	P value
Gender	1	22	0.86	0.365
Eye	1	154	3.59	0.860
Visit	3	154	1.30	0.278
Worst Eye	1	154	0.20	0.652

Effect	Degrees of Freedom Numerator	Degrees of Freedom Denominator	F value	P value
Gender	1	22	0.86	0.365
Eye	1	154	3.58	0.060
Visit	3	154	1.30	0.278

Effect	Degrees of Freedom Numerator	Degrees of Freedom Denominator	F value	P value
Eye	1	154	3.58	0.060
Visit	3	154	1.30	0.278

Effect	Degrees of Freedom Numerator	Degrees of Freedom Denominator	F value	P value
Eye	1	154	3.58	0.060

Table 5.24 The Analysis of Variance Summary Table for the PMS to the CMS (CFF) index over the Four Visits.

The ANOVA summary table for the ratio of the Peripheral Mean Sensitivity (PMS) to the Central Mean Sensitivity (CMS) for CFF with the TOP algorithm over the four visits is given in Table 5.24. None of the variables achieved statistical significance.

5.11.9 Catch Trials

The summary statistics for the incorrect responses to the FP and FN for SAP and for CFF perimetry over the Four visits for each eye of the 22 individuals with age-related cataract are shown in Table 5.25 and Table 5.26.

FP and FN SAP Catch trials (%)	Visit 1 TOP	Visit 2 TOP	Visit 3 TOP	Visit 4 TOP
Right Mean FP	1.14	1.52	1.52	3.03
SD	5.33	7.11	7.11	9.81
Right Median FP	0.00	0.00	0.00	0.00
IQR	0.00	0.00	0.00	0.00
Left Mean FP	3.79	5.30	5.30	4.55
SD	9.87	13.98	11.66	11.71
Left Median FP	0.00	0.00	0.00	0.00
IQR	0.00	0.00	0.00	0.00
Right Mean FN	0.91	2.27	5.68	4.55
SD	4.26	7.36	10.52	9.87
Right Median FN	0.00	0.00	0.00	0.00
IQR	0.00	0.00	0.00	0.00
Left Mean FN	6.82	2.27	4.55	0.00
SD	13.76	7.36	.87	(0.00)
Left Median FN	0.00	0.00	0.00	0.00
IQR	0.00	0.00	0.00	0.00

Table 5.25 The summary statistics of the incorrect responses to the false-positive and false-negative catch trials at each visit for each eye of the 22 individuals with age-related cataract for SAP.

FP and FN CFF Catch trials (%)	Visit 1 TOP	Visit 2 TOP	Visit 3 TOP	Visit 4 TOP
Right Mean FP	15.73	13.11	11.82	10.23
SD	18.05	21.11	15.91	18.35
Right Median FP	13.89	0.00	0.00	0.00
IQR	25.00	25.00	25.00	18.75
Left Mean FP	11.14	16.29	10.15	7.95
SD	12.53	21.44	14.87	14.20
Left Median FP	0.00	0.00	0.00	0.00
IQR	25.00	31.25	23.75	18.75
Right Mean FN	13.26	2.95	8.64	3.18
SD	21.64	7.66	17.81	8.24
Right Median FN	0.00	0.00	0.00	0.00
IQR	20.00	0.00	15.00	0.00
Left Mean FN	5.00	6.36	5.91	3.18
SD	12.54	12.93	11.71	11.29
Left Median FN	0.00	0.00	0.00	0.00
IQR	0.00	0.00	0.00	0.00

Table 5.26 The summary statistics of the incorrect responses to the false-positive and false-negative catch trials at each visit for each eye of the 22 individuals with age-related cataract for CFF perimetry.

The number of incorrect responses to each of the two types of catch trials was insufficient to permit statistical analysis.

The number of individuals across each of the two types of perimetry exhibiting greater than 30% incorrect responses to the false-positive (FP) catch trials for each eye over each of the four visits are shown in Table 5.27. Within the limits of the dataset, the frequency was greater for CFF perimetry than for SAP.

False Positive. responses	Visit	Cataract Individuals SAP		Cataract Individuals CFF	
		Right eye	Left eye	Right eye	Left eye
>30%	**1**	0	1	4	0
>30%	**2**	1	2	3	6
>30%	**3**	1	2	3	2
>30%	**4**	2	3	3	1

Table 5.27 The number of individuals across each of the two perimetric examination procedures exhibiting greater than 30% incorrect responses to the False-positive (FP) catch trials for each eye over each of the four visits.

5.12 The change in sensitivity at each given stimulus location between Visits One and Visits Two and between Visit Two and Visit Four respectively, as a function of eccentricity for SAP and for CFF perimetry.

The change in sensitivity at each stimulus location between Visit Two and Visit One for the right eye (top) and left eye (bottom) for the 22 individuals with age-related cataract is shown for the mean (SD) in Figure 5.8 (SAP), Figure 5.9 (CFF) and for the median (IQR) in Figure 5.10 (SAP), and Figure 5.11 (CFF). In general, both measures of central tendency suggested an approximately similar magnitude of change at Visit Two with increase in eccentricity for the field of each eye for SAP. For CFF perimetry, the mean possibly suggested a greater improvement for the peripheral zones in the field of the right eye at Visit Two, however, the median was less clear in this regard. The field of the left eye showed no evidence of a greater improvement for the peripheral zones at Visit Two, compared to the central zone, either for the mean or for the median.

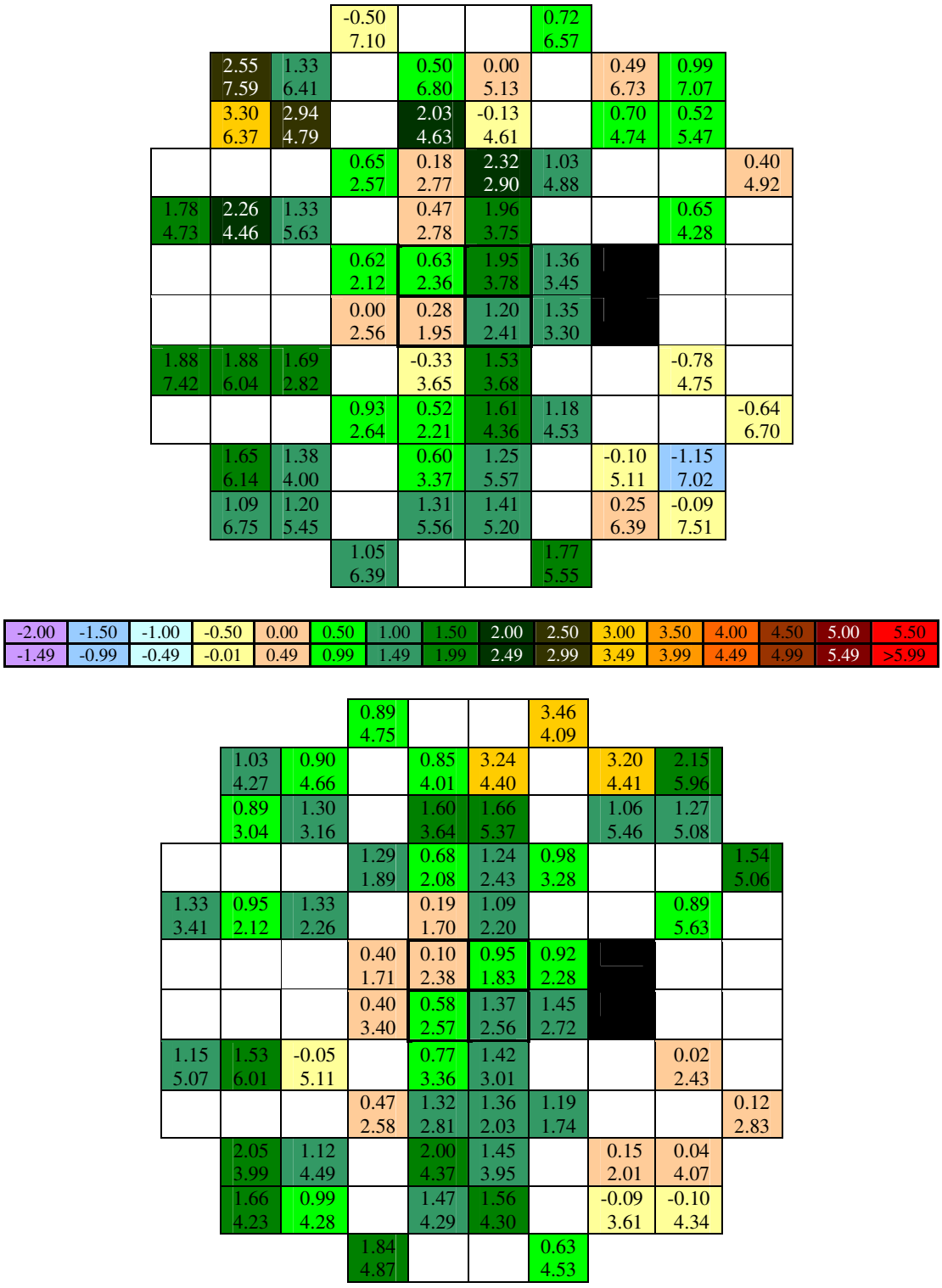

Figure 5.8 The group mean (SD) of the difference in sensitivity (SD) for SAP, Program G1 and the TOP algorithm at each stimulus location between Visit Two and Visit One for the right eye (top) and left eye (bottom) for the 22 individuals with age-related cataract. The stimulus locations for the left eye are displayed in right eye format to aid the between-eye comparison. The lower value indicates the Standard Deviation. Increasing 'warmth' of the colour at each stimulus location indicates an improvement in sensitivity at Visit Two.

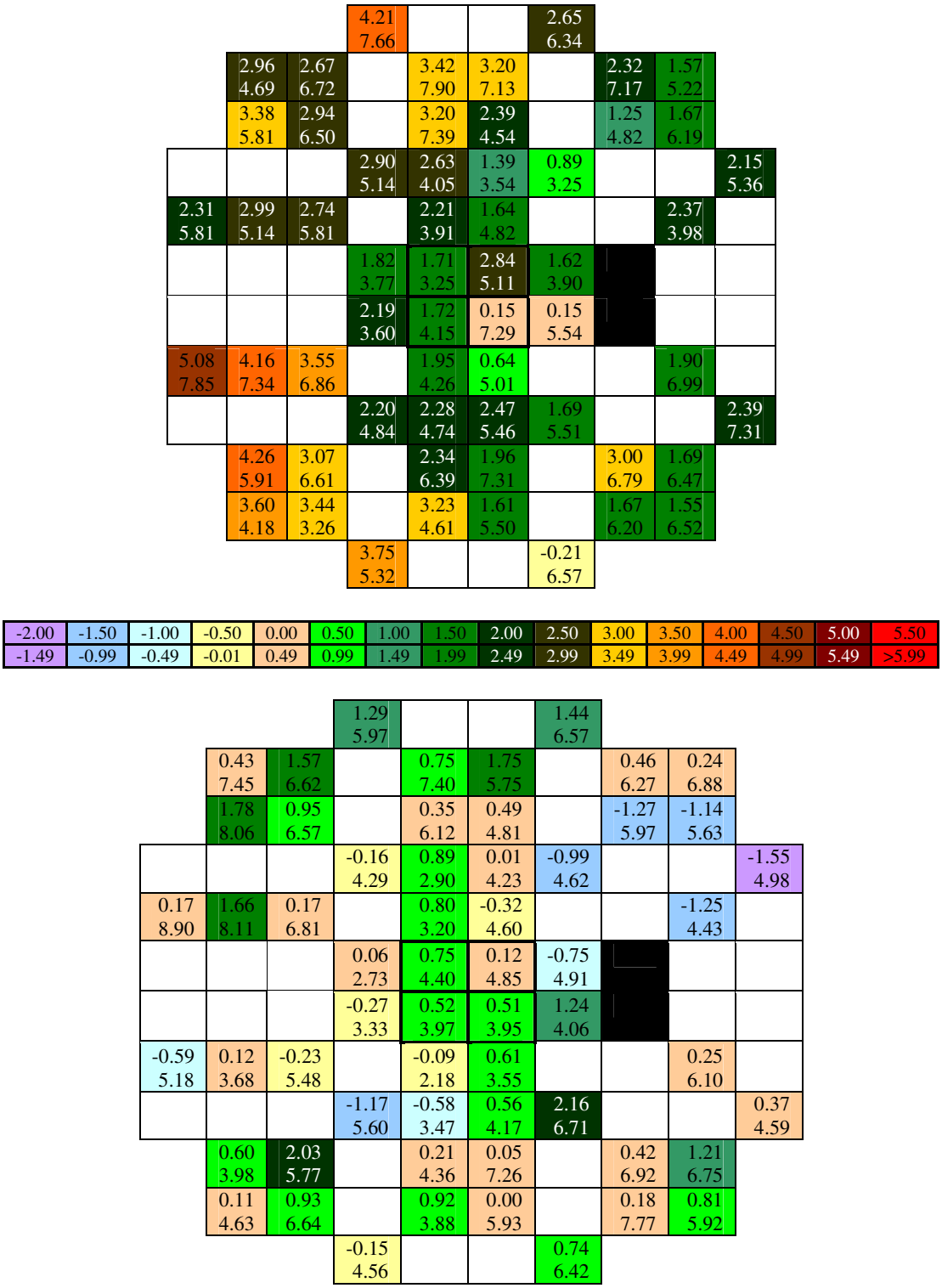

Figure 5.9 The group mean (SD) of the difference in sensitivity (SD) for CFF perimetry, Program G1 and the TOP algorithm at each stimulus location between Visit Two and Visit One for the right eye (top) and left eye (bottom) for the 22 individuals with age-related cataract. The stimulus locations for the left eye are displayed in right eye format to aid the between-eye comparison. The lower value indicates the Standard Deviation. Increasing 'warmth' of the colour at each stimulus location indicates an improvement in sensitivity at Visit Two.

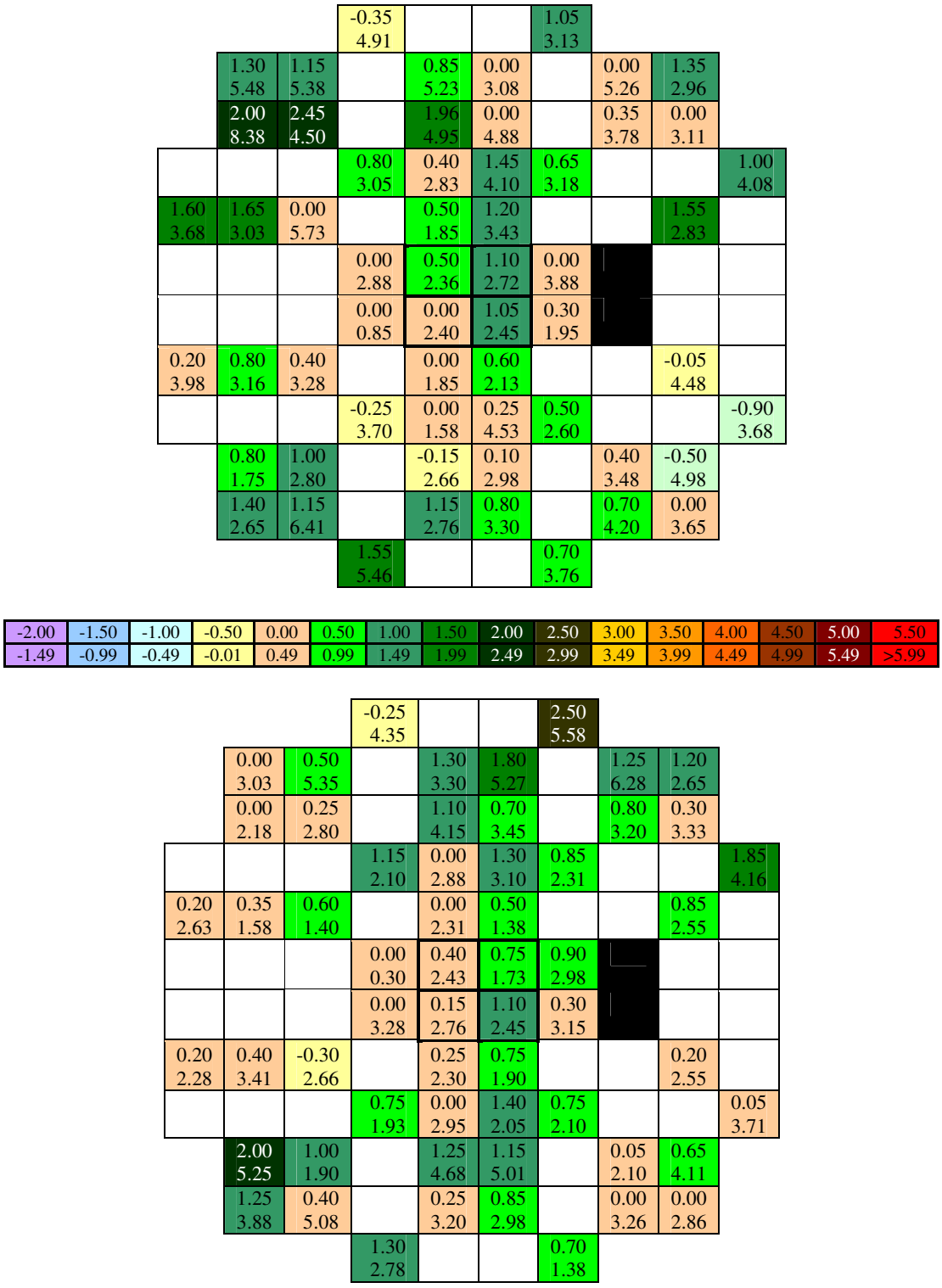

Figure 5.10 The group median (IQR) of the difference in sensitivity (SD) for SAP, Program G1 and the TOP algorithm at each stimulus location between Visit Two and Visit One for the right eye (top) and left eye (bottom) for the 22 individuals with age-related cataract. The stimulus locations for the left eye are displayed in right eye format to aid the between-eye comparison. The lower value indicates the IQR. Increasing 'warmth' of the colour at each stimulus location indicates an improvement in sensitivity at Visit Two.

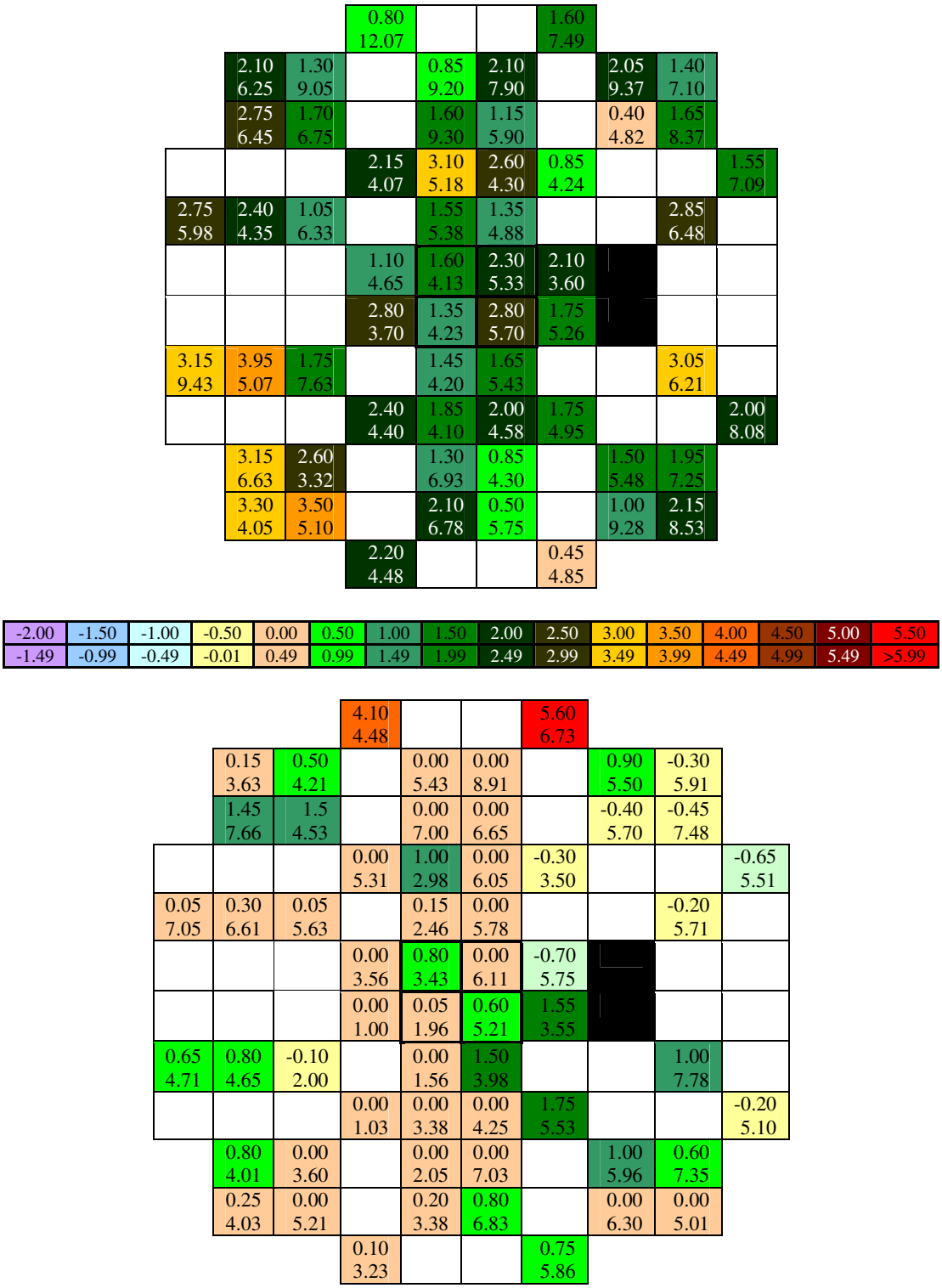

Figure 5.11 The group median (IQR) of the difference in sensitivity (SD) for CFF perimetry, Program G1 and the TOP algorithm at each stimulus location between Visit Two and Visit One for the right eye (top) and left eye (bottom) for the 22 individuals with age-related cataract. The stimulus locations for the left eye are displayed in right eye format to aid the between-eye comparison. The lower value indicates the IQR. Increasing 'warmth' of the colour at each stimulus location indicates an improvement in sensitivity at Visit Two.

The change in sensitivity at each stimulus location between Visit Four and Visit Two for the right eye (top) and left eye (bottom) for the 22 individuals with age-related cataract are shown for the mean (SD) in Figure 5.12 (SAP), Figure 5.13 (CFF) and for the median (IQR) in Figure 5.14 (SAP), Figure 5.15 (CFF).

In general, both measures of central tendency suggested an approximately similar magnitude of change at Visit Four with increase in eccentricity for the field of each eye for SAP. For CFF perimetry, the mean possibly suggested a deterioration for the peripheral zones in the field of the right eye at Visit Four, however, the median did not confirm this trend. The field of the left eye showed no evidence of a greater improvement for the peripheral zones at Visit Four either for the mean of for the median.

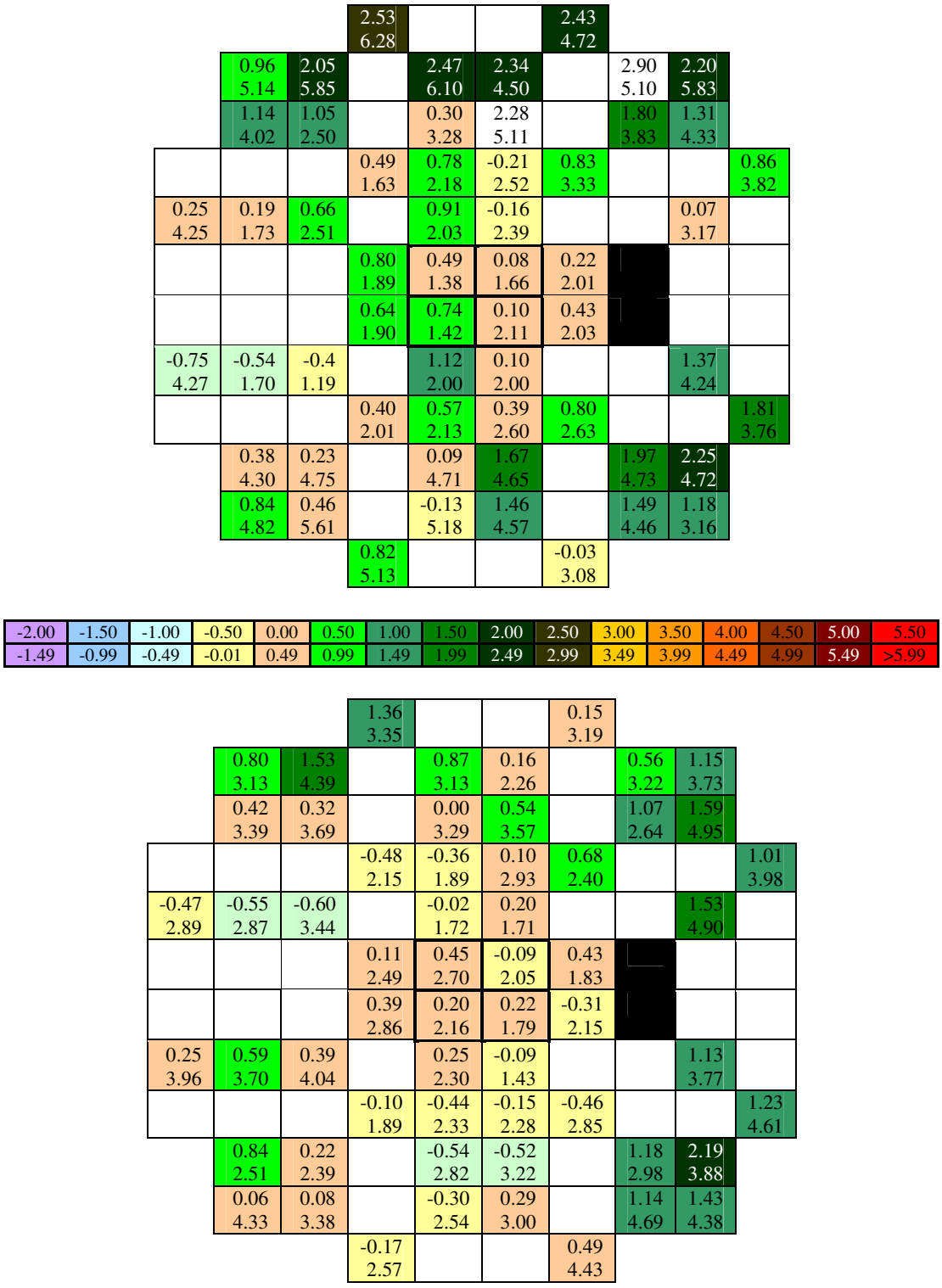

Figure 5.12 The group mean (SD) of the difference in sensitivity (SD) for SAP, Program G1 and the TOP algorithm at each stimulus location between Visit Four and Visit Two for the right eye (top) and left eye (bottom) for the 22 individuals with age-related cataract. The stimulus locations for the left eye are displayed in right eye format to aid the between-eye comparison. The lower value indicates the Standard Deviation. Increasing 'warmth' of the colour at each stimulus location indicates an improvement in sensitivity at Visit Four.

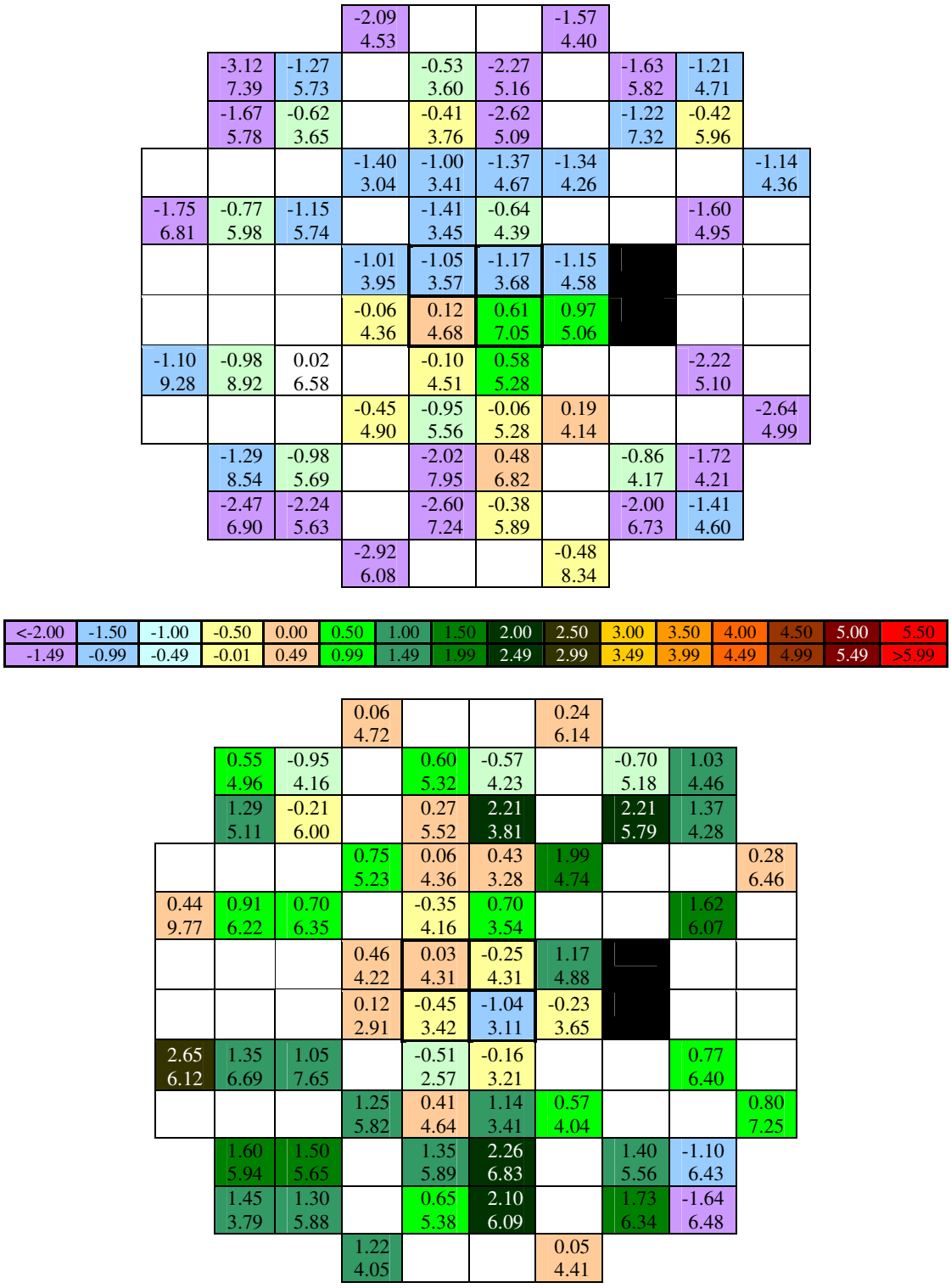

Figure 5.13 The group mean (SD) of the difference in sensitivity (SD) for CFF perimetry, Program G1 and the TOP algorithm at each stimulus location between Visit Four and Visit Two for the right eye (top) and left eye (bottom) for the 22 individuals with age-related cataract. The stimulus locations for the left eye are displayed in right eye format to aid the between-eye comparison. The lower value indicates the Standard Deviation. Increasing 'warmth' of the colour at each stimulus location indicates an improvement in sensitivity at Visit Four.

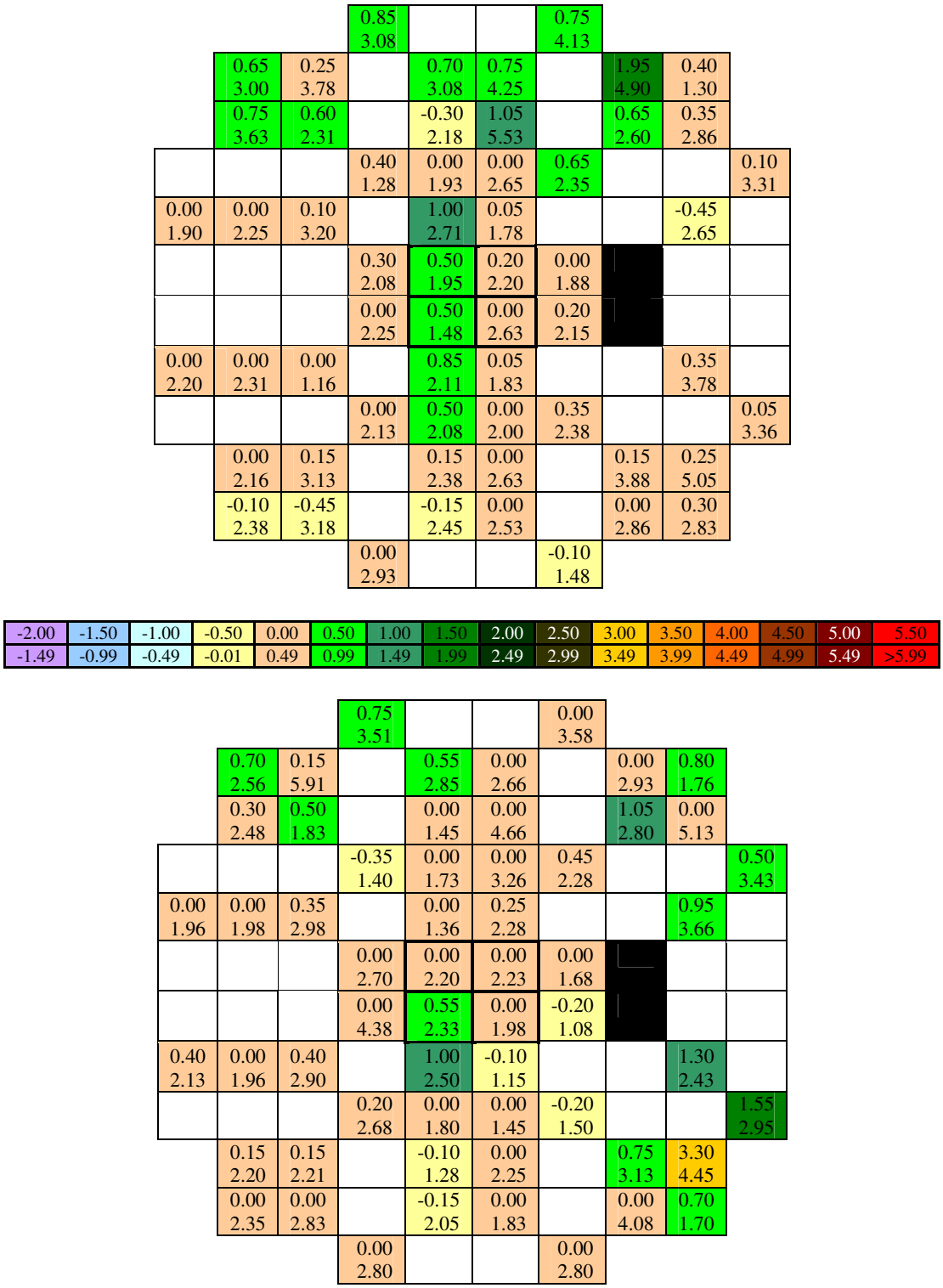

Figure 5.14 The group median (IQR) of the difference in sensitivity (SD) for SAP, Program G1 and the TOP algorithm at each stimulus location between Visit Four and Visit Two for the right eye (top) and left eye (bottom) for the 22 individuals with age-related cataract. The stimulus locations for the left eye are displayed in right eye format to aid the between-eye comparison. The lower value indicates the IQR. Increasing 'warmth' of the colour at each stimulus location indicates an improvement in sensitivity at Visit Four.

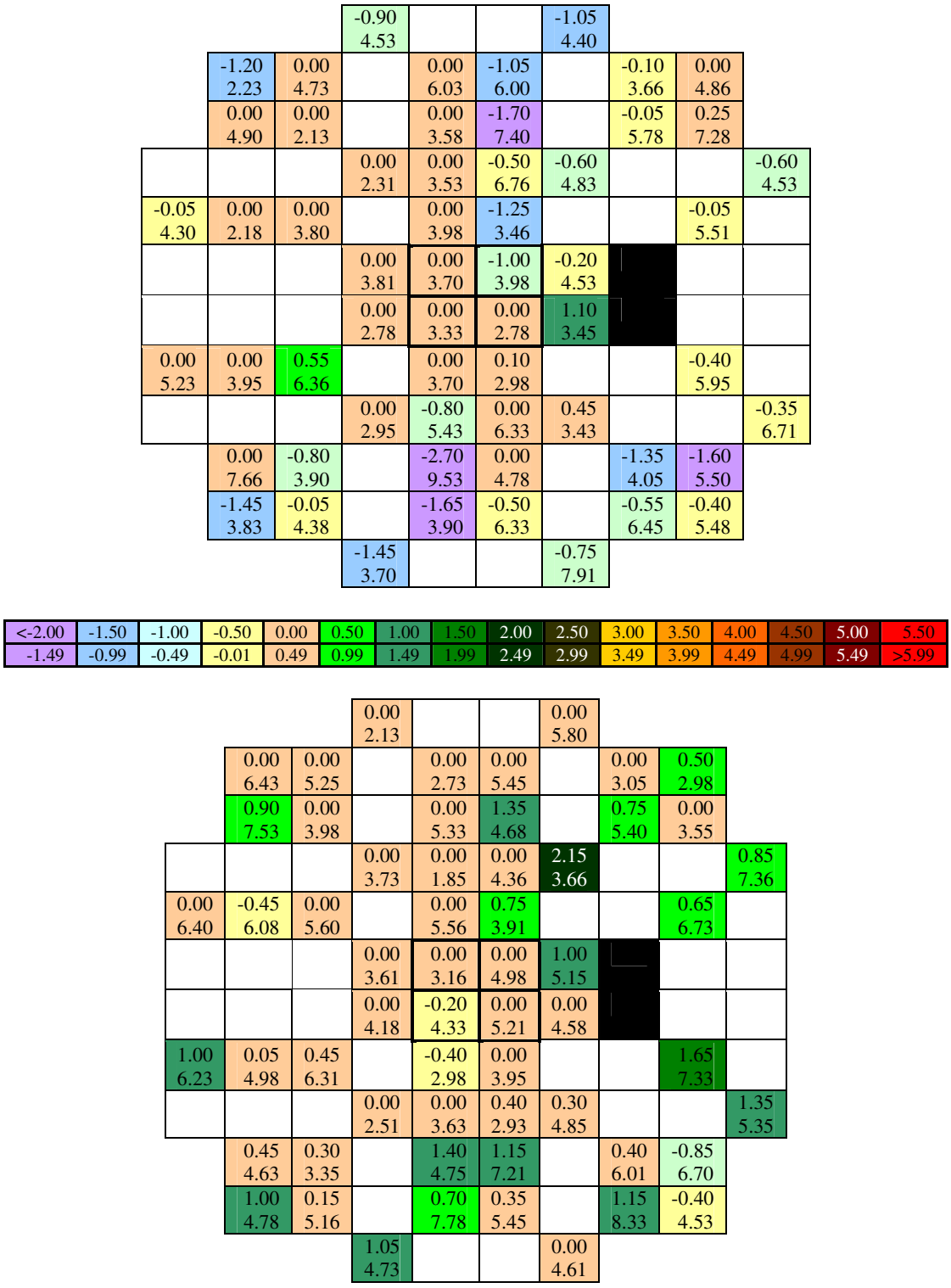

Figure 5.15 The group median (IQR) of the difference in sensitivity (SD) for CFF perimetry, Program G1 and the TOP algorithm at each stimulus location between Visit Four and Visit Two for the right eye (top) and left eye (bottom) for the 22 individuals with age-related cataract. The stimulus locations for the left eye are displayed in right eye format to aid the between-eye comparison. The lower value indicates the IQR. Increasing 'warmth' of the colour at each stimulus location indicates an improvement in sensitivity at Visit Four.

5.13 The change in sensitivity, across all stimulus locations for SAP and CFF perimetry, respectively, from Visit One to Visit Two and between Visit Four and Visit Two, respectively, as a function of the magnitude of sensitivity at the initial visit of the given paired comparison.

The change in sensitivity for SAP, across all stimulus locations, from Visit One and Visit Two as a function of the magnitude of sensitivity at Visit One for the 22 individuals with age-related cataract is given in Figure 5.16 (top) and that from Visit Two and Visit Four as a function of the magnitude of sensitivity at Visit Two in Figure 5.16 (bottom). The corresponding changes for CFF perimetry are given in Figure 5.17 Top and Bottom, respectively.

The 50^{th} percentile of the distribution of the change in sensitivity for SAP from Visits One to Two as a function of the magnitude of sensitivity at Visit One exhibited a positive slope for the field of each eye indicating a greater improvement in sensitivity for the lower values of sensitivity at Visit Two.

A similar trend was apparent for the fields of both eyes from Visit Two and Visit Four as function of the the magnitude of sensitivity at Visit Two. The range of the magnitude of sensitivity along the abscissa was less than that at Visit One due to the resultant improvement in sensitivity from Visit One to Visit Two.

The corresponding figures for CFF perimetry are shown in Figures 5.17 top and bottom. A positive slope was present for the field of each eye for the difference in sensitivity from Visit One to Visit Two as a function of the magnitude of sensitivity at Visit One and for that from Visit Two to Visit Four as a function of the magnitude of sensitivity at Visit Two. However, the data was more variable for the lower values of sensitivity for the field of the right eye compared to that of the left eye and, in general, was more variable for the fields of both eyes compared to that for SAP.

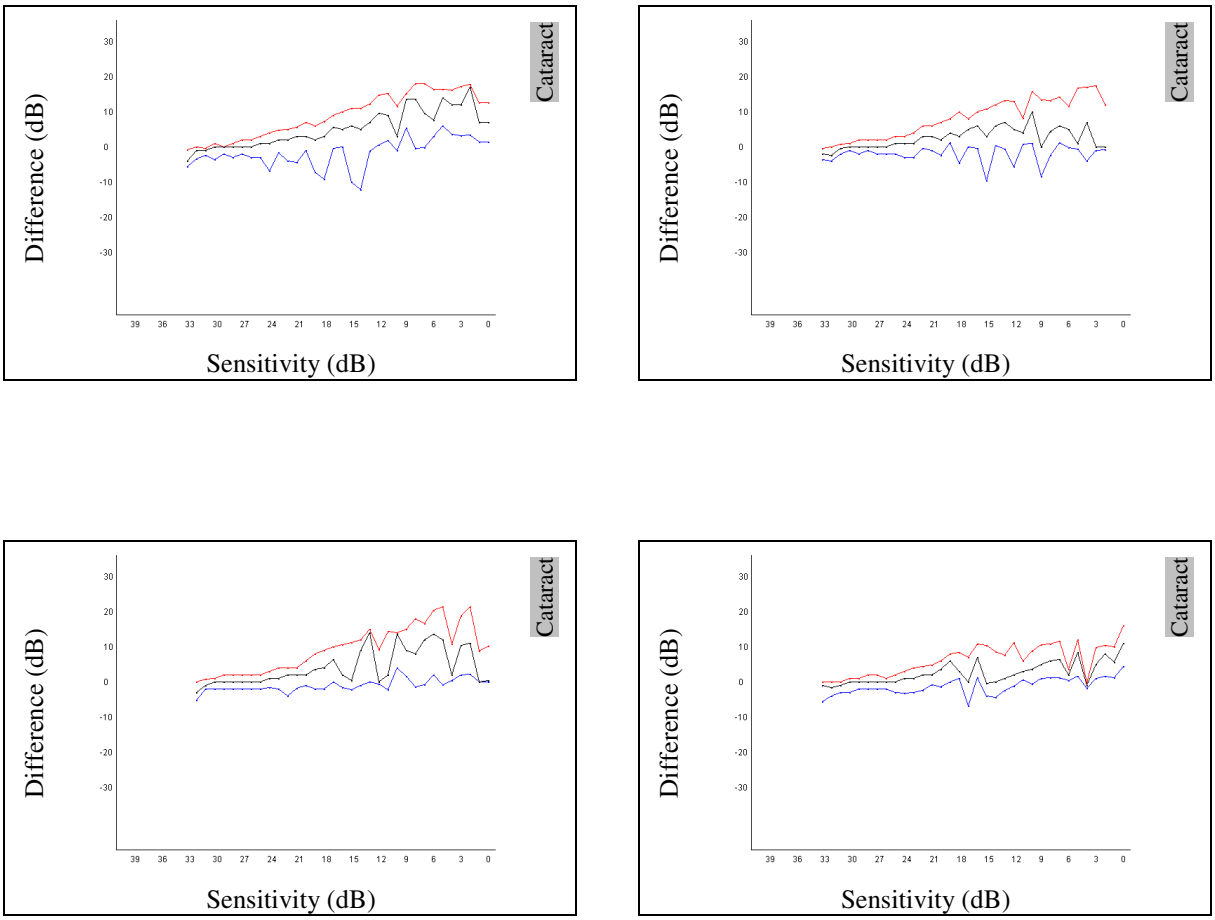

Figure 5.16 The 90th (red), 50th (black) and 10th (blue) percentiles of the distribution of the differences in sensitivity for SAP across all stimulus location from Visit One and Visit Two as a function of the sensitivity at the corresponding stimulus location recorded at Visit One (top) and from Visit Two and Visit Four as a function of the sensitivity at the corresponding stimulus location recorded at Visit Two (bottom) for the right (left column) and left (right column) eye for the 22 individuals with age-related cataract (Program G1, TOP algorithm).

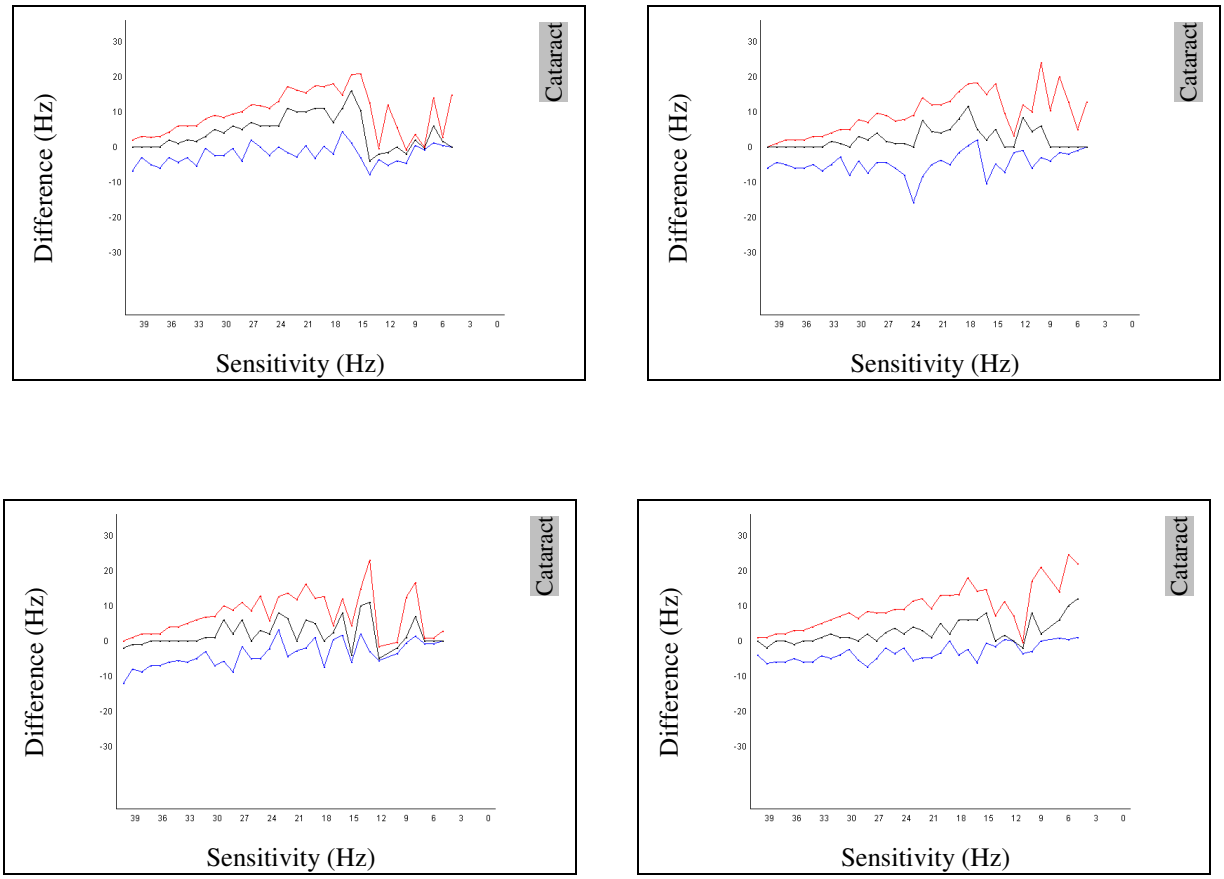

Figure 5.17 The 90th (red), 50th (black) and 10th (blue) percentiles of the distribution of the differences in sensitivity for CFF across all stimulus location from Visit One to Visit Two as a function of the sensitivity at the corresponding stimulus location recorded at Visit One (Top) and from Visit Two to Visit Four as a function of the sensitivity at the corresponding stimulus location recorded at Visit Two (bottom) for the right (left column) and left (right column) eye for the 22 individuals with age-related cataract (Program G1, TOP algorithm).

5.14 The change in the Comparison Probability value, across all given stimulus locations from Visit One to Visit Two, Visit Two to Visit Four, respectively, for the 22 individuals with age-related cataract.

The change in the Comparison Probability value across all given stimulus locations from Visit One to Visit Two for SAP and for CFF perimetry for the 22 individuals with age-related cataract, is given in the Table 5.28 top and bottom, respectively, and from Visits Two to Visit Four in Table 5.29 top and bottom, respectively.

Visit One \ Visit Two	NS	<5%	<2%	<1%	<0.5%
NS	900	30	10	8	42
<5%	56	8	6	2	6
<2%	31	5	5	1	13
<1%	13	2	1	1	7
<0.5%	71	22	12	17	29

Visit One \ Visit Two	NS	<5%	<2%	<1%	<0.5%
NS	1034	25	4	1	12
<5%	39	11	2	3	2
<2%	19	9	1	3	1
<1%	8	5	0	0	5
<0.5%	50	6	11	4	43

Visit One \ Visit Two	NS	<5%	<2%	<1%	<0.5%
NS	1084	11	3	8	7
<5%	56	4	1	2	3
<2%	31	2	2	1	3
<1%	14	3	2	0	1
<0.5%	27	2	7	3	21

Visit One \ Visit Two	NS	<5%	<2%	<1%	<0.5%
NS	1005	30	23	11	26
<5%	48	5	5	1	5
<2%	18	5	5	1	4
<1%	4	2	1	1	7
<0.5%	36	6	3	6	40

Table 5.28 The change in the Comparison Probability value across all the given stimulus locations between Visit Two and Visit One for SAP (Top) and CFF perimetry (Bottom), for the 22 individuals with age related cataract. The shading indicates the number of locations exhibiting identical probability levels at the two examinations. A reduced number of data entries above the grey line compared to that below the line represents an improvement in sensitivity from Visit One to Visit Two. The data for the field of the right eye is given in the left column and that for the left eye in the right column.

The extent of the improvement between Visits One and Two in the Comparison probability value derived by SAP for the 22 individuals with age-related cataract, as a group, (Table 5.28 top) was relatively large for each eye, (right eye, 230 locations exhibiting an improvement and 125 locations exhibiting a deterioration, i.e. a 1.8 fold improvement, from a total of 1298 locations; left eye, 151 locations exhibiting an improvement, 58 locations exhibiting a deterioration i.e. a 2.6 fold improvement). Thus, the field of the right eye showed an improvement, on average, of one or more probability levels at approximately 10 stimulus locations per individual (230 locations; 22 individuals) and a deterioration at approximately 6 locations per individual. The

field of the left eye showed an improvement at approximately 7 locations per individual and a deterioration at approximately 3 locations per individual.

The extent of the improvement between Visits One and Two in the Comparison probability value derived by CFF perimetry for the 22 individuals with age-related cataract, as a group, (Table 5.28 bottom) was also relatively high for the right eye, (right eye, 147 locations exhibiting an improvement and 40 locations exhibiting a deterioration, i.e. a 3.7 fold improvement, from a total of 1298 locations; left eye, 129 locations exhibiting an improvement, 113 locations exhibiting a deterioration i.e. a 1.1 fold improvement). Thus, the field of the right eye showed an improvement of one or more probability levels at approximately 7 stimulus locations per 22 individual (147 locations; 22 individuals) and a deterioration at approximately 2 locations per individual. The field of the left eye showed an improvement at approximately 6 locations per individual and a deterioration at approximately 5 locations per individual.

Two hundred and thirty locations in the field of the right eye exhibited an improvement in probability level between the two visits for SAP (Table 5.28 top). Of these, 171 (74.35) resulted in a normal value at Visit Two with 56 of these (32.7%) exhibiting an improvement from the 5% probability level to normal and 71 (41.5%) an improvement from the 0.5% probability level to normal. Of the 147 locations in the field of the right eye which exhibited an improvement in probability level between the two visits, 128 (87.1%) locations exhibited an improvement to normal at Visit Two with 56 of these (38.0%) exhibiting an improvement from the 5% probability level to normal and 27 (0.18%) an improvement from the 0.5% probability level to normal. A similar but less pronounced trend was present for CFF perimetry (Table 5.28 bottom) to that of SAP. Of the 128 locations in the field of the right eye which improved to normal at Visit Two, 106 locations (82.1%) exhibited an improvement to normal at Visit Two with 48

(45.2%) of these exhibiting an improvement from the 5% probability level to normal and 36 (33.9%) an improvement from the 0.5% probability level to normal. Of the 129 locations in the field of the left eye which improved to normal at Visit Two, 116 locations (89.9%) exhibited an improvement to normal at Visit Two with 56 (48.2%) of these exhibiting an improvement from the 0.5% probability level to normal and 27 (23.2%) an improvement from the 0.5% probability level to normal.

Visit Two \ Visit Four	NS	<5%	<2%	<1%	<0.5%
NS	1029	25	7	5	10
<5%	42	9	0	6	4
<2%	28	5	5	0	1
<1%	14	5	2	6	2
<0.5%	45	7	4	3	34

Visit Two \ Visit Four	NS	<5%	<2%	<1%	<0.5%
NS	1093	23	6	4	13
<5%	48	7	3	0	3
<2%	5	6	1	2	4
<1%	3	3	1	0	2
<0.5%	15	7	5	6	38

Visit Two \ Visit Four	NS	<5%	<2%	<1%	<0.5%
NS	1146	22	16	5	14
<5%	12	2	1	1	2
<2%	7	3	1	1	1
<1%	8	2	0	2	1
<0.5%	14	6	1	2	28

Visit Two \ Visit Four	NS	<5%	<2%	<1%	<0.5%
NS	1070	25	20	5	9
<5%	27	10	6	5	4
<2%	19	6	2	2	6
<1%	7	1	2	2	4
<0.5%	31	6	3	9	17

Table 5.29 The change in the Comparison probability value across all the given stimulus locations from Visit Two to Visit Four for SAP (Top) and for CFF perimetry (Bottom), for the 22 individuals with age-related cataract. The shading indicates the number of locations exhibiting identical probability levels at the two examinations. A reduced number of data entries above the grey line compared to that below the line represent an improvement in sensitivity from Visit Two to Visit Four. The data for the field of the right eye is given in the left column and that for the left eye in the right column.

The extent of the improvement from Visit Two to Visit Four in the Comparison probability value derived by SAP (Table 5.29 top) was again relatively high for each eye, (right eye, 155 locations

exhibiting an improvement and 60 locations exhibiting a deterioration, i.e. a 2.6 fold improvement, from a total of 1298 locations; left eye, 99 locations exhibiting an improvement, 60 locations exhibiting a deterioration i.e. a 1.6 fold improvement). Thus, the field of the right eye showed an improvement of one or more probability levels at approximately 7 stimulus locations per individual and deterioration at approximately 3 locations per individual. The field of the left eye showed an improvement at approximately 5 locations per individual and deterioration at approximately 3 locations per individual. Of the 155 locations exhibiting an improvement in the field of the right eye, 129 (83.2%) became normal at Visit Four. Similarly of the 99 locations exhibiting an improvement in the field of the left eye, 71 (71.7%) became normal at Visit Four.

From Visits Two to Visit Four Table 5.29 bottom), 55 locations in the field of the right eye exhibited an improvement in the Comparison probability value derived by CFF perimetry and 64 locations exhibited deterioration, i.e. a 1.2 fold deterioration, from a total of 1298 locations. For the field of the left eye, 111 locations exhibited an improvement and 86 locations exhibiting deterioration i.e. a 1.3 fold improvement). Thus, the field of the left eye showed an improvement at approximately 5 locations per individual and deterioration at approximately 4 locations per individual. Of the 111 locations exhibiting an improvement for the left eye, 84 (77.4%) improved to normal at Visit Four.

As was expected from the absence of a general height adjustment for CFF perimetry which was identified in Chapter 4, all 22 individuals exhibited identical Comparison and Corrected Comparison probability maps in both eyes at each of the 4 visits derived by CFF perimetry.

5.15 Mean Sensitivity

The difference in the Mean Sensitivity for SAP and for CFF perimetry from Visit One to Visit Two compared to the difference from Visit Two to Visit Four for each eye of the 22 individuals with age-related cataract is shown graphically in Figure 5.18 for SAP and in Figure 5.19 for CFF perimetry. The corresponding difference for each individual, is given in proportionate terms, in Table 5.30 for SAP and in Table 5.31 for CFF perimetry.

A wide variation in MS from Visits One to Visit Two, both in absolute (Figures 5.18 and 5.19), and in proportionate terms (Tables 5.30 and 5.31) was present for both types of perimetry, both between-eyes of an individual and between individuals for a given eye. A similar variation was present between Visits Two and Four not only between-eyes of an individual but also between individuals for a given eye. Considerable variation was also present between the two pairs of visits.

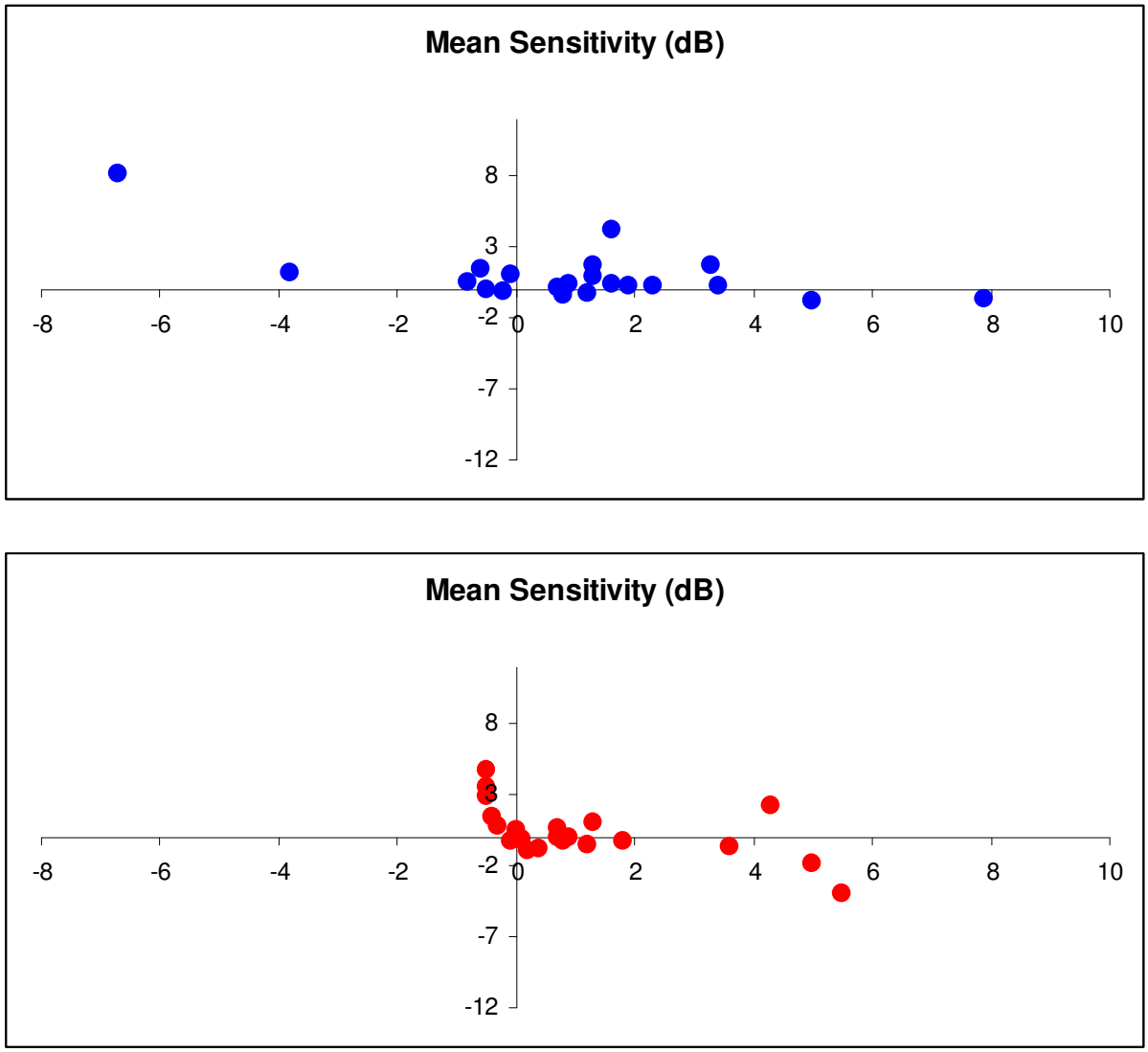

Figure 5.18 The scatter plot of the difference in the magnitude of the Mean Sensitivity$_{SAP}$ (dB) between Visit One and Visit Two (abscissa) against the difference in the magnitude between Visit Two and Visit Four (ordinate) for each of the 22 individuals with age-related cataract for the right (top), and left (bottom) eyes. A negative value represents a deterioration in performance. Data points in the superior left quadrant represent deterioration from Visit One to Visit Two and an improvement from Visit Two to Visit Four. Data points in the superior right quadrant represent an improvement from Visit One to Visit Two and also from Visit Two to Visit Four. Data points in the inferior right quadrant represent improvement from Visit One to Visit Two and deterioration from Visit Two to Visit Four. Data points in the inferior left quadrant represent deterioration both from Visit One to Visit Two and from Visit Two to Visit Four.

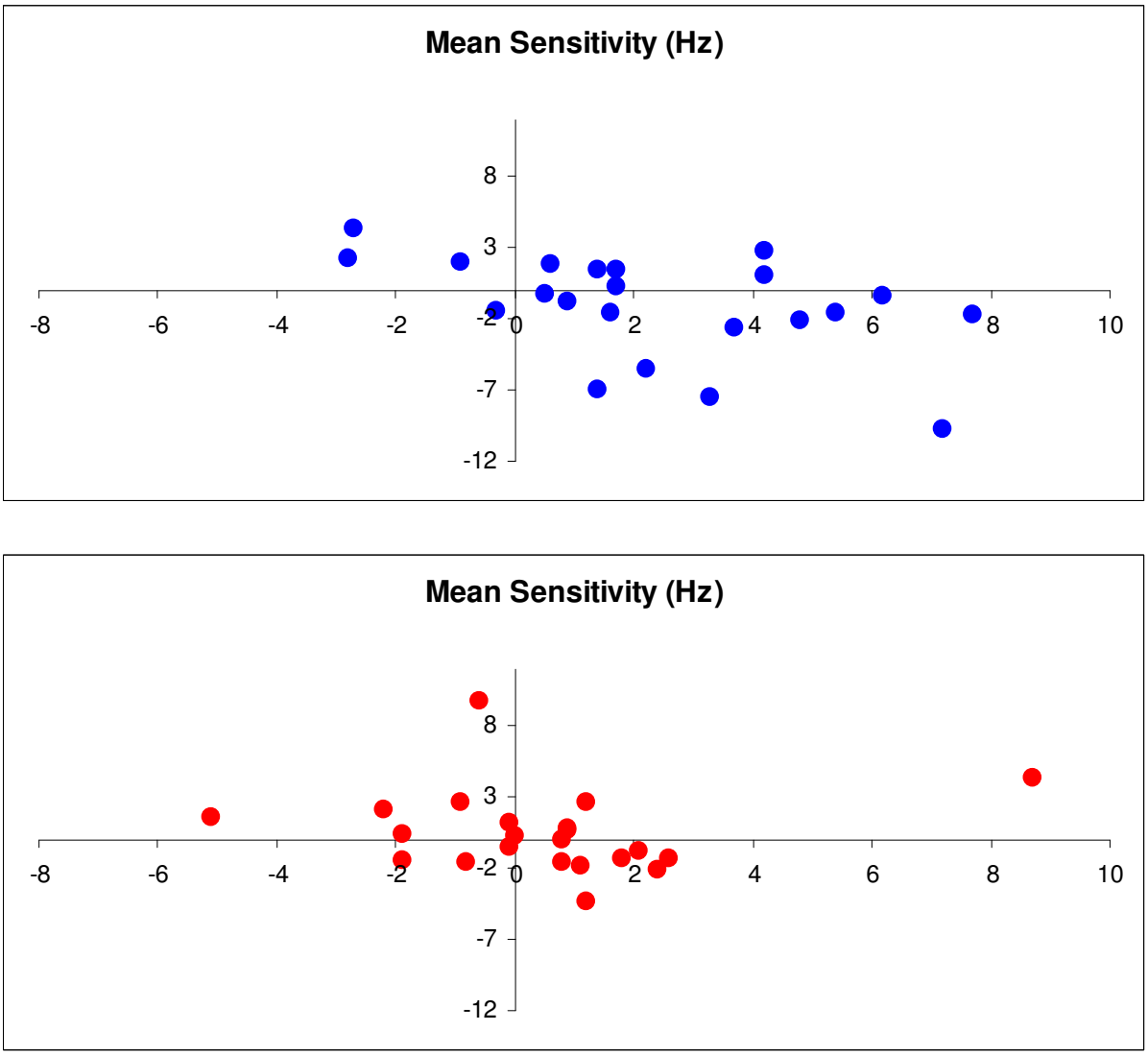

Figure 5.19 The scatter plot of the difference in the magnitude of the Mean Sensitivity$_{CFF}$ (Hz) between Visit One and Visit Two (abscissa) against the difference in the magnitude between Visit Two and Visit Four (ordinate) for each of the 22 individuals with age-related cataract for the right (top), and left (bottom) eyes. A negative value represents a deterioration in performance. Data points in the superior left quadrant represent deterioration from Visit One to Visit Two and an improvement from Visit Two to Visit Four. Data points in the superior right quadrant represent an improvement from Visit One to Visit Two and also from Visit Two to Visit Four. Data points in the inferior right quadrant represent improvement from Visit One to Visit Two and deterioration from Visit Two to Visit Four. Data points in the inferior left quadrant represent deterioration both from Visit One to Visit Two and from Visit Two to Visit Four.

Case Number	Right Eye Absolute Change (dB) V1 to V2	Right Eye Proportionate Change (%) V1 to V2	Right Eye Absolute Change (dB) V2 to V4	Right Eye Proportionate Change (%) V2 to V4	Left Eye Absolute Change (dB) V1 to V2	Left Eye Proportionate Change (%) V1 to V2	Left Eye Absolute Change (dB) V2 to V4	Left Eye Proportionate Change (%) V2 to V4
1	5	31.65	-0.8	-3.85	5	22.73	-1.9	-7.04
2	-0.2	-0.74	-0.1	-0.37	-0.1	-0.36	-0.2	-0.73
3	1.6	6.08	0.4	1.43	3.6	14.52	-0.6	-2.11
4	-0.8	-3.16	0.5	2.04	0.1	0.36	-0.1	-0.36
5	1.6	8.12	4.2	19.72	4.3	21.83	2.3	9.58
6	3.4	18.68	0.2	0.93	-0.5	-2.49	2.9	14.80
7	0.8	3.04	-0.1	-0.37	0.4	1.45	-0.8	-2.87
8	7.9	59.85	-0.7	-3.32	5.5	39.57	-3.9	-20.10
9	0.9	3.70	0.4	1.59	0.9	3.72	0.0	0.00
10	3.3	16.34	1.7	7.23	0.7	3.10	0.0	0.00
11	-6.7	-27.02	8.2	45.30	-0.5	-2.03	3.5	14.52
12	-3.8	-19.39	1.2	7.59	-0.5	-3.23	4.8	32.00
13	1.3	5.63	0.9	3.69	1.8	7.66	-0.2	-0.79
14	-0.6	-2.21	1.4	5.26	-0.3	-1.10	0.8	2.97
15	1.3	5.78	1.7	7.14	-0.4	-1.69	1.5	6.47
16	0.7	2.71	0.1	0.38	1.2	4.46	-0.5	-1.78
17	0.8	2.96	-0.4	-1.44	1.3	5.02	1.0	3.68
18	2.3	9.47	0.2	0.75	0.0	0.00	-0.1	-0.37
19	1.2	4.69	-0.3	-1.12	0.7	2.76	0.7	2.68
20	-0.1	-0.39	1.0	3.94	0.0	0.00	0.5	1.87
21	1.9	7.82	0.2	0.76	0.8	3.20	-0.3	-1.16
22	-0.5	-1.93	0.0	0.00	0.2	0.80	-0.9	-3.57

Table 5.30 The absolute (dB) and proportionate (%) change in Mean Sensitivity for each eye of the 22 individuals with age-related cataract between Visit 1 and Visit 2 and between Visit 2 and Visit 4.

Case Number	Right Eye Absolute Change (Hz) V1 to V2	Right Eye Proportionate Change (%) V1 to V2	Right Eye Absolute Change (Hz) V2 to V4	Right Eye Proportionate Change (%) V2 to V4	Left Eye Absolute Change (Hz) V1 to V2	Left Eye Proportionate Change (%) V1 to V2	Left Eye Absolute Change (Hz) V2 to V4	Left Eye Proportionate Change (%) V2 to V4
1	1.6	4.13	-1.6	-3.97	-0.1	-0.31	-0.5	-1.53
2	0.6	1.79	1.8	5.28	2.1	6.89	-0.8	-2.45
3	1.7	4.89	1.5	4.11	1.2	3.43	2.7	7.46
4	-2.8	-7.29	2.3	6.46	1.2	3.54	-4.3	-12.25
5	3.7	11.49	-2.6	-7.24	-0.8	-2.34	-1.6	-4.79
6	3.3	9.82	-7.5	-20.33	-1.9	-6.19	0.4	1.39
7	-0.3	-0.81	-1.4	-3.81	1.8	5.23	-1.3	-3.59
8	1.4	4.46	-7.0	-21.34	-5.1	-18.21	1.6	6.99
9	4.2	12.43	1.0	2.63	0.8	2.09	0.0	0.00
10	4.2	13.82	2.8	8.09	-0.9	-2.56	2.7	7.87
11	-2.7	-13.64	4.3	25.15	-0.6	-3.90	9.7	65.54
12	7.2	27.59	-9.8	-29.43	-2.2	-9.36	2.1	9.86
13	4.8	17.91	-2.1	-6.65	2.6	10.00	-1.3	-4.55
14	0.5	1.20	-0.2	-0.48	0.0	0.00	0.3	0.71
15	1.4	5.11	1.4	4.86	-0.1	-0.35	1.2	4.21
16	6.2	21.38	-0.4	-1.14	1.1	3.06	-1.8	-4.85
17	0.9	2.56	-0.8	-2.22	0.8	2.26	-1.6	-4.42
18	7.7	28.00	-1.7	-4.83	8.7	35.51	4.4	13.25
19	-0.9	-2.44	2.0	5.56	0.9	2.52	0.8	2.19
20	1.7	4.78	0.2	0.54	0.9	2.61	0.6	1.69
21	2.2	7.01	-5.5	-16.37	-1.9	-5.81	-1.5	-4.87
22	5.4	20.07	-1.6	-4.95	2.4	8.70	-2.1	-7.00

Table 5.31 The absolute (Hz) and proportionate (%) changein Mean Sensitivity for each eye of the 22 individuals with age-related cataract between Visit 1 and Visit 2 and between Visit 2 and Visit 4.

5.16 Mean Defect

The difference in the Mean Defect for SAP and for CFF perimetry from Visit One to Visit Two compared to the difference from Visit Two to Visit Four is given in Tables 5.20 and 5.21, respectively.

As would be expected from the analysis of the MS for SAP and for CFF perimetry, a wide variation was also present in the MD for both types of perimetry between Visits One and Two both between-eyes of an individual and between individuals for a given eye. A similar variation was also present between Visits Two and Four .

5.17 Square root of the Loss Variance

The difference in the Square root of the Loss Variance for SAP and for CFF perimetry from Visit One to Visit Two compared to the difference from Visit Two to Visit Four is given in Tables 5.22 and 5.23, respectively. A wide range of performance was present for both types of perimetry within each pair of visits between eyes of an individual and between individuals.

5.18 Diffuse Defect

The difference in the Diffuse Defect for SAP and CFF perimetry from Visit One to Visit Two compared to the difference from Visit Two to Visit Four is shown graphically in Figure 5.24 for SAP and in Figure 5.25 for CFF perimetry. As would be expected, the trend was similar to that for the MD but was of lower magnitude.

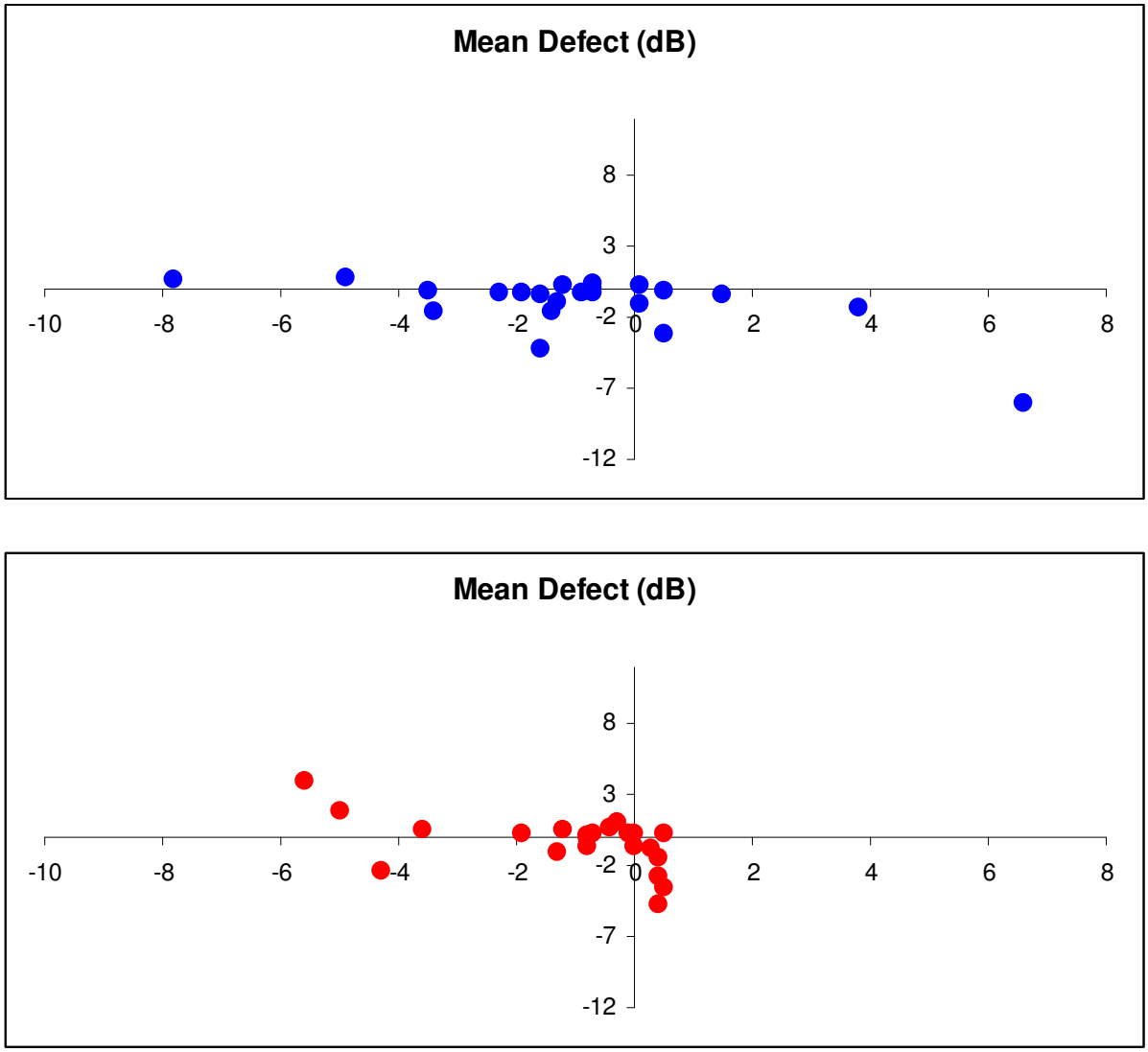

Figure 5.20 The scatter plot of the difference in the magnitude of the Mean Defect (dB) between Visit One and Visit Two (abscissa) against the difference in the magnitude between Visit Two and Visit Four (ordinate) for each of the 22 individuals with age-related cataract for the right (top), and left (bottom) eyes. A negative value represents an improvement in performance. Data points in the superior left quadrant represent an improvement from Visit One to Visit Two and deterioration from Visit Two to Visit Four. Data points in the superior right quadrant represent deterioration from Visit One to Visit Two and also from Visit Two to Visit Four. Data points in the inferior right quadrant represent deterioration from Visit One to Visit Two and an improvement from Visit Two to Visit Four. Data points in the inferior left quadrant represent an improvement both from Visit One to Visit Two and from Visit Two to Visit Four.

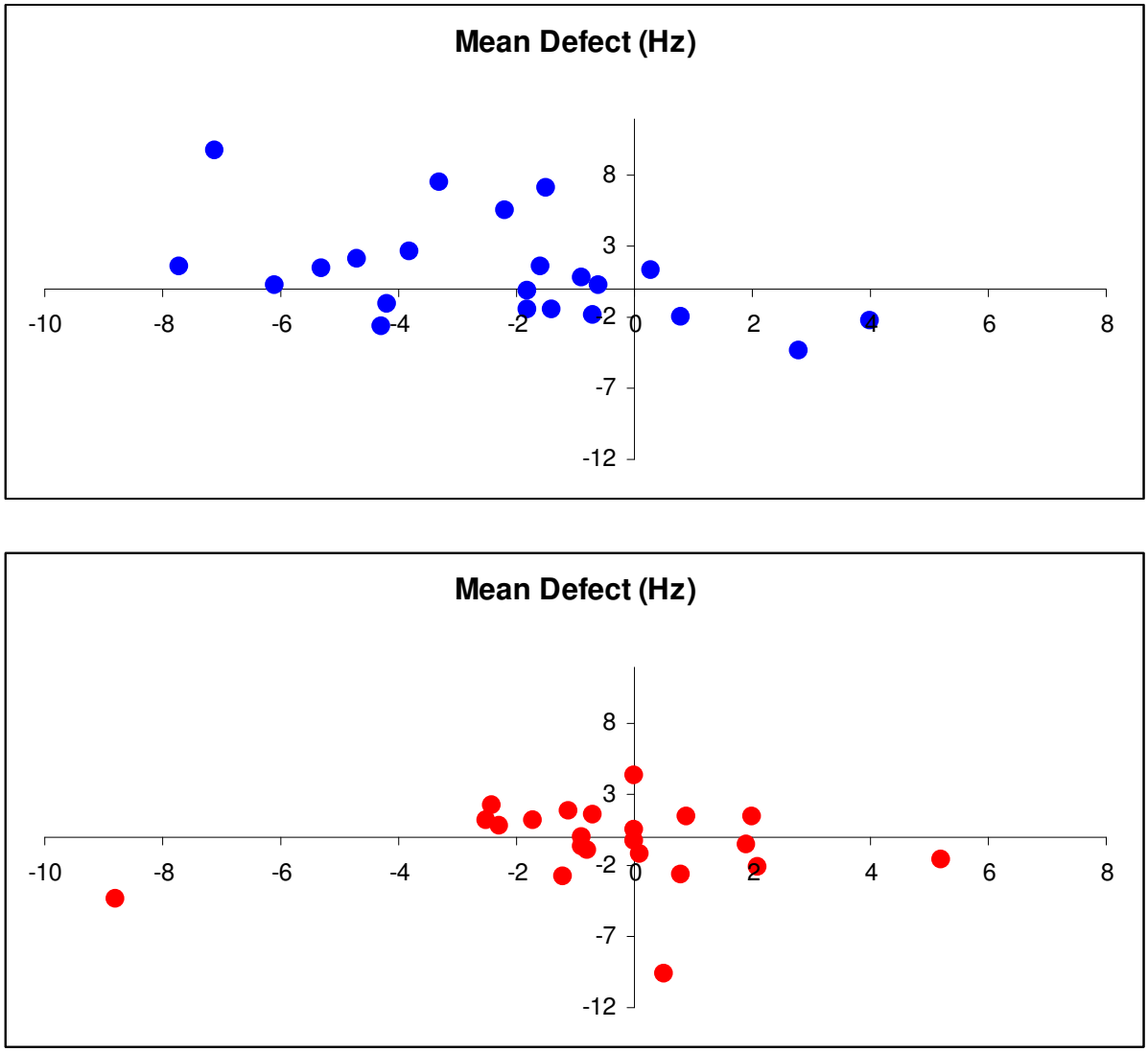

Figure 5.21 The scatter plot of the difference in the magnitude of the Mean Defect (Hz) between Visit One and Visit Two (abscissa) against the difference in the magnitude between Visit Two and Visit Four (ordinate) for each of the 22 individuals with age-related cataract for the right (top), and left (bottom) eyes. A negative value represents an improvement in performance. Data points in the superior left quadrant represent an improvement from Visit One to Visit Two and deterioration from Visit Two to Visit Four. Data points in the superior right quadrant represent deterioration from Visit One to Visit Two and also from Visit Two to Visit Four. Data points in the inferior right quadrant represent deterioration from Visit One to Visit Two and an improvement from Visit Two to Visit Four. Data points in the inferior left quadrant represent an improvement both from Visit One to Visit Two and from Visit Two to Visit Four.

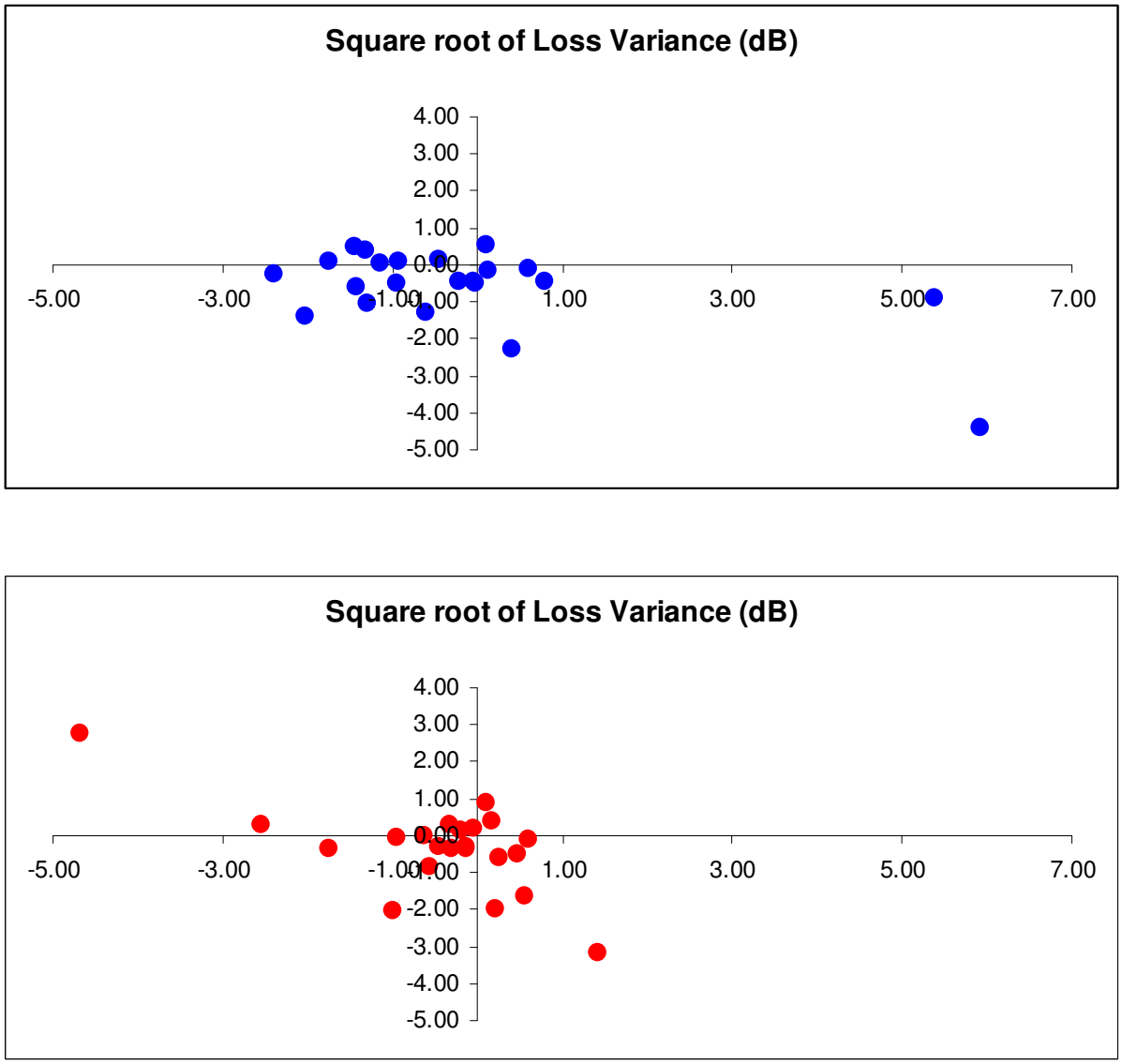

Figure 5.22 The scatter plot of the difference in the magnitude of the square root of the Loss Variance (dB) between Visit One and Visit Two (abscissa) against the difference in the magnitude between Visit Two and Visit Four (ordinate) for each of the 22 individuals with age-related cataract for the right (top), and left (bottom) eyes. A negative value represents an improvement in performance. Data points in the superior left quadrant represent an improvement from Visit One to Visit Two and a deterioration from Visit Two to Visit Four. Data points in the superior right quadrant represent a deterioration from Visit One to Visit Two and also from Visit Two to Visit Four. Data points in the inferior right quadrant represent a deterioration from Visit One to Visit Two and an improvement from Visit Two to Visit Four. Data points in the inferior left quadrant represent an improvement both from Visit One to Visit Two and from Visit Two to Visit Four.

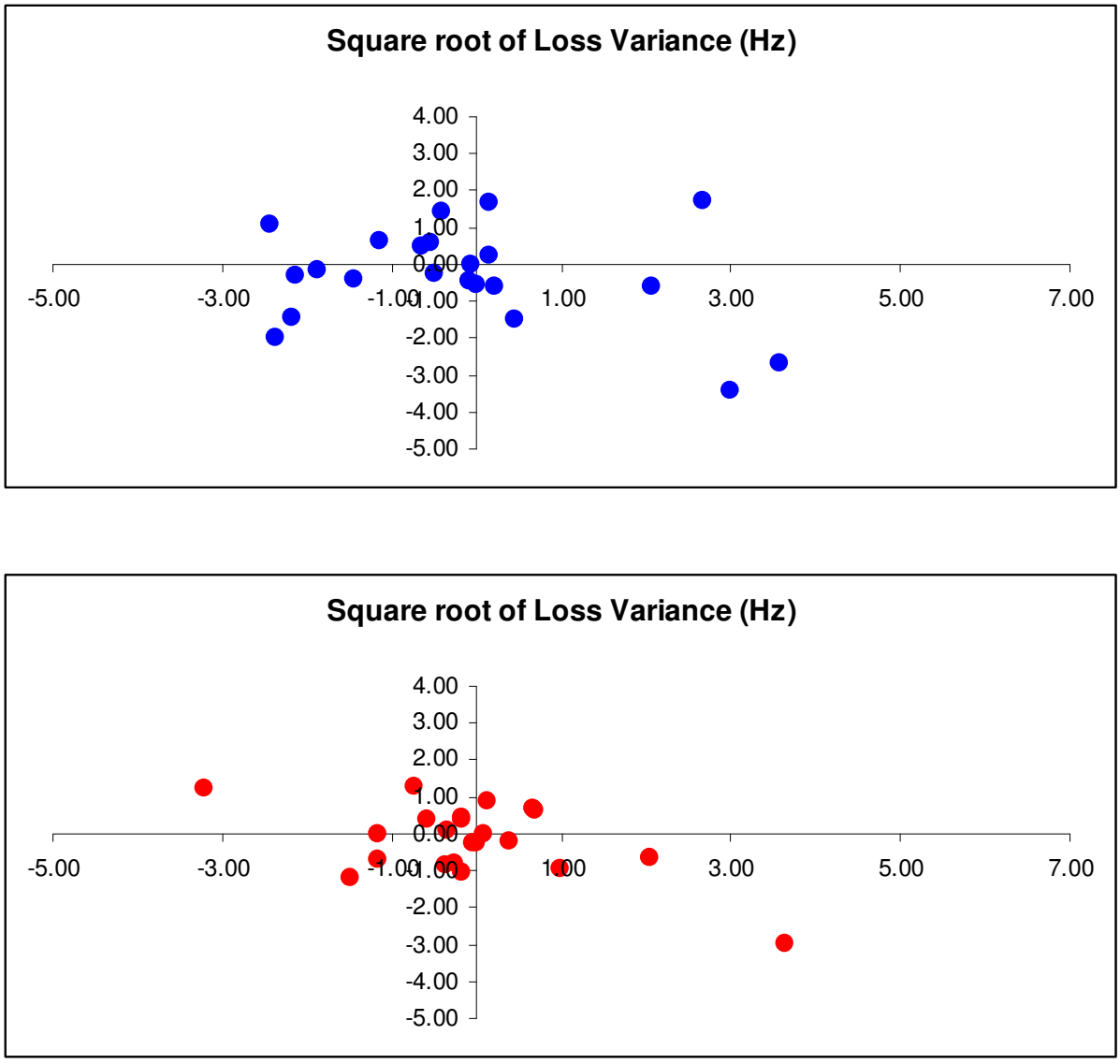

Figure 5.23 The scatter plot of the difference in the magnitude of the square root of the Loss Variance (Hz) between Visit One and Visit Two (abscissa) against the difference in the magnitude between Visit Two and Visit Four (ordinate) for each of the 22 individuals with age-related cataract for the right (top), and left (bottom) eyes. A negative value represents an improvement in performance. Data points in the superior left quadrant represent an improvement from Visit One to Visit Two and a deterioration from Visit Two to Visit Four. Data points in the superior right quadrant represent a deterioration from Visit One to Visit Two and also from Visit Two to Visit Four. Data points in the inferior right quadrant represent a deterioration from Visit One to Visit Two and an improvement from Visit Two to Visit Four. Data points in the inferior left quadrant represent an improvement both from Visit One to Visit Two and from Visit Two to Visit Four.

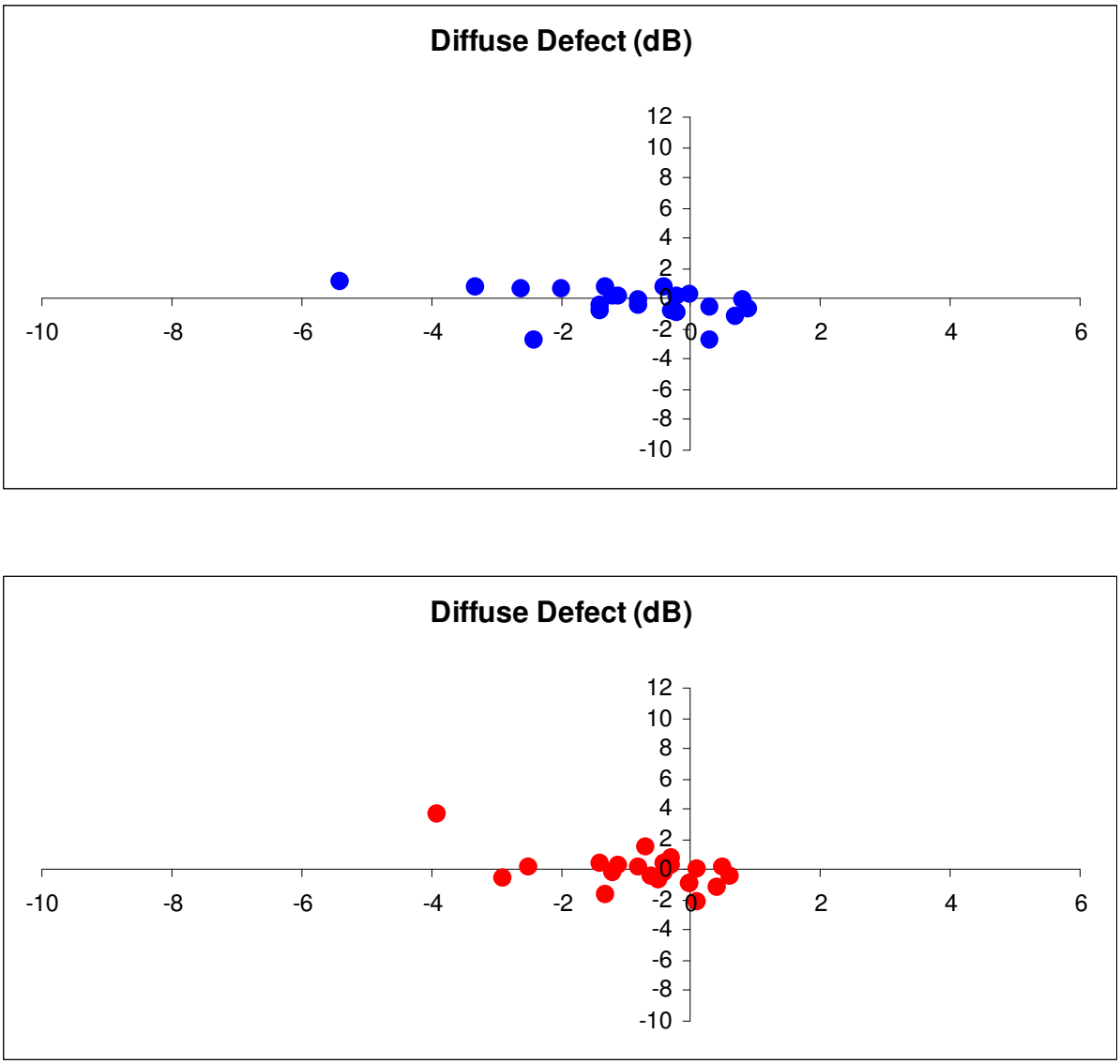

Figure 5.24 The scatter plot of the difference in the Diffuse Defect (dB) between Visit One and Visit Two (abscissa) against the difference in the magnitude between Visit Two and Visit Four (ordinate) for each of the 22 individuals with age-related cataract for the right (top), and left (bottom) eyes. A negative value represents an improvement in performance. Data points in the superior left quadrant represent an improvement from Visit One to Visit Two and deterioration from Visit Two to Visit Four. Data points in the superior right quadrant represent deterioration from Visit One to Visit Two and also from Visit Two to Visit Four. Data points in the inferior right quadrant represent deterioration from Visit One to Visit Two and an improvement from Visit Two to Visit Four. Data points in the inferior left quadrant represent an improvement both from Visit One to Visit Two and from Visit Two to Visit Four.

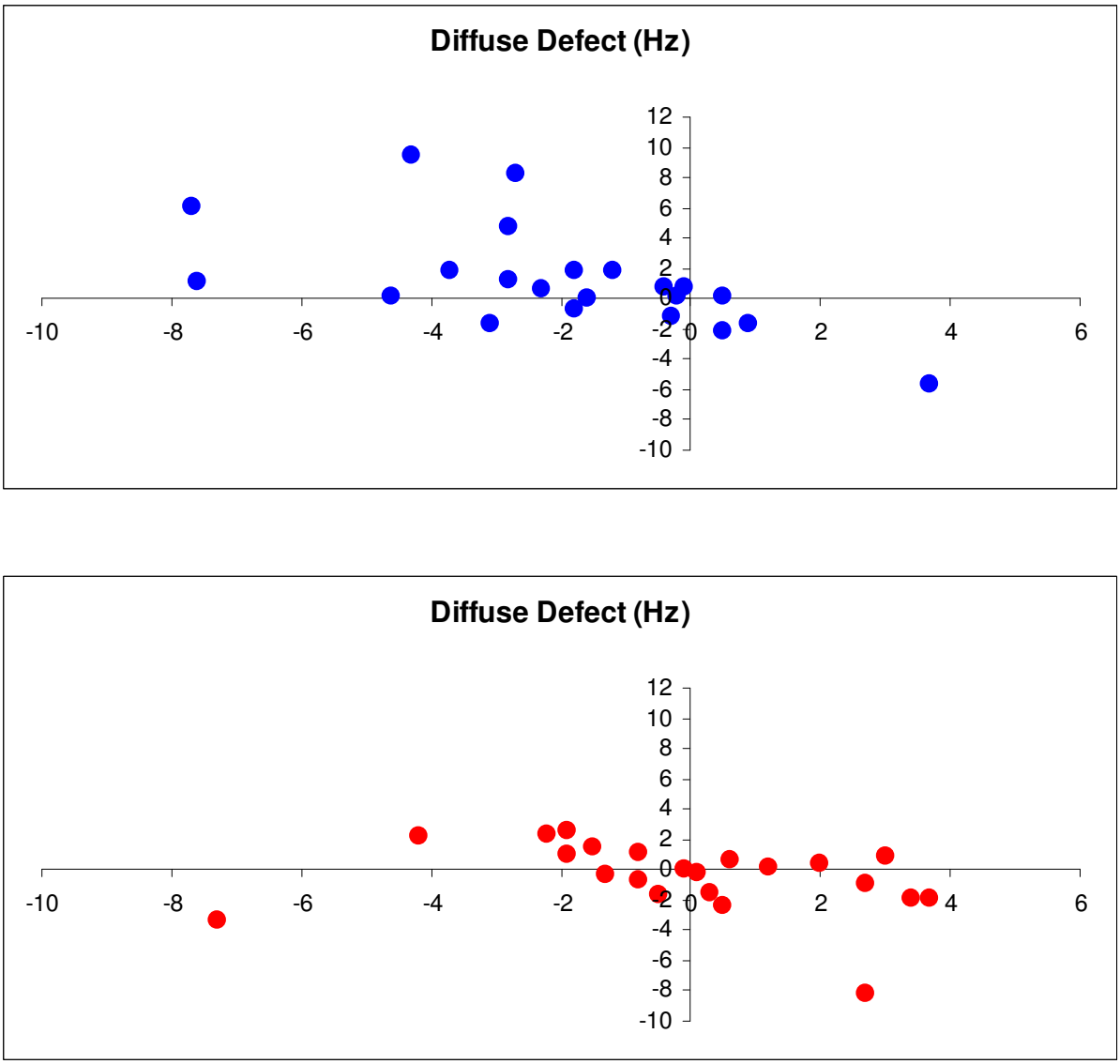

Figure 5.25 The scatter plot of the difference in the Diffuse Defect (Hz) between Visit One and Visit Two (abscissa) against the difference in the magnitude between Visit Two and Visit Four (ordinate) for each of the 22 individuals with age-related cataract for the right (top), and left (bottom) eyes. A negative value represents an improvement in performance. Data points in the superior left quadrant represent an improvement from Visit One to Visit Two and deterioration from Visit Two to Visit Four. Data points in the superior right quadrant represent deterioration from Visit One to Visit Two and also from Visit Two to Visit Four. Data points in the inferior right quadrant represent deterioration from Visit One to Visit Two and an improvement from Visit Two to Visit Four. Data points in the inferior left quadrant represent an improvement both from Visit One to Visit Two and from Visit Two to Visit Four.

5.19 Local Defect cataract individuals

The difference in the Local Defect for SAP and CFF perimetry from Visit One to Visit Two compared to the difference from Visit Two to Visit Four is shown graphically in Figure 5.26 for SAP and in Figure 5.27 for CFF perimetry.

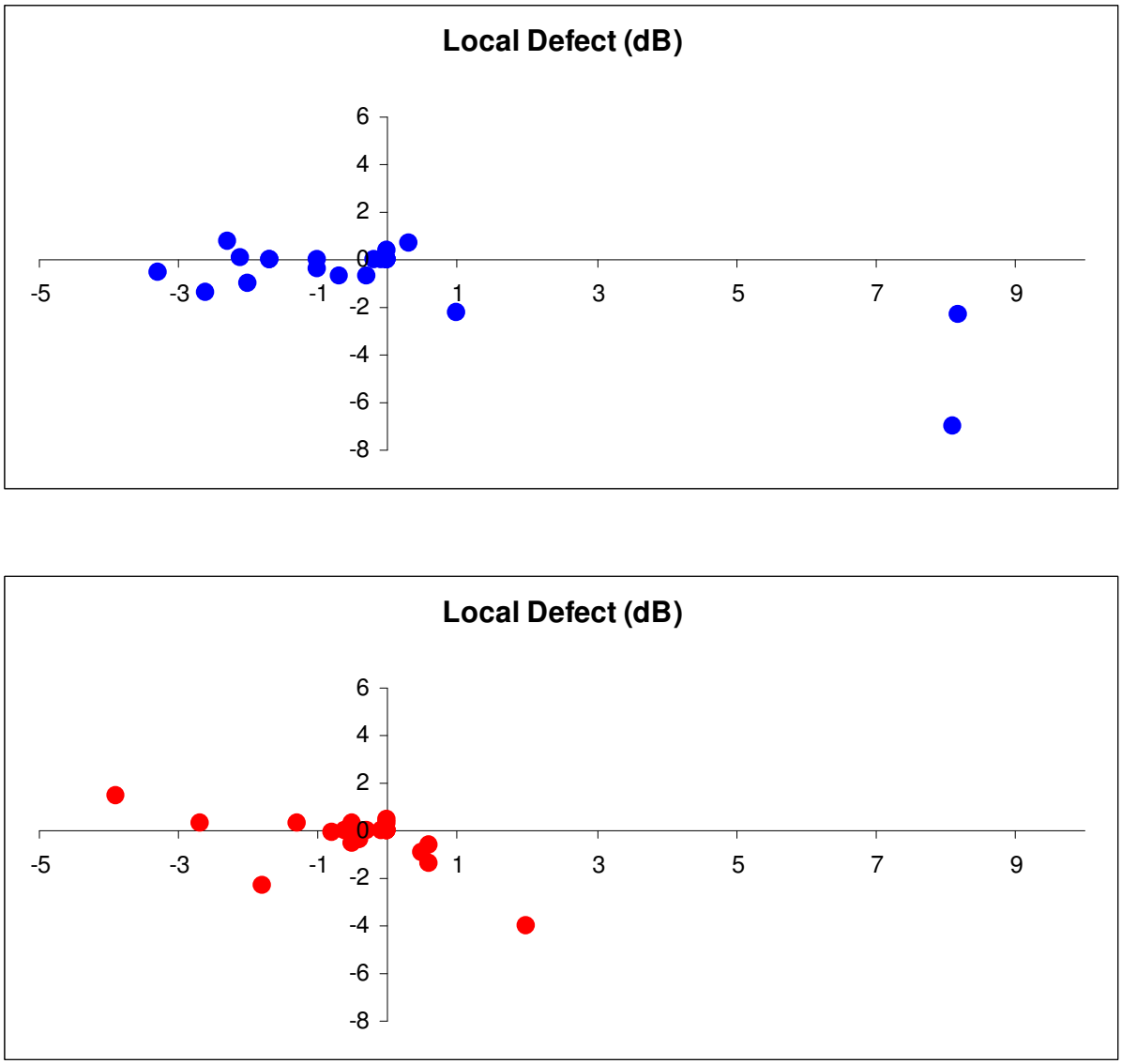

Figure 5.26 The scatter plot of the difference in the magnitude of the Local Defect (dB) between Visit One and Visit Two (abscissa) against the difference in the magnitude between Visit Two and Visit Four (ordinate) for each of the 22 individuals with age-related cataract for the right (top), and left (bottom) eyes. A negative value represents an improvement in performance. Data points in the superior left quadrant represent an improvement from Visit One to Visit Two and deterioration from Visit Two to Visit Four. Data points in the superior right quadrant represent deterioration from Visit One to Visit Two and also from Visit Two to Visit Four. Data points in the inferior right quadrant represent deterioration from Visit One to Visit Two and an improvement from Visit Two to Visit Four. Data points in the inferior left quadrant represent an improvement both from Visit One to Visit Two and from Visit Two to Visit Four.

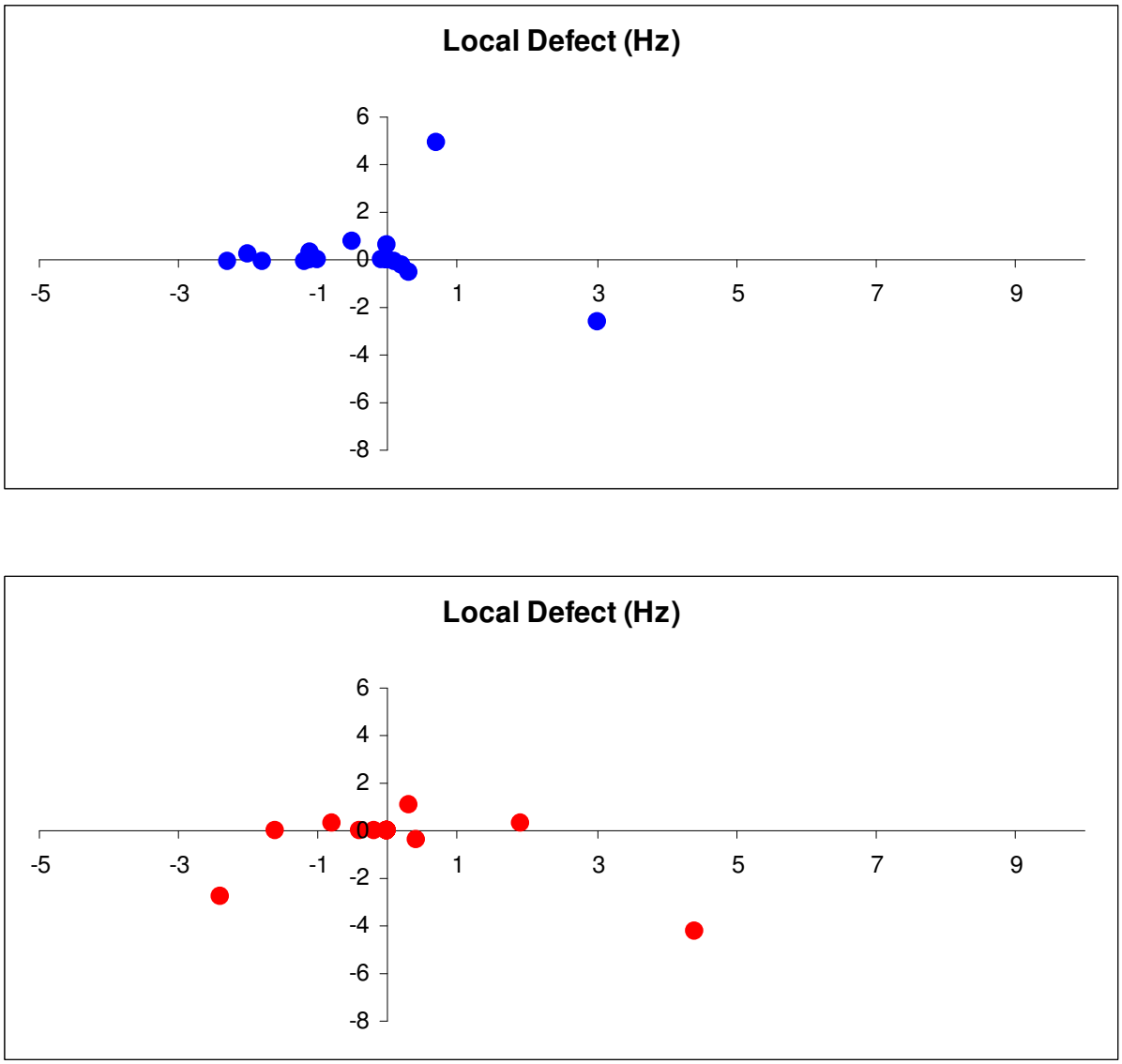

Figure 5.27 The scatter plot of the difference in the magnitude of the Local Defect (Hz) between Visit One and Visit Two (abscissa) against the difference in the magnitude between Visit Two and Visit Four (ordinate) for each of the 22 individuals with age-related cataract for the right (top), and left (bottom) eyes. A negative value represents an improvement in performance. Data points in the superior left quadrant represent an improvement from Visit One to Visit Two and deterioration from Visit Two to Visit Four. Data points in the superior right quadrant represent deterioration from Visit One to Visit Two and also from Visit Two to Visit Four. Data points in the inferior right quadrant represent deterioration from Visit One to Visit Two and an improvement from Visit Two to Visit Four. Data points in the inferior left quadrant represent an improvement both from Visit One to Visit Two and from Visit Two to Visit Four.

5.20 Glare Disability (GD)

5.20.1 LogMAR Visual Acuity in relation to Brightness Acuity Tester settings

The summary statistics for the LogMAR Visual Acuity for the 100% ETDRS (top) and for the 10% ETDRS (bottom) charts without glare and at each of the three BAT glare settings at Visit Three and at Visit Four for each eye of the 22 individuals with age-related cataract are shown in Table 5.32. LogMAR VA deteriorated with increase in disability glare and the decline was greater for the low contrast charts.

The distribution of the LogMAR VA at Visit Three and at Visit Four for each eye without glare and at each of the three glare settings is also illustrated in terms of Box and Whisker plots in Figure 5.28 (100% contrast) and in Figure 5.29 (10% contrast).

Overleaf: Table 5.32 The group mean (SD), the median and the IQR of the LogMAR Visual Acuity for the 100% ETDRS (top) and for the 10% ETDRS (bottom) charts without glare and at each of the three BAT glare settings at Visit Three and at Visit Four for each eye of the 22 individuals with age-related cataract.

LogMAR VA 100% Contrast				
Visit Three	BAT Off	BAT Low 41 cdm^{-2}	BAT Medium 343 cdm^{-2}	BAT High 1371 cdm^{-2}
Right Mean	0.28	0.28	0.33	0.41
SD	0.16	0.18	0.19	0.17
Left Mean	0.22	0.22	0.26	0.33
SD	0.11	0.10	0.12	0.13
Right Median	0.24	0.26	0.32	0.40
IQR	0.17	0.18	0.20	0.15
Left Median	0.22	0.22	0.28	0.34
IQR	0.17	0.19	0.18	0.23
Visit Four				
Right Mean	0.26	0.29	0.31	0.40
SD	0.15	0.15	0.17	0.18
Left Mean	0.24	0.25	0.27	0.32
SD	0.10	0.10	0.10	0.13
Right Median	0.27	0.31	0.32	0.37
IQR	0.18	0.15	0.14	0.18
Left Median	0.22	0.22	0.27	0.35
IQR	0.14	0.17	0.17	0.17

LogMAR VA 10% Contrast				
Visit Three	BAT open	BAT Low 41 cdm^{-2}	BAT Medium 343 cdm^{-2}	BAT High 1371 cdm^{-2}
Right Mean	0.48	0.52	0.53	0.67
SD	0.19	0.16	0.16	0.16
Left Mean	0.41	0.46	0.46	0.59
SD	0.15	0.15	0.16	0.17
Right Median	0.42	0.50	0.50	0.66
IQR	0.31	0.19	0.20	0.21
Left Median	0.40	0.50	0.45	0.54
IQR	0.20	0.22	0.22	0.18
Visit Four				
Right Mean	0.47	0.51	0.53	0.66
SD	0.15	0.15	0.13	0.18
Left Mean	0.45	0.48	0.48	0.60
SD	0.14	0.15	0.14	0.17
Right Median	0.47	0.53	0.53	0.64
IQR	0.24	0.24	0.21	0.26
Left Median	0.45	0.51	0.50	0.56
IQR	0.19	0.19	0.16	0.25

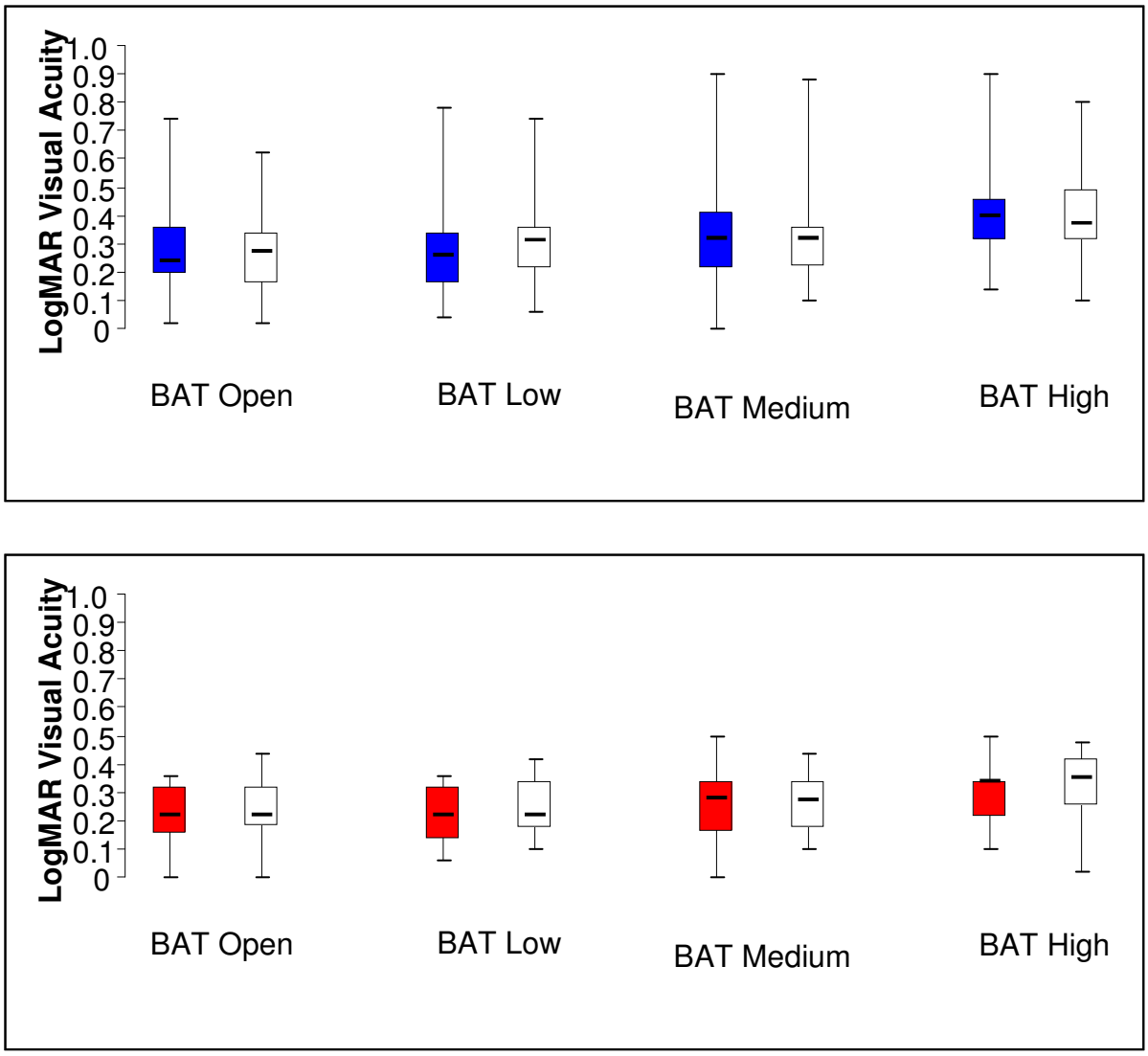

Figure 5.28 The Box and Whisker plots of the distribution of the LogMAR Visual Acuity derived with the 100% ETDRS charts without glare and at each of the three BAT settings at Visit Three (top) and at Visit Four (bottom) for each eye of the 22 individuals with age-related cataract. The median is represented by the bold line, the 25th and 75th percentiles by the lower and upper edges of the box, respectively, and the lowest and highest values by the lower and upper extremities of the whiskers, respectively. The results for the right eye are colour coded in blue at Visit Three and in red at Visit Four. The results for the left eye are colour coded in white at Visits Three and Four.

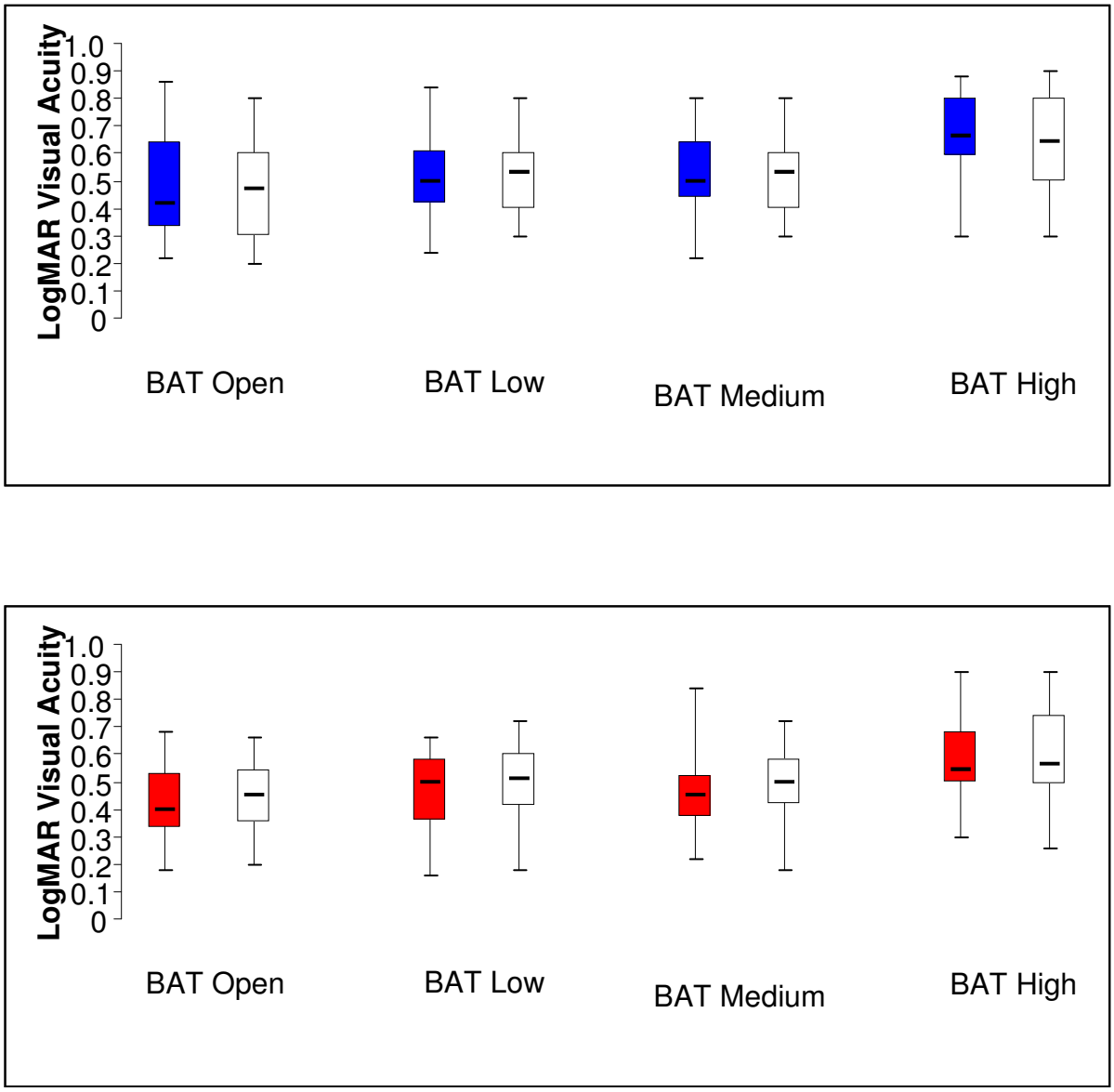

Figure 5.29 The Box and Whisker plots of the distribution of the LogMAR Visual Acuity derived with the 10% ETDRS charts without glare and at each of the three BAT settings at Visit Three (top) and at Visit Four (bottom) for each eye of the 22 individuals with age-related cataract. The median is represented by the bold line, the 25th and 75th percentiles by the lower and upper edges of the box, respectively, and the lowest and highest values by the lower and upper extremities of the whiskers, respectively. The results for the right eye are colour coded in blue at Visit Three and in red at Visit Four. The results for the left eye are colour coded in white at Visits Three and Four.

5.21 The difference in LogMAR Visual Acuity between Visit 3 and Visit 4.

The difference in LogMAR VA for the 100% and the 10% contrast charts between Visit Three and Visit Four without glare (top) and at each of the three glare (Low: middle top. Medium: middle bottom. High: bottom) for the right and for the left eye are shown in Figures 5.30 and 5.31, respectively, where the difference between the two values is plotted against the sum of the two values (Bland and Altman 1986; Bland and Altman 1999).

For the 100% contrast chart, the mean of the difference for each combination of glare source and contrast approximated to zero in all cases. The limits of agreement (i.e. the range over which 95% of the differences lie) was wider for the right eye (approximately +/- 0.2 log units) than for the left eye (between approximately +/- 0.1 - 0.2 log units) and was narrowest for the medium glare source for the left eye. A difference of 0.2 log units represents a difference of two lines in acuity.

For the 10% contrast chart, the mean of the difference for each combination of glare source and contrast again approximated to zero in all cases. The limits of agreement were approximately similar between the two eyes (approximately +/- 0.2 log units).

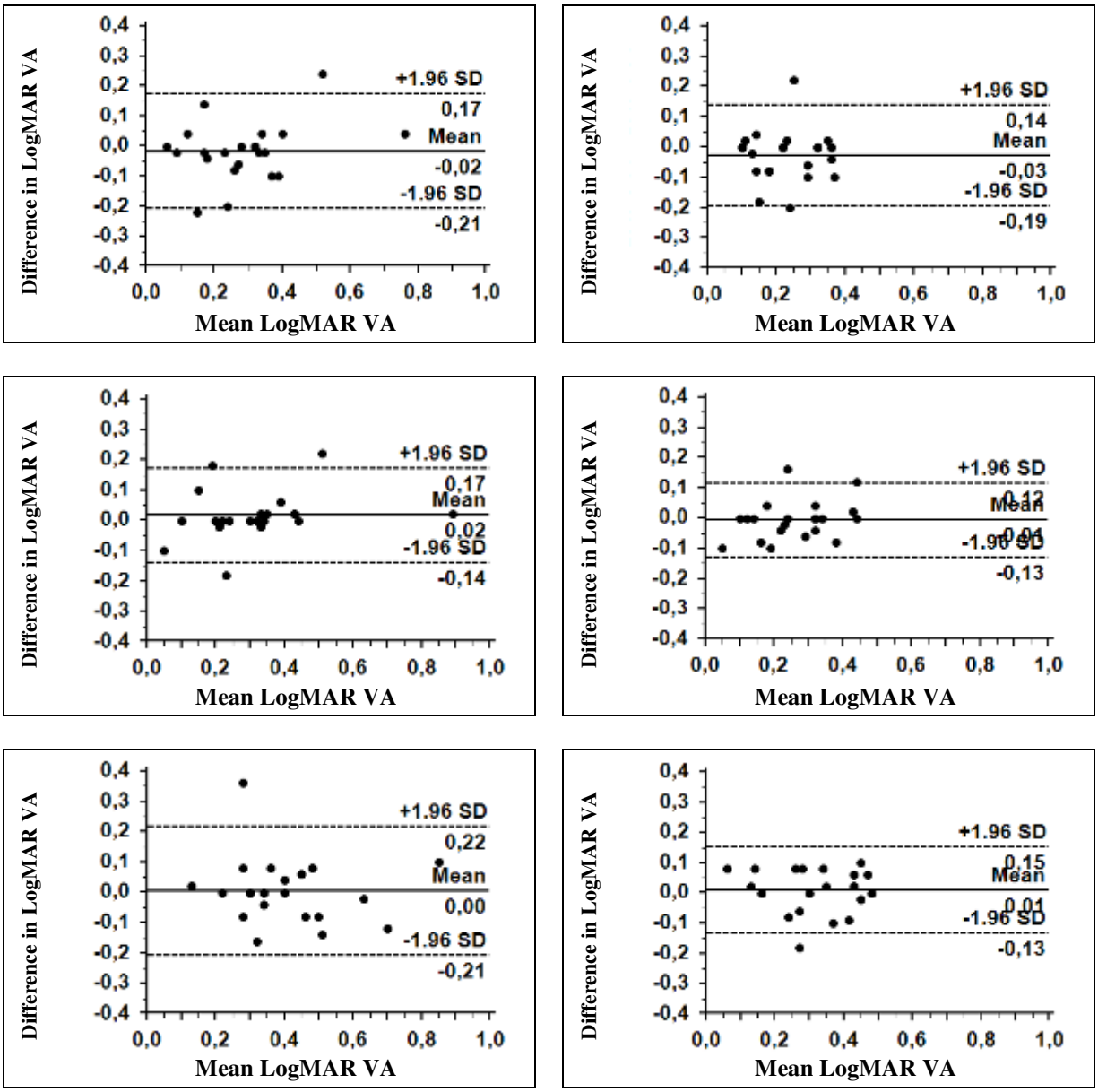

Figure 5.30 The difference in LogMAR VA for the 100% contrast ETDRS chart between Visit Three and Visit Four for the low (top) medium (middle) and high (bottom) glare sources for the Right eye (left column) and for Left eye (right column). The solid line indicates the mean of the difference and the upper and lower dotted lines the mean of the differences +/- 1.96SD, respectively.

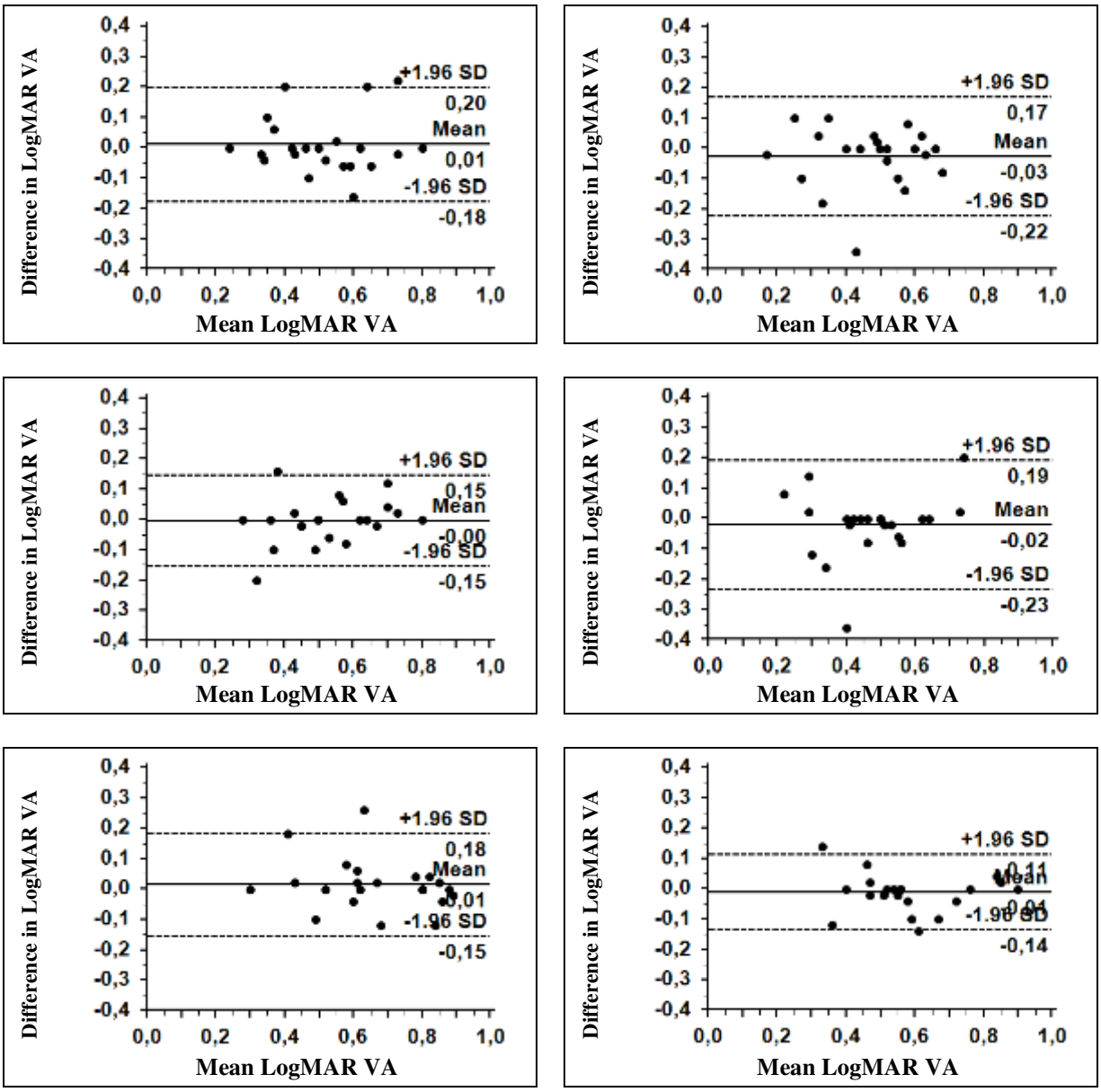

Figure 5.31 The difference in LogMAR VA for the 10% contrast ETDRS chart between Visit Three and Visit Four for the low (top) medium (middle) and high (bottom) glare sources for the Right eye (left column) and for Left eye (right column). The solid line indicates the mean of the difference and the upper and lower dotted lines the mean of the differences +/- 1.96SD, respectively.

5.22 The relationship between Mean Defect and Glare Disability

Following the completion of the learning study, four individuals were excluded from the investigation of the relationship between Mean Defect and Glare Disability. These exclusions were made on the basis of the appearance of the visual field results. One individual was excluded on the basis of an apparent central scotoma by SAP; two individuals on the basis of an abnormal field for SAP by Corrected Comparison probability analysis; and one on the basis of an apparent grossly abnormal field for CFF perimetry in the presence of a completely normal field by SAP.

The MD_{SAP} and the MD_{CFF} in the worst eye at Visit Four as a function of the high and of the low contrast logMAR VA without glare, for the remaining 18 individuals is shown in Figure 5.32. The MD_{SAP} and the MD_{CFF} were weakly correlated with the high ($r=0.16$ and $r=0.30$, respectively) and with the low ($r=0.10$ and $r=0.24$, respectively) contrast logMAR VA. The MD for both types of perimetry worsened with reduction in both types of VA. The between-individual variability was greater for CFF perimetry.

The corresponding functions, by the most severe type of cataract, for SAP are shown in Figure 5.33 and for CFF perimetry in Figure 5.34. The limited numbers within each cataract type precluded any quantitative comparison between MD for either type of perimetry and any of the three types of cataract.

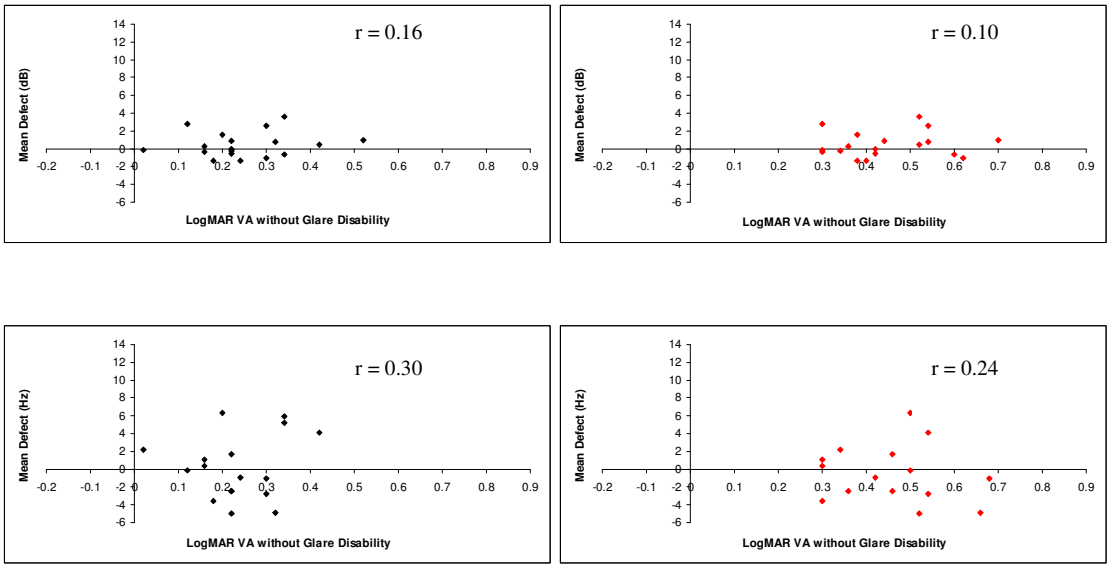

Figure 5.32 The Mean Defect for SAP (top) and for CFF (bottom) in the worst eye at Visit Four as a function of the high (right) and of the low (left) contrast logMAR VA recorded, in the absence of glare, at Visit 4 for the 18 individuals with age-related cataract.

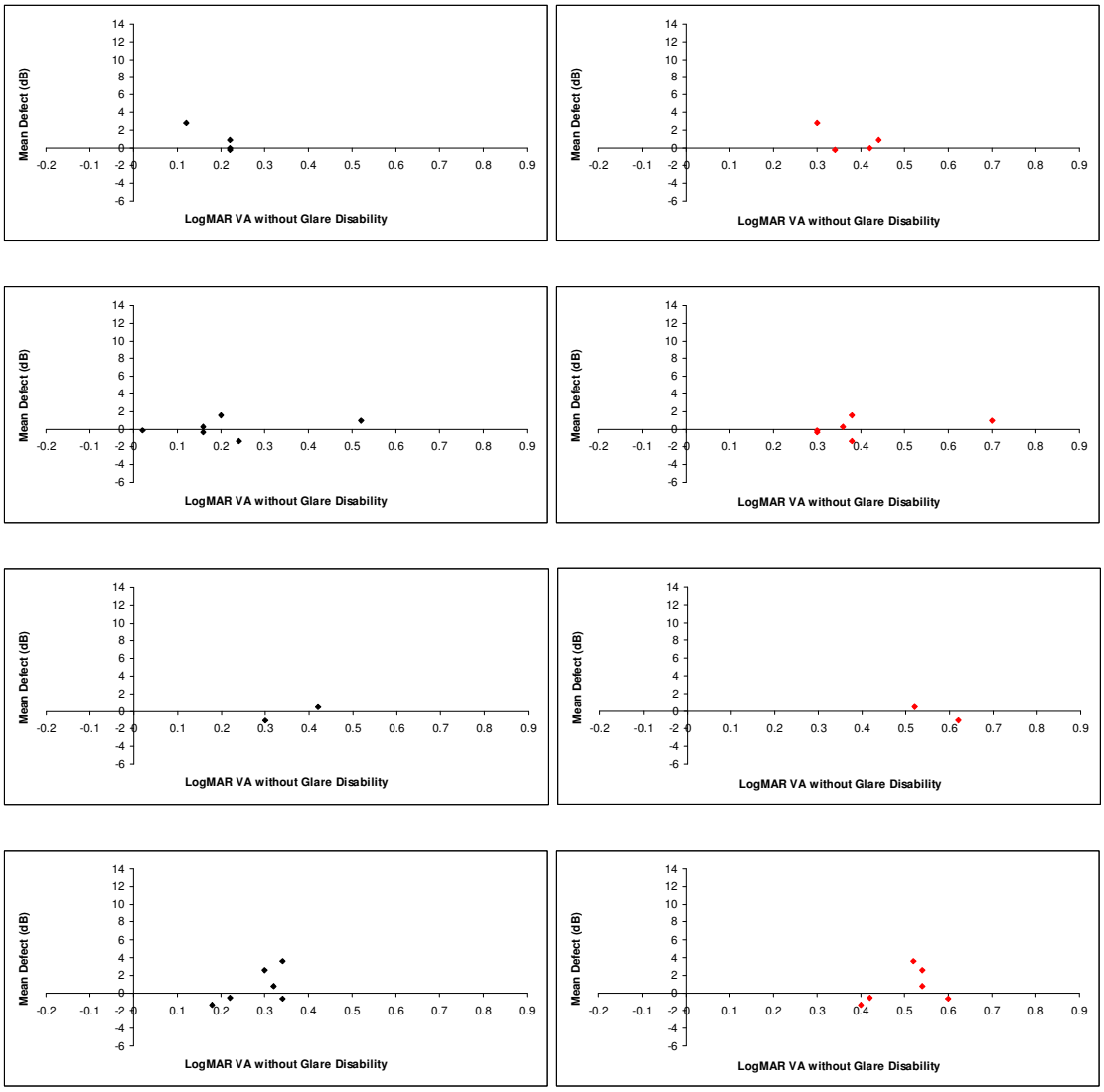

Figure 5.33 The Mean Defect for SAP in the worst eye at Visit Four as a function of the high (right) and of the low (left) contrast logMAR VA recorded at Visit 4, in the absence of glare, for each of the 4 individuals with posterior subcapsular cataract (top), the 6 individuals with anterior cortical cataract (middle top), the 2 individuals with combined cataract (C2-NO2 and C2-P2) (middle bottom) and the 6 individuals with nuclear cataract (bottom). Note the scaling of the abscissa is referenced to that of Figure 5.32.

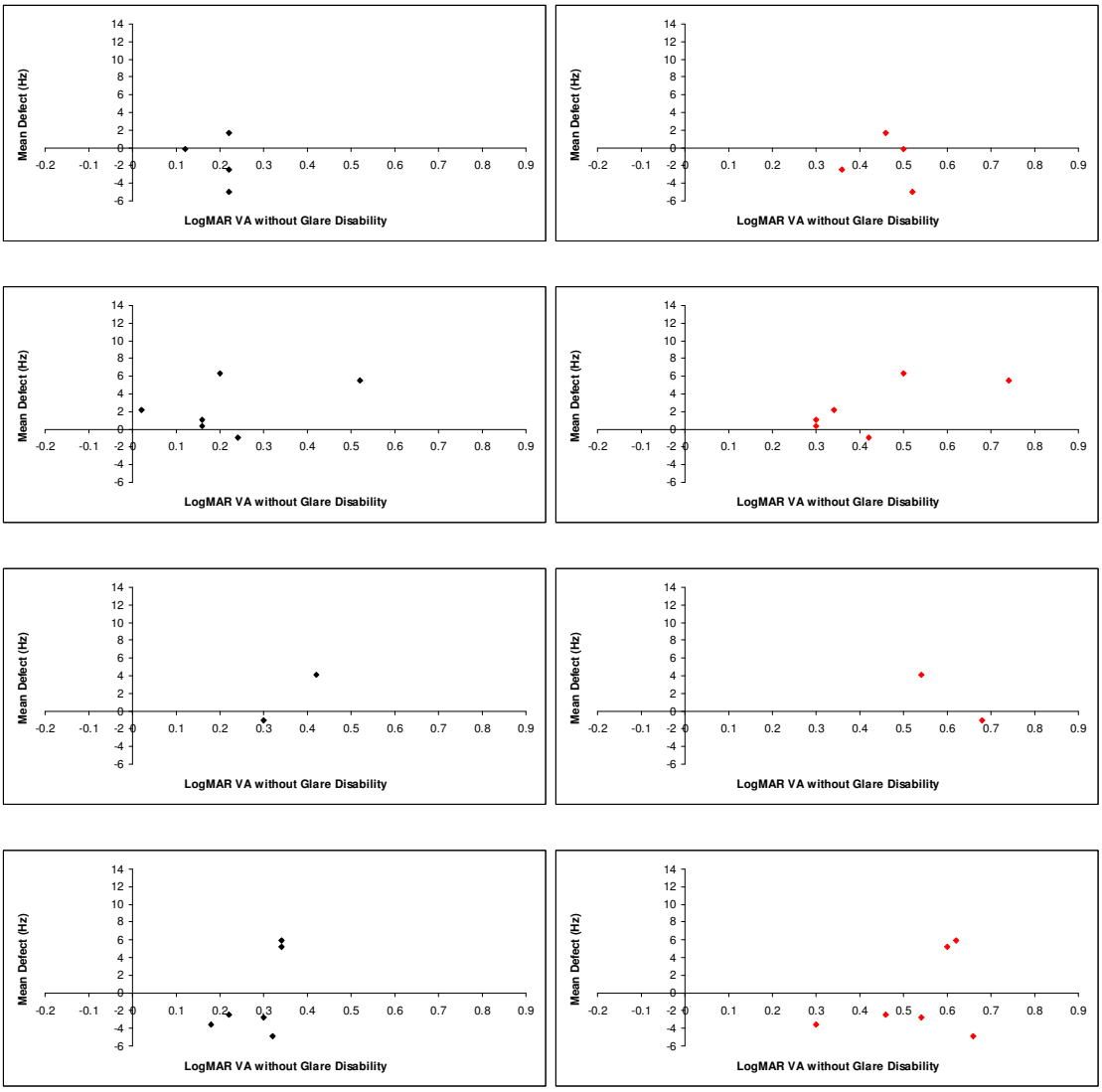

Figure 5.34 The Mean Defect for CFF in the worst eye at Visit Four as a function of the high (right) and of the low (left) contrast logMAR VA recorded at Visit 4, in the absence of glare, for each of the 4 individuals with posterior subcapsular cataract (top), the 6 individuals with anterior cortical cataract (middle top), the 2 individuals with combined cataract (C2-NO2 and C2-P2) (middle bottom) and the 6 individuals with nuclear cataract. Note the scaling of the abscissa is referenced to that of Figure 5.32.

The MD_{SAP} in the worst eye at Visit Four against each of the three Glare Disability measures calculated from the low (top), medium (middle) and high (bottom) glare sources and derived with the 100% (left column) and 10% contrast (right column) ETDRS charts for each of the 18 individuals with age-related cataract is shown in Figure 5.35.

The corresponding functions of the most severe type of cataract for SAP are shown in Figure 5.37 to 5.40. The limited numbers within each cataract type, precluded any quantitative comparison between MD for either type of perimetry and any of the measures of glare disability.

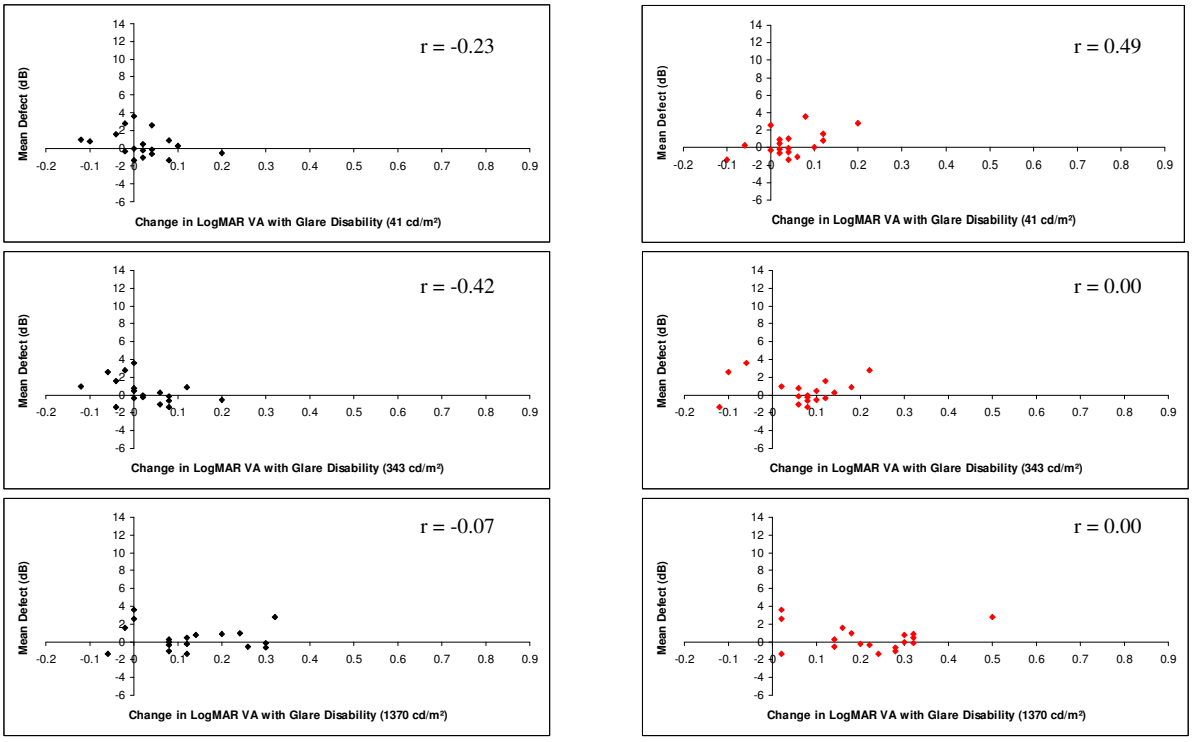

Figure 5.35 The Mean Defect for SAP in the most affected eye at Visit Four as a function of Glare Disability obtained with the low (top) medium (middle) and high (bottom) glare sources and derived with the ETDRS 100% (left) and 10% (right) contrast chart for each of the 18 individuals with age-related cataract. Note the scaling of the abscissa is referenced to that of Figure 5.32.

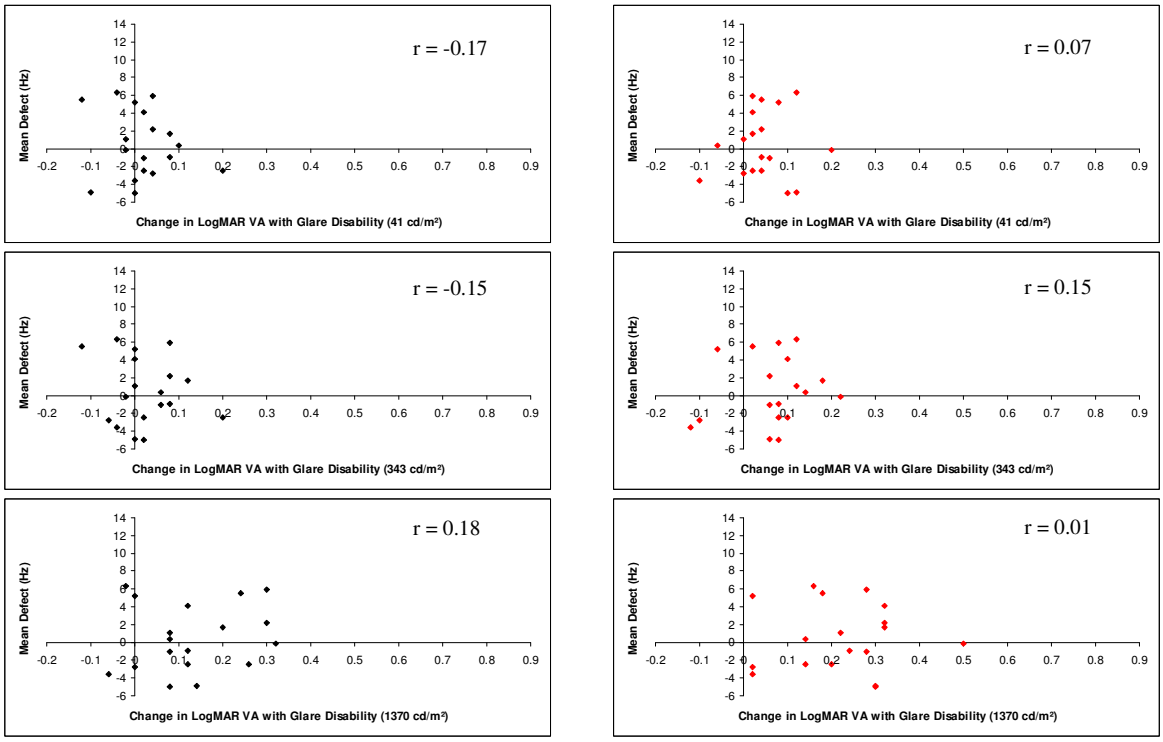

Figure 5.36 The Mean Defect for CFF in the most affected eye at Visit Four as a function of Glare Disability obtained with the low (top) medium (middle) and high (bottom) glare sources and derived with the ETDRS 100% (left) and 10% (right) contrast chart for each of the 18 individuals with age-related cataract. Note the scaling of the abscissa is referenced to that of Figure 5.32.

The Mean Defect for CFF in the worst eye at Visit Four as a function of the change in each of the three Glare Disability measures from the no-glare baseline calculated for the low (top), medium (middle) and high (bottom) glare sources and derived with the 100% (left column) and 10% contrast (right column) ETDRS charts for each of the 18 individuals with age-related cataract is shown in Figure 5.36.

The corresponding figures as a function of the most severe cataract type for CFF are shown in Figures 5.41 to 5.44. The limited numbers within each cataract type precluded any quantitative comparison between MD for either type of perimetry and any of the measures of glare disability.

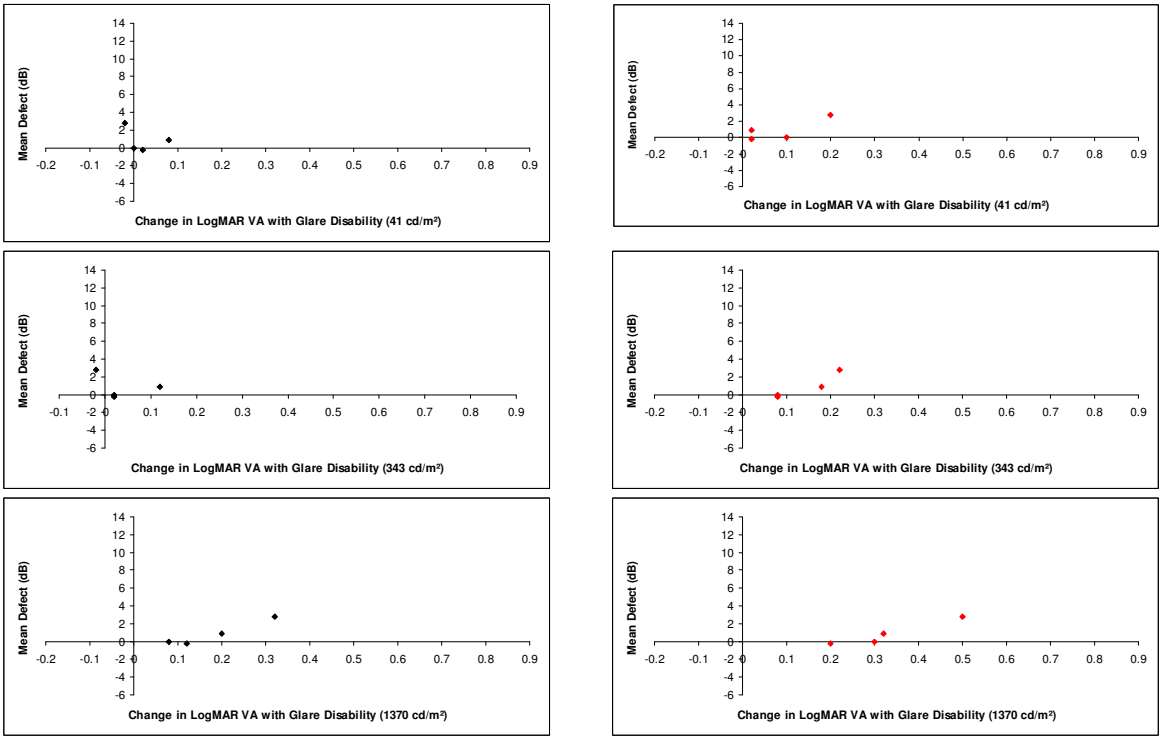

Figure 5.37 The Mean Defect for SAP in the most affected eye at Visit Four as a function of Glare Disability obtained with the low (top) medium (middle) and high (bottom) glare sources and derived with the ETDRS 100% (left) and 10% (right) contrast chart for each of the 4 individuals with posterior subcapsular cataract. Note the scaling of the abscissa is referenced to that of Figure 5.32.

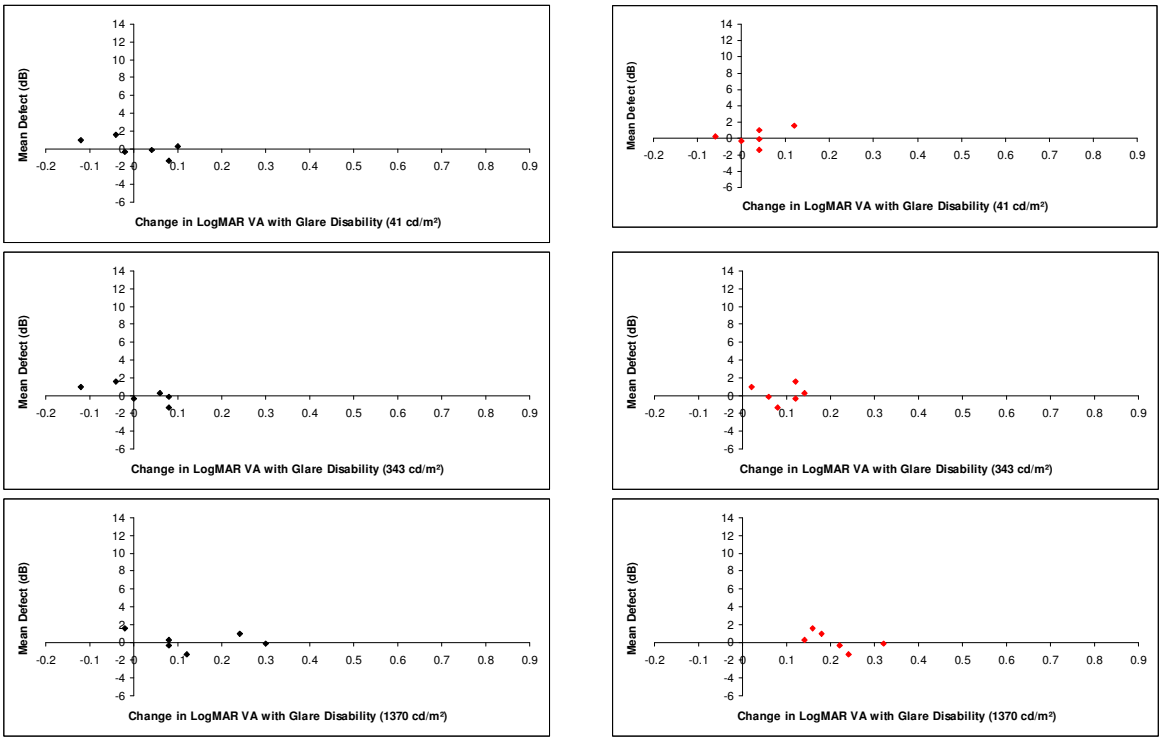

Figure 5.38 The Mean Defect for SAP in the most affected eye at Visit Four as a function of Glare Disability obtained with the low (top) medium (middle) and high (bottom) glare sources and derived with the ETDRS 100% (left) and 10% (right) contrast chart for each of the 6 individuals with anterior cortical cataract. Note the scaling of the abscissa is referenced to that of Figure 5.32.

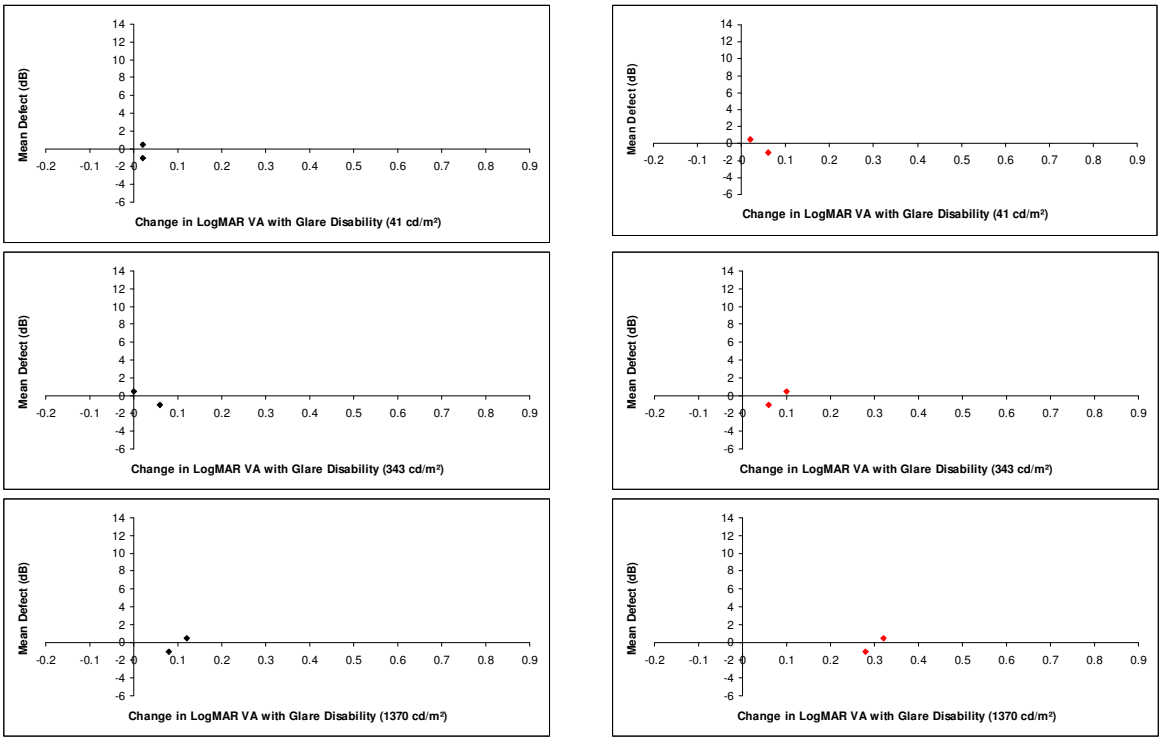

Figure 5.39 The Mean Defect for SAP in the most affected eye at Visit Four as a function of Glare Disability obtained with the low (top) medium (middle) and high (bottom) glare sources and derived with the ETDRS 100% (left) and 10% (right) contrast chart for each of the 2 individuals with combined cataract (C2-NO2 and C2-P2). Note the scaling of the abscissa is referenced to that of Figure 5.32.

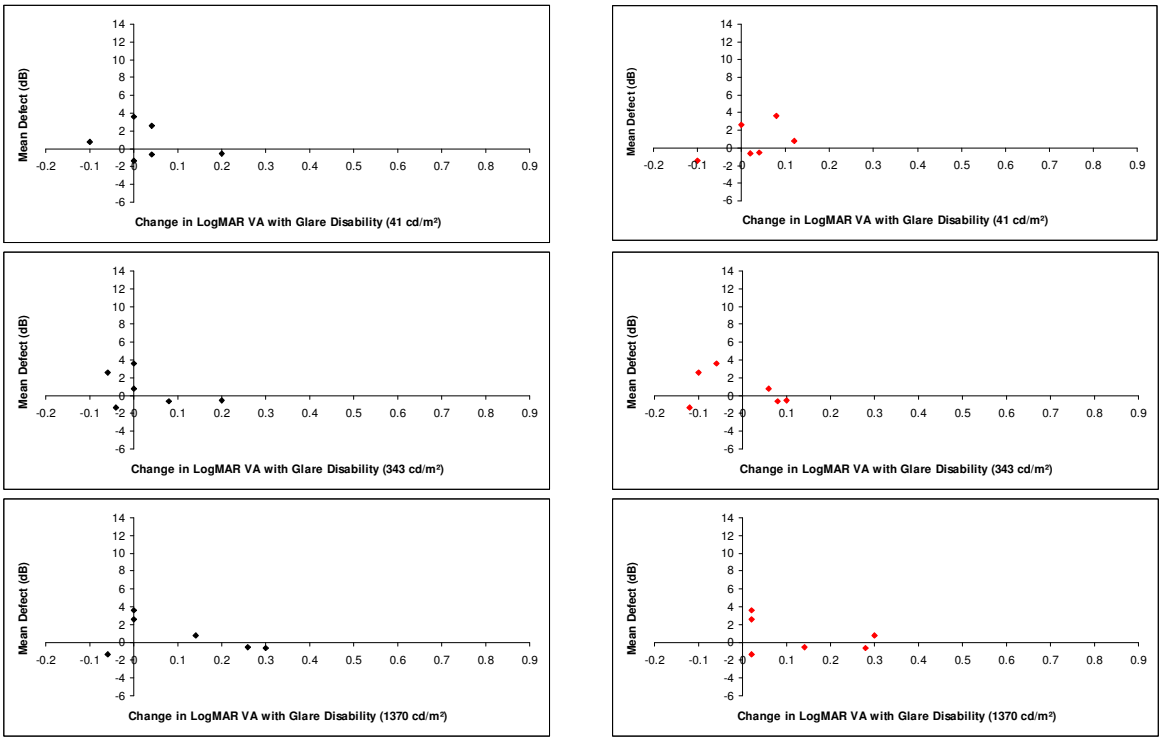

Figure 5.40 The Mean Defect for SAP in the most affected eye at Visit Four as a function of Glare Disability obtained with the low (top) medium (middle) and high (bottom) glare sources and derived with the ETDRS 100% (left) and 10% (right) contrast chart for each of the 6 individuals with nuclear cataract. Note the scaling of the abscissa is referenced to that of Figure 5.32.

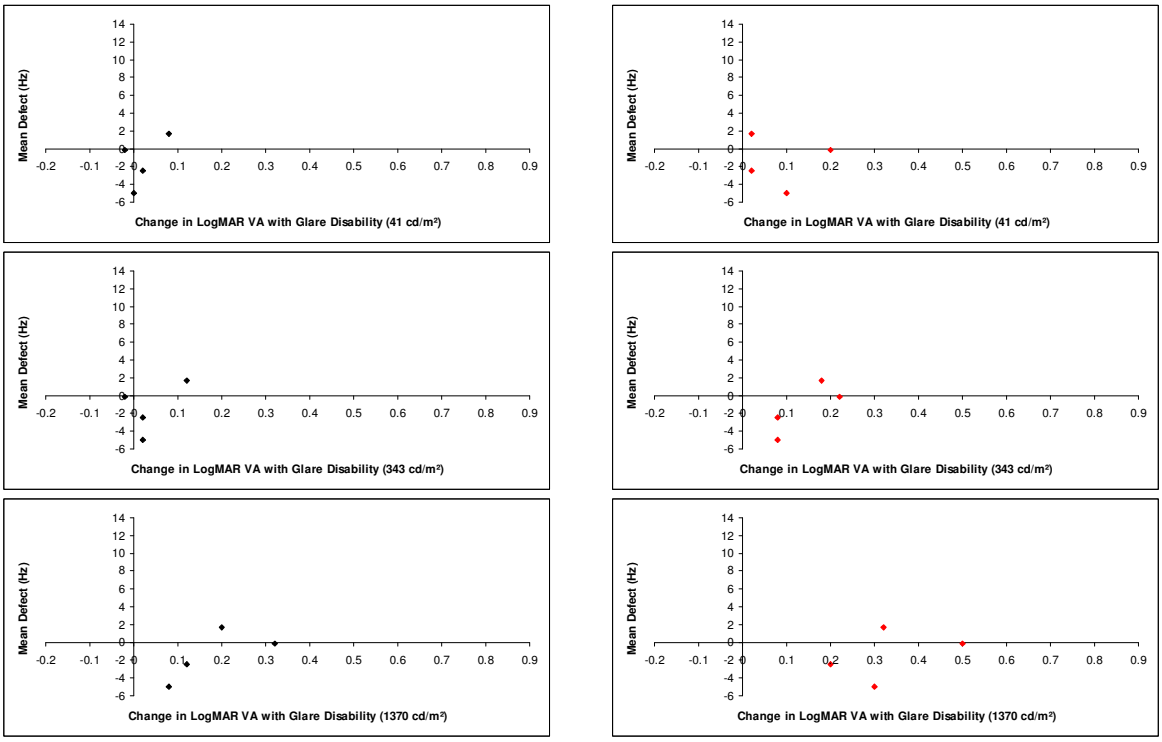

Figure 5.41 The Mean Defect for CFF in the most affected eye at Visit Four as a function of Glare Disability obtained with the low (top) medium (middle) and high (bottom) glare sources and derived with the ETDRS 100% (left) and 10% (right) contrast chart for each of the 4 individuals with posterior subcapsular cataract. Note the scaling of the abscissa is referenced to that of Figure 5.32.

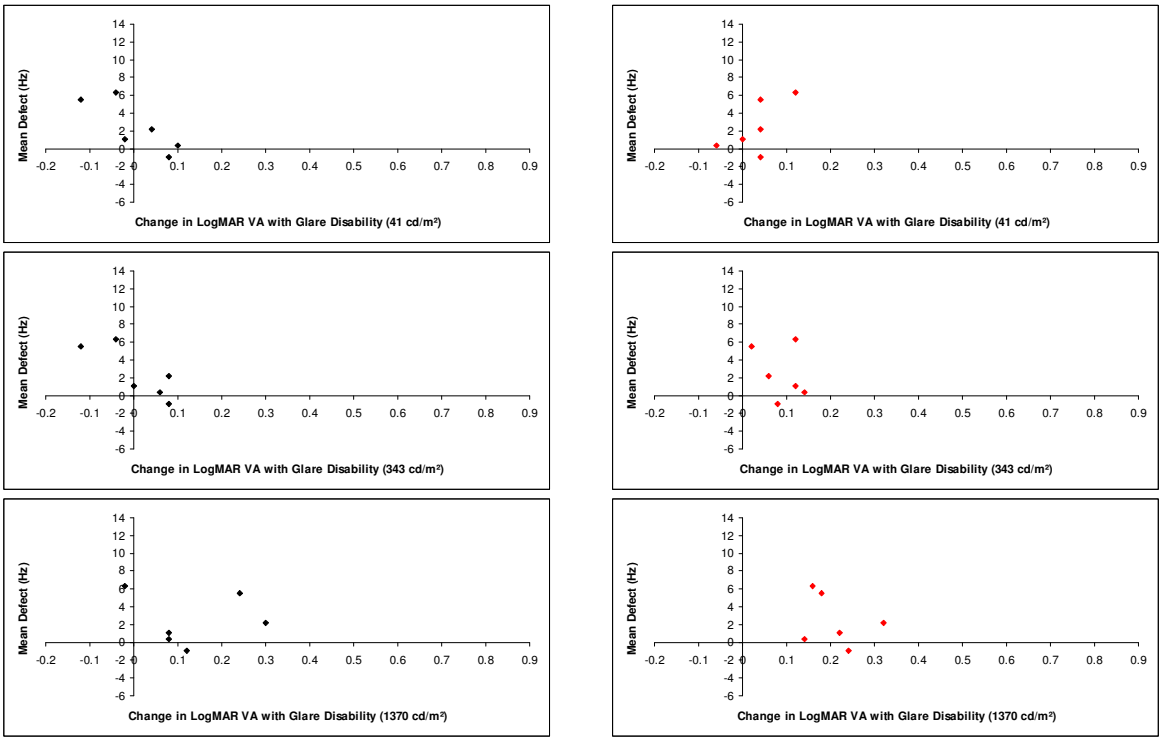

Figure 5.42 The Mean Defect for CFF in the most affected eye at Visit Four as a function of Glare Disability obtained with the low (top) medium (middle) and high (bottom) glare sources and derived with the ETDRS 100% (left) and 10% (right) contrast chart for each of the 6 individuals with anterior cortical cataract. Note the scaling of the abscissa is referenced to that of Figure 5.32.

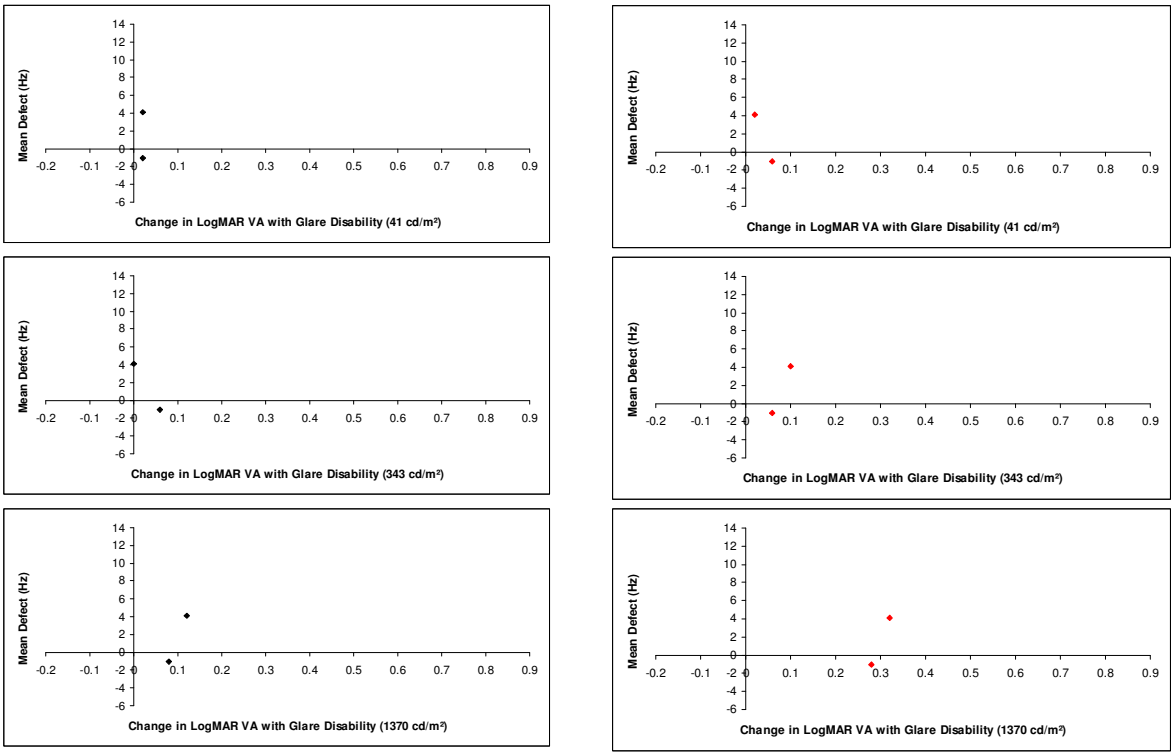

Figure 5.43 The Mean Defect for CFF in the most affected eye at Visit Four as a function of Glare Disability obtained with the low (top) medium (middle) and high (bottom) glare sources and derived with the ETDRS 100% (left) and 10% (right) contrast chart for each of the 2 individuals with combined (C2-NO2 and C2-P2) cataract. Note the scaling of the abscissa is referenced to that of Figure 5.32.

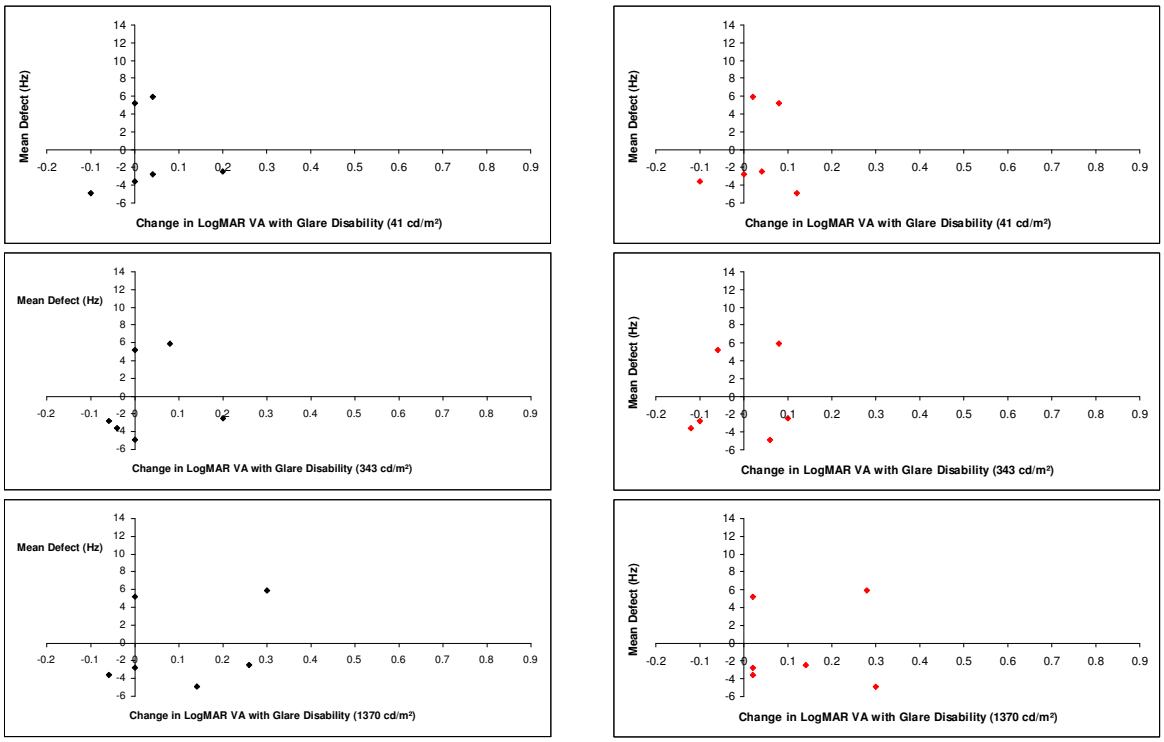

Figure 5.44 The Mean Defect for CFF in the most affected eye at Visit Four as a function of Glare Disability obtained with the low (top) medium (middle) and high (bottom) glare sources and derived with the ETDRS 100% (left) and 10% (right) contrast chart for each of the 6 individuals with nuclear cataract. Note the scaling of the abscissa is referenced to that of Figure 5.32.

Within the obvious limitations in the numbers of the data set, little correlation was present, either for the four types of cataract, combined, or for each type of cataract considered separately, between either the MD for SAP and the MD for CFF and the Glare Disability determined for any of the three glare sources for either contrast chart.

5.23 Discussion

5.24 Learning Effect

A learning effect was present for SAP. The visual field indices MS, MD and DD successively improved over the four visits indicating an increase in the overall height of the visual field. In addition, the sLV and the LD also successively improved over the four visits indicating a

reduction in the area and/ or depth of apparent non-uniform loss. This latter finding was compatible with the successive increase in the peripheral/ central mean sensitivity ratio over the four visits which indicated a greater improvement in the peripheral regions of the central field. The increase in the overall height of the field together with a proportionately greater increase peripherally compared to centrally has been previously documented for normal individuals (Wild et al 1989; Werner et al 1990; Searle et al 1991; Heijl and Bengtsson 1996; Castro, Kawase and Melo 2008). Although the learning effect for SAP has been found to be greater for the second eye examined at the initial visits both for normal individuals (Wood et al 1987b; Heijl, Lindgren and Olsson 1989; Searle et al 1991) for individuals with OHT (Wild et al 1989; Werner et al 1990; Wild et al 1991) and for individuals with OAG (Werner, Adelson and Krupin 1988; Kulze, Stewart and Sutherland 1990; Marchini, Pisano and Bertagnin 1991; Wild et al 1991; Heijl and Bengtsson 1996), any difference in the learning effect between-eyes for any of the indices in the current study did not reach statistical significance even for the worst of the two eyes. The greater peripheral improvement in the MS was not readily apparent in the analysis, by eccentricity, across each stimulus location. The learning effect from Visits One to visit Two was maximal at intermediate levels of sensitivity of approximately 12-15dB and from Visits Two to visit Four at 15-18dB. This depth-dependency of the learning effect is compatible with other studies (Wild et al 1989; Wild et al 2006). The latter findings were reflected in the number of locations exhibiting a Comparison Probability value which became statistically less severe (i.e. an improvement) by one or more probability levels from Visits One to visit Two and which was approximately 2.2 fold greater, across the two eyes, than those locations exhibiting a statistically more severe (i.e. a worsening) by one or more probability levels. A clinically similar finding was present between Visits Two and Four. The corresponding figures for the Corrected Comparison Probability value between Visits One and Two and between Visits Two and Four were 1.75 fold and 2.75 fold respectively.

The characteristics of the learning effect for CFF perimetry were similar to those described in Chapter 4 for the normal individuals and for the individuals with OHT and the individuals with OAG. The visual field indices MS, MD and DD successively improved over the first three visits indicating an increase in the overall height of the visual field. However, the sLV and the LD remained similar over the four visits confirming the clinically uniform increase in the height of the field. This similarity was also consistent with the lack of improvement in the ratio of the peripheral/ central mean sensitivity over the four visits. Within the remit of a uniform increase in the height of the field, the learning effect for CFF perimetry was also more apparent for the intermediate levels of sensitivity. From Visits One to visit Two, it was maximal at approximately 18Hz. From Visits Two to visit Four the slope of the improvement was much flatter, however, the peak was, again, at approximately 18-21Hz. As would be hypothesized with a lack of degradation to the CFF stimulus, the number of locations exhibiting abnormality by Comparison and by Corrected Comparison Probability analysis were equal for any given individual and declined over the four visits. However, a more plausible explanation for the former finding is that discussed in Chapter 4, namely, the lack of a general height adjustment for CFF perimetry. The number of locations exhibiting a Comparison, and therefore, a Corrected Comparison Probability, value which increased in magnitude (i.e. became statistically less severe, - an improvement) by one or more probability levels from Visits One to visit Two was greater for the right eye than the left eye and was approximately 2.3 fold greater, across the two eyes, than those locations exhibiting a reduction (i.e. a statistically deeper defect, - a worsening) by one or more probability levels. The corresponding value across the two eyes from Visits Two to visit Four was 1.2.

The achievement of optimum performance for CFF perimetry at Visit Three, rather than at Visit Four as with SAP, is also compatible with that for the normal individuals described in Chapter 4.

The reason for the difference in the length of the training regime required to reach optimum performance is unknown. The influence of the veiling glare, by reducing the stimulus contrast, may have had a greater effect for SAP than for CFF perimetry in terms of extending the learning outcome. It should be noted that the individuals with OHT and the individuals with OAG, both groups of which were described in Chapter 4 and who were experienced in SAP, reached optimum performance for CFF perimetry at the fourth or fifth visit. It could be argued that the neural attenuation, particularly for those with OAG, rather than the optical degradation, results in a more difficult task which requires a longer period of learning. In addition, the criterion for threshold amongst these individuals could be more critical since they have a vested interest in performing optimally.

The learning effect in both eyes was similar, in proportionate terms, between SAP and CFF perimetry. The median (IQR) improvement for SAP in each eye from Visit One to Visit Two was 4.2% (8.7%) for the right eye and 2.1% (5.2%; 42.8%) for the left eye compared with 5.0% (11.5%; 41.6%) in the right eye and 2.2% (6.0%) in the left eye for CFF. Although such magnitudes would appear to be small, they should be placed in the context that, for the SITA algorithms for SAP, 1dB may account for up to two levels of probability on the Total and Pattern Deviation probability analysis (Wild et al 1999). The median (IQR; range) improvement for SAP from Visit Two to Visit Four was 1.2% (5.2%) and -0.18% (5.13) for the right and left eyes respectively, and for CFF -1.7% (10.90%) and 0.4% (10.8%).

No evidence was present, within the remit of the types and mild nature of the cataracts in the case series, that CFF perimetry was more resistant to image degradation than SAP (Figure 5.45).

CFF Perimetry (Hz)	SAP (dB)
NO3 – NC3 Ex	
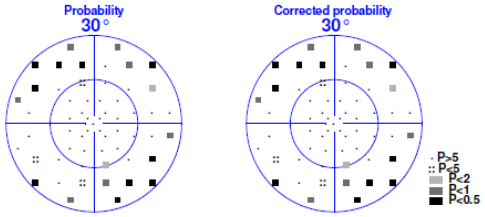	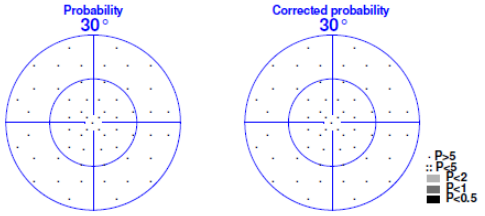
C3	
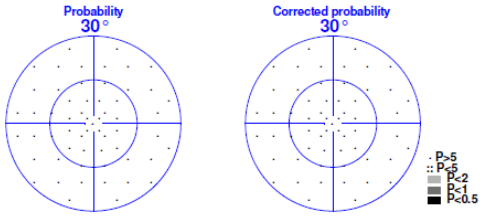	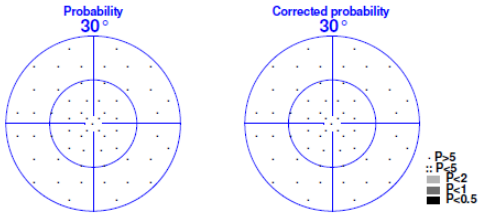
NO3 – NC4 Ex	
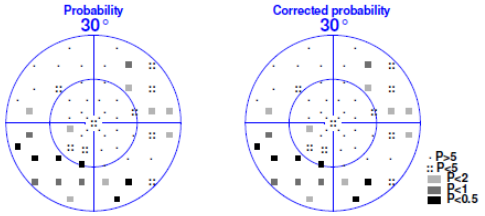	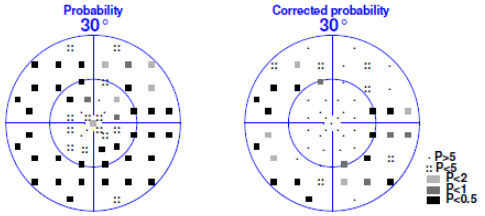
NO4	
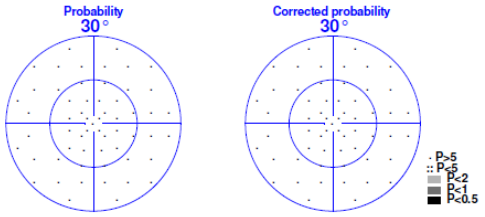	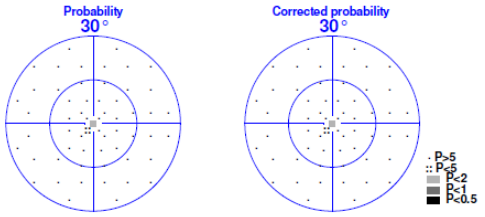
NO4 – NC4	
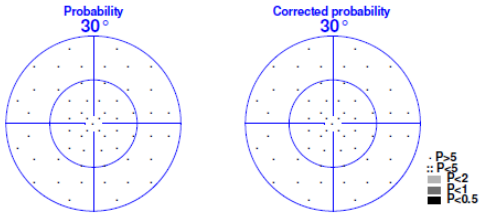	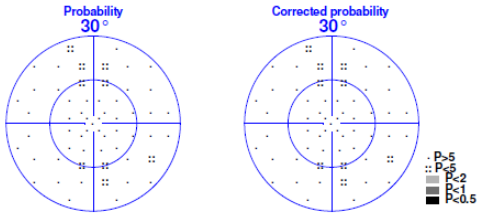
P4	
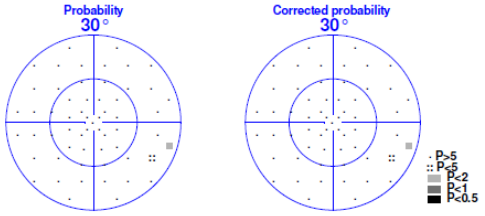	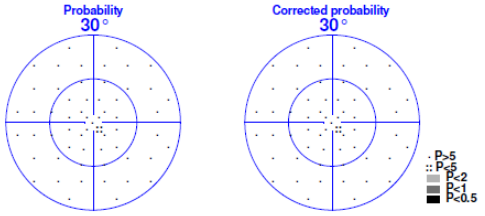

CFF Perimetry (Hz)	SAP (dB)
NO2 – NC3	
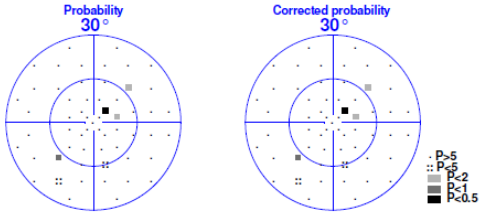	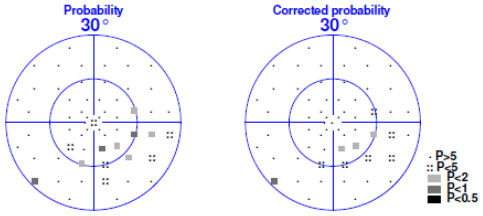
NO4 – NC4	
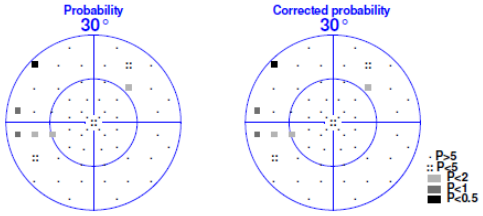	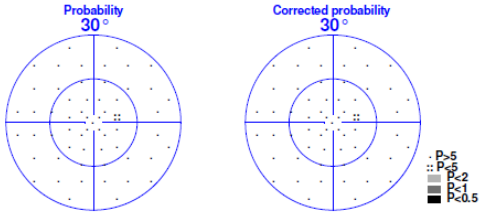
C3 Ex	
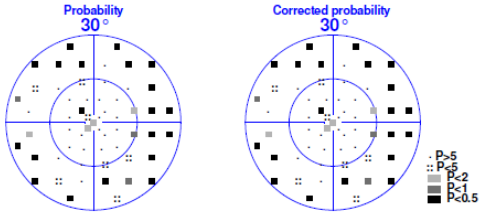	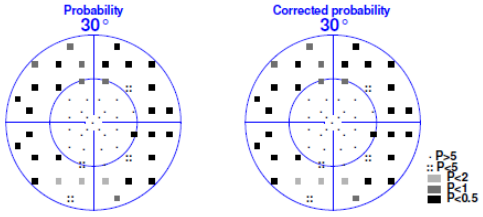
C3	
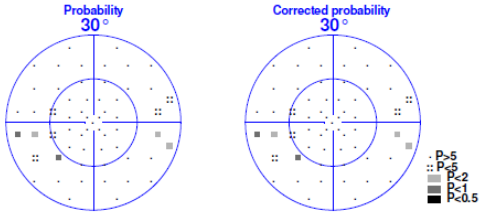	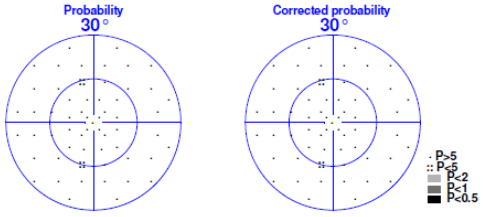
C3	
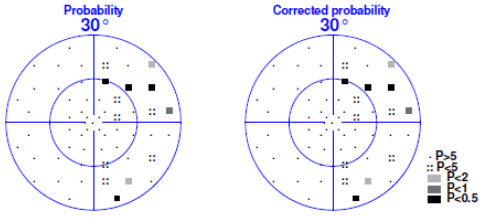	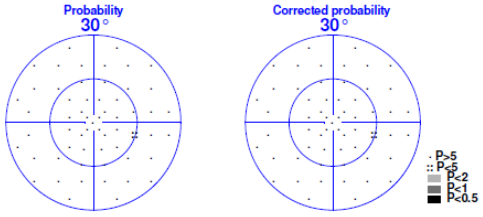
C2/P2	
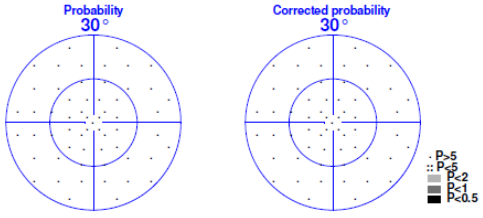	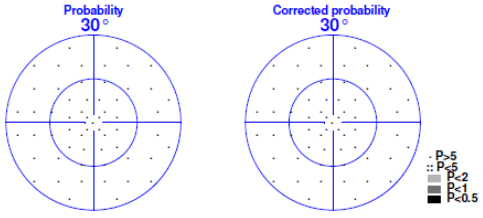

CFF Perimetry (Hz)	SAP (dB)
C4	
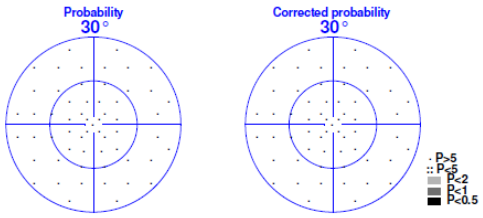	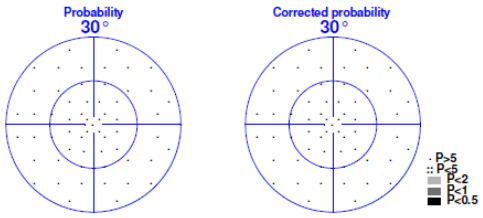
P3	
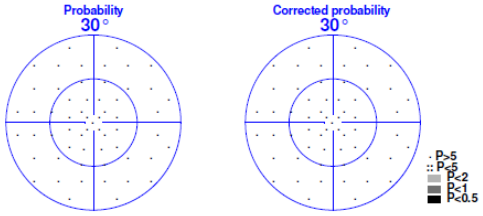	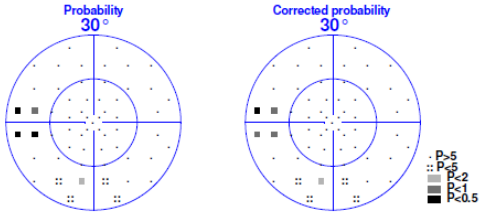
C2/N2	
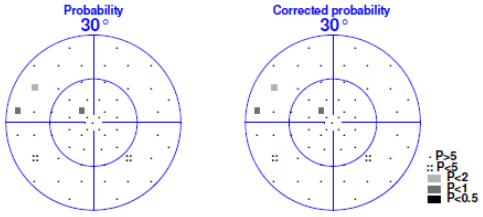	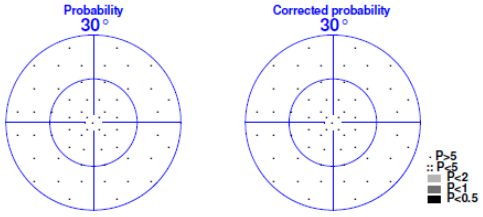
NO3/NC3	
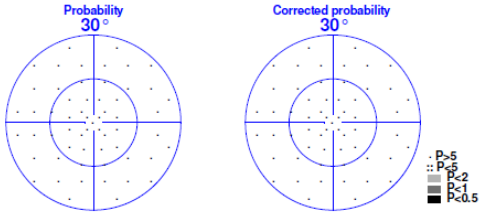	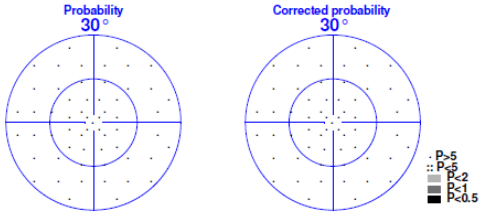
P1	
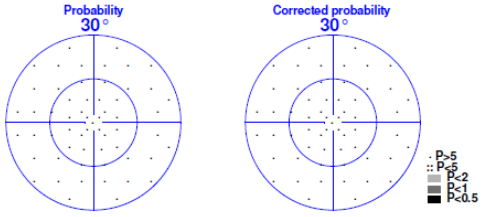	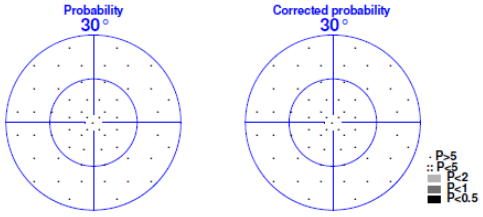
C3	
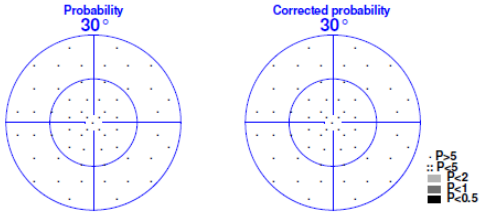	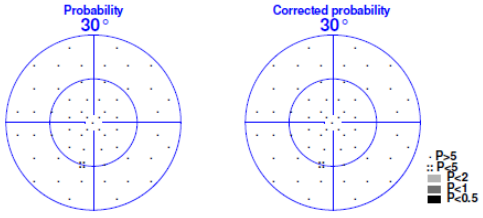

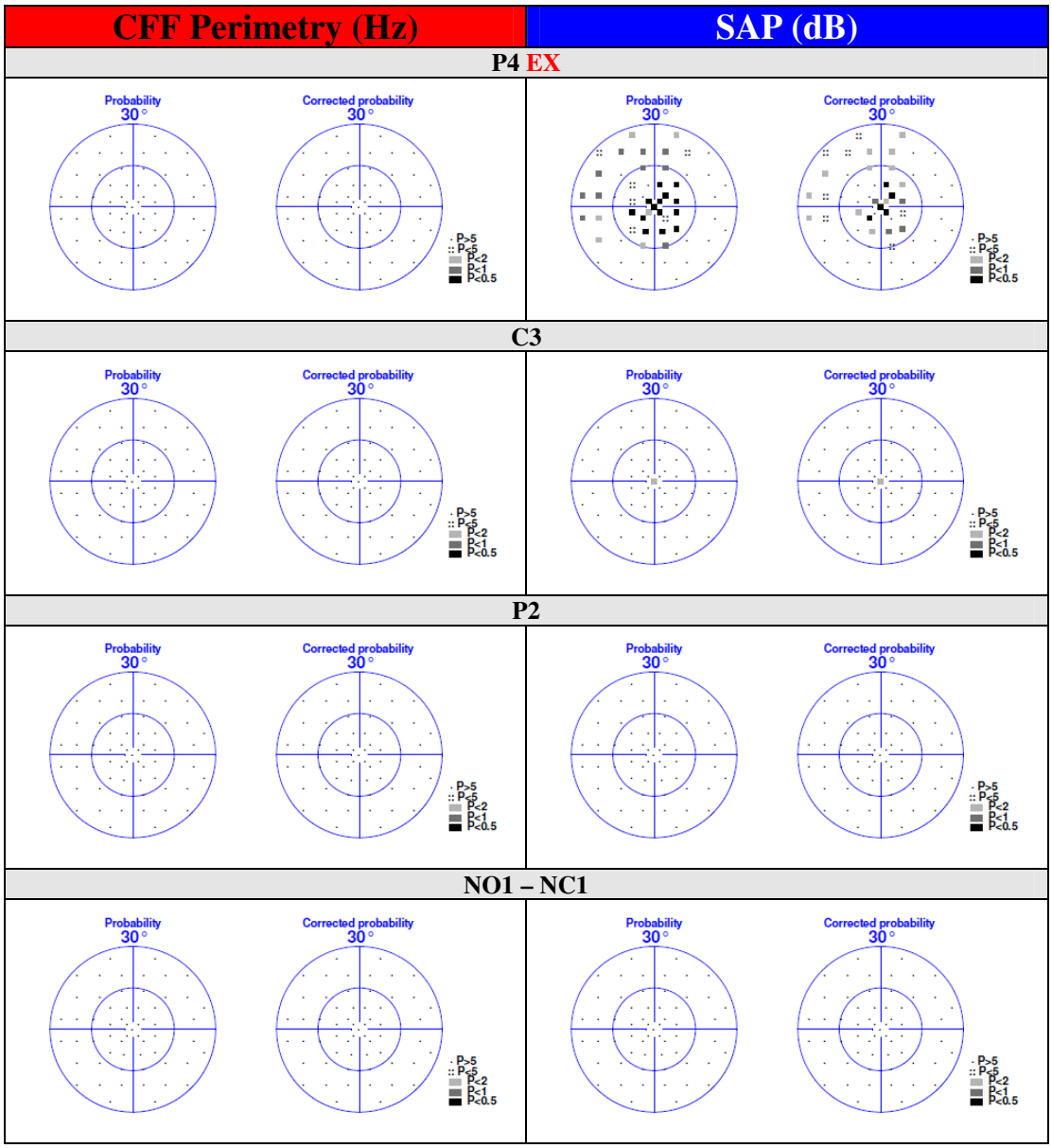

Figure 5.45 The Comparison and Corrected Comparison probability maps for CFF perimetry (left hand column) and for SAP (right hand column) for the field corresponding to the eye with the more severe cataract for each of the 22 individuals.

The three measures of Glare Disability derived from each of the two contrast charts correlated poorly with the SAP MD. Such an outcome was perhaps surprising given the close relationship between the degree of forward light scatter quantified as the stray light parameter, and expressed relative to age-correction, as the isolated cataract straylight parameter (ICSP) and the MDs for SAP and SWAP (Moss, Wild and Whitaker 1995; Bergin et al 2011). However, the two

measures of forward light scatter, calculated from the BAT and straylight meter, are not determined in the same manner. The stray light parameter determined using the straylight meter (van den Berg, IJspeert and de Waard 1991; de Waard et al 1992) involves the observer fixating the centre of a l° diameter dark target surrounded by an annulus with an outer radius of 2° and a luminance of 30 cdm^{-2}. The latter contains a yellow glare source of 137 cdm^{-2} comprised light-emitting diodes (maximum wavelength, 570 nm; half width, 30 nm) flickering at 8 Hz which are arranged in a circular display at one of each of three different glare angles (3.5°, 10°, and 28°). Because of forward light scatter, flicker is seen in the central dark area. The luminance modulation of a counterphase flickering light is adjusted to cancel the resulting central 8 Hz flicker.

The range of cataract severity would appear to have been narrower in the current study than in previous studies (Moss, Wild and Whitaker 1995). The lack of individuals with severe cataract in the current study is likely to have arisen from the improvement in access to healthcare delivery across the Western World (i.e. cataract extraction and IOL implantation is now being undertaken at an earlier stage of severity).

Both measures of light scatter do not consider the role of the pupil size in the assessment of forward light scatter. In addition, a difference in the pupil size is present between that for the assessment of forward light scatter and that operative for perimetry. The luminances of the High and Medium glare sources used for the BAT are substantially greater than that for the straylight meter. Although these higher luminances should result in greater disability glare and, therefore, a greater reduction in visual performance, the very nature of the increased glare may lead to an increased variability in the measurement of visual acuity under such glare conditions. The discrepancy in the pupil sizes between the two assessments, i.e. the light scatter and the

perimetry field, is likely to have reduced the correlation between disability glare and the MD for SAP particularly given the variation in performance arising from the interaction of the pupil size with the type of cataract. Had the pupil size been artificially maintained at the same level, both for the assessment of disability glare and for the visual field, the correlation between the two measures might have been higher but would still have been limited by the range of cataract severity.

The high and low-contrast VA measured in the absence of a glare source produced a more plausible, albeit weak, correlation with the SAP_{MD} compared to the correlation between SAP_{MD} and disability glare at any of the three glare levels. Such a finding is in agreement with that of Elliott and colleagues (Elliott and Hurst 1990) in individuals with cataract and expected normal neural function.

The concept of the BAT has been challenged on the basis of the induced pupil miosis (Tan, Spalton and Arden 1998; Wachler et al 1999). The use of the high luminance glare source has been shown to overestimate the magnitude of disability glare and can also saturate the contrast of some types of letter charts even in cases of early cataract (Neumann et al 1988a; Prager et al 1989). Nevertheless, disability glare calculated with the BAT is considered to be useful in that the outcome is independent of abnormalities in neural function (Elliott and Hurst 1990).

In conclusion, a learning effect was present in individuals with mild cataract for both SAP and CFF perimetry. In general, the effect was present over three visits for CFF and lasted slightly longer for SAP. No relationship could be determined between MD and low and high contrast visual acuity determined in the absence and in the presence, respectively, of glare. The lack of a relationship maybe attributed to the narrow range of mild cataract severity.

CHAPTER 6

THE EFFECT OF DEFOCUS ON THE VISUAL FIELD FOR CFF PERIMETRY IN NORMAL INDIVIDUALS

6.1 Introduction

It is well accepted that the magnitude of the differential light sensitivity derived by Goldmann stimulus size III reduces with increase in optical defocus for both SAP (Beneddeto et al 1985, Weinreb and Perlman 1986; Goldstick and Weinreb 1987, Heuer et al 1987) and for manual kinetic perimetry (Maguire 1971). For SAP, the gradient approximates, clinically, to 1.4dB attenuation per dioptre (Heuer et al 1987), per 1.3dB per dioptre (Weinreb and Perlman 1986) or per 2.5dB per dioptre (Lachenmayer and Gleissner 1992) of uncorrected refractive error. The effect of optical defocus increases with reduction in Goldmann stimulus size (Sloan 1961, Atchison 1987) out to 30°-40° eccentricity (Atchison 1987). The preferential effect of defocus on the smaller stimulus sizes becomes more pronounced with increase in eccentricity (Anderson et al 2001) such that, following correction for peripheral refractive error at 30° eccentricity, sensitivity to a stimulus equating to Goldmann size V is unaffected by defocus (Anderson et al 2001).

The effect of optical defocus on the 10° square stimulus size (containing a grating with a spatial frequency of 0.25 cyc/deg counterphased at 25 Hz) of Frequency-Doubling Technology perimetry is equivocal. A reduction in sensitivity of 0.05 to 0.1 log unit has been reported for a defocus of up to +/-6.00 DS (Johnson and Samuels 1997, Artes et al 2003). The impact of defocus on the smaller 4° square stimulus size (containing a grating with a spatial frequency of 0.50 cyc/deg counterphased at 18 Hz), of the Matrix perimeter is also negligible. The MD declines by 0.11dB per dioptre of defocus (Anderson and Johnson 2003).

The early research on CFF suggests that the outcome is independent of refractive error (Ong and Wong 1971), even to the extent of uncorrected aphakia, for stimuli of 2-3° in diameter. (Havener and Henderson 1954; Tyler 1991). However, it has also been suggested that defocus reduces CFF, that the reduction is most evident for a foveal stimulus of 50 min of arc in diameter and that the tolerance of CFF to blur is greater in the periphery particularly for larger stimuli (Jennings and Charman 1981). The latter results are not in accord with those of Lachemayer and Gleissner (1992) who found that the influence of defocus on CFF within the central field for a 1° diameter stimulus was minimal up to 3.00DS after which sensitivity declined almost linearly with increase in defocus up to the maximum defocus of +9.00DS. This lack of consensus is further compounded by the results of Matsumoto and colleagues (Matsumoto et al 1996) who found that CFF, for Goldmann stimulus size III, was relatively unaffected by defocus up to +10.00DS within 10-15° eccentricity after which CFF declined with increase in defocus.

The effect of defocus is less for TMP than that for SAP (Demirel 1995) and appears, in this regard, to be similar to that for CFF (Gleissner and Lachenmayr 1992).

6.2 The effect of the defocus on CFF perimetry in normal individuals

6.3 Aims

Clearly, the outcome of defocus on CFF perimetry is unclear. The aim of the study, therefore, was to determine the effect of optical defocus on CFF perimetry in normal individuals and to compare the outcome with that determined for SAP.

6.4 Methods

The study was a prospective observational case series study.

6.5 Case series

The case series comprised 16 (6 males) consecutively presenting Caucasian individuals who met the inclusion criteria for enrolment in the study and who had volunteered to take part in the study. The mean age of these individuals was 66.6 years, the median 67.0 years (IQR 12.75) and the range from 53 to 79 years. All individuals were experienced in CFF perimetry having taken part in the learning study described in Chapter 4. As with the previous studies, all individuals were provided with written and verbal information concerning the nature of the study, and gave written consent, in accordance with requirements, and approval, of the Norwegian Ethical Committee (Regional komitè for medisinsk forskningsetikk Sør- Norge [REK Sør]) and the Norwegian Datatilsynet (Enclosure nr. 4 and 5) which in turn, is in accordance with the tenets of Declaration of Helsinki. The age profile of the case series is given in Table 6.1.

Age (years)	Normal individuals
50 – 59	3
60 – 69	7
70 – 79	6

Table 6.1 The number and age distribution of the individuals within the case series.

All individuals underwent an updated standard ophthalmic examination at baseline comprising the same procedure for the normal individuals as described in Chapter 4.

The exclusion criteria were that as described in Chapter 4 for the normal individuals. Potential participants were to be excluded from the study if they exhibited in either eye: a corrected visual acuity worse than 6/9; a distance refractive error greater than +/-5.0 dioptres sphere and/or greater than +/- 2.5 dioptres cylinder; a pupil diameter smaller than 3mm; a central corneal thickness-corrected IOP of greater than 20 mm Hg; a narrow anterior chamber angle; media opacities worse than NC3.0, NO3.0, C2.0 or P2.0 by the Lens Opacities Classification System III (LOCS III) (Chylack et al 1993); any previous ocular surgery; and any ocular disorder or ocular disease. In addition, individuals with migraine with aura, diabetes; neurological disorder or disease; systemic disease, other than systemic hypertension manifesting as Grade 1 hypertensive retinopathy, or hyperthyroid disease; a family history of glaucoma or of diabetes; and previous experience of CFF perimetry; were also excluded.

The images of the optic nerve head and of the posterior pole and the results of the visual field plots for the normal individuals had all been designated as normal by Professor Wild who was masked to the assumed normality of the potential participants.

6.6 Examination protocol

Following recruitment, each participant underwent examination of one designated eye with the Octopus 311 perimeter for both SAP and CFF perimetry using Program G1 and the TOP algorithm on two separate occasions separated by one week. Both SAP and CFF perimetry were undertaken with the distance refractive correction, in the form of full aperture trial lenses, for the designated eye of each patient (i.e. Plano defocus), and under each of the three levels of defocus: +1.00DS, +2.00DS and +4.00DS (superimposed upon the distance correction). It will be recalled from Chapters 2 and 4 that the stimulus of the Octopus 311 is projected to infinity and, therefore,

does not require correction for near for the viewing distance. The non-examined eye was occluded with an opaque patch.

The designated eye for examination was randomized between individuals and the sequence of defocus and type of perimetry was randomized within the visit and also varied between individuals over Visit 2 and Visit 3.

Each individual adapted to the background luminance of the Octopus 311, perimeter for one minute. The influence of the fatigue effect was reduced by providing a rest period of 2 minutes between each examination. Each individual was given the same instructions at each examination at each visit in order to reduce operator bias. All examinations were undertaken by the same perimetrist, the author. The examination routine is given in Table 6.2.

Visit 1	**Ophthalmic examination**		
Visit 2	**50% of individuals**	**SAP first** Defocus first: Plano Defocus second: +1.00	**CFF second** Defocus first: +2.00 Defocus second: +4.00
	50% of individuals	**CFF first** Defocus first: Plano Defocus second: +1.00	**SAP second** Defocus first: +2.00 Defocus second +4.00
Visit 3	**50% of individuals**	**CFF first** Defocus first: Plano Defocus second: +1.00	**SAP second** Defocus first: +2.00 Defocus second +4.00
	50% of individuals	**SAP first** Defocus first: Plano Defocus second: +1.00	**CFF second** Defocus first: +2.00 Defocus second: +4.00

Table 6.2 The examination routine for SAP and CFF perimetry, undertaken by the designated eye, with Program G1 and the TOP algorithm at Visit 2 and Visit 3 for the 16 individuals.

6.7 Analysis

The extent of any change over the 4 defocus levels in the visual field indices, MS_{SAP}, MD_{SAP}, sLV_{SAP}, DD_{SAP} and LD_{SAP}; and MS_{CFF}, MD_{CFF}, sLV_{CFF}, DD_{CFF} and LD_{CFF}; in the examination duration; and in the ratio of the PMS to the CMS was separately modelled using repeated measures of Analysis of Variance (ANOVA) for each dependent variable. Age, gender, the designated eye, pupil size, order of the type of perimetry, defocus and order of defocus were each considered as separate between-subject factors. The level of defocus and the visit were considered as separate within-subject factors.

6.8 Results

The summary statistics for the incorrect responses to the FP and FN catch trials as a function of the type of perimetry for the 16 normal individuals is given in Table 6.3. All 64 visual field examinations for SAP yielded responses to the false-positive/false-negative catch trials (reliability factor [RF%]) within 14.3%. Of the 64 visual field examinations for CFF perimetry, 3 individuals each yielded, at one examination, an RF factor greater than 15% (22.2%, 22.2% and 25%).

False positive/False negative answers %	Plano DS	+1.00 DS	+2.00 DS	+4.00 DS
Mean FP	1.56	1.56	1.56	0
SD	6.25	6.25	6.25	0
Median FP	0	0	0	0
IQR	0	0	0	0
Mean FN	0	0	3.13	3.13
SD	0	0	8.54	8.54
Median FN	0	0	0	0
IQR	0	0	0	0

False positive/False negative answers %	Plano DS	+1.00 DS	+2.00 DS	+4.00 DS
Mean FP	15	5.42	4.69	9.06
SD	16.83	9.86	10.08	15.19
Median FP	12.5	0	0	0
IQR	24	4.17	0	21.25
Mean FN	0	0	1.56	2.50
SD	0	0	6.25	6.83
Median FN	0	0	0	0
IQR	0	0	0	0

Table 6.3 The summary statistics (mean, SD: median, IQR) for the incorrect responses to the FP and the FN catch trials derived by SAP and by CFF perimetry at each of the four levels of defocus, undertaken by the designated eye, with Program G1 and the TOP algorithm for the 16 individuals.

6.9 The outcome for the TOP algorithm

6.9.1 Mean Sensitivity

The summary statistics of the magnitude of the MS_{SAP} and of the MS_{CFF} in the designated eye at each of the four levels of defocus are given in Tables 6.4 for the 16 normal individuals. The distributions of the MS_{SAP} and of the MS_{CFF}, as a function of defocus, are also illustrated in terms of Box and Whisker plots in Figure 6.1.

MS_{SAP} dB	**Plano DS**	**+1.00 DS**	**+2.00 DS**	**+4.00 DS**
Mean	27.24	26.34	25.42	23.33
SD	1.32	1.26	1.07	1.14
Median	27.40	26.40	25.55	23.35
IQR	1.42	0.83	0.92	1.15

MS_{CFF} Hz	**Plano DS**	**+1.00 DS**	**+2.00 DS**	**+4.00 DS**
Mean	34.73	35.07	34.78	36.84
SD	4.80	4.91	4.70	3.91
Median	36.50	35.75	35.30	37.50
IQR	8.47	7.65	5.30	4.32

Table 6.4 The summary statistics (mean, SD: median, IQR) for MS_{SAP} (dB) (top) and for MS_{CFF} (Hz) (bottom) at each of the four levels of defocus, undertaken by the designated eye, for the 16 normal individuals.

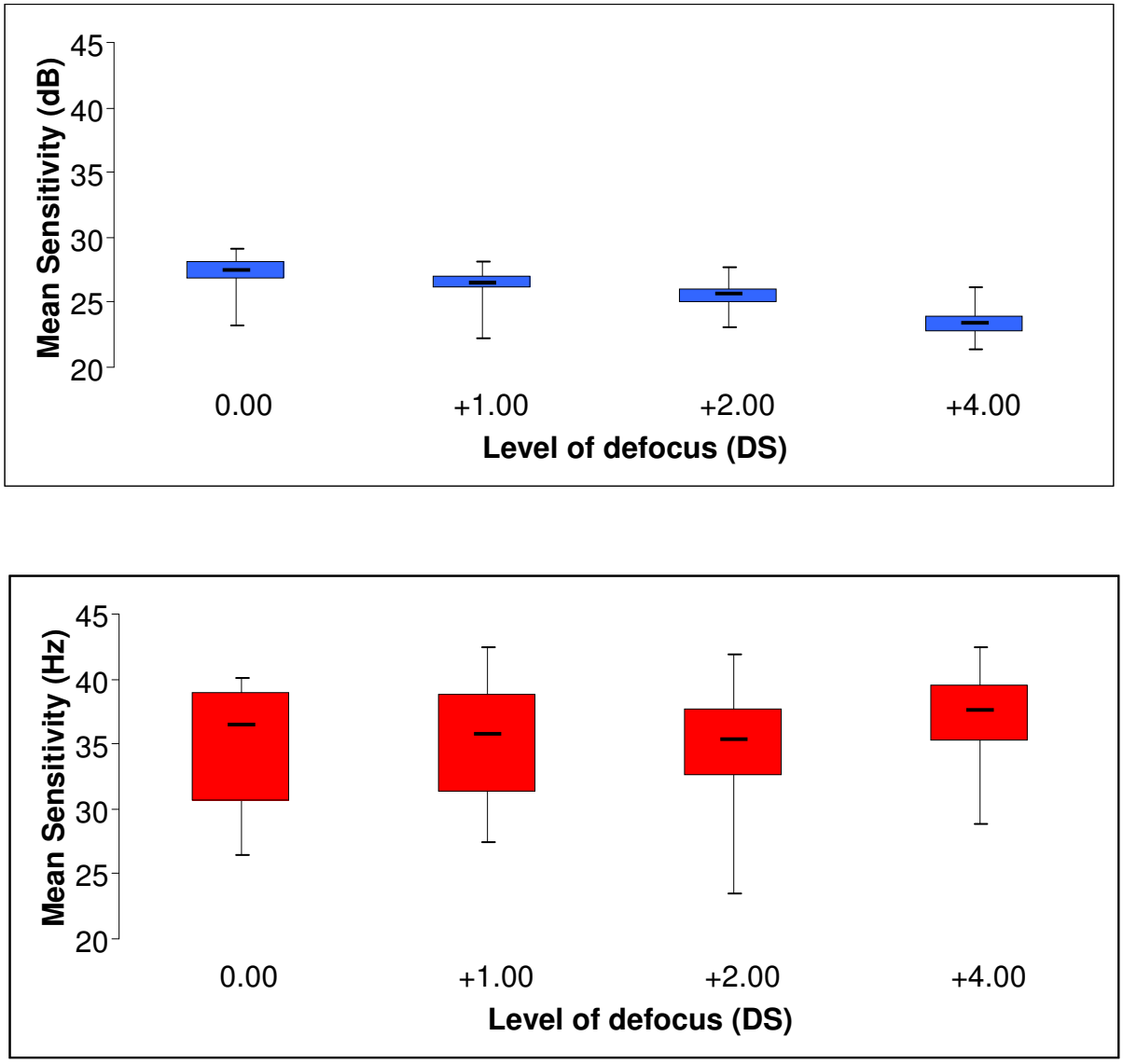

Figure 6.1 Box and whisker plots for the distributions of MS_{SAP} (dB) (top) and of MS_{CFF} (Hz) (bottom) at each of the four levels of defocus, undertaken by the designated eye, for the 16 normal individuals. The median is represented by the black line, the 25th and 75th percentile by the edges of the box and the range by the extremities of the whiskers.

Effect	Degrees of Freedom Numerator	Degrees of Freedom Denominator	F value	P value
Age	1	16	6.28	**0.023**
Gender	1	16	9.87	**0.006**
Eye	1	16	0.70	0.416
Order of Perimetry	1	16	1.50	0.238
Order of Defocus	1	48	9.57	**0.003**
Defocus	3	48	176.19	**<0.001**
Pupil size	1	16	0.45	0.510

Effect	Degrees of Freedom Numerator	Degrees of Freedom Denominator	F value	P value
Age	1	16	5.72	**0.029**
Gender	1	16	9.26	**0.008**
Eye	1	16	0.47	0.505
Order of Perimetry	1	16	1.81	0.197
Order of Defocus	1	48	9.57	**0.003**
Defocus	3	48	176.19	**<0.001**

Effect	Degrees of Freedom Numerator	Degrees of Freedom Denominator	F value	P value
Age	1	16	5.42	**0.033**
Gender	1	16	9.24	**0.008**
Order of Perimetry	1	16	1.33	0.266
Order of Defocus	1	48	9.57	**0.003**
Defocus	3	48	176.19	**<0.001**
Age x Gender	1	16	0.01	0.912
Age x Visit	1	48	4.60	**0.037**
Age x Defocus	3	48	2.15	0.107
Gender x Defocus	3	48	0.79	0.503
Gender x Visit	1	48	5.07	**0.029**
Visit x Defocus	3	41.2	0.60	0.616

Table 6.5 The Analysis of Variance Summary Table for MS_{SAP} (dB) at the four levels of defocus.

The ANOVA modelling showed that, as would be expected, the decline in MS_{SAP} and in MS_{CFF} increased with increase in age ($p< 0.033$ and $p= 0.002$, respectively). In the case of MS_{SAP}, the influence of age on the MS_{SAP} was greater at the first of the two visits ($p=0.037$). An interesting

interaction was present within the ANOVA model, namely that the difference in sensitivity between males and females was different between the two visits ($p=0.029$).

As would be expected, the influence of defocus was also highly significant for both types of perimetry ($p<0.001$ and $p< 0.001$, respectively).

Effect	Degrees of Freedom Numerator	Degrees of Freedom Denominator	F value	P value
Age	1	16	5.90	0.270
Gender	1	16	1.01	0.330
Eye	1	16	3.09	0.098
Order of Perimetry	1	16	0.76	0.396
Order of Defocus	1	48	1.22	0.275
Defocus	3	48	6.46	**<0.001**
Pupil size	1	16	0.06	0.806

Effect	Degrees of Freedom Numerator	Degrees of Freedom Denominator	F value	P value
Age	1	16	6.26	0.024
Gender	1	16	0.96	0.341
Eye	1	16	3.48	0.080
Order of Perimetry	1	16	0.70	0.415
Order of Defocus	1	48	1.22	0.275
Defocus	3	48	6.46	**<0.001**

Effect	Degrees of Freedom Numerator	Degrees of Freedom Denominator	F value	P value
Age	1	16	6.47	0.022
Gender	1	16	0.82	0.378
Eye	1	48	2.78	0.115
Order of Defocus	1	48	1.22	0.275
Defocus	3		6.46	**<0.001**

Effect	Degrees of Freedom Numerator	Degrees of Freedom Denominator	F value	P value
Age	1	16	5.71	**0.030**
Eye	1	16	2.60	0.126
Defocus	3	48	6.30	**0.001**

Effect	Degrees of Freedom Numerator	Degrees of Freedom Denominator	F value	P value
Age	1	16	13.14	**0.002**
Defocus	3	48	6.30	**0.001**
Age x Defocus	3	48	0.99	0.410

Table 6.6 The Analysis of Variance Summary Table for MS_{CFF} (Hz) at the four levels of defocus.

6.9.2 Mean Defect

The summary statistics of the magnitude of the MD_{SAP} and of the MD_{CFF} in the designated eye at each of the four levels of defocus are given in Table 6.7 for the 16 normal individuals. The

distributions of the MD_{SAP} and of the MD_{CFF}, as a function of defocus, are also illustrated in terms of Box and Whisker plots in Figure 6.2.

MD_{SAP} dB	**Plano DS**	**+1.00 DS**	**+2.00 DS**	**+4.00 DS**
Mean	-0.61	0.26	1.18	3.30
SD	1.15	1.11	1.05	1.16
Median	0.80	0.00	1.15	3.50
IQR	0.97	1.04	1.00	1.60

MD_{CFF} Hz	**Plano DS**	**+1.00 DS**	**+2.00 DS**	**+4.00 DS**
Mean	0.88	0.55	0.83	-1.21
SD	4.27	4.24	4.14	3.29
Median	-1.55	-0.25	0.05	-1.80
IQR	7.29	7.34	4.22	4.12

Table 6.7 The summary statistics (mean, SD: median, IQR) for MD_{SAP} (dB) (top) and for MD_{CFF} (Hz) (bottom) at each of the four levels of defocus, undertaken by the designated eye, for the 16 normal individuals.

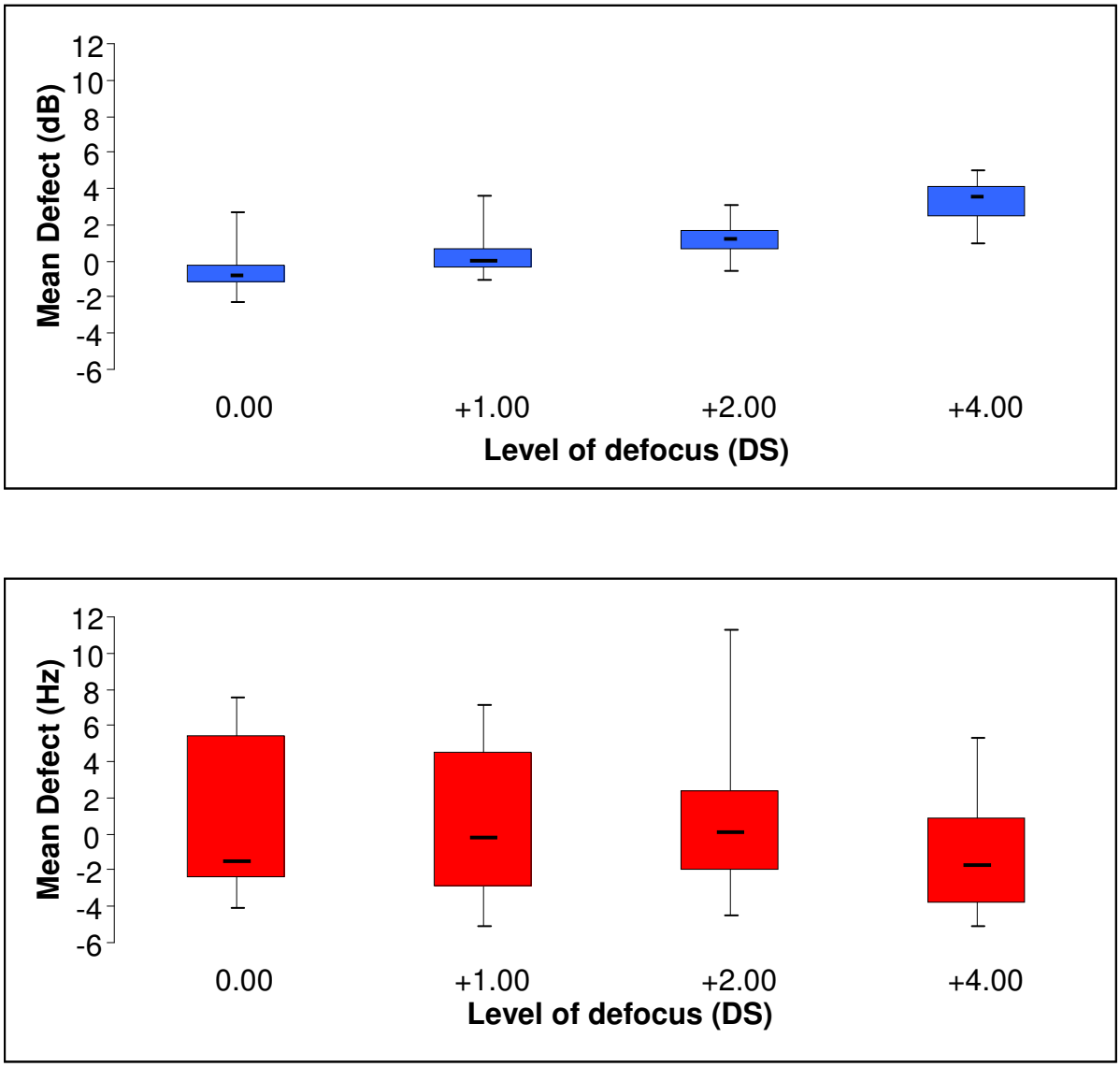

Figure 6.2 Box and whisker plots for the distributions of MD_{SAP} (dB) (top) and of MD_{CFF} (Hz) (bottom) at each of the four levels of defocus, undertaken by the designated eye, for the 16 normal individuals. The median is represented by the black line, the 25th and 75th percentile by the edges of the box and the range by the extremities of the whiskers.

The ANOVA modelling showed that, as would be expected, the MD_{SAP} and the MD_{CFF} did not alter with age (p=0.685 and p= 0.222, respectively). The MD_{SAP} was more negative (i.e. better) for females (p=0.010). The MD_{CFF} was more negative (i.e. better) when the right eye was the designated eye (p=0.019). As would be expected, the influence of defocus was also highly significant for both types of perimetry (p<0.001 and p=0.001, respectively). The influence of

defocus on MD_{SAP} was greater (i.e. the MD_{SAP} was worse) when the lower powered lenses were used first (p=0.005).

Effect	Degrees of Freedom Numerator	Degrees of Freedom Denominator	F value	P value
Age	1	16	0.17	0.685
Gender	1	16	9.64	0.007
Eye	1	16	0.69	0.419
Order of Perimetry	1	16	1.39	0.255
Order of Defocus	1	48	8.85	**0.005**
Defocus	3	48	178.58	**<0.001**
Pupil size	1	16	0.47	0.505

Effect	Degrees of Freedom Numerator	Degrees of Freedom Denominator	F value	P value
Gender	1	16	9.37	0.008
Eye	1	16	0.51	0.484
Order of Perimetry	1	16	1.32	0.267
Order of Defocus	1	48	8.85	**0.005**
Defocus	3	48	178.58	**<0.001**
Pupil size	1	16	0.38	0.546

Effect	Degrees of Freedom Numerator	Degrees of Freedom Denominator	F value	P value
Gender	1	16	8.89	**0.009**
Eye	1	16	0.37	0.553
Order of Perimetry	1	16	1.62	0.221
Order of Defocus	1	48	8.85	**0.005**
Defocus	3	48	178.58	**<0.001**

Effect	Degrees of Freedom Numerator	Degrees of Freedom Denominator	F value	P value
Gender	1	16	9.29	**0.008**
Order of Perimetry	1	16	1.29	0.273
Order of Defocus	1	48	8.85	**0.005**
Defocus	3	48	178.58	**<0.001**

Effect	Degrees of Freedom Numerator	Degrees of Freedom Denominator	F value	P value
Gender	1	16	8.60	**0.010**
Order of Defocus	1	48	8.85	**0.005**
Defocus	3	48	178.58	**<0.001**
Gender x Order of Defocus	1	48	4.11	**0.048**
Gender x Defocus	3	48	0.85	0.471
Order x Defocus	3	41.2	0.65	0.588

Table 6.8 The Analysis of Variance Summary Table for MD_{SAP} at the four levels of defocus.

Effect	Degrees of Freedom Numerator	Degrees of Freedom Denominator	F value	P value
Age	1	16	1.85	0.192
Gender	1	16	1.11	0.307
Eye	1	16	3.06	0.099
Order of Perimetry	1	16	0.79	0.389
Order of Defocus	1	48	1.26	0.266
Defocus	3	48	6.48	**0.001**
Pupil size	1	16	0.07	0.789

Effect	Degrees of Freedom Numerator	Degrees of Freedom Denominator	F value	P value
Age	1	16	1.82	0.196
Gender	1	16	1.06	0.320
Eye	1	16	3.47	0.081
Order of Perimetry	1	16	0.72	0.410
Order of Defocus	1	48	1.26	0.266
Defocus	3	48	6.48	**0.001**

Effect	Degrees of Freedom Numerator	Degrees of Freedom Denominator	F value	P value
Age	1	16	1.61	0.222
Eye	1	16	2.55	0.130
Defocus	3	48	6.31	**0.001**

Effect	Degrees of Freedom Numerator	Degrees of Freedom Denominator	F value	P value
Eye	1	16	6.80	**0.019**
Defocus	3	48	6.31	**0.001**
Eye x Defocus	3	48	1.02	0.390

Table 6.9 The Analysis of Variance Summary Table for MD_{CFF} (Hz) at the four levels of defocus.

6.9.3 Square root of the Loss Variance (sLV)

The summary statistics of the magnitude of the sLV_{SAP} and of the sLV_{CFF} in the designated eye at each of the four levels of defocus are given in Table 6.10 for the 16 normal individuals. The distributions of the sLV_{SAP} and of the sLV_{CFF}, as a function of defocus, are also illustrated in terms of Box and Whisker plots in Figure 6.3.

sLV_{SAP} dB	Plano DS	+1.00 DS	+2.00 DS	+4.00 DS
Mean	1.44	1.54	1.79	1.86
SD	0.47	0.69	0.45	0.50
Median	1.32	1.35	1.90	1.88
IQR	0.50	0.65	0.35	0.45

sLV_{CFF} Hz	Plano DS	+1.00 DS	+2.00 DS	+4.00 DS
Mean	3.09	2.99	3.41	3.43
SD	1.11	1.45	1.26	1.83
Median	2.83	3.11	3.42	3.08
IQR	1.17	2.03	1.09	2.25

Table 6.10 The summary statistics (mean, SD: median, IQR) for sLV_{SAP} (dB) (top) and for sLV_{CFF} (Hz) (bottom) at each of the four levels of defocus, undertaken by the designated eye, for the 16 normal individuals.

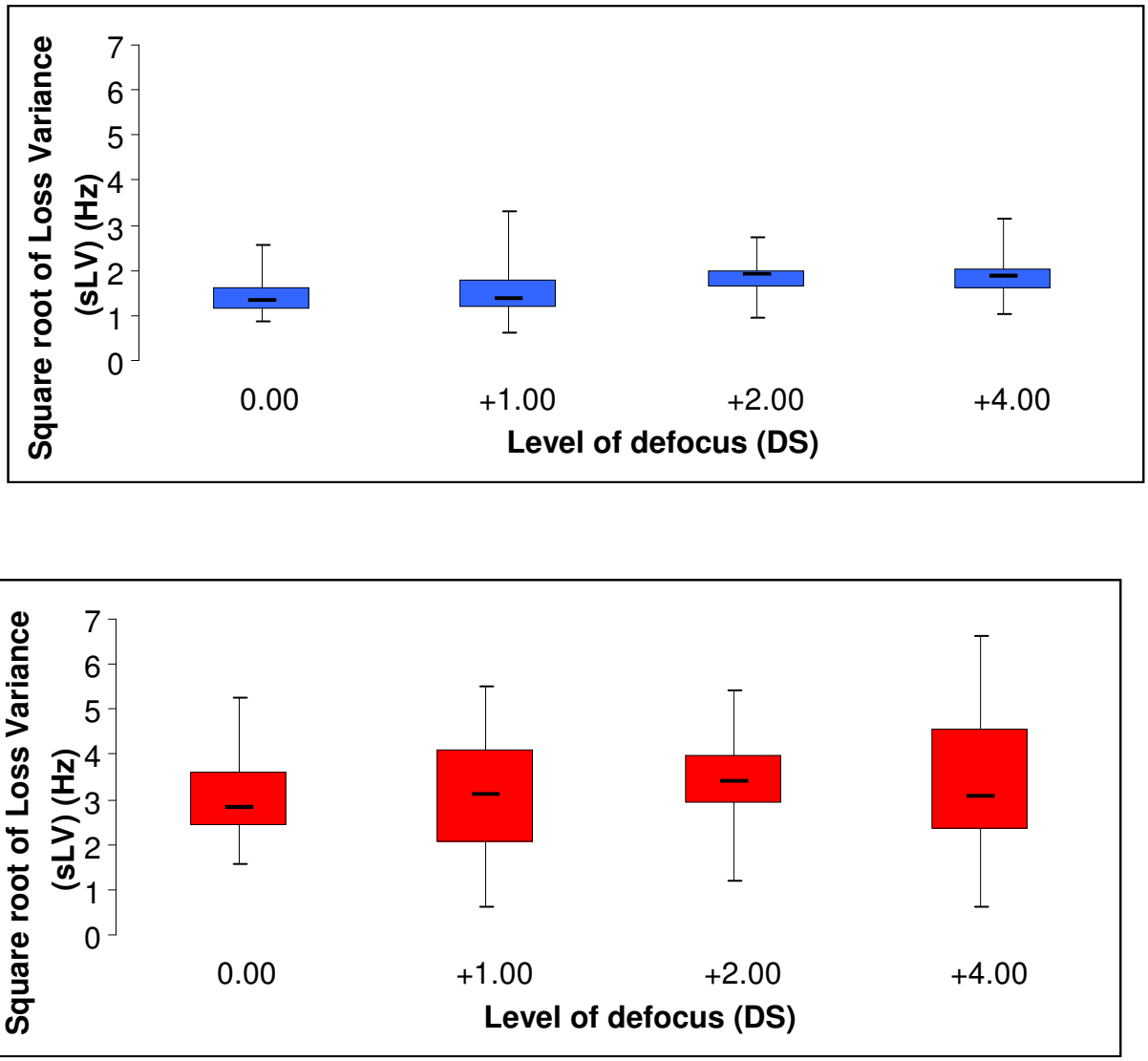

Figure 6.3 Box and whisker plots for the distributions of sLV_{SAP} (dB) (top) and of sLV_{CFF} (Hz) (bottom) at each of the four levels of defocus, undertaken by the designated eye, for the 16 normal individuals. The median is represented by the black line, the 25th and 75th percentile by the edges of the box and the range by the extremities of the whiskers.

Interestingly, the sLV_{CFF} increased with age ($p<0.001$).

The sLV_{SAP} was attenuated by defocus ($p=0.033$); however, the influence of defocus on the sLV_{CFF} did not reach statistical significance ($p=0.343$). The sLV_{CFF} was larger (i.e. worse) when the higher powered lenses were used first ($p=0.013$).

Effect	Degrees of Freedom Numerator	Degrees of Freedom Denominator	F value	P value
Age	1	16	0.87	0.366
Gender	1	16	0.98	0.337
Eye	1	16	0.24	0.630
Order of Perimetry	1	16	0.29	0.595
Order of Defocus	1	48	0.04	0.852
Defocus	3	48	3.18	**0.032**
Pupil size	1	16	0.50	0.489

Effect	Degrees of Freedom Numerator	Degrees of Freedom Denominator	F value	P value
Age	1	16	0.87	0.366
Gender	1	16	0.98	0.337
Eye	1	16	0.24	0.630
Order of Perimetry	1	16	0.29	0.595
Defocus	3	48	3.18	**0.032**
Pupil size	1	16	0.50	0.489

Effect	Degrees of Freedom Numerator	Degrees of Freedom Denominator	F value	P value
Age	1	16	0.62	0.444
Gender	1	16	0.99	0.335
Order of Perimetry	1	16	0.11	0.746
Defocus	3	48	3.18	**0.032**
Pupil size	1	16	0.72	0.410

Effect	Degrees of Freedom Numerator	Degrees of Freedom Denominator	F value	P value
Age	1	16	0.83	0.376
Gender	1	16	1.04	0.322
Defocus	3	48	3.18	**0.033**

Effect	Degrees of Freedom Numerator	Degrees of Freedom Denominator	F value	P value
Gender	1	16	0.88	0.361
Defocus	3	48	3.18	**0.032**

Effect	Degrees of Freedom Numerator	Degrees of Freedom Denominator	F value	P value
Defocus	3	48	3.18	**0.033**

Table 6.11 The Analysis of Variance Summary Table for sLV_{SAP} at the four levels of defocus.

Effect	Degrees of Freedom Numerator	Degrees of Freedom Denominator	F value	P value
Age	1	16	15.17	**0.001**
Gender	1	16	2.51	0.133
Eye	1	16	2.84	0.111
Order of Perimetry	1	16	4.21	**0.057**
Order of Defocus	1	48	7.15	**0.010**
Defocus	3	48	1.14	0.343
Pupil size	1	16	0.15	0.702

Effect	Degrees of Freedom Numerator	Degrees of Freedom Denominator	F value	P value
Age	1	16	16.03	**0.001**
Gender	1	16	2.37	0.143
Eye	1	16	3.33	0.087
Order of Perimetry	1	16	4.02	0.062
Order of Defocus	1	48	7.15	**0.010**
Defocus	3	48	1.14	0.343

Effect	Degrees of Freedom Numerator	Degrees of Freedom Denominator	F value	P value
Age	1	16	12.93	**0.002**
Eye	1	16	2.65	0.123
Order of Perimetry	1	16	3.16	0.095
Order of Defocus	1	48	6.68	**0.013**

Effect	Degrees of Freedom Numerator	Degrees of Freedom Denominator	F value	P value
Age	1	16	22.29	**<0.001**
Order of Perimetry	1	16	0.87	0.366
Order of Defocus	1	48	6.68	**0.013**

Effect	Degrees of Freedom Numerator	Degrees of Freedom Denominator	F value	P value
Age	1	16	20.46	**<0.001**
Order of Defocus	1	48	6.68	**0.013**
Age x Order of Defocus	1	48	0.030	0.869

Table 6.12 The Analysis of Variance Summary Table for sLV_{CFF} at the four levels of defocus.

6.9.4 Diffuse Defect

The summary statistics of the magnitude of the DD_{SAP} and of the DD_{CFF} in the designated eye at each of the four levels of defocus are given in Table 6.13 for the 16 normal individuals. The distributions of the DD_{SAP} and of the DD_{CFF}, as a function of defocus, are also illustrated in terms of Box and Whisker plots in Figure 6.4.

Diffuse Defect dB	Plano DS	+1.00 DS	+2.00 DS	+4.00 DS
Mean	-0.33	0.56	1.24	3.36
SD	1.07	0.82	0.89	1.29
Median	-0.55	0.55	1.30	3.45
IQR	1.46	1.05	0.55	2.53

Diffuse Defect Hz	Plano DS	+1.00 DS	+2.00 DS	+4.00 DS
Mean	0.51	0.16	0.14	-1.68
SD	3.65	3.20	3.62	2.26
Median	-1.65	-0.90	-0.65	-2.45
IQR	5.31	5.55	3.70	2.20

Table 6.13 The summary statistics (mean, SD: median, IQR) for DD_{SAP} (dB) (top) and for DD_{CFF} (Hz) (bottom) at each of the four levels of defocus, undertaken by the designated eye, for the 16 normal individuals.

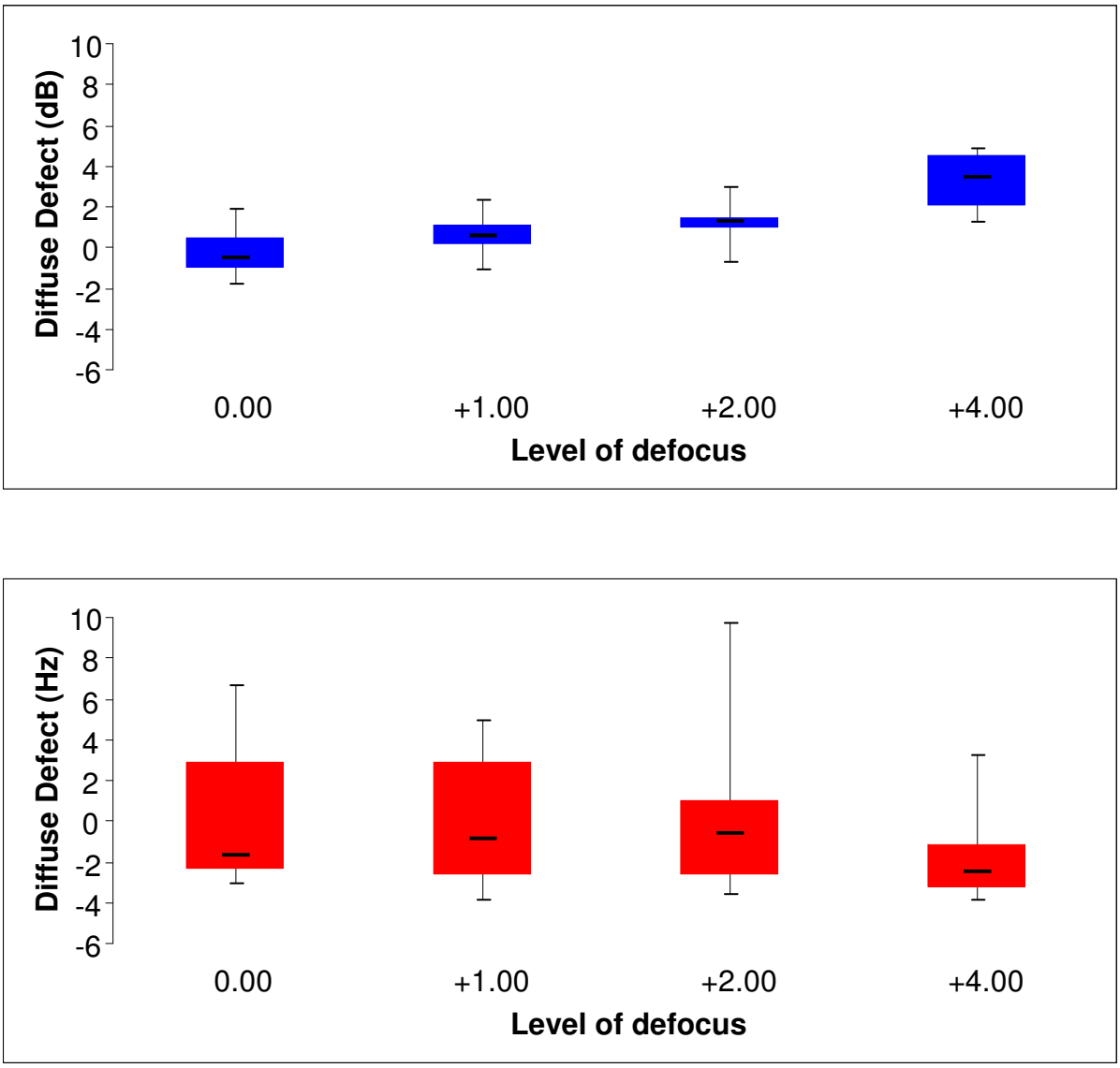

Figure 6.4 Box and whisker plots for the distributions of DD_{SAP} (dB) (top) and of DD_{CFF} (Hz) (bottom) at each of the four levels of defocus, undertaken by the designated eye, for the 16 normal individuals. The median is represented by the black line, the 25th and 75th percentile by the edges of the box and the range by the extremities of the whiskers.

The ANOVA modeling showed that the DD_{SAP} was worse in males (P=0.005). The DD_{CFF} was worse when the left eye was the designated eye (p=0.034).

As would be expected, the influence of defocus was also highly significant for both types of

perimetry ($p<0.001$ and $p< 0.001$, respectively). The influence of defocus on MD_{SAP} was greater (i.e. the DD_{SAP} was worse) when the higher powered lenses were used first ($p=0.018$).

Effect	Degrees of Freedom Numerator	Degrees of Freedom Denominator	F value	P value
Age	1	16	0.01	0.941
Gender	1	16	13.69	**0.002**
Eye	1	16	1.51	0.237
Order of Perimetry	1	16	3.26	0.090
Order of Defocus	1	48	6.01	**0.018**
Defocus	3	48	109.29	**<0.001**
Pupil size	1	16	1.32	0.268

Effect	Degrees of Freedom Numerator	Degrees of Freedom Denominator	F value	P value
Gender	1	16	14.00	**0.002**
Eye	1	16	2.17	0.160
Order of Perimetry	1	16	3.29	0.089
Order of Defocus	1	48	6.01	**0.018**
Defocus	3	48	109.29	**<0.001**
Pupil size	1	16	1.39	0.256

Effect	Degrees of Freedom Numerator	Degrees of Freedom Denominator	F value	P value
Gender	1	16	12.26	**0.003**
Eye	1	16	1.51	0.237
Order of Perimetry	1	16	3.95	0.064
Order of Defocus	1	48	6.01	**0.018**
Defocus	3	48	109.29	**<0.001**

Effect	Degrees of Freedom Numerator	Degrees of Freedom Denominator	F value	P value
Gender	1	16	12.41	**0.003**
Order of Perimetry	1	16	2.24	0.154
Order of Defocus	1	48	6.01	**0.018**
Defocus	3	48	109.29	**<0.001**

Effect	Degrees of Freedom Numerator	Degrees of Freedom Denominator	F value	P value
Gender	1	16	10.89	**0.005**
Order of Defocus	1	48	6.01	**0.018**
Defocus	3	48	109.29	**<0.001**
Gender x Order of Defocus	1	48	0.62	0.434
Gender x Defocus	3	48	0.45	0.722
Order of Defocus x Defocus	3	41.2	1.05	0.379

Table 6.14 The Analysis of Variance Summary Table for DD_{SAP} at the four levels of defocus.

Effect	Degrees of Freedom Numerator	Degrees of Freedom Denominator	F value	P value
Age	1	16	0.78	0.390
Gender	1	16	0.93	0.348
Eye	1	16	2.29	0.150
Order of Perimetry	1	16	0.38	0.544
Order of Defocus	1	48	0.00	0.966
Defocus	3	48	7.54	**<0.001**
Pupil size	1	16	0.17	0.685

Effect	Degrees of Freedom Numerator	Degrees of Freedom Denominator	F value	P value
Age	1	16	0.78	0.390
Gender	1	16	0.93	0.348
Eye	1	16	2.29	0.150
Order of Perimetry	1	16	0.38	0.544
Defocus	3	48	7.54	**<0.001**
Pupil size	1	16	0.17	0.685

Effect	Degrees of Freedom Numerator	Degrees of Freedom Denominator	F value	P value
Age	1	16	0.61	0.445
Gender	1	16	0.84	0.372
Eye	1	16	2.72	0.118
Order of Perimetry	1	16	0.30	0.594
Defocus	3	48	7.54	**<0.001**

Effect	Degrees of Freedom Numerator	Degrees of Freedom Denominator	F value	P value
Gender	1	16	0.58	0.456
Eye	1	16	5.91	0.027
Defocus	3	48	7.54	**<0.001**

Effect	Degrees of Freedom Numerator	Degrees of Freedom Denominator	F value	P value
Eye	1	16	5.41	**0.034**
Defocus	3	48	7.54	**<0.001**
Eye x Defocus	3	48	0.89	0.451

Table 6.15 The Analysis of Variance Summary Table for DD_{CFF} at the four levels of defocus.

6.9.5 Local Defect

The summary statistics of the magnitude of the LD_{SAP} and of the LD_{CFF} in the designated eye at each of the four levels of defocus are given in Table 6.16 for the 16 normal individuals. The

distributions of the LD_{SAP} and of the LD_{CFF}, as a function of defocus, are also illustrated in terms of Box and Whisker plots in Figure 6.5.

Summary Statistics (dB)	Plano DS	+1.00 DS	+2.00 DS	+4.00 DS
Mean	0.16	0.28	0.36	0.43
SD	0.31	0.54	0.31	0.62
Median	0.00	0.05	0.30	0.30
IQR	0.20	0.23	0.60	0.53

Summary Statistics (Hz)	Plano DS	+1.00 DS	+2.00 DS	+4.00 DS
Mean	0.26	0.40	0.41	0.51
SD	0.59	0.66	0.65	0.88
Median	0.00	0.05	0.05	0.00
IQR	0.10	0.45	0.63	0.63

Table 6.16 The summary statistics (mean, SD: median, IQR) for LD_{SAP} (dB) (top) and for LD_{CFF} (Hz) (bottom) at each of the four levels of defocus, undertaken by the designated eye, for the 16 normal individuals.

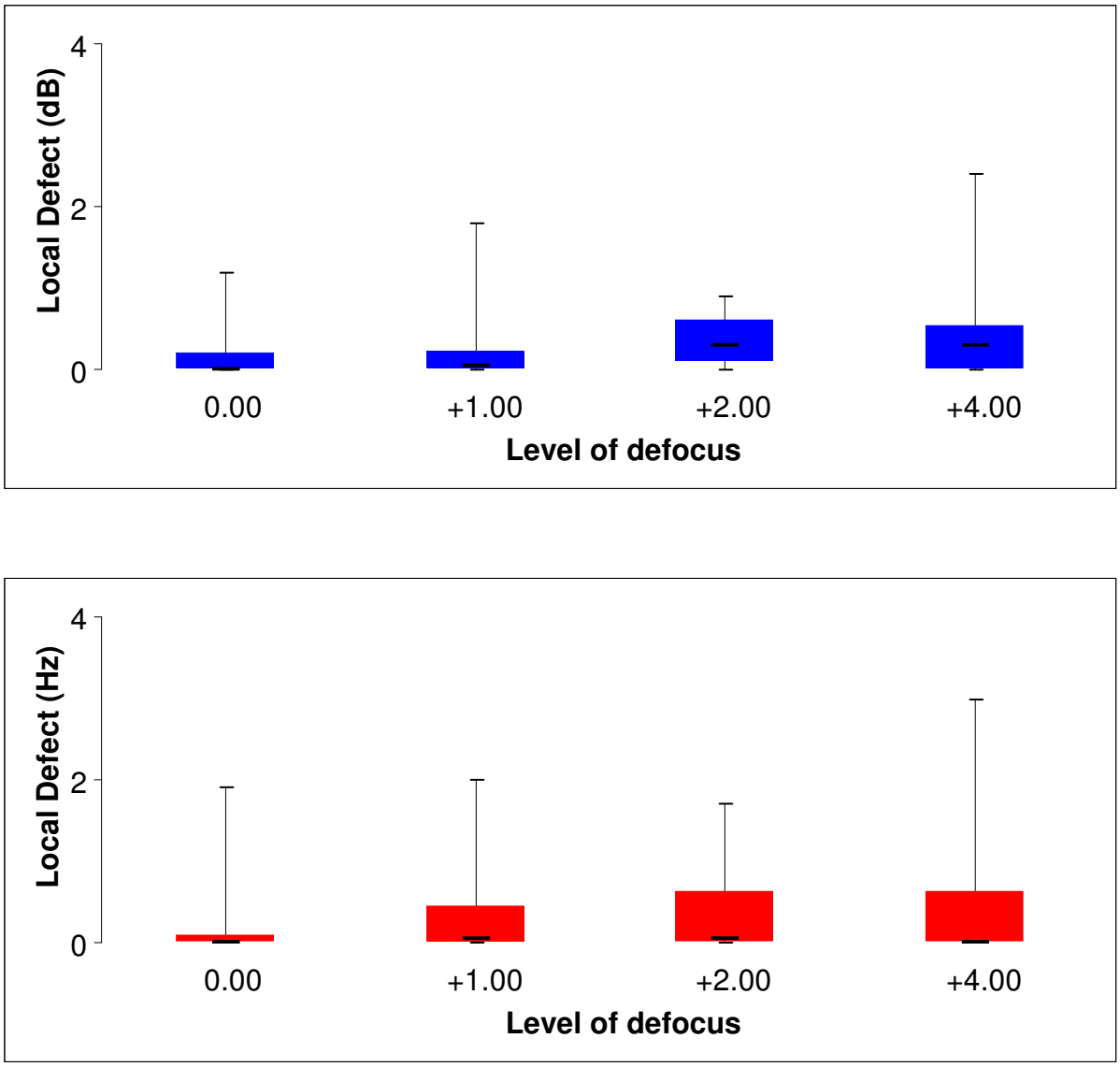

Figure 6.5 Box and whisker plots for the distributions of LD_{SAP} (dB) (top) and of LD_{CFF} (Hz) (bottom) at each of the four levels of defocus, undertaken by the designated eye, for the 16 normal individuals. The median is represented by the black line, the 25th and 75th percentile by the edges of the box and the range by the extremities of the whiskers.

The LD_{CFF} increased (i.e. worsened) with increase/ decrease in age (p=0.002).

The LD_{SAP} and the LD_{CFF} were not influenced by defocus (p=0.198 and 0.513 respectively).

Effect	Degrees of Freedom Numerator	Degrees of Freedom Denominator	F value	P value
Age	1	16	0.14	0.714
Gender	1	16	2.00	0.176
Eye	1	16	0.17	0.685
Order of Perimetry	1	16	0.09	0.767
Order of Defocus	1	48	0.50	0.481
Defocus	3	48	1.63	0.194
Pupil size	1	16	0.34	0.570

Effect	Degrees of Freedom Numerator	Degrees of Freedom Denominator	F value	P value
Age	1	16	0.15	0.699
Gender	1	16	1.94	0.183
Eye	1	16	0.09	0.770
Order of Defocus	1	48	0.50	0.481
Defocus	3	48	1.63	0.194
Pupil size	1	16	0.41	0.531

Effect	Degrees of Freedom Numerator	Degrees of Freedom Denominator	F value	P value
Age	1	16	0.46	0.509
Gender	1	16	1.95	0.182
Order of Defocus	1	48	0.50	0.481
Defocus	3	48	1.63	0.194
Pupil size	1	16	0.32	0.579

Effect	Degrees of Freedom Numerator	Degrees of Freedom Denominator	F value	P value
Gender	1	16	1.80	0.198
Order of Defocus	1	48	0.50	0.481
Defocus	3	48	1.63	0.194

Effect	Degrees of Freedom Numerator	Degrees of Freedom Denominator	F value	P value
Gender	1	16	1.80	0.198
Defocus	3	48	1.62	0.198

Effect	Degrees of Freedom Numerator	Degrees of Freedom Denominator	F value	P value
Defocus	3	48	1.62	0.198

Table 6.17 The Analysis of Variance Summary Table for LD_{SAP} at the four levels of defocus.

Effect	Degrees of Freedom Numerator	Degrees of Freedom Denominator	F value	P value
Age	1	16	6.48	**0.019**
Gender	1	16	1.12	0.306
Eye	1	16	1.85	0.193
Order of Perimetry	1	16	0.29	0.595
Order of Defocus	1	48	6.22	**0.016**
Defocus	3	48	0.88	0.460
Pupil size	1	16	0.38	0.548

Effect	Degrees of Freedom Numerator	Degrees of Freedom Denominator	F value	P value
Age	1	16	6.84	**0.019**
Gender	1	16	1.12	0.306
Eye	1	16	1.85	0.193
Order of Defocus		48	0.29	0.595
Defocus	3	48	0.78	0.513
Pupil size	1	16	0.38	0.549

Effect	Degrees of Freedom Numerator	Degrees of Freedom Denominator	F value	P value
Age	1	16	6.77	**0.019**
Gender	1	16	1.01	0.330
Eye	1	16	1.56	0.230
Defocus	3	48	0.78	0.513
Pupil size	1	16	0.26	0.618

Effect	Degrees of Freedom Numerator	Degrees of Freedom Denominator	F value	P value
Age	1	16	6.64	**0.020**
Gender	1	16	0.90	0.357
Eye	1	16	2.52	0.132

Effect	Degrees of Freedom Numerator	Degrees of Freedom Denominator	F value	P value
Age	1	16	5.83	**0.028**
Eye	1	16	2.34	0.146

Effect	Degrees of Freedom Numerator	Degrees of Freedom Denominator	F value	P value
Age	1	16	13.16	**0.002**

Table 6.18 The Analysis of Variance Summary Table for LD_{CFF} at the four levels of defocus.

6.9.6 Examination duration

The summary statistics of the magnitude of the examination duration for SAP and of the examination duration for CFF perimetry, in the designated eye, at each of the four levels of

defocus are given in Table 6.19 for the 16 normal individuals. The distributions of the examination duration for SAP and of the examination duration for CFF perimetry, as a function of defocus, are also illustrated in terms of Box and Whisker plots in Figure 6.6.

Examination Duration (sec)	Plano DS	+1.00 DS	+2.00 DS	+4.00 DS
Mean	141	150	148	158
SD	9.92	30.40	13.40	16.70
Median	140	140	143	151
IQR	9.25	12.50	14.00	20.25

Examination Duration (sec)	Plano DS	+1.00 DS	+2.00 DS	+4.00 DS
Mean	205	212	211	220
SD	19.56	58.94	39.71	36.46
Median	204	201	205	214
IQR	28.25	21.75	57.25	58.00

Table 6.19 The summary statistics (mean, SD: median, IQR) for the examination duration for SAP (seconds) (top) and the examination duration for CFF (seconds) (bottom) at each of the four levels of defocus, undertaken by the designated eye, for the 16 normal individuals.

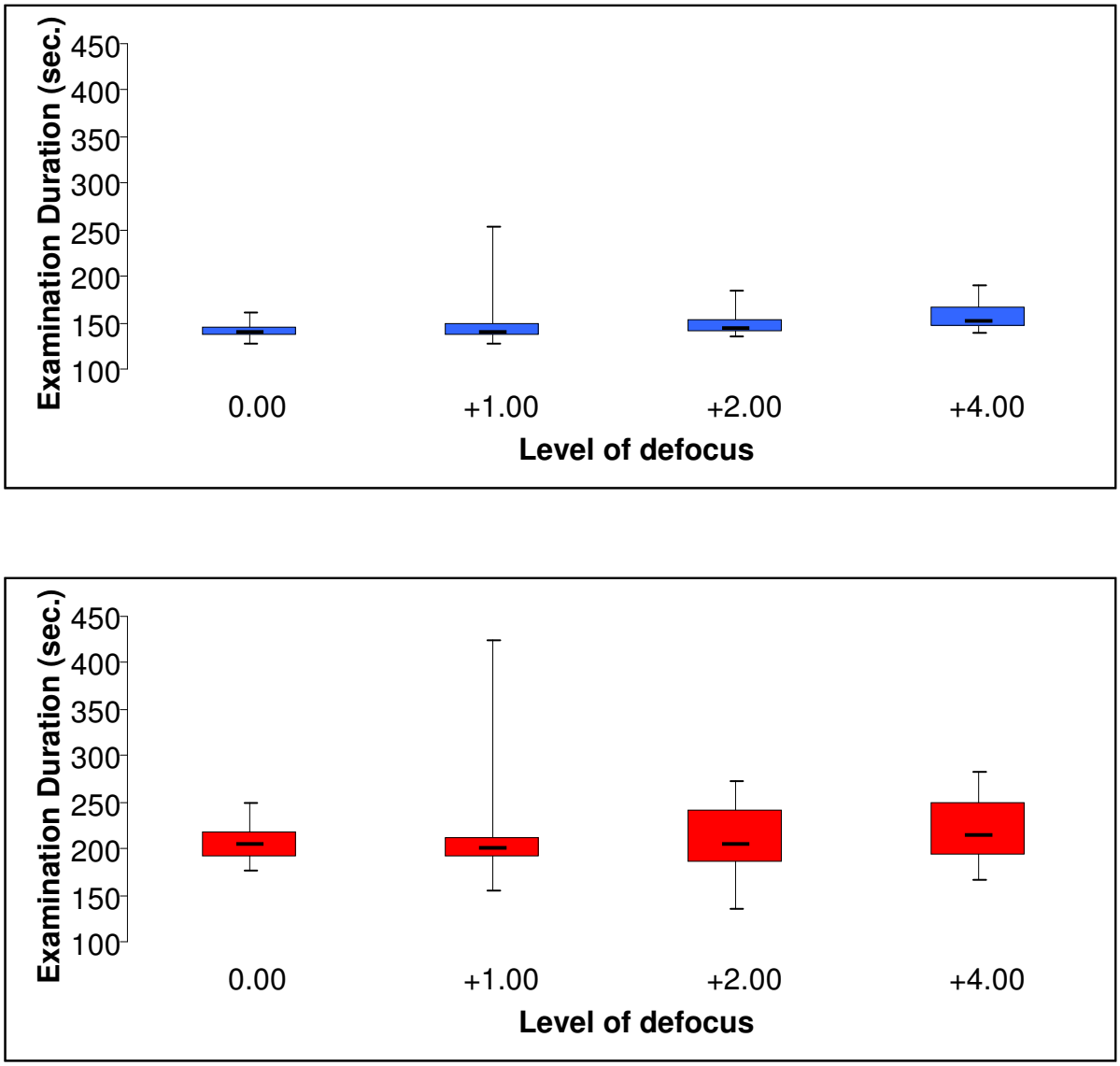

Figure 6.6 Box and whisker plots for the distributions of the examination duration (sec.) for SAP (top) and for CFF perimetry (bottom) at each of the four levels of defocus, undertaken by the designated eye, for the 16 normal individuals. The median is represented by the black line, the 25th and 75th percentile by the edges of the box and the range by the extremities of the whiskers.

The ANOVA modelling showed that the examination duration for SAP was shorter in males (p=0.004). The examination duration for SAP increased with increase in defocus (P=0.024) and this increase was greater for females when the higher powered lenses were used first (p=0.026).

Effect	Degrees of Freedom Numerator	Degrees of Freedom Denominator	F value	P value
Age	1	16	0.44	0.514
Gender	1	16	4.45	**0.051**
Eye	1	16	0.34	0.567
Order of Perimetry	1	16	1.36	0.261
Order of Defocus	1	48	2.98	0.091
Defocus	3	48	3.43	**0.024**
Pupil size	1	16	0.03	0.862

Effect	Degrees of Freedom Numerator	Degrees of Freedom Denominator	F value	P value
Age	1	16	0.42	0.528
Gender	1	16	4.58	0.480
Eye	1	16	0.31	0.585
Order of Perimetry	1	16	1.33	0.266
Order of Defocus	1	48	2.98	0.091
Defocus	3	48	3.43	**0.024**

Effect	Degrees of Freedom Numerator	Degrees of Freedom Denominator	F value	P value
Age	1	16	0.18	0.678
Gender	1	16	4.39	**0.053**
Order of Perimetry	1	16	3.36	0.085
Order of Defocus	1	48	2.98	0.091
Defocus	3	48	3.43	**0.024**

Effect	Degrees of Freedom Numerator	Degrees of Freedom Denominator	F value	P value
Gender	1	16	4.74	**0.045**
Order of Perimetry	1	16	3.16	0.095
Order of Defocus	1	48	2.98	0.091
Defocus	3	48	3.43	**0.024**
Gender x Order of Perimetry	1	16	0.13	0.722
Gender x Order of Defocus	1	48	5.25	**0.026**
Gender x Defocus	3	48	0.42	0.740
Order of Perimetry X Defocus	2	48	2.52	0.091
Order of Defocus x Defocus	2	48	2.52	0.091

Table 6.20 The Analysis of Variance Summary Table for the examination duration for SAP at the four levels of defocus.

Effect	Degrees of Freedom Numerator	Degrees of Freedom Denominator	F value	P value
Age	1	16	3.05	0.100
Gender	1	16	0.32	0.580
Eye	1	16	0.00	0.982
Order of Perimetry	1	16	0.05	0.818
Order of Defocus	1	48	0.22	0.638
Defocus	3	48	0.55	0.652
Pupil size	1	16	1.18	0.294

Effect	Degrees of Freedom Numerator	Degrees of Freedom Denominator	F value	P value
Age	1	16	4.19	0.058
Gender	1	16	0.32	0.578
Order of Perimetry	1	16	0.07	0.799
Order of Defocus	1	48	0.22	0.638
Defocus	3	48	0.55	0.653
Pupil size	1	16	1.24	0.283

Effect	Degrees of Freedom Numerator	Degrees of Freedom Denominator	F value	P value
Age	1	16	5.22	**0.036**
Gender	1	16	0.35	0.561
Order of Defocus	1	48	0.22	0.638
Defocus	3	48	0.55	0.652
Pupil size	1	16	1.74	0.206

Effect	Degrees of Freedom Numerator	Degrees of Freedom Denominator	F value	P value
Age	1	16	5.22	**0.036**
Gender	1	16	0.35	0.561
Order of Defocus	1	48	0.22	0.643
Pupil size	1	16	1.74	0.206

Effect	Degrees of Freedom Numerator	Degrees of Freedom Denominator	F value	P value
Age	1	16	5.22	**0.036**
Gender	1	16	0.35	0.561
Pupil size	1	16	1.74	0.206

Effec	Degrees of Freedom Numerator	Degrees of Freedom Denominator	F value	P value
Age	1	16	4.80	0.044
Pupil size	1	16	1.57	0.223

Effec	Degrees of Freedom Numerator	Degrees of Freedom Denominator	F value	P value
Age	1	16	3.74	0.071

Table 6.21 The Analysis of Variance Summary Table for the examination duration for CFF at the four levels of defocus.

6.9.7 Ratio of the peripheral mean sensitivity to the central mean sensitivity

The summary statistics of the magnitude of the PMS_{SAP}/CMS_{SAP} ratio and of the PMS_{CFF}/CMS_{CFF} ratio in the designated eye at each of the four levels of defocus are given in Table 6.22 for the 16 normal individuals. The distributions of the PMS_{SAP} and of the PMS_{CFF}, as a function of defocus, are also illustrated in terms of Box and Whisker plots in Figure 6.7.

Peripheral/Central (dB)	Plano DS	+1.00 DS	+2.00 DS	+4.00 DS
Mean	0.91	0.90	0.89	0.88
SD	0.04	0.05	0.04	0.03
Mean Median	0.92	0.91	0.89	0.88
IQR	0.04	0.04	0.05	0.03

Peripheral/Central (Hz)	Plano DS	+1.00 DS	+2.00 DS	+4.00 DS
Mean	0.95	0.94	0.94	0.92
SD	0.07	0.07	0.06	0.07
Mean Median	0.93	0.96	0.95	0.95
IQR	0.11	0.05	0.05	0.07

Table 6.22 The summary statistics (mean, SD: median, IQR) for the PMS_{SAP}/CMS_{SAP} ratio (top) and the PMS_{CFF}/CMS_{CFF} ratio (bottom) at each of the four levels of defocus, undertaken by the designated eye, for the 16 normal individuals.

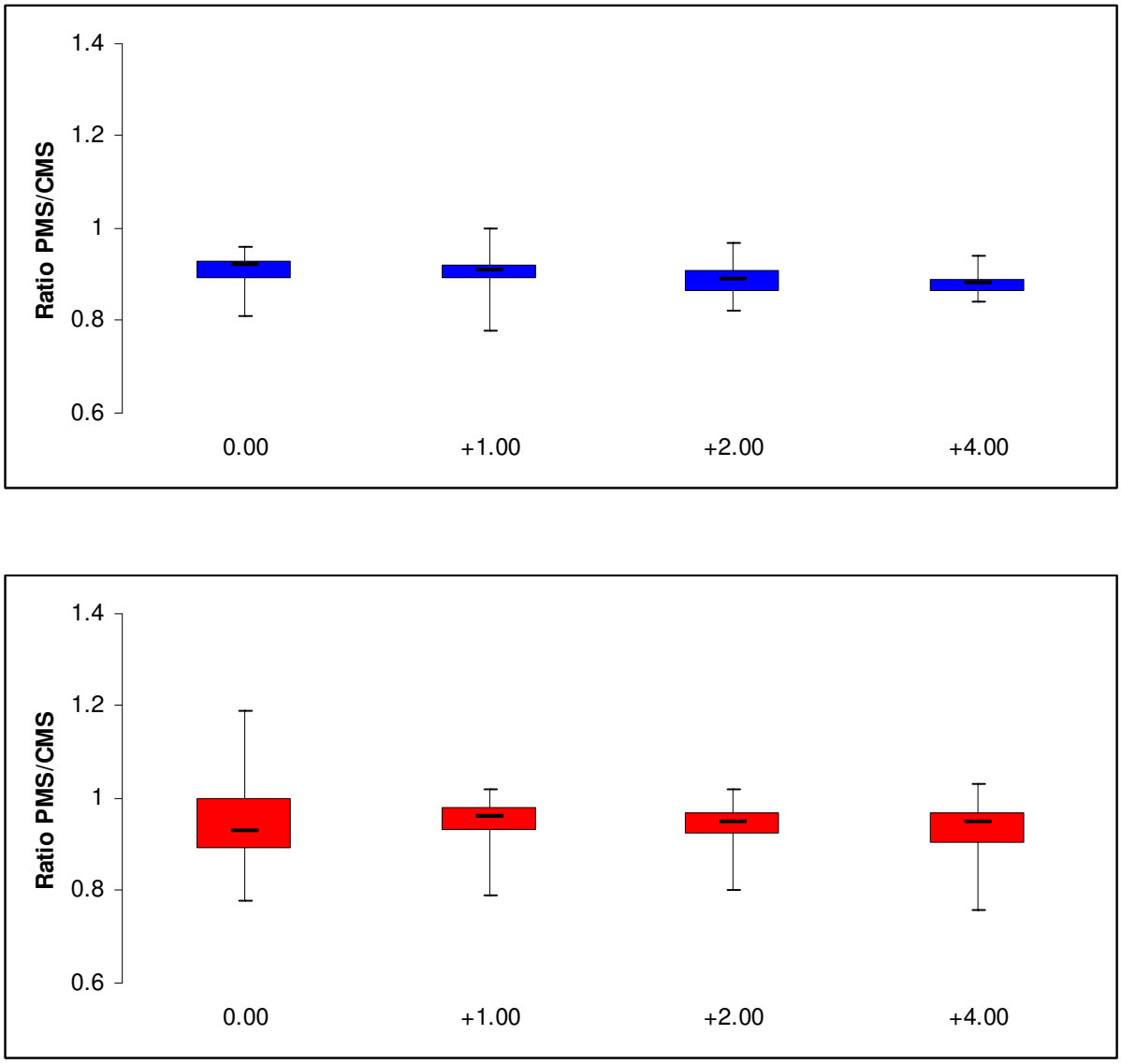

Figure 6.7 Box and whisker plots for the distributions of the PMS_{SAP}/CMS_{SAP} ratio (top) and of the PMS_{CFF}/CMS_{CFF} ratio (bottom) at each of the four levels of defocus, undertaken by the designated eye, for the 16 normal individuals. The median is represented by the black line, the 25th and 75th percentile by the edges of the box and the range by the extremities of the whiskers.

Neither the PMS_{SAP}/CMS_{SAP} ratio nor the PMS_{CFF}/CMS_{CFF} ratio were influenced by any of the independed variables included in the ANOVA modelling.

Effect	Degrees of Freedom Numerator	Degrees of Freedom Denominator	F value	P value
Age	1	16	8.05	**0.012**
Gender	1	16	0.35	0.563
Eye	1	16	2.44	0.138
Order of Perimetry	1	16	4.36	**0.053**
Order of Defocus	1	48	1.96	0.168
Defocus	3	48	4.33	**0.009**
Pupil size	1	16	1.14	0.302

Effect	Degrees of Freedom Numerator	Degrees of Freedom Denominator	F value	P value
Age	1	16	7.58	**0.014**
Eye	1	16	2.43	0.139
Order of Perimetry	1	16	4.51	**0.050**
Order of Defocus	1	48	1.96	0.168
Defocus	3	48	4.33	**0.009**
Pupil size	1	16	1.27	0.276

Effect	Degrees of Freedom Numerator	Degrees of Freedom Denominator	F value	P value
Age	1	16	8.18	**0.011**
Eye	1	16	3.33	0.087
Order of Perimetry	1	16	3.57	0.077
Order of Defocus	1	48	1.96	0.168
Defocus	3	48	4.33	**0.009**

Effect	Degrees of Freedom Numerator	Degrees of Freedom Denominator	F value	P value
Age x Eye	1	16	0.48	0.500
Age x Order of Perimetry	1	16	1.13	0.303
Age x Defocus	3	48	0.79	0.503
Eye x Order of Perimetry	1	16	4.26	**0.056**
Eye x Defocus	3	48	0.51	0.676
Order of Perimetry x Defocus	3	48	2.49	0.080

Table 6.23 The Analysis of Variance Summary Table for the PMS_{SAP}/CMS_{SAP} ratio.

Effect	Degrees of Freedom Numerator	Degrees of Freedom Denominator	F value	P value
Age	1	16	0.69	0.418
Gender	1	16	0.55	0.469
Eye	1	16	1.08	0.315
Order of Perimetry	1	16	0.70	0.414
Order of Defocus	1	48	0.99	0.323
Defocus	3	48	1.16	0.333
Pupil size	1	16	1.12	0.306

Effect	Degrees of Freedom Numerator	Degrees of Freedom Denominator	F value	P value
Age	1	16	0.51	0.484
Eye	1	16	1.01	0.330
Order of Perimetry	1	16	0.58	0.457
Order of Defocus	1	48	0.99	0.324
Defocus	3	48	1.16	0.333
Pupil size	1	16	0.92	0.353

Effect	Degrees of Freedom Numerator	Degrees of Freedom Denominator	F value	P value
Eye	1	16	2.65	0.123
Order of Perimetry	1	16	0.60	0.451
Order of Defocus	1	48	0.99	0.324
Defocus	3	48	1.16	0.333
Pupil size	1	16	0.55	0.468

Effect	Degrees of Freedom Numerator	Degrees of Freedom Denominator	F value	P value
Eye	1	16	2.74	0.117
Order of Perimetry	1	16	0.38	0.548
Order of Defocus	1	48	0.99	0.324
Defocus	3	48	1.16	0.333

Effect	Degrees of Freedom Numerator	Degrees of Freedom Denominator	F value	P value
Eye	1	16	2.61	0.126
Order of Defocus	1	48	0.99	0.324
Defocus	3	48	1.16	0.333

Effect	Degrees of Freedom Numerator	Degrees of Freedom Denominator	F value	P value
Eye	1	16	2.61	0.126
Order of Defocus	1	48	0.93	0.341

Effect	Degrees of Freedom Numerator	Degrees of Freedom Denominator	F value	P value
Eye	1	16	2.61	0.126

Table 6.24 The Analysis of Variance Summary Table for the PMS_{CFF}/CMS_{CFF} ratio.

6.10 The change in sensitivity with defocus

The gradients of the overall group means for the MS_{SAP}, MS_{CFF}, MD_{SAP}, and MD_{CFF} with increase in defocus, are given in Table 6.25 for the 16 normal individuals.

Perimetry	MS dB per dioptre	MD dB per dioptre
SAP gradient	-0.9803	0.982
R^2	0.9985	0.9976
	MS Hz per dioptre	**MD Hz per dioptre**
CFF gradient	0.5149	-0.5106
R^2	0.7712	0.7721

Table 6.25 The gradients, and the corresponding value of the Coefficient of Determination (R^2), of the decline in the group mean MS_{SAP}, MS_{CFF}, MD_{SAP}, and MD_{CFF} with increase in defocus, for the 16 normal individuals.

The gradient for MS_{SAP} was negative whilst that for MS_{CFF} was positive. The gradients for MD_{SAP} and MD_{CFF} exhibited the reverse polarity, as would be expected. The gradients of the group mean MS_{SAP} and MD_{SAP} with increase in defocus were approximately unity. Those for CFF perimetry and were approximately 0.5Hz per dioptre.

6.11 The change in sensitivity at each stimulus locations with defocus

The gradients of the group mean $MS_{SAP,}$ and of the group mean MS_{CFF}, with increase in defocus, at each stimulus location for the 16 normal individuals are given in Figure 6.8. The gradients of the group mean MS_{SAP} tended to steepen with increase in eccentricity, particularly superiorly. The gradients of the group mean MS_{CFF} were approximately unity, centrally, and, in general, became less positive with increase in eccentricity.

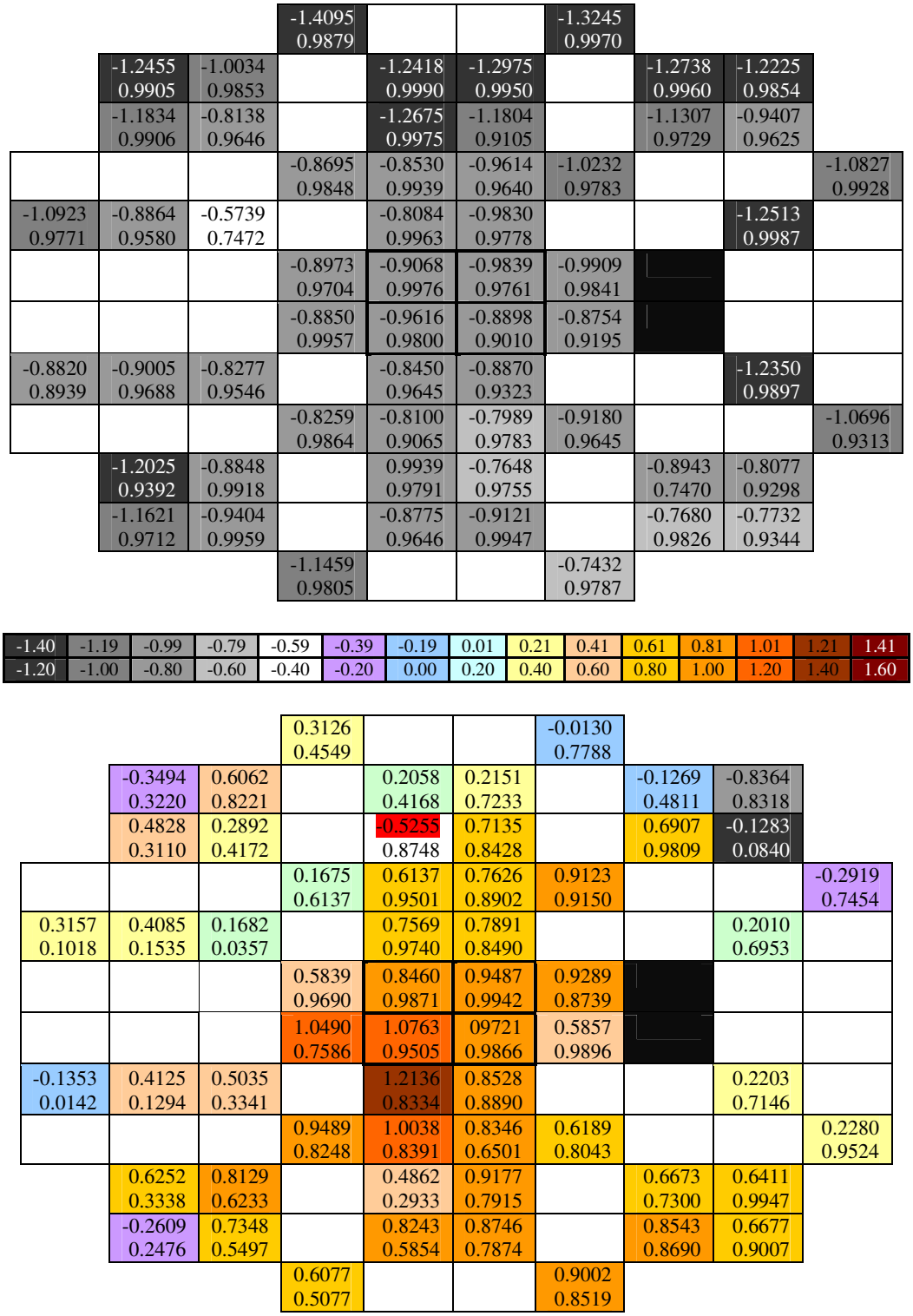

Figure 6.8 The gradient of the group mean MS_{SAP} (top) and the group mean MS_{CFF} (bottom), as a function of increasing defocus, at each stimulus location for the 16 normal individuals. The lower value is the Coefficient of Determination (R^2). The results are presented in right eye format.

6.12 Discussion

The decline in the overall group mean MS_{SAP} with increase in defocus was 0.98dB per dioptre. This figure is compatible with that of 1.3dB per dioptre (Weinreb and Perlman 1986) and 1.25dB per dioptre (Heuer et al 1987) but not with that of 2.5dB per dioptre (Lachenmayer and Gleissner 1992). In the current study, the decline in MS_{SAP} at each stimulus location tended to steepen with increase in eccentricity, particularly superiorly. This is contrary to that of Heuer and colleagues (1987) who found that the gradients at fixation, and at 5°, 10°, 15°, 20°, and 25° eccentricities along the nasal meridian, to be of similar magnitude.

The overall group mean MS_{CFF} increased with increase in defocus. A positive gradient was present at the majority of stimulus locations; however, the magnitude of the gradient, in general, declined with increase in eccentricity and became negative at the superior extremities of the central field. The positive gradient is contrary to the findings of Lachenmayer and Gleissner (1992) who found that defocus of +9.00 only attenuated the 1° diameter stimulus by 0.5Hz. However, the presence of positive gradients beyond 10-15° eccentricity has been reported by Matsumoto et al (1997).

The outcome of CFF perimetry is essentially dependent upon the Granit-Harper Law which states that sensitivity increases with increase in the logarithm of the stimulus area (Berger 1953; Kugelmass and Landis 1955; Roehrig 1959a; Roehrig 1959b) for stimulus areas up to 13.6° and eccentricities up to 50° (Brown 1945). The linearity of the Granit-Harper Law beyond eccentricities of 15° has been questioned (Hartmann, Lachenmayr and Brettel 1979). The Granit-Harper Law is considered to be valid for defocused images (Roehrig 1959a).

The gradient of the increase in MS_{CFF} with increase in defocus was approximately 0.5Hz per dioptre. The reason for the positive gradient for CFF perimetry with increase in defocus can be attributed to the increase in retinal image size of the blurred stimulus which increases with increase in defocus and is most profound for the +4.00DS defocus. A blur circle is formed on the retina when the image of an object is focused either in front of, or behind, the retina or when excessive aberrations are present in the optical system of the eye. The size of the blur circle at the fovea increases as a function of the distance of the image from the retina and as a function of pupil diameter. The diameter of the blur circle, α, can be expressed in angular terms (in min arc) as:

$$\alpha = 3.48 \,.\, XF \,.\, d$$

where 3.48 is a constant, XF is the defocus (in dioptres) with respect to the object point, and d the pupil diameter (in mm).

In the current study, the equation for a defocus of +4.00DS and a pupil diameter of 4.0mm solves as:

$$\alpha = 3.48 \,.\, 4 \,.\, 4 = 55.68 \text{ min of arc}$$

which is equivalent to 0.93° and is slightly larger than the diameter of Goldmann size IV which is 0.86°.

In addition, the retinal image is magnified by the defocus lens, itself (Pascal 1955). The vergence of the light prior to entering the eye, Lc, can be expressed as:

$$Lc = \frac{L}{1 - \left(\frac{d}{n}\right)L}$$

where L = the power of the defocusing lens (in this instance +4.00DS), d = distance of the defocusing lens from the eye and n = refractive index of air. Solving this equation:

$$Lc = \frac{4.0}{1-\left(\frac{0.015}{1.0}\right)L} = \frac{4}{1-0.06} = \frac{4}{0.94} = 4.25$$

.

and, $$M = \frac{Lc}{L'}$$

where, in this instance, L' = the vergence of the light from the Goldmann stimulus. Solving this equation:

$$M = \frac{4.25}{64.17} = 0.066$$

Thus, a +4.00DS defocusing lens leads to an additional 6.6% magnification of the Goldmann size III stimulus. The net result of the increases in the size of the perceived Goldmann size III is illustrated in Figure 6.9.

The increase in the size of the Goldmann size III stimulus to that slightly larger than Goldmann size IV, for example, occurs in the presence of the same stimulus luminance and is applicable to both SAP and CFF perimetry. However, in the case of CFF, the flicker is present over the entire magnified stimulus and, as a consequence of the Granit-Harper Law, results in an increase in sensitivity.

Figure 6.9 The Goldmann size III stimulus, as projected on the perimeter bowl of the Octopus 311, in the absence of defocus (top) and arising from a defocus of +4.00DS (bottom). Note the corresponding increase in the size of the fixation cross with defocus.

A comparison of the CFF stimulus generated by Goldmann size IV in the absence of defocus with that generated by Goldmann size III in the presence of +4.00DS would be of interest. However, the software of the Octopus 311 perimeter does not permit CFF perimetry to be undertaken with Goldmann size IV.

It can be speculated that the discrepancy between the positive gradient of the current study and the negative gradient of Lachenmayer and Gleisser (1992) can be explained, at least in part, on the basis of the difference in age of the individuals, and in the stimulus size, between the two studies and, therefore, the corresponding difference in the magnitude of sensitivity to the CFF stimulus. The mean age of the individuals generating the negative gradient in the study of Lachenmayer and Gleisser (1992) was 26.7 years (median 26.5, range 23 to 32 years). With the 1° stimulus diameter, such young individuals exhibit close to the maximum sensitivity for CFF (i.e. saturation) before defocus and, therefore, do not manifest an increased CFF, via the Granit-Harper Law, from the increase in stimulus area arising from the defocus. The mean age of the individuals generating the positive gradient in the current study was 66 years (SD 7.9, median 67.0, IQR 12.75). With the 0.431° stimulus diameter, such older individuals exhibit a sensitivity in the region of 35Hz before defocus, compared to approximately 45Hz for those aged 25 years. Thus, the stimulus is not saturated for the older age group and these individuals exhibit an increase in CFF, via the Granit-Harper Law, from the increase in stimulus area arising from the defocus. The age of the case series used by Matsumoto et al (1997) was not stated in the publication.

It is clear from the results illustrated in Figure 6.8 that the magnitude of the gradient of the local group mean MS_{CFF} becomes less positive with increase in stimulus eccentricity. However, considerable between-stimulus variability is present within the dataset. Such variability could, perhaps, be overcome by the utilization of smaller and more numerous increments in defocus over a wider range of defocus. The validity of the Grant-Harper Law as a function of stimulus eccentricity would be an interesting area for future study.

In summary, the decline in the group mean MS_{SAP} within increase in defocus, of approximately 1.00dB per dioptre, was compatible with that of previous estimates, 1.40dB per dioptre found by Heuer et al (1987). The increase in the MS_{CFF} and in the local MS_{CFF} with increase in defocus was attributed to the Granit-Harper Law whereby CFF increases linearly with increase in stimulus area irrespective of defocus. From a clinical perspective, the utilization of the appropriate refractive correction is essential for CFF perimetry.

CHAPTER 7
SUMMARY, CONCLUSIONS AND SUGGESTIONS FOR FURTHER RESEARCH

7.1 Results summary and conclusions

Critical Flicker Fusion perimetry determines the highest flicker frequency that can be distinguished from a uniform steady stimulus. A number of studies have reported that CFF perimetry to be superior to that of SAP for the detection of glaucomatous visual field loss in that the technique identifies loss at an earlier stage and is resistant to image degradation arising from cataract (Lachenmayr et al 1991; Lachenmayr et al 1991; Lachenmayr and Drance 1992; Lachenmayr and Gleissner 1992; Lachenmayr, Drance and Airaksinen 1992b; Lachenmayr 1994; Lachenmayr et al 1994; Matsumoto et al 2006).

In this Thesis, four groups of individuals were investigated in three different studies. The normal individuals and the individuals with age-related cataract were naïve to SAP and to CFF perimetry. The individuals with either OAG or OHT were experienced in SAP and naïve to CFF perimetry.

The study of the learning effect for CFF perimetry was undertaken in 28 normal individuals, 10 individuals with OHT and in 11 individuals with OAG. Each individual attended for 5 examinations each separated by one week. The visual field indices MS, MD and DD for the normal individuals exhibited a sustained improvement over the first four visits. A learning effect was also present for the individuals with OHT and for the individuals with OAG. The greatest improvement for these individuals occurred between the two first visits after which they also exhibited a sustained improvement over the remaining three visits. The examination duration

became shorter over the five visits for all three groups and, in general, was shortest for the second (left) eye examined at any given examination. The ratio PMS/CMS was similar across the five examinations for each of the three groups.

The magnitude of the improvement in the visual field over the five visits was modest for the normal individuals amounting to, for example an improvement of approximately 2.3Hz in the median MS across the two eyes. The corresponding improvement for the individuals with OHT and for the individuals with OAG was greater amounting to approximately 3.5Hz and 6.1Hz, respectively.

The majority of the improvement in CFF perimetry for the individuals with OHT and for the individuals with OAG occurred between the first and second visits. This finding is compatible with that for SAP (Wood et al 1987b; Werner, Adelson and Krupin 1988; Heijl, Lindgren and Olsson 1989; Wild et al 1989; Autzen and Work 1990; Kulze, Stewart and Sutherland 1990; Marchini, Pisano and Bertagnin 1991; Searle et al 1991; Wild et al 1991; Heijl and Bengtsson 1996), for FDT (Matsuo et al 2002; Contestabile et al 2007; Hong et al 2007; Centofanti et al 2008; Pierre-Filho et al 2010) and for SWAP (Wild, Moss and O'Neill 1996; Rossetti et al 2006; Gardiner, Demirel and Johnson 2008; Zhong et al 2008; Fogagnolo et al 2010). However, the continued improvement for CFF over the remaining three visits is not conducive to the implementation of the technique into clinical practice. The lack of an improvement in the PMS/CMS is contrary to that for SAP (Wood et al 1987b; Heijl, Lindgren and Olsson 1989; Wild et al 1989; Werner et al 1990; Searle et al 1991; Heijl and Bengtsson 1996) and indicates an improvement in the height, only, of the visual field for CFF perimetry.

The magnitudes of each of the indices were generally worse for the TOP algorithm at Visit Five compared to those of the Dynamic algorithm at Visit Six and the defect depth expressed, in terms of Comparison Probability values, also yielded a statistically deeper defect depth for the TOP algorithm, particularly in OAG. These findings would pose a problem in the interpretation of a series of visual fields if a mixture of the two algorithms were to be used. The reason for the difference in magnitude of the indices undoubtedly lies in the difference between the two algorithms in determining the threshold estimate including the cut-off by the TOP algorithm for CFF at a sensitivity of 9/8 above the age-corrected normal value above (i.e. a higher sensitivity). However, it could be expected that the values for the indices such as the MD, which reference the result for any given algorithm to that of the corresponding age-corrected normal field, to be similar between the TOP and Dynamic algorithms compared to those of the Dynamic algorithm. The difference in terms of the Comparison Probability values between the two algorithms can be explained by the narrower confidence limits for the TOP algorithm in CFF perimetry. Interestingly, the Dynamic Strategy for SAP, undertaken prior to enrolment, on the 11 individuals with OAG yielded a greater abnormality by Comparison Probability analysis compared to the Dynamic Strategy for CFF at Visit Six. Thus, it would appear that the confidence limits for normality are narrower for SAP than for CFF and that, within CFF, the confidence limits are narrower for the TOP algorithm compared to the Dynamic Strategy algorithm. Thus, in addition to the clinically unacceptable long time course of the learning effect for CFF perimetry in individuals experienced in SAP and with either OHT or OAG, the wider confidence limits for CFF compared to SAP provides further evidence for the lack of clinical plausibility of the technique.

The study of the influence of age-related cataract on the CFF perimetry, undertaken on 22 individuals naïve to any form of perimetry, used an experimental protocol which was intended to

minimize the influence of any potential learning effect for CFF and included a comparison with that of SAP.

The learning effect for SAP expressed in the proportionate change in the median, was 5% and 6% for the fields of the right and left eyes, respectively. The corresponding improvement in the field of the right eye for CFF was 6.7%; no improvement was present in the field of the left eye (the second eye examined) and, since the median MS was consistently lower than that for the field of the right eye, the absence of such an effect may have arisen from the fatigue effect.

No evidence was present, in terms of the results of the Comparison probability analysis, to suggest that CFF perimetry recorded with the TOP algorithm was more resistant to image degradation than SAP. Little relationship was present between the MD and low and high contrast visual acuity determined either in the presence, or in the absence of, disability glare. The lack of an unequivocal outcome is likely to have arisen from the lack of individuals with severe cataract in the case series. The clinical utility of CFF perimetry in this regard requires further study with respect to the influence of severe age-related cataract. However, it could be argued that, in the healthcare operative in the developed world where surgery for the extraction of early cataract is widely available, the utility of CFF perimetry is minimal since it does not offer any advantage over SAP in the presence of mild cataract and, seemingly in the context of the current study, in the evaluation of glaucomatous field loss.

The study of the influence of optical defocus on CFF perimetry was undertaken on 16 of the normal individuals who had taken part in the study of the learning effect described in Chapter 4. A comparison was made with the outcome for that for SAP. It was assumed that these individuals were experienced in CFF perimetry and, having undergone SAP at two previous

visits as part of the protocols for the studies described in Chapters 4 and 6, were also reasonably experienced in SAP. The group mean MS for SAP, MS_{SAP}, exhibited a linear decline with increase in defocus of approximately 1.00dB per dioptre. The slope was compatible with that of a previous estimate for SAP of 1.25dB per dioptre (Heuer et al 1987). The corresponding function for CFF increased linearly by 0.52Hz per dioptre of defocus. The increase in the global and in the local MS_{CFF} with increase in defocus was attributed to the Granit-Harper Law. This law states that CFF increases linearly with increase in stimulus area (regardless of whether the increase in size results from defocus). Since the outcome of any form of perimetry is dependent upon a comparison of the measured result with that of the age-corrected normal result, the utilization of the appropriate refractive correction would appear to be particularly necessary for CFF perimetry.

The compilation of the individuals for the studies described in Chapters 4 and 5 were based upon the number needed (n=27) to detect, with 95% power, a difference in the MD for SAP of 3.00dB. The difficulty in, and lack of, recruitment of sufficient individuals with either OHT or OAG limited the inferences from some outcomes which could have potentially been attributable to differences between diagnostic groups. However, as the general trends were so strong in most cases, the numbers of individuals were clearly sufficient for these purposes.

Due to the diversity of the between-individual variation in the magnitude of the perimetric learning effect for SAP and for SWAP, the results from Chapters 4 and 5 were analyzed using an in-depth approach involving various levels of sophistication which concentrated both on the summary statistics for the given group, as a whole, and on the performance of the given individual. For the identification of an individual's performance, the most useful would appear to be those of the absolute and proportionate change in performance between Visit One and

Visit Two plotted against that between Visits Two and Five. This approach enabled a rapid appreciation of the extent to which the majority of the expected learning effect (i.e., between Visits One and Two) should have occurred. It also enabled a rapid appreciation of the magnitude of the remaining improvement in sensitivity over the remaining visits. Equally, the approach immediately identifies those individuals who exhibit a decline in performance. For the identification of the performance of the group, as a whole, the most useful would appear to be that of the summary statistic of MS. A comparison of the Comparison probability values at each stimulus location between the appropriate visits and displayed as a contingency table is also of benefit.

The study of the learning effect for CFF perimetry could have been undertaken for SAP, as a control. However, such a study would have required an unrealistic examination time per visit. It was felt that knowledge of the between-eye learning effect for CFF perimetry was more useful than that, which could have been obtained within the same time constraints, namely the difference in the learning effect, for one eye, between CFF perimetry and SAP.

A necessary feature for any kind of novel perimetric technique is the requirement for minimal short- and long-term variability of the threshold estimate. Both measures require a second threshold estimate at fixed locations within the given examination. The option for a second estimate of threshold at a given location is not available for either the TOP or the Dynamic Strategy algorithms using CFF perimetry with the Octopus 300 series perimeters. Nevertheless, a study both of the short- and long-term fluctuation for CFF perimetry would be of academic, if not clinical, interest.

The relation between defocus of the CFF stimulus and the Granit-Harper Law could be further investigated to establish the range of linearity by the use of additional optical defocus of +6.00DS and +9.00DS. A useful control would require a change in software of the Octopus 311 perimeter which would permit the use of Goldmann size IV as well as the available Goldmann III and V. This would enable a comparison of the slope of CFF against the area of the variously defocused size III stimulus with that of the CFF against the actual (i.e. non-defocused) Goldmann III, IV and V area. Little is known about the age-dependency of the Granit-Harper Law and this should also be investigated.

CFF perimetry is a difficult task for the 'typical' patient. It is possible that an increase in the stimulus duration from the default of 1000msec to 1500msec or even 2000msec might render the judgement of flicker easier and thereby reduce both the requirement for a learning period and also the inherent variability associated with the threshold estimate. Eye tracking technology could be used to negate the influence of eye movements on the outcome of the examination. It is also possible that the task could be made easier for the patient by the use of Goldmann size V rather than the default size III. The variability of response might also be improved by a real-time feedback to the patient throughout the examination concerning the number of incorrect responses to the false-positive and false-negative catch trials.

The major strengths of the study were the robust control over the exacting schedule of a weekly separation of visits within each of the three studies, the consistency of the same perimetrist (the author) for all 1146 visual field examinations and of the same instruction for each individual. To the author's knowledge, it remains the most extensive study of fully automated CFF perimetry within the age range representative of those attending secondary and tertiary eye care.

7.2 Conclusion

CFF perimetry is unlikely to become the technique of choice for perimetry. Such a conclusion is based upon the finding that the outcome of CFF perimetry in individuals with either OHT or OAG, and experienced in SAP, requires in the region of four visits to overcome the perimetric learning effect. It is also based upon the fact that the advantage claimed for CFF perimetry in regard to the earlier detection of glaucomatous field loss compared to SAP was not found in the limited case series studies in this Thesis. Similarly, the apparent resistance to image degradation of the CFF stimulus compared to that of SAP was not present within the case series exhibiting mild cataract. The CFF stimulus was also not resistant to optical defocus.

APPENDIX: A.1 ABSTRACTS

Luraas K, Wild JM (2007). Where Is the Learning Effect for CFF Perimetry in Normal Individuals? *ARVO*. E-5897

Luraas K, Wild JM (2009). Is CFF Perimetry Affected by Cataract? *ARVO*. E-2011

Luraas K, Uchermann B, Wild JM (2010). Is CFF Perimetry Affected by Optical Defocus? *ARVO*. E-1821

APPENDIX: A.2 LECTURES

Luraas K (2007). Aspekter ved Standard Automatisert Perimetri (SAP), „Klinisk verdi i optometrisk praksis". *Meeting of the locale group of ophthalmologists and optometrists*. Haugesund, Norway.

Luraas K (2008). Is there a learning effect in CFF perimetry? *Octopus symposium*. October 29-November 1, 2008, Berne, Switzerland.

Luraas K (2009). Is CFF Perimetry Affected by the Learning Effect?, *Kongsberg Vision Meeting* Kongsberg, Norway.

Luraas K (2010). The comparative performance of standard automated perimetry and critical flicker frequency perimetry in individuals with cataract. *Imaging and Perimetry Society*, March 23-26, 2010, Puerto de La Cruz, Tenerife.

ENCLOSURES

1 Comments to the project from the Norwegian Ethical Committee (REK Sør, 20.12.05).

2 Approval to the project from the Norwegian Ethical Committee (REK Sør, 11.01.06).

3 Approval to alteration to the project from the Norwegian Ethical Committee (REK Sør, 20.11.06).

4 Approval to alteration to the project from the Norwegian Ethical Committee (REK Sør, 12.07.07).

5 Approval in regards to keeping personal information from the Norwegian Datatilsynet (03.03.06).

1

UNIVERSITETET I OSLO

DET MEDISINSKE FAKULTET

Optiker M.Sc Knut Luraas
Rjukan Synssenter AS
Sam Eydesg 57
3660 Rjukan

Regional komité for medisinsk forskningsetikk
Sør- Norge (REK Sør)
Postboks 1130 Blindern
NO-0318 Oslo

Telefon: 228 44 666
Telefaks: 228 44 661
E-post: rek-2@medisin.uio.no
Nettadresse: www.etikkom.no

Dato: 20.12.05
Deres ref.:
Vår ref.: S-05382

S-05382 **The Learning Effect for Critical Flicker Fusion (CFF) Perimetry in normal individuals**

Komiteen behandlet søknaden i sitt møte torsdag 15.12.05.

Komiteen har følgende merknader til prosjektsøknaden:

1. Komiteen ber om en revidert prosjektbeskrivelse på alminnelig og forståelig norsk språkform.
2. Prosjektets tittel skal normalt foreligge på norsk.
3. Komiteen ønsker svar på at undersøkelsesmetodene er metoder som friske personer er vant med, slik det fremgår i informasjonsskrivet.
4. Pkt 18: Det er ikke krysset av for melding til Datatilsynet/NSD. Det er meldeplikt til Datatilsynet for forskningsprosjekter med personsensitive pasientopplysninger (Dette gjelder også vanlige journalopplysninger etc. som samles selv om de er avidentifiserte. Eventuelt kan det meldes til personvernombudet. Det er ikke nødvendig å melde til Datatilsynet når melding gis personverneombudet. Mer opplysninger om dette finnes på Datatilsynets hjemmeside: www.datatilsynet.no og NSDs hjemmeside: http://www.nsd.uib.no/personvern/

Komiteen har følgende merknad til informasjonsskrivet:

1. Samtykkeerklæringen skal kun inneholde samtykket. Deltakerne skal ved sin underskrift ikke behøve å stadfeste annet enn å ha mottatt informasjon om prosjektet og at de ønsker å delta. Deltakerne skal ha kopi av både informasjonsskriv og samtykkeerklæring.

Vedtak:
"Komiteen ber om svar på merknader samt revidert informasjonsskriv og samtykkeerklæring. Forutsatt tilfredsstillende tilbakemelding, vil prosjektet tilrås. Komiteens leder tar stilling til dette ved mottatt svar."

Med vennlig hilsen

Hans Erik Rugstad
Professor dr.med.
Leder

Tone Haug
Rådgiver
Sekretær

UNIVERSITETET I OSLO

DET MEDISINSKE FAKULTET

2

Optiker M.Sc Knut Luraas
Rjukan Synssenter AS
Sam Eydesg 57
3660 Rjukan

Regional komité for medisinsk forskningsetikk
Sør- Norge (REK Sør)
Postboks 1130 Blindern
NO-0318 Oslo

Telefon: 228 44 666
Telefaks: 228 44 661
E-post: rek-2@medisin.uio.no
Nettadresse: www.etikkom.no

Dato: 11.01.06
Deres ref.:
Vår ref.: S-05382

S-05382 **The Learning Effect for Critical Flicker Fusion (CFF) Perimetry in normal individuals**

Vi viser til brev datert 04.01.05 med vedlegg: skjema for protokolltillegg og endringer.

Komiteen har ingen merknader til revidert prosjektbeskrivelse.

Komiteen har følgende merknad til revidert informasjonsskriv:

1. Deler av skrivet kan synes noe overtalende, for eksempel "Kjære Prosjektdeltaker. Du inviteres…". Komiteen anbefaler å bruke forespørres i stedet for inviteres. Setningen "Vi ser frem til å høre fra deg" bes strøket.

Komiteen forutsetter at merknaden tas til etterretning, og tilrår at prosjektet gjennomføres.

Vi ønsker lykke til med prosjektet!

Med vennlig hilsen

Kristian Hagestad (sign)
Fylkeslege cand.med., spes. i samf.med
Fungerende leder

Tone Haug
Rådgiver
Sekretær

UNIVERSITETET I OSLO
DET MEDISINSKE FAKULTET

3

Optiker M.Sc Knut Luraas
Rjukan Synssenter AS
Sam Eydesg 57
3660 Rjukan

Regional komité for medisinsk forskningsetikk
Sør- Norge (REK Sør)
Postboks 1130 Blindern
NO-0318 Oslo

Telefon: 228 44 666
Telefaks: 228 44 661
E-post: rek-2@medisin.uio.no
Nettadresse: www.etikkom.no

Dato: 20.11.06
Deres ref.:
Vår ref.: S-05382

S-05382 **The Learning Effect for Critical Flicker Fusion (CFF) Perimetry in normal individuals**

Vi viser til brev datert 1.11.06 med følgende vedlegg, skjema for protokolltillegg og endringer datert 1.11.06, informasjonsskriv med samtykkeerklæring og prosjektinformasjon.

Komiteen har ingen merknader til de foreslåtte endringene i studien.

Komiteen har ingen merknader til revidert informasjonsskriv og samtykkeerklæring.

Komiteen tilrår at prosjektet gjennomføres med de foreslåtte endringene.

Vi ønsker fortsatt lykke til med prosjektet.

Med vennlig hilsen

Kristian Hagestad (sign)
Fylkeslege cand.med., spes. i samf.med
Leder

Jørgen Hardang
Sekretær

UNIVERSITETET I OSLO

DET MEDISINSKE FAKULTET

4

Optiker M.Sc Knut Luraas
Rjukan Synssenter AS
Sam Eydesg 57
3660 Rjukan

Regional komité for medisinsk forskningsetikk
Sør- Norge (REK Sør)
Postboks 1130 Blindern
NO-0318 Oslo

Telefon: 228 44 666
Telefaks: 228 44 661
E-post: rek-2@medisin.uio.no
Nettadresse: www.etikkom.no

Dato: 12.07.07
Deres ref.:
Vår ref.: S-05382

S-05382 **The Learning Effect for Critical Flicker Fusion (CFF) Perimetry in normal individuals**

Vi viser til brev datert 3.7.07 med følgende vedlegg: skjema for protokolltillegg og endringer, invitasjon, samtykkeerklæring og prosjektinformasjon.

Komiteen har ingen merknader til revidert informasjonsskriv med samtykkeerklæring.

Komiteen tilrår at prosjektet videreføres med de endringer som er beskrevet i skjema for protokolltillegg og endringer.

Med vennlig hilsen

Kristian Hagestad (sign)
Fylkeslege cand.med., spes. i samf.med
Leder

Jørgen Hardang
Sekretær

5

Datatilsynet

Rjukan Synssenter as
Sam Eydesgt 57
3660 RJUKAN

Deres ref.

Vår ref. (bes oppgitt ved svar)
06/00112-2 /CAO

3. mars 2006

KONSESJON TIL Å BEHANDLE HELSEOPPLYSNINGER - THE LEARNING EFFECT FOR CRITICAL FLICKER FUSION (CFF) PERIMETRY IN NORMAL INDIVIDUALS

Datatilsynet viser til Deres søknad av 21.januar 2006 om konsesjon til å behandle helseopplysninger.

Datatilsynet har vurdert søknaden og gir Dem med hjemmel i helseregisterloven § 5, jf. personopplysningsloven § 33, jf. § 34, konsesjon til å behandle helseopplysninger til følgende formål: *The Learning Effect for Critical Flicker Fusion (CFF) Perimetry in normal individuals.*

Databehandlingsansvarlig er Rjukan Synssenter AS ved øverste leder. Gjennomføringen av det daglige ansvaret kan delegeres.

Konsesjonen er gitt under forutsetning av at behandlingen foretas i henhold til søknaden og de bestemmelser som følger av helseregisterloven med forskrifter.

Dersom det skjer endringer i behandlingen i forhold til de opplysninger som er gitt i søknaden, må dette fremmes i ny konsesjonssøknad.

Datatilsynet tar forbehold om at konsesjonen kan bli trukket tilbake eller at nye og endrede vilkår kan bli gitt dersom dette er nødvendig ut fra personvernhensyn.

Med hilsen

Hanne P. Gulbrandsen
seniorrådgiver

Christine Ask Ottesen
rådgiver

Postadresse: Postboks 8177 Dep 0034 OSLO
Kontoradresse: Tollbugt 3
Telefon: 22 39 69 00
Telefaks: 22 42 23 50
Org.nr: 974 761 467
Hjemmeside: www.datatilsynet.no

REFERENCES

Adams AJ, Heron G and Husted R. Clinical measures of central vision function in glaucoma and ocular hypertension. *Archives of Ophthalmology* 1987;105:782-787.

Akarsu C, Yazici B, Taner P and Ergin A. Effects of moderate smoking on the central visual field. *Acta Ophthalmogica* 2004;82:432-435.

Allen F. Effect upon the persistence of vision of exposing the eye to light of various wavelengths. *Physical Review* 1900;11:257-290.

Allen F. The persistence of vision. *American Journal of Physiological Optics* 1926;7:439-457.

Anderson AJ and McKendrick A. Quantifying adaptation and fatigue effects in Frequency Doubling perimetry. *Investigative Ophthalmology and Visual Science* 2007;48:943-948.

Anderson AJ. Spatial resolution of the Tendency-Oriented Perimetry algorithm. *Investigative Ophthalmology and Visual Science* 2003;44:1962-1968.

Anderson AJ and Johnson CA. Frequency-Doubling Technology perimetry and optical defocus. *Investigative Ophthalmology and Visual Science* 2003;44:4147-4152.

Anderson AJ and Johnson CA. Comparison of the ASA, MOBS, and ZEST threshold methods. *Vision Research* 2006;46:2403-2411.

Anderson AJ, Johnson CA, Fingeret M, Keltner JL, Spry PG, Wall M and Werner JS. Characteristics of the normative database for the Humphrey Matrix perimeter *Investigative Ophthalmology and Visual Science* 2005;46:1540-1548.

Anderson AJ and Vingrys AJ. Interactions between flicker thresholds and luminance pedestals. *Vision Research* 2000;40:2579-2588.

Anderson AJ and Vingrys AJ. Effect of eccentricity on luminance-pedestal flicker thresholds. *Vision Research* 2002;42:1149-1156.

Anderson C, Blaha GR and Marx JL. Humphrey visual field findings in hydroxychloroquine toxicity. *Eye* 2011;25:1535-1345.

Anderson DR and Patella VM. Automated Static Perimetry. St. Louis, MI: Mosby; 1999.

Anderson RS. The psychophysics of glaucoma: improving the structure/ function relationship. *Progress in Retinal and Eye Research* 2006;25:79-97.

Anderson RS, Ennis F and McDowell DR. Detection and resolution thresholds in the fovea and periphery for high-pass tumbling E's. In: Wall M, Wild JM, eds. *Perimetry Update 1998/1999* Amsterdam, The Netherlands: Kugler Publications; 1999. 177-178.

Anderson RS and O'Brien C. Psychophysical evidence for a selective loss of M ganglion cells in glaucoma. *Vision Research* 1997;37:1079-1083.

Anderson RS, Redmond T, McDowell DR, Breslin KM and Zlatkova MB. The robustness of various forms of perimetry to different levels of induced intraocular stray light. *Investigative Ophthalmology and Visual Science* 2009;50:4022-4028.

Ang GS, Shunmugam M and Azuara-Blanco A. Effect of cataract extraction on the glaucoma progression index (GPI) in glaucoma patients. *Journal of Glaucoma* 2010;19:275-278.

Aoki Y, Takahashi G and Kitahara K. Comparison of Swedish Interactive Threshold Algorithm and Full Threshold algorithm for glaucomatous visual field loss. *European Journal of Ophthalmology* 2007;17:196-202.

Armaly MF. Visual field defects in early open angle glaucoma. *Transactions of the American Ophthalmological Society* 1971;69:147-162.

Artes PH and Chauhan BC. Longitudinal changes in the visual field and optic disc in glaucoma. *Progress in Retinal and Eye Research* 2005;24:333-354.

Artes PH, Henson DB, Harper R and McLeod D. Multisampling suprathreshold perimetry: a comparison with conventional suprathreshold and Full Threshold strategies by computer simulation. *Investigative Ophthalmology and Visual Science* 2003;44:2582-2587.

Artes PH, Hutchison DM, Nicolela MT, LeBlanc RP and Chauhan BC. Threshold and variability properties of Matrix Frequency-Doubling Technology and standard automated perimetry in glaucoma. *Investigative Ophthalmology and Visual Science* 2005;46:2451-2457.

Artes PH, Iwase A, Ohno Y, Kitazawa Y and Chauhan BC. Propertes of perimetric threshold estimates from Full Threshold, SITA Standard and SITA Fast strategies. *Investigative Ophthalmology and Visual Science* 2002;43:2654-2659.

Artes PH, Nicolela MT, McCormick TA, LeBlanc RP and Chauhan BC. Effects of blur and repeated testing on sensitivity estimates with Frequency Doubling Perimetry. *Investigative Ophthalmology and Visual Science* 2003;44:646-652.

Artes PH, O'Leary N, Hutchison DM, Heckler L, Sharpe GP, Nicolela MT and Chauhan BC. Properties of the Statpac visual field index. *Investigative Ophthalmology and Visual Science* 2011;8:4030-4038.

Arvind H, George R, Baskaran M, Raju P, Ramesh SV, Paul PG and Vijaya L. Effect of cataract surgery with intraocular lens implant on Frequency Doubling Perimetry. *Current Eye Research* 2005;30:123-128.

Asman P, Britt JM, Mills RP and Heijl A. Evaluation of adaptive spatial enhancement in suprathreshold visual field screening. *Ophthalmology* 1988;95:1656-1662.

Asman P, Fingeret M, Robin A, Wild JM, Pacey IE, Greenfield D, Liebmann J and Ritch R. Kinetic and static fixation methods in automated threshold perimetry. *Journal of Glaucoma* 1999;8:290-296.

Asman P and Heijl A. Glaucoma Hemifield Test, automated visual field evaluation. *Archives of Ophthalmology* 1992a;110:812-819.

Asman P and Heijl A. Weighting according to location in computer-assisted glaucoma visual field analysis. *Acta ophthalmologica* 1992b;70:671-678.

Asman P and Heijl A. Diffuse visual field loss and glaucoma. *Acta Ophthalmologica* 1994;72:303-308.

Asman P and Olsson J. Physiology of cumulative defect curves; consequences in glaucoma perimetry. *Acta Ophthalmologica Scandinavica* 1995;73:197-201.

Asman P, Wild JM and Heijl A. Appearance of the Pattern Deviation map as a function of change in area of localized field loss. *Investigative Ophthalmology and Visual Science* 2004;45:3099-3106.

Atchison DA. Effect of defocus on visual field measurement. *Ophthalmic and Physiological Optics* 1987;7:259-265.

Aulhorn E and Harms H. Handbook of Sensory Physiology. Vol. VII: Springer-Verlag, Berlin, 1972; 102-145.

Autzen T and Work K. The effect of learning and age on short-term fluctuation and mean sensitivity of automated static perimetry. *Acta Ophthalmologica* 1990;68:327-330.

Baez KA, McNaught AI, Dowler JG, Poinoosawmy D, Fitzke FW and Hitchings RA. Motion detection threshold and field progression in normal tension glaucoma. *British Journal of Ophthalmology* 1995;79:125-128.

Balazsi AG, Rootman J, Drance SM, Schulzer M and Douglas GR. The effect of age on the nerve fiber population of the human optic nerve. *American Journal of Ophthalmology* 1984;97:760-766.

Ballon BJ, Echelman DA, Shields MB and Ollie AR. Peripheral visual field testing in glaucoma by automated kinetic perimetry with the Humphrey Field Analyzer. *Archives of Ophthalmology* 1992;110:1730-1732.

Baraldi P, Enoch JM and Raphael S. A Comparison of visual impairment caused by nuclear (NC) and posterior subcapsular (PSC) cataracts. In Greve EL and Heijl A eds Proceedings of the Seventh International Visual Field Symposium, Amsterdam, September 1986. Documenta Ophthalmologica Proceedings Series. The Hague, The Netherlands: Martinus Nijhoff/ Dr W Junk Publishers; Documenta Ophthalmologica Proceedings Series, 1987; 49:363-366.

Barlow HB. Temporal and spatial summation in human vision at different background intensities. *Journal of Physiology* 1958;141:337-350.

Baumgardt E. Visual spatial and temporal summation. *Nature* 1959;184:1951-1952.

Bebie H, Fankhauser F and Spahr J. Static perimetry: Strategies. *Acta Ophthalmologica* 1976;54:325-338.

Bebie H, Flammer J and Bebie T. The Cumulative Defect curve: separation of local and diffuse components of visual field damage. *Graefe's Archive of Clinical and Experimental Ophthalmology* 1989;227:9-12.

Beerthuizen JJ, Franssen L, Landesz M and van den Berg TJ. Straylight values 1 month after laser in situ keratomileusis and photorefractive keratectomy. *Journal of Cataract and Refractive Surgery* 2007;33:779-783.

Bek T and Lund-Andersen H. The influence of stimulus size on perimetric detection of small scotoma. *Graefe's Archive of Clinical and Experimental Ophthalmology* 1989;227:531-534.

Bengtsson B. Reliability of computerized perimetric threshold tests as assessed by reliability indices and threshold reproducibility in patients with suspect and manifest glaucoma. *Acta Ophthalmolgica Scandinavica* 2000;78:519-522.

Bengtsson B and Heijl A. SITA Fast, a new rapid perimetric threshold test. Description of methods and evaluation in patients with manifest and suspect glaucoma. *Acta Ophthalmologica Scandinavica* 1998a;76:431-437.

Bengtsson B and Heijl A. Evaluation of a new perimetric threshold strategy SITA, in patients with manifest and suspect glaucoma. *Acta Ophthalmolgica Scandinavica* 1998b;76:268-272.

Bengtsson B and Heijl A. False-negative responses in glaucoma perimetry: indicators of patient performance or test reliability. *Investigative Ophthalmology and Visual Science* 2000;41:2201-2204.

Bengtsson B and Heijl A. Normal inter-subject threshold variability and normal limits of the SITA SWAP and Full Threshold SWAP perimetric programs. *Investigative Ophthalmology and Visual Science* 2003;44.

Bengtsson B and Heijl A. Diagnostic sensitivity of fast blue-yellow and standard automated perimetry in early glaucoma: a comparison between different test programs. *Ophthalmology* 2006;113:1092-1097.

Bengtsson B and Heijl A. A visual field index for calculation of glaucoma rate of progression. *American Journal of Ophthalmology* 2008;145:343-353.

Bengtsson B, Heijl A and Olsson J. Evaluation of a new threshold visual field strategy, SITA, in normal subjects. *Acta Ophthalmologica Scandinavica* 1998;76:165-169.

Bengtsson B, Lindgren A, Heijl A, Lindgren G and Asman P. Perimetric probability maps to separate change caused by glaucoma from that by cataract. *Acta Ophthalmologica Scandinavica* 1997;75:184-188.

Bengtsson B, Olsson J, Heijl A and Rootzen H. A new generation of algorithms for computerized threshold perimetry SITA. *Acta Ophthalmologica Scandinavica* 1997;75:368-375.

Berger C. Area of retinal image and flicker fusion frequency. *Acta Physiology Scandinavica* 1953;28:224-233.

Berger C. Illumination of surrounding field and flicker fusion frequency with foveal images of different sizes. *Acta Physiology Scandinavica* 1954;30:161-170.

Bergin C, Redmond T, Nathwani N, Verdon-Roe GM, Crabb DP, Anderson RS and Garway-Heath DF. The effect of induced intraocular straylight on perimetric tests. *Investigative Ophthalmology and Visual Science* 2011;52:3676-3682.

Bernardi L, Costa VP and Shiroma LO. Flicker perimetry in healthy subjects: influence of age and gender, learning effect and short-term fluctuation. *Arquivos Brasileiros de Oftalmologia* 2007;70:91-99.

Bettelheim FA and Ali S. Light scattering of normal human lens. III. Relationship between forward and back scatter of whole excised lenses. *Experimental Eye Research* 1985;41:1-9.

Bettelheim FA and Chylack LT. Light scattering of whole excised human cataractous lenses. Relationships between different light scattering parameters. *Experimental Eye Research* 1985;41:19-30.

Bickler-Bluth M, Trick GL, Kolker AE and Cooper DG. Assessing the utility of reliability indices for automated visual fields. *Ophthalmology* 1989;96:616-619.

Bigger JF and Becker B. Cataracts and open angle glaucoma. *American Journal of Ophthalmology* 1971;71:335-340.

Bland JM and Altman DG. Statistical methods for assessing agreement between two methods of clinical measurement. *Lancet* 1986;8:307-310.

Bland JM and Altman DG. Measuring agreement in method comparison studies. *Statistical Methods in Medical Research* 1999;8:135-160.

Bloch A. Expèriences sur la vision. Paris. Société de Biologie Mémoires 1885;37:493-495.

Blum FG, Gates LK and James BR. How important are peripheral fields? *Archives of Ophthalmology* 1959;61:1-8.

Blumenthal EZ, Sample PA, Berry CC, Lee AC, Girkin CA, Zangwill L, Caprioli J and Weinreb RN. Evaluating several sources of variability for standard and SWAP visual fields in glaucoma patients, suspects, and normals. *Ophthalmology* 2003;110:1895-1902.

Blumenthal EZ, Sample PA, Zangwill L, Lee AC, Kono Y and Weinreb RN. Comparison of long-term variability for standard and short-wavelength automated perimetry in stable glaucoma patients. *American Journal of Ophthalmology* 2000;129:309-313.

Boeglin RJ, Caprioli J and Zulauf M. Long-term fluctuation of the visual field in glaucoma. *American Journal of Ophthalmology* 1992;113:396-400.

Bosworth CF, Sample PA, Gupta N, Bathija R and Weinreb RN. Motion automated perimetry identifies early glaucomatous field defects. *Archives of Ophthalmology* 1998;116:1153-1158.

Bowd C, Zangwill LM, Berry CC, Blumenthal EZ, Vasile C, Sanchez-Galeana C, Bosworth CF, Sample PA and Weinreb RN. Detecting early glaucoma by assessment of retinal nerve fiber layer thickness and visual function. *Investigative Ophthalmology and Visual Science* 2001;42:1993-2003.

Bozkurt B, Ylmaz PT and Irkec M. Relationship between Humphrey 30-2 SITA Standard test, Matrix 30-2 threshold test, and Heidelberg Retina Tomograph in ocular hypertensive and glaucoma patients. *Journal of Glaucoma* 2008;17:203-210.

Brechner RJ and Whalen WR. Creation of the transformed Q statistic probability distribution to aid in the detection of abnormal computerized visual fields. *Ophthalmic Surgery* 1984;15:833-836.

Brenton RS and Argus WA. Fluctuations on the Humphrey and Octopus perimeters. *Investigative Ophthalmology and Visual Science* 1987;28:767-771.

Brenton RS and Phelps CD. The normal visual field on the Humphrey Field Analyzer. *Ophthalmologica* 1986;193:56-74.

Britt JM and Mills RP. The black hole effect in perimetry. *Investigative Ophthalmology and Visual Science* 1988;29:795-801.

Brooke RT. The variation of critical fusion frequency with brightness of various retinal locations. *Journal of the Optical Society of America* 1951;41:1010-1016.

Brown HC. The relationship of flicker to stimulus area in peripheral vision. *Archives of Psychology* 1945;41:1-61.

Brown NA. The morphology of cataract and visual performance. *Eye* 1993;7:63-67.

Brusini P, Salvetat ML, Parisi L and Zeppieri M. Probing glaucoma visual damage by Rarebit perimetry. *British Journal of Ophthalmology* 2005;89:180-184.

Brusini P, Salvetat ML, Zeppieri M and Parisi L. Frequency Doubling Technology perimetry with the Humphrey Matrix 30-2 test. *Journal of Glaucoma* 2006;15:77-84.

Budenz DL, Feuer WJ and Anderson DR. The effect of simulated cataract on the glaucomatous visual field. *Ophthalmology* 1993;100:511-517.

Budenz DL, Rhee P, Feuer WJ, McSoley J, Johnson CA and Anderson DR. Sensitivity and specificity of the Swedish Interactive Threshold Algorithm for glaucomatous visual field defects. *Ophthalmology* 2002;109:1052-1058.

Buerki E and Monhart M. An update to Octopus perimetry. *European Ophthalmic Review* 2007;12:20-22.

Burgansky-Eliash Z, Wollstein G, Patel A, Bilonick RA, Ishikawa H, Kagemann L, Dilworth WD and Schuman JS. Glaucoma detection with Matrix and standard achromatic perimetry. *British Journal of Ophthalmology* 2007;91:933-938.

Burk ROW and Rendon R. Clinical detection of optic nerve damage: measuring changes in cup steepness with use of a new image alignment algorithm. *Survey of Ophthalmology* 2001;45:297-303.

Calkins DJ. Seeing with S cones. *Progress in Retinal and Eye Research* 2001;20:255-287.

Campbell FW and Green DG. Optical and retinal factors affecting visual resolution. *Journal of Physiology* 1965;181:576-593.

Caprioli J and Spaeth GL. Static threshold examination of the peripheral nasal visual field in glaucoma. *Archives of Ophthalmology* 1985;103:1150-1154.

Capris P, Autuori S, Capris E and Papadia M. Evaluation of threshold estimation and learning effect of two perimetric strategies, SITA Fast and CLIP, in damaged visual fields. *European Journal of Ophthalmology* 2008;18:182-190.

Carrillo MM, Artes PH, Nicolela MT, LeBlanc RP and Chauhan BC. Effect of cataract extraction on the visual fields of patients with glaucoma. *Archives of Ophthalmology* 2005;123:929-932.

Cascairo MA, Stewart WC and Sutherland SE. Influence of missed catch trials on the visual field in normal subjects. *Graefe's Archive for Clinical and Experimental Ophthalmology* 1991;229:437-441.

Casson EJ and Johnson CA. Temporal modulation perimetry in glaucoma and ocular hypetension. In: Mills R, ed. *Perimetry Update, 1992/1993*. Amsterdam, The Netherlands: Kugler Publications; 1993. 443-450.

Casson EJ, Johnson CA and Nelson-Quigg JM. Temporal modulation perimetry: the effects of aging and eccentricity on sensitivity in normals. *Investigative Ophthalmology and Visual Science* 1993;34:3096-3102.

Casson EJ, Johnson CA and Shapiro LR. Longitudinal comparison of temporal-modulation perimetry with white-on-white and blue-on-yellow perimetry in ocular hypertension and early glaucoma. *Journal of the Optical Society of America* 1993;10:1792-1806.

Casson RJ and James B. Effect of cataract on Frequency Doubling perimetry in the screening mode. *Journal of Glaucoma* 2006;15:23-25.

Casson RJ, James B, Rubinstein A and Ali H. Clinical comparison of Frequency Doubling Technology perimetry and Humphrey perimetry. *British Journal of Ophthalmology* 2000;85:360-362.

Castro DP, Kawase J and Melo LAJ. Learning effect of standard automated perimetry in healthy individuals. *Arquivos Brasileiros de Oftalmologia* 2008;71:523-528.

Celebisoy N, Oztürk T and Köse T. Rarebit perimetry in the evaluation of visual field defects in idiopathic intracranial hypertension. *European Journal of Ophthalmology* 2010;20:756-762.

Cello KE, Nelson-Quigg JM and Johnson CA. Frequency Doubling Technology perimetry for detection of glaucomatous visual field loss. *American Journal of Ophthalmology* 2000;129:314-322.

Centofanti M, Fogagnolo P, Oddone F, Orzalesi N, Vetrugno M, Manni G and Rossetti L. Learning effect of Humphrey Matrix Frequency Doubling Technology perimetry in patients with ocular hypertension. *Journal of Glaucoma* 2008;17:436-441.

Chaturvedi N, Hedley-Whyte ET and Dreyer EB. Lateral geniculate nucleus in glaucoma. *American Journal of Ophthalmology* 1993;116:182-188.

Chauhan BC, Drance SM and Douglas GR. The use of visual field indices in detecting changes in the visual field in glaucoma. *Investigative Ophthalmology and Visual Science* 1990;31:512-520.

Chauhan BC, Drance SM and Lai C. A cluster analysis for threshold perimetry. *Graefe's Archive for Clinical and Experimental Ophthalmology* 1989;227:216-220.

Chauhan BC, Henson DB and Hobley AJ. Cluster analysis in visual field quantification. *Documenta Ophthalmologica* 1988;69:25-39

Chauhan BC, House PH, McCormick TA and LeBlanc RP. Comparison of conventional and High-pass Resolution perimetry in a prospective study of patients with glaucoma and healthy controls. *Archives of Ophthalmology* 1999;117:24-33.

Chauhan BC, LeBlanc RP, McCormick TA and Rogers JB. Comparison of High-pass Resolution perimetry and Pattern Discrimination perimetry to conventional perimetry in glaucoma. *Canadian Journal of Ophthalmology* 1993;28:306-311.

Chauhan BC, LeBlanc RP, Shaw AM, Chan AB and McCormick TA. Repeatable diffuse visual field loss in open-angle glaucoma. *Ophthalmology* 1997;104:532-538.

Chauhan BC, Tompkins JD, Le Blanc RP and McCormick TA. Characteristics of Frequency-of-seeing curves in normal subjects, patients with suspected glaucoma and patients with glaucoma. *Investigative Ophthalmology and Visual Science* 1993;34:3534-3540.

Chen PP and Budenz DL. The effects of cataract extraction on the visual field of eyes with chronic open-angle glaucoma. *American Journal of Ophthalmology* 1998;125:325-333.

Chin CF, Yip LW, Sim DC and Yeo AC. Rarebit perimetry: normative values and test-retest variability. *Clinical and Experimental Ophthalmology* 2011;39:752-759.

Choplin N and Edwards R. Visual Fields. Thorofare, NJ: Slack; 1998.

Choplin N, Sherwood M and Spaeth G. The effect of stimulus size on the measured threshold values in automated perimetry. *Ophthalmology* 1990;97:371-374.

Chylack LT, Wolfe JK, Singer DM and Leske C. The Lens Opacities Classification System III. *Archives of Ophthalmology* 1993;111:831-836.

Cinotti AA. Evaluation of indications for cataract surgery. *Ophthalmic Surgery* 1979;10:25-31.
Contestabile MT, Perdicchi A, Amodeo S, Recupero V and Recupero SM. The influence of learning effect on Frequency Doubling Technology perimetry (Matrix). *Journal of Glaucoma* 2007;16:297-301.

Coops A and Henson DB. A new reliability index for threshold visual field tests utilizing a filtering technique. Investigative Ophthalmology and Visual Science, 2005; E-Abstract 3736.

Corallo G, Iester M, Scotto R, Calabria G and Traverso CE. Rarebit perimetry and Frequency Doubling Technology in patients with ocular hypertension. *European Journal of Ophthalmology* 2008;18:2005-2211.

Croswell HH, Stewart WC, Cascairo MA and Hunt HH. The effect of background intensity on the components of fluctuation as determined by threshold-related automated perimetry. *Graefe's Archive for Clinical and Experimental Ophthalmology* 1991;229:119-122.

Curcio CA, Allen KA, Sloan KR, Lerea CL, Hurley JB, Klock IB and Milam AH. Distribution and morphology of human cone photoreceptors stained with anti-blue opsin. *Journal of Comparative Neurology* 1991;312:610-624.

Dacey DM. Morphology of a small-field bistratified ganglion cell type in the macaque and human retina. *Visual Neuroscience* 1993;10:1081-1098.

Dacey DM. The mosaic of midget ganglion cells in the human retina. *Journal of Neuroscience* 1993;13:5334-5355.

Dacey DM. Physiology, morphology and spatial densities of identified ganglion cell types in primate retina. *Ciba Foundation Symposium* 1994;184:12-28.

Dacey DM and Lee BB. The 'blue-on' opponent pathway in primate retina originates from a distinct bistratified ganglion cell type. *Nature* 1994;367:731-735.

Daly SJ and Normann RA. Temporal information processing in cones: effects of light adaptation on temporal summation and modulation. *Vision Research* 1985;25:1197-1206.

de Jong LAMS, Snepvangers CEJ, Van Den Berg TJTP and Langerhorst CT. Blue-yellow perimetry in the detection of early glaucomatous damage. *Documenta Ophthalmologica* 1990;75:303-314.

de la Rosa MG, Gonzalez-Hernandez M, Lozano-Lopez V, Mendez MS and de la Vega RR. Optic disc tomography and perimetry in controls, glaucoma suspects, and early and established glaucomas. *Optometry and Vision Science* 2007;84:33-41.

de Monasterio FM, McCrane EP, Newlander JK and Schein SJ. Density profile of blue-sensitive cones along the horizontal meridian of macaque retina. *Investigative Ophthalmology and Visual Science* 1985;26:289-302.

de Vries NE, Franssen L, Webers CA, Tahzib NG, Cheng YY, Hendrikse F, Tjia KF, van den Berg TJ and Nuijts RM. Intraocular straylight after implantation of the multifocal AcrySof ReSTOR SA60D3 diffractive intraocular lens. *Journal of Cataract and Refractive Surgery* 2008;34:957-962.

de Waard PW, IJspeert JK, van den Berg TJ and de Jong PT. Intraocular light scattering in age-related cataracts. *Investigative Ophthalmology and Visual Science* 1992;33:618-625.

del Romo GB, Douthwaite WA and Elliott DB. Critical Flicker Frequency as a potential vision technique in the presence of cataracts. *Investigative Ophthalmology and Visual Science* 2005;46:1107-1112.

Demirel S. Optimising the reliability of automated perimetry for the early detection of visual disorders. PhD Thesis. Melbourne University, 1995.

Demirel S and Vingrys AJ. Acceptable false response rates for reliable perimetric outcomes. In: Mills RP, Wall M, eds. Perimetry Update 1994/1995. Amsterdam, The Netherlands: Kugler Publications; 1996, 83-88.

Dengler-Harles M, Wild JM, Cole MD, O'Neill EC and Crews SJ. The influence of forward light scatter on the visual field indices in glaucoma. *Graefe's Archive for Clinical and Experimental Ophthalmology* 1990;228:326-331.

Desjardins D and Anderson DR. Threshold variability with an automated LED perimeter. *Investigative Ophthalmology and Visual Science* 1988;29:915-921.

Devaney KO and Johnson HA. Neuron loss in the aging visual cortex of man. *Journal of Gerontology* 1980;35:836-841.

Dolman CL, McCormick AQ and Drance SM. Aging of the optic nerve. *Archives of Ophthalmology* 1980;98:2053-2058.

Douthwaite WA, Vianya-Estopà M and Elliott DB. Predictions of postoperative visual outcome in subjects with cataract: a preoperative and postoperative study. *British Journal of Ophthalmology* 2007;91:638-643.

Drance SM, Douglas GR, Airaksinen PJ, Schulzer M and Hitchings RA. Diffuse visual field loss in chronic open angle and low-tension glaucoma. *American Journal of Ophthalmology* 1987;104:577-580.

Drance SM, Wheeler C and Pattullo M. The use of static perimetry in the early detection of glaucoma. *Canadian Journal of Ophthalmology* 1967;2:249-258.

Dudzinski A, Zawojska I and Kinasz R. Flicker perimetry (CFF) in glaucoma diagnosis. *Klinika Oczna* 2003;105:283-287.

Eisner A, Austin DF and Samples JR. Short-wavelength automated perimetry and tamoxifen use. *British Journal of Ophthalmology* 2004;88:125-130.

Eke T, Talbot JF and Lawden MC. Severe persistent visual field constriction associated with vigabatrin. *British Medical Journal* 1997;314:180-181.

Elliott DB and Bullimore MA. Assessing the reliability, discriminative ability, and validity of disability glare tests. *Investigative Ophthalmology and Visual Science* 1993;34:108-119.

Elliott DB, Bullimore MA and Bailey IL. Improving the reliability of the Pelli-Robson contrast sensitivity test. *Clinical Vision Sciences* 1991;6:471-475.

Elliott DB, Gilchrist J and Whitaker D. Contrast sensitivity and glare sensitivity changes with three types of cataract morphology: are these techniques necessary in a clinical evaluation of cataract? *Ophthalmic and Physiological Optics* 1989;9:25-30.

Elliott DB and Hurst MA. Simple clinical techniques to evaluate visual function in patients with early cataract. *Optometry and Vision Science* 1990;67:822-825.

Essock EA, Williams RA, Enoch JM and Raphael S. The effects of image degradation by cataract on vernier acuity. *Investigative Ophthalmology and Visual Science* 1984;25:1043-1050.

Fankhauser F. Problems related to the design of automatic perimeters. *Documenta Ophthalmologica* 1979;47:89-138.

Fankhauser F. Influence of missed catch-trials on the visual field in normal subjects. *Graefe's Archive for Clinical and Experimental Ophthalmology* 1993;231:58-59.

Fankhauser F and Bebie H. Threshold fluctuations, interpolations and spatial resolution in perimetry. In Greve EL ed Proceedings of the Fourth international Visual Field Symposium, Bristol, UK, 13-16 April, 1980. Documenta Ophthalmologica Proceedings Series, Springer-Verlag, New York, NY. 1980; 19: 295-309.

Fankhauser F and Haeberlin H. Dynamic range and stray light. An estimate of the falsifying effects of stray light in perimetry. *Documenta Ophthalmologica* 1980;50:143-167.

Fankhauser F, Koch P and Roulier A. On automation of perimetry. *Albrecht von Graefes Archiv fu̇r Klinische und Experimentelle Ophthalmologie* 1972;184:126-150.

Farber DB, Flannery JG, Lolley RN and Bok D. Distribution patterns of photoreceptors, protein, and cyclic nucleotides in the human retina. *Investigative Ophthalmology and Visual Science* 1985;26 1558-1568.

Farrell DF. Retinal toxicity to antimalarial drugs: chloroquine and hydroxychloroquine: a neurophysiologic study. *Clinical Ophthalmology* 2012;6:377-383.

Feghali JG, Bocquet X, Charlier J and Odom JV. Static flicker perimetry in glaucoma and ocular hypertension. *Current Eye Research* 1991;10:205-212.

Fiorelli VM, Kasahara N, Cohen R, França AS, Della Paolera M, Mandia CJ and de Almeida GV. Improved automated perimetry performance following exposure to Mozart. *British Journal of Ophthalmology* 2006;90:543-545.

Flammer J. The Concept of visual field indices. *Graefe's Archive for Clinical and Experimental Ophthalmology* 1986;224:389-392.

Flammer J, Drance SM, Augustiny L and Funkhouser A. Quantification of glaucomatous visual field defects with automated perimetry. *Investigative Ophthalmology and Visual Science* 1985;26:176-181.

Flammer J, Drance SM, Fankhauser F and Augustiny L. Differential light threshold in automated static perimetry: Factors influencing short-term fluctuation. *Archives of Ophthalmology* 1984;102:876-879.

Flammer J, Drance SM and Schulzer M. The estimation and testing of the components of long-term fluctuation of the differential light threshold. In Greve EL and Heijl A eds. Proceedings of the Fifth international Visual Field Symposium, Sacramento, CA, October 20-23,1982. Documenta Ophthalmologica Proceedings Series. The Hague, The Netherlands: Dr W Junk Publishers; 1983 35:383-389.

Flammer J, Drance SM and Schulzer M. Covariates of the long-term fluctuation of the differential light threshold. *Archives of Ophthalmology* 1984;102:880-882.

Flammer J, Drance SM and Zulauf M. Differential light threshold: short- and long-term fluctuation in patients with glaucoma, normal controls, and patients with suspected glaucoma. *Archives of Ophthalmology* 1984;102:704-706.

Flammer J, Jenni F, Bebie H and Keller B. The Octopus glaucoma G1 program. *Glaucoma* 1987;9:67-72.

Flanagan JG, Moss ID, Wild JM, Hudson C, Prokopich L, Whitaker D and O'Neill EC. Evaluation of FASTPAC : A new strategy for threshold estimation with the Humphrey Field Analyser. *Graefe's Archive for Clinical and Experimental Ophthalmology* 1993;231:465-469.

Flanagan JG, Wild JM and Trope GE. The visual field indices in primary open-angle glaucoma. *Investigative Ophthalmology and Visual Science* 1993;34:2266-2274.

Flanagan JG, Williams-Lyn GE, Trope GE, Hatch W and Harrison E. The phantom contour illusion letter test: a new psychophysical test for glaucoma? In: Mills RP, Wall M, eds. Perimetry Update 1994/1995. Amsterdam, The Netherlands: Kugler Publications; 1996, 405-410.

Fogagnolo P, Tanga L, Rossetti L, Oddone F, Manni G, Orzalesi N and Centofanti M. Mild learning effect of short-wavelength automated perimetry using SITA program. *Journal of Glaucoma* 2010;19:319-323.

Franssen L, Coppens JE and van den Berg TJ. Compensation comparison method for assessment of retinal straylight. *Investigative Ophthalmology and Visual Science* 2006;47:768-776.

Fraser S, Bunce C and Wormald R. Risk factors for late presentation in chronic glaucoma. *Investigative Ophthalmology and Visual Science* 1999;40:2251-2257.

Frisén L. A computer graphics visual field screener using high-pass spatial frequency resolution targets and multiple feedback devices. In Greve EL and Heijl A eds Proceedings of the Seventh International Visual Field Symposium, Amsterdam, September 1986. Documenta Ophthalmologica Proceedings Series. The Hague, The Netherlands: Martinus Nijhoff/ Dr W Junk Publishers; Documenta Ophthalmologica Proceedings Series, 1987; 49:441-446.

Frisén L. High-pass resolution targets in peripheral vision. *Ophthalmology* 1987;94:1104-1108.

Frisén L. High-pass resolution perimetry. *Documenta Ophthalmologica* 1993;83:1-25.

Frisén L. New, sensitive window on abnormal spatial vision: Rarebit probing. *Vision Research* 2002;42:1931-1939.

Frisén L and Jensen C. How robust is the optic chiasm? Perimetric and neuro-imaging correlations. *Acta Neurologica Scandinavica* 2008;117:198-204.

Fry GA and Bartley SH. The effect of steady stimulation of one part of the retina upon the critical frequency in another. *Journal of Experimental Psychology* 1936;19:351-356.

Fujimoto N and Adachi-Usami E. Frequency Doubling Perimetry in resolved optic neuritis. *Investigative Ophthalmology and Visual Science* 2000;41:2558-2560.

Funkhouser A and Fankhauser F. The effects of weighting the Mean Defect visual field index according to threshold variability in the central and mid-peripheral visual field. *Graefe's Archive for Clinical and Experimental Ophthalmology* 1991;229:228-231.

Funkhouser AT, Fankhauser F and Weale RA. Problems related to diffuse versus localized loss in the perimetry of glaucomatous visual fields. *Graefe's Archive for Clinical and Experimental Ophthalmology* 1992;230:243-247.

Gardiner SK, Demirel S and Johnson CA. Is there evidence for continued learning over multiple years in perimetry? *Optometry and Vision Science* 2008;85:1043-1048.

Gardiner SK, Demirel S and Johnson CA. Perimetric indices as predictors of future glaucomatous functional change. *Optometry and Vision Science* 2011;88:56-62.

Gardiner SK, Johnson CA and Spry PG. Normal age-related sensitivity loss for a variety of visual functions throughout the visual field. *Optometry and Vision Science* 2006;83:438-443.

Gartner S and Henkind P. Aging and degeneration of the human macula. 1. Outer nuclear layer and photoreceptors. *British Journal of Ophthalmology* 1981;65:23-28.

Garway-Heath DF, Caprioli J, Fitzke FW and Hitchings RA. Scaling the hill of vision: the physiological relationship between light sensitivity and ganglion cell numbers. *Investigative Ophthalmology and Visual Science* 2000;41:1774-1782.

Gasch AT, Wang P and Pasquale LR. Determinants of glaucoma awareness in a general eye clinic. *Ophthalmology* 2000;107:303-308.

Gedik S, Akman A and Akova YA. Efficiency of Rarebit perimetry in the evaluation of homonymous hemianopia in stroke patients. *British Journal of Ophthalmology* 2007;91:1065-1069.

Gilpin LB, Stewart WC, Hunt HH and Broom CD. Threshold variability using different Goldmann stimulus sizes. *Acta Ophthalmogica* 1990;68:674-676.

Glass E, Schaumberger M and Lachenmayr BJ. Simulations for FASTPAC and the standard 4-2 dB full-threshold strategy of the Humphrey Field Analyzer. *Investigative Ophthalmology and Visual Science* 1995;36:1847-1854.

Gleissner M and Lachenmayr BJ. Light perception and flicker perimetry. Effect of refractive error, artificial media opacities and pupillary size. *Der Ophthalmologe* 1992;89:162-165.

Glovinsky Y, Quigley HA and Dunkelberger GR. Retinal ganglion cell loss is size dependent in experimental glaucoma. *Investigative Ophthalmology and Visual Science* 1991;32:484-491.

Glovinsky Y, Quigley HA and Pease ME. Foveal ganglion cell loss is size dependent in experimental glaucoma. *Investigative Ophthalmology and Visual Science* 1993;34:395-400.

Goldstick BJ and Weinreb RN. The effect of refractive error on automated global analysis program G-1. *American Journal of Ophthalmology* 1987;104:229-232.

Gonzales de la Rosa M, Morales J, Dannheim F, Papst E, Papst N, Seiler TJ, Matsumoto C, Lachkar Y, Mermoud A and Prünte C. Multicenter evaluation of Tendency Oriented Perimetry (TOP) using the G1 grid. *European Journal of Ophthalmology* 2003 13:32-41.

Gonzalez-Hernandez M, de la Rosa MG, de la Vega RR and Hernandez-Vidal A. Long-term fluctuation of standard automatic perimetry, Pulsar perimetry and Frequency-Doubling Technology in early glaucoma diagnosis. *Ophthalmic Research* 2007;39:338-343.

González-Hernández M, García-Feijoó J, Mendez MS and de la Rosa MG. Combined spatial, contrast, and temporal functions perimetry in mild glaucoma and ocular hypertension. *European Journal of Ophthalmology* 2004;14:514-522.

Gonzalez-Hernandez M, Rios AP, Rodriguez M and Gonzalez de la Rosa M. Combined spatial resolution and contrast perimetry in normal subjects. In Wall M, Mills RP eds *Perimetry Update 2000/ 2001*. Amsterdam, The Netherlands: Kugler Publications; 2001 PAGES.

Gonzalez de la Rosa M, Gonzalez-Hernandez M, Sanchez-Mendez M, Medina-Mesa E and Rodriguez de la Vega R. Detection of morphological and functional progression in initial glaucoma. *British Journal of Ophthalmology* 2009;94:414-418.

Gonzalez de la Rosa M, Martinez A, Sanchez M, Mesa C, Cordoves L and Losada MJ. Accuracy of the Tendency-Oriented Perimetry with the Octopus 1-2-3 perimeter. In: Wall M, Heijl A, eds. *Perimetry Update 1996/97.* Amsterdam, The Netherlands: Kugler Publications;1997: 119-123.

Gonzalez de la Rosa M and Pareja A. Influence of the fatigue effect on the Mean Deviation measurement in perimetry. *European Journal of Ophthalmology* 1997;7:29-34.

Gordon MO, Beiser JA, Brandt JD, Heuer DK, Higginbotham EJ, Johnson CA, Keltner JL, Miller JP, Parrish RK, Wilson MR and Kass MA. The Ocular Hypertension Treatment Study: Baseline factors that predict the onset of primary open-angle glaucoma. *Archives of Ophthalmology* 2002;120:714-720.

Gordon MO, Torri V, Miglior S, Beiser JA, Floriani I, Miller JP, Gao F, Adamsons I, Poli D, D'Agostino RB and Kass MA. Validated prediction model for the development of primary open angle glaucoma in individuals with ocular hypertension. *Ophthalmology* 2007;114:10-19.

Goren D and Flanagan JG. Is flicker-defined form (FDF) dependent on the contour? *Journal of Vision* 2008;8:1-11.

Graham SL and Drance SM. Interpretation of High-pass Resolution perimetry with a probability plot. *Graefe's Archive for Clinical and Experimental Ophthalmology* 1995;233:140-149.

Granit R. Two types of retinae and their electrical responses to intermittent stimuli in light and dark adaptation. *Journal of Physiology* 1935b;85:421-438.

Granit R and Harper P. Comparative studies on the peripheral and central retina: II. Synaptic reactions in the eye. *American Journal of Physiological Optics* 1930;95:211-227.

Granit R and Riddell LA. The electrical responses of light- and dark-adapted frogs eyes to rhythmical and continuous stimuli. *Journal of Physiology* 1934;81:1-28.

Granit R and Therman PO. Excitation and inhibition in the retina and in the optic nerve. *Journal of Physiology* 1935;83:359-381.

Greve EL. Single and multiple stimulus static perimetry in glaucoma; the two phases of perimetry. Documenta Ophthalmologica, 1973; 36. 1-355.

Greve EL. Static Perimetry. *Journal International d'Ophtalmologie* 1975;171:26-38.

Greve EL. Visual field, glaucoma and cataract. Documenta Ophthalmologica Proceedings Series. 1979; 22. 79-88.

Greve EL, Dannheim F and Bakker D. The Peritest, a new automatic and semi-automatic perimeter. *International Ophthalmology* 1982;5:201-214.

Guthauser U and Flammer J. Quantifying visual field damage caused by cataract. *American Journal of Ophthalmology* 1988;106:480-484.

Hackett DA and Anderson AJ. Determining mechanisms of visual loss in glaucoma using Rarebit perimetry. *Optometry and Vision Science* 2011;88:48-55.

Haeberlin H and Fankhauser F. Adaptive programs for analysis of the visual field by automatic perimetry - basic problems and solutions Efforts oriented towards the realisation of the generalised spatially adaptive Octopus program Sapro. *Documenta Ophthalmologica* 1980;50:123-141.

Haefliger IO and Flammer J. Fluctuation of the differential light threshold at the border of absolute scotomas - comparison between glaucomatous visual field defects and blind spots. *Ophthalmology* 1991;98:1529-1532.

Ham WTJ, Mueller HA, Ruffolo JJ, Guerry D and Guerry RK. Action spectrum for retinal injury from near-ultraviolet radiation in the aphakic monkey. *American Journal of Ophthalmology* 1982;93:299-306.

Hamill TR, Post RB, Johnson CA and Keltner JL. Correlation of color vision deficits and observable changes in the optic disc in a population of ocular hypertensives. *Archives of Ophthalmology* 1984;102:1637-1639.

Hankins MW, Peirson SN and Foster RG. Melanopsin: An exciting photopigment. *Trends in Neurosciences* 2008;31:27-36.

Hart WM, Silverman SE, Trick GL, Nesher R and Gordon MO. Glaucomatous visual field damage. Luminance and color-contrast sensitivities. *Investigative Ophthalmology and Visual Science* 1990;31:359-367.

Hartmann E, Lachenmayr BJ and Brettel H. The peripheral critical flicker frequency. *Vision Research* 1979;19:1019-1023.

Harwerth RS, Carter-Dawson L, Shen F, Smith EL and Crawford MLJ. Ganglion cell losses underlying visual field defects from experimental glaucoma. *Investigative Ophthalmology and Visual Science* 1999;40:2242-2250.

Harwerth RS, Carter-Dawson L, Smith EL, Barnes G, Holt WF and Crawford MLJ. Neural losses correlated with visual losses in clinical perimetry. *Investigative Ophthalmology and Visual Science* 2004;45:3152-3160.

Harwerth RS, Wheat JL, Fredette MJ and Anderson DR. Linking structure and function in glaucoma. *Progress in Retinal and Eye Research* 2010 29:249-271.

Havener WH and Henderson JW. Comparison of flicker perimetry with standard perimetric methods. *Archives of Ophthalmology* 1954;52:91-105.

Hayashi K, Hayashi H, Nakao F and Hayashi F. Influence of cataract surgery on automated perimetry in patients with glaucoma. *American Journal of Ophthalmology* 2001;132:41-46.

Haymes SA, Hutchison DM, McCormick TA, Varma DK, Nicolela MT, LeBlanc RP and Chauhan BC. Glaucomatous visual field progression with Frequency-Doubling Technology and standard automated perimetry in a longitudinal prospective study. *Investigative Ophthalmology and Visual Science* 2005;46:547-554.

Heider HW, Seez KJ and Schnaudigel OE. Changes in the visual field caused by lens opacities. *Klinische Monatsblätter für Augenheilkunde* 1991;198:15-19.

Heijl A. The Humphrey Field Analyzer, construction and concepts. In: Greve EL, Heijl A, eds. Proceedings of the Sixth International Visual Field Symposium. Santa Margherita, Ligure, Italy, 1984. Documenta Ophthalmologica Proceedings Series: 1985; 42: 77-84.

Heijl A. Lack of diffuse loss of differential light sensitivity in early glaucoma. *Acta Ophthalmologica* 1989;67:353-360.

Heijl A and Bengtsson B. The effect of perimetric experience in patients with glaucoma. *Archives of Ophthalmology* 1996;114:19 - 22.

Heijl A and Drance SM. A clinical comparison of three computerized automatic perimeters in the detection of glaucoma defects. *Archives of Ophthalmology* 1981;99:832-836.

Heijl A and Drance SM. Changes in differential threshold in patients with glaucoma during prolonged perimetry. *British Journal of Ophthalmology* 1983;67:512-516.

Heijl A and Krakau CET. An automatic static perimeter, design and pilot study. *Acta Ophthalmogica* 1975;53:293-310.

Heijl A, Lindgren G and Olsson J. Normal variability of static perimetric threshold values across the central visual field. *Archives of Ophthalmology* 1987a;105:1544-1549.

Heijl A, Lindgren G and Olsson J. A package for the statistical analysis of visual fields. *Documenta Ophthalmologica Proceedings Series* 1987b;45:153-168.

Heijl A, Lindgren G and Olsson J. The effect of perimetric experience in normal subjects. *Archives of Ophthalmology* 1989;107:81-86.

Hendry SH and Reid R, C. The koniocellular pathway in primate vision. *Annual Review of Neuroscience* 2000;23:127-153.

Henson DB, Artes PH and Chauhan BC. Diffuse loss of sensitivity in early glaucoma. *Investigative Ophthalmology and Visual Science* 1999;40:3147-3151.

Henson DB, Chauhan BC and Hobley A. Screening for glaucomatous visual field defects: the relationship between sensitivity and specificity and the number of test locations. *Ophthalmic and Physiological Optics* 1988;8:123-127.

Heron G, Adams AJ and Husted R. Central visual fields for short-wavelength sensitive pathways in glaucoma and ocular hypertension. *Investigative Ophthalmology and Visual Science* 1988;29:64-72.

Hess R and Woo G. Vision through cataracts. *Investigative Ophthalmology and Visual Science* 1978;17:428-435.

Heuer DK, Anderson DR, Feuer WJ and Gressel MG. The influence of refraction accuracy on automated perimetric threshold measurements. *Ophthalmology* 1987;94:1550-1553.

Hodapp E, Parrish RK, Anderson DR and Perkins TW. Clinical decisions in glaucoma. St. Louis, MI: Mosby, 1993; 52-61.

Holló G, A. S and Vargha P. Scanning Laser Polarimetry versus Frequency-Doubling Perimetry and conventional threshold perimetry: changes during a 12-month follow-up in preperimetric glaucoma. A pilot study. *Acta Ophthalmogica Scandinavia* 2001;79:403-407.

Hong S, Na K, Kim CY and Seong GJ. Learning effect of Humphrey Matrix perimetry. *Canadian Journal of Ophthalmology* 2007;42:707-711.

Hong S, Yeom HY, Kim CY and Seong GJ. Comparison between indices of Humphrey Matrix and Humphrey perimetry in early glaucoma patients and normal subjects. *Annals of Ophthalmology* 2007;39:318-320.

Hood DC, Anderson SC, Wall M and Kardon RH. Structure versus function in glaucoma: an application of a linear model. *Investigative Ophthalmology and Visual Science* 2007;48:3662-3668.

Horani A, Frenkel S, Yahalom C, Farber MD, Ticho U and Blumenthal EZ. The learning effect in visual field testing of healthy subjects using Frequency Doubling Technology. *Journal of Glaucoma* 2002;11:511-516.

Hudson C, Wild JM and Archer-Hall J. Maximizing the dynamic range of the Humphrey Field Analyzer for blue-on-yellow perimetry. *Ophthalmic and Physiological Optics* 1993;13:405-408.

Hudson C, Wild JM and O'Neill EC. Fatigue effects during a single session of automated static threshold perimetry. *Investigative Ophthalmology and Visual Science* 1994;35:268-280.

Hutchings N, Hosking SL, Wild JM and Flanagan JG. Long-term fluctuation in short-wavelength automated perimetry in glaucoma suspects and glaucoma patients. *Investigative Ophthalmology and Visual Science* 2001;42:2332-2337.

Hutchings N, Wild JM, Hussey MK and Trope GE. The homogeneous and heterogeneous components of the long-term fluctuation in glaucomatous field loss. *Investigative Ophthalmology and Visual Science* 1993;34:1263.

Hylkema BS. Examination of the visual field by determining the fusion frequency. *Acta Ophthalmologica* 1942;20:181-193.

Haas A, Flammer J and Schneider U. Influence of age on the visual fields of normal subjects. *American Journal of Ophthalmology* 1986;101:199-203.

Interzeag AG. OCTOPUS, Visual Field Digest. Interzeag AG, Schliren, Switzerland, 1998.

Jaffe GJ, Alvarado JA and Juster RP. Age-related changes of the normal visual field. *Archives of Ophthalmology* 1986;104:1021-1025.

Jampel HD, Singh K, Lin SC, Chen TC, Francis BA, Hodapp E, Samples JR and Smith SD. Assessment of visual function in glaucoma: a report by the American Academy of Ophthalmology. *Ophthalmology* 2011;118:986-1002.

Jennings JA and Charman WN. The effects of central and peripheral refraction on critical fusion frequency. *Ophthalmic and Physiological Optics* 1981;1:91-96.

Johnson CA. Selective versus nonselective losses in glaucoma. *Journal of Glaucoma* 1994;3:532-544.

Johnson CA. FDT Perimetry for the detection of glaucomatous visual field loss. The effectiveness of the FDT and Humphrey Matrix Perimeters. *Glaucoma Today* 2008;6:26-28.

Johnson CA, Adams AJ, Casson EJ and Brandt JD. Blue-on-yellow perimetry can predict the development of glaucomatous visual field loss. *Archives of Ophthalmology* 1993a;111:645-650.

Johnson CA, Adams AJ, Casson EJ and Brandt JD. Progression of early glaucomatous visual field loss as detected by blue-on-yellow and standard white-on-white automated perimetry. *Archives of Ophthalmology* 1993b;111:651-656.

Johnson CA, Adams AJ and Lewis RA. Evidence for a neuronal basis of age-related visual field loss in normal observers. *Investigative Ophthalmology and Visual Science* 1989;30:2056-2064.

Johnson CA, Adams AJ, Twelker JD and Quigg JM. Age-related changes in the central visual field for short-wavelength-sensitive pathways. *Journal of the Optical Society of America* 1988;5:2131-2139.

Johnson CA, Adams CW, Lewis RA and Keltner JL. Fatigue effects in automated perimetry. *Applied Optics* 1988;27:1030-1037.

Johnson CA, Brandt JD, Khong AM and Adams AJ. Short-wavelength automated perimetry in low, medium, and high risk ocular hypertensive eyes. *Archives of Ophthalmology* 1995;113:70-76.

Johnson CA, Cioffi GA, Liebmann JR, Sample PA, Zangwill LM and Weinreb RN. The relationship between structural and functional alterations in glaucoma: a review. Seminars in Ophthalmology, 2000.

Johnson CA and Marshall DJ. Aging effects for opponent mechanisms in the central visual field. *Optometry and Vision Science* 1995;72:75-82.

Johnson CA, Sample PA, Cioffi GA, Liebmann JR and Weinreb RN. Structure and Function Evaluation (SAFE): I. Criteria for glaucomatous visual field loss using standard automated perimetry (SAP) and short-wavelength automated perimetry (SWAP). *American Journal of Ophthalmology* 2002;134:177-185.

Johnson CA and Samuels SJ. Screening for glaucomatous visual field loss with Frequency-Doubling Perimetry. *Investigative Ophthalmology and Visual Science* 1997;38:413-425.

Johnson MA and Choy D. On the definition of age-related norms for visual function testing. *Applied Optics* 1987;26:1449-1454.

Kalaboukhova L, Fridhammar V and Lindblom B. Glaucoma follow up by the Heidelberg Retina Tomograph - new graphical analysis of optic disc topography changes. *Graefe's Archive for Clinical and Experimental Ophthalmology* 2006;244:654-662.

Kandel H, Adhikari P, Shrestha GS, Ruokonen EL and Shah DN. Visual function in patients on ethambutol therapy for tuberculosis. *Journal of Ocular Pharmacology and Therapeutics* 2012;28:174-178.

Kanski JJ. Clinical Ophthalmology, a systematic approach. Oxford, UK: Butterworth-Heinemann, 2003.

Kaplan E and Shapley RM. X and Y cells in the lateral geniculate nucleus of macaque monkeys. *Journal of Physiology* 1982;330:125-143.

Kass MA, Heuer DK, Higginbotham EJ, Johnson CA, Keltner JL, Miller JP, Parrish RK, Wilson MR and Gordon MO. The Ocular Hypertension Treatment Study: A randomized trial determines that topical ocular hypotensive medication delays or prevents the onset of primary open angle glaucoma. *Archives of Ophthalmology* 2002;120:701-713.

Katsanos A, Labiris G, Fanariotis M, Tsirouki T and Chatzoulis D. The relationship between Rarebit perimetry and OCT-derived retinal nerve fibre layer thickness in glaucoma. *Acta Ophthalmologica* 2008;86:871-876.

Katz J and Sommer A. Asymmetry and variation in the normal hill of vision. *Archives of Ophthalmology* 1986;104:65-68.

Katz J and Sommer A. A longitudinal study of the age-adjusted variability of automated visual fields. *Archives of Ophthalmology* 1987;105:1083-1086.

Katz J and Sommer A. Reliability indexes of automated perimetric tests. *Archives of Ophthalmology* 1988;106:1252-1254.

Katz J and Sommer A. Reliability of automated perimetric tests (letter, comment). *Archives of Ophthalmology* 1990;108:777-778.

Katz J, Sommer A and Gaasterland DE. Comparison of analytic algorithms for detecting glaucomatous visual field loss. *Archives of Ophthalmology* 1991;109:1684-1689.

Katz J, Sommer A and Witt K. Reliability of visual field results over repeated testing. *Ophthalmology* 1991;98:70-75.

Kaufmann H and Flammer J. Clinical experimence with the Bebie curve. In: Heijl A, ed. *Perimetry Update 1988/1989.* Amsterdam, The Netherlands: Kugler Publications; 1989; 235-238.

Kelly DH. Frequency Doubling in visual responses. *Journal of the Optical Society of America* 1966;56:1628-1633.

Kelly DH. Nonlinear visual responses to flickering sinusoidal gratings. *Journal of the Optical Society of America* 1981;71:1051-1055.

Keltner JL and Johnson CA. Short-wavelength automated perimetry in neuro-ophthalmological disorders. *Archives of Ophthalmology* 1995;113:475-481.

Keltner JL, Johnson CA and Balestrery FG. Suprathreshold static perimetry. Initial clinical trials with the Fieldmaster automated perimeter. *Archives of Ophthalmology* 1979;97:260-272.

Kerrigan-Baumrind LA, Quigley HA, Pease ME, Kerrigan DF and Mitchell RS. Number of ganglion cells in glaucoma eyes compared with threshold visual field tests in the same persons. *Investigative Ophthalmology and Visual Science* 2000;41:741-748.

Keunen JE, van Norren D and van Meel GJ. Density of foveal cone pigments at older age. *Investigative Ophthalmology and Visual Science* 1985;28:985-991.

Kho RC, Al-Obailan M and Arnold AC. Bitemporal visual field defects in ethambutol-induced optic neuropathy. *Journal of Neuro-Ophthalmology* 2011;31:121-126.

Khong JJ, Dimitrov PN, Rait J and McCarty CA. Can the specificity of the FDT for glaucoma be improved by confirming abnormal results? *Journal of Glaucoma* 2001;10:199-202.

Kilbride PE, Hutman LP, Fishman M and Read JS. Foveal cone pigment density difference in the aging human eye. *Vision Research* 1986;26:321-325.

Kim JH and Kee C. The Effect of myopic optical defocus on the Humphrey Matrix 30-2 threshold test. *Journal of the Korean Ophthalmological Society* 2008;49:119-124.

Kim YY, Kim JS, Shin DH, Kim C and Jung HR. Effect of cataract extraction on blue-on-yellow visual field. *American Journal of Ophthalmology* 2001;132:217-220.

King-Smith PE, Grigsby SS, Vingrys AJ, Benes SC and Supowit A. Efficient and unbiased modifications of the QUEST threshold method: theory, simulations, experimental evaluation and practical implementation. *Vision Research* 1994;34:885-912.

King AJW, Taguri A, Wadood AC and Azuara-Blanco A. Comparison of two fast strategies, SITA Fast and TOP, for the assessment of visual fields in glaucoma patients. *Graefe's Archive for Clinical and Experimental Ophthalmology* 2002;240:481-487.

King D, Drance SM, Douglas GR and Wijsman K. The detection of paracentral scotomas with varying grids in computed perimetry. *Archives of Ophthalmology* 1986;104:524-525.

Klein BE, Klein R and Jensen SC. Visual sensitivity and age-related eye diseases. The Beaver Dam Eye Study. *Ophthalmic Epidemiology* 1996;3:47-55.

Klein BEK, Klein R, Sponsel WE, Franke T, Cantor LB, Martone J and Menage MJ. Prevalence of glaucoma. The Beaver Dam Eye Study. *Ophthalmology* 1992;99:1499-1504.

Knox GW. Investigations of flicker fusion. I. The effect of practice, under the influence of various attitudes, on the CFF. *Journal of General Psychology,* 1945;33:121-129.

Koch DD. Glare and contrast sensitivity testing in cataract patients. *Journal of Cataract and Refractive Surgery* 1989;15:158-164.

Koch P, Roulier A and Fankhauser F. Perimetry - The information theoretical basis for its automation. *Vision Research* 1972;12:1619-1630.

Kogure S, Toda Y and Tsukahara S. Prediction of future scotoma on conventional automated static perimetry using Frequency Doubling Technology perimetry. *British Journal of Ophthalmology* 2006;90:347-352.

Kook MS, Yang SJ, Kim S, Chung J, Kim ST and Tchah H. Effect of cataract extraction on Frequency Doubling Technology perimetry. *American Journal of Ophthalmology* 2004;138:85-90.

Kosmin AS. Apparent glaucomatous visual field defects caused by dermatochalasis. *Eye* 1997;11:682-686.

Koucheki B, Nouri-Mahdavi K, Patel G, Gaasterland D and Caprioli J. Visual field changes after cataract extraction: The AGIS experience. *American Journal of Ophthalmology* 2004;138:1022-1028.

Kratochvilová P. Computer perimetry - rapid TOP (Tendency Oriented Perimetry) and normal threshold methods in clinical practice - comparison of results. *Ceská a Slovenská Oftalmologie* 2002;58:187-193.

Kugelmass S and Landis C. The relation of area and luminance to the threshold for critical flicker fusion. *American Journal of Psychology* 1955;68:1-19.

Kulze JC, Stewart WC and Sutherland SE. Factors associated with a learning effect in glaucoma patients using automated perimetry. *Acta Ophthalmologica* 1990;68:681-686.

Kutzko KE, Brito CF and Wall M. Effect of instructions on conventional automated perimetry. *Investigative Ophthalmology and Visual Science* 2000;41:2006-2013.

Lachenmayr BJ. The role of temporal threshold criteria in psychophysical testing in glaucoma. *Current Opinion in Ophthalmology* 1994;5:58-63.

Lachenmayr BJ and Drance SM. Diffuse field loss and central visual function in glaucoma. *German Journal of Ophthalmology* 1992;1:67-73.

Lachenmayr BJ, Drance SM and Airaksinen PJ. Diffuse field loss and diffuse retinal nerve fiber loss in glaucoma. *German Journal of Ophthalmology* 1992;1:22-25.

Lachenmayr BJ, Drance SM, Chauhan BC, House PH and Lalani S. Diffuse and localized glaucomatous field loss in light sense, flicker and resolution perimetry. *Graefe's Archive for Clinical and Experimental Ophthalmology* 1991;229:267-273.

Lachenmayr BJ, Drance SM, Douglas GR and Mikelberg FS. Light sense, flicker and resolution perimetry in glaucoma: a comparative study. *Graefe's Archive for Clinical and Experimental Ophthalmology* 1991;229:246-251.

Lachenmayr BJ and Gleissner M. Flicker perimetry resists retinal image degradation. *Investigative Ophthalmology and Visual Science* 1992;33:3539-3542.

Lachenmayr BJ, Kojetinsky S, Ostermaier N, Angstwurm K, Vivell PM and Schaumberger M. The different effects of aging on normal sensitivity in flicker and light-sense perimetry. *Investigative Ophthalmology and Visual Science* 1994;35:2741-2748.

Lachkar Y, Barrault O, Lefrançois A and Demailly P. Rapid Tendency Oriented Perimetry (TOP) with the Octopus visual field analyzer. *Journal Français d'Ophtalmologie* 1998;21:180-184.

Lam BL, Alward WL and Kolder HE. Effect of cataract on automated perimetry. *Ophthalmology* 1991;98:1066-1070.

Lamparter J, Schulze A, Schuff AC, Berres M, Pfeiffer N and Hoffmann EM. Learning curve and fatigue effect of flicker defined form perimetry. *American Journal of Ophthalmology* 2011;151:1057-1064.

Langerhorst CT, Thomas JTP, Van Den Berg TJTP and Greve EL. Is there a general reduction of sensitivity in glaucoma? *International Ophthalmology* 1989;3:31-35.

Langerhorst CT, Van Den Berg TJTP, Van Spronsen R and Greve EL. Results of a fluctuation analysis and defect volume program for automated static threshold perimetry with the scoperimeter. In: Greve EL, Heijl A, eds. Proceedings of the 6th International Visual Field Symposium. Santa Margherita, Ligure, Italy, 1984. Documenta Ophthalmologica Proceedings Series: 1985. 1-6.

LeClaire J, Nadler MP, Weiss S and Miller D. A new glare tester for clinical testing. Results comparing normal subjects and variously corrected aphakic patients. *Archives of Ophthalmology* 1982 100:153-158.

Leite MT, Zangwill LM, Weinreb RN, Rao HL, Alencar LM and Medeiros FA. Structure-function relationships using the Cirrus spectral domain optical coherence tomograph and standard automated perimetry. *Journal of Glaucoma* 2012;21:49-54.

Lennie P. Parallel visual pathways: A review. *Vision Research* 1980;20:561-594.

Leung CK, Liu S, Weinreb RN, Lai G, Ye C, Cheung CY, Pang CP, Tse KK and Lam DS. Evaluation of retinal nerve fiber layer progression in glaucoma: a prospective analysis with neuroretinal rim and visual field progression. *Ophthalmology* 2011;118 1551-1557.

Lewis RA, Johnson CA and Keltner JL. Variability of quantitatitve automated perimetry in normal observers. *Ophthalmology* 1986;93:878-881.

Li J, Tripathi RC and Tripathi BJ. Drug-induced ocular disorders. *Drug Safety* 2008;31:127-141.

Lindenmuth KA, Skuta GL, Rabbani R and Musch DC. Effects of pupillary constriction on automated perimetry in normal eyes. *Ophthalmology* 1989;96:1298-1301.

Lindenmuth KA, Skuta GL, Rabbani R, Musch DC and Bergstrom TJ. Effects of pupillary dilation on automated perimetry in normal patients. *Ophthalmology* 1990;97:367-370.

Liu S, Lam S, Weinreb RN, Ye C, Cheung CY, Lai G, Lam DS and Leung CK. Comparison of standard automated perimetry, Frequency-Doubling Technology perimetry, and short-wavelength automated perimetry for detection of glaucoma. *Investigative Ophthalmology and Visual Science* 2011;52:7325-7331.

Livingstone MS and Hubel DH. Psychophysical evidence for separate channels for the perception of form, color, movement, and depth. *The Journal of Neuroscience* 1987;7:3416-3468.

Livingstone MS and Hubel DH. Segregation of form, color, movement, and depth: anatomy, physiology, and perception. *Science* 1988;240:740-749.

Lyne AJ and Phillips CI. Visual field defects due to opacities in the optical media. *British Journal of Ophthalmology* 1996;53:119-122.

Lythgoe RJ and Tansley K. The relation of the critical frequency of flicker to the adaptation of the eye. *Proceedings of the Royal Society of London* 1929;105:60-92.

Maddess T, Goldberg I, Dobinson J, Wine S, Welsh AH and James AC. Testing for glaucoma with the spatial frequency doubling illusion. *Vision Research* 1999;39:4258-4273.

Maddess T and Henry GH. Performance of nonlinear visual units in ocular hypertension and glaucoma. *Clinical Vision Sciences* 1992;7:371-383.

Maeda H, Nakaura M and Negi A. New perimetric threshold test algorithm with Dynamic Strategy and Tendency Oriented Perimetry (TOP) in glaucomatous eyes. *Eye* 2000;14 747-751.

Maguire MJ, Hemming K, Wild JM, Hutton JL and Marson AG. Prevalence of visual field loss following exposure to vigabatrin therapy: a systematic review. *Epilepsia* 2010;51:2423-2431.

Mahneke A. Flicker-fusion thresholds; comparison between the continuous and the discontinuous method. *Acta Ophthalmologica* 1957;35:53-61.

Maltzman BA, Horan C and Rengel A. Penlight test for glare disability of cataracts. *Journal of Ophthalmic Nursing and Technology* 1988;7:137-139.

Mandava S, Zulauf M, Zeyen T and Caprioli J. An evaluation of clusters in the glaucomatous visual field. *American Journal of Ophthalmology* 1993;116:684-691.

Marchini G, Pisano F and Bertagnin F. Perimetric learning effect in glaucoma patients. *Glaucoma* 1991;13:102-106.

Marmor MF, Kellner U, Lai TY, Lyons JS and Mieler WF. Revised recommendations on screening for chloroquine and hydroxychloroquine retinopathy. *Ophthalmology* 2011;118:415-422.

Martin-Boglind LM. Computer-assisted interpretation of resolution visual fields from patients with chiasmal and retrochiasmal lesions. *Ophthalmologica* 1993;207:148-154.

Martin DD, Vonthein R, Wilhelm H and Schiefer U. Pupil size and Perimetry - a pharmacological model using increment and decrement stimuli. *Graefe's Archive for Clinical and Experimental Ophthalmology* 2005;243:1091-1097.

Martin L. Cataract and High-pass resolution perimetry. *Acta Ophthalmogica Scandinavia* 1997;75:174-177.

Martin L. Intraocular pressure before and after visual field examination. *Eye* 2007;21:1479-1481.

Martin L, Magnusson G, Popovic Z and Sjöstrand J. Resolution visual fields in children surgically treated for bilateral congenital cataract. *Investigative Ophthalmology and Visual Science* 2008;49:3730-3733.

Martin L and Wanger P. New perimetric techniques: A comparison between Rarebit and Frequency Doubling Technology perimetry in normal subjects and glaucoma patients. *Journal of Glaucoma* 2004;13:268-272.

Martinez GA, Sample PA and Weinreb RN. Comparison of High pass resolution perimetry and standard automated perimetry in glaucoma. *American Journal of Ophthalmology* 1995;119:195-201.

Mastropasqua L, Brusini P, Carpineto P, Ciancaglini M, Di Antonio L, Zeppieri MW and Parisi L. Humphrey Matrix Frequency Doubling Technology perimetry and optical coherence tomography measurement of the retinal nerve fiber layer thickness in both normal and ocular hypertensive subjects. *Journal of Glaucoma* 2006;15:328-335.

Matsumoto C, Okuyama S, Iwagaki A, Otsuki T, Uyama K and Otori T. The influence of target blur on perimetric threshold values in automated light-sensitive perimetry and flicker perimetry. In: Wall M, Heijl A, eds. *Perimetry Update 1996/1997. Amsterdam, The Netherlands,* Kugler, 1997:191-199.

Matsumoto C, Okuyama S, Iwagaki A, Takada S and Otori T. Automated flicker perimetry in glaucoma and retinal detachment patients. In: Wall M, Wild JM, eds. *Perimetry Update 1998/1999 Amsterdam, The Netherlands,* Kügler, 2000:85-82,.

Matsumoto C, Takada S, Okuyama S, Arimura E, Hashimoto S and Shimomura Y. Automated flicker perimetry in glaucoma using Octopus 311: a comparative study with the Humphrey Matrix. *Acta Ophthalmologica Scandinavica* 2006;84:210-215.

Matsuo H, Tomita G, Suzuki Y and Araie M. Learning effect and measurement variability in Frequency-Doubling Technology perimetry in chronic open-angle glaucoma. *Journal of Glaucoma* 2002;11:467-473.

Mayer MJ, Spiegler SJ, Ward B, Glucs A and Kim CB. Foveal flicker sensitivity discriminates ARM risk from healthy eyes. *Investigative Ophthalmology and Visual Science* 1992a;33:3143-3149.

Mayer MJ, Spiegler SJ, Ward B, Glucs A and Kim CB. Mid-frequency loss of foveal flicker sensitivity in early stages of age-related maculopathy. *Investigative Ophthalmology and Visual Science* 1992b;33:3136-3142.

Mayer MJ, Ward B, Klein R, Talcott JB, Dougherty RF and Glucs A. Flicker sensitivity and fundus appearance in pre-exudative age-related maculopathy. *Investigative Ophthalmology and Visual Science* 1994;35:1138-1149.

McAlinden C, Gothwal VK, Khadka J, Wright TA, Lamoureux EL and Pesudovs K. A head-to-head comparison of 16 cataract surgery outcome questionnaires. *Ophthalmology* 2011;118:2374-2381.

McKendrick AM. Recent developments in perimetry: test stimuli and procedures. *Clinical and Experimental Optometry* 2005;88:73-80.

McKendrick AM and Turpin A. Combining perimetric suprathreshold and threshold procedures to reduce measurement variability in areas of visual field loss. *Optometry and Vision Science* 2005;82:43-51.

Medeiros FA, Sample PA and Weinreb RN. Frequency Doubling Technology perimetry abnormalities as predictors of glaucomatous visual field loss. *American Journal of Ophthalmology* 2004;137:863-871.

Medeiros FA, Weinreb RN, Sample PA, Gomi CF, Bowd C, Crowston JG and Zangwill LM. Validation of a predictive model to estimate the risk of conversion from ocular hypertension to glaucoma. *Archives of Ophthalmology* 2005;123:1351-1360.

Medeiros FA, Zangwill LM, Girkin CA, Liebmann JM and Weinreb RN. Combining structural and functional measurements to improve estimates of rates of glaucomatous progression. *American Journal of Ophthalmology* 2012;Epub ahead of print.

Menon V, Jain D, Saxena R and Sood R. Prospective evaluation of visual function for early detection of ethambutol toxicity. *British Journal of Ophthalmology* 2009;93:1251-1254.

Merigan WH, Byrne CE and Maunsell JH. Does primate motion perception depend on the magnocellular pathway? *Journal of Neuroscience* 1991;11:3422-3429.

Meyer DR, Stern JH, Jarvis JM and Lininger LL. Evaluating the visual field effects of blepharoptosis using automated static perimetry. *Ophthalmology* 1993;100:651-659.

Meyer JH and Funk J. High-pass resolution perimetry and light-sense perimetry in open-angle glaucoma. *German Journal of Ophthalmology* 1995;4:222-227.

Michaelides M, Stover NB, Francis PJ and Weleber RG. Retinal toxicity associated with hydroxychloroquine and chloroquine: risk factors, screening, and progression despite cessation of therapy. *Archives of Ophthalmology* 2011;129:30-39.

Midena E. Psychophysics and visual aging. *Metabolic, Pediatric and Systemic Ophthalmology* 1989;12:28-31.

Miller BA and Gelber EC. Aphakic visual fields by automated perimetry. *Annals of Ophthalmology* 1990;22:419-422.

Miller D, Jernigan ME, Molnar S, Wolf E and Newman J. Laboratory evaluation of a clinical glare tester. *Archives of Ophthalmology* 1972 87:324-332.

Mills RP. A comparison of Goldmann, Fieldmaster 200, and Dicon AP2000 perimeters used in a screening mode. *Ophthalmology* 1984;91:347-354.

Mills RP. Usefulness of peripheral testing in automated screening perimetry. In: Heijl A, Greve EL, eds. Proceedings of the 6th International Visual Field Symposium. Santa Margherita, Ligure, Italy, 1984. Documenta Ophthalmologica Proceedings Series. 1985:207-211.

Mills RP, Barnebey HS, Migliazzo CV and Li Y. Does saving time using FASTPAC or suprathreshold testing reduce quality of visual fields? *Ophthalmology* 1994;101:1596-1603.

Morales J, Weitzman ML and Gonzalez de la Rosa M. Comparison between Tendency-Oriented Perimetry (TOP) and Octopus threshold perimetry. *Ophthalmology* 2000;107:134-142.

Morgan JE. Selective cell death in glaucoma: does it really occur? *British Journal of Ophthalmology* 1994;78:875-879.

Morgan JE. Retinal ganglion cell shrinkage in glaucoma. *Journal of Glaucoma* 2002;11:365-370.

Morgan JE, Uchida H and Caprioli J. Retinal ganglion cell death in experimental glaucoma. *British Journal of Ophthalmology* 2000;84:303-310.

Moss ID and Wild JM. The influence of induced forward light scatter on the normal blue-on-yellow perimetric profile. *Graefe's Archive for Clinical and Experimental Ophthalmology* 1994;232:409-414.

Moss ID, Wild JM and Whitaker DJ. The influence of age-related cataract on blue-on-yellow perimetry. *Investigative Ophthalmology and Visual Science* 1995;36:764-773.

Musch DC, Lichter PR, Guire KE, Standardi CL and Group CS. The collaborative initial glaucoma treatment study. *Ophthalmology* 1999;106:653-662.

Mutlu FM, Akay F and Bayer A. Effect of pseudophakia on standard perimetry parameters. *Current Eye Research* 2009;34:711-716.

Neumann AC, McCarty GR, Locke J and Cobb B. Glare disability devices for cataractous eyes: a consumer's guide. *Journal of Cataract and Refractive Surgery* 1988;14:212-216.

Neumann AC, McCarty GR, Steedle TO, Sanders DR and Raanan MG. The relationship between cataract type and glare disability as measured by the Miller-Nadler glare tester. *Journal of Cataract and Refractive Surgery* 1988;14:40-45.

Newkirk MR, Gardiner SK, Demirel S and Johnson CA. Assessment of false-positives with the Humphrey Field Analyzer II Perimeter with the SITA Algorithm. *Investigative Ophthalmology and Visual Science* 2006;47:4632-4637.

Ng M, Racette L, Pascual JP, Liebmann JM, Girkin CA, Lovell SL, Zangwill LM, Weinreb RN and Sample PA. Comparing the Full-Threshold and Swedish Interactive Thresholding Algorithms for Short-wavelength automated perimetry. *Investigative Ophthalmology and Visual Science* 2009;50:1726-1733.

Nilsson M, Abdiu O, Laurell CG and Martin L. Rarebit perimetry and fovea test before and after cataract surgery. *Acta Ophthalmologica* 2010;88:479-482.

Nowomiejska K, Brzozowska A, Zarnowski T, Rejdak R, R.G. W and Schiefer U. Variability in isopter position and fatigue during semi-automated kinetic perimetry. *Ophthalmologica* 2012;227:166-172.

Oleszczuk JD, Bergin C and Sharkawi E. Comparative resilience of clinical perimetric tests to induced levels of intraocular straylight. *Investigative Ophthalmology and Visual Science* 2012;53:1219-1224.

Olsson J, Bengtsson B, Heijl A and Rootzen H. An improved method to estimate frequency of false-positive answers in computerized perimetry. *Acta Ophthalmologica Scandinavica* 1997;75:181-183.

Olsson J, Heijl A, Bengtsson B and Rootzen H. Freqency-of-seeing in computerized perimetry. In: Mills RP, ed. *Perimetry update 1992/1993*. Amsterdam, The Netherlands. Kugler. 1993:551-556.

Olsson J, Rootzen H and Heijl A. Maximum likelihood estimation of the frequency of false-positive and false-negative answers from the up-and-down staircases of computerized threshold perimetry. In: Heijl A, ed. *Perimetry Update 1988/1989* Amsterdam, The Netherlands. Kugler. 1988:245-251.

Olsson J, Åsman P and Heijl A. A perimetric learner's index. *Acta Ophthalmogica Scandinavia* 1997;75:665-668.

Ong J and Wong T. Effect of ametropias on critical fusion frequency. *American Journal of Optometry and Archives of American Academy of Optometry* 1971;48:736-739.

Paczka JA, Friedman DS, Quigley HA, Barron Y and Vitale S. Diagnostic capabilities of Frequency-Doubling Technology, scanning laser polarimetry, and nerve fiber layer photographs to distinguish glaucomatous damage. *American Journal of Ophthalmology* 2001;131:188-197.

Parrish RK, Schiffman J and Anderson DR. Static and kinetic visual field testing; Reproducibility in normal volunteers. *Archives of Ophthalmology* 1984;102:1497-1502.

Pascal JI. Retinal image in axial and refractive ametropia. *British Journal of Ophthalmology* 1955;39:380-381.

Paulsson LE and Sjøstrand J. Contrast sensitivity in the presence of a glare light. Theoretical concepts and preliminary clinical studies. *Investigative Ophthalmology and Visual Science* 1980;19:401-406.

Pearson PA, Baldwin LB and Smith TJ. The Q-Statistic in glaucoma and ocular hypertension. In: Heijl A, ed. *Perimetry update 1988/1989.* In: Heijl A, ed. *Perimetry Update 1988/1989* Amsterdam, The Netherlands. Kugler. 1989: 229-233.

Peckham RH and Arner WJ. Visual acuity, contrast, and flicker, as measures of retinal sensitivity. *Journal of the Optical Society of America* 1952;42:621-625.

Pennebaker GE, Stewart WC, Stewart JA and Hunt HH. The effect of stimulus duration upon the components of fluctuation in static automated perimetry. *Eye* 1992;6:353-355.

Perez PC, Gil-Arribas L, Ferreras A, Altemir I, Otin S, Fernandez S, Garcia E and Monclus NG. Relationship between FDF perimetry and standard automated perimetry. *Acta Ophthalmogica* 2010;88:Supplement 246.

Philipson B. Light scattering in lenses with experimental cataract. *Acta Ophthalmologica* 1969;47:1089-1101.

Phipps JA, Dang TM, Vingrys AJ and Guymer RH. Flicker perimetry losses in age-related macular degeneration. *Investigative Ophthalmology and Visual Science* 2004;45:3355-3360.

Phipps JA, Guymer RH and Vingrys AJ. Temporal sensitivity deficits in patients with high-risk drusen. *Australian and New Zealand Journal of Ophthalmology* 1999;27:265-267.

Pieron H. Neurophysiological mechanisms of critical flicker frequency and harmonic phenomena. *Journal of the Optical Society of America* 1962;52:475-475.

Pierre-Filho PT, Gomes PR, E.T. P and Pierre LM. Learning effect in visual field testing of healthy subjects using Humphrey Matrix Frequency Doubling Technology perimetry. *Eye* 2010;24:851-856.

Pierre-Filho PT, Gomes PR, Pierre ET and Pierre LM. Learning effect of Humphrey Matrix Frequency Doubling Technology perimetry in patients with open angle glaucoma. *European Journal of Ophthalmology* 2010;20:538-541.

Prager TC, Urso RG, Holladay JT and Stewart RH. Glare testing in cataract patients: instrument evaluation and identification of sources of methodological error. *Journal of Cataract and Refractive Surgery* 1989;15:149-157.

Quigley HA. Chronic glaucoma selectively damages large optic nerve fibers. *Investigative Ophthalmology and Visual Science* 1987;28:913-920.

Quigley HA. Number of people with glaucoma worldwide. *British Journal of Ophthalmology* 1996;80:389-393.

Quigley HA and Broman AT. The number of people with glaucoma worldwide in 2010 and 2020. *British Journal of Ophthalmology* 2006;90:262-267.

Quigley HA, Dunkelberger GR and Green R. Chronic human glaucoma causing selectively greater loss of large optic nerve fibers. *Ophthalmology* 1988;95:357-363.

Racette L, Medeiros FA, Zangwill LM, Ng D, Weinreb RN and Sample PA. Diagnostic accuracy of the Matrix 24-2 and original N-30 Frequency-Doubling Technology tests compared with standard automated perimetry. *Investigative Ophthalmology and Visual Science* 2008;49:954-960.

Rao HL, Jonnadula GB, Addepalli UK, Senthil S and Garudadri CS. Effect of cataract extraction on visual field index in glaucoma. *Journal of Glaucoma* 2011; Epub ahead of print.

Rao HL, Zangwill LM, Weinreb RN, Leite MT, Sample PA and Medeiros FA. Structure-function relationship in glaucoma using spectral-domain optical coherence tomography. *Archives of Ophthalmology* 2011a;129:864-871.

Rebolleda G, Muñoz FJ, Fernández Victorio JM, Pellicer T and del Castillo JM. Effects of pupillary dilation on automated perimetry in glaucoma patients receiving pilocarpine. *Ophthalmology* 1992;99:418-423.

Reed H and Drance SM. The essentials of perimetry. Oxford: Oxford University Press, 1972; 177.

Regan D. The Charles F. Prentice Award Lecture 1990: specific tests and specific blindnesses: keys, locks, and parallel processing. *Optometry and Vision Science* 1991;68:489-512.

Rehman Siddiqui MA, Khairy HA and Azuara-Blanco A. Effect of cataract extraction on SITA perimetry in patients with glaucoma. *Journal of Glaucoma* 2007;16:205-208.

Reitner A, Tittl M, Ergun E and Baradaran-Dilmaghani R. The efficient use of perimetry for neuro-ophthalmic diagnosis. *British Journal of Ophthalmology* 1996;80:903-905.

Reus NJ and Lemij HG. Scanning laser polarimetry of the retinal nerve fiber layer in perimetrically unaffected eyes of glaucoma patients. *Ophthalmology* 2004;111:2199-2203.

Reynolds M, Stewart WC and Sutherland S. Factors that influence the prevalence of positive catch trials in glaucoma patients. *Graefe's Archive for Clinical and Experimental Ophthalmology* 1990;228:338-341.

Riemann CD, Hanson S and Foster JA. A comparison of manual kinetic and automated static perimetry in obtaining ptosis fields. *Archives of Ophthalmology* 2000;118:65-69.

Roehrig WC. The influence of the portion of the retina stimulated on the critical flicker fusion threshold. *Journal of Psychology* 1959a;48:57-63.

Roehrig WC. The influence of area on the critical flicker fusion threshold. *Journal of Physiology* 1959b;47:317-330.

Rogers-Ramachandran DC and Ramachandran VS. Psychophysical evidence for boundary and surface systems in human vision. *Vision Research* 1998;38:71-77.

Ross DF, Fishman GA, Gilbert LD and Anderson RJ. Variability of visual field measurements in normal subjects and patients with retinitis pigmentosa. *Archives of Ophthalmology* 1984;102:1004-1010.

Ross RT. The fusion frequency in different areas of the visual field: II. The regional gradient of fusion frequency. *Journal of General Psychology* 1936;15:161-170.

Rossetti L, Fogagnolo P, Miglior S, Centofanti M, Vetrugno M and Orzalesi N. Learning effect of short-wavelength automated perimetry in patients with ocular hypertension. *Journal of Glaucoma* 2006;15:399-404.

Rota-Bartelink A. The diagnostic value of automated flicker threshold perimetry. *Current Opinion in Ophthalmology* 1999;10:135-139.

Rucker JC, Hamilton SR, Bardenstein D, Isada CM and Lee MS. Linezolid-associated toxic optic neuropathy *Neurology* 2006;66:595-598.

Rutishauser C and Flammer J. Retests in static perimetry. *Graefe's Archive for Clinical and Experimental Ophthalmology* 1988;226:76-77.

Salvetat ML, Zeppieri M, Parisi L and Brusini P. Rarebit perimetry in normal subjects: test–retest variability, learning effect, normative range, influence of optical defocus, and cataract extraction. *Investigative Ophthalmology and Visual Science* 2007;48:5320-5331.

Salvetat ML, Zeppieri M, Parisi L, Johnson CA, Sampaolesi R and Brusini P. Learning effect and test-retest variability of Pulsar perimetry. *Journal of Glaucoma* 2011;Epub ahead of print.

Sample PA, Bosworth CF, Blumenthal EZ, Girkin C and Weinreb RN. Visual function-specific perimetry for indirect comparison of different ganglion cell populations in glaucoma. *Investigative Ophthalmology and Visual Science* 2000;41:1783-1790.

Sample PA, Bosworth CF and Weinreb RN. Short-wavelength automated perimetry and motion automated perimetry in patients with glaucoma. *Archives of Ophthalmology* 1997 115 1129-1133.

Sample PA, Boynton RM and Weinreb RN. Isolating the color vision loss in primary open-angle glaucoma. *American Journal of Ophthalmology* 1988;106:686-691.

Sample PA, Martinez GA and Weinreb RN. Short-wavelength automated perimetry without lens density testing. *American Journal of Ophthalmology* 1994;118:632-641.

Sample PA, Medeiros FA, Racette L, Pascual JP, Boden C, Zangwill LM, Bowd C and Weinreb RN. Identifying glaucomatous vision loss with visual-function-specific perimetry in the Diagnostic Innovations in Glaucoma Study. *Investigative Ophthalmology and Visual Science* 2006;47:3381-3389.

Sample PA, Taylor JDN, Martinez GA, Lusky M and Weinreb RN. Short-wavelength color visual fields in glaucoma suspects at risk. *American Journal of Ophthalmology* 1993;115:225-233.

Sample PA and Weinreb RN. Color perimetry for assessment of primary open angle glaucoma. *Investigative Ophthalmology and Visual Science* 1990;31:1869-1875.

Sample PA and Weinreb RN. Progressive color visual field loss in glaucoma. *Investigative Ophthalmology and Visual Science* 1992;33:2068-2071.

Sample PA, Weinreb RN and Boynton RM. Acquired dyschromatopsia in glaucoma. *Survey of Ophthalmology* 1986;31:54-64.

Sanabria O, Feuer WJ and Anderson DR. Pseudo-loss of fixation in automated perimetry. *Ophthalmology* 1991;98:76-78.

Saunders RM. The critical duration of temporal summation in the human central fovea. *Vision Research* 1975;15:699-703.

Schaumberger M, Schafer B and Lachenmayr BJ. Glaucomatous visual fields. FASTPAC versus Full Threshold strategy of the Humphrey Field Analyzer. *Investigative Ophthalmology and Visual Science* 1995;36:1390-1397.

Scheibel ME, Lindsay RD, Tomiyasu U and Scheibel AB. Progressive dendritic changes in aging human cortex. *Experimental Neurology* 1975;47:392-403.

Schiefer U, Pascual JP, Edmunds B, Feudner E, Hoffmann EM, Johnson CA, Lagrèze WA, Pfeiffer N, Sample PA, Staubach F, Weleber RG, Vonthein R, Krapp E and Paetzold J. Comparison of the new perimetric GATE strategy with conventional Full Threshold and SITA Standard strategies. *Investigative Ophthalmology and Visual Science* 2009;50:488-494.

Schmied U. Automatic (Octopus) and manual (Goldmann) perimetry in glaucoma. *Graefe's Archive for Clinical and Experimental Ophthalmology* 1980;213:239-244.

Searle AE, Wild JM, Shaw DE and O'Neill EC. Time-related variation in normal automated static perimetry. *Ophthalmology* 1991;98:701-707.

Sekhar GC, Naduvilath TJ, Lakkai M, Jayakumar AJ, Pandi GT, Mandal AK and Honavar SG. Sensitivity of Swedish Interactive Threshold Algorithm compared with standard Full Threshold algorithm in Humphrey visual field testing. *Ophthalmology* 2000;107:1303-1308.

Serguhn S and Spiegel D. Comparison of Frequency Doubling perimetry and standard achromatic computerized perimetry in patients with glaucoma. *Graefe's Archive for Clinical and Experimental Ophthalmology* 2001;239:351-355.

Shankar H and Pesudovs K. Critical flicker fusion test of potential vision. *Journal of Cataract and Refractive Surgery* 2007;33:232-239.

Shapley R. Visual sensitivity and parallel retinocortical channels. *Annual Review of Psychology* 1990;41:635-658.

Shapley R and Perry VH. Cat and monkey retinal ganglion cells and their functional roles. *Trends in Neuroscience* 1986;9:229-235.

Sharma AK, Goldberg I, Graham SL and Moshin M. Comparison of the Humphrey Swedish Interactive Thresholding Algorithm (SITA) and Full Threshold strategies. *Journal of Glaucoma* 2000;9:20-27.

Sherafat H, Spry PGD, Waldock A, Sparrow JM and Diamond JP. Effect of a patient training video on visual field test reliability. *British Journal of Ophthalmology* 2003;87:153-156.

Sheu SJ, Chen YY, Lin HC, Chen HL, Lee IY and Wu TT. Frequency-Doubling Technology perimetry in retinal diseases - preliminary report. *The Kaohsiung Journal of Medical Sciences* 2001;17:25-28.

Shue B, Chatterjee A, Fudemberg S, Katz LJ, Moster MR, Navarro MJ, Pro M, Schmidt C, Spaeth GL, Stirbu O, Yalcin A and Myers JS. The effects of Mozart's music on the performance of glaucoma patients on automated perimetry. *Investigative Ophthalmology and Visual Science* 2011;52:7347-7349.

Siatkowski RM, Lam BL, Anderson DR, Feuer WJ and Halikman AM. Automated suprathreshold static perimetry screening for detecting neuro-ophthalmologic disease. *Ophthalmology* 1996;103:907-917.

Siddiqui MA, Azuara-Blanco A and Neville S. Effect of cataract extraction on Frequency Doubling Technology perimetry in patients with glaucoma. *British Journal of Ophthalmology* 2005;89:1569-1571.

Siddiqui MA, Khairy HA and Azuara-Blanco A. Effect of cataract extraction on SITA perimetry in patients with glaucoma. *Journal of Glaucoma* 2007;16:205-208.

Silverman SE, Trick GL and Hart WMJ. Motion perception is abnormal in primary open angle glaucoma and ocular hypertension. *Investigative Ophthalmology and Visual Science* 1990;31:722-729.

Simakova IL and Boĭko EV. Impact of cataract and age-related macular degeneration on the results of various perimetry techniques. *Vestnik Oftalmologii* 2010;126:10-14.

Sloan LL. Area and luminance of test object as variables in examination of the visual field by projection perimetry. *Vision Research* 1961;1:121-138.

Smith SD, Katz J and Quigley HA. Effect of cataract extraction on the results of automated perimetry in glaucoma. *Archives of Ophthalmology* 1997;115:1515-1519.

Sommer A, Tielsch JM, Katz J, Quigley HA, Gottsch JD, Javitt J and Singh K. Relationship between intraocular pressure and primary open angle glaucoma among white and black Americans. The Baltimore Eye Survey. *Archives of Ophthalmology* 1991;109:1090-1095.

Spahr J. Optimization of the presentation pattern in automated static perimetry. *Vision Research* 1975;15:1275-1281.

Sponsel WE, Ritch R, Stamper R, Higginbotham EJ, Anderson DR, Wilson MR and Zimmerman TJ. Prevent Blindness America visual field screening study. The Prevent Blindness America Glaucoma Advisory Committee. *American Journal of Ophthalmology* 1995;120:699-708.

Spry PG, Hussin HM and Sparrow JM. Clinical evaluation of Frequency Doubling Technology perimetry using the Humphrey Matrix 24-2 threshold strategy. *British Journal of Ophthalmology* 2005;89:1031-1035.

Spry PG, Johnson CA, Mansberger SL and Cioffi GA. Psychophysical investigation of ganglion cell loss in early glaucoma. *Journal of Glaucoma* 2005;14:11-19.

Stavrou EP and Wood JM. Central visual field changes using flicker perimetry in Type 2 diabetes mellitus. *Acta Ophthalmologica Scandinavica* 2005 83:574-580.

Stewart WC, Rogers GM, Crinkley CMC and Carlson AN. Effect of cataract extraction on automated fields in chronic open-angle glaucoma. *Archives of Ophthalmology* 1995;113:875-879.

Stewart WC, Shields MB and Ollie AR. Full Threshold versus Quantification of Defects for visual field testing in glaucoma. *Graefe's Archive for Clinical and Experimental Ophthalmology* 1989;227:51-54.

Tafreshi A, Sample PA, Liebmann JM, Girkin CA, Zangwill LM, Weinreb RN, Lalezary M and Racette L. Visual function-specific perimetry to identify glaucomatous visual loss using three different definitions of visual field abnormality. *Investigative Ophthalmology and Visual Science* 2009 50:1234-1240.

Takada S, Matsumoto C, Arimura E, Hashimoto S, Okuyama S and Shimomura Y. Influence of media opacities on SAP, SWAP, HRP, FDP and flicker perimetry. *Investigative Ophthalmology and Visual Science* 2004;45:E-Abstract 4330.

Tan JC, Spalton DJ and Arden GB. Comparison of methods to assess visual impairment from glare and light scattering with posterior capsule opacification. *Journal of Cataract and Refractive Surgery* 1998;24:1626-1631.

Tanga L, Centofanti M, Oddone F, Parravano M, Parisi V, Ziccardi L, Kroegler B, Perricone R and Manni G. Retinal functional changes measured by Frequency-Doubling Technology in patients treated with hydroxychloroquine. *Graefe's Archive for Clinical and Experimental Ophthalmology* 2011;249:715-721.

Tanna AP, Abraham C, Lai J and Shen J. Impact of cataract on the results of Frequency Doubling Technology perimetry. *Ophthalmology* 2004;111:1504-1507.

Tate GW. The physiological basis for perimetry. Orlando, FL: Grune & Stratton Inc, 1985; 1-28.

Taylor MM. On the efficiency of psychophysical measurement. *Journal of the Acoustical Society of America* 1971;49:505-508.

Thibos LN, Cheney FE and Walsh DJ. Retinal limits to the detection and resolution of gratings. *Journal of the Optical Society of America* 1987;4:1524-1529.

Thomas D, Thomas R, Muliyil JP and George R. Role of Frequency Doubling Perimetry in detecting neuro-ophthalmic visual field defects. *American Journal of Ophthalmology* 2001;131:734-741.

Topouzis F, Coleman AL, Yu F, Mavroudis L, Anastasopoulos E, Koskosas A, Pappas T, Dimitrakos S and Wilson MR. Sensitivity and specificity of the 76-suprathreshold visual field test to detect eyes with visual field defect by Humphrey threshold testing in a population-based setting: the Thessaloniki eye study. *American Journal of Ophthalmology* 2004;137:420-425.

Turpin A, McKendrick AM, Johnson CA and Vingrys AJ. Performance of efficient test procedures for Frequency-Doubling Technology perimetry in normal and glaucomatous eyes. *Investigative Ophthalmology and Visual Science* 2002;43:709-715.

Turpin A, McKendrick AM, Johnson CA and Vingrys AJ. Properties of perimetric threshold estimates from Full Threshold, ZEST, and SITA-like strategies, as determined by computer simulation. *Investigative Ophthalmology and Visual Science* 2003;44:4787-4795.

Tyler CW. Specific deficits of flicker sensitivity in glaucoma and ocular hypertension. *Investigative Ophthalmology and Visual Science* 1981;20:204-212.

Tyler CW. Analysis of normal flicker sensitivity and its variability in the visuogram test. *Investigative Ophthalmology and Visual Science* 1991;32:2552-2560.

Tyler CW, Ryu S and Stamper R. The relation between visual sensitivity and intraocular pressure in normal eyes. *Investigative Ophthalmology and Visual Science* 1984;25:103-105.

Tyrrell RA and Owens DA. A rapid technique to assess the resting states of the eyes and other threshold phenomena: The Modified Binary Search (MOBS). *Behavior Research Methods, Instruments and Computers* 1988;20:137-141.

Ueda T, Ota T, Yukawa E and Hara Y. Frequency Doubling Technology perimetry after clear and yellow intraocular lens implantation. *American Journal of Ophthalmology* 2006;142:856-858.

Van Coevorden RE, Mills RP, Chen YY and Barnebey HS. Continuous visual field test supervision may not always be necessary. *Ophthalmology* 1999;106:178-181.

van den Berg TJ. On the relation between glare and straylight. *Documenta Ophthalmologica Proceedings Series* 1991;78:177-181.

van den Berg TJ, IJspeert JK and de Waard PW. Dependence of intraocular straylight on pigmentation and light transmission through the ocular wall. *Vision Research* 1991;31:1361-1367.

van Den Berg TJTP, van Spronsen R, van Veenendaal WG and Bakker D. Psychophysics of intensity discrimination in relation to defect volume examination on the scoperimeter. In: Heijl A, Greve EL, eds. Proceedings of the Sixth International Visual Field Symposium. Santa Margherita, Ligure, Italy, 1984. Documenta Ophthalmologica Proceedings Series 1985:147-151.

van der Schoot J, Reus NJ, Colen TP and Lemij HG. The ability of short-wavelength automated perimetry to predict conversion to glaucoma. *Ophthalmology* 2010;117:30-34.

Van Toi V, Grounauer PA and Burckhardt CW. Artificially increasing intraocular pressure causes flicker sensitivity losses. *Investigative Ophthalmology and Visual Science* 1990;31:1567-1574.

Vidal-Fernández A, García Feijoó J, González-Hernández M, González De La Rosa M and García Sánchez J. Initial findings with Pulsar perimetry in patients with ocular hypertension. *Archivos de la Sociedad Española de Oftalmología* 2002;77:321-326.

Vingrys AJ and Demirel S. False-response monitoring during automated perimetry. *Optometry and Vision Science* 1998;75:513-517.

Vingrys AJ and Pesudovs K. Localized scotomata detected with temporal modulation perimetry in central serous chorioretinopathy. *Australian and New Zealand Journal of Ophthalmology* 1999;27:109-116.

Vislisel JM, Doyle CK, Johnson CA and Wall M. Variability of Rarebit and standard perimetry sizes I and III in normals. *Optometry and Vision Science* 2011;88:635-639.

Wabbels BK, Diehm S and Kolling G. Continuous light increment perimetry compared to Full Threshold strategy in glaucoma. *European Journal of Ophthalmology* 2005;15:722-729.

Wabbels BK and Wilscher S. Feasibility and outcome of automated static perimetry in children using continuous light increment perimetry (CLIP) and fast threshold strategy. *Acta Ophthalmologica Scandinavica* 2005;83:664-669.

Wachler BSB, Durrie DS, Assil KK and Krueger RR. Improvement of visual function with glare testing after photorefractive keratectomy and radial keratotomy. *American Journal of Ophthalmology* 1999;128:582-587.

Wall M. High-pass Resolution perimetry in optic neuritis. *Investigative Ophthalmology and Visual Science* 1991;32:2525-2529.

Wall M, Brito CF, Woodward KR, Doyle CK, Kardon RH and Johnson CA. Total Deviation probability plots for stimulus size V perimetry: a comparison with size III stimuli. *Archives of Ophthalmology* 2008;126:473-479.

Wall M, Chauhan B, Frisén L, House PH and Brito C. Visual Field of High-pass Resolution perimetry in normal subjects. *Journal of Glaucoma* 2004;13:15-21.

Wall M, Conway MD, House PH and Allely R. Evaluation of sensitivity and specificity of spatial resolution and Humphrey automated perimetry in pseudotumor cerebri patients and normal subjects. *Investigative Ophthalmology and Visual Science* 1991;32:3306-3312.

Wall M, Doyle CK, Brito CF, Woodward KR and Johnson CA. A comparison of catch-trial methods used in standard automated perimetry in glaucoma patients. *Journal of Glaucoma* 2008;17:626-630.

Wall M, Jennisch CS and Munden PM. Motion perimetry identifies nerve fiber bundle like defects in ocular hypertension. *Archives of Ophthalmology* 1997 115:26-33.

Wall M, Johnson CA, Kardon RH and Crabb DP. Use of a continuous probability scale to display visual field damage. *Archives of Ophthalmology* 2009;127:749-756.

Wall M, Kardon R and Moore P. Large size stimuli of automated perimetry have lower variability. *Investigative Ophthalmology and Visual Science* 1993;34:1262.

Wall M, Kutzko KE and Chauhan BC. Variability in patients with glaucomatous visual field damage is reduced using size V stimuli. *Investigative Ophthalmology and Visual Science* 1997;38:426-435.

Wall M and White WN. Asymmetric papilledema in idiopathic intracranial hypertension: prospective interocular comparison of sensory visual function. *Investigative Ophthalmology and Visual Science* 1998;39:134-142.

Wall M, Woodward KR, Doyle CK and Artes PH. Repeatability of automated perimetry: a comparison between standard automated perimetry with stimulus size III and V, Matrix, and Motion perimetry. *Investigative Ophthalmology and Visual Science* 2009;50:974-979.

Wall M, Woodward KR, Doyle CK and Zamba G. The effective dynamic ranges of standard automated perimetry sizes III and V and Motion and Matrix perimetry. *Archives of Ophthalmology* 2010;128:570-576.

Walsh TJ. Visual Fields. San Francisco, CA: American Academy of Ophthalmology, 1996; 309.

Weber J and Klimaschka T. Test time and efficiency of Dynamic Strategy in glaucoma perimetry. *German Journal of Ophthalmology* 1995;4:25-31.

Weijland A, Fankhauser F, Bebie H and Flammer J. Automated Perimetry Visual Field Digest. Haag-Streit AG, 2004.

Weinreb RN, Friedman DS, Fechtner RD, Cioffi GA, Coleman AL, Girkin CA, Liebmann JM, Singh K, Wilson MR, Wilson R and Kannel WB. Risk assessment in the management of patients with ocular hypertension. *American Journal of Ophthalmology* 2004;138:458-467.

Weinreb RN and Perlman JP. The effect of refractive error on automated global analysis program G-1. *American Journal of Ophthalmology* 1986;104:229-232.

Werner EB, Adelson A and Krupin T. Effect of patient experience on the results of automated perimetry in clinically stable glaucoma patients. *Ophthalmology* 1988;95:764-767.

Werner EB and Drance SM. Early visual field disturbances in glaucoma. *Archives of Ophthalmology* 1977;95:1173-1175.

Werner EB, Krupin T, Adelson A and Feitl ME. Effect of patient experience on the results of automated perimetry in glaucoma suspect patients. *Ophthalmology* 1990;97:44-48.

Westcott MC, McNaught AI, Crabb DP, Fitzke FW and Hitchings RA. High spatial resolution automated perimetry in glaucoma. *The British Journal of Ophthalmology* 1997;81:452-459.

Wetherill GB and Levitt H. Seqential estimation of points on a psychometric function. *British Journal of Mathematical and Statistical Psychology* 1965;18:1-10.

White AJ, Sun H, Swanson WH and Lee BB. An examination of physiological mechanisms underlying the Frequency-Doubling illusion. *Investigative Ophthalmology and Visual Science* 2002;43:3590-3599.

Wild JM. Short-wavelength automated perimetry. *Acta Ophthalmologica Scandinavica* 2001;79:546-559.

Wild JM, Betts TA and Shaw DE. The Influence of a social dose of alcohol on the central visual field. *Japanese Journal of Ophthalmology* 1990;34:291-297.

Wild JM, Cubbidge RP, Pacey IE and Robinson R. Statistical aspects of the normal visual field in short-wavelength automated perimetry. *Investigative Ophthalmology and Visual Science* 1998;39:54-63.

Wild JM, Dengler-Harles M, Searle AE, O'Neill EC and Crews SJ. The influence of the learning effect on automated perimetry in patients with suspected glaucoma. *Acta Ophthalmologica* 1989;67:537-545.

Wild JM, Kim LS, Pacey IE and Cunliffe IA. Evidence for a learning effect in short-wavelength automated perimetry. *Ophthalmology* 2006;113:206-215.

Wild JM, Martinez C, Reinshagen G and Harding FA. Characteristics of a unique visual field defect attributed to Vigabatrin. *Epilepsia* 1999;40:1784-1794.

Wild JM, Moss ID and O'Neill EC. Baseline alterations in blue-on-yellow normal perimetric sensitivity. *Graefe's Archive for Clinical and Experimental Ophthalmology* 1996;234:141-149.

Wild JM, Moss ID, Whitaker DJ and O'Neill EC. The statistical interpretation of blue on yellow visual field loss. *Investigative Ophthalmology and Visual Science* 1995;36:1398-1410.

Wild JM, Pacey IE, Hancock SA and Cunliffe IA. Between-algorithm, between-individual differences in normal perimetric sensitivity: Full Threshold, FASTPAC, and SITA. *Investigative Ophthalmology and Visual Science* 1999a;40:1152-1161.

Wild JM, Pacey IE, O'Neill EC and Cunliffe IA. The SITA Perimetric Threshold Algorithms in glaucoma. *Investigative Ophthalmology and Visual Science* 1999b;40:1998-2009.

Wild JM, Searle AE, Dengler-Harles M and O'Neill EC. Long-term follow-up of baseline learning and fatigue effects in the automated perimetry of glaucoma and ocular hypertensive patients. *Acta Ophthalmologica* 1991;69:210-216.

Wilensky JT and Joondeph BC. Variation in visual field measurements with an automated perimeter. *American Journal of Ophthalmology* 1984;97:328-331.

Wilson ME. Invariant features of spatial summation with changing locus in the visual field. *Journal of Physiology* 1970;2007:611-622.

Winther C and Frisén L. A compact Rarebit test for macular diseases. *British Journal of Ophthalmology* 2010;94:324-327.

Wood JM, Wild JM, Bullimore MA and Gilmartin B. Factors affecting the normal perimetric profile derived by automated static threshold LED perimetry. I. Pupil size. *Ophthalmic and Physiological Optics* 1988;8:26-31.

Wood JM, Wild JM and Crews SJ. Induced intraocular light scatter and the sensitivity gradient of normal visual field. *Graefe's Archive for Clinical and Experimetal Ophthalmology* 1987a;225:369-373.

Wood JM, Wild JM, Hussey MK and Crews SJ. Serial examination of the normal visual field using Octopus automated projection perimetry. Evidence for a learning effect. *Acta Ophthalmologica* 1987b;65:326-333.

Wood JM, Wild JM, Smerdon DL and Crews SJ. Alterations in the shape of the automated perimetric profile arising from cataract. *Graefe's Archive for Clinical and Experimental Ophthalmology* 1989;227:157-161.

Wu LL, Suzuki Y, Kunimatsu S, Araie M, Iwase A and Tomita G. Frequency-Doubling technology and confocal scanning ophthalmoscopic optic disc analysis in open-angle glaucoma with hemifield defects. *Journal of Glaucoma* 2001;10:256-260.

Yenice O and Temel A. Evaluation of two Humphrey perimetry programs: Full Threshold and SITA Standard testing strategy for learning effect. *European Journal of Ophthalmology* 2005;15:209-212.

Yoshiyama KK and Johnson CA. Which method of flicker perimetry is most effective for detection of glaucomatous visual field loss? *Investigative Ophthalmology and Visual Science* 1997;38:2270-2277.

Zalta AH. Lens rim artifact in automated threshold perimetry. *Ophthalmology* 1989;96:1302-1311.

Zalta AH. Use of a central 10 degrees field and size V stimulus to evaluate and monitor small central islands of vision in end stage glaucoma. *British Journal of Ophthalmology* 1991;74:289-293.

Zalta AH and Burchfield JC. Detecting early glaucomatous field defects with the size I stimulus and Statpac. *The British Journal of Ophthalmology* 1990;74:289-293.

Zeppieri M, Brusini P, Parisi L, Johnson CA, Sampaolesi R and Salvetat ML. Pulsar perimetry in the diagnosis of early glaucoma. *American Journal of Ophthalmology* 2010;149:102-112.

Zeppieri M, Demirel S, Kent K and Johnson CA. Perceived spatial frequency of sinusoidal gratings. *Optometry and Vision Science* 2008;85:318-329.

Zhong Y, Chen L, Cheng Y and Huang P. Influence of learning effect on blue-on-yellow perimetry. *European Journal of Ophthalmology* 2008;18:392-399.

Zulauf M, Caprioli J, Hoffman DC and Tressler CS. Fluctuation of the differential light senstivity in clinically stable glaucoma. In: Mills RP, Heijl A, eds. *Perimetry Update 1990/1991* Proceedings of the IXth International Perimetric Society Meeting. Malmø, Sweden: Kugler and Ghedini; 1991, 183-188.

Zulauf M, Fehlmann P and Flammer J. Perimetry with normal Octopus technique and Weber 'Dynamic' technique. Initial results with reference to reproducibility of measurements in glaucoma patients. *Ophthalmologe* 1996;93:420-427.

Zulauf M, Flammer J and Signer C. The influence of alcohol on the outcome of automated static perimetry. *Graefe's Archive for Clinical and Experimental Ophthalmology* 1986;224:525-528.

Zulauf M, LeBlanc RP and Flammer J. Normal visual fields measured with Octopus program G1 II. Global visual field indices. *Graefe's Archive for Clinical and Experimental Ophthalmology* 1994;232:516-522.